

**A POWERFUL COMBINATION OF COMPUTATIONAL METHODS
ON THE ROAD TOWARD POTENT NON-STEROIDAL
INHIBITORS OF STEROIDOGENIC ENZYMES
INVOLVED IN
HORMONE-DEPENDENT DISEASES.**

Dissertation

zur Erlangung des Grades des Doktors der Naturwissenschaften

der Naturwissenschaftlich-Technischen Fakultät III

Chemie, Pharmazie, Bio- und Werkstoffwissenschaften

der Universität des Saarlandes

von

Matthias Negri

Saarbrücken

2010

Day of oral dissertation defense: 04.06.2010

chairwoman: Prof. Dr. Alexandra Kiemer (Saarland University)

commission Prof. Dr. Rolf W. Hartmann (Saarland University)
Prof. Dr. Maurizio Recanatini (University of Bologna)
Prof. Dr. Marinella Roberti (University of Bologna)
Dr. Matthias Engel (Saarland University)

This doctoral thesis was performed from July 2005 until Dezember 2009 in “co-tutele” under the supervision of Prof. Dr. Rolf W. Hartmann and Prof. Dr. Maurizio Recanatini at the Faculty of Natural Sciences and Technology III of Saarland University and at the Department of Pharmaceutical Sciences of the “Alma Mater Studiorum” University of Bologna, respectively.

„Die Schlange, welche sich nicht häuten kann, geht zugrunde. Ebenso die Geister, welche man verhindert, ihre Meinungen zu wechseln; sie hören auf, Geist zu sein.“

Friedrich Wilhelm Nietzsche

”Il serpente che non può cambiar pelle muore. Lo stesso accade agli spiriti ai quali s'impedisce di cambiare opinione: cessano di essere spiriti.”

...FOR MY SON AMOR LEONARD AND MY WIFE MONIKA

ABSTRACT

Different computational methods have been applied to the development of non-steroidal inhibitors of steroidogenic enzymes for the treatment of hormone-sensitive diseases, like breast and prostate cancer and hypertension.

A high-quality homology model of CYP17 was created and used for docking studies. Three binding modes were identified and SAR for different CYP17-inhibitor classes, substantiated by *ab initio* calculations, could be derived and used in further drug design leading to improved potency.

Docking studies and ligand cluster analysis for a series of CYP19 inhibitors resulted in a binding mode, well explaining their different inhibitory potencies. The derived SAR were used in ongoing drug design, resulting so far in highly potent CYP19 inhibitors.

The kinetic cycle of 17 β -HSD1 was hypothesized based on biochemical data, analysis of the crystal structures and a multi-trajectory MD approach and provided insights in protein motion. These were translated into the drug design process. An ensemble docking study was performed for bis(hydroxyphenyl)-arenes, potent 17 β -HSD1 inhibitors, and two conformation-dependent binding modes were identified. MD simulations and quantum-chemical calculations identified one of them as the more plausible, suggesting this class of compounds to dysfunction the enzyme dynamics.

Two pharmacophore models were derived from CYP11B2 inhibitors and combined into a ligand- and structure-based approach, which led to a new class of potent CYP11B2 inhibitors.

ZUSAMMENFASSUNG

Verschiedene computergestützte Methoden wurden in der Entwicklung von nicht-steroidalen Hemmstoffen steroidogener Enzyme angewandt. Diese Inhibitoren sollen zur Behandlung hormon-abhängiger Krankheiten eingesetzt werden.

Ein qualitativ-hochwertiges CYP17 Homologiemodell wurde erstellt und in Docking Studien verwendet. Drei Bindungsmodi konnten identifiziert werden und Struktur-Wirkungsbeziehungen wurden für verschiedene CYP17 Hemmstoffklassen abgeleitet und erfolgreich in eine weitere Hemmstoffentwicklung eingebaut.

Dockingstudien und Clusteranalysen einer Reihe von CYP19 Inhibitoren ergaben einen plausiblen Bindungsmodus und die daraus gewonnenen Erkenntnisse führten in laufenden Projekten zu höchst potenten Hemmstoffen.

Der kinetische Zyklus von 17β -HSD1 wurde postuliert basierend auf biochemischen Literaturdaten, Kristallstrukturenanalyse und einem multiplen MD-Ansatz, welcher wichtige Einblicke in die Dynamik des Enzyms lieferte. Diese wurden als ensemble docking Ansatz in die Entwicklung einer Klasse hochpotenter 17β -HSD1 Inhibitoren eingebaut und ergaben zwei Enzymkonformations-abhängige Bindungsmodi. MD-Simulationen und quantenchemische Methoden identifizierten einen davon als plausibler. Dabei scheinen Substanzen dieser Klasse die Enzymdynamik zu stören.

Zwei Pharmakophormodelle wurden basierend auf CYP11B2-Hemmstoffen erstellt und in einen Ligand- und Struktur-basierten Ansatz eingebaut. Dieser führte zu einer neuen Klasse von potenten und selektiven CYP11B2-Inhibitoren.

PAPERS INCLUDED IN THIS THESIS

This thesis is divided into 14 publications, which are referred to in the text by their Roman numerals.

CYP17:

- I.** Synthesis, biological evaluation and molecular modelling studies of novel ACD- and ABD-ring steroidomimetics as inhibitors of CYP17.
Pinto-Bazurco Mendieta MA, **Negri M**, Jagusch C, Hille UE, Müller-Vieira U, Schmidt D, Hansen K, Hartmann RW.
Bioorganic Medicinal Chemistry Letters (2008) 18(1):267-273.
- II.** Synthesis, biological evaluation and molecular modelling studies of methyleneimidazole substituted biaryls as inhibitors of human 17 α -hydroxylase-17,20-lyase (CYP17). Part I: Heterocyclic modifications of the core structure.
Jagusch C, **Negri M**, Hille UE, Hu Q, Bartels M, Jahn-Hoffmann K, Pinto-Bazurco Mendieta MA, Rodenwaldt B, Müller-Vieira U, Schmidt D, Lauterbach T, Recanatini M, Cavalli A, Hartmann RW.
Bioorganic Medicinal Chemistry (2008) 16(4):1992-2010.
- III.** Synthesis, biological evaluation, and molecular modeling of abiraterone analogues: novel CYP17 inhibitors for the treatment of prostate cancer.
Pinto-Bazurco Mendieta MA, **Negri M**, Jagusch C, Müller-Vieira U, Lauterbach T, Hartmann RW.
Journal of Medicinal Chemistry (2008) 51(16):5009-5018.
- IV.** Synthesis, biological evaluation, and molecular modeling studies of methylene imidazole substituted biaryls as inhibitors of human 17 α -hydroxylase-17,20-lyase (CYP17) - part II: Core rigidification and influence of substituents at the methylene bridge.
Hu Q, **Negri M**, Jahn-Hoffmann K, Zhuang Y, Olgen S, Bartels M, Müller-Vieira U, Lauterbach T, Hartmann RW.
Bioorganic Medicinal Chemistry (2008) 16(16):7715-7727.
- V.** CYP17 inhibitors. Annulations of additional rings in methylene imidazole substituted biphenyls: synthesis, biological evaluation and molecular modelling.
Pinto-Bazurco Mendieta MA, **Negri M**, Hu Q, Hille UE, Jagusch C, Jahn-Hoffmann K, Müller-Vieira U, Schmidt D, Lauterbach T, Hartmann RW.
Archiv der Pharmazie (Weinheim) (2008)341(10):597-609.
- VI.** Novel CYP17 inhibitors: synthesis, biological evaluation, structure-activity relationships and modelling of methoxy- and hydroxy-substituted methyleneimidazolyl biphenyls.
Hille UE, Hu Q, Vock C, **Negri M**, Bartels M, Müller-Vieira U, Lauterbach T, Hartmann RW.
European Journal of Medicinal Chemistry (2009) 44(7):2765-2775.
- VII.** Role of fluorine substitution in biphenyl methylene imidazole type CYP17 inhibitors for the treatment of prostate carcinoma.
Hu Q, **Negri M**, Olgen S, Hartmann RW
(Hu Q. and Negri M. contributed equally to the work)
Submitted to *ChemMedChem* (2010).

CYP19:

VIII. Imidazolylmethylbenzophenones as highly potent aromatase inhibitors.

Gobbi S, Cavalli A, **Negri M**, Schewe KE, Belluti F, Piazzini L, Hartmann RW, Recanatini M, Bisi A.
Journal of Medicinal Chemistry (2007) 50(15):3420-3422.

17 β -HSD1:

IX. Design, synthesis, biological evaluation and pharmacokinetics of bis(hydroxyphenyl) substituted azoles, thiophenes, benzenes, and aza-benzenes as potent and selective nonsteroidal inhibitors of 17 β -hydroxysteroid dehydrogenase type 1 (17 β -HSD1).

Bey E, Marchais-Oberwinkler S, Werth R, **Negri M**, Al-Soud YA, Kruchten P, Oster A, Frotscher M, Birk B, Hartmann RW.
Journal of Medicinal Chemistry (2008) 51(21):6725-6739.

X. New insights into the SAR and binding modes of bis(hydroxyphenyl)thiophenes and -benzenes: influence of additional substituents on 17 β -hydroxysteroid dehydrogenase type 1 (17 β -HSD1) inhibitory activity and selectivity.

Bey E, Marchais-Oberwinkler S, **Negri M**, Kruchten P, Oster A, Klein T, Spadaro A, Werth R, Frotscher M, Birk B, Hartmann RW.
Journal of Medicinal Chemistry (2009) 52(21):6724-6743.

XI. Dynamic motion investigation of 17 β -HSD1 provides deep insights in enzyme kinetics and ligand binding.

Negri M, Recanatini M, Hartmann RW.
Submitted **2010**.

CYP11B2:

XII. Development and evaluation of a pharmacophore model for inhibitors of aldosterone synthase (CYP11B2).

Ulmschneider S, **Negri M**, Voets M, Hartmann RW.
Bioorganic Medicinal Chemistry Letters (2006) 16(1):25-30.

XIII. Overcoming undesirable CYP1A2 inhibition of pyridyl-naphthalene-type aldosterone synthase inhibitors: influence of heteroaryl derivatization on potency and selectivity.

Heim R, Lucas S, Grombein CM, Ries C, Schewe KE, **Negri M**, Müller-Vieira U, Birk B, Hartmann RW.
Journal of Medicinal Chemistry (2008) 51(16):5064-5074.

XIV. Novel aldosterone synthase inhibitors with extended carbocyclic skeleton by a combined ligand-based and structure-based drug design approach.

Lucas S, Heim R, **Negri M**, Antes I, Ries C, Schewe KE, Bisi A, Gobbi S, Hartmann RW.
Journal of Medicinal Chemistry (2008) 51(19):6138-6149.

CONTRIBUTION REPORT

The author wishes to clarify his contributions to the papers **I–XIV** in the thesis.

- I-V** Performed all the computational work (molecular docking) present in the articles. Contributed to the design of new inhibitors. Significantly contributed to the interpretation of the results. Wrote the molecular modeling part of the manuscript.
- VI** Performed all the computational work and wrote the computational part of the manuscript. Interpretation of the modeling results.
- VII** Performed all the computational work present in the articles. Contributed to the design of new inhibitors. Significantly contributed to the interpretation of the results. Contributed to write the manuscript.
- VIII** Performed all molecular docking studies and contributed to interpret the results. Contributed to writing the manuscript.
- IX** Proposed, planned and performed all the quantum chemical calculations and the analysis of the different MEP maps. Significantly contributed to the establishment of the “semi-QMAR”, a quantitative MEP-activity relationship for the series of bis(hydroxyphenyl)-arenes, potent 17 β -HSD1 inhibitors. Thus, significantly contributed to the interpretation of the results and to write the manuscript.
- X** Planned and performed all molecular docking studies and was substantially involved in the design of the study. Significantly contributed to the identification of two binding modes, thus to the interpretation of the results and the write the manuscript.
- XI** Designed the study concept. Planned, performed and analyzed all the results of the computational studies. Interpreted the results. Wrote the manuscript.
- XII** Performed the set up of the pharmacophore, analyzed the results and validated them *in silico*. Wrote the pharmacophore chapter of the manuscript and contributed to the interpretation of the results.
- XIII** Performed and planned the computational studies. Contributed to the interpretation of the results. Contributed to the composition of the manuscript.
- XIV** Significantly contributed to the design of the inhibitors. Built the pharmacophore and contributed to develop a validation schedule in order to design new inhibitors. Significantly contributed to the interpretation of the results. Wrote the computational ligand-based part of the manuscript.

ABBREVIATIONS

17 β -HSDs	17 β -Hydroxysteroid dehydrogenases
17 β -HSD1	17 β -Hydroxysteroid dehydrogenase type 1
17 β -HSD2	17 β -Hydroxysteroid dehydrogenase type 2
17 β -HSD3	17 β -Hydroxysteroid dehydrogenase type 3
17 β -HSD5	17 β -Hydroxysteroid dehydrogenase type 5
17OHPreg	17 α -Hydroxypregnenolone
17OHP	17 α -Hydroxyprogesterone
3 β -HSD	3 β -hydroxysteroid dehydrogenase/ Δ 5- Δ 4 isomerase
4-Adione	Androstenedione (4-A)
ACE	Angiotensin-converting enzyme
ACTH	Adrenocorticotrophic hormone
AI	Aromatase inhibitors
AKR	Aldo keto reductases
Ang II	Angiotensin II
AUC	Area under the curve
cAMP	Cyclic adenosine monophosphate
BC	Breast cancer
CAB	Combined androgen blockade
CHF	Congestive heart failure
CNS	Central nervous system
CONSENSUS	Cooperative north scandinavian enalapril survival study
CPR	Cytochrome P450 reductase (also POR, CYPOR)
CRPC	Castration-resistant prostate cancer
CYB5	Cytochrome b5
CYB5R	Cytochrome b5 reductase (CBR)
CYP	Cytochrome P450
CYP11A1	Cholesterol desmolase
CYP11B1, P450c11 β	11 β -Hydroxylase, steroid 11 β -hydroxylase
CYP11B2, P450c18	Aldosterone synthase
CYP17, CYP17A1	17 α -Hydroxylase-17,20-lyase
CYP19, P450arom	Aromatase
CYP101	Cytochrome P450cam
CYP102A1	Cytochrome P450 BM3
CYP21	21-Hydroxylase

CYP5	Thromboxane synthase
CYP8	Prostacyclin synthase
DFT	Density functional theory
DHEA	Dehydroepiandrosterone
DHEA-S	DHEA-sulfate
DHT	Dihydrotestosterone
E1	Estrone
E2	Estradiol
EDD	Estrogen-dependent diseases
EPHESUS	Eplerenone post-acute myocardial infarction heart failure efficacy and survival study
ER	Estrogen receptor
ESI	Electrospray ionization
ESP	Electrostatic potential
Et	Ethyl
FAD	Flavin adenine dinucleotide
Fd	Fe ₂ S ₂ ferredoxin
FMN	Flavinmononucleotid
FR	Ferredoxin reductase
FSH	Follicle stimulating hormone
g	Gram
GA	Genetic algorithm
GnRH	Gonadotropin releasing hormone
Het	Heteroaryl
HSD	Hydroxysteroid dehydrogenases
IC ₅₀	Concentration required for 50 % inhibition
kDa	Kilodalton
LH	Luteinizing hormone
LHRH	Luteinizing hormone releasing hormone
Me	Methyl
MD (simulation)	Molecular dynamic (simulation), MDS
MEP	Molecular electrostatic potential
mL	Milliliter
mmol	Millimol, mM
MR	Mineralocorticoid receptor
μg	Microgram
μL	Microliter

μM	Micromolar
NAD(H)	Nicotinamide adenine dinucleotide
NADP(H)	Nicotinamide adenine dinucleotide phosphate
nm	Nanometer
nM	Nanomolar
P	Progesterone
Preg	Pregnenolone
P-450	Cytochrome P450
P450 _{sc} , P450c11a1	P450-linked side chain cleaving enzyme
Ph	Phenyl
PK	Pharmacokinetic
PKA	Protein kinase A
pM	Picomolar
QSAR	Quantitative structure activity relationship
RAAS	Renin-angiotensin-aldosterone system
RALES	Randomized aldactone evaluation study
RE	Endoplasmatic Reticulum
RMSD	Root mean square deviation
SAR	Structure activity relationship
SCR	Structurally conserved regions
SDR	Short chain dehydrogenases/reductases
SEM	Standard error of the mean
Semi-QMAR	Semi quantitative MEP-activity relationship
SERM	Selective estrogen receptor modulators
SHBG	Sex hormone binding globulin
SRS	Substrate recognition sites
StAR	Steroidogenic acute regulatory protein
SVR	Structurally variable regions
T	Testosterone
Å	Ångström

CONTENTS

Abstract	vii
Zusammenfassung	viii
Papers included in the thesis	ix
Contribution report	xi
Abbreviations	xiii
Chapter One. Introduction	1
1.1 Steroidogenesis	1
1.1.1. Biosynthesis of steroid hormones	2
1.1.2. Adrenal glands	3
1.1.3. Gonadal steroid hormones	4
1.1.4. Steroid hormones receptors	6
1.2 Endocrinology vs intracrinology - pathophysiological role of steroid hormones	7
1.2.1. Prostate cancer (PC)	9
1.2.2. Estrogen-dependent diseases (EDD)	10
1.2.2.1. Breast cancer (BC)	11
1.2.2.2. Endometriosis	12
1.2.3. Congestive heart failure (CHF)	12
1.3 Potential target enzymes involved in steroidogenesis	15
1.3.1. Cytochromes P450 (CYPs) enzymes	15
1.3.1.1. CYP17 – 17 α -Hydroxylase/17,20-Lyase	21
1.3.1.2. CYP19 – Aromatase	22
1.3.1.3. CYP11B2 – Aldosterone synthase	23
1.3.2. Hydroxysteroid dehydrogenases (HSDs)	25
1.3.2.1. 17 β -HSDs – 17 β -Hydroxysteroid dehydrogenases	26
1.3.2.2. 17 β -HSD1 – 17 β -Hydroxysteroid dehydrogenase type 1	28
Chapter Two. Aims of the study	31

Chapter Three.	Results and Discussion	33
3.1	Androgen-dependent prostate cancer (PC) – selective CYP17 inhibition	33
3.1.1.	Homology model of CYP17	33
3.1.2.	Molecular docking of CYP17 inhibitors	35
3.1.3.	Molecular electrostatic potential (MEP) distribution of CYP17 inhibitors	37
3.1.4.	Articles published in CYP17 project – paper I-VII	39
3.1.4.1.	Synthesis, biological evaluation and molecular modelling studies of novel ACD- and ABD-ring steroidomimetics as inhibitors of CYP17.	39
3.1.4.2.	Synthesis, biological evaluation and molecular modelling studies of methyleneimidazole substituted biaryls as inhibitors of human 17 α -hydroxylase-17,20-lyase (CYP17). Part I: Heterocyclic modifications of the core structure.	55
3.1.4.3.	Synthesis, biological evaluation, and molecular modeling of abiraterone analogues: novel CYP17 inhibitors for the treatment of prostate cancer.	77
3.1.4.4.	Synthesis, biological evaluation, and molecular modeling studies of methylene imidazole substituted biaryls as inhibitors of human 17 α -hydroxylase-17,20-lyase (CYP17) - part II: Core rigidification and influence of substituents at the methylene bridge.	95
3.1.4.5.	CYP17 inhibitors. Annulations of additional rings in methylene imidazole substituted biphenyls: synthesis, biological evaluation and molecular modelling.	115
3.1.4.6.	Novel CYP17 inhibitors: synthesis, biological evaluation, structure-activity relationships and modelling of methoxy- and hydroxy-substituted methyleneimidazolyl biphenyls.	131
3.1.4.7.	Role of fluorine substitution in biphenyl methylene imidazole type CYP17 inhibitors for the treatment of prostate carcinoma.	147
3.1.5.	Conclusions and Outlook	165
3.2	Estrogen-dependent breast cancer (BC) - selective CYP19 inhibition	167
3.2.1.	Molecular docking of non-steroidal aromatase inhibitors	167
3.2.2.	Articles published in CYP19 project - paper VIII	
	Imidazolylmethylbenzophenones as highly potent aromatase inhibitors.	169
3.2.3.	Conclusions and Outlook	175
3.3	Estrogen-dependent endometriosis - selective 17β-HSD1 inhibition	177
3.3.1.	X-ray Analysis	177
3.3.2.	Rapid equilibrium random bi-bi kinetic cycle – a hypothesis	179
3.3.3.	Validating the binding mode of bis(hydroxyphenyl)-arenes: docking and MDs	181
3.3.4.	Validating the binding mode of bis(hydroxyphenyl)-arenes: “semi-QMAR”	184

3.3.5. Articles published in 17 β -HSD1 project - paper IX-XI	185
3.3.5.1. Design, synthesis, biological evaluation and pharmacokinetics of bis(hydroxyphenyl) substituted azoles, thiophenes, benzenes, and aza-benzenes as potent and selective nonsteroidal inhibitors of 17 β -hydroxysteroid dehydrogenase type 1 (17 β -HSD1).	185
3.3.5.2. New insights into the SAR and binding modes of bis(hydroxyphenyl)thiophenes and - benzenes: influence of additional substituents on 17 β -hydroxysteroid dehydrogenase type 1 (17 β -HSD1) inhibitory activity and selectivity.	211
3.3.5.3. Dynamic motion investigation of 17 β -HSD1 provides deep insights in enzyme kinetics and ligand binding.	243
3.3.6. Conclusions and Outlook	255
3.4 Congestive heart failure– selective CYP11B2 inhibition	257
3.4.1. Pharmacophore-model – evolution and consequences for drug design	257
3.4.2. MEP maps and rotational energy barriers	258
3.4.3. Articles published in CYP11B2 project - paper XII-XIV	261
3.4.3.1. Development and evaluation of a pharmacophore model for inhibitors of aldosterone synthase (CYP11B2).	261
3.4.3.2. Overcoming undesirable CYP1A2 inhibition of pyridynaphthalene-type aldosterone synthase inhibitors: influence of heteroaryl derivatization on potency and selectivity.	267
3.4.3.3. Novel aldosterone synthase inhibitors with extended carbocyclic skeleton by a combined ligand-based and structure-based drug design approach.	285
3.4.4. Conclusions and Outlook	305
Chapter Four. General conclusions	307
Chapter Five. Bibliography	309
Chapter Six. Acknowledgements	319
Chapter Seven. Appendix	321

Chapter One. INTRODUCTION

1.1 Steroidogenesis

Steroidogenesis is an important step in the biosynthesis of steroids. Precisely, it describes the processes wherein desired forms of steroids are generated by transformation of other steroids. Products of steroidogenesis include steroidal hormones, generally synthesized from cholesterol in the gonads and adrenal glands, and grouped into five classes by the receptor to which they bind: progestagens (progesterone), androgens (testosterone), estrogens (17β -estradiol), glucocorticoids (cortisol) and mineralocorticoids (aldosterone). They play an important role in the regulatory mechanisms in human body, especially at the sexual level. Biosynthesis of steroid hormones (Fig. 1) requires a battery of oxidative enzymes located in both mitochondria and endoplasmic reticulum, belonging mainly to two enzyme families, namely cytochromes P450 (CYPs) and hydroxysteroid dehydrogenases (HSDs).

Because steroids and sterols are lipid-soluble, they can diffuse fairly freely from the blood through the cell membrane and into the cytoplasm of target cells. In the cytoplasm, the steroid may or may not undergo an enzyme-mediated alteration such as reduction, hydroxylation, or aromatization. In the cytoplasm these hormones can quite easily combine with a protein receptor, a large metalloprotein. Thus, the effects of the steroid hormones are mediated by slow genomic mechanisms through nuclear receptors as well as by fast nongenomic mechanisms through membrane-associated receptors and signaling cascades.

The particular steroid hormone class synthesized by a given cell type depends upon its complement of peptide hormone receptors, its response to peptide hormone stimulation and its genetically expressed complement of enzymes. The following indicates which peptide hormone is responsible for stimulating the synthesis of the most important steroid hormones:

- Luteinizing Hormone (LH): progesterone and testosterone
- Adrenocorticotrophic hormone (ACTH): cortisol
- Follicle Stimulating Hormone (FSH): estradiol
- Angiotensin II/III: aldosterone

Steroid hormones are generally carried in the blood bound to specific carrier proteins such as sex hormone-binding globulin (SHBG) or corticosteroid-binding globulin. Further conversions and catabolism occur in the liver, in other "peripheral" tissues, and in the target tissues. All steroid hormones share the same cyclopentanoperhydrophenanthrene ring structure and carbon numbering system. Depending on the total number of carbon atoms per structure, steroids are classified in C-21 (pregnenolone), C-19 (testosterone) and C-18 steroids (estradiol).

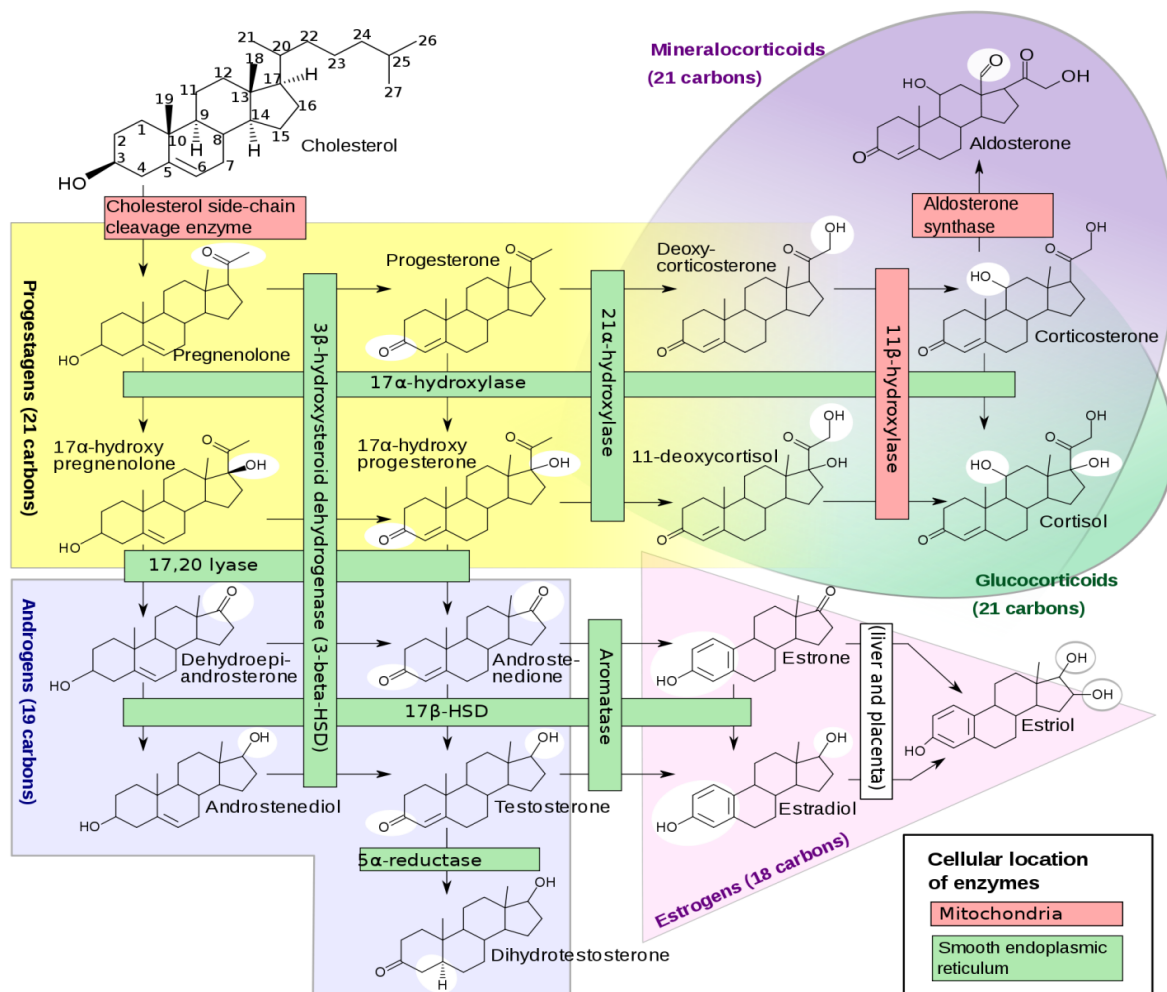


Figure 1. Steroidogenesis (taken from Wikipedia).¹

1.1.1. Biosynthesis of steroid hormones.

The first reaction in converting cholesterol to C18, C19 and C21 steroids involves the cleavage of a 6-carbon group from cholesterol and is the principal and rate-limiting step in steroid biosynthesis. The enzyme system that catalyzes the cleavage reaction is known as P450-linked side chain cleaving enzyme (P450ssc or 20,22-desmolase) and is found primarily in the mitochondria of steroid-producing cells. Chronic regulation of steroidogenesis occurs principally at the level of transcription of the gene for P450 side chain cleavage (P450scc)², which is the enzymatically rate-limiting step. Subsequent to desmolase activity, pregnenolone moves to the cytosol, where further processing depends on the cell (tissue) under consideration. At this stage the acute regulation of steroidogenesis takes place mediated by steroidogenic acute regulatory protein (StAR), which facilitates the rapid influx of cholesterol into mitochondria.

All the enzymes involved in the multi-step biosynthesis of steroid hormones act as hydroxylases, either cytochrome P450s (CYPs) or short-chain dehydrogenases/hydroxysteroid dehydrogenases (SDR/HSD), and have as such a nomenclature indicative of the site of hydroxylation (e.g. 17 α -hydroxylase (CYP17A1) and 17 β -hydroxysteroid dehydrogenase (17 β -HSD1) – hydroxylation of the carbon in 17 position, in α or β site of the steroid, respectively). The most important are:

- CYP11A1 (P450_{ssc}, P450c11a1, steroid 20 α -hydroxylase, steroid 22-hydroxylase, cholesterol side chain cleavage enzyme) - adrenal mitochondria.
- CYP11B1 (P450c11 β , steroid 11 β -hydroxylase) - inner mitochondrial membrane of adrenal cortex.
- CYP11B2 (P450c18, aldosterone synthase, 18-hydroxylase) only in mitochondria of the adrenal zona glomerulosa.
- CYP17A1 (P450c17, 17 α -hydroxylase/17,20-lyase) - endoplasmic reticulum (RE) of adrenal cortex, testes.
- CYP21A1 (21-hydroxylase) - adrenal cortex.
- CYP19A (P450_{aro}, aromatase) - RE of gonads, brain, adipose tissue.
- 3 β -HSD (3 β -hydroxysteroid dehydrogenase/ Δ 5- Δ 4 isomerase) - ubiquitous

Sex steroids (gonadal steroids, sex hormones) are steroid hormones that interact with vertebrate androgen, estrogen or progestin receptors. Natural sex steroids are made by the gonads (ovaries or testes), by adrenal glands, or by conversion from other sex steroids in other tissue such as liver or fat. The two main classes of sex steroids are androgens and estrogens, of which the most important human derivatives are testosterone and estradiol, respectively. Progestagens are often included as a third class of sex steroids, distinct from androgens and estrogens. Progesterone is the most important and only naturally-occurring human progestagen. In general, androgens are considered "male sex hormones", since they have masculinizing effects, while estrogens and progestagens are considered "female sex hormones", although all types are present in each gender, albeit at different levels.³

1.1.2. Adrenal glands

The adrenal cortex is responsible for the production of the 3 major classes of steroid hormones: glucocorticoids, which regulate carbohydrate metabolism; mineralocorticoids, which regulate the body levels of sodium and potassium; and androgens, male sex hormones. The adrenal cortex is composed of 3 main tissue regions (Fig. 2): zona glomerulosa, zona fasciculata, and zona reticularis. In order to be converted to pregnenolone in the adrenal cortex cholesterol must be transported into the mitochondria where CYP11A1 (P450_{ssc}) resides. This transport process is mediated by the steroidogenic acute regulatory protein (StAR) and is the acute rate-limiting step in steroidogenesis. Although the pathway to pregnenolone synthesis is the same in all zones of the cortex, the zones are histologically and enzymatically distinct, with the exact steroid hormone product dependent on the enzymes present in the cells of each zone. This is the qualitative regulation of steroidogenesis, determining the class of steroid produced, and it is principally determined by P450c17 (CYP17):

- Zona glomerulosa. Zona glomerulosa cells are unique in the adrenal cortex in containing P450c18 (CYP11B2, aldosterone synthase), which converts the C21 deoxy steroid corticosterone to aldosterone, the principal and most potent mineralocorticoid. P450c17 is absent in this area of the adrenals, resulting in a missing pathway to the glucocorticoids (deoxycortisol and cortisol) and the androgens (dehydroepiandrosterone (DHEA) and androstenedione).

- Zona fasciculata. In the presence of the 17 α -hydroxylase, but not the 17,20 lyase, activity of CYP17 C21,17 α -hydroxy steroids are produced, leading to the glucocorticoid cortisol.
- Zona reticularis. Both 17 α -hydroxylase and 17,20 lyase activities of P450c17 are present and the androgen precursor dehydroepiandrosterone is produced. The discrimination between 17 α -hydroxylase and 17,20 lyase activities is regulated by two posttranslational events, the serine phosphorylation of CYP17 and the allosteric action of cytochrome b5, both of which act to optimize the interaction of CYP17 with its obligatory electron donor, P450 oxidoreductase.

So, pregnenolone, moving from the mitochondria to the cytosol, is converted either to androgens or to 11-deoxycortisol and 11-deoxycorticosterone by enzymes of the endoplasmic reticulum. The latter 2 compounds then re-enter the mitochondrion, where the enzymes are located for tissue-specific conversion to glucocorticoids or mineralocorticoids, respectively.

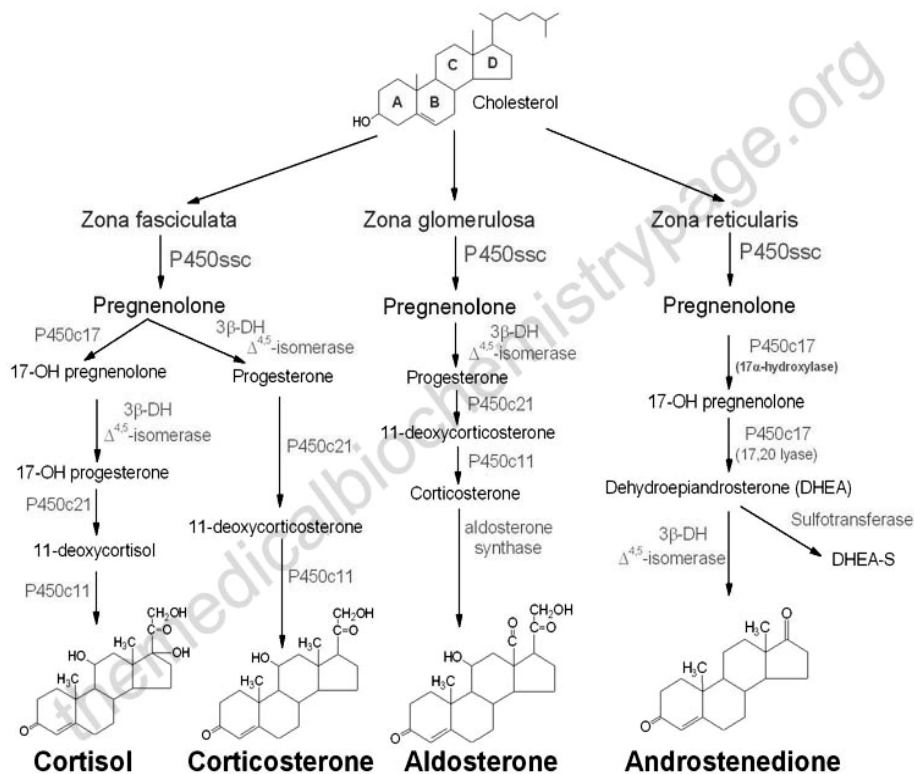


Figure 2. Adrenal synthesis of steroid hormones from cholesterol (<http://themedicalbiochemistrypage.org>).⁴

1.1.3. Gonadal steroid hormones

The biosynthetic pathway to sex hormones (Fig. 3) in male and female gonadal tissue (testes and ovaries, respectively) includes the production of the androgens androstenedione and dehydroepiandrosterone (DHEA). These are then converted into the two most important hormones testosterone (T) and estradiol (E2). T and E2 are under tight biosynthetic control, with short and long negative feedback loops that regulate the secretion of follicle stimulating hormone (FSH) and luteinizing hormone (LH) by the pituitary and gonadotropin releasing hormone

(GnRH) by the hypothalamus. Low levels of circulating sex hormone reduce feedback inhibition on GnRH synthesis (the long loop), leading to elevated FSH and LH.

In males, LH binds to Leydig cells, stimulating production of the principal Leydig cell hormone, testosterone. Testosterone (T) is secreted to the plasma and also carried to Sertoli cells by androgen binding protein. In Sertoli cells the Δ^4 double bond of testosterone is reduced, producing dihydrotestosterone (DHT), the most potent of the male steroid hormones. Testosterone and dihydrotestosterone are carried in the plasma, and delivered to target tissue, by a specific gonadal steroid binding globulin.

In females, LH binds to thecal cells of the ovary, where it stimulates the synthesis of androstenedione and testosterone by the cAMP- and PKA-regulated pathway. An additional enzyme complex known as aromatase is responsible for the final conversion of the latter androgens into the estrogens. Aromatase is a complex endoplasmic reticulum enzyme found in the ovary and in numerous other tissues in both males and females. Its action involves hydroxylations that culminate in the cleavage of the C10-C19 bond and in aromatization of the A ring of the androgens.

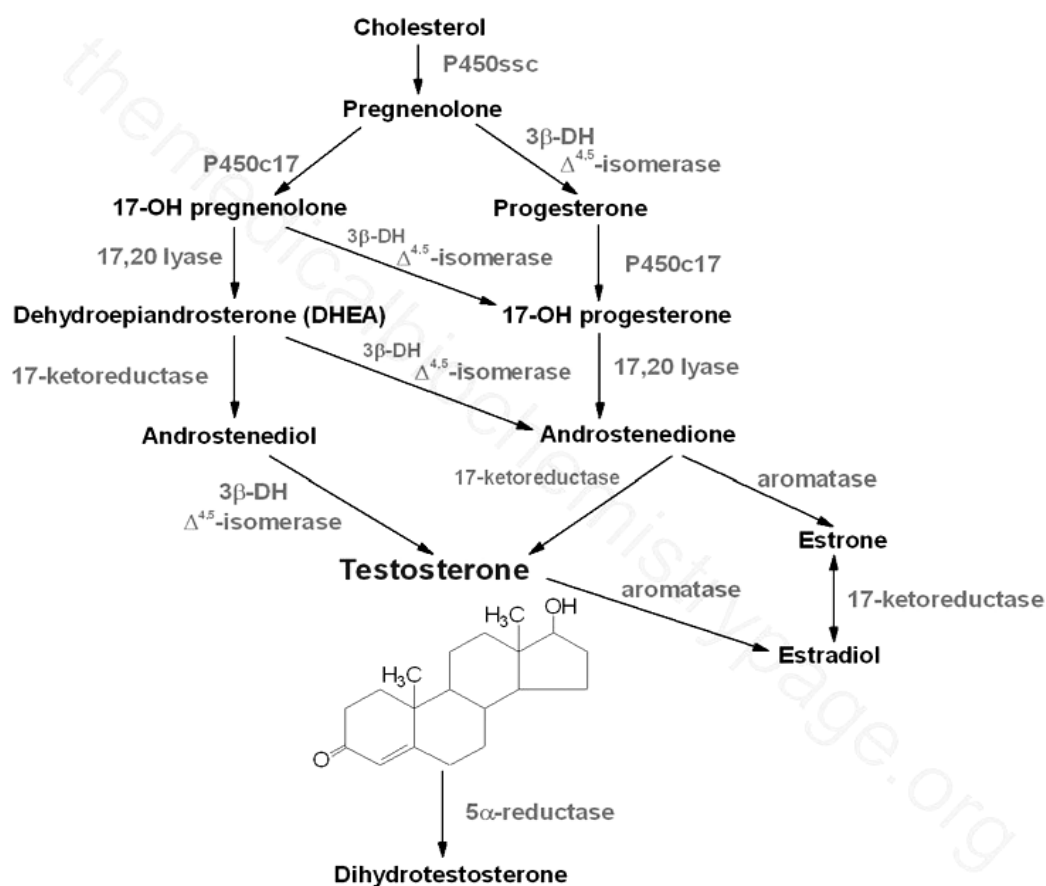


Figure 3. Biosynthesis of sex hormones from cholesterol (<http://themedicalbiochemistrypage.org>).⁵

1.1.4. Steroid hormone receptors.

Unlike peptide hormone receptors that span the plasma membrane and bind ligand outside the cell, steroid hormone receptors are found in the cytosol and the nucleus. The steroid hormone receptors belong to the steroid and thyroid hormone receptor super-family of proteins, that includes not only the receptors for steroid hormones (androgen receptor, progesterone receptor, estrogen receptor), but also for thyroid hormone, vitamin D, retinoic acid, mineralocorticoids, and glucocorticoids. These receptors are ligand-activated proteins that regulate transcription of selected genes. When a ligand binds, they undergo a conformational change that renders them activated to recognize and bind to specific nucleotide sequences. These specific nucleotide sequences in the DNA are referred to as hormone-response elements. When ligand-receptor complexes interact with DNA they alter the transcriptional level (responses can be either activation or repression) of the associated gene. Thus, the steroid-thyroid receptors family has three distinct domains: a ligand-binding domain, a DNA-binding domain and a transcriptional regulatory domain. Although there is the commonly observed effect of altered transcriptional activity in response to hormone-receptor interaction, there are family member-specific effects with ligand-receptor interaction. Several receptors are induced to interact with other transcriptional mediators in response to ligand binding. Binding of steroid hormones leads to translocation of the ligand-receptor complex from the cytosol to the nucleus.

1.2 Endocrinology vs intracrinology – pathophysiological role of steroid hormones

Biologically active hormones need to interact with their specific receptors located in the target tissues in order to unfold their physiological functions. We can distinguish four systems of hormone actions (see Fig. 4), localized on different levels.

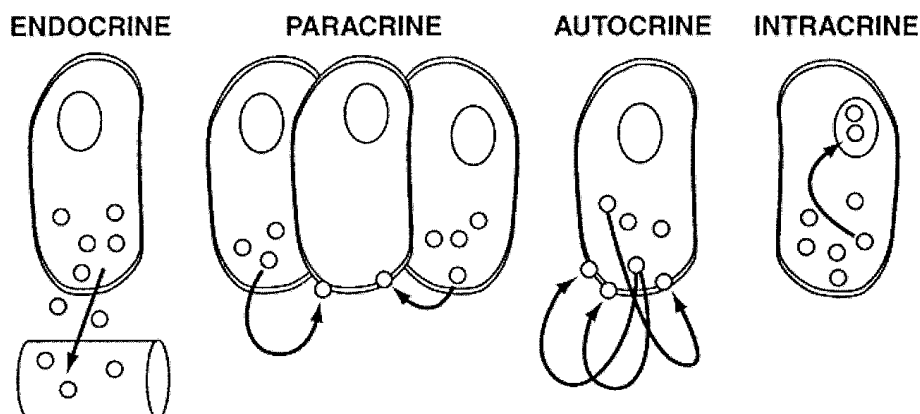


Figure 4. Endocrine, paracrine, autocrine and intracrine secretion (taken from Labrie et al. 2000).⁶

The one which is investigated most is the endocrine system, influenced at various stages by the plasma concentration of biologically active hormones. These are synthesized and secreted from endocrine organs, such as adrenal cortex, gonads (testes and ovaries) or pituitary gland, and then transported through the circulation, and act on their target tissues via binding to their specific receptors. In classical endocrine systems only a small amount of hormones produced and secreted is in general utilized in the target tissues or exerts their effects. The great majority of these hormones is actually metabolized or converted to inactive forms.

Additionally, hormones, locally produced from endocrine organs, can also act in the same cell (autocrine system) or neighboring cells (paracrine system) without their release into the circulation.

The forth, and more particular action system, is the intracrine one. The term intracrinology was created in 1988 by Labrie *et al.* focusing on the synthesis of active steroids in peripheral target tissues where steroid action is exerted in the same cells where synthesis takes place without release of the active hormones in the extracellular space and in the general circulation.⁷ A large proportion of androgens in men (approximately 50%) and estrogens in women (approximately 75% before menopause, and close to 100% after menopause) were produced in peripheral hormone target tissues from abundantly present less active circulating precursor steroids (i.e. dehydroepiandrosterone (DHEA), DHEA-S (DHEA-sulfate) and/or androstenedione (4-Adione)), where the enzymes involved in the formation of androgens and estrogens are expressed (Fig. 5).

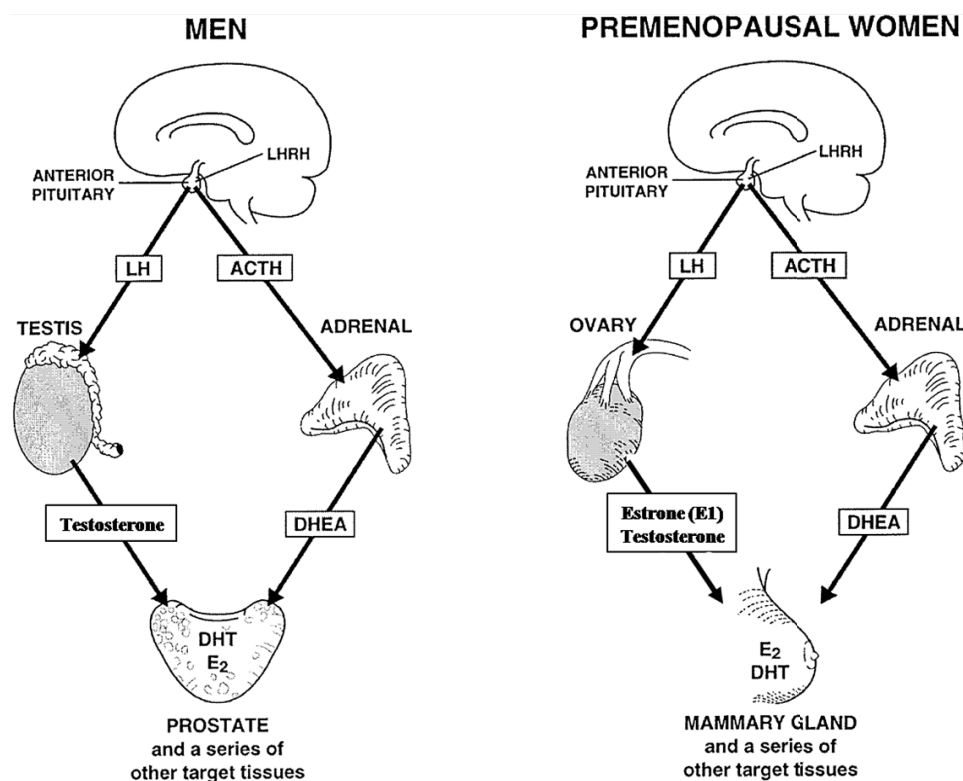


Figure 5. Role of gonadal (testicular and ovarian) and adrenal sources of sex steroids in men and premenopausal women (adapted from Labrie et al. 2000).⁶

Since these steroids are not released in the circulation, the rate of formation of each active sex steroid thus depends upon the level of expression of the specific androgen- and estrogen-synthesizing enzymes in each cell of each tissue. It is remarkable that humans, in addition to possessing a highly sophisticated endocrine system, have largely vested sex steroid formation in peripheral tissues.⁸ Active sex steroids are to a much larger degree or completely synthesized locally in peripheral tissues; this provides autonomous control to target tissues which are thus able to adjust the formation and metabolism of sex steroids according to local requirements. In contrast to the classical endocrine system, an intracrine system requires minimal amounts of biologically active hormones to exert their maximum hormonal effects. Therefore, the intracrine system is considered a remarkable efficient mode of hormone action and plays an important role, especially in the development of hormone-dependent neoplasms including human prostate, breast, endometrial, and ovarian malignancies.

The synthesis from DHEA of the most potent natural androgen, (DHT), and of the most potent natural estrogen, 17 β -estradiol (E2), involves several enzymes, namely 3 β -hydroxysteroid dehydrogenase/ Δ 5- Δ 4 isomerase (3 β -HSD), 17 β -HSD, 5 α -reductase and/or aromatase. 17 β -HSDs are required for both the synthesis of all active androgens and all active estrogens as well as for their inactivation. In the human, the continuous formation of sex steroids from DHEA in peripheral tissues is likely to play a major role in the maintenance of adequate functioning of most human tissues. It is important to mention that 40% of all cancers, namely breast, prostate, ovarian and uterine cancers, are sex steroid-sensitive and are thus prime candidates for approaches based upon control of intracrine activity.

1.2.1. Prostate cancer (PC)

Prostate cancer is the most common tumor and age-related cause of death in elder men worldwide.⁹⁻¹¹ In about 80 % of the cases it is androgen dependent. Commonly, in PC androgens exert their action via the endocrine system, being synthesized in the testes, gonads and the adrenals by the P450c17 complex. Although, it has to be mentioned that besides the uptake and conversion of circulating adrenal androgens prostate cancer metastases may also be capable of de novo androgen biosynthesis from cholesterol and/or progesterone precursors, thus involving the intracrine system.

About 90% of prostate cancers are diagnosed at an early stage. Nevertheless, the treatment selection is very difficult. Since prostate cancer is predominantly a disease of older men, many will die of other causes before a slowly growing PC can spread or cause symptoms. The age and underlying health of the man, as well as the grade and stage of the disease and response of the cancer to initial treatment, are important in prognosing the outcome of the disease. The decision whether or not to treat localized prostate cancer with curative intent is a patient trade-off between the expected beneficial and harmful effects in terms of patient survival and quality of life.

In the course of studies on the hormonal therapy of prostate cancer, a surprising observation was that, while blood levels of testosterone were reduced by 90–95%, approximately 50% of DHT, the active intracellular androgen, was left in the prostate in men who had their testicles removed or had complete blockade of testicular androgen secretion following treatment with a luteinizing hormone releasing hormone (LHRH) agonist.¹²⁻¹⁴ This suggested that, in the absence of testicles, another source continued to provide androgens to the prostate. Indeed, the remaining 5-10% of the androgens is produced in the adrenals. The objective arose to block simultaneously the androgens of both testicular and adrenal origin at the start of treatment of prostate cancer^{7b, 15}, which led to the development of the so called combined androgen blockade (CAB).

Currently the standard treatment for prostate carcinoma is CAB. This means orchiectomy or its therapeutic equivalent the medical castration by gonadotropin-releasing hormone (GnRH) analogues, which reduce the testicular androgen production, is accompanied by the use of a pure androgen receptor antagonist (flutamide, cyproterone acetate), in order to silence the stimulatory effects of the remaining androgens. However, CAB often leads to resistance which has been associated to androgen receptor mutations, causing the mutated receptor to recognize antagonists as agonist. Moreover, although the good results of CAB result in remissions lasting two to three years, nearly all patients will eventually progress to castration-resistant prostate cancer (CRPC), which is fatal in the majority of patients.¹⁶

An alternative, pharmacological therapy is the total blockage of the androgen biosynthesis, which brings P450c17 complex and its central role in the androgen biosynthesis into focus. P450c17 complex consists of two proteins anchored to the endoplasmatic reticulum: the NADPH cytochrome P450 reductase (CPR) and the cytochrome P450 17 protein (CYP17),¹⁷ and is commonly located in both testicular and adrenal tissue but not in the prostate. CYP17 is a key branch point in androgen production and in the system of adrenal steroid hormone synthesis: as 17 α -hydroxylase, it distinguishes in the adrenal cortex between the synthesis of mineralocorticoids (e.g. aldosterone) and that of glucocorticoids (cortisol); as 17,20-lyase it distinguishes between the synthesis of glucocorticoids and C-19 precursors of androgens such as

DHEA. Thus, the therapies that inhibit the systemic biosynthesis of androgens through the targeting of CYP17 may represent a promising alternative, suitable for early and advanced (metastatic) PC, to the CAB approach and a rational approach in the treatment of CRPC. Indeed, blocking the biological pathway of androgen biosynthesis at an early stage, production of testosterone and all other androgens will be stopped in the testes, adrenals and in the castration-resistant prostatic tumor, thus preventing the tumor from growing further and, according to recent studies, even delaying the development of bone metastasis for a period of up to eight years.¹⁸

1.2.2. Estrogen-dependent diseases (EED)

Estradiol originates from different sources before and after the menopause in women. In premenopausal women, the ovary or *membrana granulosa* of dominant follicles is the main source of abundant circulating estrogens. However, after menopause, the secretion of estradiol by the ovaries ceases and 100% of sex steroids are made locally in peripheral target intracrine tissues, primarily through conversion of androgens of both adrenal and ovarian origins, especially of *zona reticularis* origin of adrenal cortex. This conversion is catalyzed by the aromatase enzyme complex.

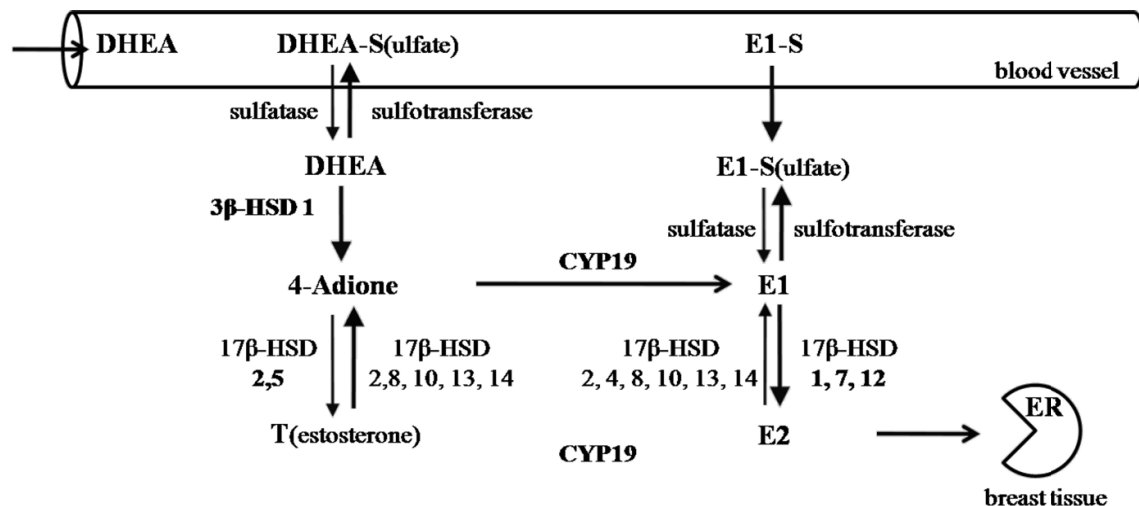


Figure 6. Local production of sex steroids in breast tissues.

Aromatase takes part in both the endo- and the intracrine biosynthesis of estrogens, while 17β-HSD1 only in the intracrine (Fig. 6).¹⁹ Proof of the role of estrogen formation in peripheral intracrine tissues is well illustrated in women by the important benefits on breast cancer observed in postmenopausal women treated by a series of aromatase inhibitors.²⁰ It is worth mentioning, that these two enzymes are not the only sources of 17β-estradiol to the hormone-sensitive cancer.

1.2.2.1. Breast cancer (BC)

Breast cancer is the widest hormone-dependent disease in women. It is asymptomatic and can be recognized only by analysis thorough mammography.

The great majority of human breast carcinomas express estrogen receptor (ER) in carcinoma or parenchymal cells. These cases are termed hormone- or estrogen-dependent breast carcinoma, and estrogens, especially 17β -estradiol (E2), a biologically potent estrogen, contribute to a great extend to the growth and development of carcinoma cells and some of these carcinoma actually require estrogens for their continued growth and other biological processes.²¹ Breast carcinomas can be divided in two categories: estrogen receptor positive (ER+) and estrogen receptor negative (ER-) tumors. Around 50% of breast cancers in premenopausal women and 75% of breast cancers in postmenopausal women are ER+, i.e. the progression of the tumor is dependent on the physiological concentration of estrogens present in the diseased tissue.²²

In addition to surgery, chemotherapy and radiotherapy, hormone-dependent breast cancers can be treated via different endocrine therapies: SERMs (Selective Estrogen Receptor Modulators), like tamoxifene and raloxifene constrain the estrogen action at the receptor level, aromatase inhibitors (AI, e.g. fadrozole, letrozole) suppress the estrogen formation by inhibiting the last step of E1 biosynthesis and GnRH analogues completely block the ovarian steroid formation. (Fig. 7).²³

These strategies are already used in therapy but they show some limitations. Many breast tumors fail to respond to anti-estrogen therapy or progress after a period of time. SERMs are also known to induce carcinoma in other tissues like endometrium, where tamoxifene acts as an estrogen agonist. Aromatase inhibitors block the formation of estrogens but do not prevent the formation of the non-aromatic estrogen 5-androstene-3 β -diol from DHEA which also stimulates the proliferation of cancer cells after binding to the ER. Aromatase inhibitors are restricted to postmenopausal women because in premenopausal women they induce a strong ovarian stimulation by hypothalamic/pituitary feedback. GnRH analogues do not affect adrenal formation of androgens which are converted into estrogens by peripheral aromatase.

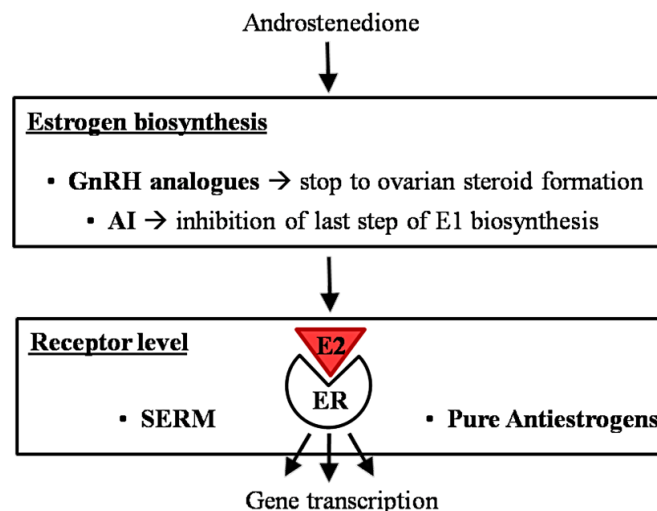


Figure 7. Existing endocrine therapies.

1.2.2.2. Endometriosis

Endometriosis was first described by Rokitansky²⁴ and is one of the most common causes of pelvic pain and infertility in women. Endometriosis can affect any woman, from premenarche to postmenopause. It is primarily a disease of the reproductive years. Estimates about its prevalence vary, but 5–10% is a reasonable number, more common in women with infertility (20–50%) and women with chronic pelvic pain (about 80%). As an estrogen-dependent process, it can persist beyond menopause and persists in up to 40% of patients following hysterectomy. Endometriosis in postmenopausal women does occur and has been described as an aggressive form of this disease characterized by complete progesterone resistance and extraordinarily high levels of aromatase expression.²⁵

In endometriotic tissue aromatase and 17 β -HSD1, but not 17 β -HSD2, are overexpressed, which leads to an increased concentration of estradiol, which further stimulates the proliferation of these tissues. Attar et al. describe a positive feed-back mechanism, which leads to a permanent estradiol production in the endometrium, thus resulting in stimulation of growth and inflammation processes in the tissue.²⁶

In this condition endometrial tissue grows abnormally outside the uterus, often in locations such as the ovaries, fallopian tubes and abdominal cavity. It causes adhesions and scarring, pain, heavy bleeding and can damage the reproductive organs leading to infertility. The specific causes of endometriosis are still not clear. The most widely accepted theory developed by Sampson is that the disorder originates from retrograde menstruation of endometrial tissue through the fallopian tubes into the peritoneal cavity.²⁷⁻²⁸

Currently available medical therapies are designed to suppress the estrogen biosynthesis. Oral contraceptives, androgenic agents and GnRH-analogues are used to inhibit the menstruation, a source of much of the pain associated with endometriosis and to restrain the growth of endometriotic tissue.²⁹ Analgesics are also applied in combination to the classical hormonal therapy in order to relieve the pain triggered by endometriosis. However, the available therapies focused on the symptoms of the disease but do not provide a cure. Due to the alteration of the hormone balance, it leads also to several side effects such as weight gain and acne.³⁰

1.2.3. Congestive heart failure.

Congestive heart failure (CHF) is a condition of insufficient cardiac output and reduced systemic blood flow, most frequently provoked by arterial hypertension and coronary artery disease, and goes along with dispnoea, fatigue and edema. The prognosis is poor: 30 % of the patients die within one year and the mortality rises to 60–70 % after five years.³¹ The progressive nature of the disease is a consequence of a neurohormonal imbalance and involves a chronic activation of the renin-angiotensin-aldosterone system (RAAS) in response to the reduced cardiac output and the reduced renal perfusion. Aldosterone and angiotensin II (Ang II) are released excessively, leading to increased blood volume and blood pressure as a consequence of epithelial sodium retention as well as Ang II mediated vasoconstriction and finally to a further reduction of cardiac output. The RAAS is pathophysiologically stimulated leading to a vicious circle of neurohormonal activation that counteracts the normal negative feedback loop regulation (Fig. 8). Aldosterone plays an important physiological role in the regulation of electrolyte homeostasis

and thereby blood pressure, exerting its function by binding to the mineralocorticoid receptor. Upon ligand binding, the protein-ligand complex is translocated to the cell nucleus, where it modulates the gene expression of proteins involved in electrolyte homeostasis.³²

Recently, various studies on the pathophysiology of heart failure have revealed that aldosterone plays a role in the formation of myocardial hypertrophy, reactive myocardial fibrosis, vascular remodelling and electrolyte imbalance.³³ This may contribute to the development of arrhythmias, hypertension and congestive heart failure.³⁴⁻³⁶

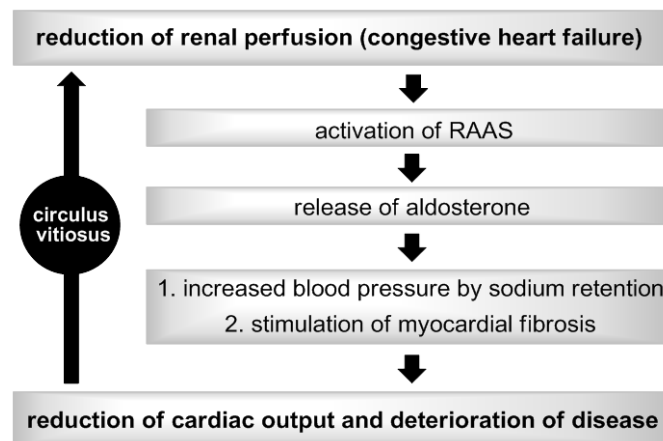


Figure 8. Pathophysiology of the renin-angiotensin-aldosterone system.

Until today, various drug classes targeting the RAAS have been developed, acting either by inhibition of the key regulator enzymes or by blocking the actions of the effector hormones (i.e. aldosterone, Ang II) by functional antagonism, affording a successful treatment of heart failure and hypertension. Their efficacy had been proven in two clinical studies, CONSENSUS trial³⁷ and SOLVD trial.³⁸

First successes were gained by inhibiting the biosynthesis of Ang II with enalapril, an ACE inhibitor, but still a high level of mortality remained. Moreover, ACE independent pathways to AngII are not blocked and ACE inhibitors can indeed trigger an initial downregulation of circulating aldosterone, but increased levels of aldosterone may be seen after several months of therapy, presumably due to potassium stimulated secretion.³⁹ This phenomenon termed ‘aldosterone escape’ is a limiting factor of ACE inhibitors and shows that novel therapeutic concepts combating the effects of elevated aldosterone levels are needed.

On the other hand, in the two recent clinical studies RALES⁴⁰ and EPHEBUS⁴¹ the aldosterone receptor antagonists spironolactone and eplerenone were found to reduce mortality in patients with chronic congestive heart failure and in patients after myocardial infarction, respectively. From this it can be derived that reducing aldosterone action is highly beneficial in the treatment of heart-failure and that it is particularly worthwhile to find new pharmacological ways to interfere with this hormone. The treatment with these antagonists, however, is accompanied with severe side effects like hyperkalemia.⁴²

A novel therapy option, targeting cardiovascular diseases by interruption of the RAAS, is the blockade of aldosterone production, preferably by inhibiting CYP11B2, the key enzyme of its biosynthesis. Aldosterone synthase was proposed as a potential pharmacological target as early

as 1994 by our group ⁴³, hypothesizing that inhibitors of CYP11B2 could serve for the treatment of hyperaldosteronism, congestive heart failure, and myocardial fibrosis.⁴⁴

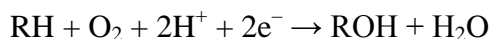
Although the net outcome of aldosterone receptor blockade versus aldosterone synthesis inhibition apparently is similar, a number of potential advantages for the latter approach exists:⁴⁵ reduction of side effects as particularly observed for the antagonist spironolactone, prevention of compensatory aldosterone synthesis inherent to mineralocorticoid receptor blockade, and the fact, that no nonsteroidal inhibitor of a steroidogenic CYP enzyme is known to have affinity for a steroid receptor (fewer side effects on the endocrine system can be expected).

Some aldosterone effects are not mediated by classical MR binding. These rapid actions are referred to as nongenomic effects, they are independent of gene transcription and translation, and, in most cases, they proved to be insensitive to specific MR antagonists.⁴⁶ This because MR antagonists interfere at receptor level, one step after aldosterone biosynthesis, thus leaving aldosterone levels unaffected. Differently, CYP11B2 inhibition can reduce the pathologically elevated aldosterone levels induced by both genomic and non-genomic effects.

1.3 Potential target enzymes involved in steroidogenesis

1.3.1. Cytochrome P450 (CYP) enzymes

The cytochrome P450 proteins (CYPs) are a large ubiquitous monooxygenase heme protein family, which have a large and diverse set of substrate specificities and catalyze a range of biochemical transformations. The most common reactions catalyzed include monooxygenase reactions, e.g. insertion of one atom of oxygen into an organic substrate (RH) while the other oxygen atom is reduced to water:



The name **cytochrome P450** is derived from the fact that these are colored ('chrome') cellular ('cyto') proteins, with a "pigment at 450 nm", so named for the characteristic Soret peak formed by absorbance of light at wavelengths near 450 nm when the heme iron is reduced and complexed to carbon monoxide.

CYPs are present in nearly every form of life and in february 2008 the CYP superfamily consisted of more than 7,000 named sequences in animals, plants, bacteria and fungi (<http://drnelson.utm.edu/CytochromeP450.html>). In particular, human CYPs (57 CYP genes present in human genome; see Appendix A for full list) play a prominent role since they contribute massively to the metabolism of xenobiotics, such as drugs, environmental pollutants, and carcinogens. Moreover, biosynthesis of steroid hormones, bioavailability, bioactivation, toxicity, and drug-drug interactions may be associated with CYP-mediated bioconversions.⁴⁷

Seven of these 57 CYPs are targeted to mitochondria (type 1 P450s) and 50 are targeted to the endoplasmic reticulum (type 2 P450s). Among these 50, about 15 are involved in hepatic metabolism of drugs and xenobiotics, about 20 participate in the synthesis of steroids, sterols, bile acids, prostaglandins, retinoids and other endogenous compounds, and about 15 are 'orphan' enzymes, whose activity is yet unknown.⁴⁸ The P450 proteins are categorized into families (>50%) and subfamilies (>60%) according to their sequence similarities, respectively.

All structures of cytochrome P450s known so far show the same tertiary fold. The active site of the enzyme is next to the heme cofactor, buried in the core of the protein. It is usually isolated from the surrounding solvent.⁴⁹

The structure of mammalian CYPs is mainly α -helical with orthogonal bundle architecture with almost the same number of α -helices (A-L) and β -sheets (10) (Fig. 9). Nevertheless, despite a highly conserved ternary structure, these enzymes share only a low sequence identity (<20 %) and homology (<30-40 %), underlining the functional importance of the conserved 20%. Typical structural features of CYPs are the F/G segment (F helix, F/G loop, G helix) perpendicular to the highly structurally conserved I helix with the segment housing the heme cofactor. This F/G segment, together with the B/C-loop control access to the CYP active site. The long I helix, extending through the whole CYP structure, presents a kink in proximity of the heme. Close to this kink we find a conserved acidic residue (Asp or Glu) and the catalytic threonine, presumably involved in the catalytic mechanism, by stabilizing the proton transfer. Moreover, several basic amino acids on the proximal side of the enzyme are maintained in nearly all CYPs, responsible for the anchoring of the redox partner of the CYP enzymes.

The active site of cytochrome P450 contains a heme iron center. The iron is tethered to the P450 protein via a thiolate ligand derived from a cysteine residue. This cysteine and a dozen flanking residues (Cys pocket) are highly conserved in known CYPs, forming a short, characteristic loop (meander) which undergoes interactions with the redox partner and presumably plays a notable role in the conformational rearrangement of the CYP active site after the first electron-transfer. This conserved loop is the so-called “P450 signature” motif of 10 amino acids, including the invariant cysteine residue that ligates the heme iron to the protein, Phe-XX-Gly-Xb-XX-Cys-X-Gly. The amino acid Xb is usually a basic amino acid that plays a key role in interactions with the reductase partner.⁵⁰

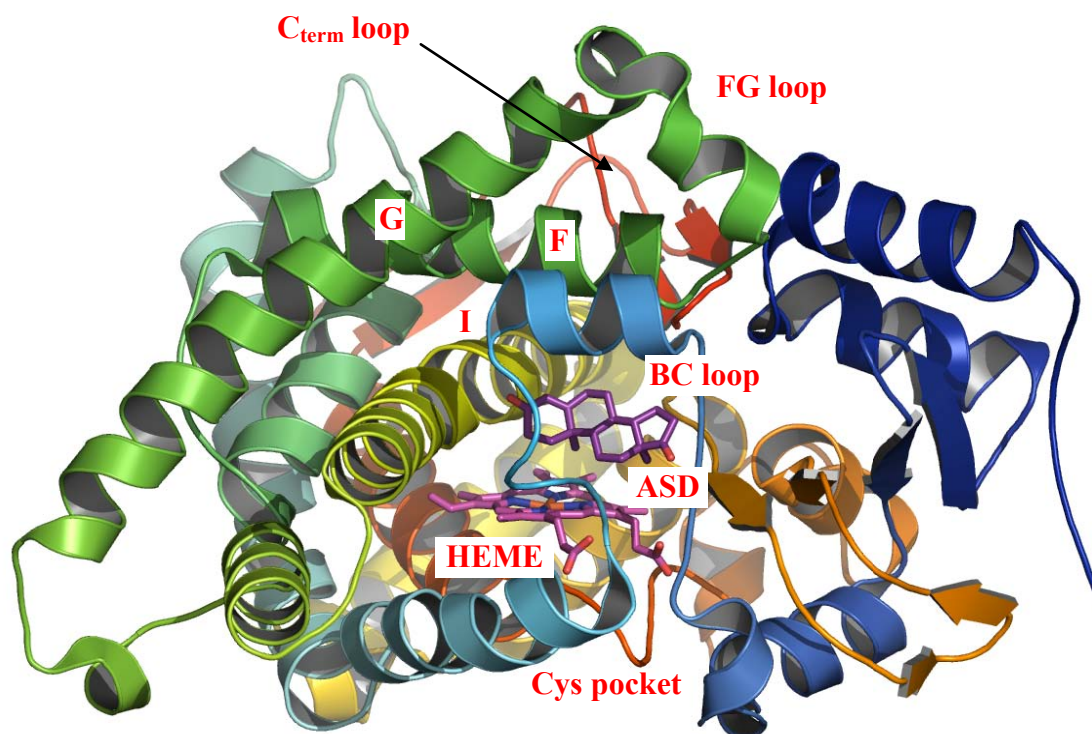


Figure 9. Common fold of typical mammalian CYP19 (PDB code 3EQM) as front view with the most important secondary structure elements labeled.

While prokaryotic, bacterial P450s are soluble proteins, most eukaryotic P450s are membrane-bound enzymes and are attached via a transmembrane N-terminal helix to either the endoplasmic reticulum or mitochondrial membranes. Additionally the F/G-segment, presenting two short α -helices F' and G', is merged into the membrane for a couple of Angstroms. These two helices place one active site substrate access in the lipid bilayer, enabling passive diffusion of lipophilic substrates (i.e. steroids) from the lumen directly into the active site. This is one of the entrance pathways for the CYPs, but several other have been described (Fig. 10).^{49, 51-52}

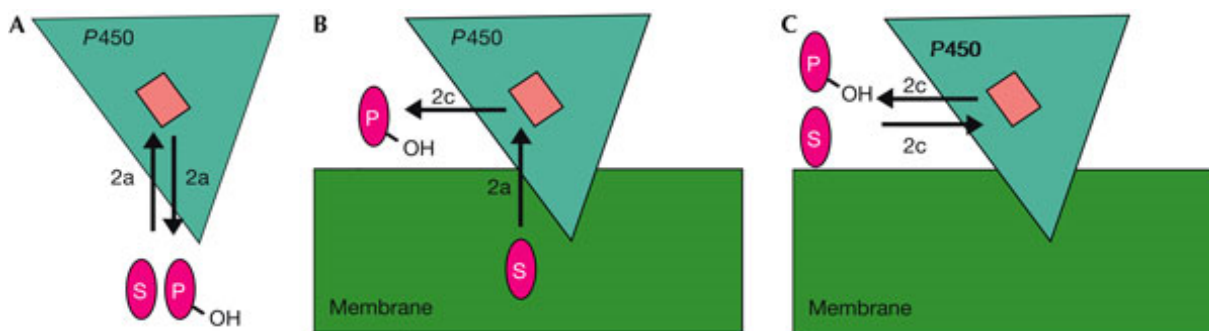


Figure 10 (taken from Schleinkofer et al. 2005).⁵¹ Schematic representation of putative substrate access and product egress routes in P450s. (A) substrate access and product egress channel in soluble P450s. (B) One-way route through mammalian membrane-bound P450 (C) Soluble substrates access the active site. Substrate (S) and product (P) are depicted in magenta, heme cofactor (active site) in light pink and P450 in turquoise.

Although CYPs all have the heme-iron porphyrin ring, they are capable of very specific and selective hydroxylations. This is especially true for CYPs involved in steroidogenesis, which yield very high substrate specificity. Since the tertiary structure is highly conserved and all CYPs present the heme group, the active cavity needs to present specific pockets in order to accommodate the substrate in a specific way, which allows only particular hydroxylation pattern. The difference in substrate conversion is likely to be caused by a difference in the relative positioning of the substrate above the heme in the active site. To be more specific, as exemplified by Roumen et al. for CYP11B2/B1,⁵³ there should be a correlation between substrate selectivity and substrate hydroxylation distance, the distance between the heme iron and the substrate carbon. In other words, the binding mode of the natural substrate dictates which carbon atom is oxidized first, with conversion taking place on the carbon atom which is in closest proximity to the iron-oxygen complex (Fig. 11).

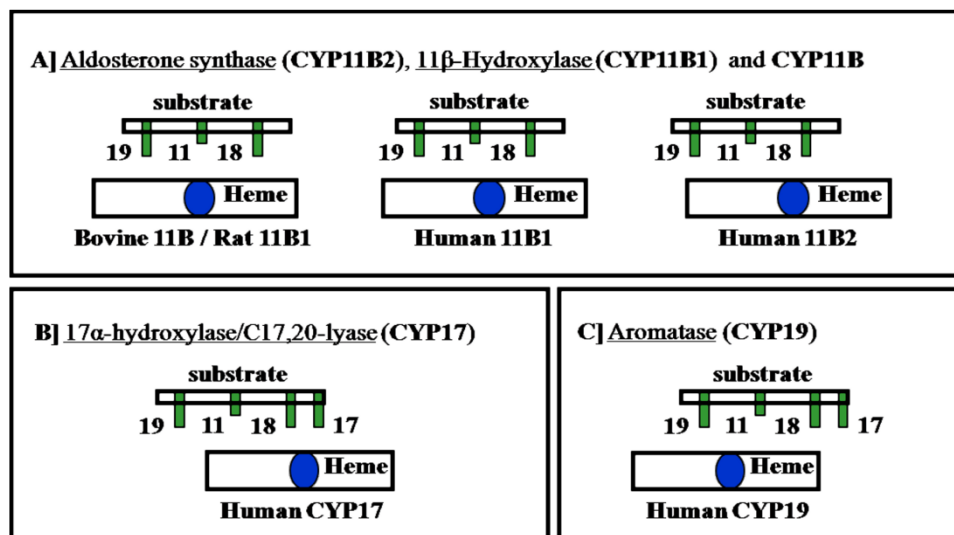


Figure 11. Localization of the steroidal substrate over the Fe=O (blue dot) exemplified for the steroidogenic enzymes CYP11B (11B2 – 11β-hydroxylation/18-hydroxylation/18-methyl oxidation; 11B1 - 11β-hydroxylation), CYP17 (17α-hydroxylation/17,20-lyase) and CYP19 (19-hydroxylation/aromatization).

The reaction cycle of the heme proteins (Fig. 12) runs through an unstable intermediate, called compound I or [Fe=O]-iron-oxo species. This is generally assumed to be a high valent iron-oxo derivative, where the iron is present in an oxidized, oxyferryl (Fe(IV)) form with a triplet spin state.⁵⁴ Additionally, there might be either an oxidized porphyrin- π -cation radical or a tyrosine radical, the latter more likely since tyrosine and tryptophans close to the heme can reduce by intramolecular electron transfer the transiently formed porphyrin- π -cation radical.

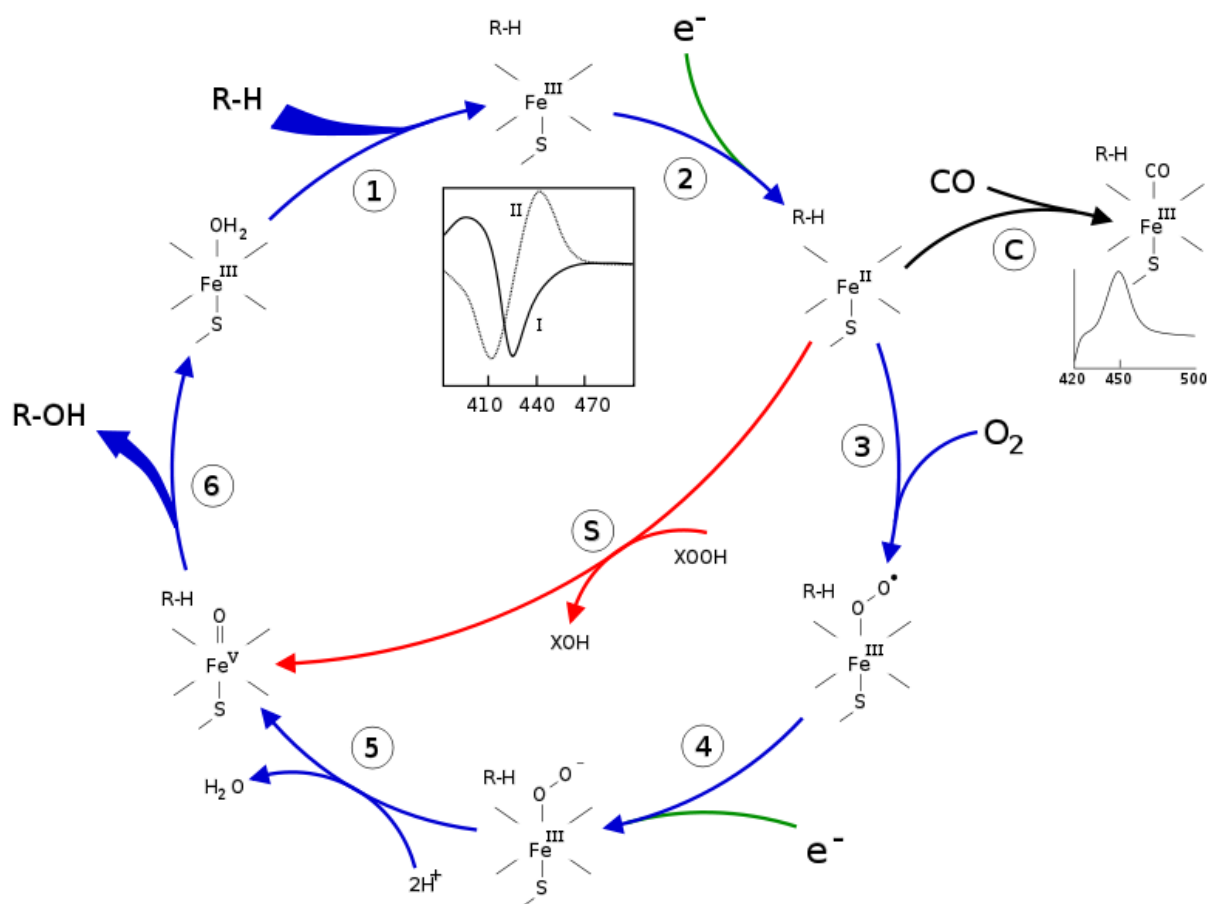
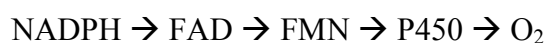


Figure 12. The P450 catalytic cycle (see Appendix B for further descriptions).

Most CYPs require protein partners, which deliver one or more electrons to reduce the iron (and eventually molecular oxygen). Five general schemes are known:

- 1. CPR/cyb5/P450 systems** (Fig. 13): employed by most eukaryotic microsomal CYPs, involve the reduction of cytochrome P450 reductase (variously CPR, POR, or CYPOR) by NADPH, and the transfer of reducing power as electrons to the CYP. Cytochrome b5 (cyp b5) can also contribute reducing power to this system after being reduced by cytochrome b5 reductase (CYB5R). The general scheme of electron flow in the CPR/P450 system is:



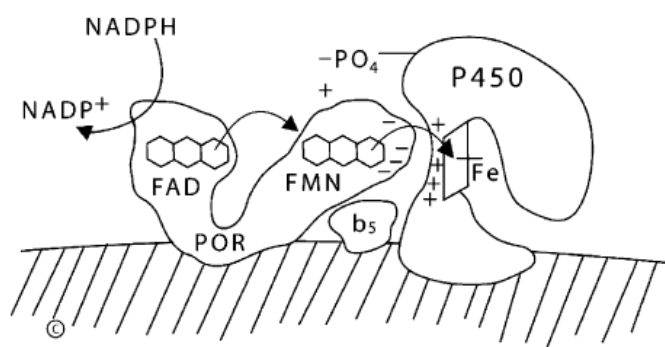
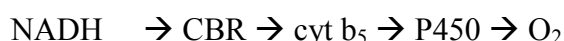
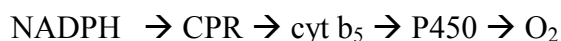


Figure 13. Electron transport to microsomal forms of cytochrome P450. (Copyright W.L. Miller).⁵⁵

- 2. CYB5R/cyb5/P450 systems:** both electrons required by the CYP come from cytochrome b5. The ubiquitous electron-transport protein cytochrome b5 can serve as an effector (activator or inhibitor) of P450s. It was hypothesized that cytochrome b5 is involved in the transfer of the second electron to P450, either from CPR or NADH:cytochrome b5 reductase (CBR):



- 3. FR/Fd/P450 systems** (Fig 14): mitochondrial and some bacterial P450 systems employ soluble Fe_2S_2 ferredoxins (Fd) that act as single electron carriers between FAD-containing ferredoxin reductase (FR) and P450. Adrenodoxin functions as a soluble electron carrier between NADPH, adrenodoxin reductase and several membrane-bound P450s (CYP11A, CYP11B, CYP27). The general scheme of electron flow in the P450 systems containing adrenodoxin-type ferredoxins is:

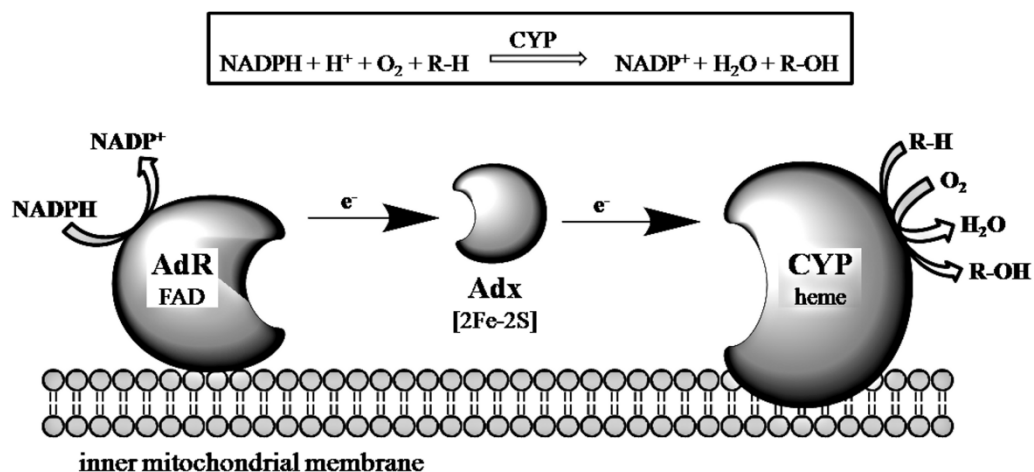


Figure 14. Electron transport to mitochondrial forms of cytochrome P450.

- 4. P450-only systems:** prostacyclin synthase (CYP8) and thromboxane synthase (CYP5) are examples of P450 enzymes which do not require a reductase or molecular oxygen for their catalytic activity. Substrates for all these enzymes are fatty acid derivatives containing partially reduced dioxygen (either hydroperoxy or epidioxy groups).

CYPs have been extensively examined in mice, rats, and dogs, and less so in zebra fish, in order to facilitate use of these model organisms in drug discovery and toxicology. CYPs have also been heavily studied in insects, often to understand pesticide resistance.

Bacterial cytochrome P450s are often soluble enzymes and are involved in critical metabolic processes. Two examples that have contributed significantly to structural and mechanistic studies are cytochrome P450cam (CYP101), the first CYP solved by x-ray crystallography, and cytochrome P450 BM3 (CYP102A1), which unlike almost every other known CYP (except CYP505A1, cytochrome P450 foxy) constitutes a natural fusion protein between the CYP domain and an electron donating cofactor.

Substrate recognition sites. The active site of the CYP enzymes consists of the heme ring at one wall and six common substrate recognition sites (SRS), as defined by Gotoh for CYP2 family enzymes (Fig. 15).⁵⁶ SRS-1 is located between the B- and C-helices, where an additional B'-helix is observed in some CYP enzymes. SRS-2 and SRS-3, or the C-terminus of the F-helix and the N-terminus of the G-helix, are located on the opposite wall of the active site from the heme ring. This area varies among CYP family members showing helices and loops of different lengths and with none, one or two additional helices (F' and G'). SRS-4 is located in the I-helix, which protrudes through the whole enzyme and includes residues that are highly conserved among the CYP enzymes. Often in SRS-4 a so-called I-helix kink is present, leading to a break in the I-helix with two resulting segments. The active-site wall opposite the I-helix consists mainly of SRS-5, the hydrophobic coil between the K-helix and the β 1-4-strand. SRS-6 is located in the β -sheet 4 or, more accurately, in the hairpin turn between the two strands β 4-1 and β 4-2. This site includes amino acids thought to be important not only to substrate recognition but also to the catalytic activity.

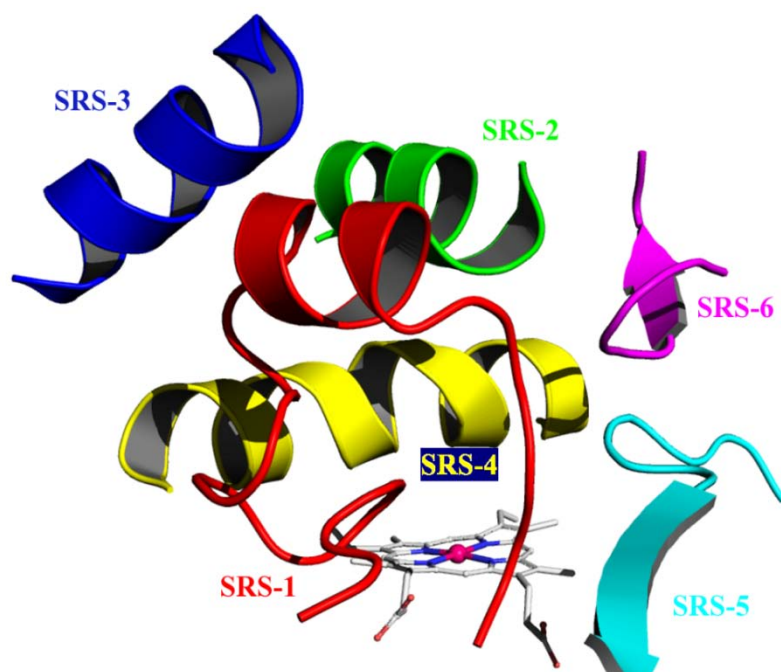


Figure 15. Structural elements corresponding to the substrate recognition sites (SRS) of CYP19. SRS-1 is coloured red, SRS-2 green, SRS-3 blue, SRS-4 yellow, SRS-5 cyan and SRS-6 magenta. Heme is represented as sticks.

1.3.1.1. CYP17 - 17 α -hydroxylase/17,20 lyase

CYP17A1 (17 α -hydroxylase/17,20 lyase/17,20 desmolase; steroid 17-alpha-monooxygenase; P450-C17) is a single member of the CYP17 family, coded by the CYP17A1 gene and consisting of 508 amino acid residues with total molecular weight of 57.4 kDa. It is involved in steroidogenesis, where it converts pregnenolone and progesterone to their 17 α -hydroxy forms. The CYP17 enzyme localizes to the endoplasmic reticulum of the Leydig cells in the testis, theca interna region of the ovaries, and zona fasciculata and reticularis in the adrenal glands. It is a key enzyme in the generation of androgens and estrogens in the adrenal glands and tumor tissue, and works by the catalysis of two independently regulated steroid reactions: 17 α -hydroxylase and 17,20-lyase. CYP17 needs to be activated by a post-translational phosphorylation;⁵⁷ although this seems to be required only for the 17,20-lyase, but not for the 17 α -hydroxylase step. Moreover, the 17,20-lyase activity of CYP17 can be explicated only in presence of cytochrome b5, as mutagenesis studies confirm.⁵⁸ Cyt b5 also acts as a second electron-donor in the catalytic cycle of CYP17, in addition to CPR, requested by most of the other CYPs.

No crystal structure exists of CYP17, but several homology models have been build in the past in order to solve its catalytic mechanism and to study how substrates and inhibitors bind into the active site.⁵⁹

The 17 α -hydroxylase activity converts pregnenolone (Preg) to 17 α -hydroxypregnenolone (17OHPreg) and progesterone (P) to 17 α -hydroxyprogesterone (17OHP), while C17,20-lyase converts 17OHPreg to dehydroepiandrosterone (DHEA) and 17OHP to androstenedione.⁶⁰⁻⁶²

P450c17 can drive sex steroid production by acting along the Δ^5 pathway (Preg \rightarrow 17OHPreg \rightarrow DHEA \rightarrow T) or, alternatively, along Δ^4 pathway (P \rightarrow 17OHP \rightarrow Δ^4 A) (Fig. 16). Both clinical observations of human adrenal physiology and direct biochemical assays of recombinant human P450c17 demonstrate that the 17, 20-lyase activity of the human enzyme strongly prefers the Δ^5 pathway, catalyzing the conversion of 17OHPreg to DHEA approximately 20 times more efficiently than the conversion of 17OHP to Δ^4 A.⁶³

Summarizing, the hydroxylase reactions are part of the synthetic pathway to cortisol as well as sex steroids, but the lyase reaction is only necessary for sex steroid synthesis.

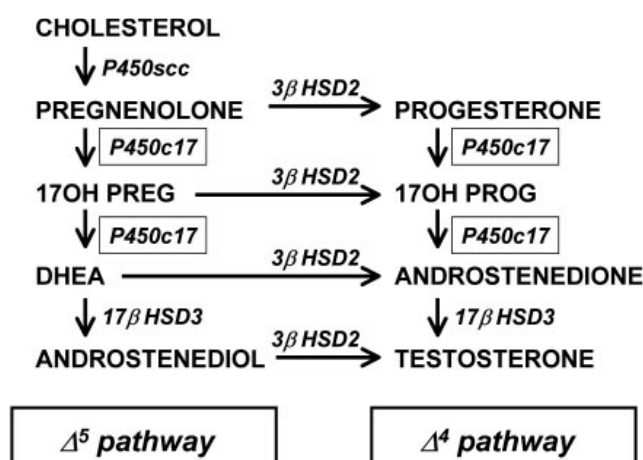


Figure 16. Potential pathways of testosterone synthesis in the human testis (taken from Flück CE et al. 2003).⁶³

In congenital CYP17 deficiencies (congenital adrenal hyperplasia, CAH, less than 5%), the production of cortisol, androgens and estrogens is impaired, leading to the lack of sexual development.⁶² Nonetheless, the synthesis of corticosterone, a weaker glucocorticoid, is preserved. Hence, patients do not develop symptoms of adrenal insufficiency. However, higher levels of adrenocorticotrophic hormone (ACTH) are required before a new steady state is reached as corticosterone is a weaker glucocorticoid than cortisol. Raised levels of ACTH result in a syndrome of secondary mineralocorticoid excess, characterised by fluid overload, hypertension and hypokalaemia (Fig. 17).

This syndrome may be effectively managed with mineralocorticoid antagonists, with or without low doses of glucocorticoids to suppress ACTH generation. ACTH suppression in turn leads to normalization of mineralocorticoid levels and a return of serum potassium and blood pressure to normal. A similar syndrome was observed with the selective inhibition of CYP17, for example by abiraterone acetate, confirming that CYP17 is inhibited.⁶⁴

Since prostate cancer is typically a disease in older men, often presenting cardiovascular problems as well, we propose a selective dual-inhibition approach of CYP17 and CYP11B2, in order to manage the mineralocorticoid side effects, rising by the inhibition of CYP17.

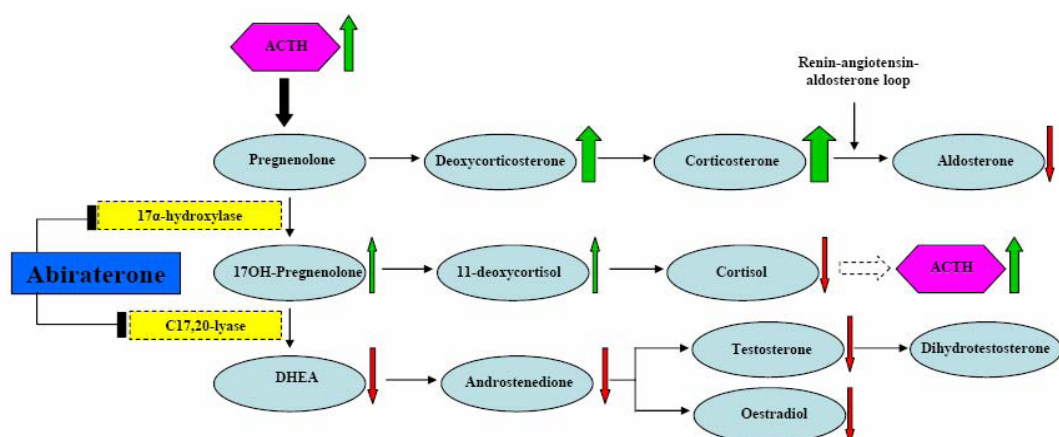


Figure 17. The physiological effects of abiraterone acetate on the androgen biosynthesis pathway are indicated by arrows next to each steroid precursor (taken from Yap TA et al. 2008).⁶⁴

1.3.1.2. CYP19 - Aromatase

Aromatase (estrogen synthetase, P450arom) is a single member of the CYP19 family, coded by the CYP19A1 gene and consisting of 503 amino acid residues with total molecular weight of 57.9 kDa. It catalyzes the conversion of the androgens androstenedione, testosterone and 16 α -hydroxytestosterone to the aromatic estrogenic steroids estrone, 17 β -estradiol and 17 β ,16 α -estriol, respectively, through the aromatization of the A ring of the substrate (three step process), being the only enzyme in vertebrates known to catalyze the biosynthesis of all estrogens from androgens. Aromatase inhibitors therefore constitute a frontline therapy for estrogen-dependent breast cancer, representing the first successful hormone therapy targeting steroidogenesis as proven by various drugs on the market (letrozole, anastrozole, exemestane).

Very recently the crystal structure of aromatase in complex with its natural substrate androstenedione at a resolution of 2.9 Å was published (PDB code 3eqm), becoming the first steroidogenic CYP enzyme being crystallized.⁶⁵

The catalytic complex consists of the aromatase enzyme and a NADPH cytochrome P450 reductase, and facilitates the reaction with the required molar amount of NADPH.⁶⁶ The whole complex is bound to the endoplasmic reticulum membrane in the cell. Aromatase is mostly expressed in the ovaries of pre-menopausal women, in the placenta of pregnant women and additionally in the peripheral adipose tissue, breast tissue and brain.⁶⁷ It is overexpressed in or near breast cancer tissue and is responsible for the local estrogen production and proliferation of breast tumors.⁶⁸ Peripherally synthesized estrogens act locally in an intracrine or paracrine manner without being released into the circulation and act by binding to specific estrogen receptor α (ER α) in the tumor cells thereby mediating transcription of genes regulating proliferation.⁶⁹

For the same reason, they were likely to cause fewer side-effects in patients. Aromatization of androgens to estrogens is the last in the series of reactions in steroid biosynthesis and is rate-limiting for estrogen synthesis. Therefore, there are no steroids produced downstream to be affected by inhibition of aromatase. Also, although aromatase shares common features with other P-450 enzymes, the unique characteristics of the aromatization reaction, involving loss of the C-19 carbon and conversion of the steroidal A ring to an aromatic ring, provide the opportunity to develop inhibitors selective for P450arom.

Tamoxifen, an estrogen receptor antagonist blocks the action of estrogens by binding to the ER. For the past 30 years, tamoxifen has proven to be an effective first-line or adjuvant endocrine treatment for advanced breast cancer.^{23a} Compounds selectively targeting aromatase and lacking estrogenic activity⁷⁰ were envisaged as being more effective than the antiestrogens.^{23b, 71}

Today, three aromatase inhibitors have been approved by the FDA exemestane (Aromasin), a steroidal inhibitor similar to formestane and two non-steroidal inhibitors anastrozole (Arimidex), and letrozole (Femara). All have high potency and specificity for aromatase. The latter two inhibitors were based on inhibition of P-450 enzymes and were derived from drugs used as antifungal agents, such as ketoconazole, an inhibitor of fungal P-450 enzymes. Triazole and imidazole compounds possess a heteroatom, such as nitrogen containing heterocyclic moiety. This interferes with steroidal hydroxylation by binding with the heme iron of CYPs. These nonsteroidal compounds are reversible inhibitors of aromatase, whereas the steroidal inhibitors cause irreversible inactivation of the enzyme. Aromatase inhibitors are proving to be superior to tamoxifen in the advanced setting and are now replacing tamoxifen as first-line therapy.⁷²

1.3.1.3. CYP11B2 - Aldosterone synthase

In humans the final steps of cortisol and aldosterone synthesis are catalyzed by 11 β -hydroxylase (CYP11B1) and aldosterone synthase (CYP11B2), respectively.⁷³ The corticosteroid synthesizing enzymes CYP11B2 and CYP11B1 are not coexpressed within the adrenal cortex. CYP11B1 is expressed at high levels in the *zona fasciculata/reticularis* of the adrenal cortex and oxidizes its substrate 11-deoxycortisol, giving rise to cortisol, the principal human glucocorticoid. Cortisol regulates energy mobilisation, stress response and is additionally involved in the immune response of the human body. In contrast, aldosterone is secreted and

CYP11B2 is expressed in low levels in the *zona glomerulosa* of the adrenal cortex and its synthesis of the former steroid involves three consecutive reactions: initial 11 β -hydroxylation of 11-deoxycorticosterone to yield corticosterone, plus two subsequent CYP11B2 catalyzed oxidations at C₁₈ and water release to form the mineralocorticoid aldosterone. So, a major difference between CYP11B1 and CYP11B2 is the lacking 18-hydroxylase activity. CYP11B1 can only introduce a hydroxy group in 11 β -position in both 11-deoxycortisol and 11-deoxycorticosterone whereas CYP11B2 can also carry out oxidations in 18-position.

The zonal distribution of CYP11B1 and 2 in the adrenal gland has recently been further investigated with surgically removed human adrenal gland cells, showing a higher concentration of CYP11B1 in the *zona fasciculata* than in the *zona reticularis*. Cortisol is usually secreted 100- to 1000-fold in excess over aldosterone, but this is not only due to transcriptional regulation of these enzymes, but also to differences in catalytic activities.⁷⁴

The primary protein sequences of CYP11B2 and CYP11B1 differ only in 32 out of 503 amino acid positions and in the mature enzymes which are bound to the inner mitochondrial membrane, only 29 out of 479 residues are not identical.⁷⁵ This high sequence identity (approximately 93 %) is reflected in the shared 11 β -hydroxylase function of both CYP11B isoforms. However, CYP11B1 is a pure 11 β -hydroxylase catalyst without 18-hydroxylase activity and cannot even 11 β -hydroxylate 18-hydroxy-11-deoxycorticosterone.⁷⁶ By contrast, CYP11B2 catalyzes also oxidations at the steroidal 18-position, mainly in the course of converting corticosterone to 18-hydroxycorticosterone and subsequently to aldosterone, but it can also 18-hydroxylate cortisol.

A series of site-directed mutagenesis experiments was performed affecting the putative I-helix. It was demonstrated by Böttner et al.⁷⁷ that the aldosterone synthase activity decreases to approximately 10 % compared to the CYP11B2 wild type in the case of modifying the positions 301 (leucine to proline), 302 (glutamic to aspartic acid), and 320 (alanine to valine) whereas the 11 β -hydroxylase activity simultaneously increases. Vice versa swapping the aldosterone synthase specific amino acid at position 320 of CYP11B1 from valine to alanine induced aldosterone synthase activity without significant impact on the 11 β -hydroxylase efficacy.⁷⁷

Since no X-ray structure of CYP11B2, located in the inner mitochondrial membrane, is available, several homology models have been established,^{53, 59b, 75b, 78} providing elementary insight into the protein structures and inhibitor binding modes. It has been shown by our group that docking into the homology models of CYP11B2 built on the X-ray structure of human CYP2C9 is a useful tool to explain differences in activity and selectivity of nonsteroidal aldosterone synthase inhibitors.⁷⁹

Aldosterone participates in the regulation of the salt and water household of the body and thus in the regulation of blood pressure. Pathological elevations in plasma aldosterone levels (hyperaldosteronism) increase blood pressure and play a detrimental role in cardiovascular diseases.⁸⁰ Several mineralocorticoid receptor blockers had been developed so far to treat this pathological conditions, but all presented severe side-effects.⁸¹ Thus, inhibition of aldosterone formation with CYP11B2-inhibitors was proposed as a new pharmacological approach for the treatment of hyperaldosteronism, congestive heart failure, and myocardial fibrosis.⁸² Non-steroidal, selective inhibitors are to be preferred, because they can be expected to have less side effects on the endocrine system. The inhibitors must not affect other P450 (CYP) enzymes, like

11 β -hydroxylase (key enzyme of glucocorticoid biosynthesis, CYP11B1) and other hepatic ones, responsible for drug metabolism.

1.3.2. Hydroxysteroid dehydrogenases (HSDs)

The hydroxysteroid dehydrogenases (HSDs) have molecular weights of about 35 to 45 kDa, do not have heme groups, and require NAD(H) or NADP(H) as cofactors. Most steroidogenic reactions catalyzed by P450 enzymes are due to the action of a single form of P450, but each of the reactions catalyzed by HSDs can be catalyzed by at least two, often very different isozymes. These enzymes include the 3 α - and 3 β -hydroxysteroid dehydrogenases, the two 11 β -HSDs, and the 17 β -HSDs.

The hydroxysteroid dehydrogenases (HSDs) catalyze stereoselective reactions at specific positions of the steroid backbone.⁸³ In fact, for each sex hormone an isoform pair is responsible for either inactivation or provision of an active ligand. This is achieved either by the oxidation of the alcohol group (oxidase activity) or by the reduction of the keto function (reductase activity, Fig. 18) on the steroid skeleton. These reductase/oxidase activities allow, therefore, the HSDs to function as a molecular switch.

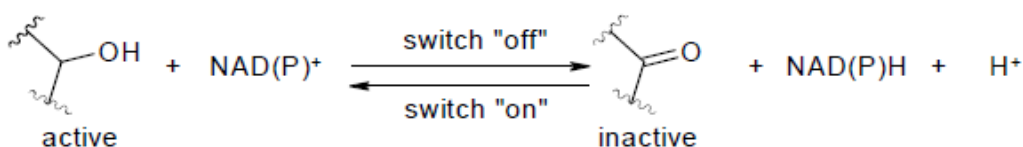


Figure 18: general reaction catalyzed by hydroxysteroid dehydrogenases

The HSD family is split into 2 superfamilies: the short-chain dehydrogenase/reductase (SDR) family, characterized by a Rossmann fold, and the aldo-keto reductase (AKR) family, characterized by a triosephosphate isomerase (TIM) barrel motif.⁸⁴ The SDR family members often function as multimers and share a low sequence identity (less than 25%). Despite to this relatively low homology, SDR family members share identical protein folds.⁸⁵ Part of the protein fold includes an arrangement of α -helix and β -strands (β - α - β) to produce the “Rossmann fold” motif for cofactor binding. They also contain a conserved catalytic motif of Tyr-X-X-X-Lys where Tyr is the catalytic general acid/base of the reaction.⁸⁶

In contrast, the AKRs are monomeric, soluble enzymes utilising NAD(P)(H) as cofactor. They share a high amino acid sequence identity (>67%) compared to the SDR subfamily. Invariant to their active site is a catalytic tetrad consisting of Asp, Tyr, Lys and His motif. Site-directed mutagenesis supports the crucial role for the amino acids Tyr and Lys in the catalytic mechanism in a manner similar to that described for the SDR family but the disposition of these residues on the enzyme structure is different compared to the SDRs.⁸⁷

The SDR enzymes include 11 β HSDs 1 and 2, and 17 β HSDs 1, 2, 3, and 4; the AKR enzymes include 17 β HSD5 (AKR1C3), which is important in activation of androgenic precursors in peripheral tissues, such as the prostate.⁸⁸

We can classify HSDs physiologically based on their activities as dehydrogenases or reductases. The dehydrogenases use NAD⁺ as their cofactor to oxidize hydroxysteroids to ketosteroids, and

the reductases mainly use NADPH to reduce ketosteroids to hydroxysteroids. Although these enzymes are typically bidirectional *in vitro*, they tend to function in only one direction in intact cells, with the direction determined by the cofactor(s) available.⁸⁴

1.3.2.1. 17 β -Hydroxysteroid dehydrogenases (17 β -HSDs)

As mentioned in chapter I, the synthesis from DHEA of the most potent natural androgen, DHT and of the most potent natural estrogen, 17 β -estradiol (E2) involves several enzymes, namely 3 β -hydroxysteroid dehydrogenase/ Δ 5- Δ 4 isomerase (3 β -HSD), 17 β -HSD, 5 α -reductase and/or aromatase.

17 β -hydroxysteroid dehydrogenases (17 β -HSDs) catalyze the interconversion between the active and inactive forms of specific steroidal hormones on the final steps of their biosynthesis, playing the key role in the last step of androgen and estrogen formation. 17 β -HSDs are responsible for the stereospecific oxido-reduction reaction of hydroxy or carbonyl groups at position 17 of the steroid backbone using NAD(P)H or NAD(P)⁺ as cofactor.⁸⁹ They are expressed in the gonads as well as in peripheral tissues. This enzyme family is responsible for the pre-receptor activation/inactivation of hormones *in vivo*, thus regulating the amount of active hormone available to bind to the specific receptor.

Up to now, 15 mammalian 17 β -HSDs are reported in vertebrates of which 12 are also present in humans, while 17 β -HSD6 and 9 are only reported for rodents. With the exception of 17 β -HSD5, which is a member of the aldoketo-reductase (AKR) family, all 17 β -HSDs belong to the short chain dehydrogenase/reductase (SDR) superfamily.⁹⁰ In vertebrates the enzymes show generally low sequence homology (15–20%) but some elements characteristic for SDR members are strongly maintained, e.g. the Rossmann fold. Despite this structural conservation, substrate specificities among the family members are diverse and for some 17 β -HSDs substrates such as fatty acids or bile acids are preferred over sex steroids.⁹¹

17 β -HSDs drive unidirectional reactions in intact cells while in cell homogenates it has been shown that these enzymes are able to catalyze either the oxidation or the reduction depending on which cofactor form (reducent or oxidant) is present. In cells, NADPH is a major source for electrons, and reducing equivalents from NADPH are used in different metabolic reactions. In contrast NAD⁺ is a versatile electron acceptor, and most enzymatic oxidations deposit these electrons on NAD⁺. To maintain this cofactor abundance, the cell constantly recycles these compounds from other oxidation states.

As shown in Figure 19, the cellular concentration of NADPH is higher (500 times) than the NADP⁺ concentration. In contrast for the non phosphorylated cofactor NAD⁺ is generally 700 times more abundant in cells than NADH.⁹²

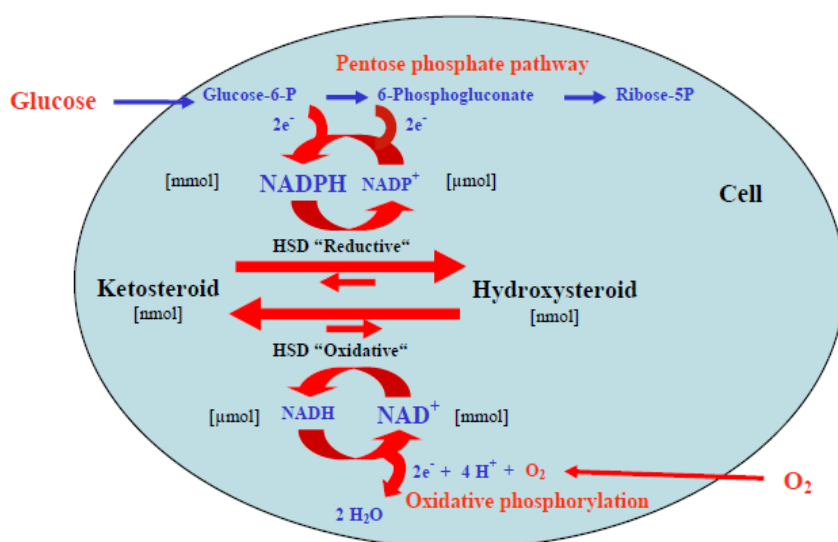


Figure 19. Interplay between metabolism and HSD reactions

Besides these cofactor concentration differences observed in intact cells, kinetic studies showed that the 17 β -HSDs exhibit huge K_M value differences between NADP(H) and NAD(H). This implicates that it in the cofactor binding sites of each 17 β -HSD isoform amino acids must be present which allow the enzyme to distinguish the non-phosphorylated from the phosphorylated cofactor form.⁹²

Crystal structure analysis of reductive HSD enzymes, such as 17 β -HSD1, show that an arginine residue in the N-terminal region (R37 in 17 β -HSD1) of the Rossmann fold is responsible for this discrimination.⁹³ The positively charged guanidinium group of the arginine forms a salt bridge with the 2'-phosphate moiety of NADPH, which further enhances the affinity of these enzymes for NADPH (Fig. 20).

In contrast, oxidative SDRs like 17 β -HSD2, contain a negatively charged amino acid at the position corresponding to the stabilizing arginine of the reductive enzymes: the carboxylate groups of aspartate and glutamate induce repulsive interactions with the 2'-phosphate group of NADP⁺ but might be able to form hydrogen bonds with the 2'-OH function of NAD⁺ (Fig. 20) enhancing therefore the affinity for the non-phosphorylated cofactor form.

Site-directed mutagenesis experiments demonstrated that exchanging this arginine with an aspartate moiety in the case of a reductive HSD enzyme increases the affinity for NADH (vs. NADPH), while exchanging this aspartate with arginine moiety in the case of an oxidative HSD enzyme enhances the affinity for NADP⁺ (vs. NAD⁺).⁹⁴⁻⁹⁵

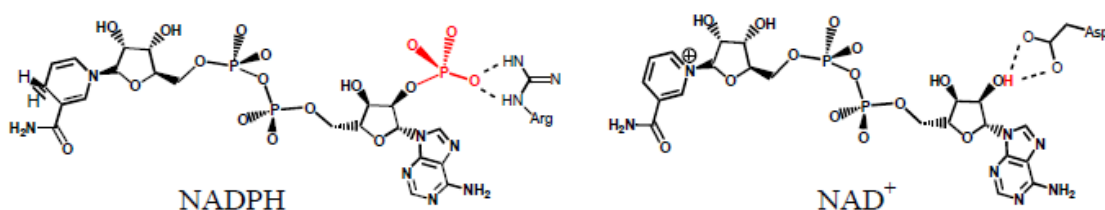


Figure 20. Binding preferences of NADPH and NAD⁺ for reductive/oxidative HSDs.

1.3.2.2. 17 β Hydroxysteroid dehydrogenases type 1 (17 β -HSD1)

17 β -HSD type 1 (EC 1.1.1.62) was first described in 1958 by Langer & Engel.⁹⁶ It is active as a soluble cytosolic homodimer, both subunits having a molecular mass of 34.9 kDa and containing 327 amino acids.⁹⁷⁻⁹⁸

It catalyzes predominantly the final step of the E2 biosynthesis, reducing estrone (E1) to estradiol (E2) and using NADPH as cofactor.⁹⁹ As this reaction is the last step of the biosynthetic pathway to estradiol E2, which has a far stronger estrogenicity than E1, 17 β -HSD1 plays a key role in activating estrogens and regulating their concentrations.

17 β -HSD1 is abundantly expressed in the ovaries (in granulosa cells of developing follicles and placenta),¹⁰⁰⁻¹⁰¹ but also present and active in peripheral tissues, among those breast and endometrium.¹⁰² Therein, E2 is biosynthesized in an intracrine pathway, i.e. 17 β -HSD1 is expressed *in situ* and catalyzes the biosynthesis of E2 on-site. In the aforementioned tissues, estradiol can exert effects that cause or facilitate the progression of estrogen-dependent diseases, especially breast cancer and endometriosis. Thus, the discovery of inhibitors of 17 β -HSD1 is of high pharmacological interest for the treatment of hormone-sensitive diseases, because reduced systemic effects can be expected compared to aromatase inhibitors (AI) which act both at an intracrine and at an endocrine level.

The first X-ray structure of 17 β -HSD1 as native form was published in 1995.¹⁰³ Since then 18 crystal structures of binary or ternary complexes with estrogenic and androgenic ligands or with steroid based inhibitors have been deposited in the Protein Data Bank (PDB).

The core of the monomeric form of 17 β -HSD1 is a seven-stranded parallel β -sheet (β A to β G), surrounded by 6 parallel α -helices, three on each side of the β -sheet (Fig. 21), bearing the classical Rossmann fold, which is associated with the NADPH binding. Five additional α -helices are located around the steroid binding domain.¹⁰³

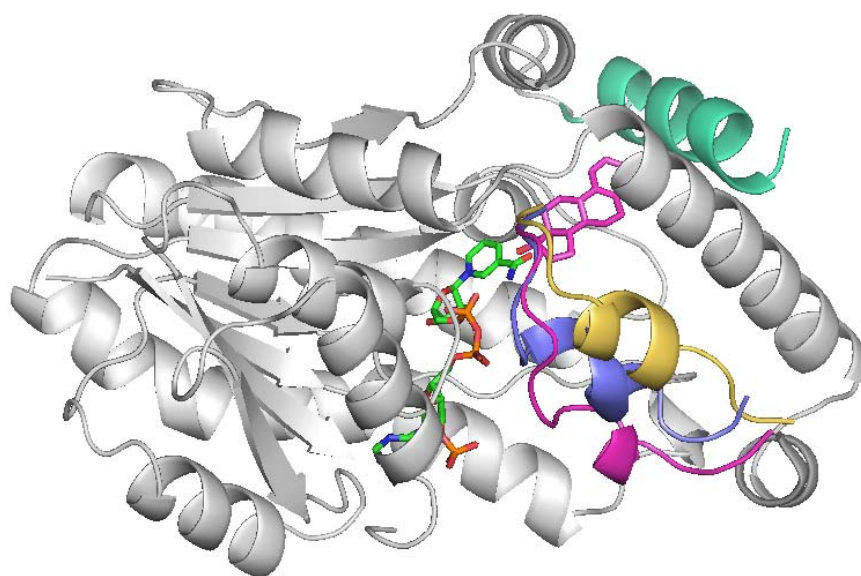


Figure 21. Common fold of 17 β -HSD1 rendered as cartoon. The cofactor NADP(H) and the co-crystallized product E2 are presented as sticks in green and magenta, respectively. The three main dispositions of the highly flexible β F- α G'-loop are depicted in yellow, blue and magenta, the C-terminal helix in cyan.

The analysis of the available crystal structures furnishes useful informations about the enzyme architecture: a substrate binding site, a cofactor binding pocket and an entry channel can be defined. As a member of the SDR superfamily, 17 β -HSD1 contains the highly conserved and catalytically crucial tetrad Tyr-x-x-x-Lys sequence (Asn114, Ser 142, Tyr155 and Lys 159; Fig. 22). The steroid binding pocket of 17 β -HSD1, a narrow hydrophobic tunnel showing a high degree of complementarity to the substrate E1, can be divided into three regions: the first region recognizes the steroidal phenolic A-ring and contains His221 and Glu282, which could form hydrogen bonds with O3 of the steroid. The second region binds to the central hydrophobic core of the steroid and contributes to the main thermodynamic force favoring the binding of substrate (hydrophobic interactions with Val143, Leu149, Pro187, Val225, Phe226 and Phe259). Interestingly, two polar amino acids (Tyr218 and Ser 222) are located in this region without any interaction with the substrate. The third region (catalytic region) surrounds the D-ring and contains Ser142, Tyr155, and Lys159.

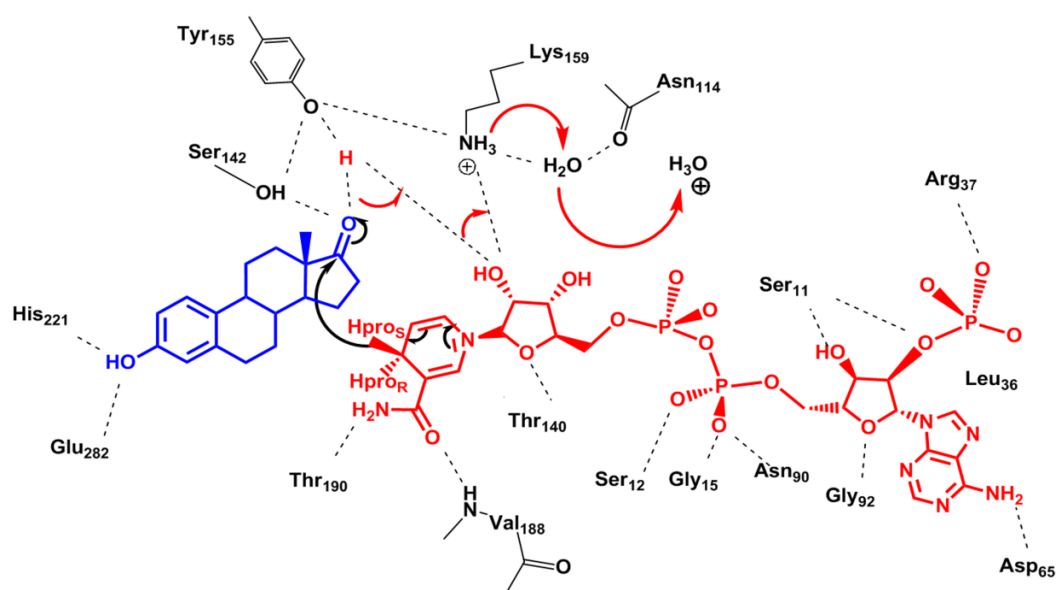


Figure 22. Postulated mechanism of the reduction of E1 to E2 (13). The substrate E1 is represented in blue, the cofactor NADPH in red. The amino acids, which are either involved in the catalysis or are responsible for ligand/cofactor stabilization, are colored in black and residue labelled. The hydrogen bonds are in dashed lines while the proton transfers are highlighted with arrows.

17 β -HSD1 shows a clear preference for estrogen substrates, but has also the ability to reduce some androgens, such as DHEA, into dihydrotestosterone.¹⁰⁴⁻¹⁰⁶ Because both estrogens and androgens (with C19) have 3- and 17-hydroxy or ketone groups, the critical residues that are expected to determine specificity for the estrogenic substrates must lie within the hydrophobic binding region.

For dihydrotestosterone and dehydroepiandrosterone, crystallization experiments (PDB code 1DHT and 3DEY) confirmed this hypothesis by showing that the C19 methyl group causes a shift of the substrate compounds away from NADP⁺, resulting in a lower k_{cat} value.¹⁰⁶ Especially the rigidity of the fork-like side chain Leu149 forced the androgens to occupy a slightly different site than estradiol in the PDB complex 1FDT. Subsequently, a decrease of the binding affinity was observed, probably due to reduced Van der Waals interactions between Phe259 and the

ligand. Indeed, the K_m value for dehydroepiandrosterone is more than 1000-fold greater than that for estrone, and the K_m for dihydrotestosterone is about 10-fold greater than that for estradiol.

In several site directed mutagenesis experiments the importance of Leu149 for substrate specificity as well as the identification of critical amino acid residues (Ser142, Tyr155, His221, Glu282) for enzyme activity and substrate binding could be determined.^{95, 107, 108}

17 β -HSD1 can be inhibited at several sites, including the substrate binding pocket and the cofactor binding region including part of the Rossmann fold.¹⁰⁹ The large majority of known 17-HSD1 inhibitors, mainly steroids, was shown to compete with the natural substrate for its binding site. Although, so-called hybrid compounds have been synthesized, that combine moieties from NAD(P)H and estradiol analogs, occupying both the steroid and the cofactor binding site.¹¹⁰

The major disadvantage of steroidal inhibitors lies in their generally unfavorable ADMET characteristics and low specificity due to cross-reactivity with other steroid metabolizing enzymes and steroid hormone receptors. Moreover, metabolizing enzymes might modify steroidal inhibitors at several positions of their steroid scaffold, leading to potentially bioactive metabolites and possible disturbances of steroid hormone metabolism. Therefore, there is currently a great interest for the identification of novel nonsteroidal 17 β -HSD1 inhibitors.

Chapter Two. Aims of the study.

Steroidal hormones play a predominant role in various hormone-sensitive events, like breast (BC) or prostate cancer (PC) and hypertension. The binding of these steroids to their specific receptors results in slow genomic or fast nongenomic effects, often crucial for cell proliferation or maintenance of physiological balance. This occurs especially in hormone-dependent diseases, where the steroidogenic enzymes are highly overexpressed in relation to normal tissues, like in case of BC or PC. Sex steroids, in particular, are well recognized to play a predominant role in the regulation of cell growth and differentiation of normal mammary glands. Interestingly, while estrogens stimulate the proliferation of hormone sensitive breast cancer tumor,¹¹¹ androgens exert an antiproliferative action in these cells.¹¹² In other hormone-sensitive pathologies, however, like in hypertension, no overexpression of the steroidogenic enzymes was observed, whereas a systemic overproduction of mineralocorticoids could be responsible for a marked disbalance in the regulation of the systemic circulation.

First-choice strategies, which are currently applied for the treatment of hormone-dependent disorders, can be roughly classified into surgical, i.e. castration, and pharmacological approaches, which consider the use of small molecules as drugs. The latter can be further subdivided into drugs affecting the production (biosynthesis) of the steroids (inhibitors), *de facto* eliminating the “source” of induced genomic and non-genomic effects, or hampering the steroid-receptor interaction (agonists, antagonists), thus suppressing the “effects” induced by receptor-ligand binding. Most of the strategies concerning the effects are associated with systemic side-effects, resulting from an indiscriminated, widespread silencing of the receptor functionalities. The reason therefore is that different ligands can stimulate the same receptor-mediated responses, acting not only in the target cells/organs, but also in other compartments, where the inhibition of the protein functions can be crucial for the survival of the investigated biological system.

There is a large body of evidence showing that in the human the local intracrine formation of active estrogens and androgens from inactive steroid precursors DHEA and DHEA-S regulates growth and function of peripheral target tissues, including the breast.⁸ Thus, the selective inhibition of steroidogenic enzymes expressed in these target organs (CYP19 and 17 β -HSD1) is regarded to be a promising strategy for the treatment of such hormone dependent diseases (BC). However, apart of the intracrine formation, most of the steroidal hormones are produced distant from their site of action. Thus, the selective inhibition of enzymes (CYP17, CYP11B2 and CYP19) involved in the biosynthetic pathways placed in endocrine organs is also a valuable strategy,¹¹³ as several clinical studies confirmed.^{20, 37, 38, 41, 64}

Computational methodologies, like docking studies, comparative modeling and molecular dynamic simulations, as well as quantum chemical methods, are a powerful addition to the classical synthesis of inhibitors of steroidogenic enzymes based on traditional medicinal chemistry strategies. They have been applied, in order to identify and validate possible binding modes of known inhibitors, to investigate the influence of their different physicochemical properties (like molecular electrostatic potential distribution) on the inhibitory potency and to rationalize drug design of new inhibitors, which was performed ligand- and structure based.

Specifically, the aims of this thesis were:

1. CYP17:

- To build a homology model of the human CYP17 enzyme.
- To dock several classes of CYP17 inhibitors in this model and to investigate the interactions formed with the enzyme, if possible, deriving suitable substitution patterns.
- To calculate the molecular electrostatic potential (MEP) distribution of a series of imidazolyl-biaryls in order to elucidate the potency differences within this class of compounds.

2. CYP19:

- To dock non steroidal CYP19 inhibitors into the homology model of CYP19 (1TQA) in order to improve and focus the drug design of novel compounds and to rationalize the SAR on a biomolecular basis.

3. 17 β -HSD1:

- To analyze the 17 (18, considering the two conformations in 1fdt) existing crystal structures of 17 β -HSD1 and highlight their differences in order to assign the different identified conformations to enzyme forms occurring along the kinetic pathway.
- To dock non steroidal 17 β -HSD1 inhibitors into various, representative crystal structures of the enzyme with the aim of identifying the most reliable binding mode for the class of bis(hydroxyphenyl)-arenes.
- To validate different binary (17 β -HSD1-NADPH) and ternary (17 β -HSD1-NADPH-E1) complexes by means molecular dynamic simulations, MM/PBSA methods and normal mode analysis in order to substantiate the hypothesis of the rapid equilibrium random bi-bi kinetic cycle and to determine the most plausible enzyme conformation at each step of the cycle.
- To perform quantum chemical investigations on the class of bis(hydroxyphenyl)-arenes ("semi"-QMAR), in order to identify a common MEP distribution pattern responsible for high potency along this series.

4. CYP11B2:

- To create a pharmacophore model based on non steroidal CYP11B2 inhibitors.
- To design a new class of non steroidal CYP11B2 inhibitors exploiting structural features derived from potent CYP19 inhibitors.

Chapter Three. Results and Discussion

3.1 Androgen-dependent prostate cancer (PC) – selective CYP17 inhibition

3.1.1. Homology model of CYP17

The CYP17 enzyme is bundled in a catalytic complex with the catalytically crucial iron-binding porphyrin ring as a prosthetic group in the active site, an NADPH–cytochrome P450 reductase, which provides the reaction with the required amount of NADPH, and with cytochrome b5, responsible for enzyme activation and electron transfer (2nd step). The whole complex is bound to the endoplasmic reticulum in the cell. Due to the membrane-bound character of the complex, the crystal structure of the enzyme is yet to be solved. The lack of an experimental structure for CYP17 requires comparative modeling methods to be used in studying the overall protein fold and the geometry of the active site. One of the most powerful tools for creating a 3D structure of a protein is homology modeling.

CYP17 is a distant relative of other CYP enzymes. Despite a low amino acid sequence identity ($\approx 23\%$) it possesses a common tertiary fold to most of the other CYP, which allows to derive its unknown structure from a known CYP one. Moreover, certain residues and the secondary structures are also conserved throughout the CYP enzyme families, thus α -helices, β -strands, turns and loops might vary in length and amino acid constitution.

After the first bacterial CYP enzyme was crystallized and its structure solved, these enzymes have been used as templates for modeling human cytochromes. Several groups have proposed CYP17 models that were based on bacterial cytochrome structures.^{59,114-116} In the past years various human mammalian CYP enzymes have been crystallized, representing better templates than the bacterial CYPs. In relation to our ongoing study concerning anti-prostate cancer drugs and enzymes deputed to androgen biosynthesis, we have built a three-dimensional model of human 17 α -hydroxylase/17,20-lyase. Moreover, the aims of this homology model are to help rationalizing and speeding up the design of novel non-steroidal inhibitors of CYP17 and to study the binding of natural substrates and various designed inhibitors.

We searched for templates evolutionally related to the target with the help of PSI-BLAST¹¹⁷ and Pcons¹¹⁸ server. The identification of structurally conserved regions (SCR) and structurally variable regions (SVR) was based on literature studies, with the assistance of secondary structure elements prediction with the PsiPred server.¹¹⁹ CYP2C9 resulted as one of the best templates among CYP enzymes with 28.9 % sequence identity. Sequence alignment is the most important part of the homology modelling process. With proteins sharing low sequence identity, this is by no means a trivial task. Gaps and insertions must be introduced to the target sequence to make the important residues match each other. The first alignment was obtained from the PSI-BLAST server and subsequently manually refined on the basis of the PsiPred secondary structure element predictions. Finally, a multiple sequence alignment was created with ESPRESSO¹²⁰ - the 3D routine of T-Coffee¹²¹ - including as templates CYP2C9, 2C8, 2A6, 3A4 and 2B4, and a secondary structure profile was extracted from it and used for the final refinements of the

CYP17-CYP2C9 alignment. Different solutions were generated by focusing on the six substrate recognition sites (SRS) defined for the CYP2 enzyme family by Gotoh (Chapter I, pg. 20).

These SRS constitute the active site of the enzyme where the substrate binds and the catalytic reaction takes place. They can differ in length and amino acid composition. For example, the sequences of CYP17 and 2C9 in SRS-1 (between B- and C-helices) have different lengths, and while PsiPred predicts a short 5-residue BC-helix for CYP17, the template 2C9 has a 7-residue helix flanking the active site. When performing the alignment, particular care has to be taken to a correct match between conserved residues in these SRS and the insertion of gaps. Problematic areas were SRS-2 and SRS-3, i.e. the C-terminus of F-helix, the N-terminus of G-helix and the loop between them. This area varies among cytochrome family members showing loops of different lengths and exhibiting one or two additional helices (F' and G'). Again the length of SRS-2 and SRS-3 is different for CYP2C9 and CYP17, as well as their amino acid sequence. SRS-4 is located in the so-called I-helix kink, directly involved in the catalytic process and presenting several residues conserved among the CYPs. Also CYP17 and CYP2C9 are highly similar in this region, as the following short extract of the alignment nicely shows (in blue the identical residues):

```
CYP2C9:  D276-L277-F278-G279-A280-G281-T282-E283-T284-T285-S286-T287-T288-L289  
CYP17:  D298-I299 -F300-G301-A302-G303-V304-E305-T306-T307-T308-S309-V310-V311
```

Conserved residues E305 and T306 of CYP17, aligned with residues E283 and T284 of 2C9 have been proven critical in mutagenesis studies.¹²²⁻¹²³ The active site wall opposite to the I-helix consists mainly of SRS-5, the coil between K-helix and β 1-4-strand. For this site the alignment between CYP17 and 2C9 matches the hydrophobic nature of the template. Ile371 decreases the overall size of the active site slightly compared to the leucines of the template. The SRS-6 is located in the C-terminal loop, or more accurately, the hairpin turn between the two strands β 4-1 and β 4-2. This last region is one of the less conserved for all CYP enzymes, and is described to be responsible for ligand binding. The final alignment is shown in Figure 22.

A set of models was built by means of MODELLER v8.0¹²⁴ based on the human mammalian CYP2C9 enzyme as template, whereas all three crystal structures of CYP2C9 deposited in the PDB, one holoenzyme (1og2, only with heme) and two ternary complexes cocrystallized with S-warfarin (1og5) and flurbiprofen (1r9o), respectively, were used as template.

Remarkably, S-warfarin is not bound close to the heme but placed in a secondary binding site, while flurbiprofen is oriented parallel to the I-helix and placed on the top of the heme.

Despite flurbiprofen does not complex with the heme iron, we chose PDB entry 1r9o as template, due to the inward turned polar residues of the BC-loop and due to the biphenyl-like core of flurbiprofen similar to that of our CYP17-inhibitors, For the missing residues of the F/G segment in 1r9o we used the crystal 1og2_B as template, presenting two nicely solved helices in the FG-loop.

```

1r9o 26 RGKLP PPGPTLP - - - - LQIGIKD - ISKSLTNLSKVYGPVFTLYFGLKPIVVLHGVEAVKEALIDLGEE 88
log2_B 30 - - - - PPGPTLPVIGNILQIGIKD - ISKSLTNLSKVYGPVFTLYFGLKPIVVLHGVEAVKEALIDLGEE 93
CYP17 24 GAKVYPKSLLS LPLVGS L PFLPRRHGHMHNFFK LQKKYGP IYSVRMGTKTTVIIVGHHQLAKEVLIKKGKD 92

1r9o 89 FSGRGIFPLAERA - - NRGFGIVFSN - GKKWKEIRRFSLMTRLNFGMGKRSIEDRVQEEARCLVEELRKT 154
log2_B 94 FSGRGIFPLAERA - - NRGFGIVFSN - GKKWKEIRRFSLMTRLNFGMGKRSIEDRVQEEARCLVEELRKT 159
CYP17 93 FSGRPFQMATLDIASNNR - KGI AFADS GAHWQLHRRLLAMATFALFKDGDQKLEKIICQEISTLCDMLATH 160

1r9o 155 KASPCDPTF IILGCAPCNVICS IIFHKRFDYKDDQFLNLMKLNENIKILSSPWI - - - - - P - I IDYFPFG 216
log2_B 160 KASPCDPTF IILGCAPCNVICS IIFHKRFDYKDDQFLNLMKLNENIEILSSPWIQVYNNFPALDYFPFG 223
CYP17 161 NGQSIDIS F P V F V A V T N V I S L L C F N T S Y K N G D P E - L N V I Q N Y N E G I - - - I D N L S K D S L V D L V P W L K I F P N 226

1r9o 217 THNKLLKNVAFMKS Y I L E K V K E - HQESMDMNNPQDFIDCF LM - KMEKEKHN - - - - QPSEFTIES - LENT 278
log2_B 229 THNKLLKNVAFMKS Y I L E K V K E - HQESMDMNNPQDFIDCF LM - KMEKEKHN - - - - QPSEFTIES - LENT 290
CYP17 227 KTLEK L K S H V K I R N D L L N K I L E N Y K E K F R S D S I T N M L D T L M Q A K M N S D N G N A G P D O S E L L S D N H I L T T 295

1r9o 279 AVDLFGAGTETTS T T L R Y A L L L L K H P E V T A K V Q E E I E R V I G R N R S P C M Q D R S H M P Y T D A V V H E V Q R Y I 347
log2_B 291 AVDLFGAGTETTS T T L R Y A L L L L K H P E V T A K V Q E E I E R V I G R N R S P C M Q D R S H M P Y T D A V V H E V Q R Y I 359
CYP17 296 I G D I F G A G V E T T S V V K W T L A F L L H N P Q V K K K L Y E E I D Q N V G F S R T P T I S D R N R L L L L E A T I R E V L R L R 364

1r9o 348 DLLFTSLPHAVTCDIKFRNYLIPKGT T I L I S L T S V L H D N K E F P N P E M F D P H H F L D E G G N - - F K K S K Y F M 414
log2_B 360 DLLFTSLPHAVTCDIKFRNYLIPKGT T I L I S L T S V L H D N K E F P N P E M F D P H H F L D E G G N - - F K K S K Y F M 426
CYP17 365 P V A P M L I P H K A N V D S S I G E F A V D K G T E V I I N L W A L H H N E K E W H Q P D Q F M P E R F L N P A G T Q L I S P S V S Y L 433

1r9o 415 PFSAGKRICVGEALAGMELF L F L T S I L Q N F N L K S L V D P K N L D T T P V V N G F A S V P P F Y Q L C F I P I / h 480
log2_B 427 PFSAGKRICVGEALAGMELF L F L T S I L Q N F N L K S L V D P K N L D T T P V V N G F A S V P P F Y Q L C F I P V / h 492
CYP17 434 P F G A G P R S C I G E I L A R Q E L F L I M A W L L Q R F D L E - - - V - P D D G Q L - - P S L E G I P K V F L I D S F K V K I / h 495

```

Figure 22. Alignment of CYP17 with the amino acid sequences of the 2 crystal structures of CYP2C9, 1r9o – cocrystallized with flurbiprofen, and log2_B – presenting a water molecule at the sixth coordination position of the heme-iron.

The C-terminus of the sequence was built using the loop-refine module of MODELLER. The prosthetic heme group was copied from the template in the modeling process and the coordination of sulfur in C442 to the heme iron was prepared for AMBER9¹²⁵ by setting the distance between sulfur and iron to 2.3Å and by assigning to the whole heme group the DFT-charges calculated by Favia et al.¹²⁶ Notably, the charge for the iron atom was adapted to docking needs, considering it 5-coordinated and with a charge of +1.58. The obtained model was put in a TIP3PBOX water box of 9 Å radius, equilibrated and simulated using MDS with AMBER9 for 200 ps. The trajectory was clustered on the basis of the backbone root mean square deviation (RMSD), and the representative structure of the biggest cluster was extracted and minimized. This structure was subjected to PROCHECK to analyze the quality of the model (Fig. 23) which was found to be good with a G-factor of -0.21 (values between 0 and -0.5 are considered to be good ones), no residues in a disallowed and > 98% in a favored region (Fig. 24).

3.1.2. Molecular docking of CYP17 inhibitors

The homology model was first validated by docking into it a set of active and inactive compounds by means of GOLD v3.0.1 software,¹²⁷ with distance restraints set between the heme-iron and the nitrogen present in the heteroring of the inhibitors. In this way we do not force the inhibitor to coordinate with the iron, because a wrong angle between heme plane and heteroring plane (optimum 90°) can still hamper the complexation. GOLD was considered as a suitable docking software because it was able to reproduce the binding conformations of the cocrystallized ligands in four CYP complexes (PDB entries 1SUO, 1Z11, 1W0G and 1J0C). The results of the docking studies are presented hereafter in paper I-VII. The homology model showed a good capacity to comprehensively rationalize the SAR of the docked inhibitors and helped to further improve the drug design, while on the contrary almost no correlation between CYP17 inhibition IC₅₀ values and GOLDScore values was observed.

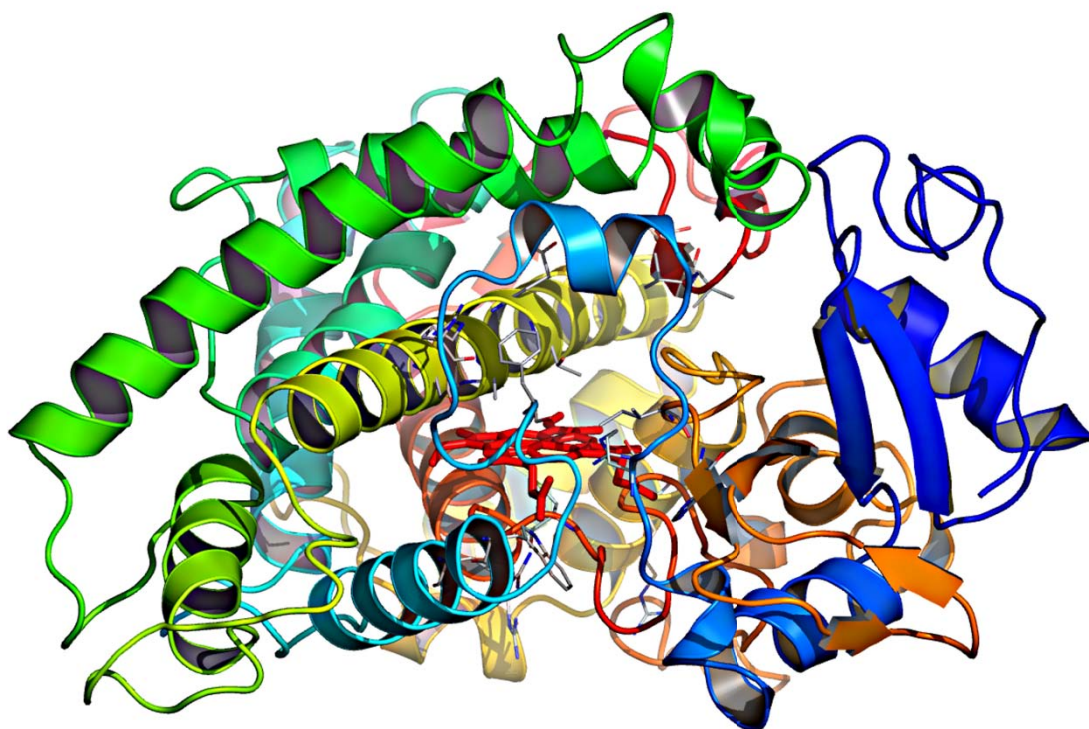


Figure 23. 3D structure of the generated CYP17 model, with the different segments rainbow color-coded (BC-loop is cyan, I-helix yellow, F/G-segment green, C-terminal loop red, etc.). Heme is represented as red sticks.

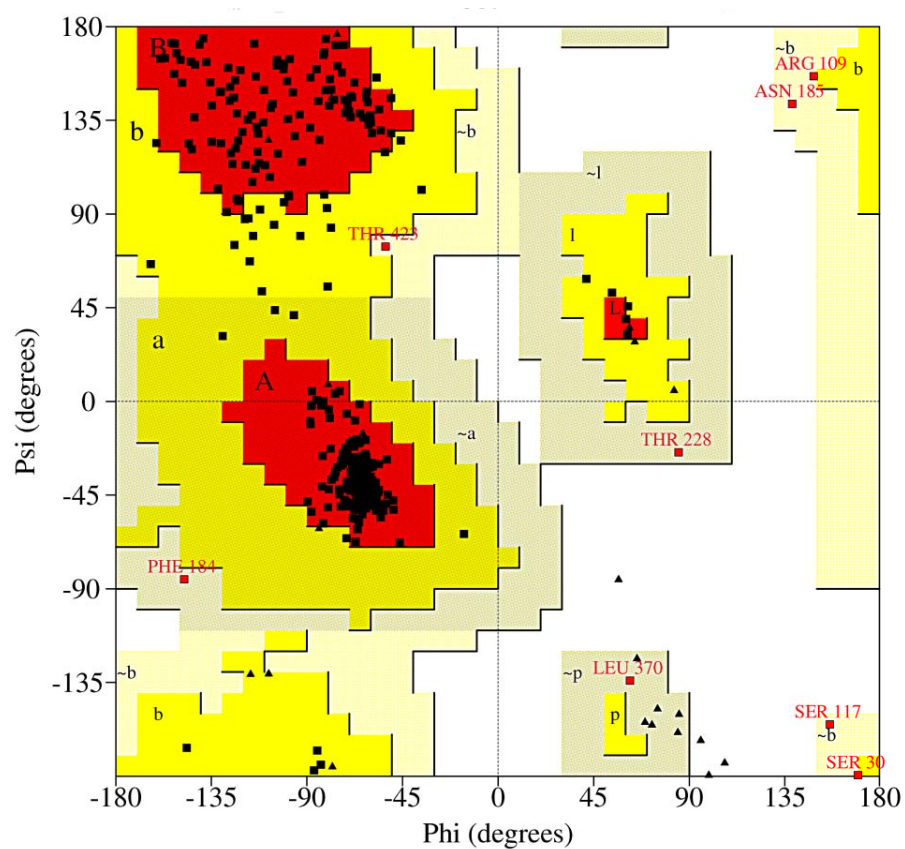


Figure 24. The Ramachandran plot of the generated CYP17 homology model (amino acids are for 90.8% in core, 7.2% in allowed, 1.9 % in generously allowed and 0% in disallowed regions, clustered by phi and psi angles).

3.1.3. Molecular electrostatic potential (MEP) distribution of CYP17 inhibitors.

“The electrostatic potential (ESP) is created in the space around a molecule by its nuclei and electrons (treated as static distributions of charge) and can be a very useful property for analyzing and predicting molecular reactive behavior. It is rigorously defined and it is particularly useful as an indicator of the sites or regions of a molecule to which an approaching electrophile, for example, is initially attracted.”¹²⁸

Several CYP17 inhibitors were investigated with regards to the MEP distribution and it could be observed that those with a biaryl-core, subject of paper **II** require a particular ESP on the two aryl rings to gain high potency. Best example is the deleterial effect of a negative electrostatic potential on the C-ring (second aryl ring, close to the N-bearing heteroring; Fig. 25) on the biological activity. Optimally, this region should be almost neutral, to better fit to the I-helix and to interact with G301-A302-G303.

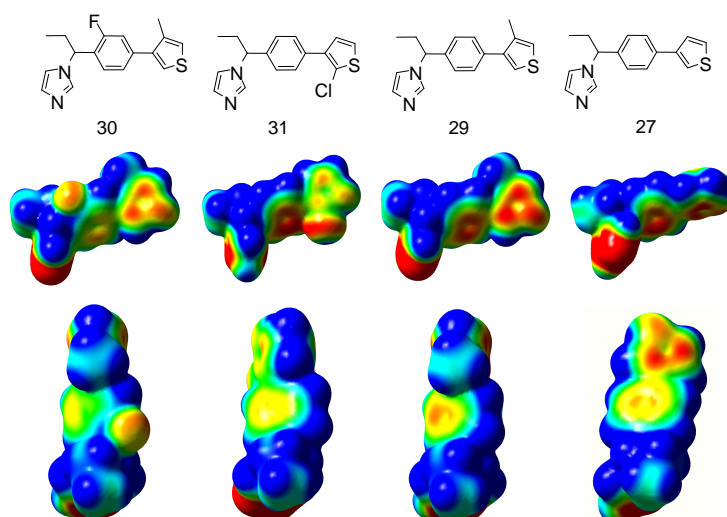


Figure 25. MEP maps of compounds **27**, **29**, **30** and **31**. The ESP surfaces were plotted with GaussView 3.0 in a range of $\pm 12,5$ kcal/mol.

3.1.4. Articles published in CYP17 project – paper I-VII

3.1.4.1. Paper I.

Synthesis, Biological Evaluation and Molecular Modelling Studies of Novel ACD- and ABD-Ring Steroidomimetics as Inhibitors of CYP17

Mariano A. E. Pinto-Bazurco Mendieta, Matthias Negri, Carsten Jagusch, Ulrike E. Hille, Ursula Müller-Vieira, Dirk Schmidt, Klaus Hansen, and Rolf W. Hartmann

This article is protected by copyrights of ‘Bioorganic and Medicinal Chemistry Letters.’

Bioorg. Med. Chem. Lett. **2008**, *18*, 267–273

Abstract

Two novel classes of non-steroidal substrate mimetics were synthesised and examined for their potency as inhibitors of human CYP17. Selected compounds were tested for inhibition of hepatic CYP enzymes 3A4, 1A2, 2C9 and 2C19. The most promising compound **15** showed a good inhibition of the target enzyme (31% and 66% at 0.2 and 2 μ M, respectively), and little inhibition of the most important hepatic enzyme CYP3A4 (6% and 19% inhibition at 0.2 and 2 μ M, respectively) and the key enzyme of glucocorticoid biosynthesis CYP11B1 (3% and 23% inhibition at 0.2 and 2 μ M, respectively). Docking studies revealed that this compound does not assume the same binding mode as steroidal ligands.

Introduction

Prostate cancer is the most common disease and age-related cause of death in elder men worldwide.¹ Since it is in over 80% of the cases androgen dependent, the standard treatment is orchiectomy or its medicinal equivalent the chemical castration by gonadotropin-releasing hormone analogues, which reduce the testicular androgen production.² Because these treatments do not affect adrenal androgen production, they are frequently combined with androgen receptor antagonists (flutamide, cyproterone acetate) to reduce the stimulatory effects of the remaining androgens.³ However, due to mutations in the androgen receptor, anti-androgens might be recognised as agonists,^{4,5} making this so-called ‘combined androgen blockade’ therapy not suitable for all patients.

The antimycotic ketoconazole has proven itself clinically as a good adjuvant therapy by reducing testosterone biosynthesis through inhibition of CYP17.^{6,7} Nevertheless, the toxicity drawbacks it showed have forced to suspend it from use.⁸ On the other hand, the steroidal CYP17 inhibitor abiraterone (Fig. 1) passed phase II clinical trials showing high activity in post-docetaxel castration refractory PC patients and seems to have no dose-limiting toxicity.⁹ All this makes CYP17 an interesting target, since it catalyses both the 17 α -hydroxylation of pregnenolone and progesterone and the subsequent 17,20-lyase reaction cleaving the C17-C20 bond to yield the 17-keto androgens androstendione and dehydroandrostendione, the precursors of testosterone (Fig. 2).¹⁰ We also developed highly active steroidal inhibitors, which showed up to 3-fold higher activities against human CYP17 than abiraterone *in vitro*.¹¹ In order to selectively inhibit CYP17 without the potential side effects of steroidal drugs¹² non-steroidal substrate mimetics have been prepared before.¹²⁻¹⁶ In this work, in order to find a new core structure, two different classes of substrate analogues were synthesised (Fig. 3) which mimic the A-, C- and D-rings (compounds 1-11), and the A-, B- and D-rings of the substrate with benzene nuclei (compounds 12-17). Different nitrogen bearing heterocycles were introduced at different positions, since the heme complexation by an aromatic nitrogen is an important prerequisite for a high binding affinity.¹⁷ From previous work,¹⁴⁻¹⁶ it was known that the introduction of a fluorine in the A-ring strongly contributed to a better inhibition of our target enzyme. Hydroxyl groups were introduced, too, in order to mimic the oxygen functionality of the steroidal substrates. In the following, the synthesis, biological activities and molecular modelling studies are presented. Besides the CYP17 activity, inhibition of other CYP enzymes was examined, that is, selectivity towards hepatic CYP enzymes and CYP11B1 was

determined, since the latter is the key enzyme in glucocorticoid biosynthesis. The most promising structure was docked into our protein model, and the key interactions with the enzyme were elucidated.

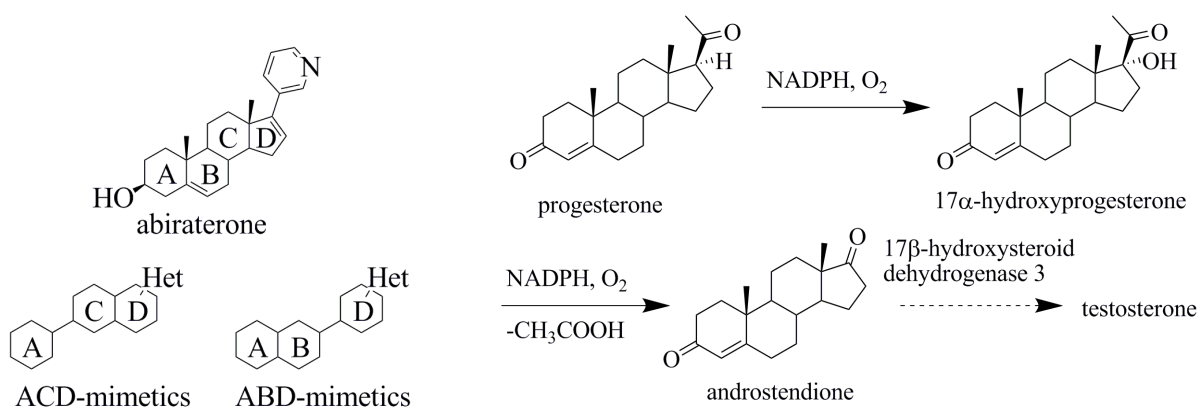


Figure 1. The steroidal CYP17 inhibitor abiraterone and ACD- and ABD-ring mimetics. Het: N-containing

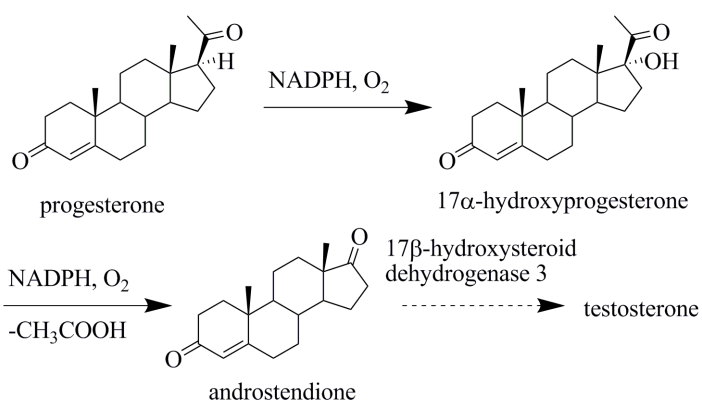
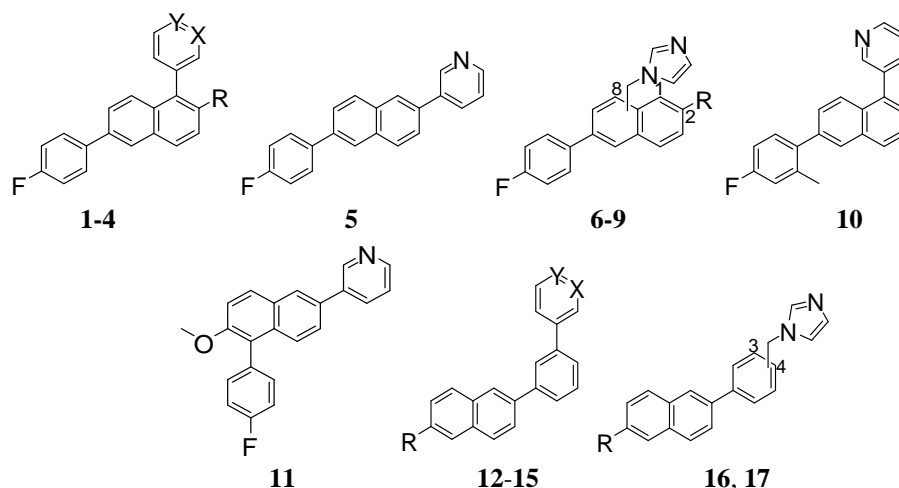


Figure 2. The role of CYP17 in androgen biosynthesis.

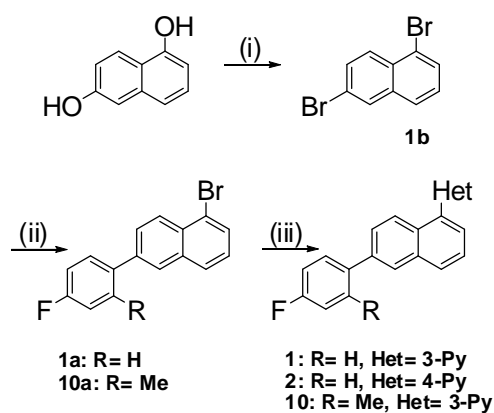


Compound	R	X	Y	subst. pos.
1	H	N	CH	
2	H	CH	N	
3	OMe	N	CH	
4	OH	N	CH	
6	H			1
7	OMe			1
8				2
9	H			8
12	OMe	N	CH	
13	OMe	CH	N	
14	OH	N	CH	
15	OH	CH	N	
16	OMe			3
17	OH			4

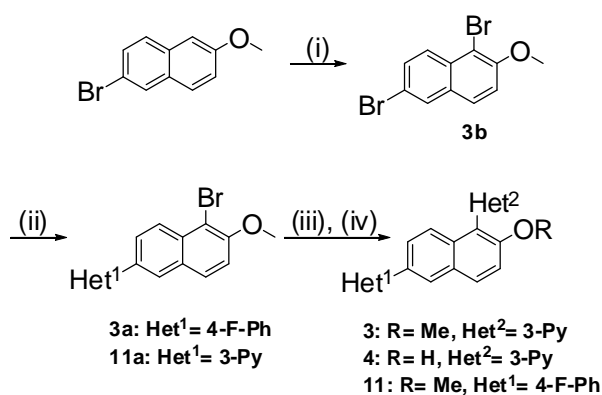
Figure 3. List of synthesised compounds 1-17.

Chemistry

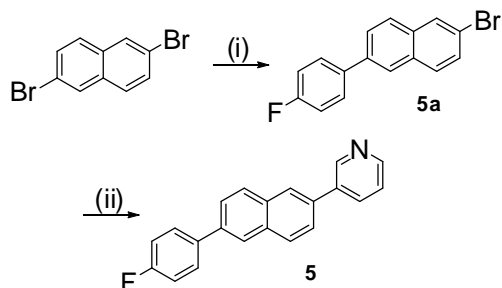
The syntheses of compounds **1-17** are shown in Schemes 1-9. In our aim to find the correct pattern for progesterone mimetics, different core structure alignments were synthesised, hence the diverse synthetic pathways. The substances can be divided in pyridyl (Schemes 1, 2, 3, 7) and imidazolyl (Schemes 4, 5, 6, 8, 9) compounds. The introduction of the pyridine moiety was achieved by means of Suzuki coupling¹⁸ (Method A), as well as the coupling of the naphthalenes and the phenyl rings. When the necessary bromides for the couplings were not commercially available, they were prepared either by bromination using NBS (Scheme 2) or with triphenylphosphine dibromide (Scheme 1). The imidazoles were introduced by performing a $S_{\text{N}}\text{T}$ reaction with 1,1-carbonyl diimidazole (CDI) and the corresponding alcohol¹⁹ (Method D) in the last step. The alcohols were obtained from either the carboxylic acids (Method C) or from the aldehydes (Method E). In some cases the carbonyl group had first to be introduced (Scheme 5) or modified (Scheme 4) before reducing it to the corresponding alcohol. In some cases the methoxy-substituted compounds were submitted to an ether cleavage (Method B). For the preparation of compound **17**, the hydroxyl group on the naphthalene had to be protected before the Suzuki coupling due to otherwise very low yields.¹⁸



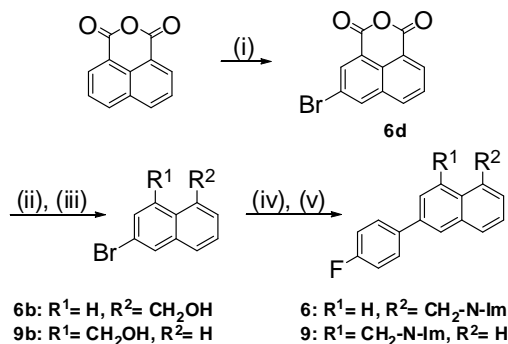
Scheme 1. Reagents and conditions: (i) Br_2 , PPh_3 , acetonitrile, μw , 240°C , 10 min; (ii) **Method A:** **1a:** 4-fluorophenylboronic acid (**5a:** 2-methyl-4-fluorophenylboronic acid), Na_2CO_3 , $\text{Pd}(\text{PPh}_3)_4$, toluene, 110°C , 16 h; (iii) **Method A:** **1, 5:** 3-pyridineboronic acid, Na_2CO_3 , $\text{Pd}(\text{PPh}_3)_4$, toluene, 110°C , 16 h, **for 2:** 4-pyridineboronic acid, NaHCO_3 , $\text{Pd}(\text{PPh}_3)_4$, DMF, H_2O , μW , 150°C , 15 min.



Scheme 2. Reagents and conditions: (i) NBS, THF, 75°C , 2 h; (ii) **Method A:** **4a:** 4-fluorophenylboronic acid (**11a:** 3-pyridineboronic acid), Na_2CO_3 , $\text{Pd}(\text{PPh}_3)_4$, toluene, 110°C , 16 h; (iii) **Method A:** **4:** 3-pyridineboronic acid (**11:** 4-fluorophenylboronic acid), Na_2CO_3 , $\text{Pd}(\text{PPh}_3)_4$, PhMe, 110°C , 16 h; (iv) **Method B:** BBr_3 , DCM, -78°C to 0°C , 16 h.

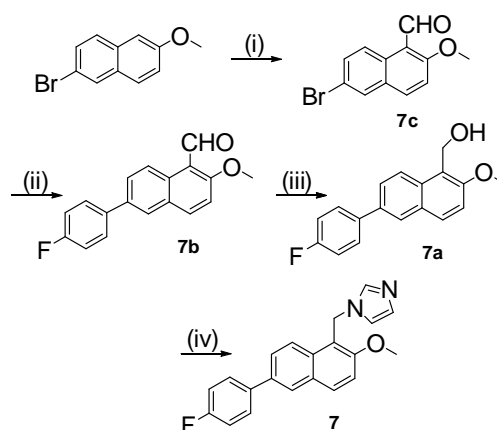


Scheme 3. Reagents and conditions: (i) **Method A:** 4-fluorophenylboronic acid, Na_2CO_3 , $\text{Pd}(\text{PPh}_3)_4$, toluene, 110°C , 16 h; (ii) **Method A:** 3-pyridineboronic acid, Na_2CO_3 , $\text{Pd}(\text{PPh}_3)_4$, toluene, 110°C , 16 h.



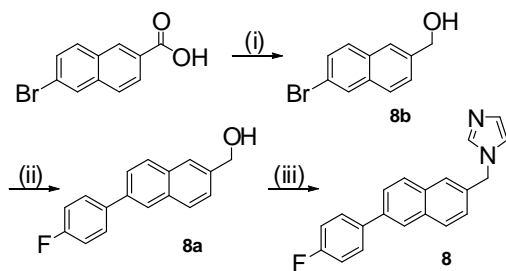
Scheme 4.

Reagents and conditions: (i) Br₂, Ag₂SO₄, H₂SO₄, 65°C, 6 h; (ii) NaOH, HgO, acetic acid, H₂O, 100°C, 4 d; (iii) **Method C:** LiAlH₄, THF, 75°C, 2 h; (iv) **Method A:** 4-fluorophenylboronic acid, Na₂CO₃, Pd(PPh₃)₄, toluene, 110°C, 16 h; (v) **Method D:** CDI, imidazole, NMP, 170°C, 3 h.



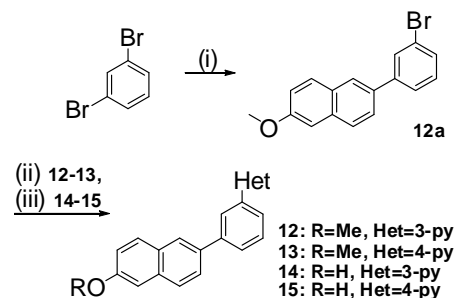
Scheme 5.

Reagents and conditions: (i) TiCl₄, 1,1-dichloromethylmethylether, DCM, 70°C, 2 h; (ii) **Method A:** 4-fluorophenylboronic acid, Na₂CO₃, Pd(PPh₃)₄, toluene, 110°C, 16 h; (iii) **Method E:** NaBH₄, MeOH, THF, rt, 1 h; (iv) **Method D:** CDI, MeCN, 85°C, 2 d.



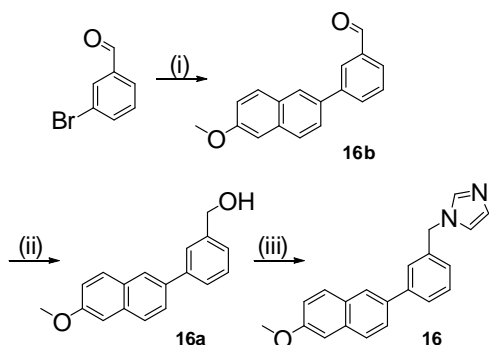
Scheme 6.

Reagents and conditions: (i) **Method C:** LiAlH₄, Et₂O, 35°C, 4 h; (ii) **Method A:** 4-fluorophenylboronic acid, Na₂CO₃, Pd(PPh₃)₄, toluene, 110°C, 16 h; (iii) **Method D:** CDI, imidazole, NMP, 180°C, 16 h.



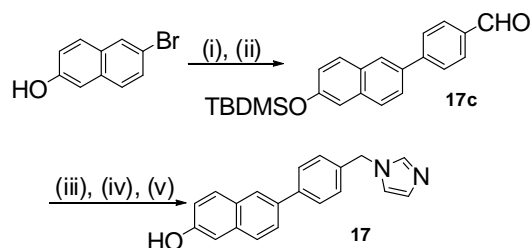
Scheme 7.

Reagents and conditions: (i) **Method A:** 6-methoxynaphthalen-2-ylboronic acid, Na₂CO₃, Pd(PPh₃)₄, toluene, 110°C, 16 h; (ii) **Method A:** 12: 3-pyridineboronic acid (13: 4-pyridineboronic acid), Na₂CO₃, Pd(PPh₃)₄, toluene, 110°C, 16 h; (iii) **Method B:** BBr₃, DCM, -78°C to 0°C, 16 h.



Scheme 8.

Reagents and conditions: (i) **Method A:** 6-methoxynaphthalen-2-ylboronic acid, Na₂CO₃, Pd(PPh₃)₄, toluene, 110°C, 16 h; (ii) **Method E:** NaBH₄, MeOH, THF, rt, 1 h; (iii) **Method D:** CDI, acetonitrile, 85°C, 16 h.



Scheme 9.

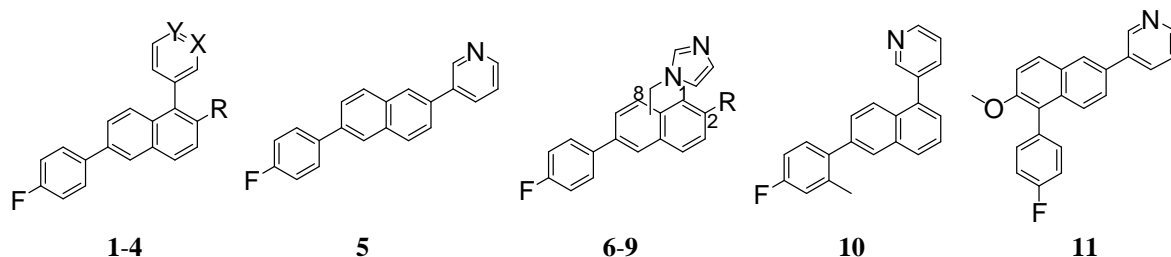
Reagents and conditions: (i) TBDMSCl, imidazole, DCM, rt, 16 h; (ii) **Method A:** Na₂CO₃, Pd(OAc)₂, TBAB, toluene, EtOH, H₂O, 110°C, 16 h; (iii) **Method E:** NaBH₄, MeOH, rt, 16 h; (iv) **Method D:** CDI, NMP, 170°C, 6 h; (v) TBAF, THF, rt, 16 h.

Results

Biological Results. Inhibition of human CYP17 was determined by performing our previously described assay²⁰ at inhibitor concentrations of 0.2 and 2 μM . As source of human CYP17, our *Escherichia coli* system²¹ (coexpressing human CYP17 and NADPH-P450 reductase) stably expressing human CYP17 was used. After homogenisation the 50,000g sediment was incubated with progesterone and NADPH as previously described.²² Separation of the product was performed by HPLC using UV-detection.

The 3- and the 4-pyridyl-substituted ACD mimetics (**1-5**) showed no or little inhibition, respectively, in contrast to the reference compounds ketoconazole and abiraterone (Table 1). Amongst our methylene-imidazolyl-substituted compounds (**6-9**), the 8-substituted one showed the best result (**9**). It can also be observed that the introduction of a 2-methoxy group in compound **6** leads to a higher activity (**7**). Neither the introduction of a methyl substituent in the A-ring of **1** (**10**), nor the switch of the position of the A-ring from 6- to 5- (**11**) resulted in an active compound.

Table 1. Inhibition of CYP17 by steroidal ACD-ring mimetics (compounds **1-11**)



Compound	R	X	Y	subst. pos.	CYP17 % Inhibition ^{a,b}	
					0.2 μM	2 μM
1	H	N	CH		2	3
2	H	CH	N		1	28
3	OMe	N	CH		6	7
4	OH	N	CH		0	0
5					0	22
6	H			1	2	19
7	OMe			1	13	45
8				2	3	14
9	H			8	9	50
10					3	3
11					0	1

^a Ketoconazole ($\text{IC}_{50} = 2780 \text{ nM}$); abiraterone ($\text{IC}_{50} = 72 \text{ nM}$).

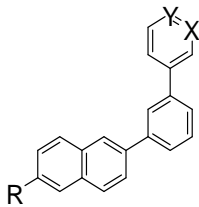
^b Data shown are the mean of at least one independent test in duplicate. Concentration of progesterone (substrate): 25 μM . The deviations were within $< \pm 5 \%$

Regarding the ABD mimetics (Table 2) it is striking that the class of the 4-pyridyl compounds (**13**, **15**) showed again activity while the 3-pyridyl compounds (**12**, **14**) were inactive. The cleavage of their methyl ether led to an enhancement of inhibition (**14**, **15**). An increase in activity for compound **13** with 23 - 66% inhibition at 2 μM (**15**) could be observed, leading to the most active compound of this study. Analogous to the work done in the ACD class, the heterocycle was replaced by a methylene-imidazole moiety, and moderate activities for compounds **16** and **17** were observed.

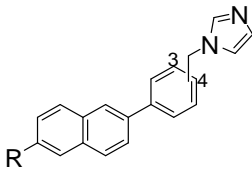
Since CYP3A4 is the hepatic enzyme responsible for the metabolism of lipophilic substances and therefore of about 50% of current prescription drugs,²³ a broader spectrum of our compounds were studied for their effects on this enzyme. Critical is the fact that this enzyme together with CYP2D6 and CYP1A2 shows pronounced genetic polymorphism.²⁴ Selected compounds (**3**, **7**, **15**, **16**) showed moderate to high activity towards the mentioned hepatic CYP enzymes (Table 3). Since compound **15** exhibited a very low activity of 19% inhibition at 10 μM towards CYP3A4²⁵ it was further tested on 2D6. At this enzyme, it showed inhibitions of 80% at 1 μM and 85% at 10 μM .

In further terms of selectivity, compound **15** was additionally tested on the steroidogenic CYP enzyme CYP11B1 which is involved in the glucocorticoid biosynthesis. For the assay,²⁶ V79MZh11B1 cells expressing human CYP11B1 were used. Compound **15** showed very low activities of 3% at 0.2 μ M and 23% at 2 μ M.

Table 2. Inhibition of CYP17 by steroidal ABD-ring mimetics (compounds **12-17**)



12-15



16, 17

Compound	R	X	Y	subst. pos.	CYP17 % Inhibition ^{a,b}	
					0.2 μ M	2.0 μ M
12	OMe	N	CH		3	4
13	OMe	CH	N		4	23
14	OH	N	CH		0	8
15	OH	CH	N		31	66
16	OMe			3	0	28
17	OH			4	24	61

^a Ketoconazole (IC₅₀ = 2780 nM); abiraterone (IC₅₀ = 72 nM).

^b Data shown are the mean of at least one independent test in duplicate. Concentration of progesterone (substrate): 25 μ M. The deviations were within $\pm 5\%$

Table 3. Inhibition of hepatic CYP enzymes (1A2, 2C9, 2C19, 3A4) by compounds **3, 7, 15, 16**

Compound	CYP1A2 % Inhibition ^a		CYP2C9 % Inhibition ^a		CYP2C19 % Inhibition ^a		CYP3A4 % Inhibition ^a	
	1.0 μ M	10.0 μ M	1.0 μ M	10.0 μ M	1.0 μ M	10.0 μ M	1.0 μ M	10.0 μ M
	3	40	87	66	54	68	28	64
7	80	85	100	100	93	96	93	95
15	98	98	94	97	86	89	6	19
16	96	97	97	100	95	97	91	96
KTZ ^b	8	38	21	75	24	1	1	4
ABT ^b	36	53	17	51	3	7	7	7

^a Data shown are the mean of three independent tests.

^b KTZ: ketoconazole; ABT: abiraterone. The deviations were within $\pm 5\%$

Molecular Modelling. Since there is no crystal structure of CYP17 available we built a homology model of CYP17 using the X-ray structure of human CYP2C9 (PDB code 1r9o) as template, as described before by us.²⁸ Docking simulations were carried out by means of the GOLD v3.0.1 software. For the docking studies, our homology model was used running Linux Suse 10.1 on Intel® P4 CPU 3.00 GHz, and the energy minimisation was also performed as previously described.²⁸ Compound **15** and the steroidal inhibitor abiraterone were docked as shown in Figure 4.

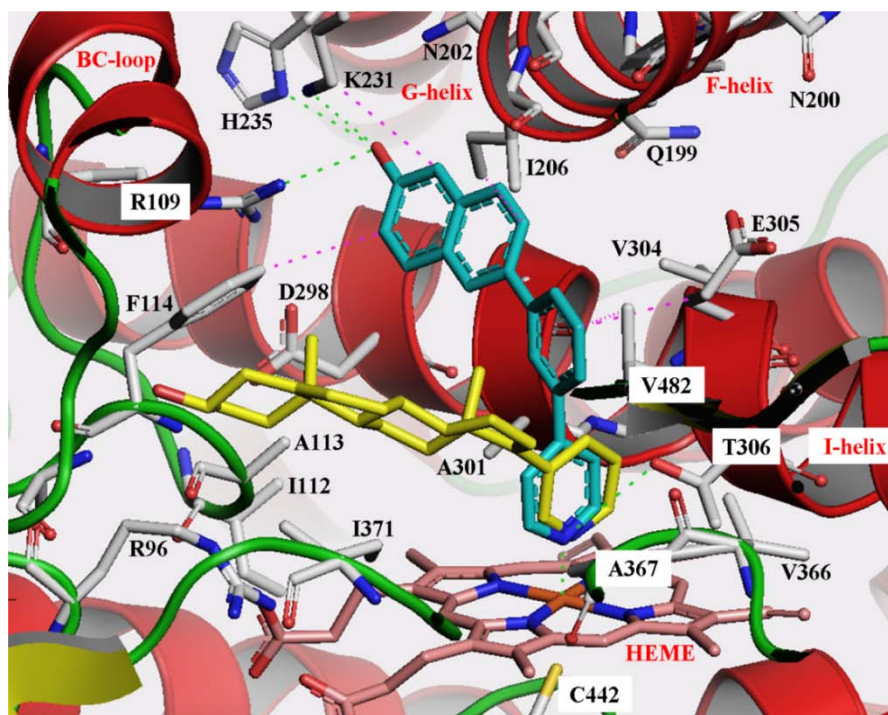


Figure 4. Docking complex between CYP17 and compounds **15** (cyan) and abiraterone (yellow). Heme, interacting residues and ribbon rendered tertiary structure of the active site are shown. Figure was generated with Pymol (<http://www.pymol.org>).

Besides the already described interaction between the sp^2 hybridised nitrogen and the heme iron, the key interaction for compound **15** seems to be the H-bond net of the hydroxyl group on the naphthalene with the amino acids Arg109, His235, Lys231 and Asn202 in the active site of our target enzyme. Further, hydrophobic interactions between the aromatic core and Ile206, Gly301, Ala302, Glu305, Val366 and Val482 were observed.

For abiraterone, the same binding mode as described for the substrates was found.^{29,30} The lone pair of the sp^2 hybridised nitrogen pointed perpendicular towards the heme iron. The steroidal scaffold was oriented almost parallel to the heme plane in the direction of the BC-loop. This pose was stabilised by hydrophobic interactions with Ile371, Ile112, Ala113 and Phe114.^{29,30} Additionally, the highly conserved Arg96 which is important for substrate binding and recognition, as shown by sitedirected mutagenesis,³¹ presented interactions of the same kind with the steroidal A-ring. Another important interaction was the H-bond between the hydroxyl group in C3 position and the backbone carbonyl group of Gln98.

Discussion and Conclusion

Relying on our molecular modelling studies, the inhibitory activity of compound **15** is supposed to be increased by introducing other polar groups like an H-bond donor in 7 position of the naphthalene, which could interact with Asp298. Other possible substitutions to increase activity and perhaps also selectivity towards hepatic CYP enzymes are chlorine or fluorine at the 1 position of the naphthalene, which should improve the hydrophobic interactions with the I-helix. Also a substituent at 3 position capable of undergoing H-bonds could interact with Glu204.

The selectivity against CYP1A2 and CYP2D6 could also be enhanced through different medicinal chemistry strategies. It is described that planar, lipophilic structures³² like compound **15** have a great affinity towards CYP1A2. This planarity could be abolished by either dearomatizing one of the benzene rings, or by specific ortho-substitutions. Regarding CYP2D6, its high inhibition is not surprising, since compound **15** bears three important pharmacophores responsible for its inhibition: the aromatic nitrogen, the H-bond donor and the lipophilic core structure.³³ Since CYP2D6 has a relatively small binding site, most of the changes or substitutions made on compound **15** might increase its selectivity against this enzyme.

Summarising, we have discovered compound **15** which shows good inhibition values, a good selectivity towards the steroidogenic CYP11B1 and a modest selectivity against CYP3A4, the most relevant hepatic enzyme in xenobiotic metabolism. Compound **15** might therefore be a good candidate for further structure optimisation. Using our protein model, we made some suggestions of how to further increase activity and selectivity towards hepatic CYP enzymes. Molecular docking calculations were performed for compound **15**. Since the GOLD docking program allows flexible docking of the compounds, no conformational search was employed to the ligand structures. GOLD gave the best poses by a genetic algorithm (GA) search strategy, and then various molecular features were encoded as a chromosome.

Experimental Section

Chemistry. Melting points were determined on a Mettler FP1 melting point apparatus and are uncorrected. IR spectra were recorded neat on a Bruker Vector 33FT-infrared spectrometer. ¹H-NMR spectra were measured on a Bruker DRX-500 (500 MHz). Chemical shifts are given in parts per million (ppm), and TMS was used as an internal standard for spectra obtained in CDCl₃. All coupling constants (J) are given in Hz. ESI (ElectroSpray Ionisation) and APCI (Atmospheric Pressure Chemical Ionisation) mass spectra were determined on a TSQ quantum (Thermo Electron Corporation) instrument. EI (Electron Ionisation) mass spectra were determined on a Trace GC Ultra (Thermo Electron Corporation) instrument. All reactions in the microwave were performed in a closed vessel in a CEM Discovery™ instrument equipped with an IR-sensor for temperature control. Column chromatography was performed using silica-gel 60 (50-200 μm), and reaction progress was determined by TLC analysis on Alugram® SIL G/UV₂₅₄ (Macherey-Nagel). Boronic acids and bromoaryls and other compounds used as starting materials were commercially obtained (CombiBlocks, Chempur, Aldrich, Acros).

1,6-Dibromonaphthalene, 1b. To an ice-cooled solution of triphenylphosphine (16.40 g, 62.50 mmol) in acetonitrile (30 mL) was carefully dropped bromine (3.20 mL, 62.50 mmol). Then naphthalene-1,6-diol (5.00 g, 31.25 mmol) was added and the resulting mixture was heated for 2 hours at 80 °C. After that the solvent was evaporated under reduced pressure and the residue was heated in the microwave at 240 °C for 5 minutes. The crude was boiled in ethanol for 30 minutes, followed by hot and cold filtration. After evaporation under reduced pressure, the desired product was purified by chromatography on silica gel; yield: 6.35 g (71 %); white solid; *R*_f = 0.69 (hexane / EtOAc, 80:20); δ_H (CDCl₃, 500 MHz) 7.32-7.35 (m, 2H), 7.65 (dd, *J* = 1.2, 9.0 Hz, 1H), 7.70 (d, *J* = 8.2 Hz, 1H), 7.78 (d, *J* = 7.4 Hz, 1H), 7.99 (s, 1H), 8.10 (d, *J* = 9.0 Hz, 1H); MS (EI): *m/z* = 283.8, 285.8, 287.8 [*M*⁺+H].

Method A: Suzuki-Coupling. The corresponding brominated aromatic compound (1 eq) was dissolved in toluene (7 mL / mmol), a 10 % Na₂CO₃ aq solution (2 eq) and the corresponding boronic acid (1.5-2.0 eq) were added. The mixture was deoxygenated under reduced pressure and flushed with nitrogen. After repeating this cycle several times, Pd(PPh₃)₄ (5 mol%) was added and the resulting suspension was heated under reflux for 16 hours. After cooling and phase separation, the aqueous phase was extracted with ethyl acetate (3 x 25 mL). The combined organic phases were washed with brine, dried over Na₂SO₄, filtered over a short plug of celite® and evaporated under reduced pressure. The compounds were purified by flash chromatography on silica gel.

1-Bromo-6-(4-fluorophenyl)naphthalene, 1a. Synthesised according to Method A using compound **1b** (0.75 g, 2.62 mmol) and 4-fluorophenylboronic acid (0.45 g, 3.22 mmol); yield: 0.33 g (42 %); white solid; *R*_f = 0.78 (hexane / EtOAc, 80:20); MS (EI): *m/z* = 312.9, 316.0 [*M*⁺+H].

3-(6-(4-Fluorophenyl)naphthalen-1-yl)pyridine, 1. Synthesised according to Method A using compound **1a** (0.18 g, 0.58 mmol) and 3-pyridineboronic acid (0.15 g, 1.16 mmol); yield: 0.05 g (31 %); light-yellow oil; *R*_f = 0.57 (DCM / MeOH, 98:2); IR (ATR) ν (cm⁻¹) 3038 (w), 1602 (w), 1517 (m), 1501 (s), 1407 (w), 1229 (s), 1159 (m), 1100 (w), 1026 (w), 965 (w), 888 (w), 844 (m), 823 (s), 792 (s), 759 (m), 715 (s), 659 (m), 539 (m); δ_H (CDCl₃, 500 MHz) 7.16-7.20 (m, 2H), 7.43 (dd, *J* = 1.1, 7.0 Hz, 1H), 7.47 (dd, *J* = 4.5, 7.7 Hz, 1H), 7.59 (dd, *J* = 7.1, 8.2 Hz, 1H), 7.66-7.69 (m, 2H), 7.84-7.88 (m, 1H), 7.88-7.89 (m, 1H), 7.96 (d, *J* = 8.3 Hz, 1H), 8.07 (d, *J* = 1.8 Hz, 1H), 8.71 (d, *J* = 3.6 Hz, 1H), 8.79 (d, *J* = 1.1 Hz, 1H); δ_C (CDCl₃, 125 MHz) 115.7, 115.9, 123.2, 125.9, 126.0, 126.1, 127.5, 128.7, 128.9, 129.0, 130.6, 134.1, 136.2, 136.3, 136.79, 136.81, 137.3, 137.8, 148.5, 148.7, 150.6, 162.7 (d, *J* = 247.0 Hz, C-F); MS (ESI): *m/z* = 299.9 [*M*⁺+H].

4-(6-(4-Fluorophenyl)naphthalen-1-yl)pyridine, 2. Synthesised according to Method A using compound **1a** (0.10 g, 0.33 mmol) and 4-pyridineboronic acid (0.06 g, 0.43 mmol); yield: 0.09 g (94 %); light-yellow oil; *R*_f =

0.69 (DCM / MeOH, 95:5); IR (ATR) ν (cm⁻¹) 3054 (w), 1732 (w), 1601 (m), 1504 (s), 1432 (w), 1409 (w), 1264 (w), 1231 (s), 1159 (m), 879 (w), 823 (s), 794 (s), 760 (s), 654 (m), 605 (w), 518 (w); δ_{H} (CDCl₃, 500 MHz) 7.16-7.20 (m, 2H), 7.43 (dd, $J = 1.0, 7.1$ Hz, 1H), 7.56-7.60 (m, 3H), 7.66-7.70 (m, 3H), 7.89 (d, $J = 8.8$ Hz, 1H), 7.98 (d, $J = 8.3$ Hz, 1H), 8.08 (d, $J = 1.8$ Hz, 1H), 8.84 (d, $J = 3.3$ Hz, 2H); δ_{C} (CDCl₃, 125 MHz) 115.8, 115.9, 125.5, 125.6, 125.9, 126.2, 126.3, 127.0, 128.9, 129.0, 129.4, 129.6, 134.0, 136.5, 136.6, 138.0, 149.5, 150.0, 162.7 (d, $J = 247.1$ Hz, C-F); MS (ESI): $m/z = 300.0$ [M⁺+H].

1-Bromo-6-(4-fluorophenyl)-2-methoxynaphthalene, 3a. Synthesised according to Method A using compound **3b** (1.00 g, 3.17 mmol) and 4-fluorophenylboronic acid (0.45 g, 3.17 mmol); yield: 0.84 g (84 %); white solid; $R_{\text{f}} = 0.57$ (hexane / EtOAc, 80:20); δ_{H} (CDCl₃, 500 MHz) 4.05 (s, 3H), 7.15-7.19 (m, 2H), 7.31 (d, $J = 9.0$ Hz, 1H), 7.66 (dd, $J = 5.3, 8.8$ Hz, 2H), 7.77 (dd, $J = 1.9, 8.9$ Hz, 1H), 7.86 (d, $J = 9.0$ Hz, 1H), 7.93 (d, $J = 1.7$ Hz, 1H), 8.28 (d, $J = 8.9$ Hz, 1H); δ_{C} (CDCl₃, 125 MHz) 57.1 (CH₃), 108.6, 114.1, 115.7, 115.9, 125.6, 126.9, 127.2, 128.76, 128.83, 129.1, 130.0, 132.3, 136.1, 136.6, 136.7, 152.9, 162.6 (d, $J = 246.7$ Hz, C-F); MS (EI): $m/z = 329.9, 332.9$ [M⁺+H].

3-(6-(4-Fluorophenyl)-2-methoxynaphthalen-1-yl)pyridine, 3. Synthesised according to Method A using compound **3a** (0.30 g, 0.91 mmol) and 3-pyridineboronic acid (0.14 g, 1.09 mmol); yield: 0.20 g (66 %); white solid; mp 147 °C; $R_{\text{f}} = 0.57$ (DCM / MeOH, 95:5); IR (ATR) ν (cm⁻¹) 2926 (m), 1599 (m), 1516 (m), 1496 (m), 1460 (w), 1344 (w), 1257 (s), 1164 (w), 1134 (w), 1067 (s), 1025 (w), 823 (s), 804 (s), 750 (w), 717 (m), 626 (w), 522 (w); δ_{H} (CDCl₃, 500 MHz) 3.87 (s, 3H), 7.14-7.17 (m, 2H), 7.41 (d, $J = 9.1$ Hz, 1H), 7.47 (dd, $J = 4.9, 7.7$ Hz, 1H), 7.53 (d, $J = 8.9$ Hz, 1H), 7.59 (dd, $J = 1.9, 8.9$ Hz, 1H), 7.65 (dd, $J = 5.3, 8.8$ Hz, 2H), 7.76 (td, $J = 1.9, 7.8$ Hz, 1H), 7.97-7.99 (m, 2H), 8.66 (d, $J = 1.5$ Hz, 1H), 8.68 (dd, $J = 1.5, 4.9$ Hz, 1H); MS (APCI): $m/z = 320.3$ [M⁺+H].

2-Bromo-6-(4-fluorophenyl)naphthalene, 5a. Synthesised according to Method A using 2,6-dibromonaphthalene (0.70 g, 2.47 mmol) and 4-fluorophenylboronic acid (0.35 g, 2.47 mmol); yield: 0.23 g (37 %); white solid; $R_{\text{f}} = 0.80$ (hexane / EtOAc, 80:20); δ_{H} (CDCl₃, 500 MHz) 7.16-7.19 (m, 2H), 7.58 (dd, $J = 2.0, 8.7$ Hz, 1H), 7.66 (dd, $J = 5.3, 8.8$ Hz, 2H), 7.71 (dd, $J = 1.8, 8.6$ Hz, 1H), 7.75 (d, $J = 8.7$ Hz, 1H), 7.82 (d, $J = 8.6$ Hz, 1H), 7.95 (d, $J = 1.0$ Hz, 1H), 8.03 (d, $J = 1.7$ Hz, 1H); δ_{C} (CDCl₃, 125 MHz) 115.7, 115.9, 119.9, 125.5, 126.5, 127.6, 128.88, 128.94, 129.70, 129.74, 129.8, 132.1, 133.6, 136.78, 136.80, 138.1, 162.7 (d, $J = 247.0$ Hz, C-F); MS (EI): $m/z = 299.8, 302.9$ [M⁺+H].

3-(6-(4-Fluorophenyl)naphthalen-2-yl)pyridine, 5. Synthesised according to Method A using compound **5a** (0.15 g, 0.50 mmol) and 3-pyridineboronic acid (0.08 g, 0.65 mmol); yield: 0.07 g (47 %); light-yellow solid; mp 126 °C; $R_{\text{f}} = 0.72$ (DCM / MeOH, 95:5); IR (ATR) ν (cm⁻¹) 2961 (m), 1728 (s), 1605 (m), 1516 (m), 1487 (m), 1377 (w), 1286 (s), 1240 (s), 1122 (s), 1072 (s), 981 (w), 896 (m), 812 (s), 744 (m), 706 (m), 666 (m), 544 (w), 527 (m); δ_{H} (CDCl₃, 500 MHz) 7.17-7.21 (m, 2H), 7.46 (dd, $J = 4.9, 7.7$ Hz, 1H), 7.53 (dd, $J = 3.3, 5.7$ Hz, 1H), 7.69 (dd, $J = 5.3, 8.8$ Hz, 2H), 7.73 (dd, $J = 3.3, 5.7$ Hz, 1H), 7.75 (dd, $J = 1.9, 4.7$ Hz, 1H), 7.77 (dd, $J = 1.9, 4.7$ Hz, 1H), 7.98-8.02 (m, 2H), 8.03 (d, $J = 1.2$ Hz, 1H), 8.05-8.08 (m, 2H), 8.65 (d, $J = 3.7$ Hz, 1H), 9.01 (s, 1H); δ_{C} (CDCl₃, 125 MHz) 115.7, 115.9, 123.8, 125.4, 125.5, 126.0, 126.2, 128.84, 128.89, 128.92, 128.99, 132.7, 133.2, 134.97, 135.02, 136.94, 136.97, 138.3, 147.92, 147.94, 162.7 (d, $J = 247.2$ Hz, C-F); MS (ESI): $m/z = 300.2$ [M⁺+H].

6-(4-Fluorophenyl)-1-naphthoic acid, 6a. Synthesised according to Method A using compound **6b** (0.50 g, 2.11 mmol) and 4-fluorophenylboronic acid (0.39 g, 2.74 mmol); yield: 0.45 g (85 %); white solid; $R_{\text{f}} = 0.44$ (DCM / MeOH, 98:2); δ_{H} (CDCl₃, 500 MHz) 5.16 (s, 2H), 7.16-7.20 (m, 2H), 7.46-7.53 (m, 2H), 7.68 (dd, $J = 5.3, 8.7$ Hz, 2H), 7.75 (dd, $J = 1.9, 8.7$ Hz, 1H), 7.86 (d, $J = 8.0$ Hz, 1H), 8.02 (d, $J = 1.7$ Hz, 1H), 8.19 (d, $J = 8.8$ Hz, 1H); δ_{C} (CDCl₃, 125 MHz) 63.7 (CH₂), 115.7, 115.8, 124.4, 125.4, 125.8, 126.0, 126.3, 128.8, 128.9, 130.3, 134.0, 136.2, 136.91, 136.93, 137.5, 162.6 (d, $J = 246.8$ Hz, C-F); MS (EI): $m/z = 252.0$ [M⁺+H].

6-(4-Fluorophenyl)-2-methoxy-1-naphthaldehyde, 7b. Synthesised according to Method A using compound **7c** (1.00 g, 3.77 mmol) and 4-fluorophenylboronic acid (0.54 g, 3.77 mmol); yield: 0.63 g (60 %); white solid; $R_{\text{f}} = 0.32$ (hexane / EtOAc, 80:20); δ_{H} (CDCl₃, 500 MHz) 4.08 (s, 3H), 7.15-7.19 (m, 2H), 7.34 (d, $J = 9.2$ Hz, 1H), 7.66 (dd, $J = 5.3, 8.8$ Hz, 2H), 7.84 (dd, $J = 2.1, 9.0$ Hz, 1H), 7.92 (d, $J = 2.0$ Hz, 1H), 8.11 (d, $J = 9.1$ Hz, 1H), 9.34 (d, $J = 9.0$ Hz, 1H); MS (APCI): $m/z = 322.2$ [M⁺+H].

(6-(4-Fluorophenyl)naphthalen-2-yl)methanol, 8a. Synthesised according to Method A using compound **8b** (0.40 g, 1.69 mmol) and 4-fluorophenylboronic acid (0.29 g, 2.03 mmol); yield: 0.36 g (84 %); white solid; $R_{\text{f}} = 0.52$ (DCM / MeOH, 98:2); δ_{H} (CDCl₃, 500 MHz) 4.88 (s, 2H), 7.16-7.19 (m, 2H), 7.51 (dd, $J = 1.4, 8.4$ Hz, 1H), 7.68 (dd, $J = 5.3, 8.7$ Hz, 2H), 7.70 (dd, $J = 1.8, 8.5$ Hz, 1H), 7.83 (s, 1H), 7.89 (dd, $J = 5.2, 8.4$ Hz, 2H), 7.98 (s, 1H); δ_{C} (CDCl₃, 125 MHz) 65.4 (CH₂), 115.6, 115.8, 125.2, 125.4, 125.7, 128.5, 128.6, 128.86, 128.93, 132.4, 133.1, 137.10, 137.12, 137.6, 138.5, 162.5 (d, $J = 246.6$ Hz, C-F); MS (APCI): $m/z = 235.1, 236.0, 237.0$ [M⁺+H].

3-(4-Fluorophenyl)-1-naphthoic acid, 9a. Synthesised according to Method A using compound **9b** (0.50 g, 2.11 mmol) and 4-fluorophenylboronic acid (0.39 g, 2.74 mmol); yield: 0.42 g (78 %); white solid; $R_{\text{f}} = 0.50$ (DCM

/ MeOH, 98:2); δ_{H} (CDCl₃, 500 MHz) 5.22 (s, 2H), 7.16-7.19 (m, 2H), 7.52-7.58 (m, 2H), 7.69 (dd, $J = 5.3, 8.8$ Hz, 2H), 7.76-7.77 (m, 1H), 7.92-7.94 (m, 1H), 7.96 (s, 1H), 8.11-8.13 (m, 1H); δ_{C} (CDCl₃, 125 MHz) 63.7 (CH₂), 103.2, 115.7, 115.8, 123.5, 126.0, 126.42, 126.44, 128.86, 128.92, 130.3, 134.1, 137.0, 162.6 (d, $J = 246.9$ Hz, C-F); MS (EI): $m/z = 252.0$ [M⁺+H].

1-Bromo-6-(4-fluoro-2-methylphenyl)naphthalene, 10a. Synthesised according to Method A using compound **1b** (0.75 g, 2.62 mmol) and 2-methyl-4-fluorophenylboronic acid (0.50 g, 3.28 mmol); yield: 0.26 g (31 %); white solid; $R_{\text{f}} = 0.85$ (hexane / EtOAc, 80:20); δ_{H} (CDCl₃, 500 MHz) 2.29 (s, 3H), 6.98 (dt, $J = 2.3, 8.4$ Hz, 1H), 7.03 (dd, $J = 2.5, 9.7$ Hz, 1H), 7.27 (dd, $J = 5.9, 8.6$ Hz, 1H), 7.34-7.37 (m, 1H), 7.54 (dd, $J = 1.7, 8.7$ Hz, 1H), 7.74 (d, $J = 1.5$ Hz, 1H), 7.80 (dd, $J = 1.0, 7.6$ Hz, 1H), 7.82 (d, $J = 8.3$ Hz, 1H), 8.28 (d, $J = 8.7$ Hz, 1H); δ_{C} (CDCl₃, 125 MHz) 20.6 (CH₃), 112.6, 112.8, 116.8, 116.9, 117.0, 122.7, 126.5, 126.6, 126.8, 127.0, 127.3, 127.7, 127.9, 128.19, 128.23, 128.7, 129.1, 129.4, 129.9, 130.1, 130.2, 130.6, 130.9, 131.3, 131.4, 131.6, 134.5, 137.09, 137.12, 137.9, 138.0, 139.5, 162.2 (d, $J = 246.0$ Hz, C-F); MS (ESI): $m/z = \text{not ionisable}$ [M⁺+H].

3-(6-(4-Fluoro-2-methylphenyl)naphthalen-1-yl)pyridine, 10. Synthesised according to Method A using compound **10a** (0.15 g, 0.48 mmol) and 3-pyridineboronic acid (0.09 g, 0.71 mmol); yield: 0.05 g (31 %); colourless oil; $R_{\text{f}} = 0.51$ (DCM / MeOH, 98:2); IR (ATR) ν (cm⁻¹) 3049 (w), 1585 (w), 1493 (s), 1408 (w), 1270 (m), 1222 (s), 1186 (w), 1152 (m), 1025 (w), 965 (m), 866 (m), 836 (w), 810 (s), 794 (s), 761 (s), 717 (s), 657 (m), 583 (m); δ_{H} (CDCl₃, 500 MHz) 2.30 (s, 3H), 6.98 (dt, $J = 2.7, 8.4$ Hz, 1H), 7.02 (dd, $J = 2.6, 9.8$ Hz, 1H), 7.28 (dd, $J = 6.0, 8.4$ Hz, 1H), 7.42 (dd, $J = 1.8, 8.7$ Hz, 1H), 7.45 (dd, $J = 0.9, 7.1$ Hz, 1H), 7.46 (dd, $J = 4.9, 7.8$ Hz, 1H), 7.60 (dd, $J = 7.1, 8.2$ Hz, 1H), 7.83 (d, $J = 1.6$ Hz, 1H), 7.85 (d, $J = 8.8$ Hz, 1H), 7.87 (td, $J = 1.8, 7.8$ Hz, 1H), 7.93 (d, $J = 8.3$ Hz, 1H), 8.71 (dd, $J = 1.6, 4.9$ Hz, 1H), 8.80 (d, $J = 2.1$ Hz, 1H); δ_{C} (CDCl₃, 125 MHz) 20.6, 20.7, 112.0, 112.6, 112.7, 116.8, 117.0, 123.2, 125.1, 125.9, 127.4, 128.4, 128.5, 128.6, 130.4, 130.8, 131.3, 131.4, 133.7, 136.3, 137.3, 137.4, 138.0, 138.9, 148.6, 150.6, 162.2 (d, $J = 245.9$ Hz, C-F); MS (ESI): $m/z = 313.9$ [M⁺+H].

3-(5-Bromo-6-methoxynaphthalen-2-yl)pyridine, 11a. Synthesised according to Method A using compound **3b** (0.75 g, 2.41 mmol) and 3-pyridineboronic acid (0.36 g, 2.89 mmol); yield: 0.19 g (25 %); white solid; $R_{\text{f}} = 0.22$ (DCM / MeOH, 98:2); δ_{H} (CDCl₃, 500 MHz) 3.98 (s, 3H), 7.26 (d, $J = 9.0$ Hz, 1H), 7.34 (ddd, $J = 0.7, 4.8, 7.9$ Hz, 1H), 7.72 (dd, $J = 1.9, 8.8$ Hz, 1H), 7.82 (d, $J = 9.0$ Hz, 1H), 7.90-7.92 (m, 2H), 8.25 (d, $J = 8.8$ Hz, 1H), 8.56 (dd, $J = 1.5, 4.8$ Hz, 1H), 8.90 (d, $J = 1.9$ Hz, 1H); δ_{C} (CDCl₃, 125 MHz) 57.1, 108.5, 114.2, 123.6, 126.1, 126.8, 127.2, 129.3, 129.9, 132.7, 133.6, 134.4, 136.0, 148.4, 148.6, 154.2, 190.7; MS (EI): $m/z = 314.9, 316.0$ [M⁺+H].

3-(5-(4-Fluorophenyl)-6-methoxynaphthalen-2-yl)pyridine, 11. Synthesised according to Method A using compound **11a** (0.10 g, 0.32 mmol) and 4-fluorophenylboronic acid (0.07 g, 0.48 mmol); yield: 0.08 g (77 %); white solid; $R_{\text{f}} = 0.23$ (DCM / MeOH, 98:2); IR (ATR) ν (cm⁻¹) 2840 (w), 1735 (w), 1599 (w), 1512 (m), 1488 (m), 1463 (w), 1281 (w), 1256 (s), 1214 (m), 1159 (w), 1132 (w), 1068 (s), 1018 (w), 914 (w), 900 (w), 833 (m), 808 (s), 758 (w), 715 (s), 689 (w), 625 (w), 556 (m), 535 (m); δ_{H} (CDCl₃, 500 MHz) 3.87 (s, 3H), 7.19-7.23 (m, 2H), 7.36 (dd, $J = 5.5, 8.7$ Hz, 2H), 7.42 (dd, $J = 4.9, 7.8$ Hz, 1H), 7.43 (d, $J = 9.1$ Hz, 1H), 7.56-7.60 (m, 2H), 7.96-8.00 (m, 2H), 8.04 (s, 1H), 8.63 (dd, $J = 1.3, 4.8$ Hz, 1H), 8.96 (d, $J = 1.8$ Hz, 1H); δ_{C} (CDCl₃, 125 MHz) 56.6, 114.3, 115.2, 115.3, 123.7, 124.1, 125.5, 126.1, 126.2, 129.1, 129.7, 131.79, 131.81, 132.48, 132.54, 132.6, 133.2, 134.6, 136.6, 148.2, 148.3, 154.3, 162.1 (d, $J = 245.9$ Hz, C-F); MS (ESI): $m/z = 329.9$ [M⁺+H].

2-(3-Bromophenyl)-6-methoxynaphthalene, 12a. Synthesised according to Method A using 1,3-dibromobenzene (0.93 mL, 7.43 mmol) and 3-methoxyphenylboronic acid (1.50 g, 7.43 mmol); yield: 1.82 g (78 %); white solid; $R_{\text{f}} = 0.68$ (DCM / MeOH, 98:2); δ_{H} (CDCl₃, 500 MHz) 4.88 (s, 2H), 7.17 (d, $J = 2.5$ Hz, 1H), 7.19 (dd, $J = 2.6, 8.9$ Hz, 1H), 7.32-7.35 (m, 2H), 7.47-7.49 (m, 1H), 7.61-7.63 (m, 1H), 7.66 (dd, $J = 1.8, 8.4$ Hz, 1H), 7.79-7.82 (m, 2H), 7.84-7.85 (m, 1H), 7.95 (d, $J = 1.7, 1\text{H}$); δ_{C} (CDCl₃, 125 MHz) 55.4 (CH₃), 105.6, 119.4, 123.0, 125.7, 125.78, 125.82, 127.4, 128.5, 129.1, 129.8, 129.9, 130.2, 130.3, 131.1, 134.1, 134.8, 143.4, 158.0; MS (EI): $m/z = 312.9, 316.0$ [M⁺+H].

3-(3-(6-Methoxynaphthalen-2-yl)phenyl)pyridine, 12. Synthesised according to Method A using compound **12a** (0.30 g, 0.96 mmol) and 3-pyridineboronic acid (0.15 g, 1.15 mmol); yield: 0.22 g (74 %); light-yellow solid; mp 157 °C; $R_{\text{f}} = 0.71$ (DCM / MeOH, 95:5); IR (ATR) ν (cm⁻¹) 2925 (w), 1605 (w), 1483 (w), 1385 (w), 1268 (w), 1244 (m), 1205 (s), 1165 (m), 1026 (m), 858 (s), 819 (s), 792 (s), 714 (s); δ_{H} (CDCl₃, 500 MHz) 3.95 (s, 3H), 7.19-7.21 (m, 2H), 7.42 (dd, $J = 4.9, 7.7$ Hz, 1H), 7.59 (m, 2H), 7.73-7.77 (m, 2H), 7.82 (d, $J = 8.7$ Hz, 1H), 7.85 (d, $J = 8.5$ Hz, 1H), 7.90 (s, 1H), 7.99 (td, $J = 1.6, 7.9$ Hz, 1H), 8.03 (s, 1H), 8.63 (d, $J = 4.1$ Hz, 1H), 8.95 (d, $J = 1.3$ Hz, 1H); δ_{C} (CDCl₃, 125 MHz) 55.4, 105.6, 119.3, 123.7, 125.80, 125.84, 125.9, 126.1, 127.1, 127.4, 129.1, 129.6, 129.7, 134.0, 134.7, 135.8, 142.2, 148.2, 148.3, 157.9; MS (ESI): $m/z = 312.2$ [M⁺+H].

4-(3-(6-Methoxynaphthalen-2-yl)phenyl)pyridine, 13. Synthesised according to Method A using compound **12a** (0.40 g, 1.28 mmol) and 4-fluorophenylboronic acid (0.19 g, 1.53 mmol); yield: 0.26 g (67 %); white solid; $R_{\text{f}} =$

0.54 (DCM / MeOH, 95:5); IR (ATR) ν (cm⁻¹) 3058 (w), 1593 (s), 1546 (w), 1489 (m), 1386 (w), 1268 (w), 1244 (m), 1205 (s), 1164 (w), 1025 (m), 895 (w), 857 (s), 828 (w), 816 (s), 795 (s), 707 (w), 616 (m), 573 (w), 537 (w), 510 (w); δ_{H} (CDCl₃, 500 MHz) 3.95 (s, 3H), 7.18 (d, $J = 2.5$ Hz, 1H), 7.20 (dd, $J = 2.5, 8.9$ Hz, 1H), 7.58-7.63 (m, 4H), 7.76 (dd, $J = 1.8, 8.5$ Hz, 1H), 7.77 (td, $J = 1.5, 7.4$ Hz, 1H), 7.81 (d, $J = 8.9$ Hz, 1H), 7.84 (d, $J = 8.5$ Hz, 1H), 7.93-7.94 (m, 1H), 8.02 (d, $J = 1.5$ Hz, 1H), 8.69-8.70 (m, 2H); δ_{C} (CDCl₃, 125 MHz) 55.3, 105.5, 119.3, 121.6, 121.7, 125.6, 125.7, 125.8, 125.9, 126.9, 127.4, 127.8, 129.05, 129.07, 129.1, 129.5, 129.7, 133.9, 135.7, 138.7, 142.1, 148.3, 150.18, 150.24, 157.9; MS (ESI): $m/z = 312.1$ [M⁺+H].

3-(6-Methoxynaphthalen-2-yl)benzaldehyde, 16b. Synthesised according to Method A using 3-bromobenzaldehyde (1.50 g, 7.58 mmol) and 3-methoxyphenylboronic acid (1.00 mL, 8.33 mmol); yield: 1.81 g (91 %); white solid; $R_{\text{f}} = 0.51$ (hexane / EtOAc, 80:20); MS (EI): $m/z = 262.0$ [M⁺+H].

4-(6-tert-Butyldimethylsilyloxy)naphthalen-2-yl)benzaldehyde, 17c. Synthesised according to Method A using compound **17d** (6.18 g, 18.30 mmol) and 4-formylphenylboronic acid (4.13 g, 27.50 mmol). Then the desired product was taken to the next step without further purification; yield: 6.07 g (91 %); $R_{\text{f}} = 0.43$ (hexane / EtOAc, 90:10).

1,6-Dibromo-2-methoxynaphthalene, 3b. To a solution of 2-bromo-6-methoxynaphthalene (3.65 g, 15.24 mmol) in THF (30 mL) was added N-bromosuccinimide (3.01 g, 16.76 mmol). Then the solution was heated to reflux for 2 hours. After cooling to ambient temperature, it was diluted with water (50 mL) and extracted with ethyl acetate (3 x 25 mL). The combined organic phases were washed with 1 N HCl, brine, dried over Na₂SO₄ and evaporated under reduced pressure. Then the desired product was taken to the next step without further purification; yield: 4.82 g (100 %); white solid; $R_{\text{f}} = 0.48$ (hexane / EtOAc, 80:20); δ_{H} (CDCl₃, 500 MHz) 4.02 (s, 3H), 7.27 (d, $J = 9.5$ Hz, 1H), 7.60 (d, $J = 9.1$ Hz, 1H), 7.71 (d, $J = 8.8$ Hz, 1H), 7.92 (s, 1H), 8.08 (d, $J = 9.1$ Hz, 1H); δ_{C} (CDCl₃, 125 MHz) 57.0 (CH₃), 108.7, 114.5, 118.1, 128.0, 129.8, 130.6, 130.9, 131.7, 154.0, 171.0; MS (ESI): $m/z = \text{not ionisable}$ [M⁺+H].

Method B: Ether cleavage with BBr₃. To a solution of the corresponding ether (1 eq) in DCM (5 mL / mmol) at -78 °C was added 1 M borontribromide in DCM (5 eq). The resulting mixture was stirred at rt for 16 hours. Then water (25 mL) was added and the emulsion was stirred for further 30 minutes. The resulting mixture was extracted with ethyl acetate (3 x 25 mL). The combined organic phases were washed with brine, dried over Na₂SO₄ and evaporated under reduced pressure. Then the desired product was purified by chromatography on silica gel.

6-(4-Fluorophenyl)-1-(pyridin-3-yl)naphthalen-2-ol, 4. Synthesised according to Method B using **3** (0.14 g, 0.43 mmol) and BBr₃ (2.20 mL, 2.20 mmol); yield: 0.10 g (75 %); light-yellow solid: mp 234 °C; $R_{\text{f}} = 0.42$ (DCM / MeOH, 95:5); IR (ATR) ν (cm⁻¹) 2922 (w), 1595 (w), 1498 (s), 1350 (m), 1324 (w), 1291 (m), 1257 (w), 1228 (m), 1188 (w), 1159 (w), 1052 (w), 943 (m), 846 (w), 816 (s), 769 (w), 710 (s), 662 (w), 638 (m), 520 (m); δ_{H} (CDCl₃ + CD₃OD, 500 MHz) 7.01-7.04 (m, 2H), 7.16 (d, $J = 8.9$ Hz, 1H), 7.34 (d, $J = 8.8$ Hz, 1H), 7.42-7.46 (m, 2H), 7.51-7.53 (m, 2H), 7.72 (d, $J = 8.9$ Hz, 1H), 7.78 (dd, $J = 1.6, 7.8$ Hz, 1H), 7.84 (s, 1H), 8.48 (d, $J = 4.6$ Hz, 1H), 8.51 (s, 1H); δ_{C} (CDCl₃ + CD₃OD, 125 MHz) 115.8, 116.0, 117.59, 117.60, 118.8, 124.1, 124.7, 126.1, 126.4, 128.87, 128.94, 129.1, 130.5, 133.0, 133.4, 135.2, 137.29, 137.32, 140.2, 147.4, 151.2, 152.4, 162.7 (d, $J = 245.9$ Hz, C-F); MS (ESI): $m/z = 314.0$ [M⁺+H].

6-(3-(Pyridin-3-yl)phenyl)naphthalen-2-ol, 14. Synthesised according to Method B using **12** (0.09 g, 0.29 mmol) and BBr₃ (1.00 mL, 1.00 mmol); yield: 0.06 g (67 %); light-yellow solid: mp 223 °C; $R_{\text{f}} = 0.47$ (DCM / MeOH, 95:5); IR (ATR) ν (cm⁻¹) 2962 (w), 1626 (w), 1596 (m), 1482 (w), 1428 (m), 1396 (w), 1260 (m), 1236 (m), 1199 (m), 1104 (s), 1020 (s), 848 (w), 783 (s), 703 (s), 674 (w); δ_{H} (CDCl₃ + CD₃OD 500 MHz) 7.11 (dd, $J = 2.4, 8.8$ Hz, 1H), 7.14 (d, $J = 2.3$ Hz, 1H), 7.45-7.48 (m, 1H), 7.50-7.52 (m, 2H), 7.52-7.56 (q, $J = 7.6$ Hz, 1H), 7.65-7.67 (dd, $J = 1.8, 8.6$ Hz, 1H), 7.70-7.72 (m, 2H), 7.74 (d, $J = 8.8$ Hz, 1H), 7.83-7.84 (m, 1H), 7.95 (s, 1H), 8.04 (d, $J = 7.9$ Hz, 1H), 8.56 (s, 1H), 8.88 (s, 1H); δ_{C} (CDCl₃ + CD₃OD, 125 MHz) 109.0, 113.1, 118.8, 125.6, 125.7, 125.8, 126.0, 127.0, 127.3, 128.6, 129.6, 129.8, 134.3, 135.0, 149.9, 155.0, 156.9, 160.2; MS (ESI): $m/z = 298.3$ [M⁺+H].

6-(3-(Pyridin-4-yl)phenyl)naphthalen-2-ol, 15. Synthesised according to Method B using **13** (0.20 g, 0.64 mmol) and BBr₃ (2.60 mL, 2.60 mmol); yield: 0.16 g (86 %); light-yellow solid; $R_{\text{f}} = 0.38$ (DCM / MeOH, 95:5); IR (ATR) ν (cm⁻¹) 3300-2450 (w), 1625 (w), 1598 (m), 1546 (w), 1494 (w), 1450 (w), 1398 (w), 1240 (m), 1218 (w), 1203 (m), 1126 (w), 1069 (w), 1007 (m), 981 (w), 860 (m), 835 (m), 812 (w), 785 (s), 697 (m), 624 (m), 571 (w); δ_{H} ((CD₃)₂SO, 500 MHz) 7.13 (dd, $J = 2.4, 8.8$ Hz, 1H), 7.17 (d, $J = 2.2$ Hz, 1H), 7.63-7.65 (m, 1H), 7.77-7.81 (m, 2H), 7.84-7.88 (m, 5H), 8.13-8.14 (m, 1H), 8.22 (s, 1H), 8.66-8.68 (m, 2H), 9.83 (s, 1H); δ_{C} ((CD₃)₂SO, 125 MHz) 108.4, 119.0, 121.4, 125.0, 125.3, 125.4, 126.7, 127.4, 127.9, 129.78, 129.81, 133.7, 134.0, 137.9, 141.2, 147.0, 150.1, 155.6; MS (ESI): $m/z = 298.2$ [M⁺+H].

5-Bromobenzo[de]isochromene-1,3-dione, 6d. Synthesised according to Mitchell et al.³⁴ To a solution of benzo[de]isochromene-1,3-dione (20.00 g, 100.92 mmol) in sulfuric acid (400 mL) was added silver sulfate (16.00 g, 51.32 mmol) and then bromine (6.41 mL, 125.15 mmol) was carefully dropped. Then the resulting mixture was heated at 65 °C for 6 hours. After cooling to ambient temperature, the reaction mixture was filtered and then carefully poured into ice water (3.2 L). The precipitate was filtrated and washed first with water and then with ethanol. A further purification was not necessary; yield: 27.26 g (100 %); white-off solid; $R_f = 0.72$ (DCM / MeOH, 95:5); MS (EI): $m/z = 275.8, 278.9$ [$M^+ + H$].

6-Bromo-1-naphthoic acid, 6c. Synthesised according to Leuck et al.³⁵ To a solution of **6d** (10.10 g, 36.45 mmol) and sodium hydroxide in water (240 mL) was added a solution of yellow mercury oxide (11.00 g, 50.86 mmol) in water (30 mL) and acetic acid (10 mL). The resulting mixture was heated under reflux for 4 days. Then 5 N hydrochloric acid (200 mL) was added and the mixture heated to reflux for 4 hours. After that, the crude was filtered at 0 °C. After fractional recrystallisation from acetic acid, the more soluble **6c** remained in the mother liquor; yield: 2.10 g (23 %); white-off solid; $R_f = 0.49$ (hexane / EtOAc, 80:20); δ_H (CDCl₃, 500 MHz) 7.42-7.47 (m, 2H), 7.51-7.52 (m, 1H), 7.82 (d, $J = 8.1$ Hz, 1H), 7.96 (d, $J = 8.2$ Hz, 1H), 8.16 (d, $J = 7.3$ Hz, 1H), 8.86 (d, $J = 8.6$ Hz, 1H); δ_C (CDCl₃, 125 MHz) 124.6, 126.0, 126.2, 127.5, 127.7, 128.6, 130.6, 133.5, 134.0; MS (EI): $m/z = 249.8, 252.9$ [$M^+ + H$].

3-Bromo-1-naphthoic acid, 9c. Synthesised according to Leuck et al.³⁵ To a solution of **6d** (10.10 g, 36.45 mmol) and sodium hydroxide in water (240 mL) was added a solution of yellow mercury oxide (11.00 g, 50.86 mmol) in water (30 mL) and acetic acid (10 mL). The resulting mixture was heated under reflux for 4 days. Then 5 N hydrochloric acid (200 mL) was added and the mixture heated to reflux for 4 hours. After that, the crude was filtered at 0 °C. After fractional recrystallisation from acetic acid, the less soluble **9c** came in the early fractions; yield: 4.90 g (54 %); white-off solid; $R_f = 0.39$ (hexane / EtOAc, 80:20); δ_H (CDCl₃, 500 MHz) 7.51-7.54 (m, 1H), 7.59-7.62 (m, 1H), 7.76 (d, $J = 8.2$ Hz, 1H), 8.18 (d, $J = 2.0$ Hz, 1H), 8.40 (d, $J = 2.1$ Hz, 1H), 8.94 (d, $J = 8.7$ Hz, 1H); δ_C (CDCl₃, 125 MHz) 118.2, 126.0, 127.4, 127.8, 128.5, 130.1, 134.6, 136.2; MS (EI): $m/z = 249.8, 252.9$ [$M^+ + H$].

Method C: Reduction with LiAlH₄. To an ice-cooled solution of the corresponding carboxylic acid (1 eq) in THF or diethylether (5 mL / mmol) was carefully dropped LiAlH₄ (10 eq) in diethylether (5 mL / mmol). Then the resulting mixture was heated to reflux for 1 hour. After cooling to ambient temperature, water (25 mL) was added, and after phase separation the aqueous phase was extracted with ethyl acetate (3 x 25 mL). The combined organic phases were washed with brine, dried over Na₂SO₄ and evaporated under reduced pressure. Then the desired product was purified by chromatography on silica gel.

(6-Bromonaphthalen-1-yl)methanol, 6b. Synthesised according to Method C using **6c** (2.50 g, 9.96 mmol), LiAlH₄ (3.90 g, 99.55 mmol) and additional 25 mL THF; yield: 2.19 g (87 %); white-off solid; $R_f = 0.44$ (hexane / EtOAc, 80:20); δ_H (CDCl₃, 500 MHz) 5.09 (s, 2H), 7.44-7.47 (m, 1H), 7.51 (d, $J = 6.9$ Hz, 1H), 7.60 (dd, $J = 2.1, 9.0$ Hz, 1H), 7.70 (d, $J = 8.1$ Hz, 1H), 7.98 (d, $J = 9.0$ Hz, 1H), 8.02 (d, $J = 2.0$ Hz, 1H); MS (EI): $m/z = 235.9, 238.9$ [$M^+ + H$].

(6-Bromonaphthalen-2-yl)methanol, 8b. Synthesised according to Method C using 6-bromo-2-naphthoic acid (3.00 g, 11.95 mmol) and LiAlH₄ (4.68 g, 119.48 mmol); yield: 2.78 g (90 %); white solid; $R_f = 0.19$ (hexane / EtOAc, 80:20); δ_H (CDCl₃, 500 MHz) 4.85 (s, 2H), 7.50 (dd, $J = 1.6, 8.5$ Hz, 1H), 7.55 (dd, $J = 2.0, 8.8$ Hz, 1H), 7.70 (d, $J = 8.8$ Hz, 1H), 7.75 (d, $J = 8.5$ Hz, 1H), 7.78 (s, 1H), 8.00 (d, $J = 1.6, 1H$); δ_C (CDCl₃, 125 MHz) 65.2, 65.5, 119.8, 125.1, 125.3, 125.4, 125.9, 126.15, 126.18, 127.4, 127.7, 127.9, 128.3, 129.5, 129.6, 129.8, 131.8, 134.0, 138.9; MS (EI): $m/z = 235.9, 238.9$ [$M^+ + H$].

(3-Bromonaphthalen-1-yl)methanol, 9b. Synthesised according to Method C using **6c** (2.50 g, 9.96 mmol), LiAlH₄ (3.90 g, 99.55 mmol) and additional 25 mL THF; yield: 2.46 g (98 %); white-off solid; $R_f = 0.34$ (hexane / EtOAc, 80:20); δ_H (CDCl₃, 500 MHz) 5.14 (s, 2H), 7.52-7.56 (m, 2H), 7.65 (d, $J = 1.9$ Hz, 1H), 7.78 (dd, $J = 1.9, 7.6$ Hz, 1H), 7.97 (s, 1H), 8.03 (d, $J = 7.9$ Hz, 1H); δ_C (CDCl₃, 125 MHz) 62.8 (CH₂), 119.4, 123.6, 126.6, 126.9, 127.8, 128.1, 129.5, 130.1, 134.9, 138.4; MS (EI): $m/z = 235.9, 238.9$ [$M^+ + H$].

Method D: CDI reaction. To a solution of the corresponding alcohol (1 eq) in NMP or acetonitrile (10 mL / mmol) was added CDI (5 eq) and imidazole (2 eq). Then the solution was heated to reflux for 16 hours. After cooling to ambient temperature, it was diluted with water (50 mL) and extracted with ethyl acetate (3 x 25 mL). The combined organic phases were washed with brine, dried over Na₂SO₄ and evaporated under reduced pressure. Then the desired product was purified by chromatography on silica gel.

1-((6-(4-Fluorophenyl)naphthalen-1-yl)methyl)-1H-imidazole, 6. Synthesised according to Method D using **6a** (0.15 g, 0.60 mmol), CDI (0.39 g, 2.38 mmol) and imidazole (0.04 g, 0.60 mmol); yield: 0.12 g (67 %); white solid; $R_f = 0.39$ (DCM / MeOH, 95:5); IR (ATR) ν (cm^{-1}) 3047 (w), 1604 (w), 1502 (s), 1287 (w), 1226 (s), 1159 (m), 1107 (w), 1075 (w), 906 (w), 817 (s), 759 (m), 736 (m), 662 (m), 508 (m); δ_H (CDCl_3 , 500 MHz) 5.61 (s, 2H), 6.95 (s, 1H), 7.12 (s, 1H), 7.16-7.21 (m, 3H), 7.46-7.49 (m, 1H), 7.63 (s, 1H), 7.66 (dd, $J = 5.3, 8.6$ Hz, 2H), 7.74 (dd, $J = 1.8, 8.7$ Hz, 1H), 7.91 (d, $J = 8.6$ Hz, 1H), 7.93 (d, $J = 9.0$ Hz, 1H), 8.04 (d, $J = 1.6$ Hz, 1H); δ_C (CDCl_3 , 125 MHz) 48.8, 115.4, 115.8, 115.9, 119.4, 119.5, 123.1, 126.0, 126.3, 126.4, 126.5, 126.6, 128.9, 129.0, 129.5, 129.9, 131.1, 134.1, 136.5, 138.0, 141.2, 141.9, 162.7 (d, $J = 247.1$ Hz, C-F); MS (ESI): $m/z = 303.1$ [$\text{M}^+ + \text{H}$].

1-((6-(4-Fluorophenyl)-2-methoxynaphthalen-1-yl)methyl)-1H-imidazole, 7. Synthesised according to Method D using **7a** (0.10 g, 0.35 mmol) and CDI (0.12 g, 0.71 mmol) in acetonitrile as solvent; yield: 0.06 g (49 %); light-yellow solid; mp 128 °C; $R_f = 0.52$ (DCM / MeOH, 95:5); IR (ATR) ν (cm^{-1}) 1601 (w), 1503 (s), 1257 (s), 1235 (s), 1162 (w), 1096 (s), 1075 (w), 1056 (w), 1026 (w), 904 (w), 844 (w), 823 (w), 788 (w), 733 (w), 662 (m), 623 (m), 551 (m), 505 (s); δ_H (CDCl_3 , 500 MHz) 4.00 (s, 3H), 5.58 (s, 2H), 6.97 (d, $J = 10.7$ Hz, 2H), 7.14-7.18 (m, 2H), 7.34 (d, $J = 9.1$ Hz, 1H), 7.58 (s, 1H), 7.63 (dd, $J = 5.3, 8.7$ Hz, 2H), 7.73 (dd, $J = 1.9, 8.8$ Hz, 1H), 7.93 (d, $J = 9.1$ Hz, 1H), 7.96 (d, $J = 1.8$ Hz, 1H), 7.99 (d, $J = 8.9$ Hz, 1H); δ_C (CDCl_3 , 125 MHz) 40.6, 56.3, 113.3, 115.6, 115.7, 115.8, 119.0, 122.5, 126.4, 127.1, 128.6, 128.7, 128.9, 129.2, 131.1, 131.9, 135.5, 136.6, 137.1, 155.7, 162.5 (d, $J = 246.7$ Hz, C-F); MS (ESI): $m/z = 333.1$ [$\text{M}^+ + \text{H}$].

1-((6-(4-Fluorophenyl)naphthalen-2-yl)methyl)-1H-imidazole, 8. Synthesised according to Method D using **8a** (0.15 g, 0.60 mmol) and CDI (0.50 g, 3.08 mmol) in acetonitrile as solvent; yield: 0.12 g (67 %); white solid; mp 114 °C; $R_f = 0.50$ (DCM / MeOH, 95:5); IR (ATR) ν (cm^{-1}) 3099 (w), 1603 (m), 1503 (s), 1439 (w), 1293 (w), 1231 (s), 1160 (w), 1105 (w), 1089 (w), 910 (m), 842 (m), 816 (s), 772 (w), 657 (s), 558 (m), 519 (w); δ_H (CDCl_3 , 500 MHz) 5.29 (s, 2H), 6.96 (s, 1H), 7.13 (s, 1H), 7.15-7.19 (m, 2H), 7.29 (dd, $J = 1.5, 8.5$ Hz, 1H), 7.61 (s, 1H), 7.64-7.67 (m, 3H), 7.72 (dd, $J = 1.8, 8.5$ Hz, 1H), 7.85-7.88 (m, 2H), 7.97 (s, 1H); δ_C (CDCl_3 , 125 MHz) 51.0, 115.7, 115.9, 119.4, 125.4, 126.1, 126.2, 128.5, 128.9, 129.0, 129.2, 129.8, 132.3, 133.2, 133.7, 136.85, 136.88, 137.5, 138.3, 162.6 (d, $J = 246.9$ Hz, C-F); MS (ESI): $m/z = 302.9$ [$\text{M}^+ + \text{H}$].

1-((3-(4-Fluorophenyl)naphthalen-1-yl)methyl)-1H-imidazole, 9. Synthesised according to Method D using **9a** (0.15 g, 0.60 mmol), CDI (0.39 g, 2.38 mmol) and imidazole (0.04 g, 0.60 mmol); yield: 0.13 g (71 %); light-yellow oil; $R_f = 0.23$ (DCM / MeOH, 98:2); IR (ATR) ν (cm^{-1}) 3057 (w), 1606 (w), 1511 (s), 1229 (s), 1160 (m), 1107 (w), 1077 (w), 832 (s), 790 (w), 749 (m), 663 (m), 519 (w); δ_H (CDCl_3 , 500 MHz) 5.64 (s, 2H), 6.97 (s, 1H), 7.13 (s, 1H), 7.14-7.17 (m, 2H), 7.38 (s, 1H), 7.53-7.58 (m, 2H), 7.60 (dd, $J = 5.3, 8.6$ Hz, 2H), 7.69 (s, 1H), 7.87-7.89 (m, 1H), 7.94-7.96 (m, 1H), 8.00 (s, 1H); δ_C (CDCl_3 , 125 MHz) 48.9, 115.7, 115.8, 116.0, 119.5, 122.2, 123.6, 124.7, 125.7, 126.3, 126.79, 126.82, 127.1, 127.2, 128.8, 128.9, 129.3, 129.5, 129.9, 131.9, 132.7, 134.1, 136.27, 136.29, 137.2, 162.7 (d, $J = 247.4$ Hz, C-F); MS (ESI): $m/z = 303.0$ [$\text{M}^+ + \text{H}$].

1-(3-(6-Methoxynaphthalen-2-yl)benzyl)-1H-imidazole, 16. Synthesised according to Method D using **7a** (0.20 g, 0.76 mmol) and CDI (0.38 g, 2.27 mmol) in acetonitrile as solvent; yield: 0.12 g (51 %); white solid; mp 130 °C; $R_f = 0.38$ (DCM / MeOH, 95:5); IR (ATR) ν (cm^{-1}) 2966 (w), 1626 (w), 1603 (w), 1492 (w), 1453 (w), 1388 (w), 1256 (m), 1227 (m), 1212 (m), 1073 (m), 1022 (s), 883 (w), 855 (s), 814 (s), 791 (m), 745 (s), 662 (s); δ_H (CDCl_3 , 500 MHz) 3.94 (s, 3H), 5.20 (s, 2H), 6.97 (s, 1H), 7.13-7.16 (m, 3H), 7.19 (dd, $J = 2.5, 8.9$ Hz, 1H), 7.44-7.47 (m, 1H), 7.48-7.49 (m, 1H), 7.63-7.66 (m, 3H), 7.78-7.81 (m, 2H), 7.92 (d, $J = 1.5$ Hz, 1H); δ_C (CDCl_3 , 125 MHz) 51.0, 55.3, 105.7, 119.3, 125.7, 125.8, 125.9, 126.1, 127.2, 127.4, 129.1, 129.5, 129.7, 134.0, 135.5, 136.7, 142.1, 158.0; MS (ESI): $m/z = 315.0$ [$\text{M}^+ + \text{H}$].

1-(4-(6-(tert-Butyldimethylsilyloxy)naphthalen-2-yl)benzyl)-1H-imidazole, 17a. Synthesised according to Method D using **17b** (3.46 g, 9.50 mmol) and CDI (7.70 g, 47.40 mmol). Then the desired product was taken to the next step without further purification; yield: 3.11 g (79 %); white solid; $R_f =$ (DCM / MeOH, 98:2).

6-Bromo-2-methoxy-1-naphthaldehyde, 7c. To a solution of 2-bromo-6-methoxy-naphthalene (5.00 g, 21.09 mmol) in DCM (100 mL) was added TiCl_4 (4.00 g, 21.09 mmol) and 1,1-dichloromethylmethylether (2.43 g, 21.09 mmol). Then the resulting mixture was stirred at 40 °C for 2 hours. After complete conversion, water (25 mL) was added, the phases were separated, and the aqueous layer was extracted with ethyl acetate (3 x 25 mL). The combined organic phases were washed with brine, dried over Na_2SO_4 and evaporated under reduced pressure. Then the desired product was taken to the next step without further purification; yield: g (100 %); white solid.

Method E: Reduction with NaBH_4 . To an ice-cooled solution of the corresponding aldehyde (1 eq) in THF (5 mL / mmol) was added NaBH_4 (2 eq) in methanol (5 mL / mmol). Then the resulting mixture was stirred at rt for 1 hour. After complete conversion, the solvent was distilled off under reduced pressure. Then water (25 mL) was

added, and the resulting mixture was extracted with ethyl acetate (3 x 25 mL). The combined organic phases were washed with brine, dried over Na₂SO₄ and evaporated under reduced pressure. Then the desired product was purified by chromatography on silica gel.

(6-(4-Fluorophenyl)-2-methoxynaphthalen-1-yl)methanol, 7a. Synthesised according to Method E using **7b** (0.28 g, 0.98 mmol) and NaBH₄ (0.08 g, 1.96 mmol); yield: 0.25 g (91 %); white solid; *R*_f = 0.56 (DCM / MeOH, 98:2); δ_H (CDCl₃, 500 MHz) 4.01 (s, 3H), 5.21 (s, 2H), 7.15-7.18 (m, 2H), 7.33 (d, *J* = 9.1 Hz, 1H), 7.66 (dd, *J* = 5.3, 8.9 Hz, 2H), 7.74 (dd, *J* = 1.9, 8.9 Hz, 1H), 7.89 (d, *J* = 9.1 Hz, 1H), 7.95 (d, *J* = 1.9 Hz, 1H), 8.18 (d, *J* = 8.9 Hz, 1H); δ_C (CDCl₃, 125 MHz) 55.9, 56.5, 113.5, 115.6, 115.8, 121.2, 123.7, 126.1, 126.5, 128.66, 128.72, 129.4, 130.3, 131.9, 135.3, 136.98, 137.00, 155.3, 162.4 (d, *J* = 246.5 Hz, C-F); MS (APCI): *m/z* = 266.9 [M⁺+H].

(3-(6-Methoxynaphthalen-2-yl)phenyl)methanol, 16a. Synthesised according to Method E using **16b** (0.40 g, 1.53 mmol) and NaBH₄ (0.12 g, 3.05 mmol); yield: 0.40 g (100 %); white solid; *R*_f = 0.50 (DCM / MeOH, 98:2); MS (ED): *m/z* = 312.9, 316.0 [M⁺+H].

(4-(6-(*tert*-Butyldimethylsilyloxy)naphthalen-2-yl)phenyl)methanol, 17b. Synthesised according to Method E using **17c** (4.55 g, 12.50 mmol) and NaBH₄ (0.95 g, 25.00 mmol). Then the desired product was taken to the next step without further purification; yield: 3.46 g (76 %); white solid; *R*_f = 0.35 (hexane / EtOAc, 70:30).

(6-Bromonaphthalen-2-yloxy)(*tert*-butyl)dimethylsilane, 17d. To a solution of 6-bromonaphthalen-2-ol (10.00 g, 44.80 mmol) and imidazole (3.40 g, 49.30 mmol) in DCM (100 mL) was added dropwise a TBDMS-Cl (7.40 g, 49.30 mmol) solution in DCM (50 mL). Then the resulting mixture was stirred at rt for 16 hours. After complete conversion, water (25 mL) was added, the phases separated, and the aqueous layer extracted with ethyl acetate (3 x 25 mL). The combined organic phases were washed with brine, dried over Na₂SO₄ and evaporated under reduced pressure. Then the desired product was taken to the next step without further purification; yield: 14.81 g (98 %); white solid.

6-(4-((1*H*-Imidazol-1-yl)methyl)phenyl)naphthalen-2-ol, 17. To a solution of **17a** (3.11 g, 7.50 mmol) in THF (50 mL) was added dropwise a 1 M TBAF solution in THF (7.50 mL, 7.50 mmol). Then the resulting mixture was stirred at rt for 16 hours. After complete conversion, water (25 mL) and ethyl acetate (25 mL) were added, the phases separated, and the aqueous layer extracted with ethyl acetate (3 x 25 mL). The combined organic phases were washed with brine, dried over Na₂SO₄ and evaporated under reduced pressure. Then the desired product was purified by chromatography on silica gel; yield: 1.96 g (87 %); brown solid; *R*_f = 0.50 (EtOAc / MeOH, 95:5); IR (ATR) ν (cm⁻¹) 3113 (w), 3026 (w), 1603 (m), 1516 (m), 1235 (s), 1198 (s), 1108 (m), 1080 (m), 831 (s), 806 (s); δ_H (CDCl₃, 500 MHz) 5.21 (s, 2H), 6.90 (t, *J* = 1.0 Hz, 1H), 7.08 (dd, *J* = 2.4 Hz, *J* = 8.7 Hz, 1H), 7.11 (d, *J* = 2.3 Hz, 1H), 7.20 (t, *J* = 1.2 Hz, 1H), 7.33 (d, *J* = 8.4 Hz, 2H), 7.67 (dd, *J* = 1.8 Hz, *J* = 8.6 Hz, 1H), 7.70-7.74 (m, 3H), 7.77 (t, *J* = 0.9 Hz, 1H), 7.79 (d, *J* = 8.9 Hz, 1H), 8.03 (d, *J* = 1.3 Hz, 1H), 9.82 (s, 1H); δ_C (CDCl₃, 125 MHz) 49.1 (CH₂), 108.4, 119.0, 119.5, 125.0, 125.1, 126.7, 126.8, 127.9, 128.1, 128.7 (C_q), 129.8, 133.7 (C_q), 133.8 (C_q), 136.5 (C_q), 137.4, 139.6 (C_q), 155.5 (C-OH); MS (ESI): *m/z* = 301.0 [M⁺+H].

Molecular Modelling. Compound **15** was docked in 50 independent genetic algorithm (GA) runs using GOLD. Heme iron was chosen as active-site origin, while the radius was set equal to 19 Å. The automatic active-site detection was switched on. A distance constraint of a minimum of 1.9 and a maximum of 2.5 Å between the sp²-hybridised nitrogen of the pyridine and the iron was set. Further, some of the GOLDScore parameters were modified to improve the weight of hydrophobic interaction and of the coordination between iron and nitrogen. The genetic algorithm default parameters were set as suggested by the GOLD authors. On the other hand, the annealing parameters of fitness function were set at 3.5 Å for hydrogen bonding and 6.5 Å for Van der Waals interactions.

All 50 poses for compound **15** were clustered with ACIAP^{36, 37} and the representative structure of each significant cluster was selected. The quality of the docked representative poses was evaluated based on visual inspection of the putative binding modes of the ligands, as outcome of docking simulations and cluster analysis.

Acknowledgment. We thank the Fonds der Chemischen Industrie for financial support. U. H. is grateful to the European Postgraduate School 532 (DFG) for a scholarship. We also thank Dr. J. J. R. Hermans, Cardiovascular Research Institute, University of Maastricht (the Netherlands), for providing us with V79 cells expressing human CYP11B1.

References and Notes

- (1) Jemal, A.; Siegel, R.; Ward, E.; Hao, Y.; Xu, J.; Murray, T.; Thun, M. J. Cancer statistics, 2007. *CA Cancer J. Clin.* **2007**, *57*, 43–66.
- (2) Huhtaniemi, I.; Nikula, H.; Parvinen, M.; Rannikko, S. Histological and functional changes of the testis tissue during GnRH agonist treatment of prostatic cancer. *Am. J. Clin. Oncol.* **1988**, *11*, Suppl. 1: S11–15.
- (3) Labrie, F.; Dupont, A.; Belanger, A.; Lefebvre, F. A.; Cusan, L.; Monfette, G.; Laberge, J. G.; Emond, J. P.; Raynaud, J. P.; Husson, J. M.; Fazekas, A. T. New hormonal treatment in cancer of the prostate: combined administration of an LHRH agonist and an antiandrogen. *J. Steroid Biochem.* **1983**, *19*, 999–1007.
- (4) Nnane, I. P.; Long, B. J.; Ling, Y.-Z.; Grigoryev, D. N.; Brodie, A. M. Metabolism of ethyl methyl sulphide and sulphoxide in rat microsomal fractions. *Br. J. Cancer* **2000**, *83*, 74–82.
- (5) Schuurmans, A. L. G.; Bolt, J.; Veldscholte, J.; Mulder, E. Stimulatory effects of antiandrogens on LNCaP human prostate tumor cell growth, EGF-receptor level and acid phosphatase secretion. *J. Steroid Biochem. Molec. Biol.* **1990**, *37*, 849–853.
- (6) Harris, K. A.; Weinberg, V.; Bok, R. A.; Kakefuda, M.; Small, E. J. Low dose ketoconazole with replacement doses of hydrocortisone in patients with progressive androgen independent prostate cancer. *J. Urol.* **2002**, *168*, 542–545.
- (7) Eklund, J.; Kozloff, M.; Vlamakis, J.; Starr, A.; Mariott, M.; Gallot, L.; Jovanovic, B.; Schilder, L.; Robin, E.; Pins, M.; Bergan, R. C. Phase II study of mitoxantrone and ketoconazole for hormone-refractory prostate cancer. *Cancer* **2006**, *106*, 2459–2465.
- (8) Small, E.J.; Halabi, S.; Dawson, N. A.; Stadler, W. M.; Rini, B. I.; Picus, J.; Gable, P.; Torti, F. M.; Kaplan, E.; Vogelzang, N. J. Antiandrogen withdrawal alone or in combination with ketoconazole in androgen-independent prostate cancer patients: a phase III trial (CALGB 9583). *J. Clin. Oncol.* **2004**, *22*, 1025–1033.
- (9) <http://www.cougarbiotechnology.com/docs/052107CougarPhaseIIAUAAnnualMeeting2007.pdf>. (Cougar Biotechnology Inc.)
- (10) Kolar, N. W.; Swart, A. C.; Mason, J. I.; Swart, P. J. Functional expression and characterisation of human cytochrome P45017alpha in *Pichia pastoris*. *J. Biotechnol.* **2007**, *129*, 635–644.
- (11) Haidar, S.; Ehmer, P. B.; Barassin, S.; Batzl-Hartmann, C.; Hartmann, R. W. Effects of novel 17alpha-hydroxylase/C17, 20-lyase (P450 17, CYP 17) inhibitors on androgen biosynthesis *in vitro* and *in vivo*. *J. Steroid Biochem. Mol. Biol.* **2003**, *84*, 555–562.
- (12) Haidar, S.; Hartmann, R. W. Enzyme inhibitor examples for the treatment of prostate tumor. In *Enzymes and their Inhibition. Drug Development*; Smith, H. J.; Simons, C., Eds.; CRC Press: Boca Raton-London-New York-Singapore, **2005**, 241–253.
- (13) Matsunaga, N.; Kaku, T.; Itoh, F.; Tanaka, T.; Hara, T.; Miki, H.; Iwasaki, M.; Aono, T.; Yamaoka, M.; Kusaka, M.; Tasaka, A. C_{17,20}-lyase inhibitors I. Structure-based de novo design and SAR study of C_{17,20}-lyase inhibitors. *Bioorg. Med. Chem.* **2004**, *12*, 2251–2273.
- (14) Hartmann, R. W.; Wachall, B.; Yoshihama, M.; Nakakoshi, M.; Nomoto, S.; Ikeda, Y. Novel dihydronaphthalene compounds and process for producing the same. WO018075, 1999.
- (15) (a) Wachall, B. G.; Hector, M.; Zhuang, Y.; Hartmann, R. W. Imidazole substituted biphenyls: a new class of highly potent and *in vivo* active inhibitors of P450 17 as potential therapeutics for treatment of prostate cancer. *Bioorg. Med. Chem.* **1999**, *7*, 1913–1924. (b) Zhuang, Y.; Wachall, B. G.; Hartmann, R. W. Novel imidazolyl and triazolyl substituted biphenyl compounds: synthesis and evaluation as nonsteroidal inhibitors of human 17alpha-hydroxylase-C17, 20-lyase (P450 17). *Bioorg. Med. Chem.* **2000**, *8*, 1245–1252.
- (16) Leroux, F.; Hutschenreuter, T.; Charrière, C.; Scopelliti, R.; Hartmann, R. W. *N*-(4-Biphenylmethyl)imidazoles as potential therapeutics for the treatment of prostate cancer: Metabolic robustness due to fluorine substitution? *Helv. Chim. Act.* **2003**, *86*, 2671–2686.
- (17) Schenkman, J. B.; Sligar, S. G.; Cinti, D. L. Substrate interaction with cytochrome P-450. *Pharmacol Ther.* **1981**, *12*, 43–71.
- (18) Miyaura, N.; Suzuki, A. Palladium-catalyzed cross-coupling reactions of organoboron compounds. *Chem. Rev.* **1995**, *95*, 2457–2483.
- (19) Tang, Y.; Dong, Y.; Vennerstrom J. L. The reaction of carbonyldiimidazole with alcohols to form carbamates and *N*-alkylimidazoles *Synthesis* **2004**, *15*, 2540–2544.

- (20) Hutschenreuter, T. U.; Ehmer, P. B.; Hartmann, R. W. Synthesis of hydroxy derivatives of highly potent non-steroidal CYP 17 inhibitors as potential metabolites and evaluation of their activity by a non cellular assay using recombinant human enzyme. *J. Enzyme Inhib. Med. Chem.* **2004**, *18*, 17–32.
- (21) Ehmer, P. B.; Jose, J.; Hartmann, R. W. Development of a simple and rapid assay for the evaluation of inhibitors of human 17 α -hydroxylase-C(17,20)-lyase (P450c17) by coexpression of P450c17 with NADPH-cytochrome-P450-reductase in *Escherichia coli*. *J. Steroid Biochem. Mol. Biol.* **2000**, *75*, 57–63.
- (22) Sergejew, T.; Hartmann, R. W. Pyridyl substituted benzocycloalkenes: new inhibitors of 17 α -hydroxylase/17,20-lyase (P450 17 α). *J. Enz. Inhib.* **1994**, *8*, 113–122.
- (23) Manga, N.; Duffy, J. C.; Rowe, P. H.; Cronin, M. T. D. Structure-based methods for the prediction of the dominant P450 enzyme in human drug biotransformation: consideration of CYP3A4, CYP2C9, CYP2D6. *SAR QSAR Environ. Res.* **2005**, *16*, 43–61.
- (24) Hodgson, J. ADMET--turning chemicals into drugs. *Nat. Biotechnol.* **2001**, *19*, 722–726.
- (25) For hepatic CYPs inhibition data the recombinantly expressed enzymes from baculovirus-infected insect microsomes (Supersomes) were used and the manufacturer's instructions (www.gentest.com) were followed.
- (26) V79MZh11B1 CYP11B1 cells expressing the human enzyme were used and our assay procedure using [4-¹⁴C]-11-deoxycorticosterone was applied (Ref. 27).
- (27) Ulmschneider, S.; Müller-Vieira, U.; Mitrenga, M.; Hartmann, R. W.; Oberwinkler-Marchais, S.; Klein, C. D.; Bureik, M.; Bernhardt, R.; Antes, I.; Lengauer, T. Synthesis and evaluation of imidazolylmethylenetetrahydronaphthalenes and imidazolylmethyleneindanes: potent inhibitors of aldosterone synthase. *J. Med. Chem.* **2005**, *48*, 1796–1805.
- (28) Jagusch, C.; Negri, M.; Hille, U. E.; Hu, Q.; Bartels, M.; Jahn-Hoffman, K.; Pinto-Bazurco Mendieta, M. A. E.; Rodenwaldt, B.; Müller-Vieira, U.; Schmidt, D.; Lauterbach, T.; Recanatini, M.; Cavalli, A.; Hartmann, R. W. Synthesis, biological evaluation and molecular modelling studies of methyleneimidazole substituted biaryls as inhibitors of human 17 α -hydroxylase-17,20-lyase (CYP17) – Part I: heterocyclic modifications of the core structure. *Bioorg. Med. Chem.* **2008**, *16*, 1992–2010.
- (29) (a) Lin, D.; Zhang, L. H.; Chiao, E.; Miller, L. W. Modeling and mutagenesis of the active site of human P450c17. *Mol. Endocrinol.* **1994**, *8*, 392–402. (b) Auchus, R. J.; Miller, W. L. Molecular modeling of human P450c17 (17 α -hydroxylase/17,20-lyase): insights into reaction mechanisms and effects of mutations. *Mol. Endocrinol.* **1999**, *13*, 1169–1182.
- (30) Mathieu, A. P.; LeHoux, J. G.; Auchus, R. J. Molecular dynamics of substrate complexes with hamster cytochrome P450c17 (CYP17): mechanistic approach to understanding substrate binding and activities. *Biochim. Biophys. Acta* **2003**, *1619*, 291–300.
- (31) Brooke, A.M.; Taylor, N.F.; Shepherd, J.H.; Gore, M.E.; Ahmad, T.; Lin, L.; Rumsby, G.; Papari-Zareei, M.; Auchus, R.J.; Achermann, J.C.; Monson, J.P. A novel point mutation in P450c17 (CYP17) causing combined 17 α -hydroxylase/17,20-lyase deficiency. *J. Clin. Endocrinol. Metab.* **2006**, *91*, 2428–2431.
- (32) Lewis, D.F.; Lake, B.G.; Dickins, M. Quantitative structure-activity relationships (QSARs) in inhibitors of various cytochromes P450: the importance of compound lipophilicity. *J. Enzyme Inhib. Med. Chem.* **2007**, *22*, 1–6.
- (33) Vaz R. J.; Nayeem A.; Santone, K.; Chandrasena, G.; Gavai, A. V. A 3D-QSAR model for CYP2D6 inhibition in the aryloxypropanolamine series. *Bioorg. Med. Chem. Lett.* **2005**, *15*, 3816–3820.
- (34) Mitchell, W. J.; Topsom, R. D.; Vaughan, J. 1,8-Dimethylnaphthoic Acids. *J. Chem. Soc.* **1962**, 2526–2528.
- (35) Leuck, G. J.; Perkins, R. P.; Whitmore, F. C. The mercuriation of naphthalic acids. *J. Am. Chem. Soc.* **1929**, *51*, 1831–1836.
- (36) Bottegoni, G.; Cavalli, A.; Recanatini, M. A comparative study on the application of hierarchical-agglomerative clustering approaches to organize outputs of reiterated docking runs. *J. Chem. Inf. Mod.* **2006**, *46*, 852–862.
- (37) Bottegoni, G.; Rocchia, W.; Recanatini, M.; Cavalli, A. ACIAP, autonomous hierarchical agglomerative cluster analysis based protocol to partition conformational datasets. *Bioinformatics*, **2006**, *22*, 58–65.

3.1.4.2. Paper II.

Synthesis, biological evaluation and molecular modelling studies of methyleneimidazole substituted biaryls as inhibitors of human 17 α -hydroxylase-17,20-lyase (CYP17). Part I: Heterocyclic modifications of the core structure.

Carsten Jagusch, Matthias Negri, Ulrike E. Hille, Qingzhong Hu, Marc Bartels, Kerstin Jahn-Hoffmann, Mariano A. E. Pinto-Bazurco Mendieta, Barbara Rodenwaldt, Ursula Müller-Vieira, Dirk Schmidt, Thomas Lauterbach, Maurizio Recanatini, Andrea Cavalli, Rolf W. Hartmann

This article is protected by copyrights of ‘Bioorganic and Medicinal Chemistry.’

Bioorg. Med. Chem. **2008**, 16, 1992-2010

Abstract

Novel chemical entities were prepared via Suzuki and S_N reaction as AC-ring substrate mimetics of CYP17. The synthesised compounds **1-31** were tested for activity using human CYP17 expressed in *E. coli*. Promising compounds were tested for selectivity against hepatic CYP enzymes (3A4, 2D6, 1A2, 2C9, 2C19, 2B6). Two potent inhibitors (**27**, IC₅₀=373 nM/ **28**, IC₅₀=953 nM) were further examined in rats regarding their effects on plasma testosterone levels and their pharmacokinetic properties. Compound **28** was similarly active as abiraterone, and showed better pharmacokinetic properties (higher bioavailability, t_{1/2} 9.5 h vs 1.6 h). Docking studies revealed two new binding modes different from the one of the substrates and steroidal inhibitors.

Introduction

Prostate cancer (PC) is currently the most common malignancy and age-related cause of death in elder men worldwide. In the US about 220,000 new cases of PC are expected to be newly diagnosed in the year 2007 and about 30,000 men will die of this disease.¹ Approximately 80% of human prostatic tumors are androgen dependent. Consequently the standard treatment of PC is orchidectomy or its medicinal equivalent the chemical castration by gonadotropin-releasing hormone (GnRH) analogues, which reduce the testicular androgen production. A major disadvantage of these treatments is that they do not affect the adrenal androgen production. Therefore it is frequently combined with androgen receptor antagonists (flutamide, cyproterone acetate) to reduce the stimulatory effects of the remaining androgens. However, this so called “combined androgen blockade” is not effective in all patients as due to mutations in the androgen receptor, anti-androgens might act as agonists.^{2,3} Thus, the inhibition of CYP17 (P45017, 17 α -hydroxylase-C17,20-lyase) is a promising alternative to the combination of anti-androgens and GnRH analogues because testicular and adrenal androgen biosynthesis will both be reduced.

CYP17, the cytochrome b₅ modulated key enzyme in androgen biosynthesis,⁴ catalyses both the 17 α -hydroxylation of pregnenolone and progesterone and the subsequent 17,20-lyase reaction cleaving the C17-C20 bond to yield the 17-keto androgens androstendione and dehydroandrostendione (DHEA), the precursors of testosterone.⁵

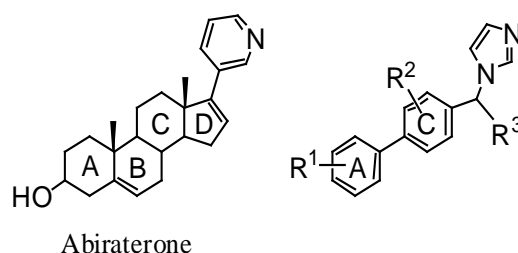
Until now the antimycotic ketoconazole was the only CYP17 inhibitor used clinically for the treatment of advanced PC to reduce testosterone biosynthesis.^{6,7} However, this drug is not a very potent inhibitor of CYP17 and relatively non-selective regarding the inhibition of other CYP enzymes. Besides it shows a number of notable side effects including liver damage. These drawbacks motivated us and others to look for more active and selective CYP17 inhibitors (for reviews see: ⁸⁻¹³).

Recently, the steroidal CYP17 inhibitor abiraterone passed phase II clinical trials showing high activity in post-docetaxel castration refractory PC patients and seems to have no dose-limiting toxicity.¹⁴ We also developed highly active steroidal inhibitors, which showed up to 3 fold higher activities against human CYP17 than abiraterone in vitro.¹⁵ Because of the fact that steroidal drugs are known to show side effects which rely on their scaffold, we also developed nonsteroidal inhibitors.¹⁶⁻¹⁸ Important for the mode of action of steroidal and nonsteroidal inhibitors is a nitrogen bearing heterocycle which is capable of complexing the heme iron of the enzyme. In the class of imidazole-methyl substituted biphenyls potent inhibitors were discovered.^{17,18} The biphenyl moiety of these inhibitors should

mimic the A- and the C-ring of the substrates (Chart I). Different substituents were introduced in the A-ring trying to achieve similar interactions as the oxygen at C3 of the substrates. In this study we exchanged the A- or the C-phenyl nuclei by different heterocycles in order to improve the potency of these AC-ring mimetics. In some compounds (**27-31**) methyl and ethyl substituents were introduced in the methylene bridge between imidazole ring and biphenyl moiety as we have seen that methyl substituents as well as the rigidified indane compounds are appropriate to increase CYP17 inhibition in some cases.^{17,18}

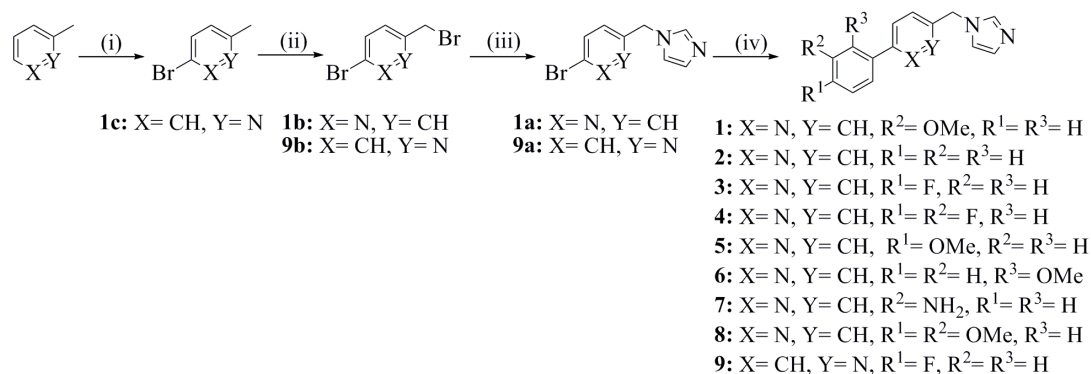
This approach was chosen to study other possible interactions between active site and ligand. In the following, the synthesis of the compounds shown in Scheme 1 and the determination of their inhibitory potency toward human CYP17 are described. Selected compounds were tested for their inhibition of hepatic CYP enzymes (3A4, 1A2, 2C9, 2C19, 2B6 and 2D6). Two potent inhibitors, compounds **27** and **28** were examined for their potential of reducing plasma testosterone levels in rats and their pharmacokinetic properties. Docking studies and molecular electrostatic potential (MEP) calculations were performed in order to elucidate some interesting structure-activity relationships.

Chart I. Schematic representation of Abiraterone and the scaffold of our biaryl inhibitors.

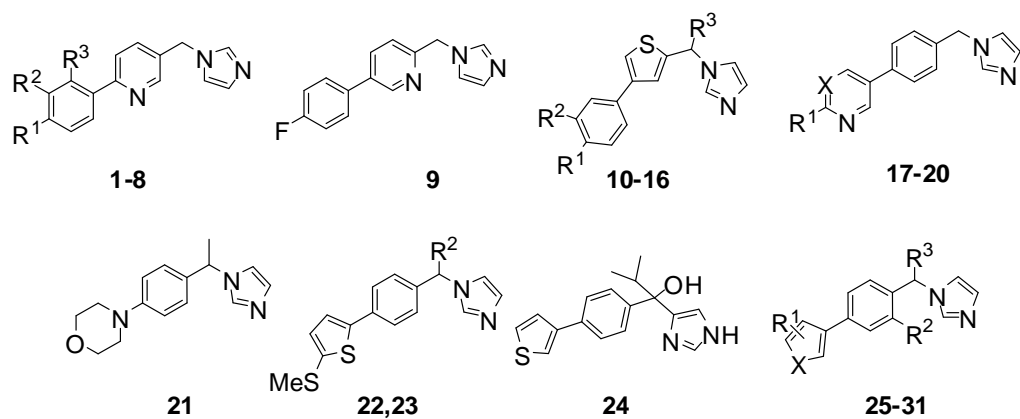


Chemistry

The syntheses of compounds **1-31** are shown in Schemes 2-8. After an eventual derivatisation of the A- or C-ring, both rings were coupled by means of a palladium catalysed Suzuki cross coupling reaction (Method B), and a nitrogen containing heterocycle was attached subsequently. The derivatisations carried out on the rings were mostly brominations and reductions of the carbonyl compounds to the corresponding alcohols, since the Suzuki coupling is described to give higher yields when using carbonyl substituted compounds instead of alcohols.¹⁹ For the synthesis of some compounds, the introduction of the imidazole moiety before the coupling was possible (Schemes 4, 5), allowing a wider range of substitution patterns. Two different reaction types for the introduction of the *1H*-imidazole were used resulting in comparable yields, an S_N2 reaction between imidazole and the corresponding bromide (Schemes 2, 5; Method A), and an S_Nt reaction between 1,1-carbonyl diimidazole (CDI) and the corresponding alcohol²⁰ (Schemes 3, 4, 6 and 8; Method E). The carbonyl compound was generally reduced with NaBH_4 (Schemes 3, 4, 6 and 8; Method C). For the synthesis of compounds **14**, **30** and **31** the introduction of the alkyl substituent at the methylene bridge was performed via Grignard reaction (Schemes 3, 8; Method D). In order to introduce the C-C linked imidazole, a protection with trityl chloride was necessary before submitting the compound to a lithium-halogen exchange (Scheme 7) like reported previously by Tasaka et al.²¹

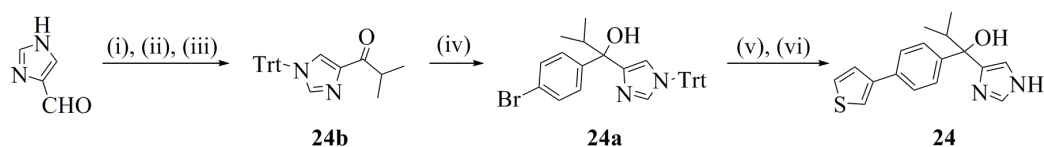


Scheme 2. Reagents: (i) AlCl_3 , Br_2 , 100°C , 2.5h; (ii) NBS, DBPO, CCl_4 , 90°C , 12h; (iii) **Method A:** imidazole, K_2CO_3 , acetonitrile, 90°C , 12h; (iv) **Method B:** Aryl-B(OH)₂, Na_2CO_3 , toluene/ MeOH/ H_2O , reflux, 5h.

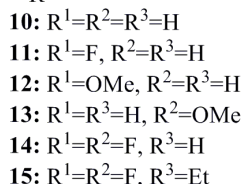
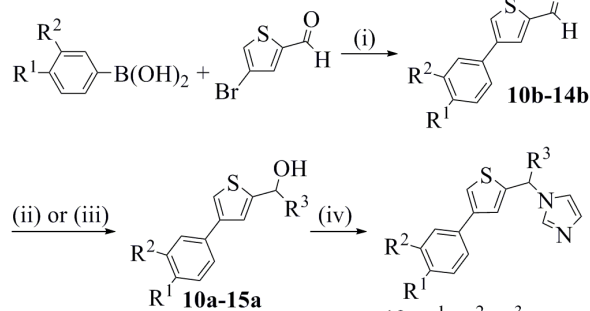


compound	R ¹	R ²	R ³	X
1	H	OMe	H	
2	H	H	H	
3	F	H	H	
4	F	F	H	
5	OMe	H	H	
6	H	H	OMe	
7	H	NH ₂	H	
8	OMe	OMe	H	
10	H	H	H	
11	F	H	H	
12	OMe	H	H	
13	H	OMe	H	
14	F	F	H	
15	F	F	Et	
16	OMe	OMe	H	
17	H			CH
18	F			CH
19	CH ₂ Cl			CH
20	H			N
22		H		
23		Et		
25	H	H	H	O
26	4-Me	H	H	S
27	H	H	Et	S
28	H	H	Me	S
29	4-Me	H	Et	S
30	4-Me	F	Et	S
31	2-Cl	H	Et	S

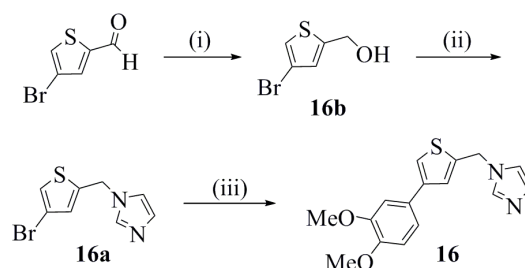
Scheme 1. List of synthesised compounds **1-31**.



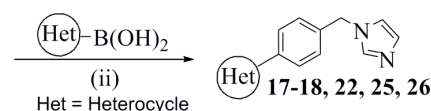
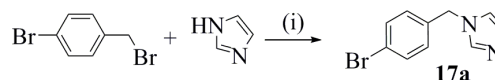
Scheme 7. (i) NH₂OHxHCl, acetanhydride, pyridine; (ii) (1) *i*-PrMgCl, THF/ Et₂O (2) H₂SO₄/ H₂O; (iii) TrtCl, Et₃N, DCM; (iv) (1) *n*-BuLi, THF/ Et₂O, (2) 1,4-dibromobenzene; (v) **Method B**: 3-thiophenylboronic acid, Pd(PPh₃)₄, Na₂CO₃, DME; (vi) pyridinexHCl, MeOH.



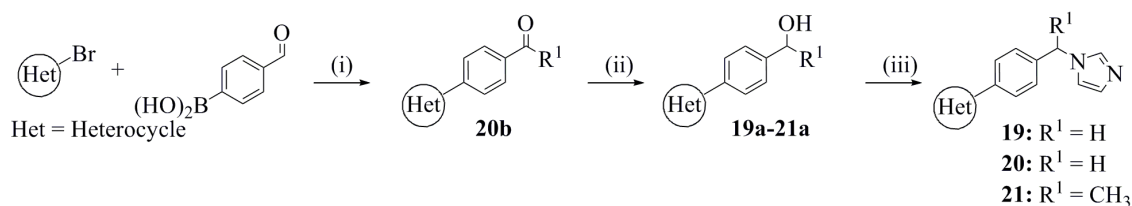
Scheme 3. (i) **Method B:** Pd(PPh₃)₄, Na₂CO₃, toluene/EtOH/H₂O, reflux, 16 h; (ii) **Method C:** **10b-14b:** NaBH₄, MeOH, 2 h, rt; (iii) **Method D:** **14b:** EtMgBr, THF, 16 h, rt; (iv) **Method E:** CDI, acetonitrile, reflux, 8 h.



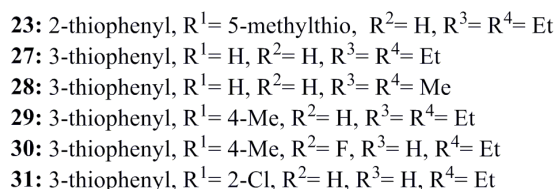
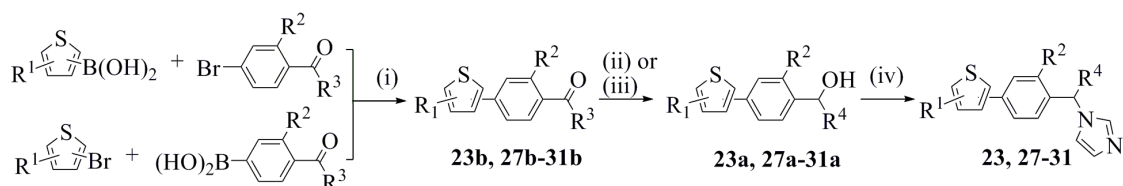
Scheme 4. (i) **Method C:** NaBH₄, MeOH, 2 h, rt; (ii) **Method E:** CDI, acetonitrile, reflux, 8 h; (iii) **Method B:** Ar-B(OH)₂, Pd(PPh₃)₄, Na₂CO₃, toluene/EtOH/H₂O, reflux, 16 h.



Scheme 5. (i) **Method A:** K₂CO₃, 18-crown-6, acetone, reflux, 2.5 h; (ii) **Method B:** Pd(PPh₃)₄, Na₂CO₃, toluene/EtOH/H₂O, reflux, 16 h.



Scheme 6. (i) **Method B:** Pd(PPh₃)₄, Na₂CO₃, toluene/EtOH/H₂O, reflux, 16 h; (ii) **Method C:** NaBH₄, MeOH, 2 h, rt; (iii) **Method E:** CDI, acetonitrile, reflux, 8 h.



Scheme 8. (i) **Method B:** Pd(PPh₃)₄, Na₂CO₃, reflux 6h; (ii) **Method C:** **23b, 27b-29b:** NaBH₄, THF, MeOH; (iii) **Method D:** **30b-31b:** EtMgCl, THF; (iv) **Method E:** CDI, NMP, reflux, 3h.

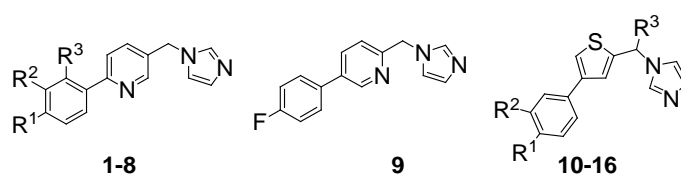
Results

Biological results

Inhibition of CYP17 was evaluated using human enzyme expressed in *E. coli*.²² The percent inhibition values of the compounds were determined with the 50,000 g sediment of the *E. coli* homogenate, progesterone (25 μ M) as substrate and the inhibitors at a concentration of 0.2 μ M and 2.0 μ M. Separation of substrate and product was accomplished by HPLC using UV detection.^{23a}

The inhibitory activities of the C-ring modified compounds **1-16** toward human CYP17 are shown in Table 1. It becomes apparent that the C-ring pyridyl compounds **1-9** are inactive, independent from their substitution pattern at the A-ring. On the contrary, the C-ring thiophenyl compounds **10-16** show low to moderate activity. In case of the methylene bridge unsubstituted compounds (**10-14**, **16**), it can be observed that the introduction of fluorine substituents and the 3-methoxy group in the A-ring does not alter the activity in regard to the unsubstituted compound whereas the 4-methoxy compounds (**12**, **16**) exhibit reduced activity. Interestingly, the introduction of an ethyl group at the methylene bridge (compound **15**) leads to a strong increase in activity for compound **14**.

Table 1. Inhibition of CYP17 by compounds 1-16



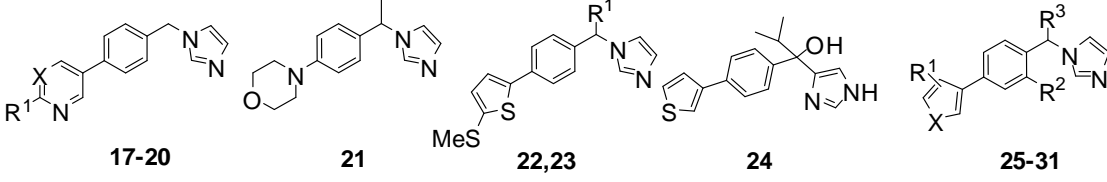
Comp.	Structures			CYP17	
	R ¹	R ²	R ³	% Inhibition ^a	
				0.2 μ M	2 μ M
1	H	OMe	H	0	1
2	H	H	H	0	4
3	F	H	H	5	5
4	F	F	H	0	0
5	OMe	H	H	0	0
6	H	H	OMe	0	5
7	H	NH ₂	H	2	3
8	OMe	OMe	H	1	2
9				0	2
10	H	H	H	0	21
11	F	H	H	0	20
12	OMe	H	H	0	13
13	H	OMe	H	0	24
14	F	F	H	7	25
15	F	F	Et	17	68
16	OMe	OMe	H	0	14

^a Concentration of progesterone (substrate): 25 μ M; standard deviations were within ± 5 %

In Table 2 the inhibition values of the A-ring modified compounds **17-31** are presented in comparison to ketoconazole and abiraterone. Neither the substitution by a pyridine (**17-19**) nor a pyrimidine (**20**) or a morpholine (**21**) leads to moderate activity. On the other hand in the class of the thiophenyl compounds **22-24** and **26-31** highly active inhibitors were obtained. The most active compounds bear an alkyl (methyl or ethyl) substituent at the methylene bridge. The ethyl compound **27** (IC₅₀ = 373 nM) has a 3 fold higher activity compared to the methyl compound **28** (IC₅₀ = 953 nM). The methyl group in 4-position of the thiophene in compound **29** (IC₅₀ = 584 nM) slightly reduces the activity of compound **27**. Both the insertion of a fluorine atom at the C-ring (compound **30**, IC₅₀ = 236 nM) and the exchange of the 4-methyl group by a 2-chloro substituent at the thiophene (compound **31**, IC₅₀ = 263 nM) increased the potency and led to the most active inhibitors of this study.

The selectivity of selected compounds toward hepatic CYP enzymes was investigated in regard of their important role in drug metabolism. The most critical one is CYP3A4 as it is involved in the metabolism of 50 % of the commercial drugs. Inhibition of this enzyme can result in severe side-effects because of a known genetic polymorphism. The compounds tested showed inhibition of this enzyme (Table 2). However, it was significantly lower than that for ketoconazole which is used clinically as an antimycotic. Besides 3A4 five other hepatic enzymes 1A2, 2C9, 2C19, 2B6 and 2D6 are also important for drug metabolism; for CYP2D6 a genetic polymorphism is described too. In contrast to ketoconazole and abiraterone our compounds showed strong inhibitory activities at concentrations of 10 μ M (Table 3).

Table 2. Inhibition of CYP17 and CYP3A4 by compounds 17-31



Comp.	Structures				Human CYP17 ^c		Rat CYP17 ^c	CYP3A4		
	R ¹	R ²	R ³	X	% Inhibition 0.2 μ M	% Inhibition 2 μ M	IC ₅₀ [nM] ^d	IC ₅₀ [nM] ^d	% Inhibition 1 μ M	% Inhibition 10 μ M
17	H			CH	2	14				
18	F			CH	4	13				
19	CH ₂ Cl			CH	9	24				
20	H			N	5	3				
21					5	12				
22	H				3	35				
23	Et				2	3				
24					7	49				
25	H	H	H	O	3	29				
26	4-Me	H	H	S	0	27				
27	H	H	Et	S	28	83	373	562	88	92
28	H	H	Me	S	21	67	953	676	80	94
29	4-Me	H	Et	S	27	84	584			
30	4-Me	F	Et	S	41	92	236		88	97
31	2-Cl	H	Et	S	40	85	263		87	97
KTZ ^a						19 ^b	2780		96	98
ABT ^a							72	220 ^e	4	25

^a **KTZ**: ketoconazole; **ABT**: abiraterone.

^b % Inhibition at 1.0 μ M

^c Concentration of progesterone (substrate): 25 μ M; standard deviations were within ± 5 %

^d Concentration of inhibitors required to give 50 % inhibition. The given values are mean values of at least three experiments. The deviations were within ± 10 %

^e Ref.: 15

Table 3. Inhibition of hepatic CYP enzymes by compounds 15, 27 and 28.

Comp.	CYP1A2		CYP2C9		CYP2C19		CYP2B6		CYP2D6	
	% Inhibition ^b		% Inhibition ^b		% Inhibition ^b		% Inhibition ^b		% Inhibition ^b	
	1 μ M	10 μ M	1 μ M	10 μ M	1 μ M	10 μ M	1 μ M	10 μ M	1 μ M	10 μ M
15	93	96	94	100	95	97				
27	98	100	81	74	95	100	60	87	24	77.
28	97	100	75	89	87	99	49	87	17	68
KTZ ^a	8	38	21	75	24	79	11	57	1	4
ABT ^a	36	53	17	51	3	21	2	11	7	7

^a **KTZ**: ketoconazole; **ABT**: abiraterone.

^b standard deviations were within $< \pm 5$ %

After it has been demonstrated that compounds **27** and **28** also inhibited the rat enzyme (Table 2), they were chosen for in vivo studies to investigate the influence of the methyl substituent versus the ethyl substituent at the methylene bridge. Both were evaluated for reduction of the plasma testosterone concentration (Table 4) and for pharmacokinetic parameters (Table 5) in male Wistar rats using abiraterone as a reference compound. All compounds reduced significantly the plasma testosterone levels. Compounds **27** and **28** showed strong effects already after 1 h. Abiraterone which was administered as a prodrug (acetate) exhibited maximum activity after 2 h. At 6 and 8 h abiraterone and compound **28** still showed high activity whereas compound **27** showed decreased effects. It is surprising that abiraterone is not more active than **28** since it is a stronger inhibitor of rat CYP17 ($IC_{50} = 220$ nM, Table 2). This finding can be explained by the pharmacokinetic properties of the compounds which differ strongly. From Table 5 it becomes apparent, that abiraterone exhibits a low bioavailability. The plasma half-lives of compound **28** (9.5 h) and abiraterone (1.6 h) are also different. The comparatively long duration of activity seen after application of abiraterone acetate is caused by the fact that the ester cleavage gradually takes place.

Table 4. Reduction of the plasma testosterone concentrations in rats by compounds 27 and 28^a

Comp.	Relative plasma testosterone level (%) ^b				
	1h	2h	4h	6h	8h
Control	143.1 \pm 13.3	76.4 \pm 13.3	81.4 \pm 24.6	109.6 \pm 31.7	90.6 \pm 22.8
27	37.6 \pm 14.8 ^c	30.5 \pm 13.9 ^c	26.9 \pm 12.1 ^d	62.6 \pm 44.6	63.0 \pm 26.4
28	30.9 \pm 7.2 ^e	n.d.	25.9 \pm 8.1 ^e	29.7 \pm 12.6 ^c	34.1 \pm 13.5 ^d
Abiraterone acetate	92.5 \pm 43.1	44.0 \pm 14.7 ^c	43.5 \pm 12.4 ^d	43.3 \pm 12.8 ^c	35.6 \pm 9.7 ^d

^a **27** and **28** were applied at a dose of 50 mg / kg body weight, abiraterone acetate at a dose of 56.02 mg / kg (corresponding to 50 mg / kg abiraterone)

^b The plasma testosterone concentrations at pre-treatment time points (-1, -0.5 and 0h) were averaged and set to 100 %. The values shown above are the relative levels compared to the pre-treatment value.

^c $P < 0.05$, ^d $P < 0.01$, ^e $P < 0.001$

n.d.: not determined

Table 5. Pharmacokinetic properties of compounds 27 and 28^a

comp.	$t_{1/2z}$ (h) ^b	t_{max} (h) ^b	C_{max} (ng / mL) ^b	$AUC_{0-\infty}$ (ng x h / mL) ^b	CL (l / kg / h) ^b
27	3.8	1.0	1745	6700	7.48
28	9.5	1.0	1277	24900	2.01
abiraterone acetate	1.6	2.0	592	4015	11.21

^a **27** and **28** were applied at a dose of 50 mg / kg body weight, abiraterone acetate at a dose of 56.02 mg / kg (corresponding to 50 mg / kg abiraterone)

^b $t_{1/2z}$: terminal half-life; t_{max} : time of maximal concentration; C_{max} : maximal concentration; $AUC_{0-\infty}$: area under the curve; CL: total body clearance (during elimination phase; assumes $F=1$)

Molecular modelling studies

No crystal structure for CYP17 is currently available, for that reason we built a homology model based on the crystal structure of human CYP2C9. Based on the different activities of compounds shown in table 1 and 2, docking simulations were carried by means of the GOLD v3.0.1 software.²⁵ The non chiral compound **22** and both enantiomers of compounds **23** and **27-31** were docked to explore the active site of the enzyme and to investigate their binding mode. Based on the suggestion that our compounds are substrate-mimetics, their binding mode was presumed to be similar to the one of the steroidal substrates and the steroidal inhibitors abiraterone and Sa40¹⁵. Abiraterone was docked into our protein model and the same binding mode as described for the substrates was found.²⁶⁻²⁷ The lone pair of the sp² hybridised nitrogen pointed perpendicular toward the heme iron. The steroidal scaffold was oriented almost parallel to the heme plane in the direction of the BC-loop. This pose was stabilized by hydrophobic interactions with Ile371, Ile112, Ala113 and Phe114.²⁶⁻²⁷ Additionally, the highly conserved Arg96 which is important for substrate binding and recognition, as shown by site directed mutagenesis,²⁸ showed interactions of the same kind with the steroidal A-ring. Another important interaction was the H-bond between the hydroxy group in C3 position and the backbone carbonyl group of Gln98.

Based on the analysis of the docking results of both enantiomers of our chiral compounds we could identify the eutomers (scoring values and deviations of docked pose of ligand to its global energetic minimum were considered). The poses of compound **22** and of the eutomers of **23** and **27-31** indicated two different orientations compared to that of the steroidal inhibitors, a primary binding mode 1 (BM1: **22**, **23 R**, GoldScore values: in a range from 48.35 to 53.45; **29 R**, **30 R**, **31 R**, GoldScore values: in a range from 67.68 to 72.02), preferred from the statistical and interaction pattern points of view, and an alternative binding mode 2 (BM2: **27 S**, **28 S**, GoldScore values: in a range from 64.85 to 69.89) (Figure 1). Compounds **22-23** and **27** showed poses in only one of the binding modes, while the other compounds were found in both ones with a clear preference for the binding mode as described above.

Starting point for these docking studies was the complexation of the heme iron by the sp² hybridized imidazole nitrogen, as it is experimentally shown that CYP inhibitors with a sterically accessible aromatic nitrogen coordinate in this way.¹⁵ Both binding modes have in common the anchoring of the alkyl substituent in a hydrophobic pocket (Figure 1A and 1B) next to the heme, which is delimited in its extent by the alkyl side-chains of Ile371, Val366, Ala367 and Thr306 (Figure 1A). The fact that compounds without methyl or ethyl substituents show no or little activity (Tables 1 and 2) indicates that interactions with this hydrophobic pocket are very important for inhibitory activity. Decisive for the different binding modes is the absence or presence of an ortho substituent at the thiophenyl ring leading to planar, thin (**27**, **28**) or twisted, thicker (**29-31**) biaryl cores of the ligands. To better understand the influence of electron-withdrawing or -releasing substituents on both A- and C-rings on the binding mode, molecular electrostatic potential (MEP) maps were plotted with GaussView 3.0⁵³ in a range of ± 12.5 kcal/mol.

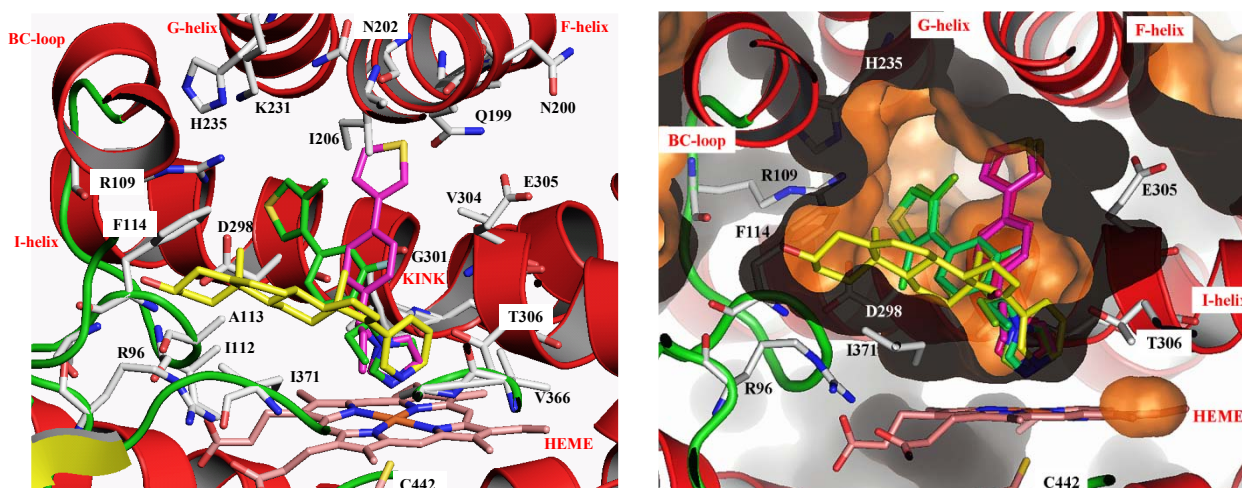


Figure 1. (A) Docking complexes between CYP17 and compounds **30** (green), **27** (magenta) and abiraterone (yellow). Further, haeme, interacting residues and ribbon rendered tertiary structure of the active site are shown. Figures were generated with Pymol (<http://www.pymol.org>). (B) A crosssection of the solvent accessible surface of CYP17 is shown in orange, revealing the active-site cavity with docked abiraterone (yellow) and all compounds in BM1 (**29-31**; green) and BM2 (**27-28** magenta).

Binding mode 2 (BM2):

Striking in this binding mode are the sterical limitations for the biaryl moiety. This is the reason why only ligands with a planar conjugated π -system (**27** and **28**) bind in this mode. The described anchoring of the alkyl substituent in the hydrophobic pocket causes the biaryl core of compounds **27** and **28** to cross the I-helix at the kink.²⁹ The thiophene-sulphur points toward the peptide bonds of Gln199 and Asn200 (F-helix), and undergoes electrostatic interactions with these amino acids. The thiophenyl ring forms hydrophobic interactions with the alkyl-groups of Gln199, Asn202, Glu203 and Ile206. The C-ring interacts with the hydrophobic alkyl side-chains of Val304 and Glu305 (Figure 1).

Binding mode 1 (BM1):

Ligands which fit in this orientation carry an ortho-substituent (**29-31**). The latter disrupts the conjugated π -system, thus twisting the angle between both rings and demanding more space. This hydrophobic, thicker biaryl core comes to lie almost parallel to the I-helix (Figure 1). The lipophilic region delimited by the kink (Gly301-Ala302-Gly303) allows good π - π -stacking with the C-ring. As MEP maps have shown, an electron withdrawing group at the C-ring, like fluorine (**30**), or in ortho-position on the thiophene, like chlorine (**31**), leads to a lower electron density on the C-ring (see Figure 2). As a consequence of this, an improvement of the π - π interactions between the π -system of this ring and the protein environment, namely the I-helix, could be observed. As a further evidence of this observation, compounds **1-9**, bearing a pyridine as C-ring, highly increasing the electron density there (MEP map not shown), shows a total loss of activity.

Additionally, the electronegative fluorine atom can form electrostatic interactions with the backbone atoms of Gly301, Ala302 and Val304, which is in agreement with the improved activity of compound **30**.

Further, in this binding mode the sulphur of the 3-thiophene points toward the polar side-chain of Arg109, allowing electrostatic interactions between the free electron pair (and perhaps d-orbitals) of the sulphur and the polar groups of Arg109 and Asp298. In addition the aromatic system of the thiophene ring undergoes T-shaped (edge-to-face) packing with Phe114, which is stabilised by Arg109, forming a very strong complex. The sulphur atom of the 2-thiophenyls (**22**, **23**) is located in a different region, thus being unable to undergo these electrostatic interactions. This might be one reason for the lack of activity of these compounds. It is striking that in this binding mode there seems to be space for the annelation of additional rings at the A- or C-ring of the biaryl moiety.

Both, the electron donating 5-ortho-methyl (**29**, **30**) and the electron withdrawing 2-ortho-chlorine (**31**) substituents decrease the electron density on the thiophene and enhance its dipole moment (negatively charged on the sulphur-C2-bond and positively on the methyl group; see MEP figure 2). The resulting relatively weak electronegativity of sulphur confers a strong aromatic character on the thiophene ring, leading to better π - π -stacking with the enzyme.

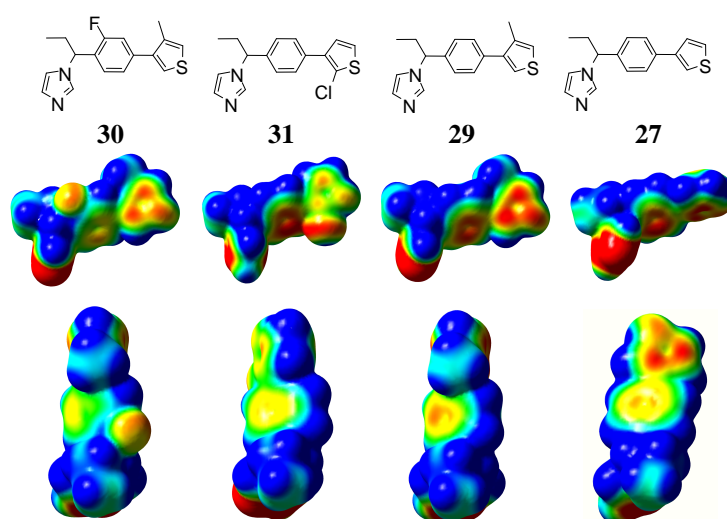


Figure 2. MEP of compounds **27**, **29**, **30** and **31**. The electrostatic potential surfaces were plotted with GaussView 3.0 in a range of $\pm 12,5$ kcal/mol.

Even more, the 5-Me group points away from the heme and could form hydrophobic interactions with Ile206. In contrast, the chlorine in 31 points toward the heme and seems to be capable of both hydrophobic (with Ile112, Ala113 and the hydrophobic CH₂-groups of Asp298) and electrostatic interactions (with the carboxylate group of Asp298, involved in a charge-cluster with Arg109 and His235).

Discussion and Conclusion

From the data shown in this paper it becomes apparent, that we succeeded in finding new lead compounds as inhibitors of CYP17. They are very potent toward the target enzyme and show less inhibition of CYP3A4 compared to ketoconazole which is used clinically. However, their inhibition of some other hepatic CYP enzymes is still too high and needs to be further improved.

The structure-activity relationships obtained in this study demonstrate that an alkyl substituent at the methylene bridge fitting into the hydrophobic pocket near the heme strongly contributes to the inhibitory potency. It also seems that electron withdrawing groups like chlorine and fluorine at the A- or C-ring are appropriate for increasing inhibition and show influence on the binding mode.

Very important is the finding that compounds of this series (**27** and **28**) showed strong in vivo activities and pharmacokinetic properties in the rat which were similar to those of abiraterone.

Interestingly, in the molecular modelling studies two distinct binding modes of our biaryl compounds were discovered, differing from the binding of the steroidal substrates and inhibitors observed by us and others.²⁶⁻²⁷ From these findings the design of modified ligands which should show a stronger interaction with the active site could be possible. On the one hand enlargement of the ligands binding in BM1 might be envisaged by annelation of additional rings to the A- or C-ring. On the other hand it could also be examined to design compounds which fill both binding cavities. Compounds modified in that way should be good candidates for showing less inhibition of hepatic CYP enzymes than the compounds of the present study. Those compounds should clinically be superior to the GnRH analogues which are presently used for the treatment of androgen dependent prostate cancer as they additionally block adrenal androgen formation thus decreasing androgen levels below those of castration.

Experimental Section

CYP17 preparation and assay

Human CYP17 was expressed in *E. coli*²² (coexpressing human CYP17 and NADPH-P450 reductase) and the assay was performed as previously described.^{23a}

Rat testicular CYP17 was obtained from adult male Sprague-Dawley rats and the assay was performed as previously described.^{23b}

Inhibition of hepatic CYP enzymes

The recombinantly expressed enzymes from baculovirus-infected insect microsomes (Supersomes) were used and the manufacturer's instructions (www.gentest.com) were followed.

In vivo study

The in vivo tests were performed in intact adult male Wistar rats (Harlan Winkelmann, Germany), 5 to 6 for each compound. These rats were cannulated with silicone tubing via the right jugular vein. The compounds were applied p.o. at 50 mg / kg body weight. The concentrations of testosterone in the rat plasma were determined using the Testosterone ELISA (EIA - 1559) from DRG Instruments according to the manufacturer's instructions. The plasma drug levels were measured by LC-MS. Non-compartmental pharmacokinetic analysis of concentration vs time data was performed for each compound on the mean plasma level using a validated computer program (PK solution 2 software; Summit Research Services, Montrose, USA). Plasma concentrations below the limit of detection were assigned a value of zero.

Chemistry Section

General

Melting points were determined on a Mettler FP1 melting point apparatus and are uncorrected. IR spectra were recorded neat on a Bruker Vector 33FT-infrared spectrometer. ¹H-NMR spectra were measured on a Bruker DRX-500 (500 MHz). Chemical shifts are given in parts per million (ppm), and TMS was used as an internal standard for spectra obtained in CDCl₃. All coupling constants (*J*) are given in Hz. ESI (electrospray ionization) mass spectra were determined on a TSQ quantum (Thermo Electron Corporation) instrument. Elemental analyses were performed at the Department of Instrumental Analysis and Bioanalysis, Saarland University. Column chromatography was

performed using silica-gel 60 (50-200 μm), and reaction progress was determined by TLC analysis on Alugram® SIL G/UV₂₅₄ (Macherey-Nagel). Boronic acids and bromoaryls used as starting materials were commercially obtained (CombiBlocks, Chempur, Aldrich, Acros).

5-Bromo-2-picoline, 1c. 2-Picoline (46.60 g, 0.50 mol) was added under nitrogen to mechanically stirred aluminium chloride (200.00 g, 1.50 mol). This slurry was heated under stirring to 100 °C, and bromine (40.00 g, 0.25 mol) was added over a period of 1 h. The heating was continued at 100 °C for 0.5 h. The reaction mixture was poured into 2 L of ice water containing 75 mL of concentrated HCl. Additional concentrated HCl was added until the mixture became acidic (pH 3). Excess NaHSO₃ (solid) was added, and the mixture was left overnight at room temperature, filtrated, and extracted with methylene chloride (3 x 150 mL). The aqueous phase was alkalisied with 50% aqueous NaOH solution and extracted with ether (4 x 150 mL). The combined organic extracts were washed with brine (100 mL) and dried. Solvent removal gave a residue, which was chromatographed on silica gel using a mixture of EtOAc / MeOH (95:5) as solvent; yield: 4.56 g (26.7 mmol, 11 % of 0.25 mol bromine used); colourless solid; R_f = 0.68 EtOAc / MeOH, 95:5); δ_H (CDCl₃, 500 MHz) 2.51 (s, 3H), 7.05 (d, J = 8.2 Hz, 1H), 7.68 (dd, J = 2.5, 8.2 Hz, 1 H), 8.55 (d, J = 2.5 Hz, 1H); δ_C (CDCl₃, 75 MHz) 23.8 (CH₃), 117.6 (C_q), 124.6 (CH), 138.8 (CH), 150.1 (CH), 156.9 (C_q); MS (ESI): m/z = 172 [M⁺+H].

2-Bromo-5-(bromomethyl)pyridine, 1b. 2-Bromo-5-methylpyridine (3.00 g, 17.40 mmol) was dissolved in 40 mL of dry carbon tetrachloride. To this solution was added *N*-bromosuccinimide (NBS) (3.41 g, 19.20 mmol) and benzoyl peroxide (0.23 g, 0.80 mmol) and the mixture was refluxed over night. After cooling, the succinimide was removed by filtration and the filtrate was concentrated under vacuum. The crude product was further purified by flash column chromatography on silica gel using a mixture of petroleum ether / EtOAc (95:5) as eluent; yield: 2.56 g (59 %); lachrymatory yellow needles; IR (ATR) ν (cm⁻¹) 3030 (m), 2923 (w), 2365 (w), 1994 (w), 1577 (s), 1556 (m), 1470 (s), 1451 (s), 1396 (m), 1379 (s), 1294 (s), 1097 (s), 920 (m), 838 (s), 810 (m), 727 (s), 645 (s), 623 (m); δ_H (CDCl₃, 500 MHz) 4.14 (s, 2H), 7.47 (d, J = 8.2 Hz, 1H), 7.59 (d, J = 8.2 Hz, 1H), 8.38 (s, 1H); MS (ESI): m/z = 252 [M⁺+H].

5-Bromo-2-(bromomethyl)pyridine, 9b. Compound **1c** (3.00 g, 17.40 mmol) was dissolved in 40 mL of dry carbon tetrachloride. To this solution was added NBS (3.41 g, 19.20 mmol) and benzoyl peroxide (0.24 g, 0.80 mmol) and the mixture was refluxed over night. After cooling, the succinimide was removed by filtration and the filtrate was concentrated under vacuum. The crude product was further purified by flash column chromatography on silica gel using petroleum ether / EtOAc (95:5) as eluent; yield: 1.70 g (39 %); lachrymatory lilac oil; IR (ATR) ν (cm⁻¹) 3038 (m), 3006 (m), 2919 (w), 2361 (w), 1983 (w), 1575 (s), 1468 (s), 1448 (s), 1374 (s), 1290 (s), 1090 (s), 1009 (s), 915 (m), 828 (s), 806 (m), 718 (s), 635 (s), 616 (m) δ_H (CDCl₃, 500 MHz) 4.24 (s, 2H), 7.16 (d, J = 8.2 Hz, 1H), 7.78 (dd, J = 2.5, 8.2 Hz, 1 H), 8.65 (d, J = 2.5 Hz, 1H); δ_C (CDCl₃, 75 MHz) 24.1 (CH₂), 118.4 (C_q), 126.5 (CH), 138.8 (CH), 151.2 (CH), 157.8 (C_q); MS (ESI): m/z = 252 [M⁺+H].

Method A: Nucleophilic Substitution with imidazole

The α -brominated compound (**1b**, **9b**), imidazole (2 eq), a catalytical amount of 18-crown-6 and anhydrous K₂CO₃ (1.5 eq) in dry acetonitrile were heated under reflux over night. After the solution was cooled down, the solvent was removed under reduced pressure. The residue was dissolved with water (10 mL / eq) and extracted three times with CH₂Cl₂ (15 mL / eq). The combined organic extracts were washed with brine, dried over anhydrous Na₂SO₄, filtered and evaporated. The crude material was purified by flash-chromatography on silica-gel, using 5% MeOH in CH₂Cl₂.

5-((1*H*-Imidazol-1-yl)methyl)-2-bromopyridine, 1a. Synthesised according to Method A using **1b** (1.32 g, 5.26 mmol), imidazole (0.75 g, 11.00 mmol), K₂CO₃ (1.13 g, 8.16 mmol) and 18-crown-6; yield: 0.75 g (60 %); yellow solid; R_f = 0.33 (EtOAc / MeOH, 9:1); δ_H (CDCl₃, 500 MHz) 5.12 (s, 2H), 6.88 (t, J = 1.2 Hz, 1H), 7.13 (s, 1H), 7.28 (d, J = 2.5 Hz, 1H), 7.48 (d, J = 8.5 Hz, 1H), 7.56 (s, 1H), 8.28 (d, J = 2.5 Hz, 1H); MS (ESI): m/z = 239 [M⁺+H].

2-((1*H*-Imidazol-1-yl)methyl)-5-bromopyridine, 9a. Synthesised according to Method A using **9b** (1.18 g, 4.70 mmol), imidazole (0.72 g, 9.60 mmol), K₂CO₃ (1.00 g, 7.24 mmol) and 18-crown-6; yield: 0.81 g (72 %); yellow solid; R_f = 0.30 (EtOAc / MeOH, 9 : 1); δ_H (CDCl₃, 500 MHz) 5.19 (s, 2H), 6.83 (d, J = 8.5 Hz, 1H), 6.96 (bs, 1H), 7.10 (s, 1H), 7.59 (s, 1H), 7.76 (dd, J = 2.1, 8.5 Hz, 1H), 8.62 (d, J = 2.1 Hz, 1H); MS (ESI): m/z = 239 [M⁺+H].

1-(4-Bromobenzyl)-1H-imidazole, 17a. Synthesised according to Method A using 1-bromo-4-(bromomethyl)benzene (6.25 g, 25.00 mmol), imidazole (6.80 g, 0.10 mol), K₂CO₃ (28.00 g, 0.20 mol) and 18-crown-6; yield: 5.06 g (85 %); *R*_f = 0.19 (EtOAc); IR (ATR) ν (cm⁻¹) 3111 (w), 1508 (m), 1489 (m), 1232 (m), 1072 (s), 1012 (m), 802 (s), 744 (s), 662 (s), 607 (m); δ _H (CDCl₃, 500 MHz) 5.00 (s, 2H), 6.81 (s, 1H), 6.94 (d, *J* = 8.4 Hz, 2H), 7.02 (s, 1H), 7.40 (d, *J* = 8.4 Hz, 2H), 7.46 (s, 1H); δ _C (CDCl₃, 125 MHz) 52.9 (CH₂), 118.2 (CH), 121.3 (C_q), 127.9 (CH), 129.0 (CH), 131.1 (CH), 134.2 (C_q), 136.3 (CH); MS (ESI): *m/z* = 239/237 [M⁺+H].

Method B: Suzuki-Coupling

The corresponding brominated aromatic compound (1 eq) was dissolved in toluene (7 mL / mmol), an aqueous 2.0 M Na₂CO₃ solution (3.2 mL / mmol) and an ethanolic solution (3.2 mL / mmol) of the corresponding boronic acid (1.5-2.0 eq) were added. The mixture was deoxygenated under reduced pressure and flushed with nitrogen. After repeating this cycle several times Pd(PPh₃)₄ (4 mol%) was added and the resulting suspension was heated under reflux for 8 h. After cooling ethyl acetate (10 mL) and water (10 mL) were added and the organic phase was separated. The water phase was extracted with ethyl acetate (2 x 10 mL). The combined organic phases were washed with brine, dried over Na₂SO₄, filtered over a short plug of celite® and evaporated under reduced pressure. The compounds were purified by flash chromatography on silica gel.

5-((1H-Imidazol-1-yl)methyl)-2-(3-methoxyphenyl)pyridine, 1. Synthesised according to Method B using compound **1a** (0.20 g, 0.84 mmol) and 3-methoxyphenylboronic acid (0.19 g, 1.26 mmol); yield: 0.05 g (18 %); yellow solid: mp 99 °C; *R*_f = 0.31 (CH₂Cl₂ / MeOH, 95:5); IR (ATR) ν (cm⁻¹) 2962 (w), 2926 (w), 1565 (m), 1477 (m), 1261 (m), 1072 (m), 1023 (s), 799 (m), 766 (s), 665 (m); δ _H (CDCl₃, 500 MHz) 3.85 (s, 3H), 5.13 (s, 2H), 6.89 (s, 1H), 6.94 (ddd, *J* = 0.9, 2.5, 8.2 Hz, 1H), 7.09 (s, 1H), 7.34 (t, *J* = 8.2 Hz, 1H), 7.44 (dd, *J* = 2.5, 8.2 Hz, 1H), 7.49 (m, 1H), 7.54 (m, 1H), 7.66 (d, *J* = 8.2 Hz, 1H), 8.53 (d, *J* = 2.2 Hz, 1H); δ _C (CDCl₃, 125 MHz) 48.0 (CH₂), 55.3 (CH₃), 112.1 (CH), 115.3 (CH), 119.0 (CH), 119.2 (CH), 120.6 (CH), 129.8 (CH), 130.1 (C_q), 130.2 (CH), 135.7 (CH), 137.2 (CH), 140.0 (C_q), 148.4 (CH), 157.3 (C_q), 160.0 (C_q); MS (ESI): *m/z* = 252 [M⁺+H].

5-((1H-Imidazol-1-yl)methyl)-2-phenylpyridine, 2. Synthesised according to Method B using compound **1a** (0.20 g, 0.84 mmol) and phenylboronic acid (0.20 g, 1.68 mmol); yield: 0.10 g (57 %); yellow solid: mp 99 °C; *R*_f = 0.35 (CH₂Cl₂ / MeOH 95:5); IR (ATR) ν (cm⁻¹) 2925 (s), 1503 (m), 1476 (s), 1344 (m), 1290 (m), 1110 (m), 1081 (s), 908 (m), 839 (s), 731 (s), 625 (m); δ _H (CDCl₃, 500 MHz) 5.19 (s, 2H), 6.94 (t, *J* = 1.3 Hz, 1H), 7.13 (s, 1H), 7.48-7.50 (m, 4H), 7.60 (s, 1H), 7.72 (d, *J* = 8.2 Hz, 1H), 7.97-7.99 (m, 1H); δ _C (CDCl₃, 125 MHz) 48.1 (CH₂), 119.0 (CH), 120.6 (CH), 126.9 (CH), 128.8 (CH), 130.0 (CH), 130.4 (C_q), 135.7 (CH), 137.3 (CH), 138.6 (C_q), 148.6 (CH) 157.7 (C_q); MS (ESI): *m/z* = 236 [M⁺+H].

5-((1H-Imidazol-1-yl)methyl)-2-(4-fluorophenyl)pyridine, 3. Synthesised according to Method B using compound **1a** (0.20 g, 0.84 mmol) and 4-fluorophenylboronic acid (0.23 g, 1.68 mmol); yield: 0.16 g (76 %); yellow solid: mp 95 °C; *R*_f = 0.15 (EtOAc / MeOH, 9:1); IR (ATR) ν (cm⁻¹) 3101 (w), 1598 (m), 1511 (m), 1478 (m), 1390 (w), 1231 (m), 1083 (m), 1026 (w), 910 (w), 824 (w), 770 (m), 737 (s), 663 (m); δ _H (CDCl₃, 500 MHz) 5.18 (s, 2H), 6.92 (s, 1H), 7.12 (bs, 1H), 7.15 (t, *J* = 8.8 Hz, 2H), 7.48 (dd, *J* = 2.2, 8.2 Hz, 1H), 7.60 (s, 1H), 7.67 (d, *J* = 8.2 Hz, 1H), 7.97 (dd, *J* = 5.4, 8.8 Hz, 2H), 8.57 (d, *J* = 1.9 Hz, 1H); δ _C (CDCl₃, 125 MHz) 48.1 (CH₂), 115.7 (d, ²*J*_{CF} = 22.1 Hz, CH), 119.0 (CH), 120.2 (CH), 128.7 (d, ³*J*_{CF} = 8.6 Hz, CH), 130.0 (C_q), 130.4 (CH), 134.7 (d, ⁴*J*_{CF} = 3.9 Hz, C_q), 135.8 (CH), 137.3 (CH), 148.6 (CH), 156.6 (C_q), 163.7 (d, ¹*J*_{CF} = 249.5 Hz, C_q); MS (ESI): *m/z* = 254 [M⁺+H].

5-((1H-Imidazol-1-yl)methyl)-2-(3,4-difluorophenyl)pyridine, 4. Synthesised according to Method B using compound **1a** (0.20 g, 0.84 mmol) and 3,4-difluorophenylboronic acid (0.27 g, 1.68 mmol); yield: 0.21 g (91 %); yellow solid: mp 100 °C, *R*_f = 0.16 (EtOAc / MeOH, 9:1); IR (ATR) ν (cm⁻¹) 3106 (w), 2930 (w), 2856 (w), 1599 (m), 1567 (m), 1523 (s), 1507 (s), 1481 (s), 784 (s); δ _H (CDCl₃, 500 MHz) 5.18 (s, 2H), 6.92 (t, *J* = 1.3 Hz, 1H), 7.13 (t, *J* = 1.3 Hz, 1H), 7.25 (ddd, *J* = 8.2, 8.5, 9.8 Hz, 1H), 7.49 (dd, *J* = 2.5, 8.2 Hz, 1H), 7.59 (s, 1H), 7.66 (dd, *J* = 0.6, 8.3 Hz, 1H), 7.69-7.73 (m, 1H), 7.86 (ddd, *J* = 2.2, 7.6, 11.4 Hz, 1 H), 8.56 (dd, *J* = 0.6, 2.3 Hz, 1H); δ _C (CDCl₃, 125 MHz) 48.0 (CH₂), 116.0 (d, ²*J*_{CF} = 18.2 Hz, CH), 117.6 (d, ²*J*_{CF} = 17.3 Hz, CH), 119.0 (CH), 120.2 (CH), 122.8 (dd, ⁴*J*_{CF} = 3.8 Hz, ³*J*_{CF} = 6.7 Hz, CH), 130.4 (CH), 130.6 (C_q), 135.6 (dd, ⁴*J*_{CF} = 3.8 Hz, ³*J*_{CF} = 5.8 Hz, C_q), 135.9 (CH), 137.3 (CH), 148.6 (CH), 150.8 (dd, ²*J*_{CF} = 20.2 Hz, ¹*J*_{CF} = 255.3 Hz, C_q), 151.3 (dd, ²*J*_{CF} = 15.4 Hz, ¹*J*_{CF} = 254.3 Hz, C_q), 155.3 (C_q); MS (ESI): *m/z* = 272 [M⁺+H].

5-((1H-Imidazol-1-yl)methyl)-2-(4-methoxyphenyl)pyridine, 5. Synthesised according to Method B using compound **1a** (0.40 g, 1.68 mmol) and 4-methoxyphenylboronic acid (0.38 g, 3.35 mmol); yield: 0.40 g (89 %); yellow solid: mp 138 °C; *R*_f = 0.15 (EtOAc / MeOH, 9:1); IR (ATR) ν (cm⁻¹) 2962 (w), 2928 (w), 1597 (m), 1478 (m), 1249 (s), 1174 (m), 1023 (m), 828 (s), 814 (s), 762 (s); δ _H (CDCl₃, 500 MHz) 3.86 (s, 3H), 5.16 (s, 2H), 6.92 (t, *J* = 1.3 Hz, 1H), 6.99 (d, *J* = 9.1 Hz, 2H), 7.11 (s, 1H), 7.46 (dd, *J* = 2.5, 8.2 Hz, 1H), 7.59 (s, 1H), 7.66 (d, *J* = 8.2

Hz, 1H), 7.94 (d, $J = 9.1$ Hz, 2H), 8.54 (d, $J = 2.5$ Hz, 1H); δ_C (CDCl₃, 125 MHz) 48.1 (CH₂), 55.4 (CH₃), 114.2 (CH), 119.0 (CH), 119.8 (CH), 128.2 (CH), 129.2 (C_q), 130.3 (CH), 131.2 (C_q), 135.7 (CH), 137.3 (CH), 148.5 (CH), 157.4 (C_q), 160.8 (C_q); MS (ESI): $m/z = 266$ [M⁺+H].

5-((1H-Imidazol-1-yl)methyl)-2-(2-methoxyphenyl)pyridine, 6. Synthesised according to Method B using compound **1a** (0.20 g, 0.84 mmol) and 2-methoxyphenylboronic acid (0.19 g, 1.68 mmol); yield: 0.21 g (92 %); yellow solid: mp 103 °C; $R_f = 0.15$ (EtOAc / MeOH, 9:1); IR (ATR) ν (cm⁻¹) 2924 (m), 2854 (m), 1598 (m), 1477 (s), 1395 (m), 1261 (m), 1237 (s), 1079 (m), 1022 (s), 835 (m), 795 (s), 665 (s); δ_H (CDCl₃, 500 MHz) 3.85 (s, 3H), 5.17 (s, 2H), 6.95 (bs, 1H), 7.00 (dd, $J = 0.6, 8.5$ Hz, 1H), 7.08 (dt, $J = 1.1, 7.6$ Hz, 1H), 7.12 (s, 1H), 7.38 (ddd, $J = 1.9, 7.6, 8.5$ Hz, 1H), 7.44 (dd, $J = 2.2, 8.5$ Hz, 1H), 7.60 (s, 1H), 7.77 (dd, $J = 1.9, 7.6$ Hz, 1H), 7.83 (d, $J = 8.2$ Hz, 1H), 8.60 (d, $J = 1.6$ Hz, 1H); δ_C (CDCl₃, 125 MHz) 48.2 (CH₂), 55.6 (CH₃), 111.4 (CH), 119.1 (CH), 121.1 (CH), 125.2 (CH), 128.3 (C_q), 129.5 (C_q), 130.2 (CH), 130.3 (CH), 131.1 (CH), 134.6 (CH), 137.3 (CH), 148.2 (CH), 156.4 (C_q), 157.0 (C_q); MS (ESI): $m/z = 266$ [M⁺+H].

3-(5-((1H-Imidazol-1-yl)methyl)pyridin-2-yl)benzenamine, 7. Synthesised according to Method B using compound **1a** (0.20 g, 0.84 mmol) and 2-methoxyphenylboronic acid (0.29 g, 1.68 mmol); yield: 0.14 g (67 %); orange solid: mp 145 °C; $R_f = 0.11$ (EtOAc / MeOH, 9:1); IR (ATR) ν (cm⁻¹) 3406 (w), 3408 (w), 3323 (w), 3212 (w), 2957 (m), 2924 (m), 2854 (m), 1630 (m), 1600 (s), 1476 (s), 1235 (m), 1105 (s), 1073 (s), 1026 (s), 787 (s), 758 (s); δ_H (CDCl₃, 500 MHz) 5.11 (s, 2H), 6.72 (ddd, $J = 0.9, 2.4, 7.6$ Hz, 1H), 6.89 (bs, 1H), 7.08 (bs, 1H), 7.21 (t, $J = 7.7$ Hz, 1H), 7.28 (dt, $J = 1.3, 7.8$ Hz, 1H), 7.33 (t, $J = 2.2$ Hz, 1H), 7.41 (dd, $J = 2.2, 8.2$ Hz, 1H), 7.55 (bs, 1H), 7.62 (d, $J = 8.2$ Hz, 1H), 8.50 (d, $J = 2.2$ Hz, 1H); δ_C (CDCl₃, 125 MHz) 48.0 (CH₂), 113.3 (CH), 116.0 (CH), 117.0 (CH), 119.0 (CH), 120.5 (CH), 129.6 (CH), 129.9 (C_q), 130.1 (CH), 135.6 (CH), 137.2 (CH), 139.5 (C_q), 146.9 (C_q), 148.3 (CH), 157.6 (C_q); MS (ESI): $m/z = 251$ [M⁺+H].

5-((1H-Imidazol-1-yl)methyl)-2-(3,4-dimethoxyphenyl)pyridine, 8. Synthesised according to Method B using compound **1a** (0.40 g, 1.68 mmol) and 3,4-dimethoxyphenylboronic acid (0.61 g, 3.36 mmol); yield: 0.47 g (94 %); yellow solid: mp 114 °C; $R_f = 0.16$ (EtOAc / MeOH 9:1); IR (ATR) ν (cm⁻¹) 3110 (w), 3086 (w), 3002 (w), 2960 (w), 2926 (w), 2855 (w), 1596 (m), 1519 (m), 1477 (m), 1280 (m), 1150 (m), 1022 (s), 808 (s), 764 (s), 666 (m); δ_H (CDCl₃, 500 MHz) 3.93 (s, 3H), 3.98 (s, 3H), 5.16 (s, 2H), 6.92 (bs, 1H), 6.94 (d, $J = 8.5$ Hz, 1H), 7.11 (bs, 1H), 7.46 (dd, $J = 2.2, 8.5$ Hz, 1H), 7.47 (dd, $J = 2.2, 8.5$ Hz, 1H), 7.58 (bs, 1H), 7.65 (d, $J = 2.2$ Hz, 1H), 7.67 (d, $J = 8.5$ Hz, 1H), 8.54 (d, $J = 2.2$ Hz, 1H); δ_C (CDCl₃, 125 MHz) 48.1 (CH₂), 56.0 (CH₃), 56.0 (CH₃), 113.3 (CH), 110.0 (CH), 111.1 (CH), 119.0 (CH), 119.5 (CH), 120.0 (CH), 129.4 (C_q), 130.3 (CH), 131.4 (C_q), 135.7 (CH), 148.4 (CH), 149.4 (C_q), 150.3 (C_q), 157.3 (C_q); MS (ESI): $m/z = 296$ [M⁺+H].

2-((1H-Imidazol-1-yl)methyl)-5-(4-fluorophenyl)pyridine, 9. Synthesised according to Method B using compound **9a** (0.20 g, 0.84 mmol) and 4-fluorophenylboronic acid (0.23 g, 1.68 mmol); yield: 0.18 g (83 %); yellow solid: mp 90 °C; $R_f = 0.11$ (EtOAc / MeOH, 9:1); IR (ATR) ν (cm⁻¹) 3116 (w), 3046 (w), 2927 (w), 1064 (m), 1519 (m), 1486 (s), 1393 (w), 1220 (s), 1163 (m), 1070 (s), 906 (w), 828 (s), 817 (s), 769 (s), 684 (s), 660 (s); δ_H (CDCl₃, 500 MHz) 5.29 (s, 2H), 7.02 (m, 2H), 7.14 (brs, 1H), 7.17 (t, $J = 8.8$ Hz, 2H), 7.52 (dd, $J = 5.4, 8.8$ Hz, 1H), 7.65 (s, 1H), 7.79 (dd, $J = 2.2, 8.2$ Hz, 2H), 8.76 (d, $J = 2.2$ Hz, 1H); δ_C (CDCl₃, 125 MHz) 52.3 (CH₂), 116.2 (d, $^2J_{CF} = 22.1$ Hz, CH), 119.5 (CH), 121.1 (CH), 128.8 (d, $^3J_{CF} = 8.6$ Hz, CH), 130.0 (CH), 130.4 (CH), 133.2 (d, $^4J_{CF} = 3.8$ Hz, C_q), 135.2 (C_q), 135.4 (CH), 148.0 (CH), 154.9 (C_q), 163.0 (d, $^1J_{CF} = 247.6$ Hz, C_q); MS (ESI): $m/z = 254$ [M⁺+H].

4-Phenylthiophene-2-carbaldehyde, 10b. Synthesised according to Method B using phenylboronic acid (0.49 g, 2.00 mmol) and 4-bromothiophen-2-carbaldehyde (0.38 g, 2.00 mmol); yield: 0.35 g (93 %); white solid: mp 57-58 °C; $R_f = 0.39$ (PE / EtOAc, 10:1); IR (ATR) ν (cm⁻¹) 3096 (w), 2838 (w), 1670 (s), 1597 (w), 1430 (m), 1247 (w), 1180 (s), 1048 (w), 755 (s), 695 (m), 660 (s); δ_H (CDCl₃, 500 MHz) 7.36 (m, 1H), 7.44 (dd, $J = 7.3, 7.9$ Hz, 2H), 7.59 (dd, $J = 1.3$ Hz, 8.5 Hz, 2H), 7.85 (dd, $J = 1.3$ Hz, 1.6 Hz, 1H), 8.03 (d, $J = 1.6$ Hz, 1H), 9.97 (d, $J = 1.3$ Hz, 1H); δ_C (CDCl₃, 125 MHz) 115.3 (CH), 126.3 (CH), 128.0 (CH), 129.1 (CH), 129.6 (CH), 134.4 (C_q), 143.7 (C_q), 144.4 (C_q), 183.0 (CH); MS (ESI): $m/z = 189$ [M⁺+H].

4-(4-Fluorophenyl)-thiophene-2-carbaldehyde, 11b. Synthesised according to Method B using 4-fluorophenylboronic acid (0.56 g, 4.00 mmol) and 4-bromothiophen-2-carbaldehyde (0.38 g, 2.00 mmol); yield: 0.38 g (92 %); white solid: mp 76-78 °C; $R_f = 0.34$ (PE / EtOAc, 10:1); IR (ATR) ν (cm⁻¹) 2945 (w), 2839 (w), 1665 (s), 1547 (m), 1507 (s), 1435 (m), 1228 (s), 1216 (s), 1181 (m), 829 (s), 666 (s), 566 (s); δ_H (CDCl₃, 500 MHz) 7.13 (dd, $J = 8.5, 8.8$ Hz, 2H), 7.55 (dd, $J = 5.4, 8.8$ Hz, 2H), 7.79 (dd, $J = 1.3, 1.6$ Hz, 1H), 7.98 (d, $J = 1.6$ Hz, 1H), 9.97 (d, $J = 1.3$ Hz, 1H); δ_C (CDCl₃, 125 MHz) 116.0 (d, $^2J_{CF} = 22.1$ Hz, CH), 128.0 (d, $^3J_{CF} = 8.6$ Hz, CH), 129.3 (CH), 130.6 (d, $^4J_{CF} = 3.6$ Hz, C_q), 134.4 (CH), 142.6 (C_q), 144.6 (C_q), 162.6 (d, $^1J_{CF} = 247.6$ Hz, C_q), 182.8 (CH); MS (ESI): $m/z = 207$ [M⁺+H].

4-(4-Methoxyphenyl)-thiophene-2-carbaldehyde, 12b. Synthesised according to Method B using 4-methoxyphenylboronic acid (0.34 g, 2.25 mmol) and 4-bromothiophene-2-carbaldehyde (0.29 g, 1.50 mmol); yield: 0.25 g (76 %); white solid; mp 72 °C; $R_f = 0.34$ (PE / EtOAc, 10:1); IR (ATR) ν (cm⁻¹) 1512 (m), 1406 (m), 1309 (m), 1246 (m), 1180 (m), 1026 (s), 832 (s), 756 (m), 521 (m); δ_H (CDCl₃, 500 MHz) 3.85 (s, 3H), 6.96 (d, $J = 8.8$ Hz, 2H), 7.52 (d, $J = 8.8$ Hz, 2H), 7.75 (dd, $J = 1.3, 1.6$ Hz, 1H), 7.98 (d, $J = 1.6$ Hz, 1H), 9.96 (d, $J = 1.3$ Hz, 1H); δ_C (CDCl₃, 125 MHz) 55.4 (CH₃), 114.5 (CH), 127.3 (C_q), 127.5 (CH), 128.4 (CH), 134.5 (CH), 143.4 (C_q), 144.3 (C_q), 159.6 (C_q), 183.0 (CH); MS (ESI): $m/z = 219$ [M⁺+H].

4-(3-Methoxyphenyl)-thiophene-2-carbaldehyde, 13b. Synthesised according to Method B using 3-methoxyphenylboronic acid (0.61 g, 4.00 mmol) and 4-bromothiophen-2-carbaldehyde (0.38 g, 2.00 mmol); yield: 0.25 g (76 %); white solid; mp 225 °C; $R_f = 0.41$ (PE / EtOAc, 10:1); IR (ATR) ν (cm⁻¹) 2836 (w), 1666 (s), 1600 (m), 1458 (m), 1258 (m), 1161 (s), 1039 (m), 850 (m), 771 (s), 689 (m), 666 (s); δ_H (CDCl₃, 500 MHz) 3.87 (s, 3H), 6.90 (ddd, $J = 1.0, 2.5, 8.5$ Hz, 1H), 7.11 (dd, $J = 1.9, 2.5$ Hz, 1H), 7.17 (ddd, $J = 1.0, 1.9, 7.9$ Hz, 1H), 7.36 (dd, $J = 7.9, 8.5$ Hz, 1H), 7.85 (dd, $J = 1.3, 1.6$ Hz, 1H), 8.02 (d, $J = 1.6$ Hz, 1H), 9.97 (d, $J = 1.3$ Hz, 1H); δ_C (CDCl₃, 125 MHz) 55.3 (CH₃), 112.3 (CH), 113.3 (CH), 118.8 (CH), 129.8 (CH), 130.1 (CH), 134.7 (CH), 135.7 (C_q), 143.5 (C_q), 144.4 (C_q), 160.1 (C_q), 182.9 (CH); MS (ESI): $m/z = 219$ [M⁺+H].

4-(3,4-Difluorophenyl)-thiophene-2-carbaldehyde, 14b. Synthesised according to Method B using 3,4-difluorophenylboronic acid (0.63 g, 4.00 mmol) and 4-bromothiophen-2-carbaldehyde (0.38 g, 2.00 mmol); yield: 0.43 g (96 %); white solid; mp 115-116 °C; $R_f = 0.35$ (PE / EtOAc, 10:1); IR (ATR) ν (cm⁻¹) 3051 (w), 1658 (s), 1517 (s), 1447 (m), 1352 (m), 1278 (s), 1190 (s), 852 (m), 816 (s), 772 (s), 670 (s), 601 (s), 574 (s); δ_H (CDCl₃, 500 MHz) 7.23 (ddd, $J = 8.2, 8.5, 10.1$ Hz, 1H), 7.29-7.32 (m, 1H), 7.38 (ddd, $J = 2.2, 7.6, 11.4$ Hz, 1H), 7.80 (dd, $J = 1.3, 1.6$ Hz, 1H), 7.95 (d, $J = 1.6$ Hz, 1H), 9.97 (d, $J = 1.3$ Hz, 1H); δ_C (CDCl₃, 125 MHz) 115.4 (d, $^2J_{CF} = 18.2$ Hz, CH), 118.0 (d, $^2J_{CF} = 18.2$ Hz, CH), 122.4 (dd, $^4J_{CF} = 3.8$ Hz, $^3J_{CF} = 6.7$ Hz, CH), 129.9 (CH), 131.6 (dd, $^4J_{CF} = 3.8$ Hz, $^3J_{CF} = 6.7$ Hz, C_q), 134.1 (CH), 141.5 (C_q), 144.8 (C_q), 150.0 (dd, $^2J_{CF} = 58.5$ Hz, $^1J_{CF} = 249.5$ Hz, C_q), 150.1 (dd, $^2J_{CF} = 59.5$ Hz, $^1J_{CF} = 249.5$ Hz, C_q), 182.7 (CH); MS (ESI): $m/z = 225$ [M⁺+H].

3-(4-((1H-Imidazol-1-yl)methyl)phenyl)pyridine, 17. Synthesised according to Method B using compound **17a** (0.24 g, 1.00 mmol) and pyridine-3-boronic acid (0.25 g, 2.00 mmol); yield: 0.17 g (73 %); $R_f = 0.20$ (EtOAc / MeOH, 9:1); IR (ATR) ν (cm⁻¹) 3384 (m), 3115 (w), 1509 (m), 1225 (s), 1081 (s), 1030 (m), 1005 (m), 804 (s), 747 (s), 708 (s), 669 (s); δ_H (CDCl₃, 500 MHz) 5.09 (s, 2H), 6.85 (s, 1H), 7.02 (s, 1H), 7.17 (d, $J = 8.2$ Hz, 2H), 7.27 (ddd, $J = 1.0, 4.7, 8.0$ Hz, 1H), 7.47 (d, $J = 8.2$ Hz, 2H), 7.50 (s, 1H), 7.76 (ddd, $J = 1.6, 2.4, 8.0$ Hz, 1H), 8.50 (dd, $J = 1.6, 4.7$ Hz, 1H), 8.73 (d, $J = 1.6$ Hz, 1H); δ_C (CDCl₃, 125 MHz) 49.4 (CH₂), 118.2, 126.6, 126.7, 128.9, 133.3, 134.8, 135.1, 136.5, 136.8, 147.0, 147.9; MS (ESI): $m/z = 236$ [M⁺+H].

5-(4-((1H-Imidazol-1-yl)methyl)phenyl)-2-fluoropyridine, 18. Synthesised according to Method B using compound **17a** (0.24 g, 1.00 mmol) and 4-fluoropyridine-3-boronic acid (0.28 g, 2.00 mmol); yield: 0.14 g (56 %); $R_f = 0.20$ (EtOAc); IR (ATR) ν (cm⁻¹) 3108 (w), 1592 (m), 1497 (s), 1250 (s), 1075 (m), 813 (s), 737 (m), 684 (s); δ_H (CDCl₃, 500 MHz) 5.10 (s, 2H), 6.85 (s, 1H), 6.91 (dd, $J = 2.6, 8.6$ Hz, 1H), 7.02 (s, 1H), 7.18 (d, $J = 8.3$ Hz, 2H), 7.43 (d, $J = 8.3$ Hz, 2H), 7.50 (s, 1H), 7.86 (ddd, $J = 2.6, 7.5, 10.1$ Hz, 1H), 8.29 (d, $J = 2.6$ Hz, 1H); δ_C (CDCl₃, 125 MHz) 49.3 (CH₂), 108.6 (d, $^2J_{CF} = 38.7$ Hz, CH), 118.3 (CH), 126.6 (CH), 127.0 (CH), 129.0 (CH), 133.0 (d, $^4J_{CF} = 4.6$ Hz, C_q), 135.3 (CH), 135.7 (C_q), 136.4 (C_q), 138.6 (d, $^3J_{CF} = 7.7$ Hz, CH), 144.7 (d, $^3J_{CF} = 15.5$ Hz, CH), 162.0 (d, $^1J_{CF} = 238.9$ Hz, C_q); MS (ESI): $m/z = 254$ [M⁺+H].

1-(4-(5-(Methylthio)thiophen-2-yl)benzyl)-1H-imidazole, 22. Synthesised according to Method B using compound **17a** (0.12 g, 0.50 mmol) and 5-(methylsulfanyl)-2-thiophenylboronic acid (0.17 g, 1.00 mmol); light brown solid; mp 139-140 °C; $R_f = 0.17$ (EtOAc / MeOH, 10:1); IR (ATR) ν (cm⁻¹) 1503 (m), 1442 (m), 1226 (m), 1078 (s), 849 (m), 802 (s), 756 (s), 741 (s), 661 (s); δ_H (CDCl₃, 500 MHz) 2.50 (d, $J = 1.0$ Hz, 3H), 5.11 (s, 2H), 6.72-6.73 (m, 1H), 6.91 (t, $J = 1.3$ Hz, 1H), 7.09 (d, $J = 1.6$ Hz, 1H), 7.10 (s, 1H), 7.13 (d, $J = 8.3$ Hz, 2H), 7.52 (d, $J = 8.3$ Hz, 2H), 7.57 (s, 1H); δ_C (CDCl₃, 125 MHz) 15.4 (CH₃), 50.5 (CH₂), 119.2 (CH), 123.3 (CH), 125.9 (CH), 126.3 (CH), 127.8 (CH), 129.8 (CH), 134.6 (C_q), 134.8 (C_q), 137.4 (CH), 140.0 (C_q), 141.0 (C_q); MS (ESI): $m/z = 255$ [M⁺+H].

1-(4-(5-Methylsulfanyl-thiophen-2-yl)-phenyl)propan-1-one, 23b. Synthesised according to Method B from 5-(methylthio)thiophen-2-yl-2-boronic acid (1.00 g, 6.30 mmol) and 1-(4-bromophenyl) propan-1-one (1.10 g, 5.20 mmol); yield: 1.19 g (88 %); white solid; $R_f = 0.63$ (Hex / EtOAc, 4:1); IR (ATR) ν (cm⁻¹) 1678 (s), 1597 (s), 1462 (s), 1409 (m), 1349 (m), 1220 (s), 1181 (s), 1112 (m), 1012 (m), 949 (s), 796 (vs); δ_H (CDCl₃, 500 MHz) 1.23 (t, $J = 7.3$ Hz, 3H, CH₃), 2.53 (s, 3H, S-CH₃), 2.99 (q, $J = 7.3$ Hz, 2H, CH₂), 6.76-6.77 (m, 1H), 7.22-7.26 (m, 1H), 7.60-7.62 (m, 2H), 7.94-7.95 (m, 2H); δ_C (CDCl₃, 125 MHz) 8.3 (CH₃), 15.1 (S-CH₃), 31.7 (CH₂), 124.5, 125.3, 128.3, 134.7, 138.3, 140.5, 141.3, 200.9 (CO); MS (ESI): $m/z = 233$ [M⁺-Et].

1-(4-Bromophenyl)-2-methyl-1-(1-trityl-1H-imidazol-5-yl)propan-1-ol, 24a. The preparation of **24a** has been reported previously by Tasaka, A. et al.²¹

1-(1H-Imidazol-5-yl)-2-methyl-1-(4-(thiophen-3-yl)phenyl)propan-1-ol, 24. Synthesised according to Method B using compound **24a** (0.17 g, 0.31 mmol) and thiophen-3-ylboronic acid (0.08 g, 0.62 mmol), and DME as solvent. The crude was then deprotected with pyridinium hydrochloride (0.05 g, 0.44 mmol) in MeOH (5 ml) at 80 °C for 5 h; yield: 0.03 g (34 %); light-yellow solid; $R_f = 0.36$ (DCM / MeOH, 9:1); IR (ATR) ν (cm^{-1}) 3122 (w), 1506 (w), 1457 (w), 1179 (w), 1003 (w), 948 (w), 865(m), 779 (s), 733, 681 (m), 669 (m), 649 (m), 567 (m), 532 (s), 517 (s); δ_H (CDCl_3 , 500 MHz) 0.77 (d, $J = 6.1$ Hz, 3H), 0.94 (d, $J = 4.8$ Hz, 3H), 2.50-2.60 (m, 1H), 6.91 (s, 1H), 7.33 (s, 2H), 7.38 (s, 1H), 7.40-7.53 (m, 5H); δ_C (CDCl_3 , 125 MHz) 17.3 (CH_3), 17.3 (CH_3), 30.3 (CH), 37.3 (C_q), 120.1 (CH), 125.2, 125.4, 125.5, 125.8, 125.9, 125.9, 126.1, 126.2, 126.3, 126.4, 126.6, 134.1 (C_q), 141.9 (C_q); MS (ESI): $m/z = [\text{M}^+ + \text{H}]$.

1-(4-(Furan-3-yl)benzyl)-1H-imidazole, 25. Synthesised according to Method B using compound **17a** (0.24 g, 1.00 mmol) and furan-3-ylboronic acid (0.22 g, 2.00 mmol); yield: 0.16 g (73 %); $R_f = 0.17$ (EtOAc); IR (ATR) ν (cm^{-1}) 3102 (w), 1518 (m), 1439 (m), 1242 (m), 1161 (m), 1071 (m), 872 (m), 784 (s), 751 (s), 662 (s), 597 (s); δ_H (CDCl_3 , 500 MHz) 5.05 (s, 2H), 6.61 (dd, $J = 1.8, 0.9$ Hz, 1H), 6.84 (t, $J = 1.2$ Hz, 1H), 7.03 (s, 1H), 7.09 (d, $J = 8.2$ Hz, 2H), 7.39 (d, $J = 8.2$ Hz, 2H), 7.41 (m, 1H), 7.49 (s, 1H), 7.66 (s, 1H); δ_C (CDCl_3 , 125 MHz) 49.5 (CH_2), 107.7 (CH), 118.2 (CH), 124.8 (C_q), 125.4 (CH), 126.8 (CH), 128.9 (CH), 131.6 (C_q), 133.7 (C_q), 136.4 (CH), 137.7 (CH), 142.8 (CH); MS (ESI): $m/z = 225 [\text{M}^+ + \text{H}]$.

1-(4-(4-Methylthiophen-3-yl)benzyl)-1H-imidazole, 26. Synthesised according to Method B using compound **17a** (0.24 g, 1.00 mmol) and furan-2-ylboronic acid (0.28 g, 2.00 mmol); red oil; bp > 200 °C; yield: 0.17 g (68 %); $R_f = 0.35$ (EtOAc / MeOH, 9:1); IR (ATR) ν (cm^{-1}) 1505 (m), 1230 (m), 1075 (m), 792 (s), 729 (m), 662 (s); δ_H (CDCl_3 , 500 MHz) 2.25 (s, 3H), 5.16 (s, 2H), 6.95 (bs, 1H), 7.02-7.03 (m, 1H), 7.12 (bs, 1H), 7.18-7.20 (m, 3H), 7.38 (d, $J = 8.2$ Hz, 2H), 7.60 (bs, 1H); δ_C (CDCl_3 , 125 MHz) 15.5 (CH_3), 50.6 (CH_2), 119.3 (CH), 122.2 (CH), 123.3 (CH), 127.2 (CH), 129.1 (CH), 129.7 (CH), 134.8 (C_q), 136.0 (C_q), 137.2 (C_q), 137.4 (CH), 142.2 (C_q).

1-(4-(4-Methylthiophen-3-yl)phenyl)propan-1-one, 29b. Synthesised according to Method B from 4-methylthiophen-3-yl-3-boronic acid (0.80 g, 6.30 mmol) and 1-(4-bromophenyl)propan-1-one (1.36 g, 6.40 mmol); yield: 0.96 g (80 %); white solid; $R_f = 0.68$ (Hex / EtOAc, 4:1); δ_H (CDCl_3 , 500 MHz) 1.25 (t, $J = 7.3$ Hz, 3H, CH_3), 2.29 (s, 3H, CH_3), 3.01-3.06 (q, 2H, CH_2), 7.05-7.06 (m, 1H), 7.26-7.27 (m, 1H), 7.48-7.50 (m, 2H), 8.00-8.02 (m, 2H); δ_C (CDCl_3 , 125 MHz) 8.3 (CH_3), 31.8 (CH_2), 122.6, 123.9, 128.1, 128.6, 135.4, 135.9, 141.6, 142.0, 200.3 (C=O); MS (ESI): $m/z = 231 [\text{M}^+ + \text{H}]$.

2-Fluoro-4-(4-methylthiophen-3-yl)benzaldehyde, 30b. Synthesised according to Method B from 4-bromo-2-fluorobenzaldehyde (1.36 g, 6.40 mmol) and 4-methylthiophen-3-yl-3-boronic acid (1.42 g, 7.10 mmol). This compound was used directly in the next step without further purification.

4-(2-Chlorothiophen-3-yl)-benzaldehyde, 31b. Synthesised according to Method B from 3-bromo-2-chlorothiophene (0.20 g, 1.00 mmol) and 4-formylphenylboronic acid (0.30 g, 2.00 mmol); yield: 0.14 g (67 %); white solid; $R_f = 0.37$ (PE / EtOAc, 10:1); δ_H (CDCl_3 , 500 MHz) 7.10 (d, $J = 5.7$ Hz, 1H), 7.20 (d, $J = 5.7$ Hz, 1H), 7.75 (d, $J = 8.5$ Hz, 2H), 7.95 (d, $J = 8.2$ Hz, 2H), 10.06 (s, 1H, CHO); δ_C (CDCl_3 , 125 MHz) 123.3, 126.5, 128.2, 129.0, 129.9, 135.3, 136.9, 140.2, 191.7 (CO); MS (ESI): $m/z = 223 [\text{M}^+ + \text{H}]$.

Method C: Reduction with NaBH_4

To an ice-cooled solution of the corresponding aldehyde or ketone (1 eq) in methanol (5 mL / mmol) was added NaBH_4 (2 eq). Then the resulting mixture was heated to reflux for 30 minutes. After cooling to ambient temperature, the solvent was distilled off under reduced pressure. Then water (10 mL) was added, and the resulting mixture was extracted with ethyl acetate (3 x 10 mL). The combined organic phases were washed with brine, dried over MgSO_4 and evaporated under reduced pressure. Then the desired product was purified by chromatography on silica gel.

4-Phenyl-2-thiophenemethanol, 10a. Synthesised according to Method C using **10b** (0.31 g, 1.60 mmol) and NaBH_4 (0.11 g, 2.90 mmol); yield: 0.27 g (88 %); white solid; mp 109-110 °C; $R_f = 0.13$ (PE / EtOAc, 10:1); IR (ATR) ν (cm^{-1}) 3290 (m), 1596 (w), 1500 (w), 1449 (m), 1195 (m), 1158 (m), 1018 (s), 837 (m), 733 (s), 688 (s); δ_H (CDCl_3 , 500 MHz) 1.89 (bs, 1H, OH), 4.86 (s, 2H, CH_2), 7.28-7.32 (m, 2H), 7.39 (d, $J = 1.6$ Hz, 1H), 7.40 (dd, $J = 7.3, 8.0$ Hz, 2H), 7.57 (dd, $J = 1.6, 8.0$ Hz, 2H); δ_C (CDCl_3 , 125 MHz) 60.3 (CH_2), 120.3 (CH), 124.7 (CH), 126.3 (CH), 127.2 (CH), 128.8 (CH), 135.8 (C_q), 142.1 (C_q), 144.8 (C_q); MS (ESI): $m/z = 191 [\text{M}^+ + \text{H}]$.

4-(4-Fluorophenyl)-2-thiophenemethanol, 11a. Synthesised according to Method C using **11b** (0.31 g, 1.50 mmol) and NaBH_4 (0.10 g, 2.70 mmol); yield: 0.27 g (87 %); white solid; mp 120-121 °C; $R_f = 0.09$ (PE / EtOAc, 10:1); IR (ATR) ν (cm^{-1}) 3354 (m), 1602 (m), 1511 (s), 1419 (m), 1246 (s), 1151 (m), 1026 (s), 839 (s), 752 (s), 566

(s); δ_{H} (CDCl₃, 500 MHz) 1.90 (bs, 1H, OH), 4.86 (s, 2H), 7.08 (dd, $J = 8.5, 8.8$ Hz, 2H), 7.24-7.25 (m, 1H), 7.32 (d, $J = 1.6$ Hz, 1H), 7.51 (dd, $J = 5.4, 8.8$ Hz, 2H); δ_{C} (CDCl₃, 125 MHz) 60.2 (CH₂), 115.6 (d, $^2J_{\text{CF}} = 21.1$ Hz, CH), 120.0 (CH), 124.6 (CH), 127.8 (d, $^3J_{\text{CF}} = 7.7$ Hz, CH), 132.0 (d, $^4J_{\text{CF}} = 3.8$ Hz, C_q), 141.1 (C_q), 145.0 (C_q), 162.2 (d, $^1J_{\text{CF}} = 246.6$ Hz, C_q); MS (ESI): $m/z = 209$ [M⁺+H].

4-(4-Methoxyphenyl)-2-thiophenemethanol, 12a. Synthesised according to Method C using **12b** (0.22 g, 1.00 mmol) and NaBH₄ (0.07 g, 1.80 mmol); yield: 0.19 g (84 %); white solid; mp 138 °C (Lit.⁴⁰ 136.5-138 °C); $R_{\text{f}} = 0.14$ (PE / EtOAc, 10:1); IR (ATR) ν (cm⁻¹) 1512 (m), 1406 (m), 1309 (m), 1246 (m), 1180 (m), 1026 (s), 832 (s), 756 (m), 521 (m); δ_{H} (CDCl₃, 500 MHz) 3.77 (s, 3H), 4.64 (d, $J = 5.4$ Hz, 2H), 5.47 (t, $J = 5.4$ Hz, 1H), 6.95 (d, $J = 8.8$ Hz, 2H), 7.31-7.32 (m, 1H), 7.57 (d, $J = 1.6$ Hz, 1H), 7.59 (d, $J = 8.8$ Hz, 2H); δ_{C} (CDCl₃, 125 MHz) 55.0 (CH₃), 58.3 (CH₂), 114.1 (CH), 117.9 (CH), 122.7 (CH), 126.9 (CH), 128.0 (C_q), 140.3 (C_q), 147.0 (C_q), 158.3 (C_q); MS (ESI): $m/z = 221$ [M⁺+H].

4-(3-Methoxyphenyl)-2-thiophenemethanol, 13a. Synthesised according to Method C using **13b** (0.31 g, 1.40 mmol) and NaBH₄ (0.10 g, 2.50 mmol); yield: 0.29 g (95 %); colourless oil; $R_{\text{f}} = 0.10$ (PE / EtOAc, 10:1); IR (ATR) ν (cm⁻¹) 3354 (m), 1600 (s), 1460 (m), 1285 (m), 1148 (s), 1038 (s), 841 (m), 784 (s), 753 (s), 688 (m); δ_{H} (CDCl₃, 500 MHz) 1.90 (bs, 1H), 3.85 (s, 3H), 4.86 (d, $J = 3.5$ Hz, 2H), 6.85 (ddd, $J = 0.6, 2.5$ Hz, $J = 8.2$ Hz, 1H), 7.10 (dd, $J = 0.6, 2.5$ Hz, 1H), 7.16 (ddd, $J = 1.0, 1.6$ Hz, 7.6 Hz, 1H), 7.29 (dd, $J = 0.6, 1.3$ Hz, 1H), 7.31 (dd, $J = 7.6, 8.2$ Hz, 1H), 7.38 (d, $J = 1.6$ Hz, 1H); δ_{C} (CDCl₃, 125 MHz) 55.3 (CH₃), 60.2 (CH₂), 112.1 (CH), 112.6 (CH), 118.9 (CH), 120.6 (CH), 124.8 (CH), 129.8 (CH), 137.1 (C_q), 142.0 (C_q), 144.7 (C_q), 160.0 (C_q); MS (ESI): $m/z = 203$ [M⁺-OH].

4-(3,4-Difluorophenyl)-2-thiophenemethanol, 14a. Synthesised according to Method C using **14b** (0.34 g, 1.50 mmol) and NaBH₄ (0.10 g, 2.70 mmol); yield: 0.27 g (80 %); white solid; mp 66 °C; $R_{\text{f}} = 0.11$ (PE / EtOAc, 10:1); IR (ATR) ν (cm⁻¹) 3264 (m), 1605 (m), 1515 (s), 1279 (s), 1224 (m), 1170 (m), 1118 (m), 1013 (s), 816 (s), 759 (s), 581 (s); δ_{H} (CDCl₃, 500 MHz) 1.93 (bs, 1H), 4.85 (s, 2H), 7.16 (ddd, $J = 1.6, 8.2, 8.5$ Hz, 1H), 7.21-7.22 (m, 1H), 7.24-7.28 (m, 1H), 7.33 (d, $J = 1.6$ Hz, 1H), 7.34 (ddd, $J = 2.2, 7.6, 11.4$ Hz, 1H); δ_{C} (CDCl₃, 125 MHz) 115.1 (d, $^2J_{\text{CF}} = 18.2$ Hz, CH), 117.5 (d, $^2J_{\text{CF}} = 18.2$ Hz, CH), 120.8 (CH), 122.3 (dd, $^4J_{\text{CF}} = 2.9$ Hz, $^3J_{\text{CF}} = 5.8$ Hz, CH), 124.3 (CH), 132.9 (dd, $^4J_{\text{CF}} = 3.8$ Hz, $^3J_{\text{CF}} = 6.7$ Hz, C_q), 140.0 (d, $^5J_{\text{CF}} = 1.9$ Hz, C_q), 145.4 (C_q), 149.0 (dd, $^2J_{\text{CF}} = 12.5$ Hz, $^1J_{\text{CF}} = 248.5$ Hz, C_q), 150.0 (dd, $^2J_{\text{CF}} = 13.4$ Hz, $^1J_{\text{CF}} = 248.5$ Hz, C_q); MS (ESI): $m/z = 209$ [M⁺-OH].

(4-Bromothiophen-2-yl)methanol, 16b. Synthesised according to Method C using 4-bromothiophene-2-carbaldehyde (1.00 g, 5.20 mmol) and NaBH₄ (0.36 g, 9.40 mmol); yield: 0.99 g (98 %); colourless oil; $R_{\text{f}} = 0.13$ (PE / EtOAc, 10:1); IR (ATR) ν (cm⁻¹) 3318 (m), 1528 (w), 1343 (w), 1147 (m), 1007 (s), 818 (s), 734 (s), 580 (s); δ_{H} (CDCl₃, 500 MHz) 2.04 (bs, 1H), 4.78 (s, 2H), 6.92 (m, 1H), 7.17 (d, $J = 1.6$ Hz, 1H); δ_{C} (CDCl₃, 125 MHz) 59.8 (CH₂), 109.3 (C_q), 122.6 (CH), 127.7 (CH), 145.3 (C_q); MS (ESI): $m/z = 177/175$ [M⁺-OH].

1-(4-(5-Methylsulfanylthiophen-2-yl)phenyl)propan-1-ol, 23a. Synthesised according to Method C from **23b** (0.79 g, 3.00 mmol); yield: 0.71 g (89 %); white solid; $R_{\text{f}} = 0.58$ (DCM / MeOH, 98:2); IR (ATR) ν (cm⁻¹) 3317 (br), 1513 (m), 1465 (w), 1416 (w), 1261 (m), 1210 (w), 1008 (m), 970 (w), 946 (w), 823 (s), 803 (s); δ_{H} (CDCl₃, 500 MHz) 0.95 (t, $J = 7.3$ Hz, 3H, CH₃), 1.82 (m, 2H, CH₂), 1.88 (d, $J = 3.1$ Hz, 1H, OH), 2.51 (s, 3H, S-CH₃), 4.58-4.61 (m, 1H, CH), 6.72-6.73 (m, 1H), 7.10-7.13 (m, 1H), 7.31-7.33 (m, 2H), 7.52-7.54 (m, 2H); δ_{C} (CDCl₃, 125 MHz) 10.1 (CH₃), 15.4 (S-CH₃), 31.8 (CH₂), 75.7 (C-OH), 122.8, 125.4, 126.1, 126.4, 133.9, 139.4, 141.7, 143.3; MS (ESI): $m/z = 217$ [M⁺-SMe].

1-(4-Thiophen-3-ylphenyl)propan-1-one, 27b. This compound is commercial available.

1-(4-Thiophen-3-ylphenyl)propan-1-ol, 27a. Synthesised according to Method C from **27b** (0.42 g, 1.90 mmol); yield: 0.41 g (91 %); white solid; $R_{\text{f}} = 0.33$ (DCM / MeOH, 98:2); IR (ATR) ν (cm⁻¹) 3307 (br), 2928 (w), 1425 (w), 1261 (w), 1092 (m), 1044 (m), 973 (m), 865 (m), 844 (s), 728 (m), 690 (m); δ_{H} (DMSO, 500 MHz) 0.83 (t, $J = 7.3$ Hz, 3H, CH₃), 1.63-1.65 (m, 2H, CH₂), 4.45-4.46 (m, 1H, CH-OH), 7.35-7.37 (m, 2H), 7.53-7.55 (dd, $J = 1.6, 3.4$ Hz, 1H), 7.63-7.64 (m, 1H), 7.66-7.68 (m, 2H), 7.81 (d, $J = 1.3$ Hz, 1.6 Hz, 1H); δ_{C} (DMSO, 125 MHz) 9.9 (CH₃), 31.8 (CH₂), 73.2 (C-OH), 120.3, 122.5, 126.0, 126.2, 126.8, 133.4, 141.3, 144.9; MS (ESI): $m/z = 201$ [M⁺-H₂O].

1-(4-Thiophen-3-ylphenyl)ethanone, 28b. This compound has been reported by Reuben, D et al.⁴¹

1-(4-Thiophen-3-ylphenyl)ethanol, 28a. Synthesised according to Method C from **28b** (1.02 g, 5.10 mmol); yield: 0.86 (83 %); white solid; $R_{\text{f}} = 0.4$ (DCM); IR (ATR) ν (cm⁻¹) 3290 (br), 1362 (w), 1290 (w), 1200 (w), 1072 (m), 892 (m), 864 (m), 835 (m), 779 (s), 731 (m); δ_{H} (DMSO, 500 MHz) 1.35 (d, $J = 6.6$ Hz, 3H, CH₃), 4.72-4.73 (m, 1H, CH-OH), 7.36-7.37 (m, 2H), 7.53 (dd, $J = 1.6, 3.4$ Hz, 1H), 7.63-7.65 (m, 1H), 7.67-7.68 (m, 2H), 7.82 (dd, $J = 1.3, 1.6$ Hz, 1H); δ_{C} (DMSO, 125 MHz) 25.8 (CH₃), 67.9 (CH-OH), 120.4, 125.8, 126.2, 127.0, 133.4, 141.5, 146.3; MS (ESI): $m/z = 187$ [M⁺-H₂O].

1-(4-(4-Methylthiophen-3-yl)-phenyl)propan-1-ol, 29a. Synthesised according to Method C from **29b** (1.23 g, 5.30 mmol); yield: 1.03 g (83 %); white solid: $R_f = 0.55$ (DCM / MeOH, 98:2); δ_H (CDCl₃, 500 MHz) 0.97 (t, $J = 7.6$ Hz, 3H, CH₃), 1.81-1.83 (m, 2H, CH₂), 2.27 (s, 3H, CH₃), 4.63-4.66 (m, 1H, CH), 7.02-7.03 (m, 1H), 7.19-7.20 (m, 1H), 7.38-7.42 (m, 4H); δ_C (CDCl₃, 125 MHz) 9.9 (CH₃), 15.3 (CH₃), 31.6 (CH₂), 121.8, 122.7, 125.7, 128.4, 135.9, 136.1, 142.6, 143.0; MS (ESI): $m/z = 233$ [M⁺+H].

Method D: Grignard reaction

Under exclusion of air and moisture a 1.0 M EtMgBr (1.2 eq) solution in THF was added dropwise to a solution of the aldehyde or ketone (1 eq) in THF (12 mL / mmol). The mixture was stirred over night at rt. Then ethyl acetate (10 mL) and water (10 mL) were added and the organic phase was separated. The organic phase was extracted with water and brine, dried over Na₂SO₄, and evaporated under reduced pressure. The crude products were purified by flash chromatography on silica gel.

1-(4-(3,4-Difluorophenyl)-2-thiophen-1-yl)-1-propanol, 15a. Synthesised according to Method D using **14b** (0.20 g, 0.89 mmol) and 1.0 M EtMgBr (0.98 mL, 0.98 mmol); yield: 0.18 g (79 %); colourless oil; $R_f = 0.14$ (PE / EtOAc, 10:1); δ_H (CDCl₃, 500 MHz) 0.93 (t, $J = 7.3$ Hz, 3H, CH₃), 1.80-1.88 (m, 2H, CH₂), 1.96 (bs, 1H, OH), 4.79 (t, $J = 6.6$ Hz, 1H, CHCH₂), 7.09-7.13 (m, 1H), 7.16-7.18 (m, 1H), 7.19-7.22 (m, 1H), 7.23 (d, $J = 1.6$ Hz, 1H), 7.27 (ddd, $J = 1.6, 2.2, 7.6$ Hz, 1H); δ_C (CDCl₃, 125 MHz) 10.0 (CH₃), 32.2 (CH₂), 71.8 (CH), 115.0 (CH), 117.4 (CH), 117.6 (CH), 119.8 (CH), 122.1 (CH), 122.6 (CH), 133.0 (C_q), 139.7 (C_q), 150.0 (C_q), 150.6 (C_q); MS (ESI): $m/z = 255$ [M⁺+H].

1-(2-Fluoro-4-(4-methylthiophen-3-yl)-phenyl)propan-1-ol, 30a. Synthesised according to Method D from **30b** (2.00 g, 4.90 mmol); yield: 0.73 g (30 %); white solid, $R_f = 0.32$ (Hex / EtOAc, 4:1); δ_H (CDCl₃, 500 MHz) 0.98 (t, $J = 7.6$ Hz, 3H, CH₃), 1.85-1.87 (m, 2H, CH₂), 2.52 (s, 3H, CH₃), 4.96 (t, $J = 6.3$ Hz, 1H, CH), 7.03-7.04 (m, 1H), 7.05-7.06 (m, 1H), 7.18-7.20 (m, 2H), 7.49-7.50 (m, 1H); δ_C (CDCl₃, 125 MHz) 10.0 (CH₃), 15.5 (CH₃), 30.9 (CH₂), 70.0 (CHOH), 115.2, 122.3, 123.4, 124.5, 127.2, 130.0, 135.9, 138.0, 160.7; MS (ESI): $m/z = 251$ [M⁺+H].

1-(4-(2-Chlorothiophen-3-yl)phenyl)propan-1-ol, 31a. Synthesised according to Method D from **31b** (1.32 g, 6.50 mmol); yield: 1.48 g (95 %); white solid: $R_f = 0.30$ (PE / EtOAc, 10:1); δ_H (CDCl₃, 500 MHz) 0.81 (t, $J = 7.6$ Hz, 3H, CH₃), 1.69-1.71 (m, 2H, CH₂), 2.07 (br, 1H, OH), 4.45 (t, $J = 6.6$ Hz, 1H, CH), 6.61-6.62 (m, 1H), 6.98-6.99 (m, 1H), 7.18-7.20 (m, 2H), 7.40-7.41 (m, 2H); δ_C (CDCl₃, 125 MHz) 10.2 (CH₃), 31.8 (CH₂), 75.7 (CH), 122.8, 125.5, 126.1, 126.5, 127.1, 128.8, 133.9, 139.4, 141.7, 143.4; MS (ESI): $m/z = 253$ [M⁺+H].

Method E: CDI reaction

To a solution of the corresponding alcohol (1 eq) in NMP or acetonitrile (10 mL / mmol) was added CDI (5 eq). Then the solution was heated to reflux for 4 to 18 h. After cooling to ambient temperature, it was diluted with water (30 mL) and extracted with ethyl acetate (3 x 10 mL). The combined organic phases were washed with brine, dried over MgSO₄ and evaporated under reduced pressure. Then the desired product was purified by chromatography on silica gel.

1-((4-Phenylthiophen-2-yl)methyl)-1H-imidazole, 10. Synthesised according to Method E using **10a** (0.19 g, 1.00 mmol) and CDI (0.24 g, 1.50 mmol); yield: 0.09 g (38 %); light brown solid: mp 112-113 °C; $R_f = 0.22$ (EtOAc); IR (ATR) ν (cm⁻¹) 3110 (w), 1504 (m), 1430 (m), 1358 (w), 1230 (m), 1084 (m), 817 (m), 744 (s), 660 (s); δ_H (CDCl₃, 500 MHz) 5.29 (s, 2H), 7.00 (t, $J = 1.3$ Hz, 1H), 7.10 (bs, 1H), 7.24-7.25 (m, 1H), 7.30 (tt, $J = 1.3, 7.5$ Hz, 1H), 7.38 (d, $J = 1.6$ Hz, 1H), 7.39 (dd, $J = 7.5, 7.8$ Hz, 2H), 7.53 (dd, $J = 1.3, 7.8$ Hz, 2H), 7.60 (s, 1H); δ_C (CDCl₃, 125 MHz) 45.7 (CH₂), 118.9 (CH), 120.8 (CH), 126.0 (CH), 126.3 (CH), 127.5 (CH), 128.9 (CH), 130.0 (CH), 135.2 (C_q), 137.0 (CH), 139.2 (C_q), 142.4 (C_q); MS (ESI): $m/z = 241$ [M⁺+H].

1-((4-(4-Fluorophenyl)thiophen-2-yl)methyl)-1H-imidazole, 11. Synthesised according to Method E using **11a** (0.21 g, 1.00 mmol) and CDI (0.24 g, 1.50 mmol); yield: 0.12 g (49 %); brown oil; $R_f = 0.20$ (EtOAc); IR (ATR) ν (cm⁻¹) 3088 (w), 1511 (s), 1224 (s), 1160 (m), 1075 (m), 830 (s), 761 (m), 661 (m), 565 (m); δ_H (CDCl₃, 500 MHz) 5.28 (s, 2H), 6.99 (t, $J = 1.2$ Hz, 1H), 7.07 (dd, $J = 8.5, 8.8$ Hz, 2H), 7.09 (bs, 1H), 7.17-7.18 (m, 1H), 7.31 (d, $J = 1.6$ Hz, 1H), 7.48 (dd, $J = 5.4$ Hz, $J = 8.8$ Hz, 2H), 7.59 (brs, 1H); δ_C (CDCl₃, 125 MHz) 45.6 (CH₂), 115.7 (d, $^2J_{CF} = 21.1$ Hz, CH), 118.9 (CH), 120.5 (CH), 125.9 (CH), 127.9 (d, $^3J_{CF} = 8.6$ Hz, CH), 129.9 (CH), 131.4 (d, $^4J_{CF} = 3.8$ Hz, C_q), 137.0 (CH), 139.4 (C_q), 141.4 (C_q), 162.3 (d, $^1J_{CF} = 246.6$ Hz, C_q); MS (ESI): $m/z = 259$ [M⁺+H].

1-((4-(4-Methoxyphenyl)thiophen-2-yl)methyl)-1H-imidazole, 12. Synthesised according to Method E using **12a** (0.16 g, 0.70 mmol) and CDI (0.16 g, 1.00 mmol); yield: 0.08 g (44 %); light brown solid: mp 140 °C; $R_f = 0.20$ (EtOAc); IR (ATR) ν (cm⁻¹) 2961 (w), 1517 (m), 1254 (m), 1077 (m), 1020 (s), 828 (s), 758 (s), 660 (m); δ_H (CDCl₃, 500 MHz) 3.83 (s, 3H), 5.28 (s, 2H), 6.92 (d, $J = 8.8$ Hz, 2H), 6.99 (bs, 1H), 7.19 (bs, 1H), 7.27 (d, $J = 1.6$ Hz, 2H), 7.45 (d, $J = 8.8$ Hz, 2H), 7.59 (bs, 1H); δ_C (CDCl₃, 125 MHz) 45.7 (CH₂), 55.3 (CH₃), 114.3 (CH), 118.9

(CH), 119.4 (CH), 126.0 (CH), 127.4 (CH), 128.1 (C_q), 129.9 (CH), 137.0 (CH), 139.0 (C_q), 142.1 (C_q), 159.1 (C_q); MS (ESI): $m/z = 271$ [M⁺+H].

1-((4-(3-Methoxyphenyl)thiophen-2-yl)methyl)-1H-imidazole, 13. Synthesised according to Method E using **13a** (0.28 g, 1.30 mmol) and CDI (0.31 g, 1.90 mmol); yield: 0.11 g (31 %); brown solid: mp 48 °C; $R_f = 0.27$ (EtOAc); IR (ATR) ν (cm⁻¹) 3076 (w), 1591 (m), 1496 (m), 1261 (m), 1222 (m), 1175 (m), 1031 (m), 784 (s), 744 (s), 659 (s); δ_H (CDCl₃, 500 MHz) 3.84 (s, 3H), 5.27 (s, 2H), 6.85 (ddd, $J = 1.0, 2.5, 8.2$ Hz, 1H), 6.98 (t, $J = 1.3$ Hz, 1H), 7.05 (dd, $J = 1.6, 2.5$ Hz, 1H), 7.09 (dd, $J = 1.0, 1.3$ Hz, 1H), 7.11 (ddd, $J = 1.0, 1.6, 7.6$ Hz, 1H), 7.22 – 7.23 (m, 1H), 7.30 (dd, $J = 7.6, 8.2$ Hz, 1H), 7.37 (d, $J = 1.6$ Hz, 1H), 7.58 (bs, 1H); δ_C (CDCl₃, 125 MHz) 45.6 (CH₂), 55.3 (CH₃), 112.1 (CH), 112.7 (CH), 118.8 (CH), 118.9 (CH), 121.0 (CH), 126.1 (CH), 129.6 (C_q), 129.9 (CH), 136.6 (C_q), 136.9 (CH), 139.1 (CH), 142.2 (C_q), 160.0 (C_q); MS (ESI): $m/z = 271$ [M⁺+H].

1-((4-(3,4-Difluorophenyl)thiophen-2-yl)methyl)-1H-imidazole, 14. Synthesised according to Method E using **14a** (0.24 g, 1.10 mmol) and CDI (0.24 g, 1.50 mmol); yield: 0.12 g (41 %); light brown solid: mp 83 °C; $R_f = 0.25$ (EtOAc); IR (ATR) ν (cm⁻¹) 3092 (w), 1605 (m), 1515 (s), 1439 (m), 1268 (m), 1226 (m), 1070 (m), 819 (s), 766 (s), 664 (m), 575 (m); δ_H (CDCl₃, 500 MHz) 5.19 (s, 2H), 6.90 (t, $J = 1.3$ Hz, 1H), 7.00 (dd, $J = 1.0, 1.3$ Hz, 1H), 7.06 (dt, $J = 8.2, 10.9$ Hz, 1H), 7.05–7.06 (m, 1H), 7.12–7.15 (m, 1H), 7.21 (ddd, $J = 1.9, 7.3, 11.4$ Hz, 1H), 7.23 (d, $J = 1.6$ Hz, 1H), 7.50 (s, 1H); δ_C (CDCl₃, 125 MHz) 45.4 (CH₂), 115.1 (d, $^2J_{CF} = 18.2$ Hz, CH), 117.5 (d, $^2J_{CF} = 17.3$ Hz, CH), 118.8 (CH), 121.2 (CH), 122.1 (dd, $^3J_{CF} = 5.8$ Hz, $^4J_{CF} = 2.9$ Hz, CH), 125.5 (CH), 129.8 (CH), 132.3 (dd, $^3J_{CF} = 5.8$ Hz, $^4J_{CF} = 3.8$ Hz, C_q), 136.9 (CH), 139.8 (C_q), 140.1 (C_q), 149.7 (dd, $^1J_{CF} = 249.5$ Hz, $^2J_{CF} = 12.5$ Hz, C_q), 150.3 (dd, $^1J_{CF} = 248.6$ Hz, $^2J_{CF} = 13.5$ Hz, C_q); MS (ESI): $m/z = 277$ [M⁺+H].

1-(1-(4-(4-Fluorophenyl)thiophen-2-yl)propyl)-1H-imidazole, 15. Synthesised according to Method E using **15a** (0.15 g, 0.60 mmol) and CDI (0.29 g, 1.80 mmol); yield: 0.08 g (45 %); brown oil; $R_f = 0.29$ (DCM / MeOH, 98:2); IR (ATR) ν (cm⁻¹) 1606 (w), 1516 (s), 1277 (m), 1222 (m), 1117 (w), 1072 (w), 815 (s), 770 (s), 662 (m); δ_H (CDCl₃, 500 MHz) 0.97 (t, $J = 7.4$ Hz, 3H), 2.22–2.34 (m, 2H), 5.26 (dd, $J = 6.3, 8.8$ Hz, 1H), 7.01 (bs, 1H), 7.09–7.10 (m, 1H), 7.11 (bs, 1H), 7.15 (ddd, $J = 8.0, 8.5, 9.9$ Hz, 1H), 7.20–7.23 (m, 1H), 7.30 (ddd, $J = 2.2, 7.5, 11.5$ Hz, 1H), 7.31 (d, $J = 1.3$ Hz, 1H), 7.65 (bs, 1H); δ_C (CDCl₃, 125 MHz) 10.9 (CH₃), 30.0 (CH₂), 58.9 (CH), 115.2 (d, $^2J_{CF} = 18.2$ Hz, CH), 117.2 (CH), 117.6 (d, $^2J_{CF} = 17.3$ Hz, CH), 120.5 (CH), 122.2 (dd, $^3J_{CF} = 6.7$ Hz, $^4J_{CF} = 3.8$ Hz, CH), 124.1 (CH), 129.8 (CH), 132.5 (dd, $^3J_{CF} = 6.7$ Hz, $^4J_{CF} = 3.8$ Hz, C_q), 136.4 (CH), 140.0 (C_q), 145.2 (C_q), 149.7 (dd, $^1J_{CF} = 247.5$ Hz, $^2J_{CF} = 12.5$ Hz, C_q), 150.5 (dd, $^1J_{CF} = 249.5$ Hz, $^2J_{CF} = 13.5$ Hz, C_q); MS (ESI): $m/z = 305$ [M⁺+H].

1-((4-Bromothiophen-2-yl)methyl)-1H-imidazole, 16a. Synthesised according to Method E using **16b** (0.74 g, 3.81 mmol) and CDI (1.24 g, 7.67 mmol); yield: 0.72 g (78 %); colourless oil; $R_f = 0.17$ (EtOAc); δ_H (CDCl₃, 500 MHz) 5.23 (s, 2H), 6.88–6.89 (m, 1H), 6.94 (s, 1H), 7.09 (s, 1H), 7.18 (d, $J = 1.6$ Hz, 1H), 7.55 (s, 1H); δ_C (CDCl₃, 125 MHz) 45.2 (CH₂), 109.8 (C_q), 118.8 (CH), 123.3 (CH), 129.2 (CH), 130.2 (CH), 137.0 (CH), 139.9 (C_q); MS (ESI): $m/z = 245/243$ [M⁺+H].

2-(4-((1H-Imidazol-1-yl)methyl)phenyl)-5-(chloromethyl)pyridine, 19. Synthesised according to Method E using compound **19a** (0.49 g, 2.10 mmol) and CDI (0.68 g, 4.20 mmol); yield: 0.22 g (37 %); $R_f = 0.15$ (EtOAc / MeOH, 95:5); IR (ATR) ν (cm⁻¹) 1507 (m), 1458 (s), 1384 (m), 1231 (m), 1104 (s), 1024 (m), 814 (m), 739 (s), 662 (s); δ_H (CDCl₃, 500 MHz) 3.94 (s, 2H), 5.09 (s, 2H), 6.89 (t, $J = 1.3$ Hz, 1H), 7.08 (t, $J = 1.3$ Hz, 1H), 7.09 (d, $J = 8.5$ Hz, 2H), 7.14 (d, $J = 8.5$ Hz, 2H), 7.23 (d, $J = 8.2$ Hz, 1H), 7.40 (dd, $J = 2.5, 8.2$ Hz, 1H), 7.53 (s, 1H), 8.24 (d, $J = 2.2$ Hz, 1H); δ_C (CDCl₃, 125 MHz) 37.8 (CH₂), 50.5 (CH₂), 119.2 (CH), 124.1 (CH), 127.8 (CH), 129.4 (CH), 129.7 (CH), 134.7 (C_q), 135.0 (CH), 137.3 (CH), 139.1 (CH), 139.5 (C_q), 149.6 (C_q), 149.7 (C_q); MS (ESI): $m/z = 284$ [M⁺+H].

5-(4-((1H-Imidazol-1-yl)methyl)phenyl)pyrimidine, 20. Synthesised according to Method E using compound **20a** (0.11 g, 0.60 mmol) and CDI (0.28 g, 1.10 mmol); yield: 0.08 g (57 %); white solid: mp 135–138 °C; $R_f = 0.29$ (EtOAc / MeOH, 10:1); δ_H (CDCl₃, 500 MHz) 5.18 (s, 2H), 6.92 (s, 1H), 7.10 (s, 1H), 7.28 (d, $J = 8.1$ Hz, 2H), 7.55 (d, $J = 8.1$ Hz, 2H), 7.57 (bs, 1H), 8.91 (s, 2H), 9.19 (s, 1H); δ_C (CDCl₃, 125 MHz) 50.3 (CH₂), 119.2 (CH), 127.5 (CH), 128.2 (CH), 130.0 (CH), 133.5 (C_q), 134.3 (CH), 137.2 (C_q), 137.4 (C_q), 154.8 (CH), 157.7 (CH); MS (ESI): $m/z = 237$ [M⁺+H].

4-(4-((1H-Imidazol-1-yl)methyl)phenyl)morpholine, 21. Synthesised according to Method E using compound **21a** (0.33 g, 1.60 mmol) and CDI (0.52 g, 3.20 mmol); light yellow oil: bp > 200 °C; $R_f = 0.22$ (EtOAc); IR (ATR) ν (cm⁻¹) 2854 (w), 1613 (m), 1518 (m), 1450 (m), 1230 (s), 1117 (s), 926 (s), 826 (s), 664 (s); δ_H (CDCl₃, 500 MHz) 1.82 (d, $J = 7.0$ Hz, 3H), 3.15 (m, 4H), 3.85 (m, 4H), 5.27 (q, $J = 7.0$ Hz, 1H), 6.86 (d, $J = 8.6$ Hz, 2H), 6.90 (bs, 1H), 7.05 (bs, 1H), 7.07 (d, $J = 8.6$ Hz, 2H), 7.56 (bs, 1H); δ_C (CDCl₃, 125 MHz) 22.0 (CH₃), 49.0 (CH₂), 56.0

(CH), 66.8 (CH₂), 115.6 (CH), 117.8 (CH), 127.1 (CH), 129.3 (CH), 132.4 (C_q), 136.0 (CH), 151.0 (C_q); MS (ESI): $m/z = 257 [M^+ + H]$.

1-(1-(4-(5-Methylsulfanyl-thiophen-2-yl)-phenyl)-propyl)-1H-imidazole, 23. Synthesised according to Method E from **23a** (0.60 g, 2.30 mmol); yield: 0.40 g (56 %); white solid: mp 86 °C; $R_f = 0.48$ (DCM / MeOH, 98:2); IR (ATR) ν (cm⁻¹) 3119 (w), 2967 (w), 1684 (w), 1512 (m), 1461 (m), 1232 (s), 1071 (s), 1022 (m), 908 (s), 836 (s), 786 (s), 741 (s), 665 (s); δ_H (DMSO, 500 MHz) 0.93 (t, $J = 7.3$ Hz, 3H, CH₃), 2.16-2.18 (m, 2H, CH₂), 2.42 (s, 3H, S-CH₃), 4.92 (t, $J = 7.6$ Hz, 1H, CH), 6.63-6.64 (m, 1H), 6.87-6.88 (m, 1H), 7.01-7.03 (m, 2H), 7.09-7.11 (m, 2H), 7.42-7.44 (m, 2H), 7.53 (s, 1H); δ_C (DMSO, 125 MHz) 11.1 (CH₃), 15.4 (S-CH₃), 28.5 (CH₂), 63.0 (C-OH), 117.6, 123.2, 125.8, 126.3, 127.0, 129.6, 134.6, 136.3, 138.9, 139.9, 141.0; MS (ESI): $m/z = 285 [M^+ - Et]$.

1-(1-(4-Thiophen-3-yl-phenyl)propyl)-1H-imidazole, 27. Synthesised according to Method E from **27a** (0.32 g, 1.40 mmol); yield: 0.37 g (87%); white solid: mp 128 °C; $R_f = 0.55$ (DCM / MeOH, 98:2); IR (ATR) ν (cm⁻¹) 3134 (w), 2930 (w), 1798 (vs), 1528 (w), 1479 (m), 1401 (vs), 1321 (s), 1265 (vs), 837 (m); δ_H (DMSO, 500 MHz) 0.91 (t, $J = 7.3$ Hz, 3H, CH₃), 1.95 (m, 1H, CH₂), 2.05-2.7 (m, 1H, CH₂), 5.83-5.85 (m, 1H, CH), 7.09-7.10 (m, 1H), 7.52-7.53 (m, 2H), 7.55 (d, $J = 8.2$ Hz, 1H), 7.63-7.65 (m, 1H), 7.67 (t, $J = 1.6$ Hz, 1H), 7.73-7.75 (m, 2H), 7.88-7.89 (m, 1H), 8.37-8.38 (m, 1H); δ_C (DMSO, 125 MHz) 9.4 (CH₃), 28.5 (CH₂), 117.4, 121.2, 126.0, 126.8, 127.0, 130.3, 135.1, 137.2, 137.6, 140.8, 147.6; MS (ESI): $m/z = 269 [M^+ + H]$.

1-(1-(4-Thiophen-3-ylphenyl)ethyl)-1H-imidazole, 28. Synthesised according to Method E from **28a** (0.50 g, 2.45 mmol); yield: 0.63 g (87 %); white solid: mp 153 °C; $R_f = 0.57$ (DCM / MeOH, 98:2); IR (ATR) ν (cm⁻¹) 3136 (w), 1745 (vs), 1476 (m), 1392 (s), 1259 (m), 836 (m); δ_H (DMSO, 500 MHz) 1.67 (d, $J = 6.3$ Hz, 3H, CH₃), 6.03-6.06 (q, 1H, CH), 7.08-7.09 (m, 1H), 7.53-7.55 (m, 3H), 7.63-7.64 (m, 2H), 7.75-7.77 (m, 2H), 7.88-7.89 (m, 1H), 8.34-8.36 (m, 1H); δ_C (DMSO, 125 MHz) 27.6 (CH₃), 121.5, 126.1, 127.6, 134.9, 137.3, 141.3, 147.5; MS (ESI): $m/z = 255 [M^+ + H]$.

1-(1-(4-(4-Methylthiophen-3-yl)phenyl)propyl)-1H-imidazole, 29. Synthesised according to Method E from **29a** (0.90 g, 3.90 mmol); yield: 0.23 (21 %); white solid; $R_f = 0.35$ (DCM / MeOH, 95:5); IR (ATR) ν (cm⁻¹) 2969 (w), 2932 (w), 1494 (m), 1455 (w), 1223 (s), 1072 (s), 906 (m), 790 (vs), 734 (s), 663 (vs); δ_H (CDCl₃, 500 MHz) 0.99 (t, $J = 7.3$ Hz, 3H, CH₃), 2.22-2.25 (m, 3H), 5.06 (t, $J = 7.6$ Hz, 1H, CH), 6.99-7.01 (m, 1H), 7.02-7.03 (m, 1H), 7.10-7.11 (m, 1H), 7.17-7.18 (m, 1H), 7.21-7.23 (m, 2H), 7.35-7.37 (m, 2H), 7.62-7.63 (m, 1H); δ_C (CDCl₃, 125 MHz) 11.1 (CH₃), 15.5 (CH₃), 28.6 (CH₂), 63.1 (CH), 117.7, 120.2, 122.2, 123.2, 126.5, 128.9, 129.6, 136.0, 136.4, 137.0, 139.0, 142.3; MS (ESI): $m/z = 283 [M^+ + H]$.

1-(1-(2-Fluoro-4-(4-methylthiophen-3-yl)phenyl)propyl)-1H-imidazole, 30. Synthesised according to Method E from **30a** (0.73 g, 2.90 mmol); yield: 0.12 g (22 %); white solid; $R_f = (PE / EtOAc, 10:1)$; IR (ATR) ν (cm⁻¹) 2970 (w), 1624 (m), 1572 (m), 1493 (m), 1446 (w), 1407 (w), 1280 (m), 1223 (s), 1111 (m), 1073 (m), 906 (m), 865 (m), 791 (vs), 732 (s); δ_H (CDCl₃, 500 MHz) 0.96 (t, $J = 7.3$ Hz, 3H, CH₃), 2.25 (m, 5H), 5.37 (t, $J = 6.9$ Hz, 1H, CH), 7.03-7.05 (m, 2H), 7.11-7.13 (m, 2H), 7.20-7.22 (m, 3H), 7.65-7.66 (m, 1H); δ_C (CDCl₃, 125 MHz) 11.1 (CH₃), 15.4 (CH₃), 27.7 (CH₂), 56.6 (CH), 115.9, 117.8, 122.6, 123.8, 124.8, 125.9, 127.1, 129.3, 135.7, 136.4, 139.1, 141.0, 158.9, 160.9; MS (ESI): $m/z = 301 [M^+ + H]$.

1-(1-(4-(2-Chlorothiophen-3-yl)-phenyl)propyl)-1H-imidazole, 31. Synthesised according to Method E from **31a** (0.81 g, 3.20 mmol); yield: 0.32 g (33 %); yellow oil; $R_f = 0.36$ (DCM / MeOH, 20:1); IR (ATR) ν (cm⁻¹) 2967 (w), 1495 (m), 1410 (w), 1260 (m), 1224 (m), 1109 (m), 1072 (s), 1024 (s), 906 (m), 876 (s), 812 (vs), 719 (vs), 663 (vs), 622 (vs), 549 (m); δ_H (CDCl₃, 500 MHz) 0.96 (t, $J = 7.3$ Hz, 3H, CH₃), 2.25 (q, $J = 7.3, 7.6$ Hz, 2H, CH₂), 5.04 (t, $J = 7.6$ Hz, 1H, CH), 6.97 (s, 1H), 7.00 (d, $J = 6.0$ Hz), 7.09 (s, 1H), 7.13 (d, $J = 5.7$ Hz, 1H), 7.23 (d, $J = 8.2$ Hz, 2H), 7.53 (d, $J = 8.2$ Hz, 2H), 7.61 (s, 1H); δ_C (CDCl₃, 125 MHz) 11.1 (CH₃), 28.5 (CH₂), 62.9 (CH), 117.6, 122.8, 125.0, 126.5, 128.2, 128.8, 129.5, 133.9, 136.3, 137.2, 139.5; MS (ESI): $m/z = 303 [M^+ + H]$, 235 [M⁺-Im].

Docking studies

Ligands. All molecular modelling studies were performed on Intel(R) P4 CPU 3.00GHz running Linux Suse 10.1. The structures of the inhibitors were built with SYBYL 7.3.2 (Sybyl, Tripos Inc., St. Louis, Missouri, USA) and energy-minimized in MMFF94s force-field⁴² as implemented in Sybyl. The resulting geometries for our compounds were then subjected to *ab initio* calculation employing the B3LYP functional⁴³⁻⁴⁴ in combination with a 6-31G* basis set using the package Gaussian03 (Gaussian, Inc., Pittsburgh, PA, 2003).

Homology modelling. A homology model was build with MODELLER v8.0,⁴⁵⁻⁴⁶ using the X-ray structure of human CYP2C9 (PDB (<http://www.rcsb.org>) code 1R9O, Res. 1.9 Å) as template. The two amino acid sequences were globally aligned with T-COFFEE⁴⁷ and then manually refined considering the predicted secondary structure of

CYP17 (secondary structure prediction by PSIPRED⁴⁸ to give an overall sequence identity percentage of approximately 30 %). The heme group was included in model building.

The resulting best homology model was first checked with the BIOPOLYMER module of SYBYL and AMBER charges were loaded. Hydrogens at histidine residues were positioned at the ϵ -nitrogen. Serine residues were considered to be neutral, whereas all basic and acidic residues were considered protonated and deprotonated, respectively. This structure was minimized for 200 steps with the steepest descent minimizer as implemented in SYBYL with the backbone atoms kept at fixed positions in order to achieve a low energy conformation and a satisfactory protein geometry containing no conformationally disallowed regions. Finally the chosen homology model was validated using different online tools (PROCHECK⁴⁹ and WHATIF⁵⁰).

Docking. Molecular docking calculations were performed for various inhibitors of Table 1 and 2. Since the GOLD docking program allows flexible docking of the compounds, no conformational search was employed to the ligand structures. GOLD gave the best poses by a genetic algorithm (GA) search strategy, and then various molecular features were encoded as a chromosome.

Ligands were docked in 50 independent genetic algorithm (GA) runs using GOLD. Heme iron was chosen as active-site origin, while the radius was set equal to 19 Å. The automatic active-site detection was switched on. A distance constraint of a minimum of 1.9 and a maximum of 2.5 Å between the sp^2 -hybridised nitrogen of the imidazole and the iron was set. Further, some of the GOLDScore parameters were modified to improve the weight of hydrophobic interaction and of the coordination between iron and nitrogen. The genetic algorithm default parameters were set as suggested by the GOLD authors. On the other hand, the annealing parameters of fitness function were set at 3.5 Å for hydrogen bonding and 6.5 Å for Van der Waals interactions.

All 50 poses for each compound were clustered with ACIAP^{51,52} and the representative structure of each significant cluster was selected. The quality of the docked representative poses was evaluated based on visual inspection of the putative binding modes of the ligands, as outcome of docking simulations and cluster analysis.

MEP. For each docked compound geometry optimization was performed at the B3LYP/6-31G* level by means of the Gaussian03 software and the molecular electrostatics potential map (MEP) was plotted using GaussView3, the 3-D molecular graphics package of Gaussian.⁵³ These electrostatic potential surfaces were generated by mapping 6-31G* electrostatic potentials onto surfaces of molecular electron density (isovalue = 0.002 electron/Å).⁵⁴

Acknowledgement. We thank the Fonds der Chemischen Industrie for financial support. U. E. H. is grateful to the European Postgraduate School 532 (DFG) for a scholarship.

References

- (1) Jemal, A.; Siegel, R.; Ward, E.; Murray, T.; Xu, J.; Thun, M. J. *CA Cancer J. Clin.* **2007**, *57*, 43.
- (2) Nnane, I. P.; Long, B. J.; Ling, Y.-Z.; Grigoryev, D. N.; Brodie, A. M. *Br. J. Cancer* **2000**, *83*, 74.
- (3) Schuurmans, A. L. G.; Bolt, J.; Veldscholte, J.; Mulder, E.; *J. Steroid Biochem. Molec. Biol.* **1990**, *37*, 849.
- (4) Akhtar, M. K.; Kelly, S. L.; Kaderbhai, M. A. *J. Endocrinol.* **2005**, *187*, 267.
- (5) Kolar, N. W.; Swart, A. C.; Mason, J. I.; Swart, P. J. *J. Biotechnol.* **2007**, *129*, 635.
- (6) Harris, K. A.; Weinberg, V.; Bok, R. A.; Kakefuda, M.; Small, E. J. *J. Urol.* **2002**, *168*, 542.
- (7) Eklund, J.; Kozloff, M.; Vlamakis, J.; Starr, A.; Mariott, M.; Gallot, L.; Jovanovic, B.; Schilder, L.; Robin, E.; Pins, M.; Bergan, R. C. *Cancer* **2006**, *106*, 2459.
- (8) Baston, E.; Leroux, F. R. *Recent Pat. Anti-Cancer Drug Discovery* **2007**, *2*, 31.
- (9) Leroux, F. *Curr. Med. Chem.* **2005**, *12*, 1623.
- (10) Bruno, R. D.; Njar, V. C. O. *Bioorg. Med. Chem.* **2007**, *15*, 5047.
- (11) Matsunaga, N.; Kaku, T.; Itoh, F.; Tanaka, T.; Hara, T.; Miki, H.; Iwasaki, M.; Aono, T.; Yamaoka, M.; Kusaka, M.; Tasaka, A. *Bioorg. Med. Chem.* **2004**, *12*, 2251.
- (12) Haidar, S.; Hartmann, R. W. In *Enzymes and their Inhibition, Drug Development*; Smith, H. J., Simons, C., Ed.; CRC Press: Boca Raton, 2005, 241-253.
- (13) Njar, V. C.; Brodie, A. M. *Curr. Pharm. Des.* **1999**, *5*, 163.
- (14) Cougar Biotechnology, Inc. <http://www.cougarbiotechnology.com/docs/052107CougarPhaseIIAUAAnnualMeeting2007.pdf>
- (15) Samer, H.; Ehmer, P. B.; Barassin, S.; Batzl-Hartmann, C.; Hartmann, R. W. *J. Steroid Biochem. Mol. Biol.* **2003**, *84*, 555.

- (16) Hartmann, R. W.; Wachall, B.; Yoshihama, M.; Nakakoshi, M.; Nomoto, S.; Ikeda, Y. *WO018075*, 1999.
- (17) a) Zhuang, Y.; Wachall, B. G.; Hartmann, R. W. *Bioorg. Med. Chem.* **2000**, *8*, 1245. b) Wachall, B. G.; Hector, M.; Zhuang, Y.; Hartmann, R. W. *Bioorg. Med. Chem.* **1999**, *7*, 1913.
- (18) Leroux, F.; Hutschenreuter, T. U.; Charrière, C.; Scopelliti, R.; Hartmann, R. W. *Helv. Chim. Acta* **2003**, *86*, 2671.
- (19) Miyaura, N.; Suzuki, A. *Chem. Rev.* **1995**, *95*, 2457.
- (20) Tang, Y.; Dong, Y.; Vennerstrom J. L. *Synthesis* **2004**, *15*, 2540.
- (21) Tasaka, A.; Kaku, T. *WO030764*, 2001.
- (22) Ehmer, P. B.; Jose, J.; Hartmann, R. W. *J. Steroid Biochem. Mol. Biol.* **2000**, *75*, 57.
- (23) a) Hutschenreuter, T. U.; Ehmer, P. B.; Hartmann, R. W. *J. Enzyme Inhib. Med. Chem.* **2004**, *18*, 17. b) Sergejew, T. F.; Hartmann, R. W. *J. Enz. Inhib.* **1994**, *8*, 113.
- (24) Madan, R. A.; Arlen, P. M. *IDrugs*, **2006**, *9*, 49.
- (25) Jones, G.; Willett, P.; Glen, R. C.; Leach, A. R.; Taylor, R. *J. Mol. Biol.* **1997**, *267*, 727-748
- (26) a) Lin, D.; Zhang, L.; Chiao, E.; Miller, L.W. *Mol. Endo.* **1994**, *8*, 391. b) Auchus, R. J.; Miller, W. L. *Mol. Endo.* **1999**, *13*, 1169.
- (27) Mathieu, A. P.; LeHoux J.-G.; Auchus, R. J. *Biochim. Biophys. Acta* **2003**, *1619*, 291.
- (28) Brooke, A.M.; Taylor, N.F.; Shepherd, J.H.; Gore, M.E.; Ahmad, T.; Lin, L.; Rumsby, G.; Papari-Zareei, M.; Auchus, R.J.; Achermann, J.C.; Monson, J.P. *J. Clin. Endocrinol. Metab.* **2006**, *91*(6):2428–2431.
- (29) Otyepka, M.; Skopalík, J.; Anzenbacherová, E.; Anzenbacher, P. *Biochim. Biophys. Acta* **2007**, *1770*, 376.
- (30) Budisa, N. *Protein Sci.* **2001**, *10*, 1281.
- (31) Cooke, S. A.; Corlett, G. K.; Legon, A. C. *J. Chem. Soc., Faraday Trans.* **1998**, *94*, 1565.
- (32) Tsuzuki, S.; Honda, K.; Azumi, R. *J. Am. Chem. Soc.* **2002**, *124*, 12200.
- (33) Pullman, B.; Pullman, A. *Proc. Natl. Acad. Sci. U. S. A.* **1958**, *44*, 1197.
- (34) Gallivan, J. P.; Daugherty, D. A. *Proc. Natl. Acad. Sci. U. S. A.* **1999**, *96*, 9459.
- (35) Singh, J.; Thornton, J. M. *J. Mol. Biol.* **1990**, *211*, 751.
- (36) Sanchez-Sixto J. *J. Med. Chem.* **2005**, *48*, 4871.
- (37) Mitchell, J. B. O.; Nandi, C. L.; McDonald, I. K.; Thornton, J. M.; Price, S. L. *J. Mol. Biol.* **1994**, *239*, 315.
- (38) Wilson et al. *Proc. Natl. Acad. Sci. U. S. A.* **1992**, *89*, 9257.
- (39) Huang, D.-M. *Chem. Phys. Lett.* **2005**, *407*, 222.
- (40) Collington, E. W.; Hallett, P.; Wallis, C. J.; Bradshaw, J.; EP 81-300078, 1981.
- (41) Reuben D.; *J. Org. Chem.* **1997**, *62*, 6921.
- (42) Halgren, T. A. *J. Comput. Chem.* **1999**, *20*, 730.
- (43) Becke, A. D. *J. Chem. Phys.* **1993**, *98*, 5648.
- (44) Stevens, P. J.; Devlin, J. F.; Chabalowski, C. F.; Frisch, M. J. *J. Phys. Chem.* **1994**, *98*, 11623.
- (45) Blundell, T. L.; Carney, D.; Gardner, S.; Hayes, F.; Howlin, B.; Hubbard, T.; Overington, J.; Singh, D. A.; Sibanda, B. L.; Sutcliffe, M. *Eur. J. Biochem.* **1988**, *172*, 513.
- (46) Sali, A.; Overington, J. P. *Proteins Sci.* **1994**, *3*, 1582.
- (47) Notredame, C.; Higgins, D. G.; Heringa, J. *J. Mol. Biol.* **2000**, *302*, 205.
- (48) McGuffin, L. J.; Bryson, K.; Jones, D. T. *Bioinformatics*, **2000**, *16*, 404.
- (49) Laskowski, R. A.; MacArthur M.W.; Moss, D. S.; Thornton, J. M. *J. Appl. Cryst.* **1993**, *26*, 283.
- (50) WHAT IF Web Interface <http://swift.cmbi.kun.nl/WIWWWI/>
- (51) Bottegoni, G.; Cavalli, A.; Recanatini, M. *J. Chem. Inf. Mod.* **2006**, *46*, 852.
- (52) Bottegoni G.; Rocchia W.; Recanatini M.; Cavalli A. *Bioinformatics*, **2006**, *22*, 58.
- (53) GaussView, Version 3.0, Dennington I.; Roy; Keith, T.; Millam, J.; Eppinnett, K.; Hovell, W. L.; Gilliland, R.; Semichem, Inc., Shawnee Mission, KS, **2003**.
- (54) Petti, M. A.; Shepodd, T. J.; Barrans, R.E., Jr.; Dougherty, D. A. *J. Am. Chem. Soc.* **1988**, *110*, 6825.

3.1.4.3. Paper III.

Synthesis, biological evaluation, and molecular modeling of abiraterone analogues: novel CYP17 inhibitors for the treatment of prostate cancer

Mariano A. E. Pinto-Bazurco Mendieta, Matthias Negri, Carsten Jagusch, Ursula Müller-Vieira, Thomas Lauterbach, and Rolf W. Hartmann

This article is protected by copyrights of 'Journal of Medicinal Chemistry.'

J. Med. Chem. **2008**, *51*, 5009–5018

Abstract

Abiraterone, a steroidal cytochrome P450 17 α -hydroxylase-17,20-lyase inhibitor (CYP17), is currently undergoing phase II clinical trials as a potential drug for the treatment of androgen-dependent prostate cancer. Since steroidal compounds often show side effects attributable to their structure, we have tried to replace the sterane scaffold by nonsteroidal core structures. The design and synthesis of 20 new abiraterone mimetics are described. Their activities have been tested with recombinant human CYP17 expressed in *E. coli*. Promising compounds were further evaluated for selectivity against CYP11B1, CYP11B2, and the hepatic CYP3A4. Compounds **19** and **20** showed comparable activity to abiraterone (IC₅₀ values of 144 and 64 nM vs 72 nM) and similar or even better selectivity against the other CYP enzymes. Selected compounds were also docked into our homology model, and the same binding modes as for abiraterone were found.

Introduction

Prostate cancer (PC) is the most common tumor and age-related cause of death in elder men worldwide.¹ Because of the advanced age of the patients, less invasive approaches are needed. Accordingly, the treatment of choice is 'watchful waiting,'² followed by radiation therapy only when it is necessary. Since PC is androgen dependent in over 80% of the cases, another current standard treatment is orchiectomy, the surgical removal of the testes, usually applied to patients under 70 years old. The reduction of testicular androgen production by gonadotropin-releasing hormone (GnRH) analogues,³ a 'medical castration', is often preferred over the surgical one and can also be used for treating older patients. Nevertheless, castration whether surgical or medical reduces maximally 90-95% of the daily testosterone production, which is often not enough to stop the tumor from growing, since prostate levels of testosterone and dihydrotestosterone are still about 25% and 10%, respectively, even after three months of treatment with a GnRH agonist.⁴

The remaining 5-10% of the androgens are produced in the adrenals. In the 1980s, Labrie⁵ hypothesized that additionally counteracting adrenal androgens by application of antiandrogens would further inhibit tumor growth. This approach, known as 'combined androgen blockade' (CAB), has been widely used in the past. The results have been partially positive, especially in patients with minimal disease and good performance status. However, it must be mentioned that antiandrogen therapy is associated with notable side effects.⁶ Another drawback of CAB is that in refractory PC regression is observed after discontinuation of antiandrogen administration. This led to the hypothesis that under antiandrogen treatment androgen receptor mutations occur causing PC cells to recognize antagonists as agonists.⁷

An alternative target proposed in the recent past is the cytochrome P450 enzyme 17 α -hydroxylase-17,20-lyase (CYP17). This enzyme is localized in the endoplasmic reticulum in the testes as well as in the adrenals and is the key enzyme for androgen biosynthesis. Its inhibition should stop the production of androgens both in the testes and in the adrenals, and therefore, inhibitors of CYP17 should be more effective for treating androgen-dependent PC than GnRH analogues. Proof of principle was achieved by the unspecific CYP inhibitor ketoconazole, which clinically turned out to be a good adjuvant therapeutic capable of reducing testosterone levels.⁸ Nevertheless, the side effects shown by this antimycotic compound are the reason that it is not used anymore.⁹

CYP17 catalyzes two reactions, the 17 α -hydroxylation of pregnenolone and progesterone to the corresponding 17 α alcohols and the subsequent 17,20-lyase reaction cleaving the C17-C20 bond. This yields the 17-keto androgens androstendione and dehydroepiandrosterone, precursors of all other androgens, including testosterone (Chart 1).

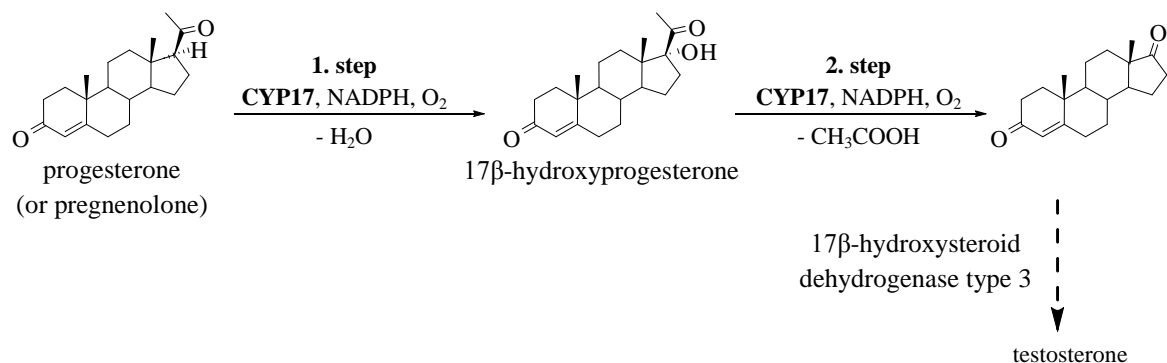


Chart 1. The role of CYP17 in androgen biosynthesis

The side effects of ketoconazole caused others¹⁰ and our group to develop steroidal¹¹ and nonsteroidal^{12,13} inhibitors. One compound, the steroidal CYP17 inhibitor abiraterone (Chart 2), is currently undergoing phase II clinical trials showing high activity in postdocetaxel castration refractory PC patients. In contrast to ketoconazole, it seems to have no dose-limiting toxicity.¹⁴

Because steroidal compounds often show side effects due to interactions with steroid receptors,¹⁵ it is our aim to develop nonsteroidal compounds. In this work, we present the design, synthesis, *in vitro* evaluation regarding activity and selectivity and modeling studies of nonsteroidal analogues of abiraterone (Chart 3).

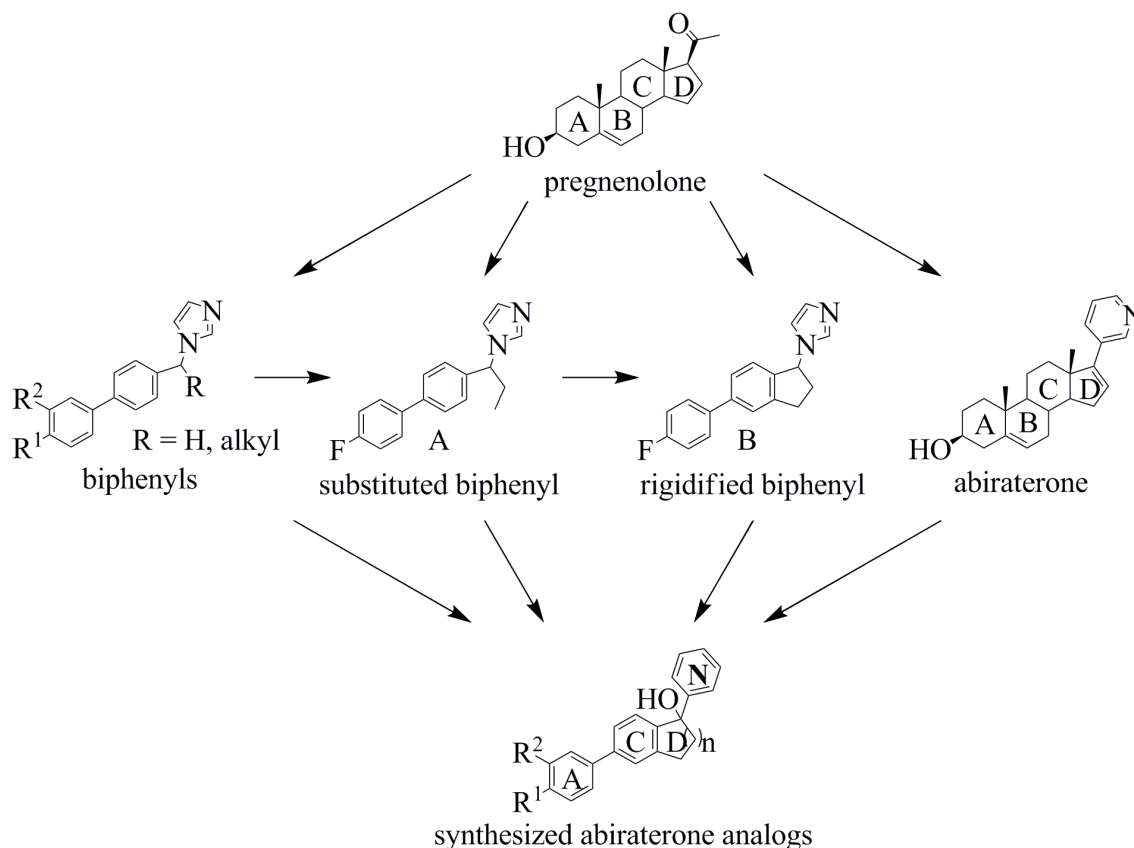
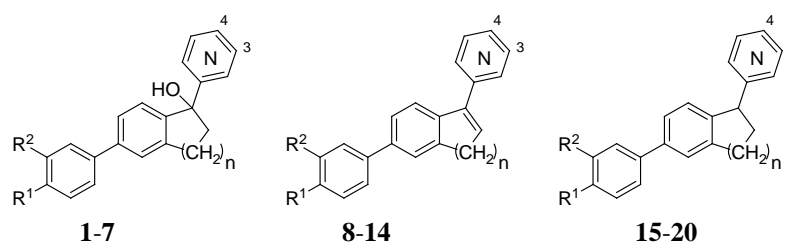


Chart 2. Substrate, abiraterone and synthesized mimetics

Design

The three most important structural features of abiraterone are the aromatic nitrogen-containing heterocycle, the hydrophobic steroidal core, and the hydroxy group mimicking the oxygen at the 3-position of the substrates. All of them are similarly important for a high affinity to the enzyme. CYP enzymes have the particularity of bearing a heme moiety in their binding site. The complexation of the Fe^{2+} of the heme with an sp^2 hybridized nitrogen as in pyridyl and imidazolyl is widely described.¹⁶ In recent studies¹³ we showed that a biphenyl moiety can replace the steroidal core AC-rings and that a biphenyl moiety furnished with an imidazolyl-methylene group ensures high CYP17 inhibitory activity (Chart 2). Introduction of alkyl substituents at the methylene bridge^{13b,f} (for example, compound **A**^{13f}) and first attempts to rigidify the structures resulting in indane compounds (like compound **B**^{13b}) increased activity. Interestingly, 4-fluoro substituted compounds in general showed very high inhibitory activity. Compound **A**, the indane ring opened analogue to compound **B**, was more active in the rat and showed a longer plasma half-life and higher bioavailability compared to abiraterone, while its *in vitro* activity with regard to potency and selectivity was not as outstanding as that of the steroidal compound. In this work we want to elucidate whether it is possible to further increase activity and especially selectivity by additional attempts to rigidify the biphenyl structure and to exchange the heterocycle. The resulting compounds are mimics of the steroidal compound abiraterone. For the design of the synthesized compounds, the steroidal core was replaced by an indane (mimicking the steroidal C- and D-rings) or tetrahydronaphthalene scaffold (for expansion of the D-ring) connected to an A-ring mimicking phenyl moiety. Electron donating and withdrawing substituents (including hydroxy and fluoro) were introduced in different positions at the phenyl ring. The iron-complexing aromatic nitrogen was represented by a 3- or 4-pyridine moiety.



Compound	R ¹	R ²	n	N
1	F	H	1	3
2	F	H	1	4
3	OMe	H	1	4
4	OMe	F	1	4
5	F	H	2	4
6	F	F	2	4
7	OMe	F	2	4
8	F	H	1	3
9	F	H	1	4
10	OMe	H	1	4
11	F	H	2	4
12	F	F	2	4
13	OH	OH	2	4
14	OH	F	2	4
15	F	H	1	3
16	F	H	1	4
17	F	H	2	4
18	F	F	2	4
19	OH	OH	2	4
20	OH	F	2	4

Chart 3. List of synthesized compounds 1-20

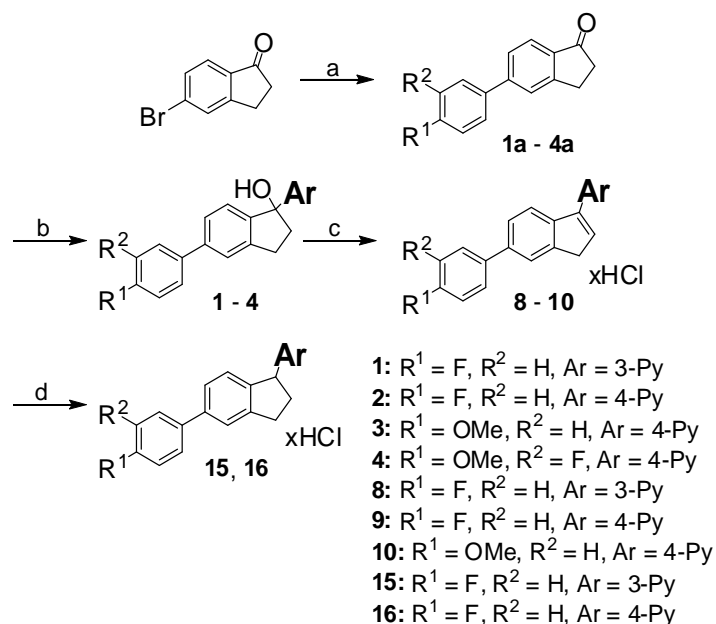
Three classes of mimetically relevant compounds were synthesized. Compounds **1-7**, hydroxylated at the C17 mimicking position, are analogues of the steroidal substrates for the second enzymatic step (lyase reaction). Compounds **7-14** bearing a double bond are structurally analogous to abiraterone. The saturated alkanes **15-20** show the highest similarity to the first-step (hydroxylase reaction) substrates.

In the following, the synthesis, determination of activity, and selectivity and molecular modeling studies of the synthesized abiraterone analogues are presented. Besides CYP17 inhibitory activity, inhibition of other CYP enzymes was examined to exclude possible side effects due to unspecific heme iron complexation. Thus, selectivity toward CYP11B1 and CYP11B2 was determined, since their biological relevance relies on the fact that CYP11B1 is involved in glucocorticoid biosynthesis while CYP11B2 catalyzes the last step in mineralocorticoid formation. Special attention was given to the most crucial hepatic enzyme CYP3A4, since it is involved in the metabolism of over 50% of all prescription drugs.¹⁷ The most interesting compounds were docked into our homology-approach derived protein model and the binding modes in the active site discussed.

Chemistry

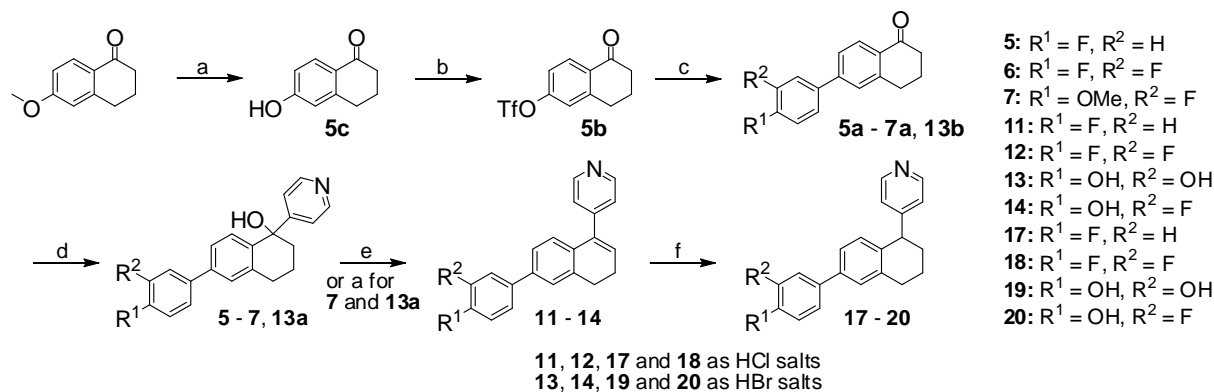
The syntheses of compounds **1-20** are shown in Schemes 1 and 2. In our aim to rigidify our biphenylic core structure by connecting the methylene bridge with the C-ring mimicking phenyl moiety, we synthesized indane derivatives (Scheme 1), which can be considered abiraterone analogues, and expanded the nonaromatic ring by one methylene group yielding tetrahydronaphthalene derivatives (Scheme 2). Different substitution patterns at the A-ring mimicking phenyl substituent were used. Suzuki coupling¹⁸ (Method A) using 5-bromoindanone for the abiraterone analogues and 1-tetralon-6-yl trifluoromethanesulfonate, synthesized from the respective alcohol, for the tetrahydronaphthalenes yielded the indanones **1a-4a** and the tetralones **5a-7a**. The pyridine moiety was introduced by means of a nucleophilic addition (Method B) with the corresponding lithium pyridinyl salt to yield the tertiary alcohols **1-7** and **13a**. The condensation to the corresponding alkenes was performed in HCl/isopropanol (**8-12**, Method C) or in HBr/H₂O (**13** and **14**, Method E). The latter method was applied when a simultaneous ether cleavage was desired. The hydration to the saturated rings was carried out with Pearlman's catalyst (Pd(OH)₂), resulting in compounds **15-20** (Method D).

Scheme 1. Synthesis of indane derivatives.



Reagents and conditions: **a: Method A:** Na₂CO₃, R¹R²C₆H₃B(OH)₂, Pd(PPh₃)₄, toluene, H₂O, reflux, 8 h; **b: Method B:** 3-iodopyridine or 4-bromopyridine, *n*-BuLi, THF, Et₂O, -78 °C - rt, 3h; **c: Method C:** HCl in *i*-propanol, rt, 2h; **d: Method D:** Pd(OH)₂, ethanol, THF, H₂, rt, 3h.

Scheme 2. Synthesis of tetrahydronaphthalene derivatives.



Reagents and conditions: **a: Method E:** HBr, reflux, 16 h; **b:** pyridine, Tf₂O, DCM, 0 °C - rt, 3h; **c: Method A:** Na₂CO₃, R¹R²C₆H₃B(OH)₂, Pd(PPh₃)₄, toluene, H₂O, reflux, 8 h; **d: Method B:** 3-iodopyridine or 4-bromopyridine, *n*-BuLi, THF, Et₂O, -78 °C - rt, 3h; **e: Method C:** HCl in *i*-propanol, rt, 2h; **f: Method D:** Pd(OH)₂, ethanol, THF, H₂, rt, 3h.

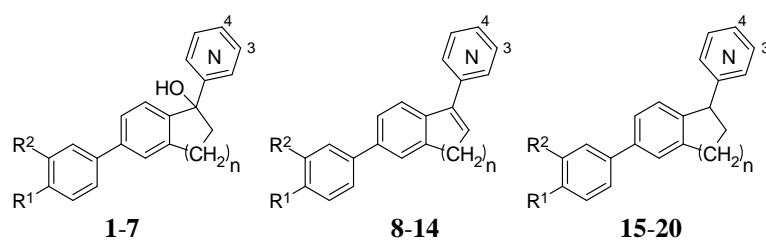
Results

Biological Results. Inhibition of human CYP17 was determined by performing our previously described assay.^{13d}

For the source of human CYP17, *E. coli*¹⁹ coexpressing human CYP17 and NADPH-P450 reductase were used. After homogenization, the 50 000 g sediment was incubated with progesterone (25 μM) and the inhibitor.^{12a} Separation of the product was performed by HPLC using UV detection. The IC₅₀ values determined for compounds **1-20** are shown in Table 1.

The compounds can be divided into two classes according to the CD-ring mimicking moiety, namely in indane and hydronaphthalene derivatives, and also into three classes regarding the pyridyl bearing C atom, that is in alcohols, alkenes, and alkanes. Most of the indane derivatives, either bearing a 3-pyridyl or a 4-pyridyl substituent, showed no or little CYP17 inhibition. Only compound **2**, with a moderate inhibition of 333 nM, and compound **16** (IC₅₀ = 233 nM) were active. Interestingly, both compounds contain a 4-pyridyl group as iron-complexing heterocycle and a fluorine at R¹.

The hydronaphthalenes were more potent than the indanes, showing a broad range of activity. The alkenes (**11-14**) were weaker inhibitors than the corresponding compounds with a single bond, the alcohols (**5-7**) and tetrahydronaphthalenes (**17-20**). The inhibition values range from about 200 to over 5000 nM, while for the single bond compounds the values range mostly from around 100 to 500 nM. An important condition for inhibitory activity in the class of the alkanes is a 4-pyridyl substituent. In the 4-position of the phenyl ring (R¹) a F or OH group and in 3-position (R²) H, F, or OH led to highly active compounds. Interestingly, the 3,4-di-F-substituted compound **18** only showed moderate activity. One explanation for this finding might be the electron withdrawing effect of the two F atoms at the phenyl ring. The most potent compounds were the 4-OH compounds **19** and **20** (IC₅₀ = 144 and 64 nM). A hydroxy substituent in 4-position of the phenyl ring also makes the alkenes from the 4-pyridyl substituted dihydronaphthalene type potent inhibitors (compounds **13** and **14**). In the class of the indenenes, 3-pyridyl substitution, as in abiraterone, led to an active compound (**8**) whereas 4-pyridyl substitution does not (**9**). It is striking, that 11 out of the 20 synthesized compounds were more active than ketoconazole. The most potent compound **20** showed a slightly higher inhibition compared to abiraterone (IC₅₀ = 72 nM). Our seven most potent compounds from this work were more active than compound **A** (345 nM), and regarding compound **B** (670 nM), nine showed significantly higher inhibitory activities for CYP17. In the whole cell assay, i.e., *E. coli* coexpressing human CYP17 and NADPH-P450 reductase,^{12f} the most active compound of this series, **20**, was also highly active (IC₅₀ < 200 nM).

Table 1. Inhibition of CYP17 by alcohols **1-7**, alkenes **8-4** and alkanes **15-20**

Structures ^a				CYP17 IC ₅₀ [nM] ^b					
R ¹	R ²	n	N	Comp. ^a	Alcohols	Comp. ^a	Alkenes	Comp. ^a	Alkanes
Indanes									
F	H	1	3	1	> 20,000	8	2346	15	> 20,000
F	H	1	4	2	333	9	> 20,000	16	233
OMe	H	1	4	3	> 20,000	10	> 5,000		
OMe	F	1	4	4	> 10,000				
Hydronaphthalenes									
F	H	2	4	5	587	11	> 5,000	17	163
F	F	2	4	6	423	12	> 5,000	18	1222
OMe	F	2	4	7	> 5,000				
OH	OH	2	4			13	307	19	144
OH	F	2	4			14	188	20	64
		KTZ ^c					2780		
		ABT ^d					72		

^a Compounds **8-12** and **15-18** were tested as HCl salts and **13, 14, 19** and **20** as HBr salts

^b Data shown were obtained by performing the tests in duplicate. The deviations were within < ±5 %. Concentration of progesterone (substrate) was 25 μM

^c **KTZ**: ketoconazole

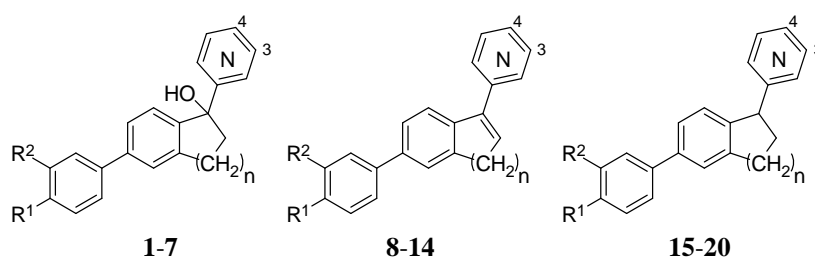
^d **ABT**: abiraterone

Since the target enzyme contains a heme in its binding site, hence CYP/P450 enzyme, which is crucial for the enzymatic reaction and for binding the iron-complexing nitrogen containing inhibitors, the latter compounds were tested for selectivity against other CYP enzymes. Accordingly, selected compounds were tested for inhibitory activity on the steroidogenic CYP enzymes CYP11B1 and CYP11B2, key enzymes in glucocorticoid and mineralocorticoid biosynthesis. For the assay,²⁰ V79MZh11B1 cells expressing human CYP11B1 and V79MZh11B2 cells expressing human CYP11B2 were used. The IC₅₀ values determined for selected compounds are shown in Table 2.

With the exception of compounds **4** and **7** showing IC₅₀ values of 291 and 686 nM toward CYP11B1, respectively, the other tested compounds exhibited IC₅₀ values above 1 μM. Most of the compounds (**2, 6, 11-14, 17-19**) turned out to be more selective than abiraterone (IC₅₀ = 1608 nM), and all compounds were more selective compared to ketoconazole (127 nM) regarding the cortisol forming enzyme. Concerning compound **A** (66% inhibition at 0.2 μM), all compounds from this study showed much higher selectivity.

The inhibition of CYP11B2 observed with the evaluated compounds was a little higher showing IC₅₀ values between 121 and 2324 nM. Compared to abiraterone (IC₅₀ = 1751 nM), compounds **6** and **13** exhibited a similar selectivity whereas compound **19** (IC₅₀ = 2324 nM) was more selective than the reference. Compared to ketoconazole (IC₅₀ = 67 nM) and compound **A** (66% inhibition at 0.2 μM), all compounds were more selective with the exception of compound **11** (IC₅₀ = 121 nM).

The synthesized compounds were also evaluated for inhibition of the most crucial hepatic CYP enzyme CYP3A4 in regard to its important role in drug metabolism. Except for compound **9** (IC₅₀ = 159 nM) and compound **13** (IC₅₀ = 357 nM), the IC₅₀ values for compounds **1-20** were between 632 and >20000 nM. These compounds were more selective than ketoconazole (72 nM) and compound **A** (88% at 1 μM). Most of the compounds were even more selective than abiraterone (IC₅₀ = 2704 nM).

Table 2. Inhibition of CYP11B1, CYP11B2 and CYP3A4 by compounds **1-20**

Comp. ^a	Structures				CYP11B1 ^b	CYP11B2 ^b	CYP3A4 ^b
	R ¹	R ²	n	N	IC ₅₀ [nM]	IC ₅₀ [nM]	IC ₅₀ [nM]
1	F	H	1	3	n.d. ^c	n.d.	> 20,000
2	F	H	1	4	> 10,000	816	3231
3	OMe	H	1	4	n.d.	n.d.	3291
4	OMe	F	1	4	291	436	3364
5	F	H	2	4	1159	840	8757
6	F	F	2	4	3109	1676	13841
7	OMe	F	2	4	686	945	15190
8	F	H	1	3	n.d.	n.d.	6947
9	F	H	1	4	n.d.	n.d.	159
10	OMe	H	1	4	n.d.	n.d.	2394
11	F	H	2	4	> 10,000	121	4199
12	F	F	2	4	> 20,000	311	3643
13	OH	OH	2	4	> 10,000	1492	357
14	OH	F	2	4	2748	991	2114
15	F	H	1	3	n.d.	n.d.	1697
16	F	H	1	4	1076	543	1093
17	F	H	2	4	> 5,000	518	2173
18	F	F	2	4	> 20,000	567	2300
19	OH	OH	2	4	2135	2324	632
20	OH	F	2	4	1370	587	3386
	KTZ^d				127	67	72
	ABT^e				1608	1751	2704

^a Compounds **8-12** and **15-18** were tested as HCl salts and **13, 14, 19** and **20** as HBr salts

^b Data shown were obtained by performing the tests in duplicate. The deviations were within $\pm 5\%$. Concentration of progesterone (substrate) was 25 μM

^c n.d.: not determined

^d **KTZ**: ketoconazole

^e **ABT**: abiraterone

Molecular Modeling. Since there is no crystal structure of CYP17 available, we recently built a homology model using the X-ray structure of human CYP2C9 (PDB ID 1r9o) as template.^{13e} Docking simulations with energy minimized compounds were carried out by means of the GOLD 3.2 software running Linux CentOS 5.1 on an Intel® P4 CPU 3.00 GHz computer, using a slightly modified GOLDScore function with goldscore.P450_pdb parameters, for a better evaluation of hydrophobic interactions. From every class, the most potent compounds were docked into this protein model, and in the case of chiral compounds, both enantiomers were docked.

In Figure 1 two binding modes of the substrate pregnenolone are shown: one already described by others²¹ (SM1 mode) and an additional one (SM2). Poses in SM1 occur more often (approximately 7:3) with an overall better scoring with respect to those in SM2. Furthermore, pregnenolone was also docked with CHEMSCORE, a scoring function with a higher assessment of the hydrophobic interactions, showing poses mostly in SM1 (>9:1). Interestingly, great similarities between SM2 and the orientation of our previously described biphenyl compound **A**

can be observed (there are actually two very similar modes described as BM1 and BM2^{13e}). Like the substrate, the steroidal inhibitor abiraterone is also able to bind in both modes but showing a good complexation with the heme iron only in SM1 (Figure 1). The same is true for compound **B**, the ring-closed analogue of compound **A** (not shown).

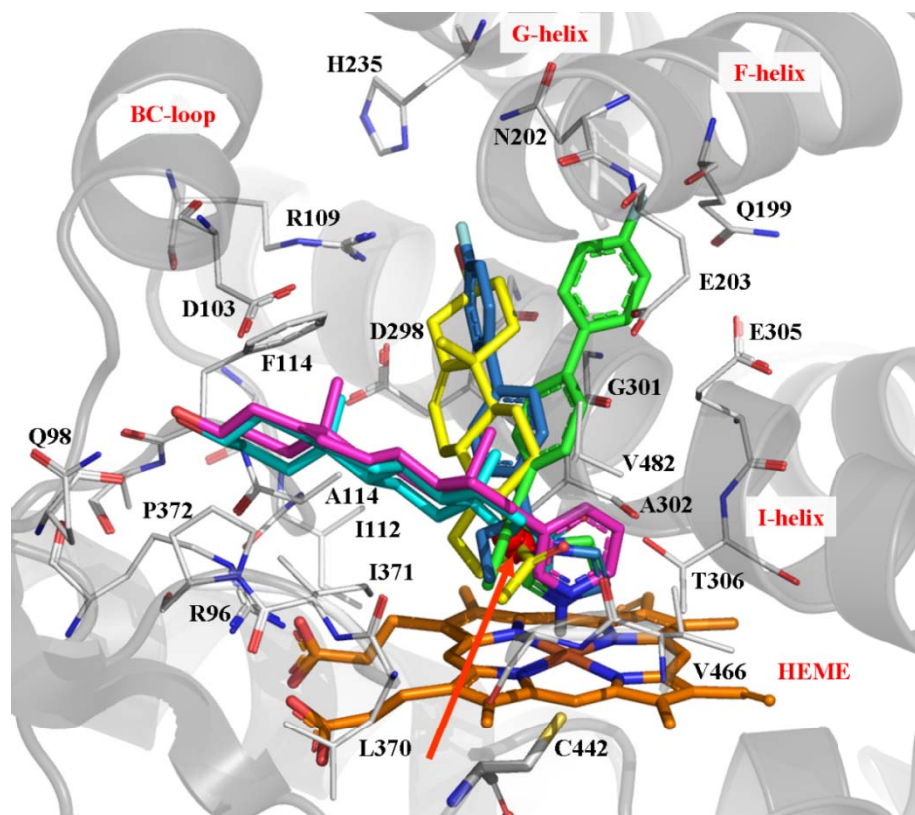


Figure 1. Both binding modes of the substrate pregnenolone (SM1, cyan, and SM2, yellow; the red arrow indicates the position of the C17 atoms, rendered as red spheres) are shown as docking complex with CYP17. For comparison, the two orientations of compound **A** (in the formerly described binding modes BM1, blue, and BM2, green^{13f}) and abiraterone (magenta) are given. Heme, interacting residues and ribbon rendered tertiary structure of the active site are also represented. Figures were generated with Pymol (<http://www.pymol.org>).

The *R* and *S* configured abiraterone analogues of the alcohol and alkane class also bind in both modes. Interestingly, a correlation between the inhibitory activities of the compounds of each class and the score values could be observed. In the case of highly active compounds, the percentage of poses presenting a good iron-nitrogen coordination is higher than for weak inhibitors. For enantiomers of a given racemic compound, one enantiomer always shows a preference for poses in one binding mode while the other enantiomer prefers to dock in the alternative one. In the case of the alcohols, in Figure 2 exemplified by compound **5**, the *R* enantiomer binds predominantly in the SM1 mode (9:1) while the *S* enantiomer binds in SM2 (8:2). The opposite relation can be seen for the alkanes (Figure 2).

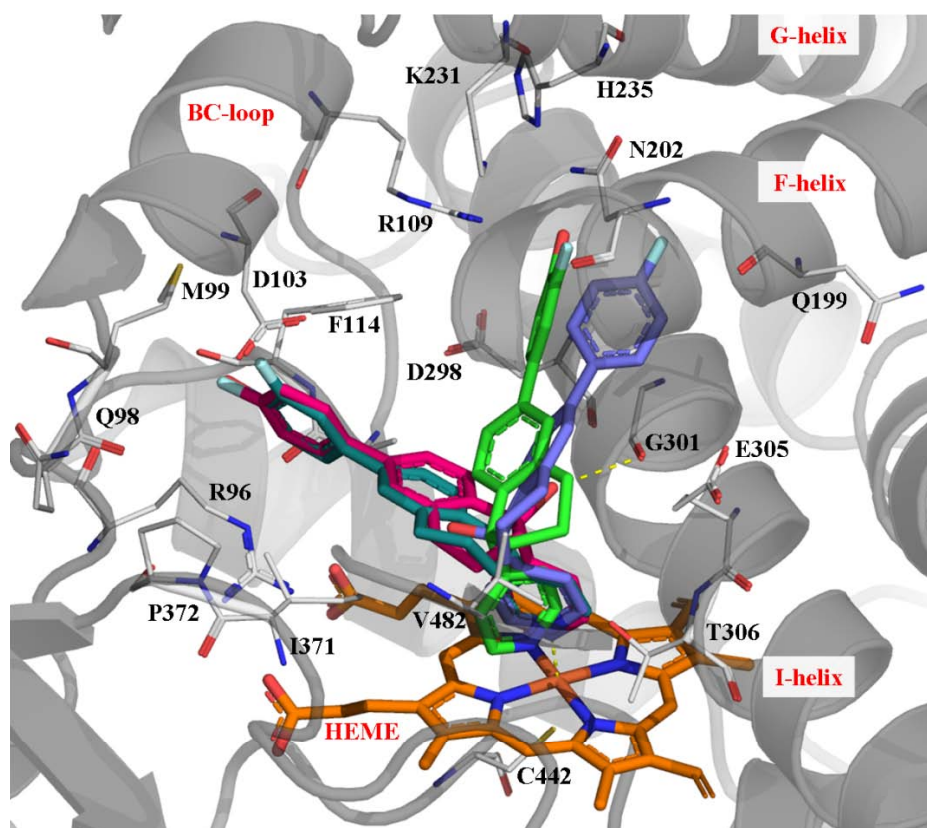


Figure 2. Docking complexes of CYP17 and compounds **5** (R enantiomer in SM1 - bluegreen; S enantiomer in SM2 - violet) and **20** (S enantiomer in SM1 - magenta; R enantiomer in SM2 - green). A dashed yellow line is representing the H-bond between the OH in C17 and the Gly301.

The most important interactions in SM1, besides heme iron complexation, are hydrophobic interactions with Ala113, Phe114, Ile371, Pro372, and Val482 and, depending on substituents R1 and R2, polar ones with the backbone of Glu98 and Met99 and the carboxyl group of Asp103. Furthermore, an H-bond formation between the OH group of R-alcohols and the backbone carbonile of Gly301 was observed, which could act as an additional stabilizing factor. Regarding SM2, the same interactions as described in refs 13e and 13f were found.

Low activity compounds did not show a real clustering in SM1 mode and were characterized by an unsuitable binding angle between the N lone electron pair and the heme plane (compound **12**, Figure 3). On the other hand, the highly active alkenes **13** and **14** bind preferentially in SM2 mode and present a good complexation of the heme iron and a strong binding due to their 3,4-di-OH or 3-F,4-OH substitution.

Discussion and Conclusion

In the class of the indanes the 3-pyridyl substituted unsaturated compound **8**, which is analogous to abiraterone, showed inhibitory activity in contrast to the respective alcohols and alkanes. In the case of the corresponding 4-pyridyl substituted compounds, it is the other way around: the alcohols and the alkanes were active, while the unsaturated compounds did not show activity. However, it became apparent that the five-membered ring, though analogous to the substrate and abiraterone, is not favorable for CYP17 inhibition. On the other hand, the expansion of this ring by one methylene group resulting in the hydronaphthalenes led to very potent and selective compounds. Summarizing, we have discovered nine very potent abiraterone analogues, four of them (**14**, **17**, **19**, and **20**) showing an IC_{50} value below 200 nM and one of them (**20**, $IC_{50} = 64$ nM) being slightly more active than abiraterone. These compounds showed low inhibition of the CYP enzymes considered for selectivity issues CYP11B1, CYP11B2 and the hepatic CYP3A4. Owing to their promising *in vitro* profile, presently compounds **20** and **19** are separated into their enantiomers and extensively evaluated for their *in vivo* activities and pharmacokinetics in the rat.

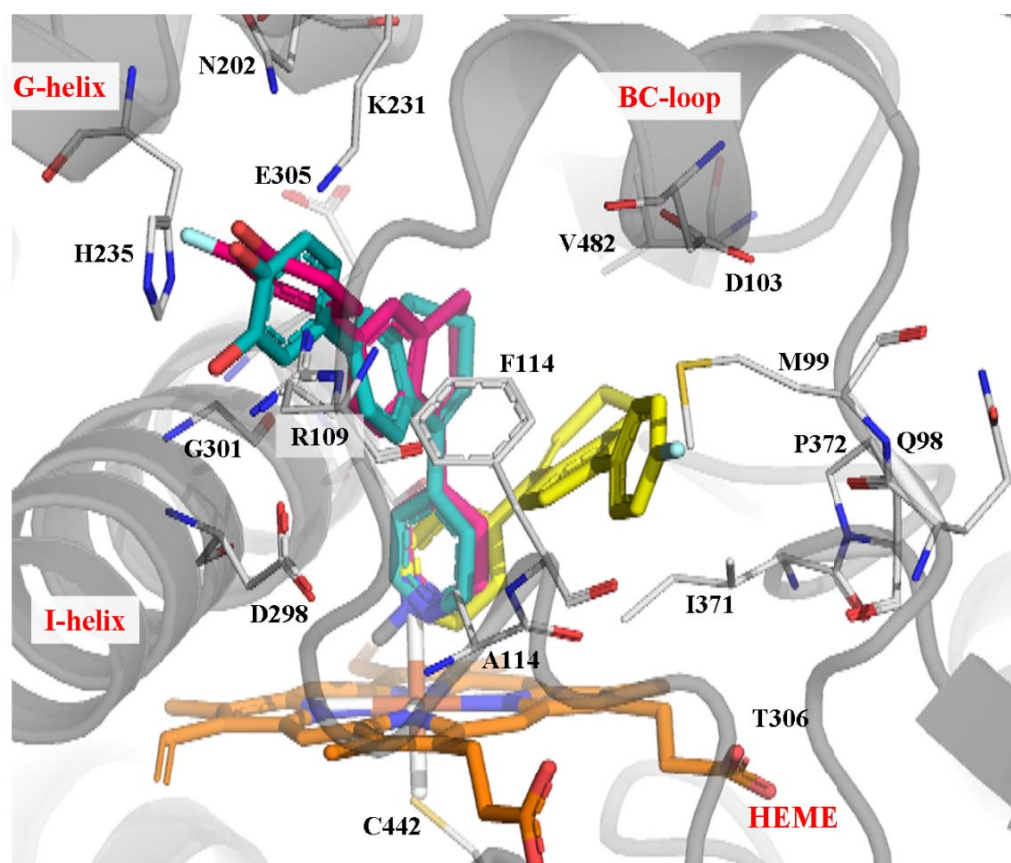


Figure 3. Docking complexes of CYP17 and compounds **11** (yellow; its lone electron pair at the nitrogen and the axis of the octahedral heme iron atom are shown), **13** (cyan) and **14** (magenta).

Experimental Section

Chemistry. IR spectra were recorded neat on a Bruker Vector 33FT-infrared spectrometer. $^1\text{H-NMR}$ spectra were measured on a Bruker DRX-500 (500 MHz). Chemical shifts are given in parts per million (ppm), and TMS was used as an internal standard for spectra obtained in CDCl_3 . All coupling constants (J) are given in Hz. ESI (electrospray ionization) mass spectra were determined on a TSQ quantum (Thermo Electron Corporation) instrument. Column chromatography was performed using silica-gel 60 (50-200 μm), and reaction progress was determined by TLC analysis on Alugram[®] SIL G/UV₂₅₄ (Macherey-Nagel). Boronic acids and bromoaryls used as starting materials were commercially obtained (CombiBlocks, Chempur, Aldrich, Acros).

Method A: Suzuki-Coupling. 5-Bromoindan-1-one (10 mmol) for compounds **1-4** or **5b** (10 mmol) for compounds **5-7** and the corresponding boronic acid (15 mmol) were dissolved in toluene (70 mL) and Na_2CO_3 (30mL, 2.0 M, aq). The mixture was deoxygenated under reduced pressure and flushed with N_2 . After repeating this 3 times, $\text{Pd}(\text{PPh}_3)_4$ (5 mol %) was added and the resulting suspension was heated under reflux for 8 h. After cooling, the phases were separated and the water phase was extracted 2 times with EtOAc. Then the combined organic extracts were dried over Na_2SO_4 , and concentrated under reduced pressure. The purification was performed by Si-gel flash-chromatography.

5-(4-Fluorophenyl)-2,3-dihydroindan-1-one (1a). Synthesized from 5-Bromoindan-1-one and 4-fluorophenylboronic acid according to Method A; yield = 95 %; δ_{H} (CDCl_3 , 500 MHz) 2.66-2.69 (m, 2H), 3.12-3.14 (m, 2H), 7.09 (t, $J = 8.7$ Hz, 2H), 7.48 (d, $J = 8.0$ Hz, 1H), 7.53 (dd, $J = 5.3$ Hz, $J = 8.7$ Hz, 2H), 7.56 (s, 1H), 7.75 (d, $J = 8.0$ Hz, 1H); δ_{C} (CDCl_3 , 125 MHz) 14.08, 22.63, 25.86, 26.97, 31.57, 36.50, 49.43, 115.84, 116.01, 124.17, 125.02, 126.62, 129.11, 129.17, 136.01, 146.64, 155.86, 162.07, 164.05, 206.40.

5-(4-Methoxyphenyl)-2,3-dihydroindan-1-one (3a). Synthesized from 5-Bromoindan-1-one and 4-methoxyphenylboronic acid according to Method A; yield = 42 %. Since the so obtained ketone was used directly for the nucleophilic addition no analytics was performed.

5-(3-Fluoro-4-methoxyphenyl)-2,3-dihydroindan-1-one (4a). Synthesized from 5-Bromoindan-1-one and 3-fluoro-4-methoxyphenylboronic acid according to Method A; yield = 99 %; δ_{H} (CDCl_3 , 500 MHz) 2.64-2.67 (m,

2H), 3.11 (t, $J = 5.7$ Hz, 2H), 3.87 (s, 3H), 6.97 (t, $J = 8.7$ Hz, 1H), 7.27-7.32 (m, 2H), 7.46 (d, $J = 8.7$ Hz, 1H), 7.53 (s, 1H), 7.71 (d, $J = 8.0$ Hz, 1H); δ_C (CDCl₃, 125 MHz) 25.85, 36.50, 56.35, 113.71, 115.01, 115.20, 123.20, 123.23, 124.17, 124.58, 126.24, 128.43, 128.55, 131.91, 131.94, 132.04, 132.14, 133.15, 133.22, 135.91, 146.03, 147.90, 148.01, 151.37, 153.82, 155.93, 206.40.

6-(4-Fluorophenyl)-3,4-dihydronaphthalen-1(2H)-one (5a). Synthesized from **5b** and 4-fluorophenylboronic acid according to Method A; yield = 89 %; δ_H (CDCl₃, 500 MHz) 2.05-2.10 (m, 2H), 2.59 (t, $J = 6.8$ Hz, 2H), 2.92 (t, $J = 6.1$ Hz, 2H), 7.05 (t, $J = 8.7$ Hz, 1H), 7.32 (s, 1H), 7.38 (dd, $J = 1.7$ Hz, $J = 8.2$ Hz, 1H), 7.48 (dd, $J = 5.3$ Hz, $J = 8.8$ Hz, 1H), 8.00 (d, $J = 8.1$ Hz, 1H); δ_C (CDCl₃, 125 MHz) 23.29, 29.91, 39.14, 115.76, 115.93, 125.33, 127.12, 127.90, 128.89, 128.96, 131.46, 136.13, 144.92, 145.01, 161.98, 163.95, 198.00.

6-(3,4-Difluorophenyl)-3,4-dihydronaphthalen-1(2H)-one (6a). Synthesized from **5b** and 3,4-difluorophenylboronic acid according to Method A; yield = 87 %. Since the so obtained ketone was used directly for the nucleophilic addition no analytics was performed.

6-(3-Fluoro-4-methoxyphenyl)-3,4-dihydronaphthalen-1(2H)-one (7a). Synthesized from **5b** and 3-fluoro-4-methoxyphenylboronic acid according to Method A; yield = 59 %; δ_H (CDCl₃, 500 MHz) 2.07-2.12 (m, 2H), 2.60 (t, $J = 6.3$ Hz, 2H), 2.94 (t, $J = 6.1$ Hz, 2H), 3.86 (s, 3H), 6.96 (t, $J = 8.7$ Hz, 1H), 7.27-7.30 (m, 2H), 7.33 (s, 1H), 7.39 (dd, $J = 1.6$ Hz, $J = 8.2$ Hz, 1H), 8.00 (d, $J = 8.2$ Hz, 1H); δ_C (CDCl₃, 125 MHz) 23.28, 29.92, 39.14, 56.33, 113.62, 114.82, 114.98, 123.01, 124.97, 126.70, 127.94, 131.37, 132.98, 133.03, 144.39, 145.04, 147.80, 147.88, 151.59, 153.55, 198.01.

6-(3,4-Dimethoxyphenyl)-3,4-dihydronaphthalen-1(2H)-one (13b). Synthesized from **5b** and 3,4-dimethoxyphenylboronic acid according to Method A; yield = 87 %. Since the so obtained ketone was used directly for the nucleophilic addition no analytics was performed.

Method B: Nucleophilic Addition of the Heterocycle. 3-Iodopyridine (4 mmol) – or either 4-Bromopyridine (4 mmol) for the 4-pyridyl compounds, after basic extraction of its hydrochloride salt with Et₂O (20 mL) and NaHCO₃ (satd, aq), followed by drying over Na₂SO₄ and concentration under reduced pressure – was prepared in Et₂O and THF (3:2, 50 mL) at -78°C. Then *n*-BuLi in hexanes (1.6 N, 4.4 mmol) was added and after 5 sec the corresponding ketone (4 mmol) in THF (20 mL) was added at once and the mixture was left stirring for additional 3 h at room temperature. After neutralization with NH₄Cl (satd, aq), the phases were separated, the aqueous layer extracted 2 times with EtOAc and the combined organic extracts dried over Na₂SO₄ and concentrated under reduced pressure. The purification was performed by Si-gel flash-chromatography.

5-(4-Fluorophenyl)-1-(pyridin-3-yl)-2,3-dihydro-1H-inden-1-ol (1). Synthesized from **1a** and 3-Iodopyridine according to Method B; yield = 55 %; IR (ATR) ν (cm⁻¹) 2925, 1604, 1516, 1482, 1418, 1223, 1159, 1060, 1027, 822, 713, 685, 605, 537, 507; δ_H (CDCl₃, 500 MHz) 2.36-2.47 (m, 2H), 2.85-2.89 (m, 1H), 3.08-3.14 (m, 1H), 6.98-7.04 (m, 3H), 7.14-7.16 (m, 1H), 7.24-7.26 (d, $J = 7.9$ Hz, 1H), 7.36 (s, 1H), 7.41-7.44 (m, 2H), 7.69 (d, $J = 7.9$ Hz, 1H), 8.29 (s, 1H), 8.48 (s, 1H); δ_C (CDCl₃, 125 MHz) 14.19, 21.03, 29.89, 44.96, 60.41, 83.55, 115.57, 115.74, 123.07, 123.69, 124.34, 126.30, 128.44, 128.54, 128.73, 128.79, 132.03, 132.11, 133.88, 137.15, 141.02, 142.31, 144.74, 146.32, 147.32, 147.77, 161.54, 163.50, 171.20; $m/z = 305.17$ [M⁺+H].

5-(4-Fluorophenyl)-1-(pyridin-4-yl)-2,3-dihydro-1H-inden-1-ol (2). Synthesized from **2a** and 4-Bromopyridine according to Method B; yield = 50 %; IR (ATR) ν (cm⁻¹) 2931, 1601, 1515, 1482, 1412, 1223, 1159, 1066, 822, 676, 601, 533, 518; δ_H (CDCl₃ + CD₃OD, 500 MHz) 2.37-2.47 (m, 2H), 2.92-2.98 (m, 1H), 3.15-3.21 (m, 1H), 7.00 (d, $J = 7.9$ Hz, 1H), 7.04 (t, $J = 8.6$ Hz, 2H), 7.29-7.31 (m, 3H), 7.41 (s, 1H), 7.41-7.47 (m, 2H), 8.38 (d, $J = 4.8$ Hz, 2H); δ_C (CDCl₃ + CD₃OD, 125 MHz) 29.90, 44.32, 83.82, 115.44, 115.61, 121.16, 123.46, 124.31, 126.17, 128.63, 128.69, 137.05, 140.95, 144.75, 145.90, 148.70, 156.88, 161.46, 163.42; $m/z = 306.21$ [M⁺+H].

5-(4-Methoxyphenyl)-1-(pyridin-4-yl)-2,3-dihydro-1H-inden-1-ol (3). Synthesized from **3a** and 4-Bromopyridine according to Method B; yield = 45 %; IR (ATR) ν (cm⁻¹) 3165, 2957, 2837, 1606, 1519, 1482, 1456, 1287, 1249, 1182, 1113, 1069, 1039, 1022, 1002, 815, 671, 510, 542; δ_H (CDCl₃ + CD₃OD, 500 MHz) 2.34-2.46 (m, 2H), 2.91-2.97 (m, 1H), 3.12-3.20 (m, 1H), 3.77 (s, 3H), 6.90 (d, $J = 8.8$ Hz, 2H), 6.98 (d, $J = 7.9$ Hz, 1H), 7.30-7.32 (m, 3H), 7.42 (s, 1H), 7.44 (d, $J = 8.8$ Hz, 2H), 8.38 (d, $J = 6.2$ Hz, 2H); δ_C (CDCl₃ + CD₃OD, 125 MHz) 29.95, 44.43, 55.29, 83.93, 114.19, 121.15, 123.15, 124.20, 125.93, 128.16, 133.49, 141.61, 144.69, 145.29, 148.81, 156.77, 159.17; $m/z = 318.18$ [M⁺+H].

5-(3-Fluoro-4-methoxyphenyl)-1-(pyridin-4-yl)-2,3-dihydro-1H-inden-1-ol (4). Synthesized from **4a** and 4-Bromopyridine according to Method B; yield = 56 %; δ_H (CDCl₃, 500 MHz) 2.39-2.48 (m, 2H), 2.93-2.98 (m, 1H), 3.14-3.19 (m, 1H), 3.85 (s, 3H), 6.93-6.98 (m, 2H), 7.21-7.30 (m, 5H), 7.40 (s, 1H), 8.40 (d, $J = 6.2$ Hz, 2H); δ_C (CDCl₃, 125 MHz) 30.03, 44.69, 56.36, 84.27, 113.65, 114.81, 114.96, 120.92, 122.74, 123.37, 124.30, 126.11,

134.09, 134.14, 140.74, 144.92, 145.99, 147.16, 147.24, 149.23, 151.57, 153.53, 155.83; $m/z = 336.11$ [$M^+ + H$].

6-(4-Fluorophenyl)-1-(pyridin-4-yl)-1,2,3,4-tetrahydronaphthalen-1-ol (5). Synthesized from **5a** and 4-Bromopyridine according to Method B; yield = 44 %; δ_H ($CDCl_3 + CD_3OD$, 500 MHz) 1.75-1.82 (m, 1H), 2.00-2.08 (m, 2H), 2.09-2.16 (m, 1H), 2.86-3.00 (m, 2H), 6.98 (d, $J = 8.1$ Hz, 1H), 7.07 (t, $J = 8.8$ Hz, 2H), 7.27 (dd, $J = 2.0$ Hz, $J = 8.1$ Hz, 1H), 7.33-7.34 (m, 3H), 7.51 (dd, $J = 5.4$ Hz, $J = 8.6$ Hz, 2H), 8.40 (d, $J = 6.3$ Hz, 2H); δ_C ($CDCl_3 + CD_3OD$, 125 MHz) 23.05, 33.68, 44.68, 77.96, 119.19, 119.40, 126.04, 128.82, 131.06, 132.35, 132.43, 133.59, 140.68, 140.71, 141.91, 143.24, 143.34, 152.16, 153.76, 165.19, 167.64; $m/z = 320.06$ [$M^+ + H$].

6-(3,4-Difluorophenyl)-1-(pyridin-4-yl)-1,2,3,4-tetrahydronaphthalen-1-ol (6). Synthesized from **6a** and 4-Bromopyridine according to Method B; yield = 40 %; IR (ATR) ν (cm^{-1}) 3063, 1603, 1568, 1525, 1492, 1411, 1320, 1272, 1230, 1198, 1119, 1068, 986, 907, 874, 816, 773, 734, 671; δ_H ($CDCl_3 + CD_3OD$, 500 MHz) 1.81-1.89 (m, 1H), 1.99-2.07 (m, 2H), 2.12-2.18 (m, 1H), 2.89-3.00 (m, 2H), 6.99 (d, $J = 8.1$ Hz, 1H), 7.19 (q, $J = 8.4$ Hz, 1H), 7.24-7.26 (m, 2H), 7.30-7.37 (m, 4H), 8.48 (d, $J = 6.0$ Hz, 2H); δ_C ($CDCl_3 + CD_3OD$, 125 MHz) 20.77, 31.35, 42.36, 117.31, 117.45, 118.95, 119.09, 123.19, 124.35, 124.38, 124.40, 124.43, 126.74, 128.95, 131.14, 139.75, 140.18, 141.49, 150.36, 159.83, 192.24; $m/z = 338.13$ [$M^+ + H$].

6-(3-Fluoro-4-methoxyphenyl)-1-(pyridin-4-yl)-1,2,3,4-tetrahydronaphthalen-1-ol (7). Synthesized from **7a** and 4-Bromopyridine according to Method B; yield = 64 %; δ_H ($CDCl_3 + CD_3OD$, 500 MHz) 1.70-1.77 (m, 1H), 1.94-2.03 (m, 2H), 2.03-2.10 (m, 1H), 2.82-2.93 (m, 2H), 3.84 (s, 3H), 6.92 (dd, $J = 2.7$ Hz, $J = 8.1$ Hz, 2H), 6.96 (dt, $J = 2.4$ Hz, $J = 8.4$ Hz, 1H), 7.19-7.28 (m, 6H), 8.35-8.36 (m, 2H); δ_C ($CDCl_3 + CD_3OD$, 125 MHz) 19.02, 29.67, 40.64, 56.06, 73.93, 113.57, 114.23, 114.42, 121.91, 122.37, 122.40, 124.55, 126.74, 129.50, 133.67, 133.73, 137.88, 138.78, 139.11, 146.84, 146.94, 148.20, 151.14, 153.58, 159.42; $m/z = 350.13$ [$M^+ + H$].

6-(3,4-Dimethoxyphenyl)-1-(pyridin-4-yl)-1,2,3,4-tetrahydronaphthalen-1-ol (13a). Synthesized from **13b** and 4-Bromopyridine according to Method B; yield = 48 %. Since the so obtained alcohol was used directly for the condensation no analytics was performed.

Method C: Condensation with HCl. The corresponding alcohol (1 mmol) was refluxed in HCl in *i*-PrOH (10 mL, 3N) for 2 h. Afterwards, the resulting solution was concentrated under reduced pressure and washed 3 times with Et_2O . No further purification was necessary.

3-(5-(4-Fluorophenyl)-3H-inden-1-yl)pyridine hydrochloride (8). Synthesized from **1** according to Method C; yield = 96 %; IR (ATR) ν (cm^{-1}) 3051, 1601, 1514, 1468, 1229, 1189, 1161, 1104, 1027, 976, 940, 879, 821, 772, 716, 678, 557, 521; δ_H ($CDCl_3$, 500 MHz) 3.53 (s, 2H), 6.61-6.62 (m, 1H), 7.06 (t, $J = 8.7$ Hz, 2H), 7.32 (dd, $J = 4.8$ Hz, $J = 7.8$ Hz, 1H), 7.44 (dd, $J = 1.4$ Hz, $J = 7.8$, 1H), 7.49-7.52 (m, 3H), 7.65 (s, 1H), 7.83-7.85 (m, 1H), 8.55-8.56 (d, $J = 4.0$ Hz, 1H), 8.81 (s, 1H); δ_C ($CDCl_3$, 125 MHz) 38.54, 115.56, 115.73, 120.16, 123.06, 123.50, 125.46, 128.70, 128.76, 131.75, 132.81, 134.83, 137.51, 137.59, 141.72, 142.47, 145.37, 148.79, 148.91, 161.41, 163.37; MS (ESI): $m/z = 288.13$ [$M^+ + H$].

4-(5-(4-Fluorophenyl)-3H-inden-1-yl)pyridine hydrochloride (9). Synthesized from **2** according to Method C; yield = 100 %; IR (ATR) ν (cm^{-1}) 3482, 3414, 3100-2500, 2075, 1997, 1632, 1602, 1679, 1555, 1469, 1383, 1262, 1221, 1190, 1157, 1097, 1029, 948, 882, 829, 819, 787, 562, 552, 527; δ_H ($CDCl_3$, 500 MHz) 3.20-3.22 (m, 2H), 7.08 (t, $J = 8.8$ Hz, 2H), 7.30 (s, 1H), 7.54 (dd, $J = 1.7$ Hz, $J = 8.1$ Hz, 1H), 7.58 (dd, $J = 5.4$ Hz, $J = 8.8$ Hz, 2H), 7.69 (d, $J = 8.1$ Hz, 1H), 7.76 (d, $J = 1.4$ Hz, 1H), 8.30 (d, $J = 6.8$ Hz, 2H), 8.81 (d, $J = 6.8$ Hz, 2H); δ_C ($CDCl_3$, 125 MHz) 116.53, 116.71, 121.29, 124.36, 126.43, 126.75, 129.90, 129.96, 138.56, 139.74, 141.01, 141.67, 142.35, 142.96, 146.93, 155.08, 162.98, 164.93; $m/z = 287.96$ [$M^+ + H$].

4-(5-(4-Methoxyphenyl)-3H-inden-1-yl)pyridine hydrochloride (10). Synthesized from **3** according to Method C; yield = 99 %; IR (ATR) ν (cm^{-1}) 3404, 3061, 1632, 1605, 1517, 1496, 1469, 1244, 1185, 1036, 1020, 815, 768, 566; δ_H ($CDCl_3 + CD_3OD$, 500 MHz) 3.24-3.27 (m, 2H), 3.78 (s, 3H), 6.92 (d, $J = 8.8$ Hz, 2H), 7.43 (s, 1H), 7.50 (d, $J = 8.8$ Hz, 2H), 7.53 (dd, $J = 1.7$ Hz, $J = 8.1$ Hz, 1H), 7.60 (d, $J = 8.1$ Hz, 1H), 7.73 (d, $J = 1.7$ Hz, 1H), 8.23 (d, $J = 6.7$ Hz, 2H), 8.80 (d, $J = 6.7$ Hz, 2H); δ_C ($CDCl_3 + CD_3OD$, 125 MHz) 54.88, 114.03, 119.55, 122.91, 124.95, 125.20, 127.89, 133.02, 138.59, 139.21, 140.25, 140.92, 141.10, 144.94, 153.90, 159.08; $m/z = 301.16$ [$M^+ + H$].

4-(6-(4-Fluorophenyl)-3,4-dihydronaphthalen-1-yl)pyridine hydrochloride (11). Synthesized from **4** according to Method C; yield = 100 %; IR (ATR) ν (cm^{-1}) 3047, 2536, 1634, 1601, 1489, 1228, 1160, 825, 754, 733; δ_H ($CDCl_3$, 500 MHz) 2.58-2.61 (m, 2H), 2.94 (t, $J = 7.8$ Hz, 2H), 6.55 (t, $J = 4.7$ Hz, 1H), 6.95 (d, $J = 7.9$ Hz, 1H), 7.14 (t, $J = 8.7$ Hz, 2H), 7.38 (d, $J = 7.9$ Hz, 1H), 7.46 (s, 1H), 7.56 (dd, $J = 5.3$ Hz, $J = 8.7$ Hz, 2H), 7.93 (d, $J = 5.6$ Hz, 2H), 8.79 (d, $J = 5.6$ Hz, 2H); δ_C ($CDCl_3$, 125 MHz) 23.92, 27.76, 115.72, 115.90, 124.88, 125.37, 125.91, 127.01, 128.50, 128.56, 130.58, 135.87, 136.21, 137.39, 140.65, 140.67, 158.45, 161.71, 163.68, 190.74; $m/z =$

302.10 [M⁺+H].

4-(6-(3,4-Difluorophenyl)-3,4-dihydronaphthalen-1-yl)pyridine hydrochloride (12). Synthesized from **5** according to Method C; yield = 98 %; IR (ATR) ν (cm⁻¹) 3067, 1634, 1604, 1522, 1493, 1276, 1200, 1119, 911, 815, 773, 729, 614; δ_{H} (CDCl₃, 500 MHz) 2.57-2.61 (m, 2H), 2.94 (t, J = 8.0 Hz, 2H), 6.57 (t, J = 4.8 Hz, 1H), 6.96 (d, J = 8.0 Hz, 2H), 7.23 (q, J = 8.5 Hz, 1H), 7.29-7.31 (m, 1H), 7.36 (d, J = 8.5 Hz, 1H), 7.37-7.41 (m, 1H), 7.44 (s, 1H), 7.92 (s, 1H), 7.93 (s, 1H), 8.81 (s, 1H), 8.82 (s, 1H); δ_{C} (CDCl₃, 125 MHz) 23.86, 27.71, 115.77, 115.91, 117.63, 117.76, 122.83, 122.85, 122.87, 122.90, 124.97, 125.35, 125.91, 126.94, 131.12, 136.10, 136.14, 137.54, 139.48, 140.73, 149.11, 149.21, 149.52, 149.62, 151.10, 151.20, 151.50, 151.60, 158.26, 190.74; m/z = 320.11 [M⁺+H].

Method D: Hydration with Pearlman's catalyst. Pearlman's catalyst (10 mass %) and the corresponding alkene was prepared in EtOH and THF (2:1, 5mL) under H₂ atmosphere. The mixture was left stirring for 3 h, then the catalyst was filtered off 3 times and the solution concentrated under reduced pressure. The obtained solid was washed 3 times with Et₂O. No further purification was necessary.

3-(5-(4-Fluorophenyl)-2,3-dihydro-1H-inden-1-yl)pyridine hydrochloride (15). Synthesized from **8** according to Method D; yield = 99 %; δ_{H} (CDCl₃, 500 MHz) 1.92-1.98 (m, 1H), 2.65-2.71 (m, 1H), 2.95-3.06 (m, 2H), 4.51 (s, 1H), 6.84 (d, J = 6.9 Hz, 1H), 7.00 (t, J = 8.6 Hz, 2H), 7.24 (d, J = 6.9 Hz, 1H), 7.38-7.41 (m, 3H), 7.76 (s, 1H), 8.13 (d, J = 5.0 Hz, 1H), 8.49 (s, 1H), 8.55 (s, 1H); δ_{C} (CDCl₃, 125 MHz) 31.60, 36.55, 48.36, 115.64, 115.66, 115.83, 115.87, 123.89, 123.91, 124.83, 126.54, 126.56, 128.78, 128.84, 140.48, 144.91, 145.03; m/z = 290.10 [M⁺+H].

4-(5-(4-Fluorophenyl)-2,3-dihydro-1H-inden-1-yl)pyridine hydrochloride (16). Synthesized from **9** according to Method D; yield = 100 %; IR (ATR) ν (cm⁻¹) 3220, 2927, 2855, 1700, 1621, 1578, 1507, 1439, 1349, 1251, 1215, 1153, 1040, 1027, 986, 914, 831, 806, 784, 748, 699, 668; δ_{H} (CDCl₃, 500 MHz) 2.03-2.09 (m, 1H), 2.72-2.78 (m, 1H), 3.03-3.13 (m, 2H), 4.60 (s, 1H), 6.93 (d, J = 7.1 Hz, 1H), 7.06 (t, J = 8.6 Hz, 2H), 7.32 (d, J = 6.7 Hz, 1H), 7.45-7.47 (m, 3H), 7.68 (s, 2H), 8.71 (s, 2H); δ_{C} (CDCl₃, 125 MHz) 31.80, 36.19, 51.29, 115.66, 115.83, 123.80, 125.02, 126.28, 126.45, 128.72, 128.78, 136.83, 140.75, 140.99, 141.34, 145.22, 161.61, 166.50; m/z = 290.17 [M⁺+H].

4-(6-(4-Fluorophenyl)-1,2,3,4-tetrahydronaphthalen-1-yl)pyridine hydrochloride (17). Synthesized from **11** according to Method D; yield = 97 %; IR (ATR) ν (cm⁻¹) 3049, 1634, 1605, 1518, 1492, 1223, 1160, 1098, 997, 911, 823, 727, 642; δ_{H} (CDCl₃, 500 MHz) 1.82-1.90 (m, 3H), 2.33-2.37 (m, 1H), 2.94-3.00 (m, 2H), 4.46 (s, 1H), 6.78 (d, J = 7.5 Hz, 1H), 7.12 (t, J = 8.6 Hz, 2H), 7.30 (d, J = 6.8 Hz, 1H), 7.39 (s, 1H), 7.53 (dd, J = 5.3 Hz, J = 8.6 Hz, 2H), 7.67 (s, 2H), 8.71 (s, 2H); δ_{C} (CDCl₃, 125 MHz) 20.06, 29.23, 32.58, 45.49, 115.54, 115.71, 125.26, 126.85, 128.21, 128.43, 128.49, 130.20, 133.17, 136.25, 136.28, 138.09, 139.61, 140.45, 161.51, 163.48, 168.11, 190.64; m/z = 304.10 [M⁺+H].

4-(6-(3,4-Difluorophenyl)-1,2,3,4-tetrahydronaphthalen-1-yl)pyridine hydrochloride (18). Synthesized from **12** according to Method D; yield = 98 %; IR (ATR) ν (cm⁻¹) 3392, 1634, 1604, 1522, 1494, 1269, 1197, 1119, 998, 925, 909, 875, 811, 772, 726, 643; δ_{H} (CDCl₃, 500 MHz) 1.82-1.90 (m, 3H), 2.33-2.37 (m, 1H), 2.94-3.00 (m, 2H), 4.46 (s, 1H), 6.79 (d, J = 6.2 Hz, 1H), 7.22 (q, J = 8.4 Hz, 2H), 7.26-7.28 (m, 2H), 7.34-7.38 (m, 2H), 7.66 (s, 2H), 8.72 (s, 2H); δ_{C} (CDCl₃, 125 MHz) 20.12, 29.31, 32.64, 45.58, 115.82, 115.96, 117.55, 117.69, 122.86, 122.88, 125.28, 126.94, 128.29, 130.45, 133.90, 138.39, 138.61, 140.64, 167.99, 190.74; m/z = 322.11 [M⁺+H].

4-(5-(Pyridin-4-yl)-5,6,7,8-tetrahydronaphthalen-2-yl)benzene-1,2-diol hydrobromide (19). Synthesized from **13** according to Method D; yield = 98 %; IR (ATR) ν (cm⁻¹) 3172, 2930, 1634, 1603, 1524, 1495, 1446, 1263, 1196, 1114, 805, 634; δ_{H} (CDCl₃ + CD₃OD, 500 MHz) 1.73-1.80 (m, 3H), 2.19-2.24 (m, 1H), 2.81-2.89 (m, 2H), 4.27-4.32 (m, 1H), 6.63-6.65 (m, 1H), 6.81 (d, J = 8.2 Hz, 1H), 6.88-6.90 (m, 1H), 7.00 (s, 1H), 7.17 (d, J = 8.0 Hz, 1H), 7.28 (s, 1H), 7.45-7.51 (m, 2H), 8.59 (s, 2H); δ_{C} (CDCl₃ + CD₃OD, 125 MHz) 20.18, 29.33, 32.56, 45.39, 113.74, 115.36, 118.77, 124.72, 126.50, 127.66, 129.98, 137.81, 144.22, 144.65; m/z = 318.65 [M⁺+H].

2-Fluoro-4-(5-(pyridin-4-yl)-5,6,7,8-tetrahydronaphthalen-2-yl)phenol hydrobromide (20). Synthesized from **14** according to Method D; yield = 96 %; IR (ATR) ν (cm⁻¹) 3066, 1635, 1607, 1525, 1494, 1366, 1293, 1215, 1117, 911, 872, 812, 780, 727, 644; δ_{H} (CDCl₃ + CD₃OD, 500 MHz) 1.84-1.92 (m, 3H), 2.34-2.40 (m, 1H), 2.92-3.00 (m, 2H), 4.48-4.50 (m, 1H), 6.76 (d, J = 8.0 Hz, 1H), 7.02 (t, J = 8.8 Hz, 1H), 7.22 (d, J = 8.4 Hz, 1H), 7.26-7.28 (m, 2H), 7.38 (s, 1H), 7.73 (s, 1H), 7.74 (s, 1H), 8.79 (s, 1H), 8.80 (s, 1H); δ_{C} (CDCl₃ + CD₃OD, 125 MHz) 24.03, 33.17, 36.48, 49.51, 118.12, 118.27, 121.90, 126.73, 128.77, 131.08, 131.69, 134.12, 136.34, 136.39, 136.79, 142.06, 143.29, 144.45, 148.04, 148.15, 154.59, 156.50, 173.21; m/z = 320.08 [M⁺+H].

Method E: Ether Cleavage and Condensation with HBr. The corresponding ether was refluxed overnight in HBr (100 mL for compound **5c**, 3 mL for compounds **13** and **14**). For compound **5c**, after reaction completion water (100 mL) was added, the mixture was cooled down and filtered. The solid was washed 3 times with water and no further purification was needed. For compounds **13** and **14**, after reaction completion the mixture was neutralized with solid NaHCO₃ and extracted 3 times with EtOAc. The combined organic extracts were dried over Na₂SO₄, concentrated under reduced pressure and purified by Si-gel flash-chromatography.

6-Hydroxy-1-tetralone (5c). Synthesized from 6-methoxy-1-tetralone according to Method E; yield = 89 %; δ_{H} (CDCl₃, 500 MHz) 2.01-2.06 (m, 2H), 2.56 (t, $J = 6.8$ Hz, 2H), 2.83 (t, $J = 6.1$ Hz, 2H), 6.66 (d, $J = 6.1$ Hz, 1H), 6.74 (dd, $J = 2.4$ Hz, $J = 8.6$ Hz, 1H), 7.38 (s, 1H), 7.91 (d, $J = 8.6$ Hz, 1H); δ_{C} (CDCl₃, 125 MHz) 23.27, 29.92, 38.80, 114.60, 114.66, 125.75, 130.20, 147.82, 161.28, 198.69.

4-(5-(Pyridin-4-yl)-7,8-dihydronaphthalen-2-yl)benzene-1,2-diol hydrobromide (13). Synthesized from **13a** according to Method E; yield = 65 %; IR (ATR) ν (cm⁻¹) 3127, 1634, 1605, 1533, 1503, 1396, 1315, 1252, 1205, 1123, 806, 788, 752, 617; δ_{H} (CDCl₃ + CD₃OD, 500 MHz) 2.53-2.55 (m, 2H), 2.87 (t, $J = 7.8$ Hz, 2H), 6.53-6.55 (m, 1H), 6.83-6.89 (m, 2H), 6.94-6.96 (m, 1H), 7.28-7.31 (m, 1H), 7.40-7.41 (m, 1H), 7.94-7.96 (m, 2H), 8.77-8.79 (m, 2H); δ_{C} (CDCl₃ + CD₃OD, 125 MHz) 27.23, 31.01, 117.13, 118.87, 122.01, 127.96, 128.02, 128.97, 129.45, 129.78, 131.43, 132.96, 135.65, 139.43, 139.55, 140.53, 144.17, 144.88, 148.02, 148.27, 162.74; $m/z = 316.18$ [M⁺+H].

2-Fluoro-4-(5-(pyridin-4-yl)-7,8-dihydronaphthalen-2-yl)phenol hydrobromide (14). Synthesized from **7** according to Method E; yield = 28 %; IR (ATR) ν (cm⁻¹) 3385, 1605, 1522, 1489, 1437, 1416, 1313, 1291, 1278, 1221, 1199, 1168, 117, 1067, 1008, 909, 891, 874, 823, 806778, 735, 667, 621; δ_{H} (CDCl₃ + CD₃OD, 500 MHz) 2.49-2.53 (m, 2H), 2.94 (t, $J = 7.9$ Hz, 2H), 6.25-6.27 (m, 1H), 7.02 (q, $J = 8.4$ Hz, 2H), 7.26 (d, $J = 8.1$ Hz, 1H), 7.31 (s, 1H), 7.34 (d, $J = 5.8$ Hz, 1H), 7.39-7.42 (m, 3H), 8.58 (d, $J = 5.7$ Hz, 2H); δ_{C} (CDCl₃ + CD₃OD, 125 MHz) 24.90, 29.47, 50.22, 50.37, 50.39, 50.55, 50.57, 115.51, 115.66, 117.44, 119.29, 124.08, 124.10, 125.27, 125.75, 126.63, 127.40, 131.57, 133.51, 134.13, 134.18, 138.60, 1388.77, 140.54, 145.40, 145.52, 150.25, 150.87, 152.09; $m/z = 318.08$ [M⁺+H].

1-Tetralon-6-yl trifluoromethanesulfonate (5b). 6-Hydroxy-1-tetralone (5 g, 30.83 mmol) was prepared with pyridine (2.77 mL, 33.91 mmol) in dry DCM (100 mL) at 0°C. After carefully adding trifluoromethanesulfonic anhydride (5.10 g, 30.83 mmol) over 1 min, the reaction mixture was left stirring for 3 h at room temperature. Afterwards, excess trifluoromethanesulfonic anhydride was neutralized and the crude was washed 2 times with water, the organic phase dried over Na₂SO₄ and concentrated under reduced pressure. Further purification was performed by Si-gel flash-chromatography; yield = 30 %; δ_{H} (CDCl₃, 500 MHz) 2.08-2.14 (m, 2H), 2.61 (t, $J = 6.8$ Hz, 2H), 2.95 (t, $J = 6.1$ Hz, 2H), 7.12-7.14 (m, 2H), 8.06 (d, $J = 8.4$ Hz, 1H); δ_{C} (CDCl₃, 125 MHz) 22.90, 29.73, 38.77, 119.68, 119.94, 121.36, 130.04, 132.39, 147.11, 152.34, 196.40.

Biological Assays. CYP17 Preparation and Assay. As source of human CYP17, our *E. coli* system¹⁹ (coexpressing human CYP17 and NADPH-P450 reductase) was used and the assay was performed as previously described^{12a} using unlabeled progesterone as substrate and applying HPLC with UV-detection for separation.

Inhibition of CYP11B1 and CYP11B2. V79MZh11B1 or V79MZh11B2²² cells expressing the respective human enzyme were used and our assay procedure using [4-¹⁴C]-11-deoxycorticosterone was performed.²⁰

Inhibition of CYP3A4. The recombinantly expressed enzymes from baculovirus-infected insect microsomes and cytochrome b5 (BD SupersomesTM) were used and the manufacturer's instructions (www.gentest.com) were followed.

Molecular Modeling. Various inhibitors of Tables 1 were docked into our CYP17 homology model by means of the GOLD v3.2 software²³ using GOLDScore and CHEMScore. Since the GOLD docking program allows flexible docking of the compounds, no conformational search was employed to the ligand structures. GOLD gave the best poses by a genetic algorithm (GA) search strategy, and then various molecular features were encoded as a chromosome.

The structures of the inhibitors were built with SYBYL 7.3.2 (Sybyl, Tripos Inc., St. Louis, Missouri, USA) and energy-minimized in MMFF94s force-field²⁴ as implemented in Sybyl.

Ligands were docked in 50 independent GA runs using GOLD. Heme iron was chosen as active site origin, while its radius was set equal to 19 Å. The automatic active site detection was switched on. Furthermore, a distance constraint of a minimum of 1.9 and a maximum of 2.5 Å between the sp²-hybridized nitrogen of the pyridine and the iron of the heme was set. Additionally, the goldscore.p450_pdb parameters were used and some of the GOLDScore parameters were modified to improve the weight of hydrophobic interaction and of the coordination between iron and nitrogen. The genetic algorithm default parameters were set as suggested by the GOLD authors.²³ On the other hand, the annealing parameters of fitness function were set at 3.5 Å for hydrogen bonding and 6.5 Å for Van der Waals interactions.

All 50 poses for each compound were clustered with ACIAP²⁵ and the representative structure of each significant cluster was selected. After the docking simulations and cluster analysis were performed, the quality of the docked representative poses was evaluated based on visual inspection of the putative binding modes of the ligands. The latter were further evaluated by means of Silver v3.1.1, the postprocessing tool of GOLD, and at last by GOLDScore.

Acknowledgement. We thank Professor J. Hermans, Cardiovascular Research Institute (University of Maastricht, The Netherlands), for providing us with V79MZh11B1 cells expressing human CYP11B1 and Professor R. Bernhardt (Saarland University, Germany) for making us the V79MZh11B2 cells expressing human CYP11B2 available. We also thank U. E. Hille and G. Schmitt for performing the CYP11B1 and CYP11B2 tests and Dr. K. Hansen and his group for the CYP3A4 data.

References

- (1) Jemal, A.; Siegel, R.; Ward, E.; Hao, Y.; Xu, J.; Murray, T.; Thun, M. J. Cancer statistics, 2008. *CA Cancer J. Clin.* **2008**, *58*, 71–96.
- (2) Pomerantz, M.; Kantoff, P. Advances in the treatment of prostate cancer. *Annu. Rev. Med.* **2007**, *58*, 205–220.
- (3) Huhtaniemi, I.; Nikula, H.; Parvinen, M.; Rannikko, S. Histological and functional changes of the testis tissue during GnRH agonist treatment of prostatic cancer. *Am. J. Clin. Oncol.* **1988**, *11*, Suppl. 1: S11–15.
- (4) Forti, G.; Salerno, R.; Moneti, G.; Zoppi, S.; Fiorelli, G.; Marinon, T.; Natali, A.; Constantini, A.; Serio, M.; Martini, L.; Motta, M. Three-month treatment with a long-acting gonadotropin-releasing hormone agonist of patients with benign prostatic hyperplasia: effects on tissue androgen concentration, 5 alpha-reductase activity and androgen receptor content. *J. Clin. Endocrinol. Metab.* **1989**, *68*, 461–468.
- (5) Labrie, F.; Dupont, A.; Belanger, A.; Cusan, L.; Lacourciere, Y.; Monfette, G.; Laberge, J. G.; Emond, J. P.; Fazekas, A. T.; Raynaud, J. P.; Husson, J. M. New hormonal therapy in prostatic carcinoma: combined treatment with LHRH agonist and an antiandrogen. *Clin. Invest. Med.* **1982**, *5*, 267–275.
- (6) Prostate Cancer Trialists' Collaborative Group. Maximum androgen blockade in advanced prostate cancer: an overview of the randomized trials. *Lancet* **2000**, *355*, 1491–1498.
- (7) Hara, T.; Miyazaki, J.; Araki, H.; Yamaoka, M.; Kanzaki, N.; Kusaka, M.; Miyamoto, M. Novel mutations of androgen receptor: a possible mechanism of bicalutamide withdrawal syndrome. *Cancer Res.* **2003**, *63*, 149–153.
- (8) (a) Harris, K. A.; Weinberg, V.; Bok, R. A.; Kakefuda, M.; Small, E. J. Low dose ketoconazole with replacement doses of hydrocortisone in patients with progressive androgen independent prostate cancer. *J. Urol.* **2002**, *168*, 542–545. (b) Eklund, J.; Kozloff, M.; Vlamakis, J.; Starr, A.; Mariott, M.; Gallot, L.; Jovanovic, B.; Schilder, L.; Robin, E.; Pins, M.; Bergan, R. C. Phase II study of mitoxantrone and ketoconazole for hormone-refractory prostate cancer. *Cancer* **2006**, *106*, 2459–2465.
- (9) Small, E.J.; Halabi, S.; Dawson, N. A.; Stadler, W. M.; Rini, B. I.; Picus, J.; Gable, P.; Torti, F. M.; Kaplan, E.; Vogelzang, N. J. Antiandrogen withdrawal alone or in combination with ketoconazole in androgen-independent prostate cancer patients: a phase III trial (CALGB 9583). *J. Clin. Oncol.* **2004**, *22*, 1025–1033.
- (10) (a) Rowlands, M. G.; Barrie, S. E.; Chan, F.; Houghton, J.; Jarman, M.; McCague, R.; Potter, G. A. Esters of 3-pyridylacetic acid that combine potent inhibition of 17 α -hydroxylase/C_{17,20}-lyase (cytochrome P45017 α) with resistance to esterase hydrolysis. *J. Med. Chem.* **1995**, *38*, 4191–4197. (b) Chan, F. C. Y.; Potter, G. A.; Barrie, S. E.; Haynes, B. P.; Rowlands, M. G.; Houghton, J.; Jarman, M. 3- and 4-pyridylalkyl adamantanecarboxylates: inhibitors of human cytochrome P450_{17 α} (17 α -hydroxylase/C_{17,20}-lyase). Potential nonsteroidal agents for the treatment of prostatic cancer. *J. Med. Chem.* **1996**, *39*, 3319–3323. (c) Barrie, S.

- E.; Haynes, B. P.; Potter, G. A.; Chan, F. C. Y.; Goddard, P. M.; Dowsett, M.; Jarman, M. Biochemistry and pharmacokinetics of potent non-steroidal cytochrome P450_{17 α} Inhibitors. *J. Steroid Biochem. Mol. Biol.* **1997**, *60*, 347–351. (d) Matsunaga, N.; Kaku, T.; Itoh, F.; Tanaka, T.; Hara, T.; Miki, H.; Iwasaki, M.; Aono, T.; Yamaoka, M.; Kusaka, M.; Tasaka, A. C_{17,20}-lyase inhibitors I. Structure-based de novo design and SAR study of C_{17,20}-lyase inhibitors. *Bioorg. Med. Chem.* **2004**, *12*, 2251–2273. (e) Matsunaga, N.; Kaku, T.; Ojida, A.; Tanaka, T.; Hara, T.; Yamaoka, M.; Kusaka, M.; Tasaka, A. C_{17,20}-lyase inhibitors. Part 2: Design, synthesis and structure–activity relationships of (2-naphthylmethyl)-1H-imidazoles as novel C_{17,20}-lyase inhibitors. *Bioorg. Med. Chem.* **2004**, *12*, 4313–4336. (f) Owen, C. P.; Dhanani, S.; Patel, C. H.; Shahid, I.; Ahmed, S. Synthesis and biochemical evaluation of a range of potent benzyl imidazole-based compounds as potential inhibitors of the enzyme complex 17 α -hydroxylase/17,20-lyase (P450_{17 α}). *Bioorg Med Chem Lett.* **2006**, *16*, 4011–4015.
- (11) (a) Njar, V. C. O.; Hector, M.; Hartmann, R. W. 20-amino and 20,21-aziridinyl pregnene steroids: development of potent inhibitors of 17 α -hydroxylase/C17,20-lyase (P450 17). *Bioorg. Med. Chem.* **1996**, *4*, 1447–1453. (b) Hartmann, R. W.; Hector, M.; Haidar, S.; Ehmer, P.; Reichert, W.; Jose, J. Synthesis and evaluation of novel steroidal oxime inhibitors of P450 17 (17 α -hydroxylase/C17-20-lyase) and 5 α -reductase types 1 and 2. *J. Med. Chem.* **2000**, *43*, 4266–4277. (c) Hartmann R. W.; Hector, M.; Wachall, B. G.; Paluszczak, A.; Palzer, M.; Huch, V.; Veith, M. Synthesis and evaluation of 17-aliphatic heterocycle-substituted steroidal inhibitors of 17 α -hydroxylase/C17-20-lyase (P450 17). *J. Med. Chem.* **2000**, *43*, 4437–4445. (d) Haidar, S.; Hartmann, R. W. C16 and C17 substituted derivatives of pregnenolone and progesterone as inhibitors of 17 α -hydroxylase-C17, 20-lyase: synthesis and biological evaluation. *Arch. Pharm. Pharm. Med. Chem.* **2002**, *335*, 526–534.
- (12) (a) Sergejew, T.; Hartmann, R. W. Pyridyl substituted benzocycloalkenes: new inhibitors of 17 α -hydroxylase/17,20-lyase (P450 17 α). *J. Enz. Inhib.* **1994**, *8*, 113–122. (b) Hartmann, R. W.; Wächter, G. A.; Sergejew, T.; Würtz, R.; Dürkop, J. 4,5-Dihydro-3-(2-pyrazinyl)naphtho[1,2-c]pyrazole: a potent and selective inhibitor of steroid-17 α -hydroxylase-C17,20-lyase (P450 17). *Arch. Pharm. (Weinheim)* **1995**, *328*, 573–575. (c) Wächter, G. A.; Hartmann, R. W.; Sergejew, T.; Grün, G. L.; Ledergerber, D. Tetrahydronaphthalenes: influence of heterocyclic substituents on inhibition of steroid enzymes P450 α and P450 17. *J. Med. Chem.* **1996**, *39*, 834–841. (d) Zhuang, Y.; Hartmann, R. W. Synthesis and evaluation of azole-substituted 2-aryl-6-methoxy-3,4-dihydronaphthalenes and -naphthalenes as inhibitors of 17 α -hydroxylase-C17,20-lyase (P450 17). *Arch. Pharm. Pharm. Med. Chem.* **1999**, *332*, 25–30. (e) Hartmann, R. W.; Ehmer, P. B.; Haidar, S.; Hector, M.; Jose, J.; Klein, C. D. P.; Seidel, S. B.; Sergejew, T.; Wachall, B. G.; Wächter, G. A.; Yhuang, Z. Synthesis, biological evaluation and molecular modelling studies of methyleneimidazole substituted biaryls as inhibitors of human 17 α -hydroxylase-17,20-lyase (CYP17) – Part I: heterocyclic modifications of the core structure. *Arch. Pharm. Pharm. Med. Chem.* **2002**, *335*, 119–128. (f) Haidar, S.; Ehmer, P. B.; Barassin, S.; Batzl-Hartmann, C.; Hartmann, R. W. Effects of novel 17 α -hydroxylase/C17, 20-lyase (P450 17, CYP 17) inhibitors on androgen biosynthesis *in vitro* and *in vivo*. *J. Steroid Biochem. Mol. Biol.* **2003**, *84*, 555–562. (g) Clement, O. O.; Freeman, C. M.; Hartmann, R. W.; Paluszczak, A.; Handratta, V. D.; Vasaitis, T. S.; Brodie, A. M. H.; Njar, V. C. O. Three dimensional pharmacophore modeling of human CYP17 inhibitors. Potential agents for prostate cancer therapy. *J. Med. Chem.* **2003**, *46*, 2345–2351. (h) Pinto-Bazurco Mendieta, M. A. E.; Negri, M.; Jagusch, C.; Hille, U. E., Müller-Vieira, U.; Schmidt, D.; Hansen, K.; Hartmann, R. W. Synthesis, biological evaluation and molecular modelling studies of novel ACD- and ABD-ring steroidomimetics as inhibitors of CYP17. *Bioorg. Med. Chem. Lett.* **2008**, *18*, 267–273.
- (13) (a) Wachall, B. G.; Hector, M.; Zhuang, Y.; Hartmann, R. W. Imidazole substituted biphenyls: a new class of highly potent and *in vivo* active inhibitors of P450 17 as potential therapeutics for treatment of prostate cancer. *Bioorg. Med. Chem.* **1999**, *7*, 1913–1924. (b) Zhuang, Y.; Wachall, B. G.; Hartmann, R. W. Novel imidazolyl and triazolyl substituted biphenyl compounds: synthesis and evaluation as nonsteroidal inhibitors of human 17 α -hydroxylase-C17, 20-lyase (P450 17). *Bioorg. Med. Chem.* **2000**, *8*, 1245–1252. (c) Leroux, F.; Hutschenreuter, T.; Charrière, C.; Scopelliti, R.; Hartmann, R. W. N-(4-Biphenylmethyl)imidazoles as potential therapeutics for the treatment of prostate cancer: Metabolic robustness due to fluorine substitution? *Helv. Chim. Act.* **2003**, *86*, 2671–2686. (d) Hutschenreuter, T. U.; Ehmer, P. B.; Hartmann, R. W. Synthesis of hydroxy derivatives of highly potent non-steroidal CYP 17 inhibitors as potential metabolites and evaluation of their activity by a non cellular assay using recombinant human enzyme. *J. Enzyme Inhib. Med. Chem.* **2004**, *18*, 17–32. (e) Jagusch, C.; Negri, M.; Hille, U. E.; Hu,

- Q.; Bartels, M.; Jahn-Hoffman, K.; Pinto-Bazurco Mendieta, M. A. E.; Rodenwaldt, B.; Müller-Vieira, U.; Schmidt, D.; Lauterbach, T.; Recanatini, M.; Cavalli, A.; Hartmann, R. W. Synthesis, biological evaluation and molecular modelling studies of methyleneimidazole substituted biaryls as inhibitors of human 17 α -hydroxylase-17,20-lyase (CYP17) – Part I: heterocyclic modifications of the core structure. *Bioorg. Med. Chem.* **2008**, *16*, 1992–2010. (f) Hu, Q.; Negri, M.; Jahn-Hoffmann, K.; Zhuang, Y.; Olgen, S.; Bartels, M.; Müller-Vieira, U.; Schmidt, D.; Lauterbach, T.; Hartmann, R. W. Synthesis, Biological Evaluation and Molecular Modelling Studies of Methylene Imidazole Substituted Biaryls as Inhibitors of Human 17 α -hydroxylase-17, 20-lyase (CYP17) – Part II: Core Rigidity and Influence of Substituents at the Methylene Bridge. *Bioorg. Med Chem* **2008**, *16*, 7715–7727.
- (14) (a) Madan, R. A.; Arlen, P. M. Abiraterone. *Cougar Biotechnology. IDrugs* **2006**, *9*, 49–55. (b) Attard, G.; Reids, A.; Molife, R.; Thompson, E.; Barrett, M.; Lee, G.; Parker, C.; Dearnaley, D.; De-Bono, J. S. Abiraterone, an oral, irreversible, CYP450C17 enzyme inhibitor appears to have activity in post-docetaxel castration refractory prostate cancer (CRCP) patients (PTS). *Ann. Oncol.* **2007**, *18*, Suppl. 9: ix173.
- (15) Haidar, S.; Hartmann, R. W. Enzyme inhibitor examples for the treatment of prostate tumor. In *Enzymes and their Inhibition. Drug Development*; Smith, H. J.; Simons, C., Eds.; CRC Press: Boca Raton-London-New York-Singapore, **2005**, 241–253.
- (16) Schenkman, J. B.; Sligar, S. G.; Cinti, D. L. Substrate interaction with cytochrome P-450. *Pharmacol Ther.* **1981**, *12*, 43–71.
- (17) Manga, N.; Duffy, J. C.; Rowe, P. H.; Cronin, M. T. D. Structure-based methods for the prediction of the dominant P450 enzyme in human drug biotransformation: consideration of CYP3A4, CYP2C9, CYP2D6. *SAR QSAR Environ. Res.* **2005**, *16*, 43–61.
- (18) Miyaura, N.; Suzuki, A. Palladium-catalyzed cross-coupling reactions of organoboron compounds. *Chem. Rev.* **1995**, *95*, 2457–2483.
- (19) Ehmer, P. B.; Jose, J.; Hartmann, R. W. Development of a simple and rapid assay for the evaluation of inhibitors of human 17 α -hydroxylase-C(17,20)-lyase (P450c17) by coexpression of P450c17 with NADPH-cytochrome-P450-reductase in *Escherichia coli*. *J. Steroid Biochem. Mol. Biol.* **2000**, *75*, 57–63.
- (20) Ehmer, P. B.; Bureik, M.; Bernhardt, R.; Müller, U.; Hartmann, R. W. Development of a test system for inhibitors of human aldosterone synthase (CYP11B2): screening in fission yeast and evaluation of selectivity in V79 cells. *J. Steroid Biochem. Mol. Biol.* **2002**, *81*, 173–179.
- (21) (a) Denner, K.; Bernhardt, R. Inhibition studies of steroid conversions mediated by human CYP11B1 and CYP11B2 expressed in cell cultures. In *Oxygen Homeostasis and Its Dynamics*; Ishimura, Y.; Shimada, H.; Suematsu, M., Eds.; Springer-Verlag: Tokyo-Berlin-Heidelberg-New York, 1998, 231–236. (b) Böttner B, Denner K, Bernhardt R. Conferring aldosterone synthesis to human CYP11B1 by replacing key amino acid residues with CYP11B2-specific ones. *Eur. J. Biochem.* **1998**, *252*, 458–466.
- (22) Jones, G.; Willett, P.; Glen, R. C.; Leach, A. R.; Taylor, R. Development and validation of a genetic algorithm for flexible docking. *J. Mol. Biol.* **1997**, *267*, 727–748.
- (23) Halgren, T. A. MMFF VII. Characterization of MMFF94, MMFF94s, and other widely available force fields for conformational energies and for intermolecular-interaction energies and geometries. *J. Comput. Chem.* **1999**, *20*, 730–748.
- (24) (a) Bottegoni, G.; Cavalli, A.; Recanatini, M. A comparative study on the application of hierarchical-agglomerative clustering approaches to organize outputs of reiterated docking runs. *J. Chem. Inf. Mod.* **2006**, *46*, 852–862. (b) Bottegoni, G.; Rocchia, W.; Recanatini, M.; Cavalli, A. ACIAP, autonomous hierarchical agglomerative cluster analysis based protocol to partition conformational datasets. *Bioinformatics*, **2006**, *22*, 58–65.

3.1.4.4. Paper IV.

Synthesis, biological evaluation, and molecular modeling studies of methylene imidazole substituted biaryls as inhibitors of human 17 α -hydroxylase-17,20-lyase (CYP17) - part II: Core rigidification and influence of substituents at the methylene bridge.

Qingzhong Hu, Matthias Negri, Kerstin Jahn-Hoffmann, Yan Zhuang, Sureyya Olgen, Marc Bartels, Ursula Müller-Vieira, Dirk Schmidt, Thomas Lauterbach, Rolf W. Hartmann

This article is protected by copyrights of 'Bioorganic and Medicinal Chemistry.'

Bioorg. Med. Chem. **2008**, 16, 7715-7727

Abstract.

Thirty-five novel substituted imidazolyl methylene biphenyls have been synthesised as CYP17 inhibitors for the potential treatment of prostate cancer. Their activities have been tested with recombinant human CYP17 expressed in *E. coli*. Promising compounds were tested for selectivity against CYP11B1, CYP11B2 and hepatic CYP enzymes 3A4, 1A2, 2B6, and 2D6. The core rigidified compounds (**30-35**) were very active however, they were also rather unselective. Another rather potent and more selective inhibitor (compound **23**, IC₅₀ = 345 nM) was further examined in rats regarding plasma testosterone levels and pharmacokinetic properties. Compared to the reference Abiraterone, **23** was more active in vivo, showed a longer plasma half-life (10 hours) and a higher bioavailability. Using our CYP17 homology protein model, docking studies with selected compounds were performed to study possible interactions between inhibitors and amino acid residues of the active site.

Introduction.

It has been illuminated that the growth of up to 80 % of prostate carcinoma, the most common malignancy and cause of death for male elders, depends on androgen stimulation. Thus, inhibition of androgen formation or prevention of androgens unfolding activity will effectively prevent cancer cell proliferation. Currently the standard therapy for prostate carcinoma is the so called "combined androgen blockade" (CAB), which means orchidectomy or treatment with gonadotropin-releasing hormone (GnRH) analogues (chemical castration) combined with androgen receptor antagonists.¹ Anti-androgens are used to prevent adrenal androgens which are not affected by the former strategies from unfolding stimulatory effects. However, CAB often leads to resistance which can be associated with androgen receptor mutations. The mutated androgen receptor recognizes antagonists as agonists, and the efficiency of this therapy is whittled away. Total blockage of the androgen biosynthesis could be a more promising alternative, which brings CYP17 and its central role in the androgen biosynthesis into focus. CYP17, located in both testicular and adrenal tissue,² is the key enzyme catalyzing 17 α -hydroxylation and subsequent C17-C20 bond cleavage of pregnenolone and progesterone to form DHEA and androstenedione, which are then converted to testosterone and DHT.³

From Ketoconazole, the first medication which has been used clinically as CYP17 inhibitor, to Abiraterone which entered into phase II clinical trial very recently, several types of CYP17 inhibitors have been synthesised and tested (representative structures are shown in Chart 1). Almost all the inhibitors, steroidal or non-steroidal, are mimics of the natural substrates pregnenolone and progesterone. Although lots of steroidal inhibitors are very potent,⁴ especially Abiraterone,⁵ the potential drawback of these compounds should not be ignored: the relative short half-life or poor bioavailability,⁶ the first pass effect when orally administered⁷ and the affinity toward steroid receptors which might result in side effect no matter acting as agonists or antagonists. All of these shortcomings indicated the necessity to develop non-steroidal CYP17 inhibitors. In the past decade, a wide variety of non-steroidal compounds has been described, the most important of these were tetrahydronaphthalenes (A),⁸ *m*-pyridinyl substituted esters (CB7645 and C),⁹ 1*H*-imidazol-4-yl substituted alcohols (D and E)¹⁰ and 1-(*m*-pyridinyl)-3-phenyl substituted heterocycles (B).¹¹

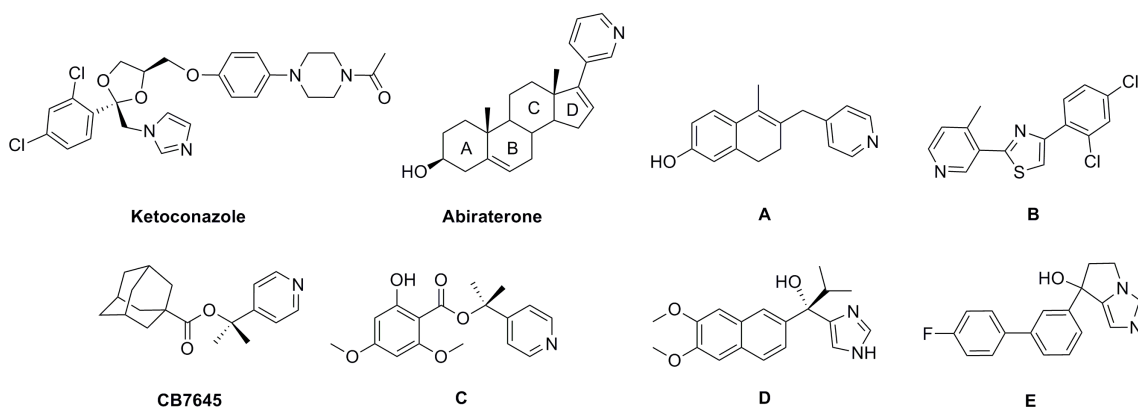


Chart 1. Structures of typical CYP17 inhibitors

Our group has reported a series of imidazolyl and triazolyl substituted biphenyls as potent CYP17 inhibitors.¹² Recently heterocyclic modifications of the core structure were performed with the more promising biphenyl methylene imidazoles. They have been published recently as part I of this study to further improve biological properties.¹³ In the present paper, modifications such as the introduction of different substituents at the methylene bridge as well as the A ring and core rigidifications have been made leading to compounds 1–35 (general structures shown in Chart 2).

Besides the syntheses and the determination of inhibitory activities towards human CYP17, the inhibitions of selected compounds against CYP11B1, CYP11B2, and hepatic CYP enzymes 3A4, 1A2, 2B6, and 2D6 are described. Furthermore, compound 23, as the most selective inhibitor, was examined for its potency of reducing plasma testosterone concentration and its pharmacokinetic properties in rats. Moreover, molecular docking studies with both enantiomers of selected compounds, if existing, were carried out using our homology model of CYP1713 for getting a closer insight into the interaction between active site amino acids and the ligands.

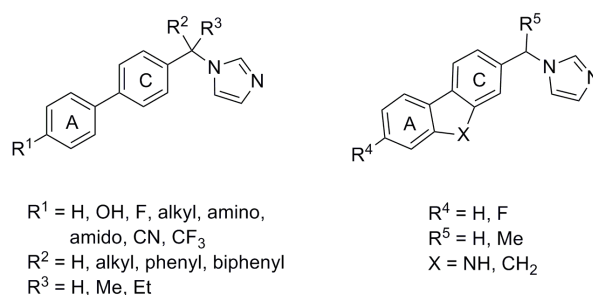
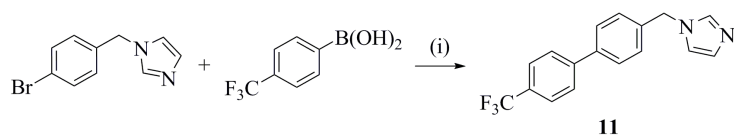


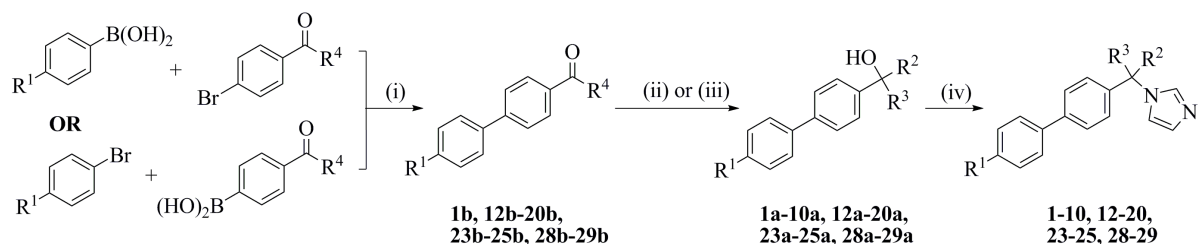
Chart 2. General structures of synthesised compounds 1-35.

Chemistry.

For the synthesis of compounds 1-10 and 12-35 (Scheme 1-7), basically the following strategy was used: the corresponding ketone or aldehyde intermediates were obtained commercially or synthesised by Suzuki coupling (Method C) from the corresponding bromides and boronic acids.¹³ Subsequently they were converted to the alcohols by reduction with NaBH_4 (Method D) or Grignard reaction (Method B). The alcohol intermediates were reacted with 1, 1-carbonyl diimidazole (CDI) (Method A) to give, in a $\text{S}_{\text{N}}1$ reaction, the desired products.¹⁴ In the case of some sensitive intermediates, certain protecting groups were employed and subsequently removed: tert-butyldimethylsilyl (TBDMS) or tert-butyldiphenylsilyl (TBDPS) for hydroxy groups and tert-butoxycarbonyl (Boc) for amino groups. The conversion of the hydroxy compound 26 to the chloro compound 27 was achieved using SOCl_2 (Scheme 5). In some cases, the carbazole core was constructed by ring closure of the o-nitro substituted biphenyl refluxed with phosphorous acid triethyl ester (Scheme 7). The only exception from this strategy was the synthesis of compound 11 (Scheme 1). This compound was simply prepared from 1-(4-bromobenzyl)-1*H*-imidazole and 4-trifluoromethylphenylboronic acid by means of Suzuki coupling (Method C).

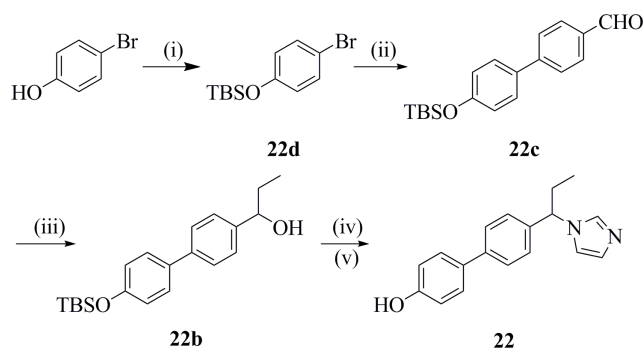


Scheme 1. (i) **Method C:** Pd(PPh₃)₄, Na₂CO₃, toluene/ EtOH/ H₂O, reflux, 16 h.

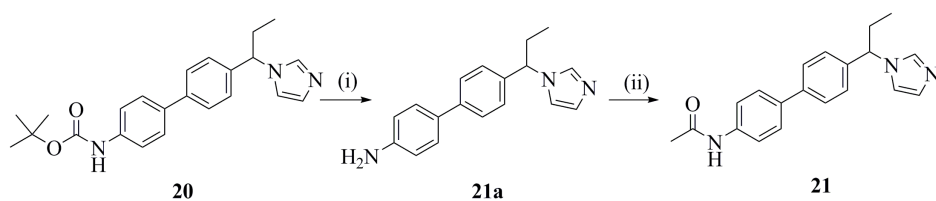


- | | | |
|---|--|--|
| 1: R ¹ = H, R ² = Et, R ³ = R ⁴ = H; | 9: R ¹ = H, R ² = phenyl, R ³ = R ⁴ = H; | 18: R ¹ = N(Et) ₂ , R ² = Et, R ³ = R ⁴ = H; |
| 2: R ¹ = H, R ² = n-Pr, R ³ = R ⁴ = H; | 10: R ¹ = H, R ² = biphenyl, R ³ = R ⁴ = H; | 19: R ¹ = morpholino, R ² = Et, R ³ = R ⁴ = H; |
| 3: R ¹ = H, R ² = i-Pr, R ³ = R ⁴ = H; | 12: R ¹ = OCF ₃ , R ² = Et, R ³ = R ⁴ = H; | 20: R ¹ = NHBoc, R ² = Et, R ³ = R ⁴ = H; |
| 4: R ¹ = H, R ² = n-Bu, R ³ = R ⁴ = H; | 13: R ¹ = SMe, R ² = Et, R ³ = R ⁴ = H; | 23: R ¹ = F, R ² = R ⁴ = Et, R ³ = H; |
| 5: R ¹ = H, R ² = i-Pr, R ³ = R ⁴ = H; | 14: R ¹ = CN, R ² = Et, R ³ = R ⁴ = H; | 24: R ¹ = F, R ² = Me, R ³ = R ⁴ = Me; |
| 6: R ¹ = H, R ² = t-Bu, R ³ = R ⁴ = H; | 15: R ¹ = Me, R ² = R ⁴ = Et, R ³ = H; | 25: R ¹ = F, R ² = Et, R ³ = R ⁴ = Et; |
| 7: R ¹ = H, R ² = cyclohexyl, R ³ = R ⁴ = H; | 16: R ¹ = Et, R ² = R ⁴ = Et, R ³ = H; | 28: R ¹ = F, R ² = CH=CH ₂ , R ³ = R ⁴ = H; |
| 8: R ¹ = H, R ² = benzyl, R ³ = R ⁴ = H; | 17: R ¹ = N(Me) ₂ , R ² = Et, R ³ = R ⁴ = H; | 29: R ¹ = H, R ² = CH=CH ₂ , R ³ = R ⁴ = H; |

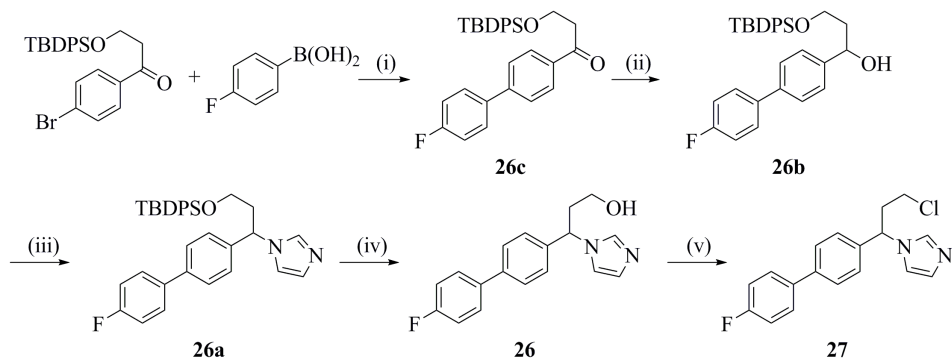
Scheme 2. (i) **Method C:** Pd(PPh₃)₄, Na₂CO₃, reflux 6h; (ii) **Method D:** 15b-16b, 23b: NaBH₄, THF, MeOH; (iii) **Method B:** 1b, 12b-14b, 17b-20b, 24b-25b, 28b-29b: corresponding Grignard reagent, THF; (iv) **Method A:** CDI, NMP



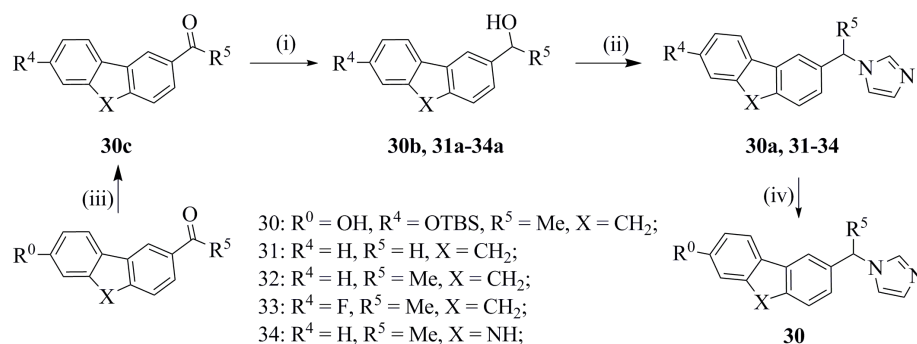
Scheme 3. (i) TBSCl, Imidazole; (ii) **Method C:** Pd(PPh₃)₄, Na₂CO₃, reflux 6h; (iii) **Method B:** EtMgBr, THF; (iv) **Method A:** CDI, NMP; (v) TBAF, THF, rt



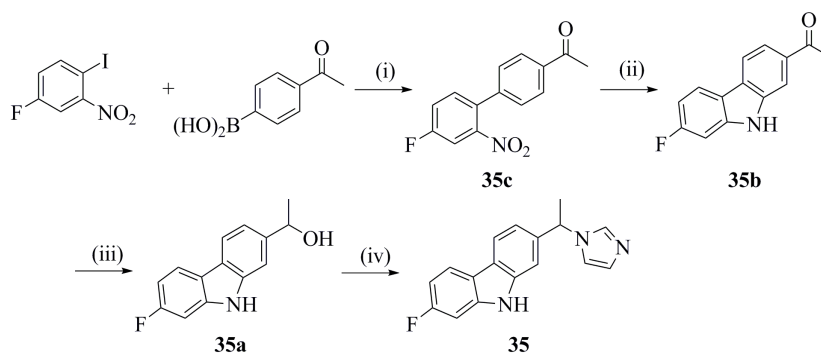
Scheme 4. (i) TFA, DCM (ii) AcCl, N(Et)₃



Scheme 5. (i) **Method C:** Pd(PPh₃)₄, Na₂CO₃, reflux 6h; (ii) **Method D:** NaBH₄, THF, MeOH; (iii) **Method A:** CDI, NMP, reflux, 3h. (iv) TBAF (v) SOCl₂



Scheme 6. (i) **Method D:** NaBH₄, THF, MeOH; (ii) **Method A:** CDI, NMP, reflux, 3h. (iii) TBSCl, imidazole; (iv) TBAF, THF



Scheme 7. (i) **Method C:** Pd(PPh₃)₄, Na₂CO₃, reflux 6h; (ii) P(OEt)₃, reflux (iii) **Method D:** NaBH₄, THF, MeOH; (iv) **Method A:** CDI, NMP, reflux, 3h.

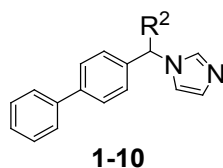
Biological Results, Modelling Studies and Discussion

CYP17 inhibition of all compounds was evaluated using the 50,000g sediment after homogenation of *E. coli* expressing human CYP17 as well as cytochrome P450 reductase.^{12d} The assay was run with progesterone (25 μM) as substrate and NADPH as cofactor. Separation of substrate and product was accomplished by HPLC using UV detection.^{15a} IC₅₀ values are presented in comparison to Ketoconazole and Abiraterone in Tables 1-4.

Inheriting from ref. compound **1**,^{12b} the influence of different substituents on the methylene bridge was investigated (Table 1). From the inhibitory activity values, it becomes apparent that increasing the length of **R**² would largely influence the potency. The introduction of two-carbon alkyl substituents, like Et (**1**), and even more bulky ones like *i*-Pr (**3**) and *t*-Bu (**6**), increased the potency of the compounds compared to ref. comp. **1** (IC₅₀ = 910 nM), resulting in inhibitors with IC₅₀ values in a range from 300 to 450 nM. Interestingly, the further prolongation of the alkyl chain by another carbon atom led to moderate (**2**, **R**²: *n*-Pr, IC₅₀ = 580 nM) or low active inhibitors (**5**, **R**²: *i*-Bu, IC₅₀ = 2100 nM). However, adding another C atom to the alkyl **R**² gave again a very potent compound (**4**, **R**²: *n*-Bu, IC₅₀ = 300 nM). Furthermore, it could be observed that the activity of the compounds with a bulky group was reduced dramatically as expected, like benzyl, phenyl (**8** and **9** with IC₅₀ values around 800 nM), cyclohexyl (**7**, IC₅₀ = 1050 nM) and biphenyl (**10**, IC₅₀ = 2300 nM).

In the modelling studies, it was observed that all docked compounds showed two binding modes, named **BM1** and **BM2**, which were identified previously for other biaryl type inhibitors.^{13, 17} These binding modes are different from the proposed substrate binding mode.^{18, 19} In **BM1** the biaryl plane is oriented almost parallel to the I-helix, and principally ligands bearing a **R**¹-substituent were found in this mode (in Fig. 1, compound **22** is taken as an example). The substituted A-ring is located next to a polar pocket¹⁸ delimited by Arg109, Lys231, His235, and Asp298, which tolerates different substitution patterns. On the other hand, in **BM2** the biaryl plane crosses the I-helix, avoiding the interaction with the polar pocket. It is a less permissive binding mode, which tolerates only planar ligands with an un- or fluorine substituted A-ring (compound **2** shown in Fig. 1).

Table 1. Inhibition of CYP17 by compounds **1-10**



Compounds	R ²	CYP17 IC ₅₀ [nM] ^b
Ref 1	Me	910
1	Et	450
2	n-Pr	580
3	i-Pr	310
4	n-Bu	300
5	i-Bu	2100
6	t-Bu	460
7	Cyclohexyl	1050
8	Benzyl	780
9	Phenyl	790
10	Biphenyl	2300
KTZ ^a		2780
ABT ^a		72

^a **KTZ**: Ketoconazole; **ABT**: Abiraterone.

^b Concentration of inhibitors required to give 50 % inhibition. The given values are mean values of at least three experiments. The deviations were within $\pm 10\%$.

Nonetheless, for both binding orientations similar hydrophobic and π - π interactions can be observed,^{13,17} namely between the biphenyl core and Phe114 as well as between the biphenyl moiety and apolar parts of amino acids of the F-helix (Asn202 and Ile206) and I-helix (Gly301, Ala302, Val304, and Glu305) (Fig. 1).

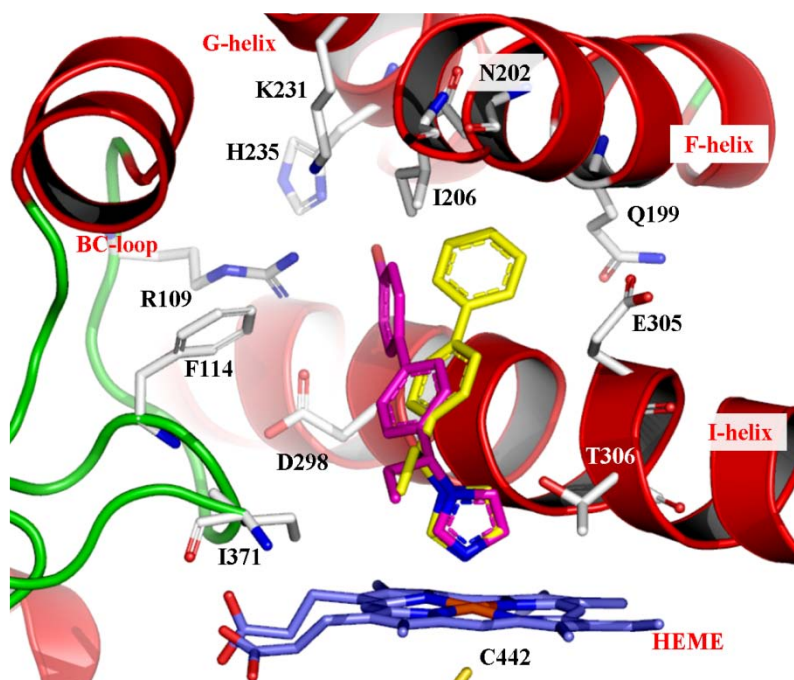


Figure 1. Representation of the two found binding modes **BM1** and **BM2**, exemplified by compounds **22** (magenta, **BM1**) and **2** (yellow, **BM2**). Furthermore, heme, interacting residues and ribbon rendered tertiary structure of the active site are shown. Figures were generated with Pymol (<http://www.pymol.org>).

Compounds **1**, **2**, **4**, **5**, **6**, and ref. compound **1** were docked into our CYP17 model with the aim of explaining the influence of the different R^2 substituents. For all R-enantiomers bearing a short alkyl substituent (Et, i-Pr, t-Bu or Me) at the methylene bridge, the preferred binding mode was **BM1**; whereas for the corresponding S-enantiomers, **BM2** seemed to be the most probable. Based on the requisites for each binding mode,^{13,17} both orientations seem to be possible for compounds **1**, **6**, and ref. compound **1**. On the other hand, although poses in **BM2** could also be observed, the preferred orientations for compounds **2**, **4**, and **5** seem to be **BM1**, regardless of which enantiomer was considered. This might be caused by the presence of a longer and bulkier substituent on the methylene bridge.

The results revealed an orientation of the R^2 group towards a tiny hydrophobic pocket, formed by amino acids Ala367-Pro368-Met369-Leu370-Ile371 (Fig. 2A). Et, i-Pr, and t-Bu substituents can undergo hydrophobic interactions with this apolar environment close to the heme without steric clashes due to their reduced length. However, for compounds **2** (n-Pr) and **5** (i-Bu) steric hindrance and hydrophobic repulsion perish the possibility of additional hydrophobic interactions, thus reducing their inhibitory potencies. As for compound **4**, the results indicate that the n-Bu group can interact not only with amino acids Ile371 and Ala367, like n-Pr does, but also with Val366, Pro368, and Val382 as additional contacts. This leads to the stabilization of its orientation, and makes it a potent inhibitor (Fig. 2A).

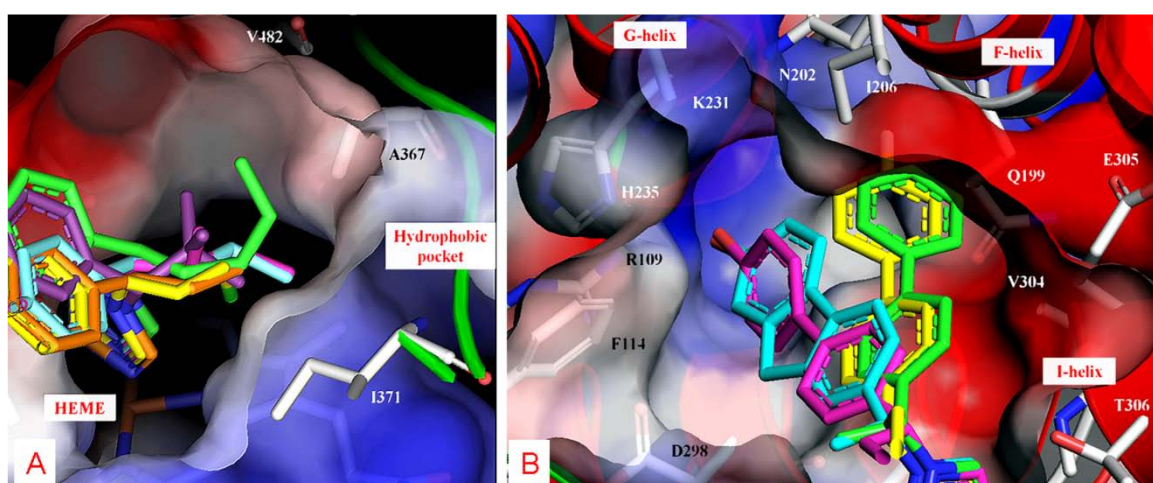
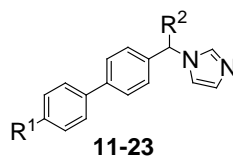


Figure 2. A cross-section of the solvent accessible surface of the active site is given with a A) closer look to the orientation of the R^2 methylene linker substituents (compounds **2** (light blue), **4** (green), **5** (magenta), **6** (violet), **23** (orange) and **27** (yellow)) with their surrounding amino acids and a B) more in-depth view of the A-ring substituents (compounds **30** (cyan), **S-23** (yellow), **R-22** (magenta) and ref. comp. **1** (**R**; green) and interacting residues.

It can also be observed that different R^1 substituents on the A ring show a strong influence on the activity of the imidazole substituted biphenyls. Exhibiting the same ethyl group at the methylene bridge, the A ring substitution dispersed the inhibitory potency of the corresponding compounds strongly ranging from no to strong inhibition (Table 2). It becomes apparent that hydrophobic and electronegative groups in R^1 led to almost inactive compounds. However, when R^1 is a small polar substituent, capable of H-bond formation, the compounds turned out to be very active (**22**, $R^1 = OH$, $IC_{50} = 375$ nM; **23**, $R^1 = F$, $IC_{50} = 345$ nM).

Docking of both enantiomers of ligands **22** and **23** into the active site of our CYP17 model revealed that **BM1** is preferred for **S-22**, **R-22**, and **R-23**. There is obviously hydrogen bond formation between R^1 and the polar surrounding of Arg109, Asp298, Lys231, and His235 (Fig. 2B). However, the S-enantiomer of compound **23** was found to bind in **BM2** as long as the small H-bond accepting fluorine group can interact with Gln199 and Asn202 (Fig. 2B).

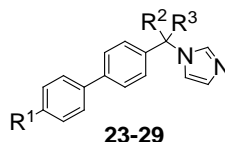
As it is known that fluorine compounds are more stable in vivo than hydroxy compounds, R^1 was sustained to be fluorine, and the influence of substituents at the methylene bridge was further investigated (Table 3). Interestingly, the single ethyl group turned out to be the best, while twin alkyl substituted analogues (**24–25**) showed lower inhibitory potency than their single substituted analogues (**23**, ref. compound **2**). This is obviously due to the steric clashes with amino acids of the I-helix kink and the reduced flexibility of these ligands. Moreover, the similar activity of compound **27** (2-chloroethyl, $IC_{50} = 756$ nM) and compound **2** (n-Pr) and the total loss of activity for the 2-hydroxyethyl analogue (**26**) demonstrate the necessity of a hydrophobic side chain on the methylene bridge.

Table 2. Inhibition of CYP17 by compounds **11-23**

Compounds	R ¹	R ²	CYP17 IC ₅₀ [nM] ^b
11	CF ₃	H	>5000
12	OCF ₃	Et	>5000
13	SMe	Et	3100
14	CN	Et	>5000
15	Me	Et	>5000
16	Et	Et	2000
17	N(Me) ₂	Et	>>5000
18	N(Et) ₂	Et	>>5000
19	morpholino	Et	2200
20	NHBoc	Et	1700
21	NHAc	Et	>5000
22	OH	Et	375
23	F	Et	345
KTZ ^a			2780
ABT ^a			72

^a **KTZ**: Ketoconazole; **ABT**: Abiraterone.

^b Concentration of inhibitors required to give 50 % inhibition. The given values are mean values of at least three experiments. The deviations were within ±10 %.

Table 3. Inhibition of CYP17 by compounds **23-29**

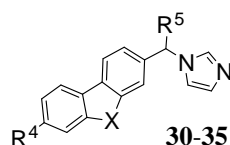
Compounds	R ¹	R ²	R ³	CYP17 IC ₅₀ [nM] ^b
Ref 2	F	Me	H	1100
23	F	Et	H	345
24	F	Me	Me	3800
25	F	Et	Et	1300
26	F	(CH ₂) ₂ OH	H	>5000
27	F	(CH ₂) ₂ Cl	H	756
28	F	CH=CH ₂	H	>5000
29	H	CH=CH ₂	H	1400
KTZ ^a				2780
ABT ^a				72

^a **KTZ**: Ketoconazole; **ABT**: Abiraterone.

^b Concentration of inhibitors required to give 50 % inhibition. The given values are mean values of at least three experiments. The deviations were within ±10 %.

Rigidification of the biphenyl core to form a carbazole or 9H-fluorene ring (Table 4) led to the most potent series of compounds (**30–35**). The planar conjugated scaffolds apparently contributed most to the inhibitory potency, probably due to the reduced degrees of freedom. Once again, inhibitors furnished with groups capable of forming hydrogen bonds turned out to be more active, with the hydroxy substituted 9H-fluorene analogue (**30**) being the most potent compound of this study ($IC_{50} = 99$ nM, 28-fold more potent than Ketoconazole). Moreover, the importance of an alkyl substituent on the spacer has been demonstrated again, as can be seen from the higher activity of the methyl compound **32** showing an IC_{50} value of 112 nM (for this compound an IC_{50} value of 4 nM is reported²³) compared to the corresponding non-substituted analogue **31** ($IC_{50} = 388$ nM).

Table 4. Inhibition of CYP17 by compounds **30–35**



Comp.	R ⁴	R ⁵	X	CYP17 IC ₅₀ [nM] ^b
30	O	M	C	99
31	H	H	C	388
32	H	M	C	112
33	F	M	C	168
34	H	M	N	282
35	F	M	N	118
KTZ ^a				2780
ABT ^a				72

^a KTZ: Ketoconazole; ABT: Abiraterone.

^b Concentration of inhibitors required to give 50 % inhibition. The given values are mean values of at least three experiments. The deviations were within ± 10 %.

For the docking studies of selected compounds from Table 4 (**30**, **32** and **35**), similar results were achieved as obtained for the non-rigidified compounds. Two binding modes, **BM1** and **BM2**, were identified. The former seemed to be preferred, based on the internal energies of the docked inhibitors and the visual inspection of possible interactions, regardless which enantiomer was considered. The same H-bond interactions were found as described above (Figs. 1 and 2B). Moreover, the poses were also stabilized by the electrostatic interactions with carbon chain of Glu305 (Fig. 3).

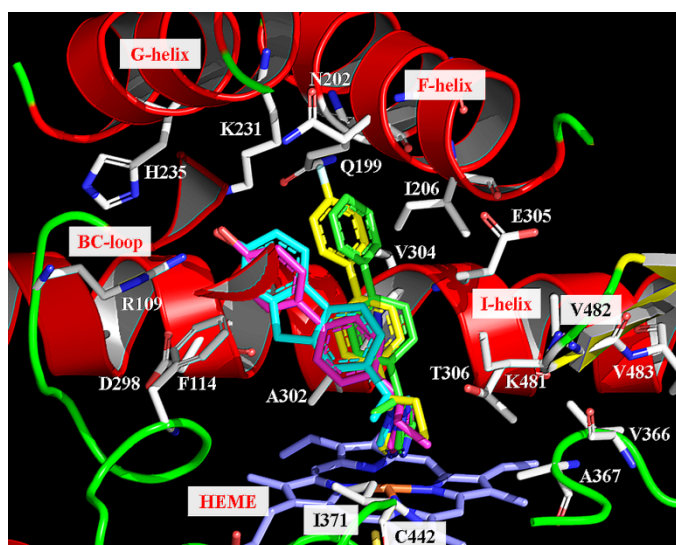


Figure 3. Docking complex between CYP17 and compounds **30** (cyan), **S-23** (yellow), **R-22** (magenta) and ref. comp. **1** (R; green). Heme, interacting residues and ribbon rendered tertiary structure of the active site are shown.

The inhibition of selected compounds toward hepatic CYP enzymes was determined (Table 5), because of their important role in drug metabolism and drug-drug interaction. Although the compounds tested showed inhibition of CYP3A4, it was lower than that of Ketoconazole. Interestingly, compound **20** showed only little inhibition (52 % at 1 μ M), possibly due to the bulky t-Boc amino group it bears. However, CYP1A2 inhibition shown by the test compounds was much higher than that of Ketoconazole. Compounds **23** and **27** showed good selectivity toward CYP 2B6 and 2D6.

Table 5. Inhibition of hepatic CYP enzymes by selected compounds.

Comp.	% Inhibition ^b			
	CYP3A4	CYP1A2	CYP2B6	CYP2D6
20	52	n.d. ^a	n.d.	n.d.
23	88	97	46	54
25	95	51	n.d.	n.d.
27	86	96	34	32
30	89	93	n.d.	n.d.
32	89	98	n.d.	n.d.
34	88	99	n.d.	n.d.
35	75	n.d.	n.d.	n.d.
KTZ ^a	96	8	11	1
ABT ^a	4	36	2	7

^a KTZ: Ketoconazole; ABT: Abiraterone; n.d.: not determined.

^b Inhibition at a concentration of 1 μ M; standard deviations were within $< \pm 5$ %; All the data are the mean values of at least 3 independent tests.

Furthermore, selectivity toward CYP11B1 and CYP11B2 - the most important steroidogenic enzymes being responsible for adrenal corticoid biosynthesis - has been determined as another criterion to evaluate safety. CYP11B1 catalyzes 11 β -hydroxylation in cortisol biosynthesis, whereas CYP11B2 is responsible for the final three steps (11 β -hydroxylation, 18-hydroxylation, and 18-oxidation) in aldosterone biosynthesis. Inhibition of these two enzymes could cause hyponatremia, hyperkalemia and a series of recessive disorders, such as adrenal hyperplasia and hypovolemic shock.²⁰ Tested at a concentration of 0.2 μ M, compound **23** showed less inhibition on both enzymes (11B2: 66 %; 11B1: 66 %) compared to compound 30 (11B1: 96 %; 11B2: 98 %). Therefore compound **23** was further tested in rats.

The in vivo evaluation of compound **23**, including the ability of reducing plasma testosterone concentration (Table 6) and the determination of pharmacokinetic properties (Table 7), was performed in male Wistar rats after oral application using Abiraterone as reference compound. The plasma concentrations of testosterone were determined by ELISA assay and plasma drug concentrations were measured using LC-MS. Although applied as acetate, only the signals of the free Abiraterone were monitored. It is obvious that both compounds significantly reduced the plasma testosterone concentration. It is striking that compound **23**, which was less active in vitro, was much more active in vivo than Abiraterone at each time point checked. Importantly, after 24 hours compound **23** still showed strong inhibitory activity, while Abiraterone exhibited at this time point plasma testosterone concentrations 6 fold higher than that of the untreated control. This activity profile can be explained by the pharmacokinetic properties of the compounds. Compound **23** exhibited a plasma half-life of 10 hours, while Abiraterone only showed 1.6 hours. The fact that Abiraterone had to be administrated as acetate prodrug, which is inactive as CYP17 inhibitor, could explain the reduced inhibitory activity of the steroidal compound. However, application of the acetate should prolong the plasma half-life having no influence on the AUC of the parent compound. The superiority of compound **23** becomes apparent by comparing the AUCs of the two compounds, leading to the conclusion that the bioavailability of compound **23** is much better.

Table 6. Reduction of the plasma testosterone concentrations in rats by compound **23**^a

Comp.	Relative plasma testosterone level (%) ^b					
	1h	2h	4h	6h	8h	24h
Control	143.1 ± 13.3	76.4 ± 13.3	81.4 ± 24.6	109.6 ± 31.7	90.6 ± 22.8	80.6 ± 21.0
23	16.5 ± 5.7 ^d	11.7 ± 5.0 ^d	13.9 ± 8.0 ^d	13.9 ± 7.1 ^d	13.4 ± 6.2 ^d	36.7 ± 27.4 ^d
ABT ^e	92.5 ± 43.1 ^d	44.0 ± 14.7 ^d	43.5 ± 12.4 ^d	43.3 ± 12.8 ^c	35.6 ± 9.7 ^d	476.0 ± 238.6

^a Compound **23** was applied at a dose of 50 mg / kg body weight; Abiraterone was administrated as Abiraterone acetate (56 mg / kg body weight, equivalent to Abiraterone 50 mg / kg body weight). 5 to 6 intact adult male Wistar rats were employed for each treatment group; each sample was tested for 3 times.

^b The average plasma testosterone concentrations (1.81 ng / mL) at pre-treatment time points (-1, -0.5 and 0 h) were set to 100 %. The values shown are the relative levels compared to the pre-treatment value.

^c P < 0.05, ^d P < 0.01. ^e ABT: Abiraterone.

Table 7. Pharmacokinetic properties of compound **23**^a

Compounds	t _{1/2 z} (h) ^b	t _{max} (h) ^b	C _{max} (ng / mL) ^b	AUC _{0-∞} (ng x h / mL) ^b	Cl _{int} (l / kg / h) ^b
23	10.0	6.0	3288	70729	0.7
Abiraterone	1.6	2.0	592	4015	11.2

^a Compound **23** was applied at a dose of 50 mg / kg body weight; Abiraterone was administrated as Abiraterone acetate (56 mg / kg body weight, equivalent to Abiraterone 50 mg / kg body weight). 5 to 6 intact adult male Wistar rats were employed for each treatment group; each sample was tested for 3 times.

^b t_{1/2 z}: terminal half-life; t_{max}: time of maximal concentration; C_{max}: maximal concentration; AUC_{0-∞}: area under the curve; Cl_{int}: intrinsic hepatic clearance.

Conclusion

Herein, we reported the synthesis and evaluation of bioactivity of a series of substituted and core rigidified biphenyl methylene imidazoles as CYP17 inhibitors. We found clearer SAR for biphenyl type CYP17 inhibitors, comparing to previous work,^{12,13} that alkyl groups at the methylene bridge, if in suitable length, can strongly improve the inhibitory potency. Analogues substituted with polar substituents at the A ring, capable of H-bond formation, always led to potent inhibitors. Besides, rigidification of the biphenyl core to form a carbazole or 9H-fluorene ring also significantly elevated the activity to give a series of CYP17 inhibitors more potent than previously reported,^{12,13} probably due to their planar conjugated scaffolds. Moreover, one of the best compounds in vitro, compound **23** showed potent activity in vivo, a long plasma half-life and a high bioavailability.

However, further structure modifications have to be performed with the aim of reducing the CYP1A2 inhibition - the enzyme responsible for the metabolism of approximately 10 % of the prescription drugs - before a candidate for the treatment of prostate cancer can be propagated. Furthermore, because of being tested as racemic mixtures, it is likely that one enantiomer of compound **23** would be more potent and selective than the other. A separation of the enantiomers is presently being performed.

Experimental Section

CYP17 preparation and assay

Human CYP17 was expressed in *E. coli* (coexpressing human CYP17 and cytochrome P450 reductase) and the assay was performed as previously described.^{12d, 16a}

Inhibition of hepatic CYP enzymes

The recombinantly expressed enzymes from baculovirus-infected insect microsomes (Supersomes) were used and the manufacturer's instructions (www.gentest.com) were followed.

Inhibition of CYP11B1 and CYP11B2

V79MZh cells expressing human CYP11B1 or CYP11B2 were incubated with [4-¹⁴C]-11-deoxycorticosterone as substrate. The assay was performed as previously described.^{16c, d}

In vivo study

The in vivo tests were performed with intact adult male Wistar rats (Harlan Winkelmann, Germany), 5-6 for each treatment group. These rats were cannulated with silicone tubing via the right jugular vein. Compound **23** was applied po at 50 mg/kg body weight, while Abiraterone was administrated as acetate at 56 mg/kg body weight

(equivalent to Abiraterone at 50 mg/kg body weight). The concentrations of testosterone in the rat plasma were determined using the Testosterone ELISA (EIA - 1559) from DRG Instruments according to the manufacturer's instructions. The plasma drug levels were measured by LC-MS. Non-compartmental pharmacokinetic analysis of concentration versus time data was performed for each compound on the mean plasma level using a validated computer program (PK solution 2 software; Summit Research Services, Montrose, USA). Plasma concentrations below the limit of detection were assigned a value of zero.

Chemistry

General

Melting points were determined on a Mettler FP1 melting point apparatus and are uncorrected. IR spectra were recorded neat on a Bruker Vector 33FT-infrared spectrometer. ¹H and ¹³C NMR spectra were measured on a Bruker DRX-500 (500 MHz). Chemical shifts are given in parts per million (ppm), and TMS was used as an internal standard for spectra obtained in CDCl₃. All coupling constants (*J*) are given in Hz. ESI (electrospray ionization) mass spectra were determined on a TSQ quantum (Thermo Electron Corporation) instrument. Elemental analyses were performed at the Department of Instrumental Analysis and Bioanalysis, Saarland University. The purities of the final compounds were controlled by Surveyor®-LC-system. Purities were greater than 98 %. Column chromatography was performed using silica-gel 60 (50-200 μm), and reaction progress was determined by TLC analysis on Alugram® SIL G/UV₂₅₄ (Macherey-Nagel). Boronic acids and bromoaryls used as starting materials were commercially obtained (CombiBlocks, Chempur, Aldrich, Acros).

Method A: CDI reaction

To a solution of the corresponding alcohol (1 eq) in N-methylpyrrolidone (NMP) or acetonitrile (10 mL / mmol) was added CDI (5 eq). Then the solution was heated to reflux for 4 to 18 h. After cooling to ambient temperature, it was diluted with water (30 mL) and extracted with ethyl acetate (3 x 10 mL). The combined organic phases were washed with brine, dried over MgSO₄ and evaporated under reduced pressure. Then the desired product was purified by chromatography on silica gel.

1-(1-Biphenyl-4-yl-propyl)-1H-imidazole, 1. Synthesised according to Method A using **1a** (0.50 g, 2.36 mmol) and CDI (1.91 g, 11.78 mmol); yield: 0.13 g (21 %); yellow solid: mp 75-77 °C; *R*_f = 0.31 (DCM / MeOH, 10:1); δ_H (CDCl₃, 500 MHz) 0.99 (t, *J* = 7.5 Hz, 3H, CH₃), 2.26-2.32 (m, 2H, CH₂), 5.09 (t, *J* = 7.5 Hz, 1H, CH), 6.99 (s, 1H), 7.11 (s, 1H), 7.25 (d, *J* = 8.4 Hz, 2H), 7.33-7.37 (m, 1H), 7.42-7.46 (m, 2H), 7.56 (d, *J* = 8.4 Hz, 2H), 7.58 (d, *J* = 8.4 Hz, 2H), 7.69 (s, 1H); MS (ESI): *m/z* = 263 [M⁺+H].

1-(1-Biphenyl-4-yl-butyl)-1H-imidazole, 2. Synthesised according to Method A using **2a** (0.50 g, 2.21 mmol) and CDI (1.79 g, 11.05 mmol); yield: 0.16 g (27 %); brownish oil; *R*_f = 0.29 (DCM / MeOH, 10:1); δ_H (CDCl₃, 500 MHz) 0.98 (t, *J* = 7.5 Hz, 3H, CH₃), 1.31-1.39 (m, 2H, CH₂), 2.14-2.28 (m, 2H, CH₂), 5.17 (t, *J* = 7.5 Hz, 1H, CH), 6.99 (s, 1H), 7.10 (s, 1H), 7.26 (d, *J* = 8.0 Hz, 1H), 7.34 (t, *J* = 7.5 Hz, 2H), 7.45 (dd, *J* = 7.5, 8.4 Hz, 2H), 7.54-7.57 (m, 4H), 7.66 (s, 1H); MS (ESI): *m/z* = 277 [M⁺+H].

1-(1-Biphenyl-4-yl-2-methyl-propyl)-1H-imidazole, 3. Synthesised according to Method A using **3a** (0.50 g, 2.36 mmol) and CDI (1.91 g, 11.78 mmol); yield: 0.20 g (33 %); white solid: mp 124-125 °C; *R*_f = 0.31 (DCM / MeOH, 10:1); δ_H (CDCl₃, 500 MHz) 0.95 (t, *J* = 7.5 Hz, 6H, (CH₃)₂), 2.56-2.65 (m, 1H, CH(Me)₂), 4.67 (d, *J* = 7.5 Hz, 1H, CH), 7.05 (s, 1H), 7.07 (s, 1H), 7.32-7.38 (m, 3H), 7.42-7.45 (m, 2H), 7.55-7.58 (m, 4H), 7.67 (s, 1H); MS (ESI): *m/z* = 277 [M⁺+H].

1-(1-Biphenyl-4-yl-pentyl)-1H-imidazole, 4. Synthesised according to Method A using **4a** (0.50 g, 2.08 mmol) and CDI (1.69 g, 10.40 mmol); yield: 0.15 g (25 %); brownish oil; *R*_f = 0.30 (DCM / MeOH, 10:1); δ_H (CDCl₃, 500 MHz) 0.89 (t, *J* = 7.5 Hz, 3H, CH₃), 1.28-1.37 (m, 2H, CH₂), 1.39-1.43 (m, 2H, CH₂), 2.20-2.26 (m, 2H, CH₂), 5.14 (t, *J* = 7.7 Hz, 1H, CH), 6.99 (s, 1H), 7.12 (s, 1H), 7.26 (d, *J* = 8.4 Hz, 2H), 7.35 (m, 1H), 7.43 (dd, *J* = 7.9, 8.4 Hz, 2H), 7.54-7.57 (m, 4H), 7.68 (s, 1H); MS (ESI): *m/z* = 291 [M⁺+H].

1-(1-Biphenyl-4-yl-3-methyl-butyl)-1H-imidazole, 5. Synthesised according to Method A using **5a** (0.50 g, 2.08 mmol) and CDI (1.69 g, 10.40 mmol); yield: 0.16 g (27 %); brownish oil; *R*_f = 0.30 (DCM / MeOH, 10:1); δ_H (CDCl₃, 500 MHz) 0.96 (d, *J* = 7.5 Hz, 6H, C(CH₃)₂), 1.46-1.53 (m, 1H, CH(Me)₂), 1.99-2.20 (m, 2H, CH₂), 5.14 (t, *J* = 9.5 Hz, 1H, CH), 6.99 (s, 1H), 7.09 (s, 1H), 7.25 (d, *J* = 8.0 Hz, 2H), 7.35 (m, 1H), 7.43 (dd, *J* = 7.9, 8.4 Hz, 2H), 7.54-7.57 (m, 4H), 7.65 (s, 1H); MS (ESI): *m/z* = 291 [M⁺+H].

1-(1-Biphenyl-4-yl-2,2-dimethyl-propyl)-1H-imidazole, 6. Synthesised according to Method A using **6a** (0.50 g, 2.08 mmol) and CDI (1.69 g, 10.40 mmol); yield: 0.15 g (25 %); white solid: mp 150-151 °C; *R*_f = 0.30

(DCM/MeOH, 10:1); δ_{H} (CDCl₃, 500 MHz) 1.07 (s, 9H, C(CH₃)₃), 4.92 (s, 1H, CH), 7.08 (s, 1H), 7.24 (s, 1H), 7.32-7.36 (m, 1H), 7.41-7.45 (m, 4H), 7.55-7.57 (m, 4H), 7.72 (s, 1H); MS (ESI): $m/z = 291$ [M⁺+H].

1-(1-Biphenyl-4-yl-cyclohexyl-methyl)-1H-imidazole, 7. Synthesised according to Method A using **7a** (0.50 g, 1.87 mmol) and CDI (1.52 g, 9.34 mmol); yield: 0.19 g (32 %); white solid: mp 118-121 °C; $R_f = 0.32$ (DCM / MeOH, 10:1); δ_{H} (CDCl₃, 500 MHz) 0.89-1.03 (m, 2H, cyclohexyl), 1.15-1.28 (m, 3H, cyclohexyl), 1.52-1.60 (m, 2H, cyclohexyl), 1.71-1.77 (m, 3H, cyclohexyl), 2.22-2.23 (m, 1H, cyclohexyl), 4.72 (t, $J = 10.1$ Hz, 1H, CH), 7.04 (s, 1H), 7.06 (s, 1H), 7.32-7.37 (m, 3H), 7.43 (dd, $J = 7.5, 8.8$ Hz, 2H), 7.54-7.57 (m, 4H), 7.63 (s, 1H); MS (ESI): $m/z = 317$ [M⁺+H].

1-(1-Biphenyl-4-yl-2-phenyl-ethyl)-1H-imidazole, 8. Synthesised according to Method A using **8a** (0.50 g, 1.82 mmol) and CDI (1.48 g, 9.11 mmol); yield: 0.14 g (23 %); yellow solid: mp 99-101 °C [Ref: 98-100 °C²²]; $R_f = 0.29$ (DCM / MeOH, 10:1); δ_{H} (CDCl₃, 500 MHz) 3.50 (d, $J = 7.5$ Hz, 2H, CH₂), 5.09 (t, $J = 7.5$ Hz, 1H, CH), 6.95(s, 1H), 7.01 (d, $J = 8.0$ Hz, 2H), 7.06 (s, 1H), 7.22-7.24 (m, 3H), 7.28 (d, $J = 8.4$ Hz, 2H), 7.35-7.37 (m, 1H), 7.42-7.45 (m, 2H), 7.48 (s, 1H), 7.56-7.58 (m, 4H); MS (ESI): $m/z = 325$ [M⁺+H].

1-(1-Biphenyl-4-yl-2-phenyl-methyl)-1H-imidazole, 9. Synthesised according to Method A using **9a** (0.50 g, 1.92 mmol) and CDI (1.56 g, 9.60 mmol); yield: 0.07 g (12 %); yellow oil; [Ref: mp 142 °C²³]; $R_f = 0.35$ (DCM / MeOH, 10:1); δ_{H} (CDCl₃, 500 MHz) 6.57 (s, 1H, CH), 6.89(s, 1H), 7.13-7.19 (m, 5H), 7.35-7.38 (m, 4H), 7.42-7.47 (m, 3H), 7.56-7.59 (m, 4H); MS (ESI): $m/z = 311$ [M⁺+H].

1-(Bis-biphenyl-4-yl-methyl)-1H-imidazole, 10. Synthesised according to Method A using **10a** (0.50 g, 1.49 mmol) and CDI (1.21 g, 7.43 mmol); yield: 0.07 g (13 %); yellow oil; [Ref: mp 120 °C²³]; $R_f = 0.37$ (DCM / MeOH, 10:1); δ_{H} (CDCl₃, 500 MHz) 6.95 (s, 1H), 7.16 (s, 1H), 7.21-7.23 (m, 4H), 7.35-7.38 (m, 2H), 7.43-7.47 (m, 4H), 7.55-7.61 (m, 10H); MS (ESI): $m/z = 387$ [M⁺+H].

1-(1-(4'-(Trifluoromethoxy)biphenyl-4-yl)propyl)-1H-imidazole, 12. Synthesised according to Method A using **12a** (0.50 g, 2.10 mmol) and CDI (2.00 g, 12.40 mmol); yield: 0.16 g (21 %); brownish oil; $R_f = 0.51$ (DCM / MeOH, 95:5); δ_{H} (CDCl₃, 500 MHz) 0.99 (t, $J = 7.5$ Hz, 3H, CH₃), 2.26-2.32 (m, 2H, CH₂), 5.09 (t, $J = 7.5$ Hz, 1H, CH), 7.00 (s, 1H), 7.13 (s, 1H), 7.28-7.31 (m, 4H), 7.54-7.59 (m, 4H), 7.66 (s, 1H); δ_{C} (CDCl₃, 125 MHz) 11.1 (CH₃), 28.6 (CH₂), 63.0 (CH), 117.6 (CH), 119.5(CF₃), 121.2 (CH), 127.0 (Im-C5), 127.5 (CH) 127.6 (CH), 128.4 (CH), 129.5 (C_q), 136.4 (C_q), 139.1 (C_q), 139.7, 139.8 (C_q) 148.8 (C_q); MS (ESI): $m/z = 347$ [M⁺+H].

1-(1-(4'-(Methylsulfonyl)biphenyl-4-yl)propyl)-1H-imidazole, 13. Synthesised according to Method A using **13a** (0.67 g, 2.6 mmol) and CDI (2.00 g, 12.40 mmol); yield: 0.12 g (15 %); beige solid; $R_f = 0.44$ (DCM / MeOH, 95:5); δ_{H} (CDCl₃, 500 MHz) 0.96 (t, $J = 7.0$ Hz, 3H, CH₃), 2.24-2.28 (m, 2H, CH₂), 2.52 (s, 3H, SCH₃), 5.04 (t, $J = 7.0$ Hz, 1H, CH), 6.97 (s, 1H), 7.10 (s, 1H), 7.23-7.26 (m, 2H), 7.30-7.33 (m, 2H), 7.47-7.50 (m, 2H), 7.52-7.54 (m, 2H), 7.63 (s, 1H); δ_{C} (CDCl₃, 125 MHz) 11.1 (CH₃), 15.8 (SCH₃), 28.6 (CH₂), 63.0 (CH), 117.7 (Im-C4), 126.9 (CH), 127.0 (CH), 127.2 (CH), 127.4 (CH), 129.5 (C_q), 136.4 (C_q), 137.1 (C_q), 138.0 (C_q), 139.2 (CH), 140.4 (CH); MS (ESI): $m/z = 309$ [M⁺+H].

4'-(1-(1H-Imidazol-1-yl)propyl)biphenyl-4-carbonitrile, 14. Synthesised according to Method A using **14a** (0.46 g, 1.93 mmol) and CDI (1.5 g, 9.30 mmol); yield: 0.14 g (25 %); brown oil; $R_f = 0.40$ (DCM/MeOH, 95:5); δ_{H} (CDCl₃, 500 MHz) 0.98 (t, $J = 7.0$ Hz, 3H, CH₃), 2.22-2.30 (m, 2H, CH₂), 5.08 (t, $J = 7.0$ Hz, 1H, CH), 6.97 (s, 1H), 7.10 (s, 1H), 7.29 (d, $J = 8.5$ Hz, 2H), 7.56 (d, $J = 8.5$ Hz, 2H), 7.61-7.68 (m, 3H), 7.73 (d, $J = 8.0$ Hz, 2H); δ_{C} (CDCl₃, 125 MHz) 11.1 (CH₃), 28.5 (CH₂), 62.9 (CH), 111.2 (C-4'), 117.6 (C-N), 118.7 (Im-C4), 127.2 (CH), 127.6 (CH), 129.6 (C_q), 132.6 (CH), 136.3 (C_q), 139.0 (CH), 140.9 (C_q), 144.7 (C_q); MS (ESI): $m/z = 288$ [M⁺+H].

1-(1-(4'-Methylbiphenyl-4-yl)propyl)-1H-imidazole, 15. Synthesised according to Method A using **15a** (0.57 g, 2.5 mmol) and CDI (2.0 g, 12.50 mmol); yield: 0.20 g (29 %); yellow solid: mp 71-72 °C; $R_f = 0.26$ (EtOAc); δ_{H} (CDCl₃, 500 MHz) 0.88 (t, $J = 7.3$ Hz, 3H, CH₃), 2.16 (q, $J = 7.3$ Hz, 2H, CH₂), 2.30 (s, 3H, PhCH₃), 4.95 (t, $J = 7.3$ Hz, 1H, CH), 6.89 (s, 1H), 7.00 (s, 1H), 7.12-7.18 (m, 4H), 7.37 (d, $J = 8.2$ Hz, 2H), 7.45 (d, $J = 8.2$ Hz, 2H), 7.54 (s, 1H); δ_{C} (CDCl₃, 125 MHz) 11.1 (CH₃), 21.0 (PhCH₃), 28.5 (CH₂), 63.0 (CH), 117.6, 126.81, 126.86, 127.3, 129.5, 136.3, 137.3, 138.9, 140.9, 142.1; MS (ESI): $m/z = 277$ [M⁺+H].

1-(1-(4'-Ethylbiphenyl-4-yl)propyl)-1H-imidazole, 16. Synthesised according to Method A using **16a** (0.64 g, 2.6 mmol) and CDI (2.1 g, 13.12 mmol); yield: 0.14 g (18 %); yellowish oil; $R_f = 0.30$ (EtOAc); δ_{H} (CDCl₃, 500 MHz) 0.89 (t, $J = 7.3$ Hz, 3H, CH₃), 1.20 (t, $J = 7.6$ Hz, 3H, CH₃), 2.18 (quint, $J = 7.3$ Hz, 2H, CH₂), 2.61 (q, $J = 7.6$ Hz, 2H, CH₂), 4.97 (t, $J = 7.3$ Hz, 1H, CH), 6.90 (s, 1H), 7.02 (s, 1H), 7.14-7.21 (m, 4H), 7.41 (d, $J = 8.2$ Hz, 2H), 7.47 (d, $J = 8.5$ Hz, 2H), 7.57 (s, 1H); δ_{C} (CDCl₃, 125 MHz) 10.1 (CH₃), 14.5 (CH₃), 27.5 (CH₂), 27.6 (CH₂), 62.1 (CH), 116.7, 125.9, 126.0, 126.4, 127.3, 128.3, 135.3, 136.7, 137.8, 140.0, 142.1; MS (ESI): $m/z = 291$ [M⁺+H].

[4'-(1H-Imidazol-1-yl-propyl)-biphenyl-4-yl]-dimethyl-amine, 17. Synthesised according to Method A using **17a** (0.59 g, 2.31 mmol) and CDI (0.56 g, 3.47 mmol); yield: 0.18 g (25 %); white solid: mp 117-119 °C; $R_f = 0.33$

(DCM / MeOH, 20:1); δ_{H} (CDCl₃, 500 MHz) 0.95 (t, $J = 7.3$ Hz, 3H, CH₃), 2.24 (q, $J = 7.3, 7.6$ Hz, 2H, CH₂), 2.99 (s, 6H, N-CH₃), 5.01 (t, $J = 7.6$ Hz, 1H, CH), 6.78 (d, $J = 9.1$ Hz, 2H), 6.97 (s, 1H), 7.09 (s, 1H), 7.20 (d, $J = 8.5$ Hz, 2H), 7.47 (d, $J = 8.8$ Hz, 2H), 7.51 (d, $J = 8.2$ Hz, 2H), 7.62 (s, 1H); δ_{C} (CDCl₃, 125 MHz) 11.1 (CH₃), 28.6 (CH₂), 40.4 (N-CH₃), 63.0 (CH), 112.6, 117.6, 126.5, 126.8, 127.6, 129.4, 136.4, 137.7, 141.0, 150.1; MS (ESI): $m/z = 306$ [M⁺+H].

Diethyl-[4'-(1*H*-imidazol-1-yl-propyl)-biphenyl-4-yl]-amine, 18. Synthesised according to Method A using **18a** (0.70 g, 2.47 mmol) and CDI (0.61 g, 3.70 mmol); yield: 0.16 g (19 %); white solid: mp 109-111 °C; $R_{\text{f}} = 0.33$ (DCM / MeOH, 20:1); δ_{H} (CDCl₃, 500 MHz) 0.95 (t, $J = 7.3$ Hz, 3H, CH₃), 1.19 (t, $J = 6.9$ Hz, 6H, N-CH₃), 2.24 (q, $J = 7.3, 7.6$ Hz, 2H, CH₂), 3.39 (q, $J = 6.9$ Hz, 4H, N-CH₂), 5.01 (t, $J = 7.6$ Hz, 1H, CH), 6.73 (d, $J = 9.1$ Hz, 2H), 6.97 (s, 1H), 7.09 (s, 1H), 7.19 (d, $J = 8.5$ Hz, 2H), 7.45 (d, $J = 8.8$ Hz, 2H), 7.50 (d, $J = 8.2$ Hz, 2H), 7.62 (s, 1H); δ_{C} (CDCl₃, 125 MHz) 11.1 (CH₃), 12.6 (N-CH₃), 28.6 (CH₂), 44.3 (N-CH₂), 63.0 (CH), 111.8, 117.6, 126.3, 126.8, 127.7, 129.4, 136.4, 137.5, 141.1, 147.3; MS (ESI): $m/z = 334$ [M⁺+H].

4-[4'-(1*H*-Imidazol-1-yl-propyl)-biphenyl-4-yl]-morpholine, 19. Synthesised according to Method A using **19a** (0.70 g, 2.37 mmol) and CDI (0.58 g, 3.55 mmol); yield: 0.27 g (33 %); white solid: mp 119-121 °C; $R_{\text{f}} = 0.17$ (DCM / MeOH, 20:1); δ_{H} (CDCl₃, 500 MHz) 0.95 (t, $J = 7.3$ Hz, 3H, CH₃), 2.24 (q, $J = 7.3, 7.6$ Hz, 2H, CH₂), 3.20 (t, $J = 4.7$ Hz, 4H), 3.86 (t, $J = 4.7$ Hz, 4H), 5.02 (t, $J = 7.6$ Hz, 1H, CH), 6.92-6.95 (m, 3H), 7.08 (s, 1H), 7.21 (d, $J = 8.5$ Hz, 2H), 7.49 (d, $J = 8.8$ Hz, 2H), 7.51 (d, $J = 8.5$ Hz, 2H), 7.61 (s, 1H); δ_{C} (CDCl₃, 125 MHz) 11.1 (CH₃), 28.5 (CH₂), 48.9, 62.9 (CH), 66.7, 115.6, 117.6, 126.7, 126.8, 127.6, 129.4, 131.5, 136.3, 138.3, 140.5, 150.6; MS (ESI): $m/z = 348$ [M⁺+H].

[4'-(1*H*-Imidazol-1-yl-propyl)-biphenyl-4-yl]-carbamic acid tert-butyl ester, 20. Synthesised according to Method A using **20a** (1.23 g, 3.75 mmol) and CDI (0.91 g, 5.63 mmol); yield: 0.33 g (23 %); white solid: mp 204-206 °C; $R_{\text{f}} = 0.29$ (DCM / MeOH, 20:1); δ_{H} (CDCl₃, 500 MHz) 0.97 (t, $J = 7.3$ Hz, 3H, CH₃), 1.53 (s, 9H, t-Bu), 2.26 (q, $J = 7.3, 7.6$ Hz, 2H, CH₂), 5.04 (t, $J = 7.6$ Hz, 1H, CH), 6.57 (s, 1H, CONH), 6.97 (s, 1H), 7.09 (s, 1H), 7.24 (d, $J = 8.2$ Hz, 2H), 7.42 (d, $J = 8.5$ Hz, 2H), 7.51-7.53 (m, 4H), 7.62 (s, 1H); δ_{C} (CDCl₃, 125 MHz) 11.1 (CH₃), 28.3 (t-Bu), 28.6 (CH₂), 63.0 (CH), 118.8, 126.9, 127.1, 127.5, 129.5, 137.9, 138.8, 140.5; MS (ESI): $m/z = 378$ [M⁺+H].

1-[1-(4'-Fluoro-biphenyl-4-yl)-propyl]-1*H*-imidazole, 23. Synthesised according to Method A using **23a** (1.23 g, 5.34 mmol) and CDI (4.33 g, 26.70 mmol); yield: 0.52 g (35 %); brown oil; $R_{\text{f}} = 0.6$ (DCM / MeOH, 95:5); δ_{H} (CDCl₃, 500 MHz) 0.97 (t, $J = 7.3$ Hz, 3H, CH₃), 2.27 (q, $J = 7.3, 7.6$ Hz, 2H, CH₂), 5.06 (t, $J = 7.6$ Hz, 1H, CH), 6.97 (s, 1H), 7.09-7.14 (m, 3H), 7.25 (d, $J = 8.9$ Hz, 2H), 7.51-7.53 (m, 4H), 7.62 (s, 1H); δ_{C} (CDCl₃, 125 MHz) 11.1 (CH₃), 28.6 (CH₂), 63.0 (CH), 115.6, 115.7, 117.7, 127.0, 127.4, 128.6, 128.7, 129.5, 136.4, 136.5, 139.3, 140.1, 161.6, 163.6; MS (ESI): $m/z = 281$ [M⁺+H].

1-(2-(4'-Fluorobiphenyl-4-yl)propan-2-yl)-1*H*-imidazole, 24. Synthesised according to Method A using **24a** (0.23 g, 1.0 mmol) and CDI (0.36 g, 2.20 mmol); yield: 0.05 g (19 %); $R_{\text{f}} = 0.27$ (DCM / MeOH, 95:5); δ_{H} (CDCl₃, 500 MHz) 1.94 (s, 6H, CH₃), 6.94-6.96 (m, 1H), 7.10-7.15 (m, 5H), 7.47-7.36 (m, 4H), 7.67-7.69 (m, 1H); δ_{C} (CDCl₃, 125 MHz) 31.5 (CH₃), 60.3 (CH), 116.1, 117.0, 125.2, 127.3, 129.2, 132.6, 139.4, 145.4, 163.7; MS (ESI): $m/z = 281$ [M⁺+H].

1-(3-(4'-Fluorobiphenyl-4-yl)pentan-3-yl)-1*H*-imidazole, 25. Synthesised according to Method A using **25a** (0.26 g, 1.00 mmol) and CDI (0.36 g, 2.20 mmol); yield: 0.13 g (43 %); $R_{\text{f}} = 0.33$ (DCM / MeOH, 95:5); δ_{H} (CDCl₃, 500 MHz) 0.75 (s, 6H, CH₃), 2.26-2.30 (q, 4H, CH₂), 6.84-6.86 (m, 1H), 7.08-7.09 (m, 1H), 7.10-7.13 (m, 2H), 7.17-7.20 (m, 2H), 7.48-7.55 (m, 4H), 7.62-7.63 (m, 1H); δ_{C} (CDCl₃, 125 MHz) 8.3 (CH₃), 30.5 (CH₂), 66.1 (CH), 116.3, 119.7, 127.6, 129.9, 136.2, 139.1, 142.8; MS (ESI): $m/z = 309$ [M⁺+H].

1-(1-(4'-Fluorobiphenyl-4-yl)allyl)-1*H*-imidazole, 28. Synthesised according to Method A using **28a** (1.14 g, 5.00 mmol) and CDI (1.80 g, 10.10 mmol); yield: 0.57 g (41 %); $R_{\text{f}} = 0.27$ (DCM / MeOH, 95:5); δ_{H} (CDCl₃, 500 MHz) 4.73-4.74 (m, 2H, CH₂), 6.30-6.35 (m, 1H, CH), 6.54-6.57 (m, 1H, CH), 6.98 (s, 1H), 7.10-7.12 (m, 3H), 7.42-7.44 (m, 2H), 7.50-7.56 (m, 5H); δ_{C} (CDCl₃, 125 MHz) 49.3 (CH), 116.5, 124.9, 127.4, 128.6, 130.8, 133.2, 135.2, 137.0, 140.3, 161.7; MS (ESI): $m/z = 279$ [M⁺+H].

1-(1-(Biphenyl-4-yl)allyl)-1*H*-imidazole, 29. Synthesised according to Method A using **29a** (0.30 g, 1.00 mmol) and CDI (0.36 g, 2.20 mmol); yield: 0.09 g (32 %); $R_{\text{f}} = 0.21$ (DCM / MeOH, 95:5); δ_{H} (CDCl₃, 500 MHz) 4.73-4.75 (m, 2H, CH₂), 6.30-6.35 (m, 1H, CH), 6.56-6.57 (m, 1H, CH), 6.98 (s, 1H), 7.12-7.13 (m, 1H), 7.34-7.37 (m, 1H), 7.43-7.46 (m, 4H), 7.56-7.60 (m, 5H); δ_{C} (CDCl₃, 125 MHz) 49.3 (CH), 119.4 (=CH₂), 123.8, 127.0, 129.4, 133.2, 134.5, 137.7, 140.9; MS (ESI): $m/z = 297$ [M⁺+H].

1-(9*H*-Fluoren-2-yl)methyl)-1*H*-imidazole, 31. Synthesised according to Method A using **31a** (0.32 g, 1.63 mmol) and CDI (0.53 g, 3.26 mmol); yield: 0.16 g (40 %); $R_{\text{f}} = 0.31$ (MeOH / EtOAc, 5:95); colourless solid: mp

183-185 °C; δ_{H} (CDCl₃, 500 MHz) 3.87 (s, 2H, CH₂), 5.18 (s, 2H), 6.94 (bs, 1H), 7.11 (bs, 1H), 7.19 (d, $J = 8.5$ Hz, 1H), 7.30-7.33 (m, 2H), 7.38 (dd, $J = 7.3, 7.6$ Hz, 1H), 7.54 (d, $J = 7.6$ Hz, 1H), 7.59 (bs, 1H), 7.75 (d, $J = 7.9$ Hz, 1H), 7.77 (d, $J = 7.6$ Hz, 1H); δ_{C} (CDCl₃, 125 MHz) 36.8 (CH₂), 51.0 (CH₂), 119.3 (CH), 120.0 (CH), 120.2 (CH), 124.0 (CH), 125.1 (CH), 126.1 (CH), 126.8 (CH), 127.1 (CH), 129.7 (CH), 134.4 (C_q), 137.4 (CH), 140.9 (C_q), 141.9 (C_q), 143.3 (C_q), 144.1 (C_q); MS (ESI): $m/z = 247$ [M⁺+H].

1-((9H-Fluoren-2-yl)ethyl)-1H-imidazole, 32. Synthesised according to Method A using **32a** (1.00 g, 4.70 mmol) and CDI (1.53 g, 9.50 mmol); yield: 0.62 g (51 %); $R_{\text{f}} = 0.58$ (MeOH / EtOAc, 5:95); light yellow solid: mp 109-110 °C; δ_{H} (CDCl₃, 500 MHz) 1.90 (d, $J = 6.9$ Hz, 3H, CH₃), 3.86 (s, 2H, CH₂), 5.41 (q, $J = 6.9$ Hz, 1H, CH), 6.96 (t, $J = 1.3$ Hz, 1H), 7.10 (bs, 1H), 7.17-7.19 (m, 1H), 7.29 (bs, 1H), 7.31 (dd, $J = 1.3, 7.6$ Hz, 1H), 7.37 (t, $J = 7.8$ Hz, 1H), 7.53 (bd, $J = 7.6$ Hz, 1H), 7.63 (bs, 1H), 7.74 (d, $J = 7.9$ Hz, 1H), 7.76 (d, $J = 7.6$ Hz, 1H); δ_{C} (CDCl₃, 125 MHz) 22.2 (CH₃), 36.9 (CH₂), 56.8 (CH), 118.0 (CH), 120.0 (CH), 120.1 (CH), 122.6 (CH), 124.8 (CH), 125.0 (CH), 126.8 (CH), 127.0 (CH), 129.2 (CH), 136.0 (CH), 139.9 (C_q), 140.9 (C_q), 141.8 (C_q), 143.3 (C_q), 144.0 (C_q); MS (ESI): $m/z = 261$ [M⁺+H].

1-[1-(7-Fluoro-9H-fluoren-2-yl)-ethyl]-1H-imidazole, 33. Synthesised according to Method A using **33a** (1.00 g, 4.38 mmol) and CDI (1.87 g, 1.16 mmol); yield: 0.44 g (36 %); $R_{\text{f}} = 0.24$ (MeOH / EtOAc, 5:95); yellow oil; δ_{H} (CDCl₃, 500 MHz) 1.90 (d, $J = 6.9$ Hz, 3H, CH₃), 3.85 (s, 2H, CH₂), 5.41 (q, $J = 7.0$ Hz, 1H, CH), 6.96 (s, 1H), 7.05-7.09 (m, 2H), 7.18 (d, $J = 7.9$ Hz, 1H), 7.22 (dd, $J = 1.8, 8.6$ Hz, 1H), 7.28 (bs, 1H), 7.63 (bs, 1H), 7.67-7.70 (m, 2H); δ_{C} (CDCl₃, 125 MHz) 22.2 (CH₃), 36.9 (CH₂), 56.8 (CH), 112.4 (d, CH), 114.1 (d, CH), 118.0 (CH), 119.8 (CH), 120.9 (CH), 122.6 (CH), 125.0 (CH), 129.2 (CH), 136.0 (CH), 137.0 (C_q), 139.7 (C_q), 141.0 (C_q), 143.7 (C_q), 145.5 (C_q), 161.6 (C_q); MS (ESI): $m/z = 279$ [M⁺+H].

2-(1-Imidazol-1-yl-ethyl)-9H-carbazole, 34. Synthesised according to Method A using **34a** (0.22 g, 1.02 mmol) and CDI (0.33 g, 2.04 mmol); yield: 0.08 g (29 %); $R_{\text{f}} = 0.40$ (MeOH / EtOAc, 5:95); δ_{H} (CDCl₃, 500 MHz) 1.90 (d, $J = 6.9$ Hz, 3H), 5.46 (q, $J = 6.9$ Hz, 1H), 6.97 (bs, 1H), 7.05-7.07 (m, 2H), 7.11 (bs, 1H), 7.22 (ddd, $J = 1.9, 6.4, 8.0$ Hz, 1H), 7.38-7.43 (m, 2H), 7.65 (bs, 1H), 8.02 (d, $J = 8.5$ Hz, 1H), 8.05 (d, $J = 7.9$ Hz, 1H); δ_{C} (CDCl₃, 125 MHz) 22.4 (CH₃), 57.2 (CH), 108.0 (CH), 110.8 (CH), 117.3 (CH), 118.3 (CH), 119.4 (CH), 120.3 (CH), 120.5 (CH), 122.7 (C_q), 123.1 (C_q), 126.0 (CH), 128.8 (CH), 136.0 (CH), 139.2 (C_q), 140.0 (C_q), 140.2 (C_q); MS (ESI): $m/z = 262$ [M⁺+H].

2-(1-(1H-Imidazol-1-yl)ethyl)-7-fluoro-9H-carbazole, 35. Synthesised according to Method A using **35a** (0.30 g, 1.30 mmol) and CDI (0.42 g, 2.60 mmol); yield: 0.08 g (23 %); $R_{\text{f}} = 0.11$ (EtOAc); δ_{H} (CDCl₃, 500 MHz) 1.93 (d, $J = 7.0$ Hz, 3H), 5.64 (q, $J = 7.0$ Hz, 1H), 6.90 (ddd, $J = 2.2, 8.5, 9.6$ Hz, 1H), 6.99 (t, $J = 1.3$ Hz, 1H), 7.07 (ddd, $J = 0.6, 1.6, 8.2$ Hz, 1H), 7.11 (dd, $J = 2.2, 9.6$ Hz, 1H), 7.18 (t, $J = 1.3$ Hz, 1H), 7.28 (d, $J = 1.6$ Hz, 1H), 7.80 (bs, 1H), 7.96-7.99 (m, 2H); δ_{C} (CDCl₃, 125 MHz) 22.5 (CH₃), 58.6 (CH), 98.2 (d, CH), 107.9 (d, CH), 109.4 (CH), 118.6 (CH), 119.7 (CH), 120.6 (C_q), 121.1 (CH), 122.2 (CH), 123.8 (C_q), 128.9 (CH), 137.4 (CH), 140.4 (C_q), 142.2 (C_q), 142.8 (C_q), 163.5 (C_q); MS (ESI): $m/z = 280$ [M⁺+H].

Method B: Grignard reaction

Under exclusion of air and moisture a 1.0 M Grignard reagent (1.2 eq) solution in THF was added dropwise to a solution of the aldehyde or ketone (1 eq) in THF (12 mL / mmol). The mixture was stirred at room temperature overnight. Subsequently ethyl acetate (10 mL) and water (10 mL) were added and the organic phase was separated. The organic phase was extracted with water and brine, dried over Na₂SO₄, and evaporated under reduced pressure. The crude products were purified by flash chromatography on silica gel.

1-Biphenyl-4-yl-3-methyl-butan-1-ol, 5a. Synthesised according to Method B using Biphenyl-4-carbaldehyde (1.00 g, 5.48 mmol) and a 1.0 M iso-butylmagnesiumbromide solution in THF (7.13 mL, 7.13 mmol); yield: 0.96 g (73 %); $R_{\text{f}} = 0.28$ (PE / EtOAc, 5:1); δ_{H} (CDCl₃, 500 MHz) 0.97 (d, $J = 4.9$ Hz, 6H, CH₃), 1.51-1.58 (m, 1H, CH), 1.72 (s, br, 1H, OH), 1.75-1.81 (m, 2H, CH₂), 4.79 (t, $J = 2.7$ Hz, 1H, CH), 7.33 (t, $J = 7.5$ Hz, 1H), 7.43 (d, $J = 8.4$ Hz, 4H), 7.57 (d, $J = 8.4$ Hz, 4H); MS (ESI): $m/z = 241$ [M⁺+H].

1-[4'-(tert-Butyl-dimethyl-silanyloxy)-biphenyl-4-yl]-propan-1-ol, 22b. Synthesised according to method B using **22c** (3.30 g, 10.6 mmol) and 1.0 M EtMgBr (12.7 mL). Yield: 1.89 g (52 %); $R_{\text{f}} = 0.40$ (PE / EtOAc, 9:1); δ_{H} (CDCl₃, 500 MHz) 0.23 (s, 6H), 0.95 (t, $J = 7.3$ Hz, 3H), 1.00 (s, 9H), 1.76-1.89 (m, 2H), 4.64 (t, $J = 6.6$ Hz, 1H), 6.90 (d, $J = 8.5$ Hz, 2H), 7.38 (d, $J = 8.5$ Hz, 2H), 7.46 (d, $J = 8.5$ Hz, 2H), 7.54 (d, $J = 8.5$ Hz, 2H); MS (ESI): $m/z = 344$ [M⁺+H].

3-(4'-Fluorobiphenyl-4-yl)pentan-3-ol, 25a. Synthesised according to Method B using **23b** (0.58 g, 2.53 mmol) and a 1.0 M ethylmagnesiumbromide solution in THF (25.0 mL, 25.0 mmol); yield: 0.58 g (89 %); $R_{\text{f}} = 0.28$

(DCM); δ_{H} (CDCl_3 , 500 MHz): 0.79-0.92 (s, 6H, CH_3), 1.68 (s, br, 1H, OH), 1.82-1.93 (m, 4H, CH_2), 7.10-7.14 (m, 2H), 7.43-7.45 (m, 2H), 7.51-7.58 (m, 4H); MS (ESI): $m/z = 259$ [M^+H].

Method C: Suzuki-Coupling

The corresponding brominated aromatic compound (1 eq) was dissolved in toluene (7 mL / mmol), an aqueous 2.0 M Na_2CO_3 solution (3.2 mL / mmol) and an ethanolic solution (3.2 mL / mmol) of the corresponding boronic acid (1.5-2.0 eq) were added. The mixture was deoxygenated under reduced pressure and flushed with nitrogen. After repeating this cycle several times $\text{Pd}(\text{PPh}_3)_4$ (4 mol%) was added and the resulting suspension was heated under reflux for 8 h. After cooling ethyl acetate (10 mL) and water (10 mL) were added and the organic phase was separated. The water phase was extracted with ethyl acetate (2 x 10 mL). The combined organic phases were washed with brine, dried over Na_2SO_4 , filtered over a short plug of celite® and evaporated under reduced pressure. The compounds were purified by flash chromatography on silica gel.

1-((4'-(Trifluoromethyl)biphenyl-4-yl)methyl)-1H-imidazole, 11. Synthesised according to Method C using 1-(4-bromobenzyl)-1H-imidazole (0.24 g, 1.00 mmol) and 4-trifluoromethylphenylboronic acid (0.38 g, 2.00 mmol); yield: 0.24 g (80 %); brown oil; $R_f = 0.14$ (EtOAc); δ_{H} (CDCl_3 , 500 MHz) 5.17 (s, 2H, CH_2), 6.93 (bs, 1H), 7.11 (bs, 1H), 7.24 (d, $J = 7.9$ Hz, 2H), 7.57 (d, $J = 7.9$ Hz, 2H), 7.59 (bs, 1H), 7.65 (d, $J = 8.5$ Hz, 2H), 7.68 (d, $J = 8.5$ Hz, 2H); δ_{C} (CDCl_3 , 125 MHz) 50.4 (CH_2), 119.2 (CH), 123.1 (C_q), 125.2 (C_q), 125.7 (CH), 127.3 (CH), 127.7 (CH), 127.8 (CH), 129.8 (CH), 136.2 (C_q), 137.4 (CH), 139.7 (C_q), 143.8 (C_q); MS (ESI): $m/z = 303$ [M^+H].

1-(4'-Fluorobiphenyl-4-yl)propan-1-one, 23b. Synthesised according to Method C using 4-bromopropiophenone (1.23 g, 6.65 mmol) and 4-fluorophenylboronic acid (1.38 g, 6.47 mmol); yield: 1.20 g (79 %); $R_f = 0.45$ (Hex / EtOAc, 10:1); δ_{H} (CDCl_3 , 500 MHz) 1.24-1.27 (t, $J = 7.3$ Hz, 3H, CH_3), 3.01-3.06 (m, 2H, CH_2), 6.97-7.01 (m, 1H), 7.06-7.11 (m, 1H), 7.58-7.61 (m, 2H), 8.02-8.04 (m, 2H); MS (ESI): $m/z = 229$ [M^+H].

1-(4'-Fluoro-2'-nitrobiphenyl-4-yl)ethanone, 35c. Synthesised according to Method C using 4-fluoro-1-iodo-2-nitrobenzene (1.20 g, 4.50 mmol) and 4-acetylbenzeneboronic acid (1.48 g, 9.00 mmol); yield: 1.01 g (87 %); $R_f = 0.19$ (petrolether / EtOAc, 10:1); δ_{H} (CDCl_3 , 500 MHz) 2.64 (s, 3H, CH_3), 7.38 (d, $J = 8.5$ Hz, 2H), 7.39-7.41 (m, 1H), 7.43 (dd, $J = 5.5, 8.5$ Hz, 1H), 7.67 (dd, $J = 2.5, 8.0$ Hz, 1H), 8.01 (d, $J = 8.5$ Hz, 2H); δ_{C} (CDCl_3 , 125 MHz) 26.6 (CH_3), 112.1 (d, CH), 119.9 (d, CH), 128.3 (CH), 128.7 (CH), 131.7 (C_q), 133.2 (CH), 136.8 (C_q), 141.3 (C_q), 161.6 (d, C_q), 197.4 (C_q); MS (ESI): $m/z = 259$ [M^+H].

Method D: Reduction with NaBH_4

To an ice-cooled solution of the corresponding aldehyde or ketone (1 eq) in methanol (5 mL / mmol) was added NaBH_4 (2 eq). Then the resulting mixture was heated to reflux for 30 minutes. After cooling to ambient temperature, the solvent was distilled off under reduced pressure. Subsequently water (10 mL) was added, and the resulting mixture was extracted with ethyl acetate (3 x 10 mL). The combined organic phases were washed with brine, dried over MgSO_4 and evaporated under reduced pressure. Then the desired product was purified by chromatography on silica gel.

1-(4'-Fluoro-biphenyl-4-yl)propan-1-ol, 23a. Synthesised according to Method D using **22b** (1.20 g, 5.26 mmol) and NaBH_4 (0.30 g, 7.89 mmol); yield: 1.15 g (95 %); the compound was directly used in the next step without further purification and characterization.

1-(9H-Carbazol-2-yl)ethanol, 34a. Synthesised according to Method D using 1-(9H-carbazol-2-yl)ethanone (0.50 g, 2.39 mmol) and NaBH_4 (0.16 g, 4.30 mmol); yield: 0.42 g (83 %); $R_f = 0.12$ (petrolether / EtOAc, 5:1); light yellow solid; mp 192-194 °C; δ_{H} (CDCl_3 , 500 MHz) 1.41 (d, $J = 6.6$ Hz, 3H, CH_3), 3.13 (bs, 1H), 4.88 (q, $J = 6.6$ Hz, 1H), 7.03 (ddd, $J = 1.2, 7.3, 7.9$ Hz, 1H), 7.07 (dd, $J = 1.6, 8.2$ Hz, 1H), 7.22 (ddd, $J = 1.2, 7.2, 8.2$ Hz, 1H), 7.30 (dt, $J = 1.0, 8.2$ Hz, 1H), 7.37-7.39 (m, 1H), 7.85 (d, $J = 8.2$ Hz, 1H), 7.88 (d, $J = 7.9$ Hz, 1H), 9.62 (bs, 1H); δ_{C} (CDCl_3 , 125 MHz) 25.5 (CH_3), 69.9 (CH_2), 107.3 (CH), 110.4 (CH), 116.4 (CH), 118.4 (CH), 119.5 (CH), 119.6 (CH), 121.8 (C_q), 122.6 (C_q), 124.9 (CH), 139.7 (C_q), 139.8 (C_q), 144.4 (C_q); MS (ESI): $m/z = 210$ [M^+H].

1-(7-Fluoro-9H-carbazol-2-yl)ethanol, 35a. Synthesised according to Method D using **35b** (0.25 g, 1.12 mmol) and NaBH_4 (0.08 g, 2.02 mmol); yield: 0.21 g (82 %); $R_f = 0.19$ (petrolether / EtOAc, 5:1); δ_{H} (CDCl_3 , 500 MHz) 1.50 (d, $J = 6.4$ Hz, 3H), 4.94 (q, $J = 6.4$ Hz, 1H), 6.85 (ddd, $J = 2.3, 8.5, 8.8$ Hz, 1H), 7.08 (dd, $J = 2.3, 9.8$ Hz, 1H), 7.15 (dd, $J = 1.2, 8.2$ Hz, 1H), 7.43 (bs, 1H), 7.91 (d, $J = 8.5$ Hz, 1H), 7.93 (dd, $J = 5.5, 8.5$ Hz, 1H); δ_{C} (CDCl_3 , 125 MHz) 26.0 (CH_3), 71.5 (CH), 98.0 (d, CH), 107.5 (d, CH), 108.6 (CH), 118.2 (CH), 120.5 (CH), 120.8 (C_q), 121.8 (d, CH), 123.2 (C_q), 142.2 (C_q), 142.4 (C_q), 145.1 (C_q), 163.2 (d, C_q); MS (ESI): $m/z = 212$ [M^+OH].

4'-(1H-Imidazol-1-yl-propyl)-biphenyl-4-ylamine, 21a. To a solution of **20** (0.32 g, 0.85 mmol) in DCM (10 mL) was added TFA (0.63 mL, 8.5 mmol) slowly in an ice bath. Subsequently it was stirred at room temperature overnight. DCM (10 mL) and water (10 mL) were added and the organic phase was separated. The organic phase

was extracted with water and brine, dried over Na₂SO₄, and evaporated under reduced pressure. The crude products were purified by flash chromatography on silica gel; yield: 0.22 g (95 %); *R*_f = 0.35 (PE / EtOAc, 2:1); the compound was directly used in the next step without further purification and analysis.

N-[4'-(1*H*-Imidazol-1-yl-propyl)-biphenyl-4-yl]-acetamide, 21. To a solution of **21a** (0.07 g, 0.25 mmol) in THF (10 mL) were added DMAP (0.02 g, 0.13 mmol) and triethylamine (0.1 mL). After cooling to 0 °C in an ice bath, acetyl chloride was dropped into the reaction solution slowly. Then it was stirred in the ambient temperature overnight. After neutralized to pH = 7 with sodium bicarbonate in an ice bath, ethyl acetate (10 mL) and water (10 mL) were added and the organic phase was separated. The organic phase was extracted with water and brine, dried over Na₂SO₄, and evaporated under reduced pressure. The crude products were purified by flash chromatography on silica gel; yield: 0.33 g (23 %); white solid: mp 221-223 °C; *R*_f = 0.27 (DCM / MeOH, 20:1); δ_H (CDCl₃, 500 MHz) 0.97 (t, *J* = 7.3 Hz, 3H, CH₃), 2.20 (s, 3H, CH₃CO), 2.26 (q, *J* = 7.3, 7.6 Hz, 2H, CH₂), 5.05 (t, *J* = 7.6 Hz, 1H, CH), 6.99 (s, 1H), 7.11 (s, 1H), 7.23 (d, *J* = 8.2 Hz, 2H), 7.49-7.58 (m, 6H), 7.72 (s, 1H); δ_C (CDCl₃, 125 MHz) 11.0 (CH₃), 24.6 (CH₃CO), 28.5 (CH₂), 63.2 (CH), 120.1, 126.9, 127.5, 127.5, 135.9, 137.6, 140.5, 168.4; MS (ESI): *m/z* = 320 [M⁺+H].

4'-(1*H*-Imidazol-1-yl-propyl)-biphenyl-4-ol, 22. To a solution of **22a** (0.85 g, 2.16 mmol) in anhydrous THF (20 mL) was added TBAF (2.4 mL, 2.4 mmol) and subsequently the solution was stirred at room temperature for 4 h. The reaction was terminated with the addition of methanol and the solvent was removed under reduced pressure. Then the desired product was purified by chromatography on silica gel. Yield: 0.22 g (37 %); Yellow solid; *R*_f = 0.21 (Hex / EtOAc, 5:1); δ_H (DMSO-d₆, 500 MHz) 0.82 (t, *J* = 7.3 Hz, 3H), 2.21 (m, 2H), 5.23 (t, *J* = 7.3 Hz, 1H), 6.82 (d, *J* = 8.8 Hz, 2H), 6.90 (s, 1H), 7.37 (d, *J* = 8.5 Hz, 2H), 7.46 (d, *J* = 8.8 Hz, 2H), 7.54 (d, *J* = 8.5 Hz, 2H), 7.82 (s, 1H), 9.55 (s, 1H); δ_C (DMSO-d₆, 125 MHz) 10.9 (CH₃), 27.4 (CH₂), 61.5 (CH), 115.6 (CH), 117.7 (CH), 126.0 (CH), 127.1 (CH), 127.6 (CH), 128.4 (C_q), 130.3 (CH), 130.7 (C_q), 139.3 (CH), 139.5 (C_q), 157.1 (C_q); MS (ESI): *m/z* = 279 [M⁺+H].

3-(4'-Fluorobiphenyl-4-yl)-3-(1*H*-imidazol-1-yl)propan-1-ol, 26. 26a (0.241 g, 0.45 mmol) was dissolved by slowly adding dropwise to 15 mL THF and 1M TBAF (0.55 mL, 0.55 mmol) in THF. 1 hour later, according to TLC (DCM / methanol, 95:5) the deprotection was quantitative. The batch was diluted with a large quantity of ethyl acetate and extracted three times with water and once with brine, then dried over MgSO₄ and the solvent removed under reduced pressure. The crude product was subsequently purified by column chromatography; yield: 0.09 g (67 %); *R*_f = 0.34 (DCM / MeOH, 9:1); δ_H (CDCl₃, 500 MHz) 2.43-2.49 (m, 2H, CH₂), 3.50-3.54 (m, 1H), 3.68-3.72 (m, 1H), 5.56-5.59 (q, 1H, CH), 6.98 (m, 1H), 7.08 (m, 1H), 7.1-7.14 (m, 2H), 7.26-7.29 (m, 2H), 7.48-7.51 (m, 4H), 7.56 (m, 1H); δ_C (CDCl₃, 125 MHz) 37.1 (CH₂), 50.5 (CH), 57.7 (CH₂-OH), 116.3, 127.6, 128.6, 129.8, 136.8, 137.2, 139.9, 140.0, 161.4; MS (ESI): *m/z* = 297 [M⁺+H].

1-(3-Chloro-1-(4'-fluorobiphenyl-4-yl)propyl)-1*H*-imidazole, 27. 26 (0.044 g, 0.148 mmol) was dissolved in 10 mL dry DCM and mixed with 13 μL thionyl chloride. The batch was stirred for 2 hours at room temperature; according to the TLC control, the reaction was quantitative (DCM as solvent). The batch was diluted with a large quantity of DCM and water. The organic phase was separated off and extracted 5 times with water and once with brine, then dried over MgSO₄ and the solvent removed under reduced pressure; yield: 0.05 g (99 %); *R*_f = 0.63 (DCM / MeOH, 9:1); δ_H (CDCl₃, 500 MHz) 2.87-2.97 (m, 2H, CH₂), 3.50-3.60 (m, 2H, CH₂Cl), 5.80-5.83 (m, 1H, CH), 7.11-7.16 (m, 2H), 7.16-7.17 (m, 1H), 7.35-7.37 (m, 1H), 7.49-7.53 (m, 4H), 7.58-7.60 (m, 2H), 9.51-9.53 (m, 1H); δ_C (CDCl₃, 125 MHz) 34.2 (CH₂), 41.4 (CH₂Cl), 61.8 (CH), 119.6, 122.9, 116.5, 128.4, 129.4, 135.7, 136.3, 137.6, 136.4, 142.5, 163.5; MS (ESI): *m/z* = 315 [M⁺+H].

1-(7-(tert-Butyldimethylsilyloxy)-9*H*-fluoren-2-yl)ethanone, 30c. Imidazole (0.17 g, 2.45 mmol) and 1-(7-hydroxy-9*H*-fluoren-2-yl)ethanone (0.50 g, 2.23 mmol) were dissolved in 20 mL DCM. Then tert-butyldimethylsilylchloride (0.37 g, 2.45 mmol) dissolved in 3 mL DCM were slowly added. The resulting mixture was stirred for 18 h at room temperature. Afterwards the mixture was extracted with water and brine. The organic phase was separated, dried over Na₂SO₄ and evaporated; yield: 0.58 g (77 %); *R*_f = 0.40 (petrolether / EtOAc, 10:1); MS (ESI): *m/z* = 339 [M⁺+H].

7-(1-(1*H*-imidazol-1-yl)ethyl)-9*H*-fluoren-2-ol, 30. 30a (0.16 g, 0.40 mmol) was dissolved in 10 mL THF and 1M TBAF (0.41 mL, 0.41 mmol) solution in THF was added dropwise. After 1 hour according to TLC (DCM / methanol 95:5) the deprotection was quantitative. The batch was diluted with a large quantity of ethyl acetate and extracted three times with water and once with brine, then dried over MgSO₄ and the solvent removed under reduced pressure; yield: 0.10 g (90 %); *R*_f = 0.12 (MeOH / EtOAc, 5:95); orange solid: mp 217-218 °C; δ_H (CDCl₃, 500 MHz) 1.81 (d, *J* = 6.9 Hz, 3H), 3.70 (s, 2H), 5.31 (q, *J* = 6.9 Hz, 1H), 6.77 (dd, *J* = 2.2, 8.2 Hz, 1H), 6.90 (s, 1H), 6.93 (s, 1H), 6.95 (s, 1H), 7.06 (d, *J* = 7.9 Hz, 1H), 7.18 (s, 1H), 7.50 (d, *J* = 8.2 Hz, 1H), 7.52 (d, *J* = 7.9 Hz,

1H), 7.55 (s, 1H); δ_C (CDCl₃, 125 MHz) 21.9 (CH₃), 36.6 (CH₂), 56.9 (CH), 112.0 (CH), 114.1 (CH), 118.1 (CH), 118.8 (CH), 120.6 (CH), 122.4 (CH), 124.7 (CH), 128.2 (CH), 132.8 (C_q), 135.6 (CH), 137.9 (C_q), 142.0 (C_q), 143.2 (C_q), 145.2 (C_q), 156.6 (C_q); MS (ESI): $m/z = 277$ [M⁺+H].

1-(7-Fluoro-9H-carbazol-2-yl)ethanone, 35b. 35c was dissolved in 3 mL P(OEt)₃ and refluxed for 16 h. The resulting mixture was directly purified using column chromatography; yield: 0.28 g (53 %); $R_f = 0.13$ (petroleum ether / EtOAc, 5:1); δ_H (CDCl₃, 500 MHz) 2.54 (s, 3H), 6.79 (ddd, $J = 2.3, 8.6, 9.5$ Hz, 1H), 7.01 (dd, $J = 2.3, 9.6$ Hz, 1H), 7.65 (dd, $J = 1.6, 8.2$ Hz, 1H), 7.85 (dd, $J = 5.4, 8.5$ Hz, 1H), 7.87 (d, $J = 8.5$ Hz, 1H), 7.93 (dd, $J = 0.6, 1.6$ Hz, 1H), 10.53 (bs, 1H); δ_C (CDCl₃, 125 MHz) 26.5 (CH₃), 97.4 (d, CH), 107.3 (d, CH), 110.9 (CH), 118.4 (C_q), 119.0 (CH), 119.2 (CH), 121.6 (d, CH), 126.2 (C_q), 133.6 (C_q), 139.7 (C_q), 142.0 (d, C_q), 162.2 (d, C_q), 197.8 (C_q); MS (ESI): $m/z = 227$ [M⁺+H].

Docking studies

All molecular modelling studies were performed on Intel(R) P4 CPU 3.00GHz running Linux Suse 10.1.

Ligands. The structures of the inhibitors were built with SYBYL 7.3.2 (Sybyl, Tripos Inc., St. Louis, Missouri, USA) and energy-minimized in MMFF94s force-field^{24a} as implemented in Sybyl. The resulting geometries for our compounds were then subjected to ab initio calculation employing the B3LYP functional^{24b-24c} in combination with a 6-31G* basis set using the package Gaussian03 (Gaussian, Inc., Pittsburgh, PA, 2003).

Docking. Various inhibitors were docked into our CYP17 homology model by means of the GOLD v3.0.1 software.²⁵ Since it is known that non-steroidal inhibitors of CYP enzymes primary interact by complexation of the heme iron with their sp² hybridized nitrogen^{16b} a distance constraint of a minimum of 1.9 and a maximum of 2.5 Å between the nitrogen of the imidazole and the iron was set.

Ligands were docked in 50 independent genetic algorithm (GA) runs using GOLD. Heme iron was chosen as active-site origin, while the active site radius was set equal to 19 Å. The automatic active-site detection was switched on. Furthermore, some of the GOLDScore parameters were modified to improve the weight of hydrophobic interaction and of the coordination between iron and nitrogen. The genetic algorithm default parameters were set as suggested by the GOLD authors. On the other hand, the annealing parameters of fitness function were set at 3.5 Å for hydrogen bonding and 6.5 Å for Van der Waals interactions.

All 50 poses for each compound were clustered with ACIAP²⁶ and the representative structure of each significant cluster was selected. The quality of the docked representative poses was evaluated based on visual inspection of the putative binding modes of the ligands, as outcome of docking simulations and cluster analysis. Further the different interaction patterns were manually analyzed using Silver 1.1,^{25b} a program included for use with GOLD and used to post-process docking results.

Acknowledgments

The authors thank Ulrike E. Hille and Dr Carsten Jagusch for their help in the synthesis of some compounds, and Maria-Christina Scherzberg for the IC₅₀ determination of some compounds. We also are grateful to Professor J. Hermans, Cardiovascular Research Institute, University of Maastricht, Netherlands, for providing us with V79MZh11B1 cells expressing human CYP11B1 and Professor R. Bernhardt, Saarland University, Germany, for making us V79MZh11B2 cells expressing human CYP11B2 available. This research was supported in part by the Fonds der Chemischen Industrie.

Supplementary data

The synthetic procedures and characterization of further intermediates and IR spectra of all compounds as well as the purities of final compounds by element analysis or HPLC can be found, in the online version, at doi:10.1016/j.bmc.2008.07.011.

References and notes

- (1) (a) Smith, J. A. *J. Urol.* **1987**, *137*, 1. (b) Crawford, E. D.; Eisenberger, M. A.; McLeod, D. G.; Spaulding, J. T.; Benson, R.; Dorr, F. A.; Blumstein, B. A.; Davis, M. A.; Goodman, P. J. *N. Engl. J. Med.* **1989**, *321*, 419.
- (2) Chung, B. C.; Picardo-Leonard, J.; Hanui, M.; Bienkowski, M.; Hall, P. F.; Shively, J. E.; Miller, W. L. *Proc. Natl. Acad. Sci. USA.* **1987**, *84*, 407.

- (3) (a) Swinney, M.; Mak, A. Y. *Biochem.* **1994**, *33*, 2185. (b) Akhtar, M.; Corina, D. L.; Miller, S. L.; Shyadehi, A. Z.; Wright, J. N. *Biochem.* **1994**, *33*, 4410.
- (4) (a) Hartmann, R.W.; Hector, M.; Haidar, M.; Ehmer, P. B.; Reichert, W.; Jose, J. *J. Med. Chem.* **2000**, *43*, 4266. (b) Hartmann, R.W.; Hector, M.; Wachall, B.G.; Palusczyk, A.; Palzer, M.; Huch, V.; Veith, M. *J. Med. Chem.* **2000**, *43*, 4437. (c) Njar, V. C. O.; Hector, M.; Hartmann, R.W. *Bioorg. Med. Chem.* **1996**, *4*, 1447.
- (5) (a) Potter, G. A.; Banie, S. E.; Jarman, M.; Rowlands, M. G. *J. Med. Chem.* **1995**, *38*, 2463. (b) Jarman, M.; Barrie, S. E.; Llera, J. M. *J. Med. Chem.* **1998**, *41*, 5375.
- (6) (a) Gambertoglio, J. G.; Amend, W. J. Jr; Benet, L. Z. *J. Pharmacokinet. Biopharm.* **1980**, *8*, 1. (b) Fotherby, K. *Contraception.* **1996**, *54*, 59. (c) Steiner, J. F. *Clin. Pharmacokinet.* **1996**, *30*, 16. (d) Hameed, A.; Brothwood, T.; Bouloux, P. *Curr. Opin. Investig. Drugs.* **2003**, *4*, 1213.
- (7) (a) Buster, J. E.; Casson, P. R.; Straughn, A. B.; Dale, D.; Umstot, E. S.; Chiamovi, N.; Abraham, G. E. *Am. J. Obstet. Gynecol.* **1992**, *166*, 1163. (b) Peterson, R. E. Metabolism of adrenal cortical steroids. In: Christy, N.P. editor. The human adrenal cortex. New York: Harper & Row, **1997**, pp. 87-189.
- (8) (a) Wächter, G. A.; Hartmann, R. W.; Sergejew, T.; Grün, G. L.; Ledergerber, D. *J. Med. Chem.* **1996**, *39*, 834. (b) Zhuang, Y.; Hartmann, R. W. *Archiv. Pharm.* **1998**, *331*, 36. (c) Zhuang, Y.; Hartmann, R. W. *Archiv. Pharm.* **1998**, *331*, 25. (d) Hartmann, R. W.; Wachall, B. WO9918075, 1998.
- (9) (a) Rowlands, M. G.; Barrie, S. E.; Chan, F.; Houghton, J.; Jarman, M.; McCague, R.; Potter, G.A. *J. Med. Chem.* **1995**, *38*, 4191. (b) Chan, F. C. Y.; Potter, G. A.; Barrie, S. E.; Haynes, B. P.; Rowlands, M. J.; Houghton, G.; Jarman, M. *J. Med. Chem.* **1996**, *39*, 3319.
- (10) (a) Matsunaga, N.; Kaku, T.; Itoh, T.; Tanaka, T.; Hara, T.; Miki, H.; Iwasaki, M.; Aono, T.; Yamaoka, M.; Kusaka, M.; Tasaka, A. *Bioorg. Med. Chem.* **2004**, *12*, 2251. (b) Matsunaga, N.; Kaku, T.; Ojida, A.; Tanaka, T.; Hara, T.; Yamaoka, M.; Kusaka, M.; Tasaka, A. *Bioorg. Med. Chem.* **2004**, *12*, 4313. (c) Tasaka, A.; Hitaka, T.; Matsunaga, N.; Kusaka, M.; Adachi, M.; Aoki, I.; Ojida, A. WO02040484, 2002.
- (11) (a) Bierer, D.; McClue, A.; Fu, W.; Achebe, F.; Ladouceur, G. H.; Burke, M. J.; Bi, C.; Hart, B.; Dumas, J.; Sibley, R.; Scott, W. J.; Johnson, J.; Asgari, D. WO03027085, 2003. (b) Ladouceur, G. H.; Burke, M. J.; Wong, W. C.; Bierer, D. WO03027094, 2003.
- (12) (a) Wachall, B. G.; Hector, M.; Zhuang, Y.; Hartmann, R. W. *Bioorg. Med. Chem.* **1999**, *7*, 1913. (b) Zhuang, Y.; Wachall, B. G.; Hartmann, R. W. *Bioorg. Med. Chem.* **2000**, *8*, 1245. (c) Leroux, F.; Hutschenreuter, T. U.; Charriere, C.; Scopelliti, R.; Hartmann, R.W. *Helv. Chim. Acta* **2003**, *86*, 2671. (d) Hutschenreuter, T. U.; Ehmer, P. E.; Hartmann, R. W. *J. Enzyme Inhibit. Med. Chem.* **2004**, *19*, 17.
- (13) Jagusch, C.; Negri, M.; Hille, U. E.; Hu, Q.; Bartels, M.; Jahn-Hoffmann, K.; Pinto-Bazurco Mendieta, M. A. E.; Rodenwaldt, B.; Müller-Vieira, U.; Schmidt, D.; Lauterbach, T.; Recanatini, M.; Cavalli, A.; Hartmann, R. W. *Bioorg. Med. Chem.* **2008**, *16*, 1992.
- (14) Miyaura, N.; Suzuki, A. *Chem. Rev.* **1995**, *95*, 2457.
- (15) Tang, Y.; Dong, Y.; Vennerstrom J. L. *Synthesis* **2004**, *15*, 2540.
- (16) (a) Ehmer, P. B.; Jose, J.; Hartmann, R. W. *J. Steroid Biochem. Mol. Biol.* **2000**, *75*, 57. (b) Hartmann, R. W.; Bayer, H.; Gruen, G. *J. Med. Chem.* **1994**, *37*, 1275. (c) Denner, K.; Bernhardt, R. Inhibition studies of steroid conversions mediated by human CYP11B1 and CYP11B2 expressed in cell cultures. In *Oxygen Homeostasis and Its Dynamics*; Ishimura, Y., Shimada, H., Suematsu, M., Eds.; Springer-Verlag: Tokyo, Berlin, Heidelberg, New York, 1998; pp 231–236; (d) Böttner, B.; Denner, K.; Bernhardt, R. *Eur. J. Biochem.* **1998**, *252*, 458.
- (17) Pinto-Bazurco Mendieta, M. A. E.; Negri, M.; Jagusch, C.; Hille, U. E.; Müller-Vieira, U.; Schmidt, D.; Hansen, K.; Hartmann, R. W. *Bioorg. Med. Chem. Lett.* **2008**, *18*, 267.
- (18) (a) Lin, D.; Zhang, L.; Chiao, E.; Miller, L. W. *Mol. Endocrinol.* **1994**, *8*, 392. (b) Auchus, R. J.; Miller, W. L. *Mol. Endocrinol.* **1999**, *13*, 1169.
- (19) Mathieu, A. P.; LeHoux, J.-G.; Auchus, R. J. *Biochim. Biophys. Acta* **2003**, *1619*, 291.
- (20) White, P. C.; Curnow, K. M.; Pascoe, L. *Endocr. Rev.* **1994**, *15*, 421.
- (21) Cuberes, M. R.; Moreno-Manas, M.; Trius, A. *Synthesis*, **1985**, *3*, 302.
- (22) Regel, E.; Draber, W.; Buechel, K. H.; Plempel, M. US4118487, 1978.
- (23) Okada, M.; Yoden, T.; Kawaminami, E.; Shimada, Y.; Ishihara, T.; Kudou, M. US5807880, 1994.
- (24) (a) Halgren, T. A. *J. Comput. Chem.* **1999**, *20*, 730. (b) Becke, A. D. *J. Chem. Phys.* **1993**, *98*, 5648. (c) Stevens, P. J.; Devlin, J. F.; Chabalowski, C. F.; Frisch, M. J. *J. Phys. Chem.* **1994**, *98*, 11623.

- (25) Jones, G.; Willett, P.; Glen, R. C.; Leach, A. R.; Taylor, R. *J. Mol. Biol.* **1997**, *267*, 727. (b) http://www.ccdc.cam.ac.uk/products/life_sciences/gold/
- (26) (a) Bottegoni, G.; Cavalli, A.; Recanatini, M. *J. Chem. Inf. Mod.* **2006**, *46*, 852. (b) Bottegoni, G.; Rocchia, W.; Recanatini, M.; Cavalli, A. *Bioinformatics*, **2006**, *22*, e58.

3.1.4.5. Paper V.

CYP17 Inhibitors. Annulations of Additional Rings in Methylene Imidazole Substituted Biphenyls: Synthesis, Biological Evaluation and Molecular Modelling

Mariano A. E. Pinto-Bazurco Mendieta, Matthias Negri, Qingzhong Hu, Ulrike E. Hille, Carsten Jagusch, Kerstin Jahn-Hoffmann, Ursula Müller-Vieira, Dirk Schmidt, Thomas Lauterbach, and Rolf W. Hartmann

This article is protected by copyrights of 'Archiv der Pharmazie - Chemistry in Life Sciences.'

Arch. Pharm. Chem. Life Sci. **2008**, *341*, 597–609

Abstract

Twenty-one novel compounds originating from two classes of annulated biphenyls were synthesised as mimetics of the steroidal A- and C-rings and examined for their potency as inhibitors of human CYP17. Selected compounds were tested for inhibition of the hepatic CYP enzyme 3A4. Potent CYP17 inhibitors were found for each class, compound **9** (17 and 71% at 0.2 and 2 μ M, respectively) and **21** (591 nM). Compound **21** showed only weak inhibition of CYP3A4 (32 and 64% at 2 and 10 μ M, respectively). Both compounds, however, exhibited moderate to strong inhibition of the glucocorticoid-forming enzyme CYP11B1. The most interesting compounds were docked into our protein model. They bound into one of the modes which we have previously published. New interaction regions were identified.

Introduction

Prostate cancer is a major cause of death in elderly men worldwide.¹ It is widely demonstrated that high androgen levels (testosterone and dihydrotestosterone) stimulate tumor growth in prostate cancer.² Thus, androgen receptor antagonists³ and gonadotropin-releasing hormone analogues⁴ are used as a standard therapy. The major drawback of these therapies is the fact that they do not reduce androgen concentrations or only affect testicular androgen production, allowing androgens still to be produced in the adrenals.

Therefore, a new promising target is 17 α -hydroxylase-17, 20-lyase (CYP17), the key enzyme for the biosynthesis of androgens. It is catalyzing the conversion of pregnenolone or progesterone to DHEA or androstenedione, respectively. Even more, this target has already clinically proven success with the antimycotic ketoconazole which is also a weak inhibitor of CYP17.⁵ In previous works, we could demonstrate in-vitro and in-vivo activity for steroidal⁶ and non-steroidal^{7-10, 11} compounds. Some of these compounds had been designed as mimetics of the steroidal AC-rings (Chart 1).^{10, 11} Since they had shown a high activity and a good selectivity, we chose them for further optimizations.

Very recently,¹² we found new highly potent and selective compounds, which showed better pharmacokinetic and pharmacodynamic profiles than abiraterone, a CYP17 inhibitor currently undergoing clinical phase II,¹³ by replacing the A-ring-mimicking benzene nucleus with different heterocycles.

In order to further explore the spatial limitations surrounding the A- and C-ring binding regions, in this work, we expand the corresponding biphenyl rings by annulations of different aromatic and non-aromatic rings. In this way, two different compound classes were synthesised (Chart 2), by either

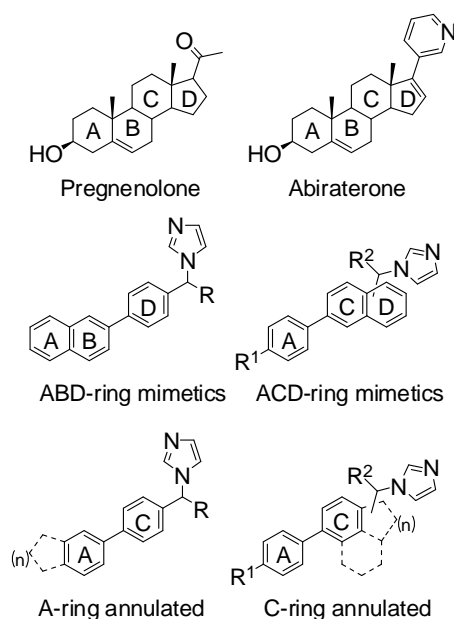


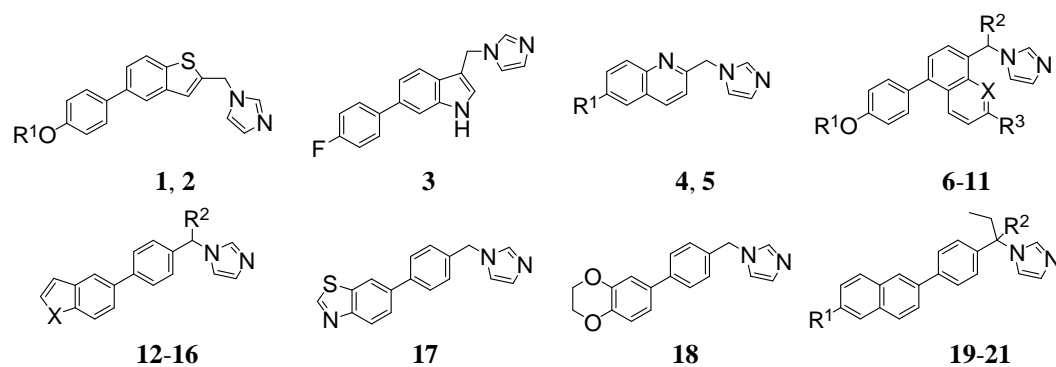
Chart 1. Substrate, abiraterone, described ABD- and ACD-ring mimetic CYP17 inhibitors and A- and C-ring annulated compounds of the present study.

annealing the C-ring (compounds **1-11**) or by otherwise annealing the A-ring (compounds **12-21**). Like in previous works,¹⁰⁻¹² 1-imidazole linked with a methylene spacer was introduced as nitrogen-bearing heterocycle, since the complexation of the heme iron by an aromatic nitrogen is an important prerequisite for inhibition of cytochrome P450 enzymes.¹⁴ We have also shown¹⁰⁻¹² that the introduction of a fluorine, hydroxy, and methoxy group in the A-ring strongly contributed to a better inhibition of our target enzyme.

In the following, the synthesis, CYP17 inhibitory activities, and molecular modelling studies are presented and these data are compared to the ones recently obtained with ABD- and ACD-ring mimetics (Chart 1).⁹ Besides, for reasons of selectivity, inhibition of the most crucial hepatic CYP enzyme CYP3A4 was monitored, and for selected compounds inhibition of the glucocorticoid-forming enzyme CYP11B1 was also determined. The most promising compounds were docked into our protein model, and the key interactions with the enzyme were elucidated.

Chemistry

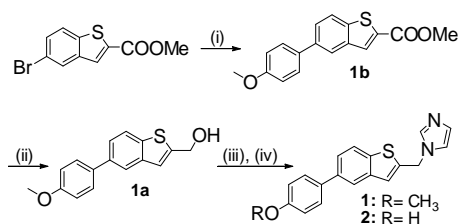
The syntheses of compounds **1-21** are shown in Schemes 1-7. In pursuing our aim to explore the binding regions surrounding the A- and C-rings, different aromatic and non-aromatic moieties were annulated to the A (Schemes 1-5) or C (Schemes 6, 7) ring. The coupling of the biphenylic moiety was achieved by means of Suzuki coupling¹⁵ (Method C) except for the synthesis of compounds **1** and **2** (Scheme 1) where a Negishi coupling had to be applied. When the necessary bromides for the couplings were not commercially available, they were prepared by bromination using NBS (N-bromosuccinimide) (Scheme 3). The imidazoles were introduced by performing a S_Nt reaction with 1,1'-carbonyldiimidazole (CDI) and the corresponding alcohol¹⁶ (Method A) or via S_N2 reaction of an alkyl bromide with imidazole (Scheme 3).



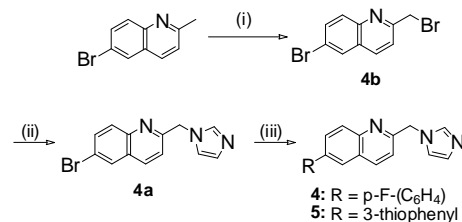
Compound	R ¹	R ²	R ³	X
1	Me			
2	H			
4	p-F-(C ₆ H ₄)			
5	3-thiophenyl			
6	Me	H	H	CH
7	H	H	H	CH
8	Me	Et	H	N
9	H	Et	H	N
10	Me	Et	Et	N
11	H	Et	Et	N
12		Et		S
13		Et		NH
14		H		O
15		H		S
16		H		NH
19	OMe	H		
20	H	H		
21	OH	Et		

Chart 2. List of synthesized compounds **1-21**.

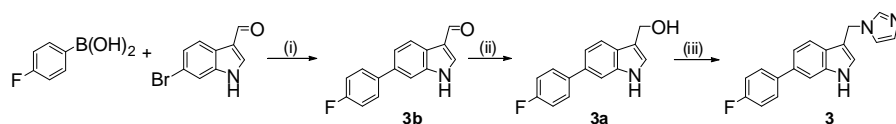
The alcohols were obtained from either the carboxylic derivatives (Schemes 1, 4) or from the aldehydes (Methods D, E). In most cases, the methoxy-substituted compounds were submitted to an ether cleavage (Method B). For the preparation of compound **21**, the hydroxyl group on the naphthalene had to be protected before the Suzuki coupling due to otherwise very low yields.¹⁵



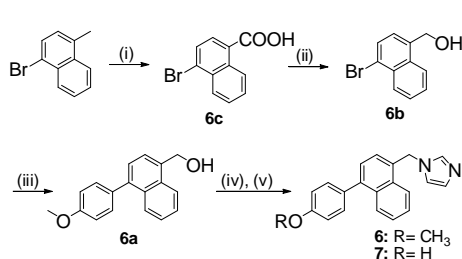
Scheme 1. Synthesis route of compounds 1 and 2
Reagent and conditions: (i) a: 4-bromo-anisole, *tert*-BuLi, THF, -78°C, 30 min; b: ZnCl₂, 0°C, 30 min; c: PdCl₂(PPh₃)₂, 16 h; (ii) LiBH₄, toluene, THF, Et₂O, 110°C, 16 h; (iii) **Method A1**: CDI, imidazole, NMP, 180°C, 16 h; (iv) **Method B**: BBr₃, DCM, -78°C to 0°C, 16 h.



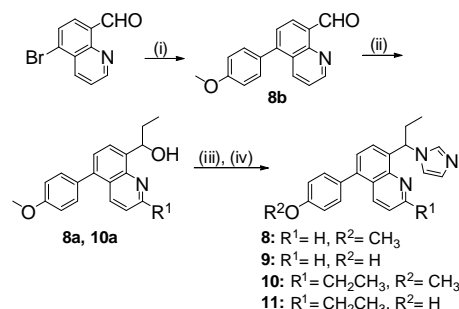
Scheme 3. Synthesis route of compounds 4 and 5
Reagents and conditions: (i) NBS, CCl₄, 75°C, 16 h; (ii) Imidazole, K₂CO₃, 18-crown-6, acetonitrile, 100°C, 16 h; (iii) **Method C1**: 4-fluorophenylboronic acid (**5**: 3-thiophenylboronic acid), Na₂CO₃, Pd(PPh₃)₄, toluene/MeOH/H₂O, 70°C, 5 h.



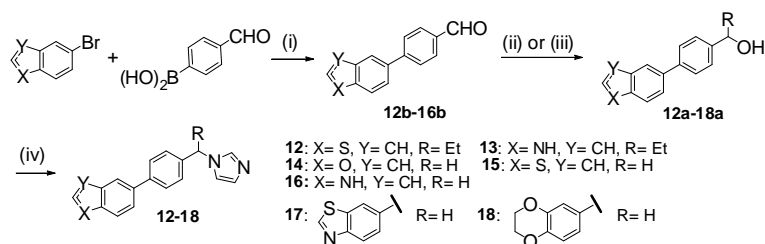
Scheme 2. Synthesis route of compound 3
Reagent and conditions: (i) **Method C1**: Na₂CO₃, Pd(PPh₃)₄, toluene/EtOH/H₂O, reflux, 5 h; (ii) **Method D**: NaBH₄, MeOH, rt, 2 h; (iii) **Method A2**: CDI, acetonitrile, reflux, 18 h.



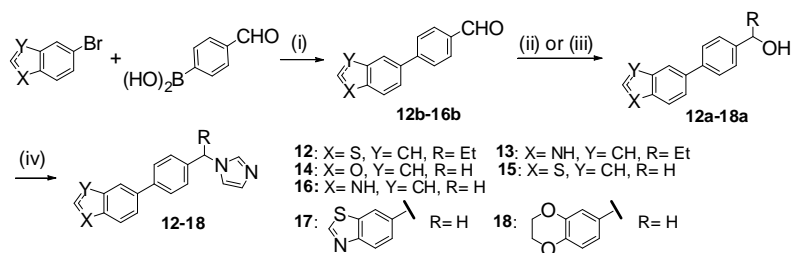
Scheme 4. Synthesis route of compounds 6 and 7
Reagents and conditions: (i) KMnO₄, pyridine, H₂O, 50°C, 4 d; (ii) LiAlH₄, Et₂O, 35°C, 16 h; (iii) **Method C2**: 4-methoxyphenylboronic acid, Cs₂CO₃, Pd(OAc)₂, TBAB, toluene/EtOH/H₂O, 110°C, 16 h; (iv) **Method A1**: CDI, imidazole, NMP, 180°C, 2 d; (v) **Method B**: BBr₃, DCM, -78°C to 0°C, 16 h.



Scheme 5. Synthesis route of compounds 8-11
Reagents and conditions: (i) **Method C2**: 4-methoxyphenylboronic acid, Cs₂CO₃, Pd(OAc)₂, TBAB, toluene/EtOH/H₂O, 110°C, 16 h; (ii) **Method E**: EtMgBr, THF, 0°C to rt, 16 h; (iii) **Method A1**: CDI, imidazole, NMP, 180°C, 1-2.5 d; (iv) **Method B**: BBr₃, DCM, -78°C to 0°C, 16 h.



Scheme 6. Synthesis route of compounds 12-18
Reagents and conditions: (i) **Method C1**: Pd(PPh₃)₄, TBAB, Na₂CO₃, toluene/EtOH/H₂O, reflux, 16 h; (ii) **Method E**: 12a-13a: EtMgBr, THF, 0°C to rt, 16 h; (iii) **Method D**: 14a-18a: NaBH₄, MeOH, reflux, 2 h; (iv) **Method A1**: CDI, NMP, reflux, 3 h.



Scheme 6. Synthesis route of compounds 12-18

Reagents and conditions: (i) **Method C1:** Pd(PPh₃)₄, TBAB, Na₂CO₃, toluene/EtOH/H₂O, reflux, 16 h; (ii) **Method E:** 12a-13a: EtMgBr, THF, 0°C to rt, 16 h; (iii) **Method D:** 14a-18a: NaBH₄, MeOH, reflux, 2 h; (iv) **Method A1:** CDI, NMP, reflux, 3 h.

Results

Biological Results. Inhibition of CYP17 was evaluated using human enzyme expressed in *E. coli*.¹⁷ The percent inhibition values of the compounds were determined with the 50,000 g sediment of the *E. coli* homogenate, progesterone (25 μM) as substrate and the inhibitors at concentrations of 0.2 and 2.0 μM. Separation of substrate and product was accomplished by HPLC using UV detection.⁷

In contrast to the reference compound ketoconazole, the C-ring-annulated compounds (**1-11**, Table 1) mostly showed moderate to no inhibition with exception of the quinoline compound **9**, which showed 71% inhibition at 2 μM. The prolongation of the C-ring in compounds **1-5** led to non-active compounds. The quinolines **8-11** bearing an ethyl moiety at the methylene linker showed an overall better activity than the naphthalenes **6** and **7**.

Table 1. Inhibition of CYP17 by C-ring annulated compounds **1-11**

Comp.	Structures				CYP17	
	R ¹	R ²	R ³	X	% Inhibition ^a	
					0.2 μM	2 μM
1	Me				0	18
2	H				6	13
3					0	12
4	p-F-(C ₆ H ₄)				1	12
5	3-thiophenyl				0	11
6	Me	H	H	CH	0	5
7	H	H	H	CH	1	12
8	Me	Et	H	N	3	32
9	H	Et	H	N	17	71 ^d
10	Me	Et	Et	N	6	57
11	H	Et	Et	N	5	57
KTZ^b						19 ^c

^a Data shown were obtained by performing the tests in duplicate. The deviations were within $\pm 5\%$. Concentration of progesterone (substrate) was 25 μM.

^b **KTZ:** ketoconazole.

^c % inhibition at 1.0 μM.

^d IC₅₀ = 817 nM

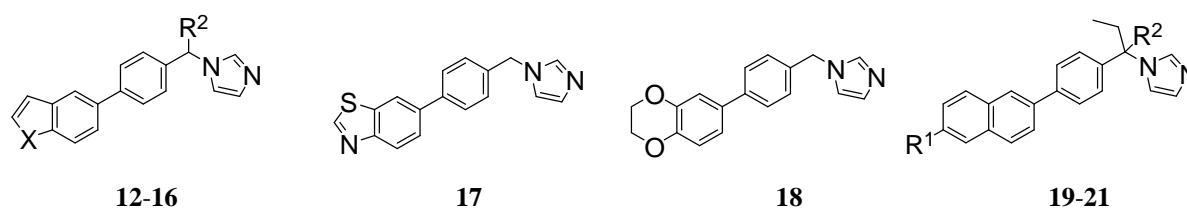
The A-ring-annulated compounds (**12-21**, Table 2) showed moderate to good activities. However, they did not exceed the activity of compound **9**. The most active compounds in this class showing percent-inhibition values of more than 70% at 2 μ M are compound **13** bearing an indole (H-bond donor) and compounds **19** and **21** bearing a methoxy group (H-bond acceptor) or a hydroxyl group (H-bond acceptor and donor), respectively, at the 6-position of a naphthalene. Absence of these substituents in the latter compounds diminishes the inhibitory activity (compound **20**). The introduction of an ethyl moiety at the methylene linker led to an increase in activity for compounds **15** to **12** and **16** to **13**. All other aromatic heterocycles resulted in only moderate inhibitors.

When comparing the activities of the compounds of this study to the ones of the parent compounds,¹¹ it must be mentioned that the structural modifications did not increase activities.

Regarding selectivity against other CYP enzymes, a broader spectrum of our compounds was tested for inhibition of the hepatic enzyme CYP3A4. This enzyme is responsible for the metabolism of lipophilic substances and, therefore, responsible for about 50% of current prescription drugs.¹⁸ While compounds **12-19** showed a strong inhibition of this enzyme (>85% inhibition at 2 μ M), compound **21** exhibited low inhibitory activity towards CYP3A4 (32% at 2 μ M and 64% at 10 μ M).

Thus, compound **21** together with the most promising compound **9** of the C-ring-annulated class of compounds, were further tested for inhibition of the steroidogenic enzyme CYP11B1. Its importance relies on the fact that it catalyzes the last step in glucocorticoid formation, namely the transformation of 11-deoxycortisol into cortisol. For the assay,¹⁹ V79MZh11B1 cells expressing human CYP11B1 were used. Both compounds showed strong inhibition of the enzyme at the tested concentrations (**9**: 86 and 94% at 0.2 and 2 μ M; **21**: 81 and 95% at 0.2 and 2 μ M).

Table 2. Inhibition of CYP17 by A-ring annulated compounds **12-21**



Comp.	Structures			CYP17	
	R ¹	R ²	X	% Inhibition ^a	
				0.2 μ M	2 μ M
12		Et	S	7	40
13		Et	NH	21	75 ^d
14		H	O	5	27
15		H	S	0	21
16		H	NH	2	39
17				5	39
18				0	17
19	OMe	H		19	74 ^e
20	H	H		7	43
21	OH	Et		16	74 ^f
KTZ ^b				19 ^c	

^a Data shown were obtained by performing the tests in duplicate. The deviations were within $< \pm 5$ %. Concentration of progesterone (substrate) was 25 μ M.

^b **KTZ**: ketoconazole.

^c % inhibition at 1.0 μ M.

^d IC₅₀ = 667 nM.

^e IC₅₀ = 703 nM.

^f IC₅₀ = 591 nM.

Molecular Modelling. Using selected compounds, we explored the binding modes of the A- and C-ring-annulated biphenyls. Several active and less active compounds (C-ring: **6-11** (R, S); A-ring: **13** (R, S), **16**, **17**, **19** (R, S) and **21**) were docked by means of the GOLD v 3.0.1 software²⁰ in the active site of our homology model of CYP17.¹²

Aware of the limitations of docking,²¹ the resulting poses of each compound were clustered with ACIAP (autonomous hierarchical agglomerative cluster analysis)²² and the representative poses of each cluster were subjected to a critical visual inspection. H-bonds, π - π , and hydrophobic interactions, as well as steric clashes were measured and evaluated. The necessity of iron-nitrogen complexation¹⁴ for inhibitory activity was also considered. Furthermore, the GOLD v 3.0.1 software, used with a slightly modified GOLDScore, was tested on different crystallised CYP enzymes. This program could reproduce quite well the correct orientation of co-crystallised ligands (data not shown). Moreover, GOLD v 3.0.1 produced reliable poses for abiraterone in our CYP17 model,¹² oriented like described for pregnenolone.²³ With these findings, the obtained results can be considered very probable.

All compounds principally showed poses in BM1 – one of two binding modes we have identified for biphenyl type inhibitors¹² – with the modified biaryl-skeleton oriented almost parallel to the I-helix (Fig. 1). Furthermore, the observed increase in activity caused by the ethyl group at the methylene spacer can be explained by the anchoring function of this substituent, namely by hydrophobic interactions with the tiny hydrophobic pocket next to the heme, as already described.¹²

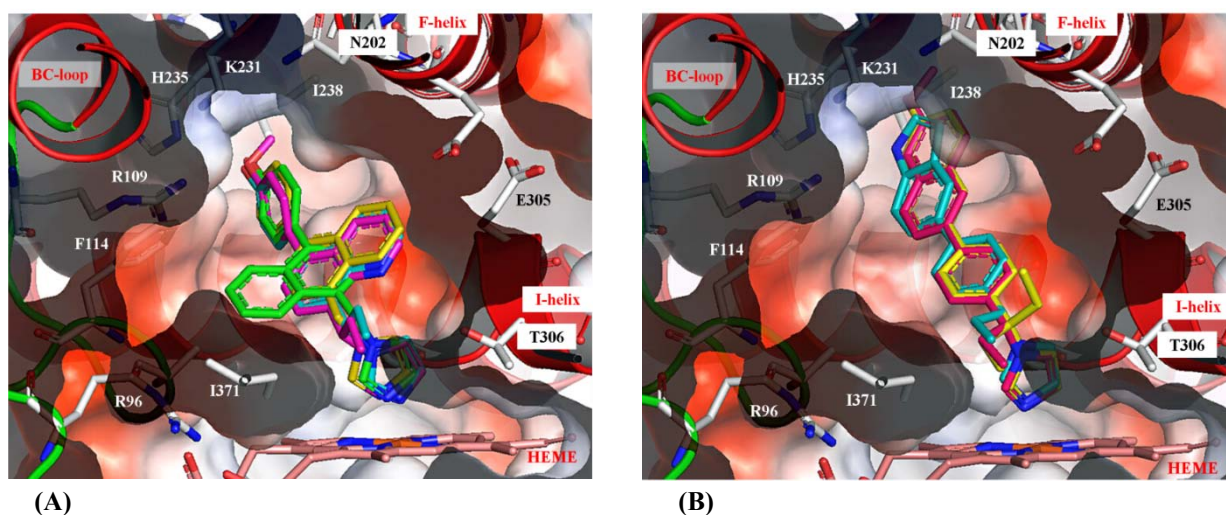


Figure 1. A cross-section of the solvent accessible surface of CYP17 is shown, revealing the active-site cavity with docked: (A) C-ring annulated **6** (green), **7** (yellow), **8** (magenta) and **9** (cyan) and (B) A-ring annulated compounds **13** (cyan), **19** (magenta) and **21** (yellow). Further, heme, interacting residues and ribbon rendered tertiary structure of the active site are shown. Figures were generated with Pymol (<http://www.pymol.org>).

Regarding the docked C-ring annulated compounds, both enantiomers of compounds **6-11** showed mainly one binding mode, except for compounds **6** and **7**, which switch the annealed ring towards or opposite the I-helix (Fig. 1A). The annealed ring is directed towards the kink of the I-helix,¹² stabilised in its orientation by π - π and hydrophobic interactions with the residues Phe114, Gly301-Ala302, Glu305, Thr306, Ile371, and Val482 (Fig. 1A). Nevertheless, for all three compound couples steric hindrance, changing in its extend from pair to pair (**8-9** < **6-7** < **10-11**) between the annulated C-ring and the surrounding amino acids, was observed. The extension of the annealed ring system, like the introduction of a space-demanding group, e. g. ethyl was crucial, as seen by the reduced activity of compounds **10** and **11** with respect to **8** and **9**.

For the inhibitory activity of compounds **8-11**, the presence of the aromatic nitrogen in the annealed C-ring was striking; it delocalizes the negative charge of the ring system and is capable of H-bond formation with the catalytically important Thr306 and the 1-N of the imidazole.

Compounds **6-11** (R, S) showed the ability of forming an H-bond net between the R¹ substituent of the A-ring (Table 1) and the amino acids Arg109 and His235, as it was already observed for their parent compounds.⁹ OH showed the highest activity values, leading to the conclusion that an H-bond donor group in this position was necessary.

As for the A-ring annulated compounds, **13** (R, S), **16** (R, S), **17**, **19** (R, S) and **21** were docked into our homology model (Fig 1B). Even these elongated compounds are basically oriented in BM1. However, the extension of the A-ring caused a shift in the interaction area. The substituent R¹ showed H-bond formations with Asn202, Lys231, His235, and, eventually, Arg109, but even hydrophobic interactions between the OMe group in R¹ and Ile198 and Ile238. Almost the same hydrophobic interactions, as reported previously,¹² between the aromatic core structure and the prevalently hydrophobic surroundings of the active site could be observed. Additionally, the extended A-ring can undergo π - π and hydrophobic interactions with Phe114, Ile205, His235, Gly297, and Thr294. Comparing compounds **13** and **16-17**, the presence of a H-bond donor hetero-atom in the annealed A-ring appeared necessary for H-bond formation with His235 and Asn202, with the intent to mimic the para-OH of some of the most active parent compounds.⁹

Discussion and Conclusion

Similar to our ABD-mimetics,⁹ the annulation at the A-ring led mostly to low to moderately active compounds with exception of **9** which showed good inhibition of CYP17. On the other hand, the annealing of an additional ring at the C-ring resulted in moderately to highly active compounds, similar to our findings in the class of ACD-ring mimetic inhibitors.⁹

The best compounds in terms of activity in each class are **9** for the A-ring-expanded and **21** for the C-ring-annulated compounds. Compound **21** is also selective against CYP3A4. Based on both biological results and molecular modelling studies (Fig. 1), we conclude that space occupancy in both the A-ring and the C-ring area is appropriate for the design of new lead structures. The presence of specific heteroatoms, especially N in the annealed rings, is recommended, since this structure modification is capable of H-bond formation and of modifying the electrostatic properties of the annealed ring system. The importance for CYP17 activity of an ethyl substituent at the methylene linker was reiterated as well.

One of our goals in this work was the discovery of a new, more complex lead structure, with the aim of increasing potency and selectivity towards other CYP enzymes. This was achieved with compounds **9** and **21**. For further increasing the activity of compound **9**, we suggest a lead structure optimised by substitution of the annealed ring with a 5-membered aromatic ring bearing a heteroatom, like imidazole, or the exchange of the whole bicyclic structure at the C-ring with a 7-membered ring. These modified compounds are likely to better fit in the active site, due to reduced steric hindrance and hydrophobic repulsion.

Experimental Section

Chemistry. Melting points were determined on a Mettler FP1 melting point apparatus and are uncorrected. IR spectra were recorded neat on a Bruker Vector 33FT-infrared spectrometer. ¹H-NMR spectra were measured on a Bruker DRX-500 (500 MHz). Chemical shifts are given in parts per million (ppm), and TMS was used as an internal standard for spectra obtained in CDCl₃. All coupling constants (*J*) are given in Hz. ESI (electrospray ionization) mass spectra were determined on a TSQ quantum (Thermo Electron Corporation) instrument. Elemental analyses were performed at the Department of Instrumental Analysis and Bioanalysis, Saarland University. Column chromatography was performed using silica-gel 60 (50-200 μ m), and reaction progress was determined by TLC analysis on Alugram® SIL G/UV₂₅₄ (Macherey-Nagel). Boronic acids and bromoaryls used as starting materials were commercially obtained (CombiBlocks, Chempur, Aldrich, Acros).

Methyl 5-(4-methoxyphenyl)benzo[*b*]thiophene-2-carboxylate, 1b. To a solution of 1-bromo-4-methoxybenzene (1.32 mL, 10.52 mmol) in dry THF (20 mL) cooled at -78 °C *t*-BuLi (1.5 M, 14.48 mL, 21.72 mmol) was added slowly. After 30 min ZnCl₂ (0.5 M, 24.53 mL, 12.26 mmol) was added carefully and after 10 min it was let to warm up to rt. After additional 20 min methyl 5-bromobenzo[*b*]thiophene-2-carboxylate (1.90 g, 7.00 mmol) and bis-(triphenylphosphine)-palladium (II)-dichloride (0.49 g, 0.70 mmol) were prepared in dry THF (30 mL) under protecting atmosphere and the reagent was added at 0 °C and the reaction mixture left stirring overnight. yield: 1.45 g (69 %); *R*_f = 0.35 (PE / EtOAc, 2:1); δ _H (CDCl₃, 500 MHz) 3.87 (s, 3H), 3.96 (s, 3H), 7.01 (d, *J* = 8.8 Hz, 2H), 7.58 (d, *J* = 8.8 Hz, 2H), 7.67 (dd, *J* = 1.8 Hz, *J* = 8.5 Hz, 1H), 7.89 (d, *J* = 8.5 Hz, 1H), 8.01 (s, 1H), 8.09 (s, 1H).

(5-(4-Methoxyphenyl)benzo[*b*]thiophen-2-yl)methanol, 1a. To a solution of **1b** (0.55 g, 1.84 mmol) in THF (30 mL), toluene (15 mL) and diethyl ether (15 mL) LiBH₄ (0.05 g, 2.21 mmol) was added and heated to reflux for 2

h. yield: 0.47 g (95 %); $R_f = 0.53$ (PE / EtOAc, 2:1); δ_H (CDCl₃, 500 MHz) 3.87 (s, 3H), 4.95-5.01 (m, 2H), 6.99-7.01 (m, 3H), 7.53 (dd, $J = 1.8$ Hz, $J = 8.4$ Hz, 1H), 7.56-7.59 (m, 2H), 7.85 (d, $J = 8.4$ Hz, 1H), 7.88 (s, 1H).

Method A: CDI reaction. To a solution of the corresponding alcohol (1 eq) in NMP or acetonitrile (10 mL / mmol) was added CDI (5 eq). Then the solution was heated to reflux for 4 to 18 h. After cooling to ambient temperature, it was diluted with water (30 mL) and extracted with ethyl acetate (3 x 10 mL). The combined organic phases were washed with brine, dried over MgSO₄ and evaporated under reduced pressure. Then the desired product was purified by chromatography on silica gel.

1-((5-(4-Methoxyphenyl)benzo[*b*]thiophen-2-yl)methyl)-1*H*-imidazole, 1. Synthesised according to Method A1 using **1a** (0.25 g, 0.93 mmol) and CDI (1.20 g, 7.40 mmol); yield: 0.20 g (68 %); white solid: mp 169 °C; $R_f = 0.44$ (EtOAc / MeOH, 95:5); IR (ATR) ν (cm⁻¹) 3106 (w), 1607 (w), 1516 (m), 1453 (w), 1436 (w), 1277 (m), 1254 (m), 1231 (m), 1194 (w), 1072 (w), 1031 (m), 1015 (w), 908 (w), 806 (s), 744 (s), 667 (m); δ_H (CDCl₃, 500 MHz) 3.86 (s, 3H), 5.35 (s, 2H), 6.99-7.01 (m, 3H), 7.12 (s, 1H), 7.17 (s, 1H), 7.52-7.56 (m, 3H), 7.62 (s, 1H), 7.80 (d, $J = 8.4$ Hz, 1H), 7.86 (s, 1H); δ_C (CDCl₃, 125 MHz) 46.3, 55.3, 114.3, 119.1, 121.5, 122.6, 123.3, 124.2, 128.3, 130.0, 133.4, 137.2, 137.9, 138.3, 139.8, 139.8, 159.1.

3-((1*H*-Imidazol-1-yl)methyl)-6-(4-fluorophenyl)-1*H*-indole, 3. Synthesised according to Method A2 using **3a** (0.25 g, 1.04 mmol) and CDI (0.34 g, 2.08 mmol); yield: 0.15 g (52 %); brown solid: mp 171-173 °C; $R_f = 0.24$ (EtOAc / MeOH, 95:5); δ_H (CDCl₃, 500 MHz) 5.29 (s, 2H), 6.91 (bs, 1H), 7.02 (bs, 1H), 7.06 (t, $J = 8.8$ Hz, 2H), 7.18 (dd, $J = 1.7$ Hz, $J = 8.3$ Hz, 1H), 7.28 (d, $J = 2.5$ Hz, 1H), 7.41 (d, $J = 8.5$ Hz, 1H), 7.50 (d, $J = 1.7$ Hz, 1H), 7.52 (dd, $J = 5.3$ Hz, $J = 8.8$ Hz, 2H), 7.71 (bs, 1H), 10.90 (bs, 1H); δ_C (CDCl₃, 125 MHz) 42.8 (CH₂), 110.1 (CH), 115.5 (CH), 118.4 (CH), 119.3 (CH), 119.8 (CH), 121.8 (C_q), 124.7 (CH), 125.5 (C_q), 128.7 (CH), 128.9 (CH), 135.1 (CH), 136.8 (C_q), 137.2 (C_q), 138.0 (C_q), 162.1 (CF); MS (ESI): $m/z = 292$ [M⁺+H].

1-((4-(4-Methoxyphenyl)naphthalen-1-yl)methyl)-1*H*-imidazole, 6. Synthesised according to Method A1 using **6a** (0.38 g, 1.42 mmol) and CDI (1.84 g, 11.35 mmol); yield: 0.37 g (83 %); white solid: mp 192 °C; $R_f = 0.25$ (EtOAc / MeOH, 95:5); IR (ATR) ν (cm⁻¹) 3109 (w), 1609 (m), 1507 (s), 1460 (w), 1392 (w), 1284 (m), 1246 (s), 1176 (w), 1108 (w), 1076 (w), 1031 (m), 830 (m), 770 (m), 735 (w), 664 (w); δ_H (CDCl₃, 500 MHz) 3.89 (s, 3H), 5.61 (s, 2H), 6.97 (s, 1H), 7.04 (d, $J = 8.6$ Hz, 2H), 7.11 (s, 1H), 7.19 (d, $J = 7.3$ Hz, 1H), 7.36 (d, $J = 7.3$ Hz, 1H), 7.39 (d, $J = 8.6$ Hz, 2H), 7.46-7.49 (m, 1H), 7.53-7.56 (m, 1H), 7.61 (s, 1H), 7.93 (d, $J = 8.4$ Hz, 1H), 7.99 (d, $J = 8.4$ Hz, 1H); δ_C (CDCl₃, 125 MHz) 48.8, 53.4, 55.3, 113.8, 119.4, 122.5, 125.7, 126.1, 126.4, 126.7, 127.3, 129.6, 130.4, 131.0, 131.1, 132.2, 132.5, 137.5, 141.2, 159.1; (ESI): $m/z = 315$ [M⁺+H].

8-(1-((1*H*-Imidazol-1-yl)propyl)-5-(4-methoxyphenyl)quinoline, 8. Synthesised according to Method A1 using **8a** (0.40 g, 1.36 mmol) and CDI (0.88 g, 5.45 mmol); yield: 0.24 g (51 %); white solid: mp 135 °C; $R_f = 0.27$ (EtOAc / MeOH, 95:5); IR (ATR) ν (cm⁻¹) 2967 (w), 1609 (m), 1515 (s), 1465 (w), 1284 (m), 1248 (s), 1176 (m), 1110 (w), 1074 (w), 1031 (m), 824 (s), 735 (w), 666 (m), 541 (w), 530 (w), 514 (w); δ_H (CDCl₃, 500 MHz) 1.06 (t, $J = 7.3$ Hz, 3H), 2.33-2.49 (m, 2H), 3.89 (s, 3H), 6.64-6.67 (m, 1H), 7.04 (d, $J = 8.7$ Hz, 2H), 7.06 (s, 1H), 7.13 (m, 1H), 7.35 (d, $J = 8.7$ Hz, 2H), 7.38 (dd, $J = 4.1$ Hz, $J = 8.6$ Hz, 1H), 7.43 (d, $J = 7.5$ Hz, 1H), 7.55 (d, $J = 7.5$ Hz, 1H), 7.79 (s, 1H), 8.25 (dd, $J = 1.7$ Hz, $J = 8.6$ Hz, 1H), 8.94 (dd, $J = 1.7$ Hz, $J = 4.1$ Hz, 1H); δ_C (CDCl₃, 125 MHz) 11.4, 28.2, 55.4, 57.0, 114.0, 118.0, 121.2, 125.3, 126.8, 127.0, 128.9, 131.0, 131.4, 134.7, 137.1, 137.8, 140.3, 145.7, 149.4, 159.3; (ESI): $m/z = 344$ [M⁺+H].

8-(1-((1*H*-Imidazol-1-yl)propyl)-2-ethyl-5-(4-methoxyphenyl)quinoline, 10. Synthesised according to Method A1 using **10a** (0.40 g, 1.25 mmol) and CDI (1.61 g, 9.96 mmol); yield: 0.27 g (59 %); white solid: mp 157 °C; $R_f = 0.24$ (EtOAc / MeOH, 95:5); IR (ATR) ν (cm⁻¹) 2969 (w), 1609 (s), 1576 (w), 1517 (s), 1498 (w), 1460 (w), 1285 (w), 1247 (s), 1177 (m), 1110 (w), 1072 (w), 1032 (m), 825 (w), 738 (m), 664 (m); δ_H (CDCl₃, 500 MHz) 1.08 (t, $J = 7.3$ Hz, 3H), 1.47 (t, $J = 7.6$ Hz, 3H), 2.37-2.51 (m, 2H), 3.06 (q, $J = 7.6$ Hz, $J = 15.1$ Hz, 2H), 3.91 (s, 3H), 6.69 (m, 1H), 7.05 (d, $J = 8.7$ Hz, 2H), 7.14 (s, 1H), 7.27 (d, $J = 3.8$ Hz, 1H), 7.35-7.39 (m, 3H), 7.55 (d, $J = 7.5$ Hz, 1H), 7.82 (s, 1H), 8.15 (d, $J = 8.7$ Hz, 1H); δ_C (CDCl₃, 125 MHz) 11.4, 13.2, 28.0, 31.9, 55.4, 57.1, 113.9, 117.9, 121.1, 125.1, 125.3, 125.8, 128.8, 131.0, 131.7, 134.7, 137.1, 137.2, 140.0, 145.2, 159.2, 162.6; (ESI): $m/z = 372$ [M⁺+H].

1-(1-(4-(Benzo[*b*]thiophen-5-yl)phenyl)propyl)-1*H*-imidazole, 12. Synthesised according to Method A1 using **12a** (1.33 g, 4.94 mmol) and CDI (4.00 g, 24.7 mmol); yield: 0.51 g (32 %); white solid: mp 101-103 °C; $R_f = 0.24$ (DCM / MeOH, 20:1); IR (ATR) ν (cm⁻¹) 1496 (m), 1223 (m), 1073 (m), 805 (vs), 758 (s), 702 (s), 663 (s); δ_H (CDCl₃, 500 MHz) 0.98 (t, $J = 7.3$ Hz, 3H, CH₃), 2.28 (q, $J = 7.3$, 7.6 Hz, 2H, CH₂), 5.08 (t, $J = 7.6$ Hz, 1H, CH), 7.00 (s, 1H), 7.13 (s, 1H), 7.29 (d, $J = 8.1$ Hz, 2H), 7.39 (d, $J = 5.4$ Hz, 1H), 7.49 (d, $J = 5.4$ Hz, 1H), 7.55 (dd, $J = 1.7$, 8.4 Hz, 1H), 7.64 (dd, $J = 1.7$, 8.3 Hz, 2H), 7.73 (s, 1H), 7.93 (d, $J = 8.4$ Hz, 1H), 8.00 (s, 1H); δ_C (CDCl₃, 125

MHz) 11.1 (CH₃), 28.6 (CH₂), 63.3 (CH), 117.8, 120.0, 121.9, 122.8, 123.7, 124.0, 127.0, 127.2, 127.8, 128.7, 136.1, 136.7, 138.8, 139.1, 139.4, 140.2, 141.3; MS (ESI): *m/z* = 319 [M⁺+H].

5-(4-(1-(*1H*-Imidazol-1-yl)propyl)phenyl)-*1H*-indole, 13. Synthesised according to Method A1 using **13a** (1.10 g, 4.38 mmol) and CDI (3.55 g, 21.88 mmol); yield: 0.33 g (25 %); white solid: mp 158-159 °C; *R_f* = 0.15 (DCM / MeOH, 20:1); IR (ATR) ν (cm⁻¹) 3143 (br), 1593 (w), 1471 (w), 1222 (w), 1075 (m), 891 (s), 805 (s), 772 (s), 739 (s), 660 (m), 574 (w), 539 (w); δ _H (CDCl₃, 500 MHz) 0.86 (t, *J* = 7.3, 3H, CH₃), 2.15 (q, *J* = 7.23, 7.6 Hz, 2H, CH₂), 4.93 (t, *J* = 7.6 Hz, 1H, CH), 6.50 (s, 1H), 6.90 (s, 1H), 7.04 (s, 1H), 7.13-7.17 (m, 3H), 7.30 (dd, *J* = 8.5, 9.5 Hz, 2H), 7.52 (d, *J* = 8.3 Hz, 2H), 7.67 (s, 1H), 7.74 (s, 1H), 8.89 (s, 1H); δ _C (CDCl₃, 125 MHz) 11.0 (CH₃), 28.4 (CH₂), 63.5 (CH), 102.6, 111.4, 119.0, 121.4, 125.2, 127.7, 128.4, 130.8, 132.1, 135.6, 135.8, 137.3, 142.6; MS (ESI): *m/z* = 302 [M⁺+H].

1-(4-(Benzofuran-5-yl)benzyl)-*1H*-imidazole, 14. Synthesised according to Method A1 using **14a** (0.50 g, 2.23 mmol) and CDI (1.81 g, 11.1 mmol); yield: 0.26 g (43 %); white solid: mp 127-129 °C; *R_f* = 0.22 (DCM / MeOH, 20:1); IR (ATR) ν (cm⁻¹) 3109 (w), 1511 (m), 1463 (m), 1439 (m), 1249 (m), 1130 (m), 1107 (m), 1083 (m), 1028 (s), 909 (m), 876 (m), 836 (m), 802 (vs), 779 (s), 748 (vs), 704 (m), 662 (vs), 631 (m), 523 (s); δ _H (CDCl₃, 500 MHz) 5.17 (s, 2H, CH₂), 6.82 (d, *J* = 3.0 Hz, 1H), 6.95 (s, 1H), 7.12 (s, 1H), 7.23 (d, *J* = 8.1 Hz, 2H), 7.49 (d, *J* = 5.4 Hz, 1H), 7.55-7.60 (m, 4H), 7.66 (d, *J* = 8.4 Hz, 1H), 7.76 (s, 1H); δ _C (CDCl₃, 125 MHz) 50.5 (CH₂), 119.7, 123.8, 127.7, 127.9, 129.9, 135.5, 137.4, 141.7, 145.7; MS (ESI): *m/z* = 275 [M⁺+H].

1-(4-(Benzo[*b*]thiophen-5-yl)benzyl)-*1H*-imidazole, 15. Synthesised according to Method A1 using **15a** (0.7 g, 2.91 mmol) and CDI (2.36 g, 14.6 mmol); yield: 0.18 g (21 %); white solid: mp 164-165 °C; *R_f* = 0.25 (DCM / MeOH, 20:1); IR (ATR) ν (cm⁻¹) 1434 (w), 908 (m), 807 (m), 759 (m), 708 (m), 663 (m); δ _H (CDCl₃, 500 MHz) 5.18 (s, 2H, CH₂), 6.95 (s, 1H), 7.12 (s, 1H), 7.25 (d, *J* = 8.1 Hz, 2H), 7.38 (d, *J* = 5.4 Hz, 1H), 7.49 (d, *J* = 5.4 Hz, 1H), 7.55 (d, *J* = 8.4 Hz, 1H), 7.59 (s, 1H), 7.64 (d, *J* = 8.3 Hz, 2H), 7.93 (d, *J* = 8.4 Hz, 1H), 8.00 (s, 1H); δ _C (CDCl₃, 125 MHz) 50.5 (CH₂), 119.3, 121.93, 122.83, 123.7, 124.1, 127.3, 127.9, 129.9, 135.0, 139.1, 140.2, 141.4; MS (ESI): *m/z* = 291 [M⁺+H].

5-(4-(*1H*-Imidazol-1-yl)methyl)phenyl)-*1H*-indole, 16. Synthesised according to Method A1 using **16a** (0.80 g, 3.58 mmol) and CDI (3.55 g, 21.88 mmol); yield: 0.24 g (25 %); white solid: mp 217-218 °C; *R_f* = 0.16 (DCM / MeOH, 20:1); IR (ATR) ν (cm⁻¹) 1509 (m), 1232 (m), 1099 (m), 1072 (m), 915 (m), 883 (m), 801 (m), 732 (s), 662 (m), 619 (m), 574 (s), 528 (m); δ _H (CDCl₃, 500 MHz) 5.16 (s, 2H, CH₂), 6.61-6.63 (m, 1H), 6.97 (s, 1H), 7.13 (s, 1H), 7.22 (d, *J* = 8.4 Hz, 2H), 7.25 (s, 1H), 7.43 (dd, *J* = 8.4, 9.4 Hz, 2H), 7.61 (s, 1H), 7.63 (d, *J* = 8.3 Hz, 2H), 7.84 (s, 1H), 8.31 (s, 1H); δ _C (CDCl₃, 125 MHz) 50.6 (CH₂), 103.0, 111.3, 119.2, 121.6, 127.6, 127.8, 128.4, 130.8, 132.4, 134.0, 135.5, 140.53, 142.63; MS (ESI): *m/z* = 274 [M⁺+H].

6-(4-(*1H*-Imidazol-1-yl)methyl)phenyl)benzo[*d*]thiazole, 17. Synthesised according to Method A1 using **17a** (0.40 g, 1.66 mmol) and CDI (2.15 g, 13.26 mmol); yield: 0.29 g (70 %); white solid: mp 143 °C; *R_f* = 0.47 (EtOAc / MeOH, 95:5); IR (ATR) ν (cm⁻¹) 3370 (w), 2927 (w), 2856 (w), 1708 (w), 1506 (m), 1468 (m), 1441 (m), 1391 (m), 1284 (w), 1232 (m), 1108 (w), 1077 (m), 1030 (w), 886 (w), 813 (s), 739 (s), 697 (w), 663 (s); δ _H (CDCl₃, 500 MHz) 5.18 (s, 2H), 6.95 (s, 1H), 7.13 (s, 1H), 7.23 (d, *J* = 8.3 Hz, 2H), 7.64 (bs, 1H), 7.71 (dd, *J* = 1.8 Hz, *J* = 8.5 Hz, 1H), 8.12 (m, 1H), 8.18 (d, *J* = 8.5 Hz, 1H); δ _C (CDCl₃, 125 MHz) 50.6, 119.3, 120.1, 123.8, 125.8, 127.9, 128.0, 134.6, 135.3, 138.1, 140.6, 152.7, 154.3.

1-((4-(2,3-Dihydrobenzo[*b*]1,4)dioxin-6-yl)phenyl)methyl)-*1H*-imidazole, 18. Synthesised according to Method A1 using **18a** (0.13 g, 0.54 mmol) and CDI (0.70 g, 4.30 mmol); yield: 0.06 g (43 %); white solid: mp 149 °C; *R_f* = 0.38 (EtOAc / MeOH, 95:5); IR (ATR) ν (cm⁻¹) 3112 (w), 3041 (w), 2930 (w), 2877 (w), 1728 (w), 1677 (w), 1588 (w), 1497 (s), 1309 (s), 1284 (m), 1246 (m), 1068 (s), 897 (m), 876 (w), 807 (m), 748 (m), 699 (w), 662 (w), 530 (w); δ _H (CDCl₃ + CD₃OD, 500 MHz) 5.13 (s, 2H), 6.88 (d, *J* = 8.3 Hz, 1H), 6.96 (bs, 1H), 7.00-7.04 (m, 3H), 7.18 (d, *J* = 8.0 Hz, 2H), 7.36 (s, 1H), 7.48 (d, *J* = 8.0 Hz, 2H), 7.64 (s, 1H); δ _C (CDCl₃ + CD₃OD, 125 MHz) 17.8, 29.8, 31.0, 51.1, 64.8, 64.8, 116.0, 117.9, 120.1, 120.3, 127.6, 128.2, 128.9, 134.1, 134.5, 137.6, 141.1, 143.8, 144.1; (ESI): *m/z* = 293 [M⁺+H].

1-(1-(4-(6-Methoxynaphthalen-2-yl)phenyl)propyl)-*1H*-imidazole, 19. Synthesised according to Method A1 using **19a** (0.75 g, 1.71 mmol) and CDI (1.50 g, 9.30 mmol); yield: 0.23 g (39 %); white solid: mp 136-138 °C; *R_f* = 0.27 (DCM / MeOH, 95:5); IR (ATR) ν (cm⁻¹) 2936 (w), 1676 (s), 1602 (m), 1502 (m), 1462 (m), 1200 (s), 1021 (m), 844 (s), 814 (s), 665 (s), 532 (m); δ _H (CDCl₃, 500 MHz) 0.98 (t, *J* = 7.25 Hz, 3H, CH₃), 2.27-2.30 (m, 2H, CH₂), 3.94 (s, 3H, OCH₃), 5.06 (t, *J* = 7.61 Hz, 1H, CH), 6.99 (s, 1H, Im-H5), 7.11 (s, 1H, Im-H4), 7.16-7.19 (m, 2H, Aromat), 7.28 (d, *J* = 8.19 Hz, 2H, Aromat), 7.65 (s, 1H, Im-H2), 7.66-7.68 (m, 3H, Aromat), 7.80 (t, *J* = 8.51 Hz, 2H, Aromat), 7.95 (d, *J* = 1.26 Hz, 1H, Aromat); δ _C (CDCl₃, 125 MHz) 11.1 (CH₃), 28.6 (CH₂), 55.3 (CH), 63.0 (OCH₃), 105.6 (C-5'), 117.7 (Im-C4), 119.2 (C-7'), 125.6, 125.7 (Im-C5, C-3'), 127.0, 127.3 (C-1', C-4'), 127.6 (C-3, C-5),

129.1 (C-2, C-6), 129.7 (C-8), 133.9 (C-2'), 135.4 (C-4), 139.0 (C-1), 141.0 (Im-C2), 157.9 (C-6'); MS (ESI): $m/z = 343 [M^+ - H]$.

1-(1-(4-(Naphthalen-2-yl)phenyl)propyl)-1H-imidazole, 20. Synthesised according to Method A1 using **20a** (0.50 g, 1.9 mmol) and CDI (1.50 g, 9.30 mmol); yield: 0.23 g (39 %); white solid: mp 136-138 °C; $R_f = 0.29$ (DCM / MeOH, 95:5); IR (ATR) ν (cm⁻¹), 1687 (m), 1499 (s), 1223 (m), 1072 (m), 1015 (m), 809 (vs), 758 (s), 733 (s), 662 (s); δ_H (CDCl₃, 500 MHz) 0.98 (t, $J = 7.25$ Hz, 3H, CH₃), 2.24-2.33 (m, 2H, CH₂), 5.08 (t, $J = 7.56$ Hz, 1H, CH), 7.00 (t, $J = 1.26$ Hz, 1H, Im-H5), 7.11 (t, $J = 1.26$ Hz, 1H, Im-H4), 7.30 (d, $J = 7.88$ Hz, 2H, arom), 7.47-7.53 (m, 2H, arom), 7.65 (s, 1H, Im-H2), 7.69-7.72 (m, 3H, arom), 7.85-7.92 (m, 3H, arom), 8.01 (d, $J = 1.57$ Hz, 1H, arom); δ_C (CDCl₃, 125 MHz) 11.1 (CH₃), 28.6 (CH₂), 63.1 (CH), 117.7 (Im-C4), 125.3 (C-3'), 125.8, 126.1, 126.4 (Im-C5, C-7', C-8'), 127.1 (C-1'), 127.6, 127.8, 128.1, 128.5 (C-3, C-5, C-5', C-8'), 129.6 (C-4'), 132.7, 132.6 (C-2, C-6), 136.4 (C-4, C-2'), 137.6 (C-1), 139.4 (Im-C2); MS (ESI): $m/z = 313 [M^+ + H]$.

1-(3-(4-(6-(tert-Butyldimethylsilyloxy)naphthalen-2-yl)phenyl)pentan-3-yl)-1H-imidazole, 21a. Synthesised according to Method A1 using **21b** (1.00 g, 2.5 mmol) and CDI (2.06 g, 12.7 mmol); brown oil; the crude product was directly used in the next step without further purification and analysis.

Method B: Ether cleavage with BBr₃. To a solution of the corresponding ether (1 eq) in DCM (5 mL / mmol) at -78 °C was added 1 M borontribromide in DCM (5 eq). The resulting mixture was stirred at rt for 16 hours. Then water (25 mL) was added and the emulsion was stirred for further 30 minutes. The resulting mixture was extracted with ethyl acetate (3 x 25 mL). The combined organic phases were washed with brine, dried over Na₂SO₄ and evaporated under reduced pressure. Then the desired product was purified by chromatography on silica gel.

4-(2-((1H-Imidazol-1-yl)methyl)benzo[*b*]thiophen-5-yl)phenol, 2. Synthesised according to Method B using **1** (0.15 g, 0.47 mmol) and BBr₃ (2.35 mL, 2.34 mmol); yield: 0.05 g (32 %); white solid: mp 211 °C; $R_f = 0.42$ (DCM / MeOH, 95:5); IR (ATR) ν (cm⁻¹) 3349 (w), 2959 (w), 1733 (w), 1609 (w), 1515 (s), 1448 (w), 1277 (s), 1242 (w), 1231 (w), 1194 (w), 1108 (m), 1030 (w), 951 (w), 885 (w), 809 (s), 749 (s), 658 (m), 547 (w); δ_H (CDCl₃ + CD₃OD, 500 MHz) 5.43 (s, 2H), 6.88 (d, $J = 8.6$ Hz, 2H), 7.02 (bs, 1H), 7.11 (bs, 1H), 7.25 (s, 1H), 7.44-7.52 (m, 3H), 7.72 (bs, 1H), 7.76 (d, $J = 8.4$ Hz, 1H), 7.85 (s, 1H); δ_C (CDCl₃ + CD₃OD, 125 MHz) 116.3, 122.0, 123.1, 124.4, 124.8, 128.9, 133.1, 138.9, 138.9, 140.3, 140.6, 157.2.

4-(4-((1H-Imidazol-1-yl)methyl)naphthalen-1-yl)phenol, 7. Synthesised according to Method B using **6** (0.15 g, 0.48 mmol) and BBr₃ (1.90 mL, 1.90 mmol); yield: 0.08 g (52 %); white solid: mp 197 °C; $R_f = 0.42$ (DCM / MeOH, 95:5); IR (ATR) ν (cm⁻¹) 3600-2900 (w), 1610 (w), 1509 (m), 1437 (w), 1391 (w), 1264 (s), 1214 (w), 1172 (w), 1091 (m), 951 (w), 834 (s), 770 (w), 734 (s), 654 (w), 574 (w); δ_H (CDCl₃ + CD₃OD, 500 MHz) 6.89 (d, $J = 8.4$ Hz, 2H), 7.04 (s, 1H), 7.15 (s, 1H), 7.21 (d, $J = 8.4$ Hz, 2H), 7.28-7.30 (m, 1H), 7.31 (s, 1H), 7.36-7.39 (m, 1H), 7.44-7.47 (m, 1H), 7.82 (d, $J = 8.4$ Hz, 1H), 7.93 (d, $J = 8.4$ Hz, 1H), 7.29 (bs, 1H); δ_C (CDCl₃ + CD₃OD, 125 MHz) 115.3, 122.4, 126.3, 126.4, 127.2, 127.6, 131.1, 131.3, 132.5, 156.6; (ESI): $m/z = 301 [M^+ + H]$.

4-(8-(1-(1H-Imidazol-1-yl)propyl)quinolin-5-yl)phenol, 9. Synthesised according to Method B using **8** (0.10 g, 0.29 mmol) and BBr₃ (1.46 mL, 1.46 mmol); yield: 0.06 g (63 %); white solid: mp 174 °C; $R_f = 0.42$ (DCM / MeOH, 95:5); IR (ATR) ν (cm⁻¹) 3500-2600 (w), 1610 (m), 1515 (s), 1458 (w), 1397 (w), 1269 (s), 1227 (w), 1172 (w), 1108 (w), 1089 (w), 826 (s), 797 (w), 736 (s), 669 (w); δ_H (CDCl₃ + CD₃OD, 500 MHz) 0.95 (t, $J = 7.2$ Hz, 3H), 2.30-2.41 (m, 2H), 6.58 (m, 1H), 6.91 (d, $J = 8.5$ Hz, 2H), 6.07 (bs, 1H), 7.14 (bs, 1H), 7.18 (d, $J = 8.5$ Hz, 2H), 7.28-7.32 (m, 1H), 7.37 (d, $J = 7.5$ Hz, 1H), 7.57 (d, $J = 7.5$ Hz, 1H), 7.99 (bs, 1H), 8.22 (d, $J = 8.5$ Hz, 1H), 8.81 (m, 1H); δ_C (CDCl₃ + CD₃OD, 125 MHz) 11.3, 27.8, 57.8, 60.7, 115.5, 115.6, 119.0, 121.4, 125.8, 125.9, 126.8, 127.2, 127.3, 130.0, 131.1, 131.1, 135.3, 135.9, 137.3, 141.4, 145.7, 149.6, 157.1; (ESI): $m/z = 330 [M^+ + H]$.

4-(8-(1-(1H-Imidazol-1-yl)propyl)-2-ethylquinolin-5-yl)phenol, 11. Synthesised according to Method B using **10** (0.15 g, 0.40 mmol) and BBr₃ (2.00 mL, 2.00 mmol); yield: 0.09 g (58 %); white solid: mp 142 °C; $R_f = 0.69$ (DCM / MeOH, 95:5); IR (ATR) ν (cm⁻¹) 3600-2800 (w), 2968 (w), 2932 (w), 1733 (s), 1608 (s), 1579 (w), 1518 (s), 1457 (w), 1398 (w), 1269 (s), 1225 (m), 1172 (m), 1108 (w), 951 (w), 824 (s), 734 (m), 659 (w); δ_H (CDCl₃ + CD₃OD, 500 MHz) 0.94 (t, $J = 7.2$ Hz, 3H), 1.30 (t, $J = 7.5$ Hz, 3H), 2.29-2.43 (m, 2H), 2.89-2.93 (m, 2H), 6.57-6.60 (m, 1H), 6.88 (d, $J = 8.1$ Hz, 2H), 6.99 (s, 1H), 7.12 (s, 1H), 7.15-7.18 (m, 3H), 7.29 (d, $J = 7.4$ Hz, 1H), 7.53 (d, $J = 7.4$ Hz, 1H), 8.08 (d, $J = 8.7$ Hz, 1H), 8.13 (s, 1H); δ_C (CDCl₃ + CD₃OD, 125 MHz) 11.0, 13.0, 27.1, 31.6, 58.1, 115.2, 119.1, 121.0, 125.2, 125.33, 125.34, 126.2, 130.2, 130.8, 134.2, 134.8, 137.5, 141.0, 145.0, 156.4, 162.9; (ESI): $m/z = 358 [M^+ + H]$.

Method C: Suzuki-Coupling. The corresponding brominated aromatic compound (1 eq) was dissolved in toluene (7 mL / mmol), an aqueous 2.0 M Na₂CO₃ solution (3.2 mL / mmol) and an ethanolic solution (3.2 mL / mmol) of the corresponding boronic acid (1.5-2.0 eq) were added. The mixture was deoxygenated under reduced

pressure and flushed with nitrogen. After repeating this cycle several times Pd(PPh₃)₄ (4 mol%) was added and the resulting suspension was heated under reflux for 8 h. After cooling ethyl acetate (10 mL) and water (10 mL) were added and the organic phase was separated. The water phase was extracted with ethyl acetate (2 x 10 mL). The combined organic phases were washed with brine, dried over Na₂SO₄, filtered over a short plug of celite® and evaporated under reduced pressure. The compounds were purified by flash chromatography on silica gel.

6-(4-Fluorophenyl)-1H-indole-3-carbaldehyde, 3b. Synthesised according to Method C1 using 6-bromo-1H-indole-3-carbaldehyde (0.45 g, 2.00 mmol) and 4-fluorophenylboronic acid (0.57 g, 4.05 mmol); yield: 0.35 g (73 %); yellow oil; $R_f = 0.57$ (petrolether / EtOAc, 1:2); IR (ATR) ν (cm⁻¹) 3228 (m), 2806 (w), 1646 (s), 1618 (m), 1518 (m), 1386 (m), 1198 (m), 1110 (s), 1083 (s), 811 (s), 670 (s), 593 (m), 517 (s); δ_H (CDCl₃, 500 MHz) 6.84 (t, $J = 8.8$ Hz, 2H), 7.15 (dd, $J = 1.6$ Hz, 8.2 Hz, 1H), 7.30 (dd, $J = 5.4$ Hz, 8.8 Hz, 2H), 7.33 (m, 1H), 7.63 (d, $J = 3.2$ Hz, 1H), 7.96 (d, $J = 8.2$ Hz, 1H), 9.71 (s, 1H), 11.42 (bs, 1H); δ_C (CDCl₃, 125 MHz) 109.7 (CH), 114.8 (CH), 118.0 (C_q), 121.0 (C_q), 121.1 (CH), 123.0 (C_q), 128.1 (CH), 135.3 (C_q), 136.8 (CH), 137.1 (C_q), 137.3 (C_q), 161.4 (CF), 184.2 (CH); MS (ESI): $m/z = 238$ [M⁺-H].

2-((1H-Imidazol-1-yl)methyl)-6-(4-fluorophenyl)quinoline, 4. Synthesised according to Method C1 using **4a** (0.24 g, 0.84 mmol) and 4-fluorophenylboronic acid (0.23 g, 1.68 mmol); yield: 0.23 g (92 %); yellow solid, $R_f = 0.15$ (EtOAc/MeOH 9/1); IR (ATR) ν (cm⁻¹) 3125 (w), 3094 (w), 2926 (w), 1602 (m), 1515 (m), 1498 (m), 1431 (m), 1224 (s), 824 (s), 771 (m), 657 (m); δ_H (CDCl₃, 500 MHz) 5.43 (s, 2H), 7.04 (t, $J = 1.3$ Hz, 1H), 7.08 (d, $J = 8.5$ Hz, 1H), 7.15 (bs, 1H), 7.18 (t, $J = 8.5$, 2H), 7.66 (m, 2H), 7.69 (bs, 1H), 7.93 (d, $J = 2.2$ Hz, 1H), 7.96 (dd, $J = 2.2$, 8.5 Hz, 1H), 8.12 (d, $J = 8.8$ Hz, 1H), 8.16 (d, $J = 8.5$ Hz, 1H); δ_C (CDCl₃, 125 MHz) 53.2 (CH₂), 115.9 (d, $^2J_{CF} = 22$ Hz, CH), 119.1 (CH), 119.6 (CH), 125.1 (CH), 127.6 (CH), 128.3 (C_q), 128.4 (CH), 129.0 (d, $^3J = 7.7$ Hz, CH), 129.6 (CH), 129.7 (CH), 130.2 (CH), 136.2 (d, $^4J_{CF} = 2.9$ Hz, C_q), 137.7 (CH), 137.8 (CH), 138.8 (C_q), 146.9 (C_q), 156.2 (C_q), 162.8 (d, $^1J_{CF} = 248.0$ Hz, CF); MS (ESI): $m/z = 304$ [M⁺+H].

2-((1H-Imidazol-1-yl)methyl)-6-(thiophen-3-yl)quinoline, 5. Synthesised according to Method C1 using **5a** (0.24 g, 0.84 mmol) and 3-thiophenylboronic acid (0.22 g, 1.68 mmol); yield: 0.22 g (88 %); yellow solid; $R_f = 0.11$ (EtOAc/MeOH 9/1); IR (ATR) ν (cm⁻¹) 3104 (w), 2963 (w), 2926 (m), 1597 (m), 1506 (m), 1318 (m), 1068 (m), 828 (s), 782 (s), 753 (s), 660 (s); δ_H (CDCl₃, 500 MHz) 5.43 (s, 2H), 7.04 (t, $J = 1.3$ Hz, 1H), 7.06 (d, $J = 8.5$ Hz, 1H), 7.15 (t, $J = 0.9$ Hz, 1H), 7.46 (dd, $J = 2.8$, 5.0 Hz, 1H), 7.52 (dd, $J = 1.6$, 5.0 Hz, 1H), 7.62 (dd, $J = 1.3$, 2.8 Hz, 1H), 7.69 (bs, 1H), 7.99 (d, $J = 1.9$ Hz, 1H), 8.02 (dd, $J = 2.2$, 8.8 Hz, 1H), 8.09 (d, $J = 8.8$ Hz, 1H), 8.14 (d, $J = 8.5$ Hz, 1H); δ_C (CDCl₃, 125 MHz) 53.2 (CH₂), 119.1 (CH), 119.6 (CH), 121.5 (CH), 124.2 (CH), 126.3 (CH), 126.8 (CH), 127.7 (C_q), 129.4 (CH), 129.6 (CH), 130.2 (CH), 134.4 (C_q), 137.6 (CH), 137.8 (CH), 141.2 (C_q), 146.9 (C_q), 155.9 (C_q); MS (ESI): $m/z = 292$ [M⁺+H].

(4-(4-Methoxyphenyl)naphthalen-1-yl)methanol, 6a. Synthesised according to Method C2 using **6b** (0.40 g, 1.69 mmol) and 4-methoxyphenylboronic acid (0.39 g, 2.53 mmol); yield: 0.42 g (94 %); white solid; $R_f = 0.57$ (petrolether / EtOAc, 1:2); δ_H (CDCl₃, 500 MHz) 3.90 (s, 3H), 5.20 (s, 2H), 7.04 (d, $J = 8.7$ Hz, 2H), 7.38 (d, $J = 7.2$ Hz, 1H), 7.40 (d, $J = 8.7$ Hz, 2H), 7.45-7.48 (m, 1H), 7.56 (d, $J = 7.2$ Hz, 2H), 7.96 (d, $J = 8.4$ Hz, 1H), 8.20 (d, $J = 8.4$ Hz, 1H); δ_C (CDCl₃, 125 MHz) 55.4, 63.8, 113.7, 123.9, 125.0, 125.9, 126.2, 126.4, 126.9, 131.1, 131.5, 132.2, 133.0, 135.4, 140.5, 159.0.

5-(4-Methoxyphenyl)quinoline-8-carbaldehyde, 8b. Synthesised according to Method C2 using 6-bromo-1H-indole-3-carbaldehyde (3.00 g, 12.71 mmol) and 4-methoxyphenylboronic acid (2.90 g, 19.06 mmol); yield: 2.75 g (82 %); white solid; $R_f = 0.63$ (petrolether / EtOAc, 1:2); δ_H (CDCl₃, 500 MHz) 7.06 (d, $J = 8.7$ Hz, 2H), 7.41 (d, $J = 8.7$ Hz, 2H), 7.45 (d, $J = 4.1$ Hz, $J = 8.6$ Hz, 1H), 7.61 (d, $J = 7.5$ Hz, 1H), 8.33-8.34 (m, 2H), 9.03-9.04 (m, 1H), 11.48 (s, 1H); δ_C (CDCl₃, 125 MHz) 55.4, 114.1, 121.5, 121.8, 126.2, 126.7, 126.9, 128.8, 129.3, 130.5, 130.9, 131.0, 134.2, 134.8, 136.3, 146.7, 148.1, 150.9, 151.3, 159.8, 192.6.

4-(Benzo[b]thiophen-5-yl)benzaldehyde, 12b. Synthesised according to Method C1 using 5-bromobenzo[b]thiophene (1.90 g, 8.92 mmol) and 4-formylphenylboronic acid (1.74 g, 11.6 mmol); yield: 1.71 g (80 %); white solid; $R_f = 0.35$ (petrolether / EtOAc, 5:1); δ_H (CDCl₃, 500 MHz) 7.41 (d, $J = 5.4$ Hz, 1H), 7.51 (d, $J = 5.4$ Hz, 1H), 7.61 (d, $J = 8.4$ Hz, 1H), 7.82 (d, $J = 7.9$ Hz, 2H), 7.97 (d, $J = 8.2$ Hz, 3H), 8.07 (s, 1H), 10.07 (s, 1H, CHO); δ_C (CDCl₃, 125 MHz) 122.3, 123.0, 123.6, 124.0, 127.5, 127.8, 130.3, 135.0, 126.1, 139.9, 140.2, 147.3, 191.9.

4-(1H-Indol-5-yl)benzaldehyde, 13b. Synthesised according to Method C1 using 5-bromo-1H-indole (0.10 g, 0.51 mmol) and 4-formylphenylboronic acid (0.1 g, 0.66 mmol); yield: 0.07 g (65 %); white solid; $R_f = 0.25$ (petrolether / EtOAc, 5:1); δ_H (CDCl₃, 500 MHz) 6.64 (t, $J = 2.8$ Hz, 1H), 7.27 (t, $J = 3.1$ Hz, 1H), 7.48 (s, 1H), 7.74 (dd, $J = 1.8$, 8.5 Hz, 2H), 7.92 (s, 1H), 8.04 (dd, $J = 1.8$, 8.5 Hz, 2H), 8.29 (s, br, 1H), 10.05 (s, 1H, CHO); δ_C (CDCl₃, 125 MHz) 103.2, 111.4, 119.6, 121.7, 125.1, 127.2, 128.4, 128.5, 132.0, 135.8, 147.0, 192.1.

4-(Benzofuran-5-yl)benzaldehyde, 14b. Synthesised according to Method C1 using 5-bromobenzofuran (1.90 g, 9.64 mmol) and 4-formylphenylboronic acid (1.88 g, 12.5 mmol); yield: 0.53 g (25 %); yellow oil; $R_f = 0.33$ (petrolether / EtOAc, 5:1); δ_H (CDCl₃, 500 MHz) 6.83-6.84 (m, 1H), 7.54-7.60 (m, 2H), 7.68 (d, $J = 2.2$ Hz, 1H), 7.76 (d, $J = 8.2$ Hz, 2H), 7.84 (d, $J = 1.6$ Hz, 1H), 7.94 (dd, $J = 1.8, 8.4$ Hz, 2H), 10.05 (s, 1H, CHO); δ_C (CDCl₃, 125 MHz) 106.8, 111.8, 120.1, 123.9, 127.8, 130.2, 134.8, 145.9, 147.6, 155.0, 191.9.

(4-(Benzo[d]thiazol-6-yl)phenyl)methanol, 17a. Synthesised according to Method C1 using 6-bromobenzo[d]thiazole (0.50 g, 2.34 mmol) and 4-(hydroxymethyl)phenylboronic acid (0.53 g, 3.50 mmol); yield: 0.50 g (89 %); white solid; $R_f = 0.26$ (petrolether / EtOAc, 1:2); δ_H (CDCl₃, 500 MHz) 4.77 (s, 2H), 7.48 (d, $J = 8.4$ Hz, 2H), 7.64-7.68 (m, 3H), 7.74 (dd, $J = 1.8$ Hz, $J = 8.5$ Hz, 1H), 8.15 (s, 1H), 8.20 (d, $J = 8.5$ Hz, 1H), 9.03 (s, 1H); δ_C (CDCl₃, 125 MHz) 64.9, 120.1, 123.6, 125.9, 127.6, 127.6, 128.5, 128.6, 132.0, 132.0, 132.1, 132.1, 134.5, 138.8, 139.7, 140.4.

(4-(2,3-Dihydrobenzo[b][1,4]dioxin-6-yl)phenyl)methanol, 18a. Synthesised according to Method C1 using 6-bromo-2,3-dihydrobenzo[b][1,4]dioxine (0.50 g, 2.33 mmol) and 4-(hydroxymethyl)phenylboronic acid (0.53 g, 3.49 mmol); yield: 0.15 g (27 %); white solid; $R_f = 0.62$ (petrolether / EtOAc, 1:2); δ_H (CDCl₃, 500 MHz) 4.29 (s, 1H), 4.71 (s, 1H), 6.93 (d, $J = 8.3$ Hz, 1H), 7.08 (dd, $J = 2.2$ Hz, $J = 8.3$ Hz, 1H), 7.12 (d, $J = 2.2$ Hz, 1H), 7.40 (d, $J = 8.3$ Hz, 2H), 7.53 (d, $J = 8.3$ Hz, 2H); δ_C (CDCl₃, 125 MHz) 64.4, 64.4, 65.1, 115.8, 117.5, 120.1, 126.9, 127.4, 134.4, 139.4, 140.0, 143.2, 143.7.

Method D: Reduction with NaBH₄. To an ice-cooled solution of the corresponding aldehyde or ketone (1 eq) in methanol (5 mL / mmol) was added NaBH₄ (2 eq). Then the resulting mixture was heated to reflux for 30 minutes. After cooling to ambient temperature, the solvent was distilled off under reduced pressure. Then water (10 mL) was added, and the resulting mixture was extracted with ethyl acetate (3 x 10 mL). The combined organic phases were washed with brine, dried over MgSO₄ and evaporated under reduced pressure. Then the desired product was purified by chromatography on silica gel.

(6-(4-Fluorophenyl)-1H-indol-3-yl)-methanol, 3a. Synthesised according to Method D using **3b** (0.30 g, 1.25 mmol) and NaBH₄ (0.86 g, 2.26 mmol); yield: 0.27 g (89 %); $R_f = 0.55$ (PE / EtOAc, 1:2); the crude product was directly used in the next step without further purification and analysis.

(4-(Benzo[b]thiophen-5-yl)phenyl)methanol, 14a. Synthesised according to Method D using **14b** (0.30 g, 1.26 mmol) and NaBH₄ (0.10 g, 2.52 mmol); yield: 0.28 g (92 %); $R_f = 0.30$ (PE / EtOAc, 2:1); the crude product was directly used in the next step without further purification and analysis.

1-(4-(Benzo[b]thiophen-5-yl)phenyl)propan-1-ol, 15a. Synthesised according to Method D using **15b** (0.30 g, 1.36 mmol) and NaBH₄ (0.11 g, 2.71 mmol); yield: 0.28 g (91 %); $R_f = 0.30$ (PE / EtOAc, 2:1); the crude product was directly used in the next step without further purification and analysis.

1-(4-(6-Methoxynaphthalen-2-yl)phenyl)propan-1-ol, 19a. Synthesised according to Method D using **19b** (1.93 g, 6.40 mmol) and NaBH₄ (0.48 g, 12.8 mmol); yield: 0.711 g (38 %); $R_f = 0.59$ (DCM / MeOH, 98:2); the crude product was directly used in the next step without further purification and analysis.

1-(4-(Naphthalen-2-yl)phenyl)propan-1-ol, 20a. Synthesised according to Method D using **20b** (1.80 g, 6.40 mmol) and NaBH₄ (0.48 g, 12.8 mmol); yield: 1.34 g (80 %); $R_f = 0.62$ (DCM / MeOH, 98:2); the crude product was directly used in the next step without further purification and analysis.

6-Bromo-2-(bromomethyl)quinoline 4b. 6-Bromo-2-methylquinoline (3.00 g, 13.5 mmol) was dissolved in 40 mL of dry carbon tetrachloride. To this solution was added NBS (2.63 g, 14.8 mmol) and dibenzoyl peroxide (0.16 g, 0.70 mmol) and the mixture was refluxed over night. After cooling, the succinimide was removed by filtration and the filtrate was concentrated under vacuum. The crude product was further purified by flash column chromatography on silica gel using petroleum ether / EtOAc (95 : 5) as eluent; yield: 1.71 g (42%); lachrymatory lilac oil; $R_f = 0.46$ (hexane / EtOAc 95 : 5); IR (ATR) ν (cm⁻¹) 3054 (w), 3038 (w), 2928 (w), 2855 (w), 1589 (m), 1484 (s), 1373 (m), 1304 (m), 1200 (s), 1190 (s), 1060 (s), 899 (s), 830 (s), 792 (s), 775 (m), 735 (s), 694 (s), 597 (s), 550 (s); δ_H (CDCl₃, 500 MHz) 4.68 (s, 2H), 7.59 (d, $J = 8.5$ Hz, 1H), 7.79 (dd, $J = 2.1, 9.1$ Hz, 1H), 7.93 (d, $J = 8.8$ Hz, 1H), 7.98 (d, $J = 2.1$ Hz, 1H), 8.08 (d, $J = 8.5$ Hz, 1H); δ_C (CDCl₃, 125 MHz) 34.0 (CH₂), 121.0 (CH), 122.0 (CH), 128.4 (C_q), 129.6 (CH), 131.0 (CH), 133.4 (CH), 136.2 (C_q), 157.4 (C_q), 157.9 (C_q); MS (ESI): $m/z = 302$ [M⁺ + H].

2-(1H-Imidazol-1-ylmethyl)-6-bromoquinoline 4a. The α -brominated compound **4b** (1.89 g, 6.28 mmol), imidazole (0.86 g, 12.55 mmol), anhydrous K₂CO₃ (1.29 g, 9.42 mmol) and a catalytical amount of 18-crown-6 in dry acetonitrile were heated under reflux over night. After the solution was cooled down, the solvent was removed under reduced pressure. The residue was dissolved with water (10 mL/eq) and extracted three times with CH₂Cl₂ (15

mL/eq). The combined organic extracts were washed with brine, dried over anhydrous Na₂SO₄, filtered, and evaporated. The crude material was purified by flash chromatography on silica-gel, using 5% MeOH in CH₂Cl₂; yield: 1.1 g (61%); *R_f* = 0.23 (EtOAc / MeOH 9 : 1); IR (ATR) ν (cm⁻¹) 3098 (w), 1593 (m), 1488 (s), 1291 (m), 1235 (m), 1086 (m), 1030 (m), 824 (s), 733 (s), 658 (s); δ_{H} (CDCl₃, 500 MHz) 5.39 (s, 2H), 7.01 (t, *J* = 1.3 Hz, 1H), 7.06 (d, *J* = 8.5 Hz, 1H), 7.13 (t, *J* = 1.3 Hz, 1H), 7.66 (s, 1H), 7.79 (dd, *J* = 2.2, *J* = 9.1 Hz, 1H), 7.91 (d, *J* = 9.1 Hz, 1H), 7.96 (d, *J* = 2.2 Hz, 1H), 8.03 (d, *J* = 8.5 Hz, 1H); δ_{C} (CDCl₃, 125 MHz) 55.0 (CH₂), 119.5 (CH), 119.5 (CH), 120.9 (CH), 129.6 (C_q), 130.2 (CH), 130.8 (CH), 133.6 (CH), 136.6 (CH), 137.7 (C_q), 146.2 (C_q), 156.6 (C_q); MS (ESI): *m/z* = 289 [M⁺ + H].

4-Bromo-1-naphthoic acid, 6c. 4-Bromo-1-methyl naphthalene (20.0 g, 88.65 mmol) was preheated to 90 °C in a water / pyridine 1 : 1 mixture (170 mL) and KMnO₄ (57.2 g, 354.6 mmol) was added over a period of 3 h every 30 min in equal portions. yield: 1.60 g (7 %); *R_f* = 0.37 (PE / EtOAc, 2:1); δ_{H} (CDCl₃ + CD₃OD, 500 MHz) 7.56-7.61 (m, 2H), 7.78 (d, *J* = 7.9 Hz, 1H), 8.00 (d, *J* = 7.9 Hz, 1H), 8.26-8.28 (m, 1H), 8.91-8.93 (m, 1H); δ_{C} (CDCl₃ + CD₃OD, 125 MHz) 126.5, 127.6, 127.7, 128.4, 128.7, 129.1, 130.5, 132.3, 132.6.

(4-Bromonaphthalen-1-yl)methanol, 6b. To a solution of **6c** (0.60 g, 2.39 mmol) in THF (10 mL) LiAlH₄ (0.91 g, 3.90 mmol) in THF (5 mL) was added slowly and heated to reflux overnight. yield: 1.65 g (83 %); *R_f* = 0.74 (PE / EtOAc, 2:1); δ_{H} (CDCl₃, 500 MHz) 5.12 (s, 2H), 7.37 (d, *J* = 7.6 Hz, 1H), 7.58-7.64 (m, 2H), 7.76 (d, *J* = 7.6 Hz, 1H), 8.11 (d, *J* = 7.8 Hz, 1H), 8.31 (d, *J* = 7.8 Hz, 1H); δ_{C} (CDCl₃, 125 MHz) 123.2, 124.0, 125.5, 127.1, 127.2, 127.9, 129.4, 132.1, 132.3, 136.3.

Method E: Grignard reaction. Under exclusion of air and moisture a 1.0 M EtMgBr (1.2 eq) solution in THF was added dropwise to a solution of the aldehyde or ketone (1 eq) in THF (12 mL / mmol). The mixture was stirred over night at rt. Then ethyl acetate (10 mL) and water (10 mL) were added and the organic phase was separated. The organic phase was extracted with water and brine, dried over Na₂SO₄, and evaporated under reduced pressure. The crude products were purified by flash chromatography on silica gel.

1-(5-(4-Methoxyphenyl)quinolin-8-yl)propan-1-ol, 8a. Synthesised according to Method E using **8b** (1.00 g, 3.80 mmol) and NaBH₄ (15.20 mL, 15.20 mmol); yield: 0.47 g (43 %); *R_f* = 0.47 (PE / EtOAc, 2:1); δ_{H} (CDCl₃, 500 MHz) 1.05 (t, *J* = 7.4 Hz, 3H), 1.97-2.20 (m, 2H), 3.90 (s, 3H), 5.04-5.07 (m, 1H), 7.04 (d, *J* = 8.6 Hz, 2H), 7.35-7.38 (m, 3H), 7.43 (d, *J* = 7.3 Hz, 1H), 7.56 (d, *J* = 7.3 Hz, 1H), 8.30 (d, *J* = 8.6 Hz, 1H), 8.82-8.83 (m, 1H); δ_{C} (CDCl₃, 125 MHz) 11.0, 31.9, 55.4, 113.9, 120.6, 126.8, 127.1, 127.4, 131.1, 131.5, 135.4, 139.2, 139.5, 146.8, 147.9, 150.3.

1-(2-Ethyl-5-(4-methoxyphenyl)quinolin-8-yl)propan-1-ol, 10a. Synthesised according to Method E using **8b** (1.00 g, 3.80 mmol) and NaBH₄ (15.20 mL, 15.20 mmol); yield: 0.43 g (39 %); *R_f* = 0.52 (PE / EtOAc, 2:1); δ_{H} (CDCl₃, 500 MHz) 1.03 (t, *J* = 7.4 Hz, 3H), 1.41 (t, *J* = 7.6 Hz, 3H), 2.02-2.19 (m, 2H), 2.98-3.03 (m, 2H), 3.89 (s, 3H), 4.95-4.98 (m, 1H), 7.03 (d, *J* = 8.6 Hz, 2H), 7.24 (d, *J* = 8.8 Hz, 1H), 7.34-7.36 (m, 3H), 7.48 (d, *J* = 7.3 Hz, 1H), 8.19 (d, *J* = 8.8 Hz, 1H).

1-(4-(Benzo[*b*]thiophen-5-yl)phenyl)propan-1-ol, 12a. Synthesised according to Method E using **12b** (0.35 g, 1.47 mmol) and a 1.0 M ethylmagnesium bromide solution in THF (1.91 mL, 1.91 mmol); yield: 0.34 g (85 %); *R_f* = 0.30 (PE / EtOAc, 2:1); the crude product was directly used in the next step without further purification and analysis.

1-(4-(1*H*-Indol-5-yl)phenyl)propan-1-ol, 13a. Synthesised according to Method E using **13b** (0.50 g, 2.26 mmol) and a 1.0 M ethylmagnesium bromide solution in THF (2.94 mL, 2.94 mmol); yield: 0.51 g (89 %); *R_f* = 0.30 (PE / EtOAc, 2:1); the crude product was directly used in the next step without further purification and analysis.

3-(4-(6-(*tert*-Butyldimethylsilyloxy)naphthalen-2-yl)phenyl)pentan-3-ol, 21b. Synthesised according to Method E using **21c** (6.07 g, 16.7 mmol) and EtMgBr (1 M, 18.4 mL, 18.4 mmol, 1.1 eq); yield: 1.37 g (21%); yellow solid; *R_f* = 0.73 (hexane / EtOAc, 7 : 3); the crude product was directly used in the next step without further purification and analysis.

(6-Bromonaphthalen-2-yloxy)(*tert*-butyl)dimethylsilane, 21d. To a solution of 6-bromonaphthalen-2-ol (10 g, 44.8 mmol) and imidazole (3.4 g, 49.3 mmol, 1.1 eq) in dichloromethane was slowly added a solution of *tert*-butyldimethylsilyl chloride (7.4 g, 49.3 mmol, 1.1 eq) in dichloromethane. After being stirred for 4 h at rt the reaction mixture was poured into water, extracted with dichloromethane, washed with water and brine, and dried over Na₂SO₄. Solvent removal under reduced pressure lead to a pale oil, which was purified by chromatography on silica gel; yield: 14.5 g, (96%); yellow oil; *R_f* = 0.63 (hexane); δ_{H} (CDCl₃, 500 MHz) 0.25 (s, 6H), 1.02 (s, 9H), 7.09 (dd, *J* = 2.2, *J* = 8.8 Hz, 1H), 7.15 (d, *J* = 2.2 Hz, 1H), 7.48 (dd, *J* = 2.2, *J* = 8.8 Hz, 1H), 7.56 (d, *J* = 8.8 Hz, 1H), 7.63 (d, *J* = 8.8 Hz, 1H), 7.92 (d, *J* = 2.2 Hz, 1H); δ_{C} (CDCl₃, 125 MHz) -4.3 (CH₃), 18.2 (C_q), 25.7 (CH₃), 114.9

(CH), 117.3 (C_{Br}), 123.1 (CH), 128.3 (CH), 128.4 (C_q), 129.4 (CH), 129.6 (CH), 130.3 (CH), 133.1 (C_q), 153.8 (C_{OR}); MS (ESI): $m/z = 337 [M^+ + H]$.

6-(4-(3-(1*H*-Imidazol-1-yl)pentan-3-yl)phenyl)naphthalen-2-ol, 21. To a solution of the silyl-protected phenol **21a** (crude product, 2.5 mmol) in anhydrous tetrahydrofuran (25 mL) was added tetrabutylammonium fluoride (3 mL, 1 M) and the solution was stirred for 4 h. The reaction was terminated with the addition of methanol and the solvent was removed under reduced pressure. Then, the desired product was purified by chromatography on silica gel; yield = 50 mg (6%); brown solid; $R_f = 0.31$ (EtOAc/MeOH 95/5); IR (ATR) ν (cm⁻¹) 2975 (w), 2874 (w), 1602 (s), 1510 (m), 1498 (m), 1251 (s), 1205 (s), 858 (s), 831 (s); δ_H (CDCl₃, 500 MHz) 0.65 (t, $J = 7.3$ Hz, 6H), 2.27-2.31 (m, 4H), 6.94 (bs, 1H), 7.06 (bs, 1H), 7.10 (dd, $J = 2.4$ Hz, $J = 8.8$ Hz, 1H), 7.14 (d, $J = 2.4$ Hz, 1H), 7.22 (d, $J = 8.8$ Hz, 2H), 7.70-7.76 (m, 4H), 7.80 (bs, 1H), 7.82 (d, $J = 8.8$ Hz, 1H), 8.07 (bs, 1H), 9.84 (s, 1H); δ_C (CDCl₃, 125 MHz) 7.6 (CH₃), 28.9 (CH₂), 65.7 (CH), 108.4 (CH), 117.1 (CH), 118.4 (CH), 119.0 (CH), 125.0 (CH), 125.0 (CH), 126.2 (CH), 126.6 (CH), 126.7 (CH), 127.9 (C_q), 128.1 (C_q), 129.7 (CH), 133.5 (C_q), 133.8 (C_q), 139.0 (C_q), 142.9 (CH), 155.5 (C_{OH}); MS (ESI): $m/z = 357 [M^+ + H]$.

Biological Assays. CYP17 Preparation and Assay. As source of human CYP17, our *E. coli* system¹⁷ (co-expressing human CYP17 and NADPH-P450 reductase) was used and the assay was performed as previously described⁷ taking unlabeled progesterone as substrate and applying HPLC with UV-detection for separation.

Inhibition of Hepatic CYP Enzymes. The recombinantly expressed enzymes from baculovirus-infected insect microsomes (BD SupersomesTM) were used and the manufacturer's instructions (www.genest.com) were followed.

Inhibition of CYP11B1. V79MZh11B1 cells expressing the respective human enzyme were used and our assay procedure using [4-¹⁴C]-11-deoxycorticosterone was applied.¹⁹

Molecular Modelling. All molecular modelling studies were performed on Intel® P4 CPU 3.00 GHz running Linux Suse 10.1.

Ligands. The structures of the inhibitors were built with SYBYL 7.3.2 (Sybyl, Tripos Inc., St. Louis, Missouri, USA) and energy-minimised in MMFF94s force-field²⁴ as implemented in Sybyl. The resulting geometries for our compounds were then subjected to ab initio calculation employing the B3LYP functional²⁵ in combination with a 6-31G* basis set using the package Gaussian03 (Gaussian, Inc., Pittsburgh, PA, USA, 2003).

Docking. Various inhibitors of Tables 1 and 2 were docked into our CYP17 homology model by means of the GOLD v 3.0.1 software.²⁰ Since the GOLD docking program allows flexible docking of the compounds, no conformational search was employed to the ligand structures. GOLD gave the best poses by a genetic algorithm (GA) search strategy, and then various molecular features were encoded as a chromosome.

Ligands were docked in 50 independent GA runs using GOLD. Heme iron was chosen as active site origin, while its radius was set equal to 19 Å. The automatic active site detection was switched on. Furthermore, a distance constraint of a minimum of 1.9 and a maximum of 2.5 Å between the sp²-hybridised nitrogen of the imidazole and the iron of the heme was set. Additionally, some of the GOLDScore parameters were modified to improve the weight of hydrophobic interaction and of the coordination between iron and nitrogen. The genetic algorithm default parameters were set as suggested by the GOLD authors.²⁰ On the other hand, the annealing parameters of fitness function were set at 3.5 Å for hydrogen bonding and 6.5 Å for van-der-Waals interactions.

All 50 poses for each compound were clustered with ACIAP²² and the representative structure of each significant cluster was selected. The quality of the docked representative poses was evaluated based on the GOLDScore values, which give a good measure of the found binding mode, and on visual inspection of the putative binding modes of the ligands, as outcome of docking simulations and cluster analysis.

Acknowledgment. We thank the Fonds der Chemischen Industrie for financial support. U. E. H. is grateful to the European Postgraduate School 532 (DFG) for a scholarship. We also thank Dr. J. J. R. Hermans, Cardiovascular Research Institute, University of Maastricht (The Netherlands), for providing us with V79MZh11B1 cells.

References

- (1) Jemal, A.; Siegel, R.; Ward, E.; Hao, Y.; Xu, J.; Murray, T.; Thun, M. J. Cancer statistics, 2008. *CA Cancer J. Clin.* **2007**, *57*, 43–66.
- (2) Huggins, C. Endocrine factors in cancer *J. Urol.* **1952**, *68*, 875–884.
- (3) Labrie, F.; Dupont, A.; Belanger, A.; Cusan, L.; Lacourciere, Y.; Monfette, G.; Laberge, J. G.; Emond, J. P.; Fazekas, A. T.; Raynaud, J. P.; Husson, J. M. New hormonal therapy in prostatic carcinoma: combined treatment with LHRH agonist and an antiandrogen. *Clin. Invest. Med.* **1982**, *5*, 267–275.
- (4) Huhtaniemi, I.; Nikula, H.; Parvinen, M.; Rannikko, S. Histological and functional changes of the testis tissue during GnRH agonist treatment of prostatic cancer. *Am. J. Clin. Oncol.* **1988**, *11*, Suppl. 1: S11–15.
- (5) (a) Harris, K. A.; Weinberg, V.; Bok, R. A.; Kakefuda, M.; Small, E. J. Low dose ketoconazole with replacement doses of hydrocortisone in patients with progressive androgen independent prostate cancer. *J. Urol.* **2002**, *168*, 542–545. (b) Eklund, J.; Kozloff, M.; Vlamakis, J.; Starr, A.; Mariott, M.; Gallot, L.; Jovanovic, B.; Schilder, L.; Robin, E.; Pins, M.; Bergan, R. C. Phase II study of mitoxantrone and ketoconazole for hormone-refractory prostate cancer. *Cancer* **2006**, *106*, 2459–2465.
- (6) (a) Njar, V. C. O.; Hector, M.; Hartmann, R. W. 20-amino and 20,21-aziridinyl pregnene steroids: development of potent inhibitors of 17 alpha-hydroxylase/C17,20-lyase (P450 17). *Bioorg. Med. Chem.* **1996**, *4*, 1447–1453. (b) Hartmann, R. W.; Hector, M.; Haidar, S.; Ehmer, P.; Reichert, W.; Jose, J. Synthesis and evaluation of novel steroidal oxime inhibitors of P450 17 (17 alpha-hydroxylase/C17-20-lyase) and 5 alpha-reductase types 1 and 2. *J. Med. Chem.* **2000**, *43*, 4266–4277. (c) Hartmann R. W.; Hector, M.; Wachall, B. G.; Paluszczak, A.; Palzer, M.; Huch, V.; Veith, M. Synthesis and evaluation of 17-aliphatic heterocycle-substituted steroidal inhibitors of 17alpha-hydroxylase/C17-20-lyase (P450 17). *J. Med. Chem.* **2000**, *43*, 4437–4445. (d) Haidar, S.; Hartmann, R. W. C16 and C17 substituted derivatives of pregnenolone and progesterone as inhibitors of 17alpha-hydroxylase-C17, 20-lyase: synthesis and biological evaluation. *Arch. Pharm. Pharm. Med. Chem.* **2002**, *335*, 526–534.
- (7) Sergejew, T.; Hartmann, R. W. Pyridyl substituted benzocycloalkenes: new inhibitors of 17 alpha-hydroxylase/17,20-lyase (P450 17 alpha). *J. Enz. Inhib.* **1994**, *8*, 113–122.
- (8) (a) Hartmann, R. W.; Wächter, G. A.; Sergejew, T., Würtz, R.; Dürkop, J. 4,5-Dihydro-3-(2-pyrazinyl)naphtho[1,2-c]pyrazole: a potent and selective inhibitor of steroid-17 alpha-hydroxylase-C17,20-lyase (P450 17). *Arch. Pharm. (Weinheim)* **1995**, *328*, 573–575. (b) Wächter, G. A.; Hartmann, R. W.; Sergejew, T., Grün, G. L.; Ledergerber, D. Tetrahydronaphthalenes: influence of heterocyclic substituents on inhibition of steroid enzymes P450 arom and P450 17. *J. Med. Chem.* **1996**, *39*, 834–841. (c) Zhuang, Y.; Hartmann, R. W. Synthesis and evaluation of azole-substituted 2-aryl-6-methoxy-3,4-dihydronaphthalenes and -naphthalenes as inhibitors of 17 α -hydroxylase-C17,20-lyase (P450 17). *Arch. Pharm. Pharm. Med. Chem.* **1999**, *332*, 25–30. (d) Hartmann, R. W.; Ehmer, P. B.; Haidar, S.; Hector, M.; Jose, J.; Klein, C. D. P.; Seidel, S. B.; Sergejew, T.; Wachall, B. G.; Wächter, G. A.; Zhuang, Y. Synthesis, biological evaluation and molecular modelling studies of methyleneimidazole substituted biaryls as inhibitors of human 17 α -hydroxylase-17,20-lyase (CYP17) – Part I: heterocyclic modifications of the core structure. *Arch. Pharm. Pharm. Med. Chem.* **2002**, *335*, 119–128. (e) Haidar, S.; Ehmer, P. B.; Barassin, S.; Batzl-Hartmann, C.; Hartmann, R. W. Effects of novel 17alpha-hydroxylase/C17, 20-lyase (P450 17, CYP 17) inhibitors on androgen biosynthesis *in vitro* and *in vivo*. *J. Steroid Biochem. Mol. Biol.* **2003**, *84*, 555–562. (f) Clement, O. O.; Freeman, C. M.; Hartmann, R. W.; Paluszczak, A.; Handratta, V. D.; Vasaitis, T. S.; Brodie, A. M. H.; Njar, V. C. O. Three dimensional pharmacophore modeling of human CYP17 inhibitors. Potential agents for prostate cancer therapy. *J. Med. Chem.* **2003**, *46*, 2345–2351.
- (9) Pinto-Bazurco Mendieta, M. A. E.; Negri, M.; Jagusch, C.; Hille, U. E., Müller-Vieira, U.; Schmidt, D.; Hansen, K.; Hartmann, R. W. Synthesis, biological evaluation and molecular modelling studies of novel ACD- and ABD-ring steroidomimetics as inhibitors of CYP17. *Bioorg. Med. Chem. Lett.* **2008**, *18*, 267–273.
- (10) Wachall, B. G.; Hector, M.; Zhuang, Y.; Hartmann, R. W. Imidazole substituted biphenyls: a new class of highly potent and *in vivo* active inhibitors of P450 17 as potential therapeutics for treatment of prostate cancer. *Bioorg. Med. Chem.* **1999**, *7*, 1913–1924.
- (11) (a) Zhuang, Y.; Wachall, B. G.; Hartmann, R. W. Novel imidazolyl and triazolyl substituted biphenyl compounds: synthesis and evaluation as nonsteroidal inhibitors of human 17alpha-hydroxylase-C17, 20-lyase (P450 17). *Bioorg. Med. Chem.* **2000**, *8*, 1245–1252. (b) Leroux, F.; Hutschenreuter, T.; Charrière, C.; Scopelliti, R.; Hartmann, R. W. *N*-(4-Biphenylmethyl)imidazoles as potential therapeutics for the treatment

- of prostate cancer: Metabolic robustness due to fluorine substitution? *Helv. Chim. Act.* **2003**, *86*, 2671–2686.
- (c) Ehmer, P. B.; Hartmann, R. W. Synthesis of hydroxy derivatives of highly potent non-steroidal CYP 17 inhibitors as potential metabolites and evaluation of their activity by a non cellular assay using recombinant human enzyme. *J. Enzyme Inhib. Med. Chem.* **2004**, *18*, 17–32.
- (12) Jagusch, C.; Negri, M.; Hille, U. E.; Hu, Q.; Bartels, M.; Jahn-Hoffman, K.; Pinto-Bazurco Mendieta, M. A. E.; Rodenwaldt, B.; Müller-Vieira, U.; Schmidt, D.; Lauterbach, T.; Recanatini, M.; Cavalli, A.; Hartmann, R. W. Synthesis, biological evaluation and molecular modelling studies of methyleneimidazole substituted biaryls as inhibitors of human 17 α -hydroxylase-17,20-lyase (CYP17) – Part I: heterocyclic modifications of the core structure. *Bioorg. Med. Chem.* **2008**, *16*, 1992–2010.
- (13) Madan, R. A.; Arlen, P. M. Abiraterone. *Cougar Biotechnology. IDrugs* **2006**, *9*, 49–55.
- (14) Schenkman, J. B.; Sligar, S. G.; Cinti, D. L. Substrate interaction with cytochrome P-450. *Pharmacol Ther.* **1981**, *12*, 43–71.
- (15) Miyaura, N.; Suzuki, A. Palladium-catalyzed cross-coupling reactions of organoboron compounds. *Chem. Rev.* **1995**, *95*, 2457–2483.
- (16) Tang, Y.; Dong, Y.; Vennerstrom J. L. The reaction of carbonyldiimidazole with alcohols to form carbamates and *N*-alkylimidazoles *Synthesis* **2004**, *15*, 2540–2544.
- (17) Ehmer, P. B.; Jose, J.; Hartmann, R. W. Development of a simple and rapid assay for the evaluation of inhibitors of human 17 α -hydroxylase-C(17,20)-lyase (P450c17) by coexpression of P450c17 with NADPH-cytochrome-P450-reductase in *Escherichia coli*. *J. Steroid Biochem. Mol. Biol.* **2000**, *75*, 57–63.
- (18) Hodgson, J. ADMET--turning chemicals into drugs. *Nat. Biotechnol.* **2001**, *19*, 722–726.
- (19) Ulmschneider, S.; Müller-Vieira, U.; Klein, C.D.; Antes, I.; Lengauer, T.; Hartmann, R. W. Synthesis and evaluation of (pyridylmethylene)tetrahydronaphthalenes/-indanes and structurally modified derivatives: potent and selective inhibitors of aldosterone synthase. *J. Med. Chem.* **2005**, *48*, 1563-1575.
- (20) Jones, G.; Willett, P.; Glen, R. C.; Leach, A. R.; Taylor, R. Development and validation of a genetic algorithm for flexible docking. *J. Mol. Biol.* **1997**, *267*, 727–748.
- (21) Warren, G.; Andrews, C.; Capelli, A.-M.; Clarke, B.; Lalonde, J.; Lambert, M.; Lindvall, M.; Nevins, N.; Semus, S.; Senger, S.; Tedesco, G.; Wall, I.; Woolven, J.; Peishoff, C.; Head, M. A critical assessment of docking programs and scoring functions. *J Med Chem.* **2006**, *49*, 5912-5931.
- (22) (a) Bottegoni, G.; Cavalli, A.; Recanatini, M. A comparative study on the application of hierarchical-agglomerative clustering approaches to organize outputs of reiterated docking runs. *J. Chem. Inf. Mod.* **2006**, *46*, 852–862. (b) Bottegoni, G.; Rocchia, W.; Recanatini, M.; Cavalli, A. ACIAP, autonomous hierarchical agglomerative cluster analysis based protocol to partition conformational datasets. *Bioinformatics*, **2006**, *22*, 58–65.
- (23) (a) Lin, D.; Zhang, L. H.; Chiao, E.; Miller, L. W. Modeling and mutagenesis of the active site of human P450c17. *Mol. Endocrinol.* **1994**, *8*, 392–402. (b) Auchus, R. J.; Miller, W. L. Molecular modeling of human P450c17 (17 α -hydroxylase/17,20-lyase): insights into reaction mechanisms and effects of mutations. *Mol. Endocrinol.* **1999**, *13*, 1169–1182. (c) Mathieu, A. P.; LeHoux, J. G.; Auchus, R. J. Molecular dynamics of substrate complexes with hamster cytochrome P450c17 (CYP17): mechanistic approach to understanding substrate binding and activities. *Biochim. Biophys. Acta* **2003**, *1619*, 291–300.
- (24) Halgren, T. A. MMFF VII. Characterization of MMFF94, MMFF94s, and other widely available force fields for conformational energies and for intermolecular-interaction energies and geometries. *J. Comput. Chem.* **1999**, *20*, 730–748.
- (25) (a) Becke, A. D. Density-functional thermochemistry. III. The role of exact exchange *J. Chem. Phys.* **1993**, *98*, 5648–5652; (b) Stevens, P. J.; Devlin, J. F.; Chabalowski, C. F.; Frisch, M. J. Ab initio calculation of vibrational absorption and circular dichroism spectra using density functional force fields *J. Phys. Chem.* **1994**, *98*, 11623–11627.

3.1.4.6. Paper VI.

Novel CYP17 inhibitors: synthesis, biological evaluation, structure-activity relationships and modelling of methoxy- and hydroxy-substituted methyleneimidazolyl biphenyls.

Ulrike Hille, Qingzhong Hu, Carsten Vock, Matthias Negri, Marc Bartels, Ursula Müller-Vierira, Thomas Lauterbach, Rolf W. Hartmann.

This article is protected by copyrights of 'European Journal of Medicinal Chemistry'

Europ. J. Med. Chem. **2009**, 44, 2765–2775.

Abstract.

Recently, the steroidal CYP17 inhibitor Abiraterone entered phase II clinical trial for the treatment of androgen dependent prostate cancer. As 17 α -hydroxylase-17,20-lyase (CYP17) catalyzes the last step in androgen biosynthesis, inhibition of this target should affect not only testicular but also adrenal androgen formation. Therefore CYP17 inhibitors should be advantageous over existing therapies, for example with GnRH analogues. However, steroidal drugs are known for side-effects which are due to affinities for steroid receptors. Therefore we decided to synthesize non-steroidal compounds mimicking the natural CYP17 substrates pregnenolone and progesterone. The synthesis and biological evaluation of a series of 15 novel and highly active non-steroidal CYP17 inhibitors are reported. The compounds were prepared via Suzuki-cross-coupling, Grignard reaction and CDI-assisted S_Nt-reaction with imidazole and their inhibitory activity was examined with recombinant human CYP17 expressed in *E. coli*. Promising compounds were further tested for their selectivity against the hepatic enzyme CYP3A4 and the glucocorticoid forming enzyme CYP11B1. All compounds turned out to be potent CYP17 inhibitors. The most active compounds **7** and **8** were much more active than Ketoconazole showing activity comparable to Abiraterone (IC₅₀ values of 90 and 52 nM vs 72 nM). Most compounds also showed higher selectivities than Ketoconazole, but turned out to be less selective than Abiraterone. Docking studies using our CYP17 protein model were performed with selected compounds to study the interactions between the inhibitors and the amino acid residues of the active site.

Introduction.

Prostate Cancer (PC) is the most prevalent cancer in men in the US and Europe [1]. Since about 80% of patients with PC have androgen-dependent disease and respond to hormonal ablation, the presently used treatment is surgical castration (orchidectomy) or its medical equivalent, the application of gonadotropin-releasing hormone (GnRH) analogs to suppress testicular androgen biosynthesis [2]. However, only testicular production of androgens is affected by these strategies, the adrenal formation of androstendione is not and even after 3 months treatment with a GnRH agonist, prostate levels of testosterone and dihydrotestosterone are still about 25 and 10%, respectively [3]. Therefore, there is frequently combination with antiandrogens to counteract the stimulatory effect of androgens on the androgen receptor [4]. However, it is speculated that due to mutations in the androgen receptor, anti-androgens might be recognized as agonists [5, 6], making this so called "combined androgen blockade" therapy not suitable for all patients.

A promising novel target for the treatment of prostate cancer is 17 α -hydroxylase-17,20-lyase (CYP17), the cytochrome b₅ modulated key enzyme [7] for the biosynthesis of androgens, catalysing the 17 α -hydroxylation of pregnenolone and progesterone and the subsequent cleavage of the C 20,21-acetyl group to yield the corresponding androgens dehydroepiandrosterone and androstendione (Fig. 1) [8]. Proof of principle was achieved by the antimycotic Ketoconazole, which clinically turned out to be a good adjuvant therapeutic capable of reducing testosterone levels through unspecific inhibition of CYP17 [9, 10]. Nevertheless, the side-effects it showed were the reason why it was not generally accepted [4]. These drawbacks motivated us and others to look for more active and selective CYP17 inhibitors (for reviews see: [11-16]). Recently, the steroidal CYP17 inhibitor Abiraterone (Fig.2)

passed phase II clinical trials showing high activity in post-docetaxel castration refractory PC patients and seems to have no dose-limiting toxicity [17].

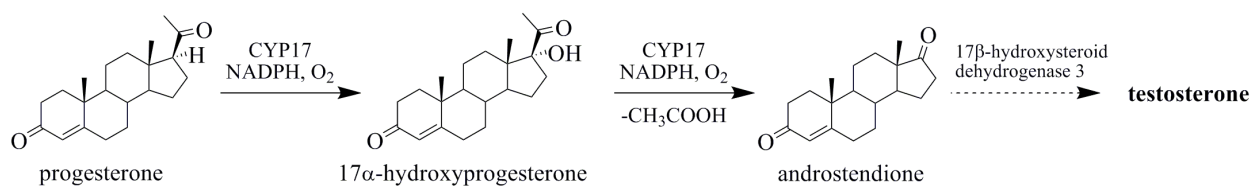


Figure 1. The role of CYP 17 in androgen biosynthesis

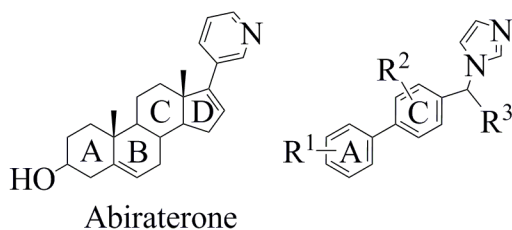


Figure 2: Schematic presentation of Abiraterone and the scaffold of our biaryl inhibitors

In previous works, we described novel *in vitro* and *in vivo* active steroidal [18-22] and non-steroidal [22-35] CYP17 inhibitors. Important for the mode of action of these compounds is a nitrogen-bearing heterocycle which is capable of complexing the heme iron of the enzyme. Very recently we demonstrated that some imidazole-methyl substituted biphenyls designed as AC-ring steroidal mimetics are good CYP17 inhibitors showing moderate selectivity toward other CYP enzymes [32].

In this work, in order to further increase the inhibitory activity of these compounds, different substitution patterns of methoxy- and hydroxy-groups in the A-ring and further selected functional groups in the A- and C-ring were examined. Methyl and ethyl substituents were introduced into the methylene bridge between the biphenyl moiety and the imidazole ring, as we found in previous works [30], that these substituents increase inhibitory potency.

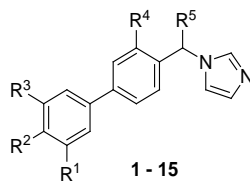
In the following we report about the synthesis of compounds **1–15** (Table 1) and the evaluation of their inhibitory activities toward CYP17 and, for reasons of selectivity, the hepatic enzyme CYP3A4 and the glucocorticoid forming enzyme CYP11B1. Furthermore molecular modelling studies were performed with selected compounds.

Chemistry

The syntheses of compounds **1 – 15** are shown in Schemes 1 and 2. Regarding the functional groups attached to the A-ring, the substances can be divided in alkoxy- and hydroxy-substituted compounds. In case of the methoxy- and ethoxy-substituted compounds **1, 2** and **9 – 12** (Scheme 1), commercially available substituted phenylboronic acids were coupled to bromopropiophenone in a *Suzuki* reaction [36] yielding the ketones **9b – 12b**, and were subsequently reduced with NaBH₄ to the corresponding secondary alcohols **1a, 2a** and **9a – 12a**. The ketones **1b** and **2b** were commercially available.

The hydroxy-substituted compounds **3–8** and **13–15** (Scheme 2) were also prepared via *Suzuki* cross-coupling reaction using phenylboronic acids carrying the carbonyl function and substituted bromophenols to yield the ketones **3b–8b, 13c–14c** and **15b**. Most of the bromophenols latter compounds (**3d, 4d, 13d–15d**) were commercially available. Demethylation of bromoveratrole and 1-bromo-3,5-dimethoxybenzene was achieved with BBr₃ (Method A) to yield **5d** and **6d**. The introduction of the ethyl substituent at the methylene bridge between the biphenylic core and the imidazole was performed by Grignard reaction, yielding the desired secondary alcohols **3a–8a** and **13a–15a**.

All these secondary alcohols **1a–15a** were subjected to a S_N1 reaction with N,N'-carbonyldiimidazole (CDI) to give the imidazole-substituted compounds **1–15** as racemates [37].

Table 1. Inhibition of CYP17 by compounds **1-15**

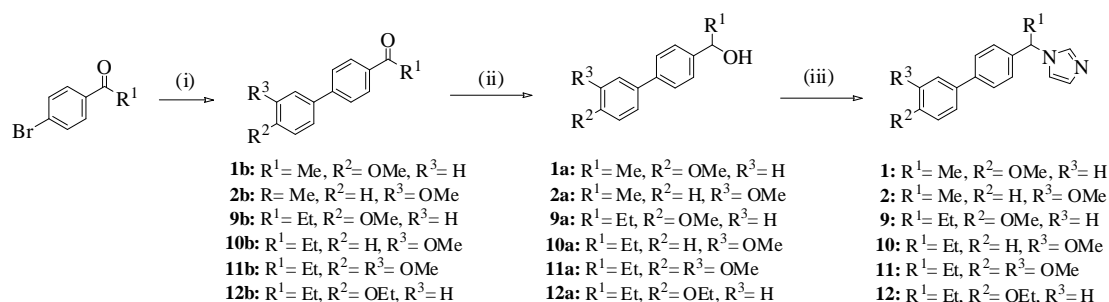
Comp.	Structures					CYP17		
	R ¹	R ²	R ³	R ⁴	R ⁵	% Inhibition ^a		IC ₅₀ ^b
						0.2 μM	2 μM	[nM]
Ref1 ^c	H	OH	H	H	H	1	32	
1	H	OMe	H	H	Me	9	40	
2	OMe	H	H	H	Me	8	59	
3	H	OH	H	H	Et	27	80	231
4	OH	H	H	H	Et	55	89	164
5	OH	OH	H	H	Et	56	91	152
6	OH	H	OH	H	Et	48	90	195
7	H	OH	H	F	Et	64	94	90
8	OH	OH	H	F	Et	69	95	52
9	H	OMe	H	H	Et	2	36	
10	OMe	H	H	H	Et	31	83	188
11	OMe	OMe	H	H	Et	9	58	
12	H	OEt	H	H	Et	3	25	
13	Me	OH	Me	H	Et	28	78	379
14	Me	OH	H	H	Et	45	89	261
15	Cl	OH	H	H	Et	44	89	217
KTZ ^d								2780
ABT ^d								72

^a Concentration of progesterone (substrate): 25 μM; standard deviations were within $\pm 5\%$

^b Concentration of inhibitors required to give 50 % inhibition. The given values are mean values of at least three experiments. The deviations were within $\pm 10\%$

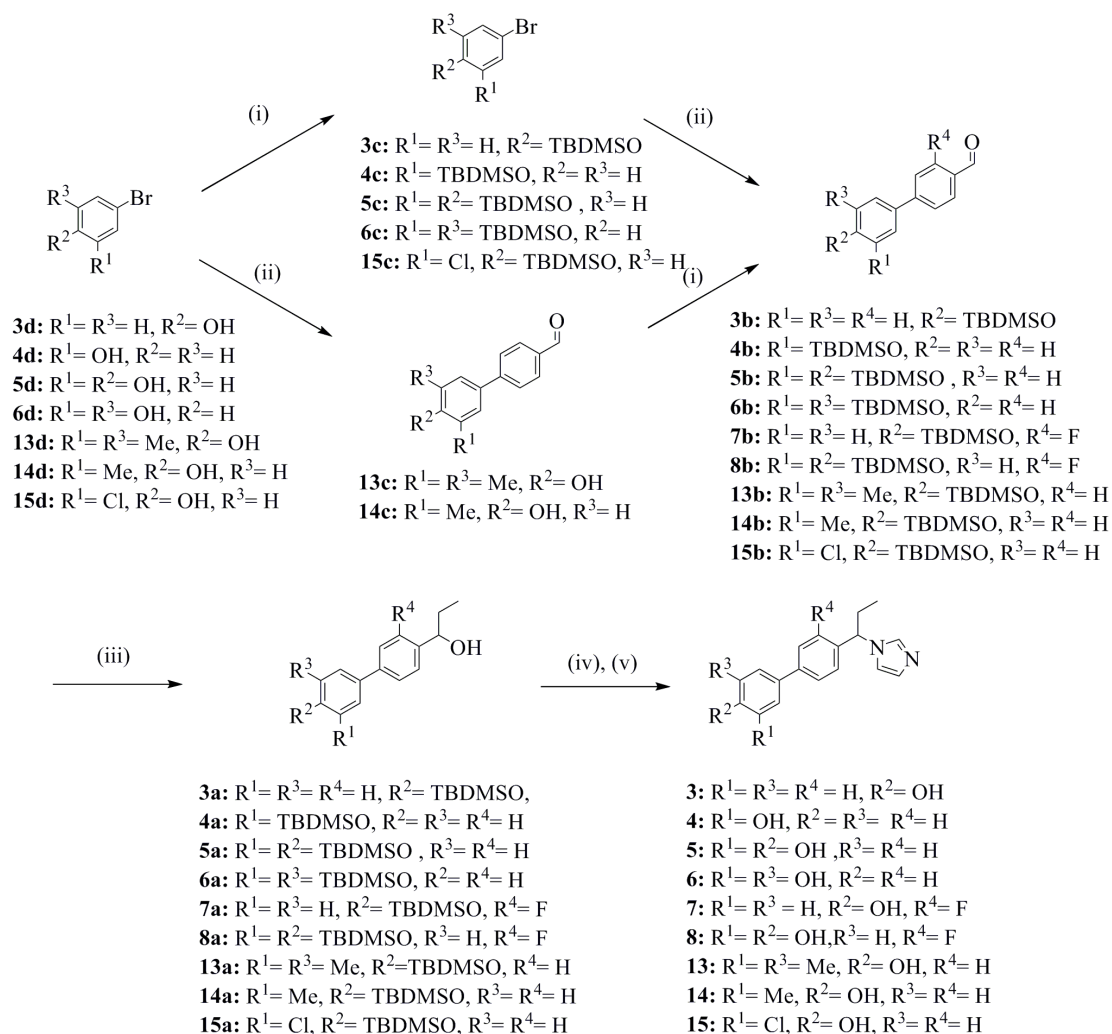
^c From Ref [32]; the IC₅₀ value of 0.31 μM cited therein was obtained using a different source of the enzyme: human testicular microsoma

^d **KTZ**: ketoconazole, **ABT**: abiraterone



Scheme 1. Reagents and conditions: (i) R²R³C₆H₃B(OH)₂, Na₂CO₃, Pd(PPh₃)₄, toluene/MeOH/H₂O, 70 °C, 5 h; (ii) NaBH₄, MeOH, reflux, 2 h; (iii) CDI, NMP, 170 °C, 7 h

The phenolic OH-groups had to be silyl-protected before the Grignard reaction. In most cases this synthetic step was performed before the Suzuki-reaction, as the chromatographic purification after the cross-coupling was easier with the protected compounds. For the final deprotection of the silylated compounds, TBAF was used as standard reagent.



Scheme 2. Reagents and conditions: (i) TBDMSCl, CH₂Cl₂, imidazole, rt, 12 h; (ii) CHOR⁴C₆H₃B(OH)₂, Na₂CO₃, Pd(PPh₃)₄, toluene/MeOH/H₂O, 70 °C, 5 h; (iii) EtMgBr, THF, rt, 5 h; (iv) CDI, NMP, 170 °C, 7 h; (v) TBAF, THF, rt, 12 h.

Results

Biological results

Inhibition of human CYP17 was determined by performing our previously described assay [33] at inhibitor concentrations of 0.2 and 2 μM. In case of the most potent inhibitors IC₅₀ values were determined. As source of human CYP17, our *E. coli* system [38] stably expressing human CYP17 and NADPH-P450 reductase was used. After homogenisation the 50,000 g sediment was incubated with progesterone (25 μM) as substrate and NADPH as previously described [27]. Separation of the product was accomplished by HPLC using UV-detection.

The inhibitory activities of compounds **1** – **15** and the reference compounds Abiraterone, Ketoconazole and **Ref1** [32] toward human CYP17 are shown in Table 1. The compounds can be divided in two classes according to the substituents at the A-ring, namely hydroxy and methoxy derivatives and also in two classes regarding substitution at the methylene bridge, in methyl and ethyl bearing compounds. All compounds were tested as racemates and showed inhibitory activity. The methoxy substituted compounds turned out to be weaker inhibitors compared to the corresponding hydroxy analogues. An exception to this is the 3-OCH₃ compound **10** which showed a similar high activity than the corresponding hydroxy compound **4** (IC₅₀ = 188 nM and 164 nM). Comparing **10** which bears an ethyl group at the methylene bridge with the correspondingly substituted methyl compound **2** clearly showed the significance of the alkyl substitution in this position, which we already have seen with similar compounds [30, 32, 34, 39]. Furthermore it is striking that methoxy substitution in para position (R₂) is not tolerated as the corresponding compounds **1**, **9** and **11** showed little activities.

The hydroxy compounds **3** - **8** and **13** - **15** showed very high inhibition ($IC_{50} = 379 - 52$ nM) with up to fifty fold better IC_{50} values than the reference Ketoconazole ($IC_{50} = 2780$ nM). They also turned out to be much more active than **Ref1** which is certainly due to the ethyl group at the methylene linker. The additional introduction of substituents in compound **3** led to interesting findings. In case of the A-ring, substitution with another OH group is favourable (**5**), while CH_3 or Cl groups did not increase activity (**13** - **15**). Introduction of a F in the C-ring, however, increased the potency and led to the most active inhibitors of this study, compounds **7** and **8** ($IC_{50} = 90$ and 52 nM), the latter even exceeding Abiraterone ($IC_{50} = 72$ nM).

Regarding selectivity against other CYP enzymes, most compounds were tested for inhibition of the hepatic enzyme CYP3A4 at concentrations of 1 and 10 μ M. This enzyme is involved in the metabolism of 50 % of the drugs. Its inhibition leads to drug-drug interactions by prolonging the half-lives of other coadministered drugs. All of the tested compounds showed inhibition of CYP3A4. The ones carrying only one hydroxy substituent at the A-ring (**Ref1** and compounds **3**, **4**, **7**; $IC_{50} > 100$ nM, data shown in supplementary material) were less potent than Ketoconazole ($IC_{50} = 72$ nM), which means they are more selective than the reference. The methoxy-substituted compounds **9**, **10** and **11** were even more selective ($IC_{50} > 200$ nM), however, not reaching Abiraterone ($IC_{50} = 2704$ nM)

Additionally, the most promising compounds were tested for inhibition of the steroidogenic CYP enzyme CYP11B1, which is catalyzing the key step in glucocorticoid biosynthesis. For the assay [40], V79MZh11B1 cells expressing human CYP11B1 were used and the compounds were tested at concentrations 0.2 and 2 μ M. While compounds **3**, **4**, **6**, **7**, **14** and **15** showed high inhibition of this enzyme at both concentrations (>89% at 0.2 μ M and >95% at 2.0 μ M, data shown in supplementary material), compounds **5**, **8** and **13** exhibited less inhibitory activity toward this enzyme (38 - 51% at 0.2 μ M). Interestingly, in contrast to the inhibition of CYP3A4, here the compounds with two vicinal OH-groups showed a very high selectivity and were better than Ketoconazole (61% at 0.2 μ M). However, they did not reach Abiraterone ($IC_{50} = 1608$ nM). Because of this lack of selectivity, the compounds were not further tested for inhibition of other steroidogenic CYP enzymes like CYP11B2 and CYP19.

Molecular modelling studies

Both enantiomers, if existing, of selected energy minimized compounds (**3-11**, **13-15**) were docked into our CYP17 model by means of the GOLD v3.2 software [41] running Linux CentOS 5.1 on Intel(R) P4 CPU 3.00GHz. A slightly modified GOLDScore function with goldscore.P450_pdb.parameters, for better evaluation of hydrophobic interactions, was used. The experimentally proven complexation of the heme iron with sp² hybridized nitrogen [22] was considered in these studies by applying a distance constraint between those two atoms.

For both enantiomers of almost all docked compounds the statistical significant binding mode was **BM1** - the alternative mode **BM2** was less prevalent (Figure 3). These two binding modes could be previously identified by us for biphenylic CYP17 inhibitors [26, 32]. In **BM1** the biaryl skeleton is oriented parallel to the I-helix pointing the A-ring next to a polar area. Hydrophobic and π - π interactions between the conjugated biphenyl core and Phe114 as well as apolar amino acid residues (Gly301, Ala302, Glu305, Ala367 and Ile371) were observed for all compounds.

The ethyl group at the methylene spacer has an important stabilizing role, as already described by us [34]. It anchors in a tiny hydrophobic pocket next to the heme, delimited in its extent by Val366 and Ile371.

The analysis of the docking results was focused on the interaction of the A-ring with the corresponding amino acid residues, since most of the variations on the compounds presented in this article are located here. Regarding the substituents in para position, it can be observed that a hydroxy group is involved in a H-bond net with Arg109, Lys231, His235 and Asp298. In contrast to this, for a methoxy group there is steric hindrance due to His235, Arg109 and the proximal I-helix residues. Depending on the different kind of substituents at the meta position, the R¹ group is oriented toward the F-/G-helix (Asn202, Lys231), if R¹ is MeO or Me or toward Asp298 for OH. The latter group forms a strong H-bond with the carboxylate ($r = 1.9$ Å). In case of the Cl-substituent, it was not possible to determine an unequivocal orientation, because of the bivalent interaction character of this halogen. Looking at the exact orientation of the MeO group, it becomes apparent that it is oriented toward a small hydrophobic pocket, delimited in its extent by Ile238, Lys231, Ile206, Asn202 and Gln199. Its methyl group is placed at about 3.5 - 5 Å from the hydrophobic interaction partners of the mentioned amino acids, while its oxygen showed a reasonable H-bond with Lys231.

Striking for compounds **7** and **8** is the influence of the fluorine in the C-ring which reduces its electrostatic potential. Thus interactions with the backbone atoms of Gly301, Ala302 and Val304 are formed as we already have observed with other inhibitors of this class [32].

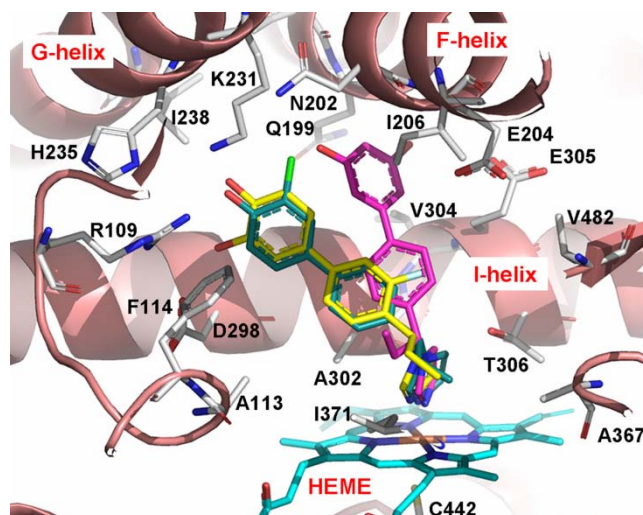


Figure 3. Presentation of the two found binding modes **BM1** (compounds **8** yellow and **15** green-blue) and **BM2** (compound **6** magenta). Heme (cyan), interacting residues and ribbon rendered tertiary structure of the active site are shown. Figure was generated with Pymol (<http://www.pymol.org>).

Discussion and Conclusion

CYP17 is the pivotal enzyme in the biosynthesis of androgens, which are known to promote prostatic tumor growth. GnRH analogs have been shown to be useful in the treatment of prostate cancer by reducing the androgen formation. As outlined above inhibitors of CYP17 could be more efficient therapeutics as they should not only affect testicular androgen formation but also adrenal biosynthesis.

The present work describes a series of new imidazole substituted biphenyls. As they are very potent inhibitors of the target enzyme, our search for new substitution patterns increasing the activity of known biphenylic compounds [30-35, 39] (e.g. **Ref1**) was successful. Regarding the structure-activity relationships obtained in this study, the importance of an ethyl substituent at the methylene bridge was demonstrated and could be explained in the modelling study. With respect to A-ring substitution a strong enhancement of the inhibitory activity was achieved by introduction of hydroxy groups, especially by two vicinal groups in R^1 and R^2 . A very important role plays the fluorine substituent in the C-ring leading to the most active compounds **7** and **8**.

All synthesized compounds are much more potent than the reference Ketoconazole and two compounds reached the inhibitory activity of Abiraterone, which is under clinical investigation. Regarding selectivity toward the hepatic CYP3A4 and the glucocorticoid forming CYP11B1, most of the compounds turned out to be superior to Ketoconazole. However, none of the novel compounds reached the selectivity of the steroidal inhibitor Abiraterone. Therefore further structural optimization has to be performed to overcome this weakness. In our opinion this should be worthwhile as nonsteroidal inhibitors should not interfere with steroid hormone receptors as steroidal drugs do. These studies are presently being performed. The structurally modified compounds will not only be tested for CYP3A4 and CYP11B1 selectivity but also for inhibition of other important hepatic CYP enzymes and steroidogenic CYPs like CYP11B2 and CYP19. As the enantioselectivity of the enzyme is an interesting aspect, the enantiomeric separation of the structural optimized compounds will be performed and the enantiomers will be evaluated.

Experimental Section

CYP17 preparation and assay.

As source of human CYP17, our *E. coli* system [38] coexpressing human CYP17 and NADPH-P450 reductase was used and the assay was performed as previously described [27] using unlabeled progesterone as substrate and applying HPLC with UV-detection for separation.

Inhibition of hepatic enzyme CYP3A4

The recombinantly expressed enzyme from baculovirus-infected insect microsomes (Supersomes) was used and the manufacturer's instructions (www.gentest.com) were followed.

Inhibition of CYP11B1

V79MZh11B1 cells expressing CYP11B1 were used and our assay procedure with [4-¹⁴C]-11-deoxycorticosterone was applied [42].

Chemistry Section

General.

Melting points were determined on a Mettler FP1 melting point apparatus and are uncorrected. IR spectra were recorded neat on a Bruker Vector 33FT-infrared spectrometer. ¹H-NMR spectra were measured on a Bruker DRX-500 (500 MHz). Chemical shifts are given in parts per million (ppm), and TMS was used as an internal standard for spectra obtained in CDCl₃. All coupling constants (*J*) are given in Hz. ESI (electrospray ionization) mass spectra were determined on a TSQ quantum (Thermo Electron Corporation) instrument. Elemental analyses were performed at the Department of Instrumental Analysis and Bioanalysis, Saarland University. Column chromatography was performed using silica-gel 60 (50-200 μm), and reaction progress was determined by TLC analysis on Alugram® SIL G/UV₂₅₄ (Macherey-Nagel). Boronic acids and bromoaryls used as starting materials were obtained commercially (CombiBlocks, Chempur, Aldrich, Acros).

Method A: Boron Tribromide Cleavage of Phenolic Methyl Ethers

To a solution of the corresponding methyl ether in dichloromethane (300 mL) cooled in an ice bath was added BBr₃ (1.5 eq per MeO) dropwise. After 2 h, the mixture was allowed to warm to room temperature and then stirred overnight. Methanol (10 mL) was added dropwise to terminate the reaction, the mixture was poured into water and stirred for another 2 h. Then saturated NaHCO₃-solution (100 mL) was added, and the mixture was extracted with dichloromethane. The extracts were washed with saturated aqueous NaHCO₃ and brine, dried over Na₂SO₄ and concentrated. The resulting crude product was subjected to flash chromatography using silica gel.

4-Bromo-benzene-1,2-diol (5d)

Synthesised according to Method A using 4-bromo-1,2-dimethoxybenzene (8.00 g, 36.9 mmol) and BBr₃ (25.00 g, 100 mmol); pale oil; yield: 6.57 g (94 %); *R*_f = 0.38 (hexane / EtOAc, 9:1); δ_H (CDCl₃, 500 MHz): 5.18 (s, 1H), 5.33 (s, 1H), 6.74 (d, *J* = 8.5 Hz, 1H), 6.93 (dd, *J* = 2.2, 8.5 Hz, 1H), 7.02 (d, *J* = 2.2 Hz, 1H); δ_C (CDCl₃, 125 MHz): 112.6, 116.7, 118.7, 124.0, 142.7, 144.4; MS (ESI): *m/z* = 190 [M⁺+H].

5-Bromo-benzene-1,3-diol (6d)

Synthesised according to Method A using 1-bromo-3,5-dimethoxybenzene (8.00 g, 36.9 mmol) and BBr₃ (25.00 g, 100 mmol); pale oil; yield: 6.77 g (97 %). *R*_f = 0.38 (DCM / MeOH, 98:2); δ_H (CDCl₃, 500 MHz): 5.20 (s, 2H), 6.28 (t, *J* = 2.2 Hz, 1H), 6.67 (d, *J* = 2.2 Hz, 2H); MS (ESI): *m/z* = 190 [M⁺+H].

Method B: Protection of Phenols as TBDMS Ethers

To a solution of the corresponding phenol and imidazole (1.1 eq per OH) in dichloromethane, a solution of *tert*-butyldimethylsilyl chloride in dichloromethane was slowly added (1.1 eq per OH). After being stirred for 4 h at rt, the reaction mixture was poured into water, extracted with dichloromethane, washed with water and brine and dried over Na₂SO₄. Solvent removal under reduced pressure led to a pale oil, which was purified by chromatography on silica gel.

(4-Bromo-phenoxy)-tert-butyl-dimethyl-silane (3c)

Synthesised according to Method B using 4-bromophenol (3d) (3.00 g, 17.3 mmol); pale oil; yield: 4.80 g (94 %); *R*_f = 0.84 (hexane / EtOAc, 9:1); δ_H (CDCl₃, 500 MHz): 0.19 (s, 6H), 0.98 (s, 9H), 6.72 (d, *J* = 8.8 Hz, 2H), 7.32 (d, *J* = 8.8 Hz, 2H); δ_C (CDCl₃, 125 MHz): -4.5, 18.2, 25.6, 113.6, 121.9, 132.3, 154.8; MS (ESI): *m/z* = 288 [M⁺+H].

(3-Bromo-phenoxy)-tert-butyl-dimethyl-silane (4c)

Synthesised according to Method B using 3-bromophenol (4d) (5.00 g, 28 mmol); pale oil; yield: 8.21 g (quant.); *R*_f = 0.81 (hexane / EtOAc, 9:1); δ_H (CDCl₃, 500 MHz): 0.19 (s, 6H), 0.98 (s, 9H), 6.79 – 6.81 (m, 1H), 7.01 – 7.12 (m, 3H); MS (ESI): *m/z* = 288 [M⁺+H].

4-Bromo-1,2-bis-(tert-butyl-dimethyl-silanyloxy)-benzene (5c)

Synthesised according to Method B using **5d** (3.57 g, 18.9 mmol); pale oil; yield: 6.64 g (84 %); $R_f = 0.59$ (hexane); δ_H (CDCl₃, 500 MHz): 0.19 (s, 6H), 0.21 (s, 6H), 0.98 (s, 9H), 0.99 (s, 9H), 6.69 (d, $J = 8.5$ Hz, 1H), 6.92 (dd, $J = 2.5, 8.5$ Hz, 1H), 6.95 (d, $J = 2.5$ Hz, 1H); δ_C (CDCl₃, 125 MHz): -4.18, -4.14, 18.42, 18.44, 25.86, 25.89, 112.7, 122.2, 124.2, 124.3, 146.4, 147.9; MS (ESI): $m/z = 418$ [M⁺+H].

1-Bromo-3,5-bis-(tert-butyl-dimethyl-silanyloxy)-benzene (6c)

Synthesised according to Method B using **6d** (7.17 g, 38.0 mmol); pale oil; yield: 14.45 g (91 %); $R_f = 0.73$ (hexane); δ_H (CDCl₃, 500 MHz): 0.20 (s, 12H), 0.97 (s, 18H), 6.26 (t, $J = 2.2$ Hz, 1H), 6.63 (d, $J = 2.2$ Hz, 2H); MS (ESI): $m/z = 418$ [M⁺+H].

4'-(tert-Butyl-dimethyl-silanyloxy)-3',5'-dimethyl-biphenyl-4-carbaldehyde (13b)

Synthesised according to Method B using **13c** (0.92 g, 4.07 mmol); white solid; yield: 1.32 g (93 %); $R_f = 0.33$ (hexane / EtOAc, 10:1); δ_H (CDCl₃, 500 MHz): 0.25 (s, 6H), 1.08 (s, 9H), 2.31 (s, 6H), 7.28 (s, 2H), 7.70 (d, $J = 8.3$ Hz, 2H), 7.89 (d, $J = 8.3$ Hz, 2H), 10.01 (s, 1H, CHO); δ_C (CDCl₃, 125 MHz): -3.2, 17.6, 18.4, 25.8, 126.7, 127.4, 128.9, 129.8, 132.0, 134.2, 146.7, 152.6, 191.4; MS (ESI): $m/z = 227$ [M⁺+H].

4'-(tert-Butyl-dimethyl-silanyloxy)-3'-methyl-biphenyl-4-carbaldehyde (14b)

Synthesised according to Method B using **14c** (0.96 g, 4.07 mmol); white solid; yield: 1.40 g (95 %); $R_f = 0.33$ (hexane / EtOAc, 10:1); δ_H (CDCl₃, 500 MHz): 0.26 (s, 6H), 1.04 (s, 9H), 2.29 (s, 3H), 6.85 (d, $J = 8.3$ Hz, 1H), 7.36 (dd, $J = 2.3, 8.3$ Hz, 1H), 7.44 (s, 1H), 7.70 (d, $J = 8.3$ Hz, 2H), 7.91 (d, $J = 8.4$ Hz, 2H), 10.03 (s, 1H); δ_C (CDCl₃, 125 MHz): -4.4, 16.8, 25.5, 118.6, 125.4, 126.8, 130.0, 134.3, 146.8, 154.4, 191.7; MS (ESI): $m/z = 227$ [M⁺+H].

(4-Bromo-2-chloro-phenoxy)-tert-butyl-dimethyl-silane (15c)

Synthesised according to Method B using 4-bromo-2-chlorophenol (**15d**) (1.00 g, 4.82 mmol); white solid; yield: 1.40 g (91 %); $R_f = 0.45$ (hexane / EtOAc, 20:1); δ_H (CDCl₃, 500 MHz): 0.22 (s, 6H), 1.02 (s, 9H), 6.75 (d, $J = 8.6$ Hz, 1H), 7.23 (dd, $J = 2.5, 8.6$ Hz, 1H), 7.48 (d, $J = 2.5$ Hz, 1H); δ_C (CDCl₃, 125 MHz): -4.7, 25.3, 112.9, 121.6, 126.6, 130.2, 132.5, 150.7; MS (ESI): $m/z = 322$ [M⁺+H].

Method C: Suzuki-Coupling

To a solution of the corresponding bromobenzene derivative (1.0 eq) in toluene (7 mL / mmol), an aqueous Na₂CO₃ solution (2.0 M; 3.2 mL / mmol) and an ethanolic solution (3.2 mL / mmol) of the corresponding boronic acid (1.5-2.0 eq) were added. The mixture was deoxygenated under reduced pressure and flushed with nitrogen. After having repeated this cycle several times, Pd(PPh₃)₄ (4 mol%) was added, and the resulting suspension was heated under reflux for 8 h. After cooling, ethyl acetate (10 mL) and water (10 mL) were added. The organic phase was separated and the water phase was extracted with ethyl acetate (2 x 10 mL). The combined organic phases were washed with brine, dried over Na₂SO₄, filtered over a short plug of celite[®] and evaporated under reduced pressure. The compounds were purified by flash chromatography using silica gel.

4'-(tert-Butyl-dimethyl-silanyloxy)-biphenyl-4-carbaldehyde (3b)

Synthesised according to Method C using **3c** (4.80 g, 16.7 mmol) and 4-formylphenylboronic acid (5.01 g, 33.4 mmol); yellow solid; yield: 3.80 g (73 %); $R_f = 0.65$ (hexane / EtOAc, 9:1); δ_H (CDCl₃, 500 MHz): 0.25 (s, 6H), 1.02 (s, 9H), 6.94 (d, $J = 8.8$ Hz, 2H), 7.53 (d, $J = 8.8$ Hz, 2H), 7.71 (d, $J = 8.2$ Hz, 2H), 7.92 (d, $J = 8.2$ Hz, 2H), 10.03 (s, 1H); δ_C (CDCl₃, 125 MHz): -4.4, 18.2, 25.6, 120.6, 127.0, 127.6, 128.4, 130.2, 134.7, 146.8, 156.4, 191.8; MS (ESI): $m/z = 297$ [M⁺+H].

3'-(tert-Butyl-dimethyl-silanyloxy)-biphenyl-4-carbaldehyde (4b)

Synthesised according to Method C using **4c** (6.66 g, 22.9 mmol) and 4-formylphenylboronic acid (5.10 g, 34.5 mmol); yellow solid; yield: 3.70 g (52 %); $R_f = 0.60$ (hexane / EtOAc 9/1); the compound was directly used in the next step without further purification and analysis.

3',4'-Bis-(tert-butyl-dimethyl-silanyloxy)-biphenyl-4-carbaldehyde (5b)

Synthesised according to Method C using **5c** (5.30 g, 12.7 mmol) and 4-formylphenylboronic acid (2.80 g, 19.0 mmol); yellow solid; yield: 3.30 g (58 %); $R_f = 0.40$ (hexane / EtOAc, 9:1); the compound was directly used in the next step without further purification and analysis.

3',5'-Bis-(tert-butyl-dimethyl-silanyloxy)-biphenyl-4-carbaldehyde (6b)

Synthesised according to Method C using **6c** (11.0 g, 26.3 mmol) and 4-formylphenylboronic acid (6.00 g, 39.4 mmol); yellow solid; yield: 7.67 g (66 %); $R_f = 0.59$ (hexane / EtOAc, 9:1); the compound was directly used in the next step without further purification and analysis.

4'-(tert-Butyl-dimethyl-silyloxy)-3-fluoro-biphenyl-4-carbaldehyde (7b)

Synthesised according to Method C using **3c** (3.50 g, 11.9 mmol) and 3-fluor-4-formylphenylboronic acid (3.00 g, 17.9 mmol); yellow solid; yield: 3.80 g (73 %); $R_f = 0.47$ (hexane / EtOAc, 9:1); the compound was directly used in the next step without further purification and analysis.

3',4'-Bis-(tert-butyl-dimethyl-silyloxy)-3-fluoro-biphenyl-4-carbaldehyde (8b)

Synthesised according to Method C using **5c** (5.0 g, 12.0 mmol) and 3-fluor-4-formylphenylboronic acid (3.00 g, 17.9 mmol); yellow solid; yield: 3.70 g (67 %); $R_f = 0.68$ (hexane / EtOAc, 9:1); the compound was directly used in the next step without further purification and analysis.

1-(4'-Methoxy-biphenyl-4-yl)-propan-1-one (9b)

Synthesised according to Method C using 4'-bromopropiophenone (2.0 g, 9.4 mmol) and 4-methoxyphenylboronic acid (2.14 g, 14.1 mmol); yellow solid; yield: 2.12 g (94 %); $R_f = 0.29$ (DCM / hexane, 1:1); δ_H (CDCl₃, 500 MHz): 1.25 (t, $J = 7.3$ Hz, 3H), 3.02 (q, $J = 7.3$ Hz, 2H), 3.86 (s, 3H), 7.00 (d, $J = 8.8$ Hz, 2H), 7.57 (d, $J = 8.8$ Hz, 2H), 7.63 (d, $J = 8.5$ Hz, 2H), 8.01 (d, $J = 8.5$ Hz, 2H); δ_C (CDCl₃, 125 MHz): 8.3, 31.8, 55.4, 114.4, 126.6, 128.3, 128.6, 132.3, 135.0, 145.1, 159.9, 200.4; MS (ESI): $m/z = 241$ [M⁺+H].

1-(3'-Methoxy-biphenyl-4-yl)-propan-1-one (10b)

Synthesised according to Method C using 4'-bromopropiophenone (2.0 g, 9.4 mmol) and 3-methoxyphenylboronic acid (2.14 g, 14.1 mmol); orange solid; yield: 2.30 g (96 %); $R_f = 0.29$ (DCM / hexane, 1:1); δ_H (CDCl₃, 500 MHz): 1.25 (t, $J = 7.3$ Hz, 3H), 3.04 (q, $J = 7.3$ Hz, 2H), 3.88 (s, 3H), 6.95 (ddd, $J = 0.6, 2.5, 8.2$ Hz, 1H), 7.15 (t, $J = 2.5$ Hz, 1H), 7.20–7.22 (m, 1H), 7.39 (t, $J = 8.2$ Hz, 1H), 7.67 (d, $J = 8.5$ Hz, 2H), 8.03 (d, $J = 8.5$ Hz, 2H); δ_C (CDCl₃, 125 MHz): 8.3, 31.8, 55.3, 113.0, 113.5, 119.7, 127.3, 128.5, 130.0, 135.8, 141.4, 160.0, 200.4; MS (ESI): $m/z = 241$ [M⁺+H].

1-(3',4'-Dimethoxy-biphenyl-4-yl)-propan-1-one (11b)

Synthesised according to Method C using 4'-bromopropiophenone (2.00 g, 9.4 mmol) and 3,4-dimethoxyphenylboronic acid (2.57 g, 14.1 mmol); orange solid; yield: 2.41 g (95 %); $R_f = 0.37$ (DCM); δ_H (CDCl₃, 500 MHz): 1.25 (t, $J = 7.3$ Hz, 3H), 3.03 (q, $J = 7.3$ Hz, 2H), 3.94 (s, 3H), 3.97 (s, 3H), 6.97 (d, $J = 8.2$ Hz, 1H), 7.14 (d, $J = 2.2$ Hz, 1H), 7.20 (dd, $J = 2.2, 8.2$ Hz, 1H), 7.64 (d, $J = 8.5$ Hz, 2H), 8.02 (d, $J = 8.5$ Hz, 2H); MS (ESI): $m/z = 271$ [M⁺+H].

1-(4'-Ethoxy-biphenyl-4-yl)-propan-1-one (12b)

Synthesised according to Method C using 4'-bromopropiophenone (0.86 g, 4.0 mmol) and 4-ethoxyphenylboronic acid (1.00 g, 6.02 mmol); yellow solid; yield: 0.96 g (94 %); $R_f = 0.32$ (hexane / EtOAc, 9:1); δ_H (CDCl₃, 500 MHz): 1.25 (t, $J = 7.3$ Hz, 3H), 1.45 (t, $J = 6.9$ Hz, 3H), 3.03 (q, $J = 7.3$ Hz, 2H), 4.10 (q, $J = 6.9$ Hz, 2H), 6.68 (d, $J = 8.8$ Hz, 2H), 7.50 (d, $J = 8.8$ Hz, 2H), 7.64 (d, $J = 8.2$ Hz, 2H), 8.01 (d, $J = 8.2$ Hz, 2H); MS (ESI): $m/z = 255$ [M⁺+H].

4'-Hydroxy-3',5'-dimethyl-biphenyl-4-carbaldehyde (13c)

Synthesised according to Method C using 4-bromo-2,6-dimethylphenol (**13d**) (1.00 g, 4.97 mmol) and 4-formylphenyl boronic acid (0.89 g, 5.9 mmol); white solid; yield: 0.92 g (82 %); $R_f = 0.30$ (hexane / EtOAc, 5:1); δ_H (CDCl₃, 500 MHz): 2.33 (s, 6H), 4.81 (bs, 1H), 7.28 (s, 2H), 7.69 (d, $J = 8.3$ Hz, 2H), 7.90 (d, $J = 8.3$ Hz, 2H), 10.03 (s, 1H); δ_C (CDCl₃, 125 MHz): 15.8, 126.4, 126.8, 127.4, 130.0, 131.4, 134.3, 152.7, 191.7; MS (ESI): $m/z = 227$ [M⁺+H].

4'-Hydroxy-3'-methyl-biphenyl-4-carbaldehyde (14c)

Synthesised according to Method C using 4-bromo-2-methylphenol (**14d**) (1.00 g, 5.35 mmol) and 4-formylphenyl boronic acid (0.96 g, 6.4 mmol); white solid; yield: 0.96 g (85 %); $R_f = 0.31$ (hexane / EtOAc, 5:1); δ_H (CDCl₃, 500 MHz): 2.34 (s, 3H), 5.23 (bs, 1H), 6.89 (d, $J = 8.3$ Hz, 1H), 7.37 (dd, $J = 2.3, 8.3$ Hz, 1H), 7.43 (bs, 1H), 7.70 (d, $J = 8.3$ Hz, 2H), 7.91 (d, $J = 8.4$ Hz, 2H), 10.03 (s, 1H); δ_C (CDCl₃, 125 MHz): 15.7, 115.2, 124.3, 125.9, 126.8, 130.1, 131.9, 134.3, 146.8, 154.4, 191.9 (CHO); MS (ESI): $m/z = 213$ [M⁺+H].

4'-(tert-Butyl-dimethyl-silyloxy)-3'-chloro-biphenyl-4-carbaldehyde (15b)

Synthesised according to Method C using **15c** (1.40 g, 4.35 mmol) and 4-formylphenyl boronic acid (0.78 g, 5.5 mmol); white solid; yield: 1.22 g (81 %); $R_f = 0.33$ (hexane / EtOAc, 10:1); δ_H (CDCl₃, 500 MHz): 0.27 (s, 6H), 1.06 (s, 9H), 6.98 (d, $J = 8.4$ Hz, 1H), 7.41 (dd, $J = 2.3, 8.4$ Hz, 1H), 7.65 (d, $J = 2.3$ Hz, 1H), 7.69 (d, $J = 8.3$ Hz, 2H), 7.93 (d, $J = 8.4$ Hz, 2H), 10.04 (s, 1H); δ_C (CDCl₃, 125 MHz): -4.4, 25.6, 121.1, 126.4, 127.1, 129.1, 130.3, 133.7, 135.1, 145.6, 152.1, 191.8; MS (ESI): $m/z = 348$ [M⁺+H].

Method D: Grignard-Reaction

Under exclusion of air and moisture, an EtMgBr-solution (1.0 M in THF, 1.2 eq) solution in THF was added dropwise to a solution of the aldehyde or ketone (1 eq) in THF (12 mL / mmol). The mixture was stirred overnight at rt. Then water (10 mL) and ethyl acetate (10 mL) were added. The organic phase was separated and washed with water and brine, dried over Na₂SO₄, and evaporated under reduced pressure. The crude products were purified by flash chromatography using silica gel.

1-[4'-(tert-Butyl-dimethyl-silyloxy)-biphenyl-4-yl]-propan-1-ol (3a)

Synthesised according to Method D using **3b** (3.30 g, 10.6 mmol) and EtMgBr (1.0 M in THF, 12.7 mL, 12.7 mmol); white solid; yield: 1.89 g (52 %); $R_f = 0.40$ (hexane / EtOAc, 9:1); δ_H (CDCl₃, 500 MHz): 0.23 (s, 6H), 0.95 (t, $J = 7.3$ Hz, 3H), 1.00 (s, 9H), 1.76 – 1.89 (m, 2H), 4.64 (t, $J = 6.6$ Hz, 1H), 6.90 (d, $J = 8.5$ Hz, 2H), 7.38 (d, $J = 8.5$ Hz, 2H), 7.46 (d, $J = 8.5$ Hz, 2H), 7.54 (d, $J = 8.5$ Hz, 2H); MS (ESI): $m/z = 344$ [M⁺+H].

1-[3'-(tert-Butyl-dimethyl-silyloxy)-biphenyl-4-yl]-propan-1-ol (4a)

Synthesised according to Method D using **4b** (3.70 g, 11.9 mmol) and EtMgBr (1.0 M, 14.3 mL, 14.3 mmol); white solid; yield: 2.02 g (45 %); $R_f = 0.40$ (hexane / EtOAc, 9:1); δ_H (CDCl₃, 500 MHz): 0.27 (s, 6H), 0.97 (t, $J = 7.3$ Hz, 1H), 1.05 (s, 9H), 1.76 – 1.91 (m, 2H), 2.15 – 2.38 (m, 1H), 4.65 (t, $J = 6.6$ Hz, 1H), 6.86 (m, 1H), 7.11 (m, 1H), 7.21 (d, $J = 7.9$ Hz, 1H), 7.31 (t, $J = 7.9$ Hz, 1H), 7.41 (d, $J = 8.2$ Hz, 2H), 7.57 (d, $J = 8.2$ Hz, 2H); δ_C (CDCl₃, 125 MHz): -4.4, 9.9, 21.2, 25.7, 29.2, 77.1, 118.8, 119.0, 120.1, 126.9, 127.1, 129.6, 139.6, 140.5, 142.2, 156.0; MS (ESI): $m/z = 344$ [M⁺+H].

1-[3',4'-Bis-(tert-butyl-dimethyl-silyloxy)-biphenyl-4-yl]-propan-1-ol (5a)

Synthesised according to Method D using **5b** (6.09 g, 13.7 mmol) and EtMgBr (1.0 M, 16.4 mL, 16.4 mmol); white solid; yield: 1.55 g (25 %); $R_f = 0.62$ (hexane / EtOAc, 7:3); δ_H (CDCl₃, 500 MHz): 0.22 (s, 6H), 0.23 (s, 6H), 0.88 (t, $J = 7.3$ Hz, 3 H), 1.00 (s, 9H), 1.01 (s, 9H), 1.68 – 1.81 (m, 2H), 2.51 (bs, 1H), 4.52 (t, $J = 6.6$ Hz, 1H), 6.86 (d, $J = 8.2$ Hz, 1H), 7.02 (dd, $J = 2.2, 8.2$ Hz, 1H), 7.08 (d, $J = 2.2$ Hz, 1H), 7.31 (d, $J = 8.2$ Hz, 2H), 7.45 (d, $J = 8.2$ Hz, 2H); δ_C (CDCl₃, 125 MHz): -4.08, -4.12, 10.1, 18.38, 18.39, 25.90, 25.92, 31.7, 75.5, 119.7, 119.9, 121.2, 126.3, 126.5, 134.3, 139.8, 143.1, 146.4, 146.9; MS (ESI): $m/z = 474$ [M⁺+H].

1-[3',5'-Bis-(tert-butyl-dimethyl-silyloxy)-biphenyl-4-yl]-propan-1-ol (6a)

Synthesised according to Method D using **6b** (6.85 g, 15.5 mmol) and EtMgBr (1.0 M, 18.6 mL, 18.6 mmol); yellow solid; yield: 3.60 g (49 %); the compound was directly used in the next step without further purification and analysis.

1-[4'-(tert-Butyl-dimethyl-silyloxy)-3-fluoro-biphenyl-4-yl]-propan-1-ol (7a)

Synthesised according to Method D using **7b** (3.01 g, 9.10 mmol) and EtMgBr (1.0 M, 10.9 mL, 10.9 mmol); white solid; yield: 1.30 g (40 %); $R_f = 0.48$ (hexane / EtOAc, 9:1); δ_H (CDCl₃, 500 MHz): 0.25 (s, 6H), 0.98 (t, $J = 7.3$ Hz, 3H), 1.03 (s, 9H), 1.79 – 1.89 (m, 2H), 2.33 (bs, 1H), 4.94 – 4.97 (m, 1H), 6.91 (d, $J = 8.8$ Hz, 2H), 7.20 (dd, $J = 1.9, 12.0$ Hz, 1H), 7.33 (dd, $J = 1.9, 8.2$ Hz, 1H), 7.44 – 7.46 (m, 3H); MS (ESI): $m/z = 361$ [M⁺+H].

1-[3',4'-Bis-(tert-butyl-dimethyl-silyloxy)-3-fluoro-biphenyl-4-yl]-propan-1-ol (8a)

Synthesised according to Method D using **8b** (3.71 g, 8.00 mmol) and EtMgBr (1.0 M, 9.6 mL, 9.6 mmol); yellow solid; yield: 1.36 g (35 %); $R_f = 0.34$ (hexane / EtOAc, 9:1); the compound was directly used in the next step without further purification and analysis.

1-[4'-(tert-Butyl-dimethyl-silyloxy)-3',5'-dimethyl-biphenyl-4-yl]-propan-1-ol (13a)

Synthesised according to Method D using **13b** (1.32 g, 3.88 mmol) and EtMgBr (1.0 M, 4.65 mL, 4.65 mmol) solution in THF. Yield: 1.24 g (86 %); $R_f = 0.15$ (hexane / EtOAc, 10:1); white solid; δ_H (CDCl₃, 500 MHz): 0.24 (s, 6H), 0.95 (t, $J = 7.4$ Hz, 3H), 1.08 (s, 9H), 1.77-1.88 (m, 2H), 1.93 (bs, 1H), 2.29 (s, 6H), 4.62 (t, $J = 6.5$ Hz, 1H), 7.23 (s, 2H), 7.37 (d, $J = 8.3$ Hz, 2H), 7.54 (d, $J = 8.3$ Hz, 2H); δ_C (CDCl₃, 125 MHz): -3.2, 9.9, 17.7, 25.8, 31.5, 75.5, 125.9, 126.4, 127.1, 128.6, 133.4, 140.0, 142.5, 151.6; MS (ESI): $m/z = 227$ [M⁺+H].

1-[4'-(tert-Butyl-dimethyl-silyloxy)-3'-methyl-biphenyl-4-yl]-propan-1-ol (14a)

Synthesised according to Method D using **14b** (1.40 g, 4.29 mmol) with EtMgBr (1.0 M, 4.71 mL, 4.71 mmol) solution in THF; white solid; yield: 1.24 g (81 %); $R_f = 0.15$ (hexane / EtOAc, 10:1); the compound was directly used in the next step without further purification and analysis.

1-[4'-(tert-Butyl-dimethyl-silyloxy)-3'-chloro-biphenyl-4-yl]-propan-1-ol (15a)

Synthesised according to Method D using **15b** (1.22 g, 3.52 mmol) with EtMgBr (1.0 M, 3.87 mL, 3.87 mmol) solution in THF; white solid; yield: 1.05 g (79 %); $R_f = 0.18$ (hexane / EtOAc, 10:1); the compound was directly used in the next step without further purification and analysis.

Method E: Reduction with NaBH₄

To an ice-cooled solution of the corresponding aldehyde or ketone (1.0 eq) in methanol (5 mL / mmol) was added NaBH₄ (2.0 eq). The resulting mixture was heated to reflux for 30 minutes. After cooling to ambient temperature, the solvent was distilled off under reduced pressure. Water (10 mL) was added, and the aqueous layer was extracted with ethyl acetate (3 x 10 mL). The combined organic phases were washed with brine, dried over MgSO₄ and evaporated under reduced pressure. The desired product was purified by chromatography using silica gel.

1-(4'-Methoxy-biphenyl-4-yl)-ethanol (1a)

Synthesised according to Method E using 1-(4'-methoxybiphenyl-4-yl)ethanone (**1b**) (0.23 g, 1.00 mmol) and NaBH₄ (0.15 g, 3.98 mmol); colourless solid; yield: 0.13 g (58 %); $R_f = 0.16$ (hexane / EtOAc, 10:1); the compound was directly used in the next step without further purification and analysis.

1-(3'-Methoxy-biphenyl-4-yl)-ethanol (2a)

Synthesised according to Method E using 1-(3'-methoxybiphenyl-4-yl)ethanone (**2b**) (0.62 g, 2.71 mmol) and NaBH₄ (0.19 g, 4.88 mmol); colourless solid; yield: 0.45 g (72 %); $R_f = 0.17$ (hexane / EtOAc, 10:1); IR (ATR) $\tilde{\nu}$ (cm⁻¹): 3388 (m), 1600 (m), 1481 (m), 1295 (m), 1214 (s), 1053 (m), 832 (s), 777 (s), 695 (m); δ_H (CDCl₃, 500 MHz): 1.54 (d, $J = 6.4$ Hz, 3H), 1.77 (bs, 1H), 3.87 (s, 3H), 4.96 (q, $J = 6.4$ Hz, 1H), 6.90 (dd, $J = 2.2, 8.2$ Hz, 1H), 7.12 (bt, $J = 2.2$ Hz, 1H), 7.17 - 7.19 (m, 1H), 7.36 (t, $J = 7.9$ Hz, 1H), 7.45 (d, $J = 8.2$ Hz, 2H), 7.58 (d, $J = 8.2$ Hz, 2H); δ_C (CDCl₃, 125 MHz): 25.1, 55.3, 70.1, 112.6, 112.8, 119.6, 125.8, 127.3, 129.7, 140.3, 142.4, 145.0, 159.9; MS (ESI): $m/z = 211$ [M⁺+H-H₂O].

1-(4'-Methoxy-biphenyl-4-yl)-propan-1-ol (9a)

Synthesised according to Method E using **9b** (2.12 g, 8.80 mmol) and NaBH₄ (0.64 g, 17 mmol); white solid; yield: 1.85 g (87 %); $R_f = 0.37$ (DCM); δ_H (CDCl₃, 500 MHz): 0.95 (t, $J = 7.6$ Hz, 3H), 1.77 - 1.89 (m, 3H), 3.85 (s, 3H), 4.64 (t, $J = 6.6$ Hz, 1H), 6.98 (d, $J = 8.5$ Hz, 2H), 7.39 (d, $J = 8.5$ Hz, 2H), 7.52 - 7.55 (m, 4H); δ_C (CDCl₃, 125 MHz): 10.2, 31.8, 55.3, 75.8, 114.2, 126.4, 126.7, 128.1, 133.4, 140.1, 143.0, 159.1; MS (ESI): $m/z = 243$ [M⁺+H].

1-(3'-Methoxy-biphenyl-4-yl)-propan-1-ol (10a)

Synthesised according to Method E using **10b** (2.30 g, 9.00 mmol) and NaBH₄ (0.76 g, 20 mmol); white solid; yield: 1.87 g (86 %); $R_f = 0.37$ (DCM); δ_H (CDCl₃, 500 MHz): 0.95 (t, $J = 7.3$ Hz, 3H), 1.78 - 1.90 (m, 3H), 3.88 (s, 3H), 4.65 (t, $J = 6.4$ Hz, 1H), 6.98 (ddd, $J = 0.6, 2.5, 8.2$ Hz, 1H), 7.17 (t, $J = 2.5$ Hz, 1H), 7.22 - 7.24 (m, 2H), 7.71 (d, $J = 8.5$ Hz, 2H), 8.06 (d, $J = 8.5$ Hz, 2H); δ_C (CDCl₃, 125 MHz): 10.3, 31.8, 55.3, 76.1, 113.0, 113.4, 119.7, 127.4, 128.2, 130.0, 135.8, 141.4, 159.9; MS (ESI): $m/z = 243$ [M⁺+H].

1-(3',4'-Dimethoxy-biphenyl-4-yl)-propan-1-ol (11a)

Synthesised according to Method E using **11b** (2.41 g, 8.90 mmol) and NaBH₄ (0.76 g, 20 mmol); yellow solid; yield: 2.03 g (84 %); $R_f = 0.31$ (DCM); δ_H (CDCl₃, 500 MHz): 0.99 (t, $J = 7.3$ Hz, 3H), 1.81 - 1.90 (m, 3H), 3.82 (s, 3H), 3.84 (s, 3H), 4.59 (t, $J = 6.6$ Hz, 1H), 6.94 (d, $J = 8.2$ Hz, 1H), 7.07 (d, $J = 2.2$ Hz, 1H), 7.11 (dd, $J = 2.2, 8.2$ Hz, 1H), 7.30 (d, $J = 8.2$ Hz, 2H), 7.55 (d, $J = 8.2$ Hz, 2H); MS (ESI): $m/z = 273$ [M⁺+H].

1-(4'-Etoxy-biphenyl-4-yl)-propan-1-ol (12a)

Synthesised according to Method E using **12b** (1.32 g, 5.20 mmol) and NaBH₄ (0.39 g, 10 mmol); white solid; yield: 1.14 g (86 %); $R_f = 0.16$ (hexane / EtOAc 9:1); δ_H (CDCl₃, 500 MHz): 0.95 (t, $J = 7.3$ Hz, 3H), 1.42 (t, $J = 6.6$ Hz, 3H), 2.22 - 2.29 (m, 2H), 4.07 (q, $J = 6.6$ Hz, 2H), 5.03 (t, $J = 7.7$ Hz, 1H), 6.97 (d, $J = 8.8$ Hz, 2H), 7.40 (d, $J = 8.2$ Hz, 2H), 7.53 - 7.56 (m, 4H); MS (ESI): $m/z = 257$ [M⁺+H].

Method F: CDI reaction (Compounds **1**, **2**, **9** - **12**)

To a solution of the corresponding alcohol (1.0 eq) in *N*-Methyl-2-pyrrolidone (NMP) or acetonitrile (10 mL / mmol), CDI (5.0 eq) was added at rt. The solution was heated to reflux for 4 to 18 h. After cooling to ambient temperature, the reaction mixture was diluted with water (30 mL) and extracted with ethyl acetate (3 x 10 mL). The combined organic phases were washed with brine, dried over MgSO₄ and evaporated under reduced pressure. The crude product was purified via chromatography using silica gel.

1-[1-(4'-Methoxy-biphenyl-4-yl)-ethyl]-1H-imidazole (**1**)

Synthesised according to Method F using **1a** (0.20 g, 0.88 mmol) and CDI (0.28 g, 1.8 mmol) in acetonitrile; colourless solid; yield: 0.12 g (49 %); $R_f = 0.15$ (EtOAc); IR (ATR) $\tilde{\nu}$ (cm⁻¹): 1605 (m), 1595 (s), 1247 (s), 1209 (m), 1185 (m), 1036 (m), 822 (s), 747 (m), 664 (s); δ_H (CDCl₃, 500 MHz): 1.89 (d, $J = 6.9$ Hz, 3H), 3.84 (s, 3H), 5.37 (q, $J = 6.9$ Hz, 1H), 6.96 (bs, 1H), 6.97 (d, $J = 9.0$ Hz, 2H), 7.10 (bs, 1H), 7.18 (d, $J = 8.2$ Hz, 2H), 7.49 (d, $J = 9.0$ Hz, 2H), 7.52 (d, $J = 8.2$ Hz, 2H), 7.61 (bs, 1H); δ_C (CDCl₃, 125 MHz): 22.0 (CH₃), 55.3 (CH), 56.3 (CH₃), 114.3 (CH),

117.9 (CH), 126.4 (CH), 127.1 (CH), 128.1 (CH), 129.4 (CH), 132.8 (C_q), 136.1 (CH), 139.8 (C_q), 140.7 (C_q), 159.4 (C_q); MS (ESI): $m/z = 279$ [M⁺+H].

1-[1-(3'-Methoxy-biphenyl-4-yl)-ethyl]-1H-imidazole (2)

Synthesised according to Method F using **2a** (0.39 g, 1.7 mmol) and CDI (0.55 g, 3.4 mmol) in acetonitrile; colourless oil; yield: 0.21 g (44 %); $R_f = 0.31$ (EtOAc / MeOH, 95:5); IR (ATR) $\tilde{\nu}$ (cm⁻¹): 1599 (w), 1566 (w), 1481 (m), 1296 (m), 1260 (m), 1220 (s), 1031 (s), 1013 (s), 787 (s); δ_H (CDCl₃, 500 MHz): 1.89 (d, $J = 6.9$ Hz, 3H), 3.85 (s, 3H), 5.39 (q, $J = 6.9$ Hz, 1H), 6.90 (ddd, $J = 1.0, 2.5, 8.2$ Hz, 1H), 6.97 (bs, 1H), 7.08 (dd, $J = 1.6, 2.5$ Hz, 1H), 7.09 (bs, 1H), 7.14 (ddd, $J = 1.0, 1.6, 7.9$ Hz, 1H), 7.20 (d, $J = 8.2$ Hz, 2H), 7.35 (t, $J = 7.9$ Hz, 1H), 7.55 (d, $J = 8.2$ Hz, 2H), 7.63 (bs, 1H); δ_C (CDCl₃, 125 MHz): 21.0 (CH₃), 55.3 (CH₃), 56.3 (CH), 112.8 (CH), 112.9 (CH), 118.0 (CH), 119.5 (CH), 126.4 (CH), 127.6 (CH), 129.3 (CH), 129.8 (CH), 136.0 (CH), 140.5 (C_q), 141.0 (C_q), 141.8 (C_q), 160.0 (C_q); MS (ESI): $m/z = 279$ [M⁺+H].

1-[1-(4'-Methoxy-biphenyl-4-yl)-propyl]-1H-imidazole (9)

Synthesised according to Method F using **9a** (2.12 g, 8.8 mmol) and CDI (7.29 g, 45.0 mmol) in NMP; yellow solid; yield: 0.28 g (11 %) $R_f = 0.52$ (EtOAc / NH₃ (aq, 25%) 97.5:2.5); IR (ATR) $\tilde{\nu}$ (cm⁻¹): 2962 (w), 2932 (w), 1605 (m), 1497 (s), 1254 (s), 818 (s); δ_H (CDCl₃, 500 MHz): 0.97 (t, $J = 7.3$ Hz, 3H), 2.24 – 2.30 (m, 2H), 3.84 (s, 3H), 5.10 (t, $J = 7.6$ Hz, 1H), 6.96 (d, $J = 8.5$ Hz, 2H), 7.00 (bs, 1H), 7.13 (bs, 1H), 7.25 (d, $J = 8.5$ Hz, 2H), 7.49 (d, $J = 8.5$ Hz, 2H), 7.52 (d, $J = 8.5$ Hz, 2H), 7.89 (bs, 1H); δ_C (CDCl₃, 125 MHz): 11.0 (CH₃), 28.4 (CH₂), 55.3 (O-CH₃), 63.4 (CH), 114.3 (CH), 117.9 (CH), 127.0 (CH), 127.1 (CH), 127.9 (C_q), 128.0 (CH), 132.7 (C_q), 136.0 (CH), 137.9 (C_q), 140.9 (C_q), 159.4 (C_{OMe}); MS (ESI): $m/z = 293$ [M⁺+H].

1-[1-(3'-Methoxy-biphenyl-4-yl)-propyl]-1H-imidazole (10)

Synthesised according to Method F using **10a** (2.30 g, 9.0 mmol) and CDI (7.29 g, 45.0 mmol) in NMP; yellow solid; yield: 0.89 g (30 %); $R_f = 0.52$ (EtOAc / NH₃ (aq, 25%) 97.5:2.5); IR (ATR) $\tilde{\nu}$ (cm⁻¹): 2967 (w), 2935 (w), 1503 (s), 1249 (s), 1218 (s), 1024 (s), 806 (s); δ_H (CDCl₃, 500 MHz): 0.95 (t, $J = 7.3$ Hz, 3H), 2.22 – 2.28 (m, 2H), 3.84 (s, 3H), 5.05 (t, $J = 7.9$ Hz, 1H), 6.89 (dd, $J = 2.2, 8.2$ Hz, 1H), 6.98 (bs, 1H), 7.08 (t, $J = 2.2$ Hz, 1H), 7.10 (bs, 1H), 7.13 (d, $J = 7.9$ Hz, 1H), 7.24 (d, $J = 7.9$ Hz, 2H), 7.34 (t, $J = 7.9$ Hz, 1H), 7.54 (d, $J = 8.2$ Hz, 2H), 7.69 (bs, 1H); δ_C (CDCl₃, 125 MHz): 11.0 (CH₃), 28.5 (CH₂), 55.2 (CH₃-O), 63.0 (CH), 112.8 (CH), 112.8 (CH), 117.7 (CH), 119.5 (CH), 126.0 (CH), 127.5 (CH), 129.0 (C_q), 129.8 (CH), 136.2 (C_q), 139.2 (C_q), 140.9 (C_q), 141.7 (CH), 159.9 (C_{OMe}); MS (ESI): $m/z = 293$ [M⁺+H].

1-[1-(3',4'-Dimethoxy-biphenyl-4-yl)-propyl]-1H-imidazole (11)

Synthesised according to Method F using **11a** (2.41 g, 8.90 mmol) and CDI (7.29 g, 45.0 mmol) in NMP; amber oil; yield: 0.69 g (24 %); $R_f = 0.47$ (EtOAc / NH₃ (aq, 25%) 97.5:2.5); IR (ATR) $\tilde{\nu}$ (cm⁻¹): 2967 (w), 2937 (w), 2875 (w), 2838 (w), 1668 (m), 1604 (m), 1583 (m), 1480 (s), 1294 (s), 1101 (s), 816 (s), 778 (s), 743 (s); δ_H (CDCl₃, 500 MHz): 0.99 (t, $J = 7.3$ Hz, 3H), 2.28- 2.35 (m, 2H), 3.92 (s, 3H), 3.94 (s, 3H), 5.21 (t, $J = 7.9$ Hz, 1H), 6.94 (d, $J = 8.2$ Hz, 1H), 7.05 (bs, 1H), 7.07 (d, $J = 2.2$ Hz, 1H), 7.11 (dd, $J = 2.2, 8.2$ Hz, 1H), 7.21 (bs, 1H), 7.30 (d, $J = 8.2$ Hz, 2H), 7.55 (d, $J = 8.2$ Hz, 2H), 8.29 (bs, 1H); δ_C (CDCl₃, 125 MHz): 11.0 (CH₃), 28.5 (CH₂), 55.9 (O-CH₃), 55.9 (O-CH₃), 62.9 (CH), 110.3 (CH), 111.4 (CH), 117.6 (CH), 119.3 (CH), 126.9 (CH), 127.1 (CH), 129.4 (CH), 133.2 (C_q), 136.3 (CH), 138.7 (C_q), 140.8 (C_q), 148.8 (C_q), 149.1 (C_q); MS (ESI): $m/z = 323$ [M⁺+H].

1-[1-(4'-Etoxy-biphenyl-4-yl)-propyl]-1H-imidazole (12)

Synthesised according to Method F using **12a** (1.14 g, 4.45 mmol) and CDI (3.61 g, 22.3 mmol) in NMP; brown solid; yield: 0.60 g (45 %); $R_f = 0.66$ (EtOAc / MeOH 95:5); IR (ATR) $\tilde{\nu}$ (cm⁻¹): 3115 (w), 2976 (w), 2936 (w), 2877 (w), 1606 (m), 1497 (s), 1245 (s), 1043 (s), 827 (s), 815 (s), 784 (s), 740 (s), 665 (s); δ_H (CDCl₃, 500 MHz) 0.95 (t, $J = 7.3$ Hz, 3H), 1.42 (t, $J = 6.9$ Hz, 3H), 2.22 - 2.29 (m, 2H), 4.07 (q, $J = 6.9$ Hz, 2H), 5.03 (t, $J = 7.7$ Hz, 1H), 6.95 (d, $J = 8.8$ Hz, 2H), 6.97 (bs, 1H), 7.09 (bs, 1H), 7.22 (d, $J = 8.2$ Hz, 2H), 7.48 (d, $J = 8.8$ Hz, 2H), 7.52 (d, $J = 8.2$ Hz, 2H), 7.63 (bs, 1H); δ_C (CDCl₃, 125 MHz): 11.1 (CH₃), 14.8 (CH₃), 28.6 (CH₂), 63.1 (CH), 63.5 (CH₂), 114.8 (CH), 117.7 (CH), 126.9 (CH), 127.0 (CH), 128.0 (CH), 129.3 (C_q), 132.6 (CH), 136.3 (CH), 138.4 (C_q), 140.7 (C_q), 158.7 (C_q); MS (ESI): $m/z = 307$ [M⁺+H].

Method G: CDI reaction and Deprotection with TBAF (Compounds 3 – 8, 13 - 15)

To a solution of the corresponding alcohol (1.0 eq) in NMP (10 mL / mmol) CDI (5.0 eq) was added at rt. The solution was heated to reflux for 4 to 18 h. After cooling to ambient temperature, the reaction mixture was diluted with water (30 mL) and extracted with ethyl acetate (3 x 10 mL). The combined organic phases were washed with brine, dried over MgSO₄ and evaporated under reduced pressure. The crude intermediate of the silyl-protected phenol was directly diluted in anhydrous THF, tetrabutylammonium fluoride solution was added (1.0 M in THF, 1.1 eq per TBDMS), and the reaction mixture was stirred for 4 h. The reaction was quenched by addition of methanol,

and the solvent was removed under reduced pressure. The crude product was purified by chromatography using silica gel.

4'-(1-Imidazol-1-yl-propyl)-biphenyl-4-ol (3)

Synthesised according to Method G using **3a** (0.85 g, 2.16 mmol); yellow solid; yield: 0.22 g (37 %); $R_f = 0.21$ (hexane / EtOAc, 5:1); IR (ATR) $\tilde{\nu}$ (cm^{-1}): 2963 (w), 2930 (w), 2364 (w), 1607 (m), 1588 (m), 1498 (s), 1272 (m), 1070 (s), 808 (s), 748 (m), 658 (m); δ_H (DMSO- d_6 , 500 MHz): 0.82 (t, $J = 7.3$ Hz, 3H), 2.21 – 2.25 (m, 2H), 5.23 (t, $J = 7.3$ Hz, 1H), 6.82 (d, $J = 8.8$ Hz, 2H), 6.90 (s, 1H), 7.37 (d, $J = 8.5$ Hz, 2H), 7.46 (d, $J = 8.8$ Hz, 2H), 7.54 (d, $J = 8.5$ Hz, 2H), 7.82 (s, 1H), 9.55 (s, 1H); δ_C (DMSO- d_6 , 125 MHz): 10.9 (CH₃), 27.4 (CH₂), 61.5 (CH), 115.6 (CH), 117.7 (CH), 126.0 (CH), 127.1 (CH), 127.6 (CH), 128.4 (C_q), 130.3 (CH), 130.7 (C_q), 139.3 (CH), 139.5 (C_q), 157.1 (C_q); MS (ESI): $m/z = 279$ [$M^+ + H$].

4'-(1-Imidazol-1-yl-propyl)-biphenyl-3-ol (4)

Synthesised according to Method G using **4a** (1.32 g, 3.36 mmol); yellow solid; yield: 0.20 g (21 %); $R_f = 0.13$ (EtOAc / MeOH, 9:1); IR (ATR) $\tilde{\nu}$ (cm^{-1}): 2963 (w), 2361 (w), 1583 (m), 1564 (m), 1477 (s), 817 (s), 781 (s), 740 (s); δ_H (DMSO- d_6 , 500 MHz): 0.83 (t, $J = 7.3$ Hz, 3H), 2.17 – 2.22 (m, 2H), 5.24 – 5.26 (m, 1H), 6.73 – 6.76 (m, 1H), 6.91 (bs, 1H), 6.99 (t, $J = 2.2$ Hz, 1H), 7.04 (ddd, $J = 0.9, 2.2, 7.6$ Hz, 1H), 7.23 (t, $J = 7.6$ Hz, 1H), 7.33 (t, $J = 1.3$ Hz, 1H), 7.41 (d, $J = 8.2$ Hz, 2H), 7.56 (d, $J = 8.2$ Hz, 2H), 7.83 (t, $J = 0.9$ Hz, 1H), 9.55 (s, 1H); δ_C (DMSO- d_6 , 125 MHz): 10.9 (CH₃), 27.4 (CH₂), 61.5 (CH), 113.4 (CH), 114.4 (CH), 117.4 (CH), 117.7 (CH), 126.7 (CH), 127.1 (CH), 128.5 (CH), 129.8 (CH), 136.4 (CH), 140.4 (C_q), 141.0 (C_q), 157.7 (C_{OH}); MS (ESI): $m/z = 279$ [$M^+ + H$].

4'-(1-Imidazol-1-yl-propyl)-biphenyl-3,4-diol (5)

Synthesised according to Method G using **5a** (1.00 g, 1.92 mmol); yellow solid; yield: 0.19 g (34 %); $R_f = 0.31$ (EtOAc / MeOH, 95:5); IR (ATR) $\tilde{\nu}$ (cm^{-1}): 3285 (m), 3157 (m), 2963 (m), 2931 (m), 2874 (m), 2828 (m), 1770 (m), 1952 (s), 1945 (s), 1495 (s), 1304 (s), 1219 (s), 1086 (s), 805 (s), 755 (s); δ_H (DMSO- d_6 , 500 MHz): 0.81 (t, $J = 7.3$ Hz, 3H), 2.18 – 2.24 (m, 2H), 5.20 – 5.23 (m, 1H), 6.79 (d, $J = 8.2$ Hz, 1H), 6.88 – 6.92 (m, 2H), 7.00 (d, $J = 2.2$ Hz, 1H), 7.31 (t, $J = 1.3$ Hz, 1H), 7.35 (d, $J = 8.2$ Hz, 2H), 7.48 (d, $J = 8.2$ Hz, 2H), 7.82 (bs, 1H), 9.01 (bs, 1H), 9.06 (bs, 1H); MS (ESI): $m/z = 295$ [$M^+ + H$].

4'-(1-Imidazol-1-yl-propyl)-biphenyl-3,5-diol (6)

Synthesised according to Method G using **6a** (2.00 g, 3.83 mmol); yellow solid; yield: 0.06 g (5 %); $R_f = 0.38$ (EtOAc / MeOH, 95 : 5); IR (ATR) $\tilde{\nu}$ (cm^{-1}): 2975 (w), 1595 (m), 1488 (m), 1351 (m), 1167 (s), 1111 (m), 1091 (m), 1077 (m), 1014 (m), 831 (s), 820 (s), 803 (s), 742 (s); δ_H (DMSO- d_6 , 500 MHz) 0.82 (t, $J = 7.3$ Hz, 3H), 2.15 - 2.28 (m, 2H), 5.23 – 5.26 (m, 1H), 6.21 (t, $J = 2.1$ Hz, 1H), 6.44 (d, $J = 2.1$ Hz, 2H), 6.91 (s, 1H), 7.31 (s, 1H), 7.38 (d, $J = 8.2$ Hz, 2H), 7.49 (d, $J = 8.2$ Hz, 2H), 7.82 (s, 1H), 9.36 (s, 2H); δ_C (DMSO- d_6 , 125 MHz): 10.9 (CH₃), 27.5 (CH₂), 61.5 (CH), 101.7 (CH), 104.7 (CH), 117.7 (CH), 126.6 (CH), 127.0 (CH), 128.5 (CH), 132.5 (C_q), 136.4 (CH), 139.9 (C_q), 141.5 (C_q), 158.7 (C_{OH}); MS (ESI): $m/z = 295$ [$M^+ + H$].

3'-Fluoro-4'-(1-imidazol-1-yl-propyl)-biphenyl-4-ol (7)

Synthesised according to Method G using **7a** (crude product); yellow solid; yield: 0.05 g; $R_f = 0.4$ (EtOAc / MeOH, 95:5); IR (ATR) $\tilde{\nu}$ (cm^{-1}): 2974 (w), 2360 (m), 2341 (m), 1607 (m), 1494 (s), 1283 (m), 1223 (m), 1077 (m), 840 (m), 827 (s), 765 (m); δ_H (DMSO- d_6 , 500 MHz): 0.84 (t, $J = 7.3$ Hz, 3H), 2.14 – 2.32 (m, 2H), 5.47 – 5.50 (m, 1H), 6.83 (d, $J = 8.5$ Hz, 2H), 6.90 (bs, 1H), 7.30 (t, $J = 1.3$ Hz, 1H), 7.41 – 7.44 (m, 3H), 7.51 (d, $J = 8.5$ Hz, 2H), 7.81 (bs, 1H), 9.67 (s, 1H); MS (ESI): $m/z = 297$ [$M^+ + H$].

3'-Fluoro-4'-(1-imidazol-1-yl-propyl)-biphenyl-3,4-diol (8)

Synthesised according to Method G using **8a** (crude product); yellow solid; yield: 0.05 g; $R_f = 0.45$ (EtOAc/MeOH, 95:5); IR (ATR) $\tilde{\nu}$ (cm^{-1}): 1500 (s), 1413 (m), 1279 (m), 1264 (s), 1109 (s), 1089 (s), 859 (s), 812 (s), 785 (m), 742 (m); δ_H (CDCl₃, 500 MHz): 1.00 (t, $J = 7.3$ Hz, 3H), 2.26 – 2.32 (m, 2H), 5.35 (t, $J = 7.9$ Hz, 1H), 6.93 – 6.97 (m, 2H), 7.01 (t, $J = 1.3$ Hz, 1H), 7.03 (d, $J = 1.9$ Hz, 1H), 7.10 (t, $J = 1.3$ Hz, 1H), 7.14 (dd, $J = 1.9, 12.0$ Hz, 1H), 7.17 (d, $J = 7.9$ Hz, 1H), 7.24 (dd, $J = 1.9, 8.2$ Hz, 1H), 7.78 (s, 1H); MS (ESI): $m/z = 313$ [$M^+ + H$].

4'-(1-Imidazol-1-yl-propyl)-3,5-dimethyl-biphenyl-4-ol (13)

Synthesised according to Method G using **13a** (0.30 g, 0.71 mmol) and TBAF solution (1.0 M in THF, 0.78 mL, 0.78 mmol); white solid; yield: 0.19 g (85 %); $R_f = 0.22$ (hexane / EtOAc, 5:1); IR (ATR) $\tilde{\nu}$ (cm^{-1}): 2927 (w), 1705 (w), 1484 (s), 1188 (m), 1076 (w), 923 (m), 817 (w), 731 (s), 662 (s), 543 (w); δ_H (CDCl₃, 500 MHz): 0.95 (t, $J = 7.3$ Hz, 3H, CH₃), 2.23 – 2.26 (m, 2H), 2.31 (s, 6H), 5.04 (t, $J = 7.6$ Hz, 1H), 6.97 (s, 1H), 7.09 (s, 1H), 7.18 (s, 2H), 7.20 (d, $J = 8.2$ Hz, 2H), 7.49 (d, $J = 8.2$ Hz, 2H), 7.63 (s, 1H); δ_C (CDCl₃, 125 MHz): 11.1 (CH₃), 16.2 (CH₂), 28.6 (CH₃), 30.9 (CH₃), 63.1 (CH), 117.7 (CH), 126.8 (C_q), 127.1 (CH), 127.2 (CH), 129.3 (CH), 136.3 (C_q), 138.2 (C_q), 141.1 (C_q); MS (ESI): $m/z = 307$ [$M^+ + H$].

4'-(1-Imidazol-1-yl-propyl)-3-methyl-biphenyl-4-ol (14)

Synthesised according to Method G using **14a** (0.24 g, 0.59 mmol) and TBAF solution (1.0 M in THF, 0.89 mL, 0.89 mmol); white solid; yield: 0.14 g (83 %); $R_f = 0.22$ (hexane / EtOAc, 5:1); IR (ATR) $\tilde{\nu}$ (cm⁻¹): 2933 (w), 2361 (w), 1602 (m), 1499 (s), 1398 (m), 1278 (s), 1129 (w), 1087 (w), 1075 (m), 927 (w), 815 (s), 739 (m), 659 (m); δ_H (CDCl₃, 500 MHz): 0.97 (t, $J = 7.3$ Hz, 3H), 2.23 – 2.29 (m, 2H), 2.32 (s, 3H), 5.04 (t, $J = 7.6$ Hz, 1H), 6.81 (d, $J = 8.3$ Hz, 1H), 7.01 (s, 1H), 7.13 (s, 1H), 7.19-7.23 (m, 3H), 7.33 (d, $J = 1.9$ Hz, 1H), 7.50 (d, $J = 8.3$ Hz, 2H), 7.67 (s, 1H); δ_C (CDCl₃, 125 MHz): 11.1 (CH₃), 16.2 (CH₂), 28.5 (CH₃), 63.3 (CH), 115.2 (CH), 117.9 (CH), 124.8 (CH), 125.4 (CH), 126.8, 127.0 (CH), 128.9 (CH), 129.6 (CH), 131.1 (CH), 136.2 (C_q), 137.9 (C_q), 141.2 (C_q), 154.9 (C_{OH}); MS (ESI): $m/z = 293$ [M⁺+H].

3-Chloro-4'-(1-imidazol-1-yl-propyl)-biphenyl-4-ol (15)

Synthesised according to Method G using **15a** (0.27 g, 0.63 mmol) and TBAF solution (1.0 M in THF, 0.91 mL, 0.91 mmol); white solid; yield: 0.18 g (86 %); $R_f = 0.25$ (hexane / EtOAc, 5:1); IR (ATR) $\tilde{\nu}$ (cm⁻¹): 2360(m), 1497 (s), 1293 (s), 1054 (m), 810 (s), 735 (m), 659 (m); δ_H (CDCl₃, 500 MHz): 0.96 (t, $J = 7.3$ Hz, 3H), 2.23 - 2.29 (m, 2H), 5.04 (t, $J = 7.3$ Hz, 1H), 6.99 (d, $J = 8.3$ Hz, 1H), 7.04 (s, 1H), 7.13 (s, 1H), 7.19-7.23 (m, 3H), 7.47 (d, $J = 1.9$ Hz, 1H), 7.52 (d, $J = 8.3$ Hz, 2H), 7.80 (s, 1H); δ_C (CDCl₃, 125 MHz): 11.0 (CH₃), 28.4 (CH₂), 63.5 (CH), 116.9 (CH), 118.1 (CH), 126.6 (CH), 127.0 (CH), 127.1(CH), 127.9 (CH), 135.8 (C_q), 139.9 (C_q); MS (ESI): $m/z = 313$ [M⁺+H].

Docking studies

Ligands

All molecular modelling studies were performed on Intel(R) P4 CPU 3.00GHz running Linux Suse 10.1. The structures of the inhibitors were built with SYBYL 7.3.2 (Sybyl, Tripos Inc., St. Louis, Missouri, USA) and energy-minimized in MMFF94s force-field [43] as implemented in Sybyl. The resulting geometries for our compounds were then subjected to *ab initio* calculation employing the B3LYP functional [44, 45] in combination with a 6-31G* basis set using the package Gaussian03 (Gaussian, Inc., Pittsburgh, PA, 2003).

Docking

Molecular docking calculations were performed for various inhibitors of Table 1. Since the GOLD docking program allows flexible docking of the compounds, no conformational search was employed to the ligand structures. GOLD gave the best poses by a genetic algorithm (GA) search strategy, and then various molecular features were encoded as a chromosome.

Ligands were docked in 50 independent genetic algorithm (GA) runs using GOLD. Heme iron was chosen as active-site origin, while the radius was set equal to 19 Å. The automatic active-site detection was switched on. A distance constraint of a minimum of 1.9 and a maximum of 2.5 Å between the sp²-hybridised nitrogen of the imidazole and the iron was set. Further, some of the GOLDScore parameters were modified to improve the weight of hydrophobic interaction and of the coordination between iron and nitrogen. The genetic algorithm default parameters were set as suggested by the GOLD authors [41]. On the other hand, the annealing parameters of fitness function were set at 3.5 Å for hydrogen bonding and 6.5 Å for Van der Waals interactions.

All 50 poses for each compound were clustered with ACIAP [46, 47] and the representative structure of each significant cluster was selected. The quality of the docked representative poses was evaluated based on visual inspection of the putative binding modes of the ligands, as outcome of docking simulations and cluster analysis.

Acknowledgement.

This work was supported by the Fonds der Chemischen Industrie. U. E. H. is grateful to the European Postgraduate School 532 (DFG) for a scholarship. We thank Professor J. Hermans, Cardiovascular Research Institute (University of Maastricht, The Netherlands), for providing us with V79MZh11B1 cells expressing human CYP11B1. Thanks are due to G. Schmitt, T. Scherzberg and J. Jung for technical assistance.

Supplementary data.

Supplementary data regarding CYP3A4 and CYP11B1 (one table) can be found in the online version, at doi:doi:10.1016/j.ejmech.2009.01.002.

References

- (1) A. Jemal, R. Siegel, E. Ward, T. Murray, J. Xu, M.J. Thun, *CA Cancer J. Clin.* 57 (2007) 43–66.
- (2) J. Huhtaniemi, H. Nikula, M. Parvinen, S. Rannikko, *Am. J. Clin. Oncol.* 11 (Suppl. 1) (1988) S11–5.
- (3) G. Forti, R. Salerno, G. Moneti, S. Zoppi, G. Fiorelli, T. Marinoni, A. Natali, A. Costantini, M. Serio, L. Martini, et al., *J. Clin. Endocrinol. Metab.* 68 (1989) 461–468.
- (4) F. Labrie, A. Dupont, A. Belanger, F.A. Lefebvre, L. Cusan, G. Monfette, J.G. Laberge, J.P. Emond, J.P. Raynaud, J.M. Husson, A.T. Fazekas, *J. Steroid. Biochem.* 19 (1983) 999–1007.
- (5) A.L. Schuurmans, J. Bolt, J. Veldscholte, E. Mulder, *J. Steroid. Biochem. Mol. Biol.* 37 (1990) 849–853.
- (6) I.P. Nnane, B.J. Long, Y.Z. Ling, D.N. Grigoryev, A. M. Brodie, *Br. J. Cancer.* 83 (2000) 74–82.
- (7) M.K. Akhtar, S.L. Kelly, M.A. Kaderbhai, *J. Endocrinol.* 187 (2005) 267–274.
- (8) N.W. Kolar, A.C. Swart, J.I. Mason, P. Swart, *J. Biotechnol.* 129 (2007) 635–644.
- (9) K.A. Harris, V. Weinberg, R.A. Bok, M. Kakefuda, E.J. Small, *J. Urol.* 168 (2002) 542–545.
- (10) J. Eklund, M. Kozloff, J. Vlamakis, A. Starr, M. Mariott, L. Gallot, B. Jovanovic, L. Schilder, E. Robin, M. Pins, R. C. Bergan, *Cancer* 106 (2006) 2459–2465.
- (11) V.C. Njar, A.M. Brodie, *Curr. Pharm. Des.* 5 (1999) 163–180.
- (12) N. Matsunaga, T. Kaku, A. Ojida, T. Tanaka, T. Hara, M. Yamaoka, M. Kusaka, A. Tasaka, *Bioorg. Med. Chem.* 12 (2004) 4313–4336.
- (13) F. Leroux, *Curr. Med. Chem.* 12 (2005) 1623–1629.
- (14) S. Haidar, R.W. Hartmann, *Enzymes and their Inhibition, Drug Development.* CRC Press: Boca Raton: 2005, pp. 241–253.
- (15) R.D. Bruno, V.C. Njar, *Bioorg. Med. Chem.* 15 (2007) 5047–5060.
- (16) E. Baston, F.R. Leroux, *Recent Patents Anticancer Drug Discov.* 2 (2007) 31–58.
- (17) R.A. Madan, P.M. Arlen, *IDrugs.* 9 (2006) 49–55.
- (18) V.C. Njar, M. Hector, R.W. Hartmann, *Bioorg. Med. Chem.* 4 (1996) 1447–1453.
- (19) R.W. Hartmann, M. Hector, B.G. Wachall, A. Paluszczak, M. Palzer, V. Huch, M. Veith, *J. Med. Chem.* 43 (2000) 4437–4445.
- (20) R.W. Hartmann, M. Hector, S. Haidar, P.B. Ehmer, W. Reichert, J. Jose, *J. Med. Chem.* 43 (2000) 4266–4277.
- (21) S. Haidar, R.W. Hartmann, *Arch. Pharm. Pharm. Med. Chem.* 335 (2002) 526–534.
- (22) S. Haidar, P.B. Ehmer, S. Barassin, C. Batzl-Hartmann, R.W. Hartmann, *J. Steroid Biochem. Mol. Biol.* 84 (2003) 555–562.
- (23) O.O. Clement, C.M. Freeman, R.W. Hartmann, V.D. Handratta, T.S. Vasaitis, A.M. Brodie, V.C. Njar, *J. Med. Chem.* 46 (2003) 2345–2351.
- (24) R.W. Hartmann, P.B. Ehmer, S. Haidar, M. Hector, J. Jose, C.D. Klein, S.B. Seidel, T.F. Sergejew, B.G. Wachall, G.A. Wächter, Y. Zhuang, *Arch. Pharm. Pharm. Med. Chem.* 335 (2002) 119–128.
- (25) R.W. Hartmann, G.A. Wächter, T. Sergejew, R. Wurtz, J. Duerkop, *Arch. Pharm. Pharm. Med. Chem.* 328 (1995) 573–575.
- (26) M.A. Pinto-Bazurco Mendieta, M. Negri, C. Jagusch, U.E. Hille, U. Müller-Vieira, D. Schmidt, K. Hansen, R.W. Hartmann, *Bioorg. Med. Chem. Lett.* 18 (2008) 267–273.
- (27) T. Sergejew, R.W. Hartmann, *J. Enzyme Inhib.* 8 (1994) 113–122.
- (28) G.A. Wächter, R.W. Hartmann, T. Sergejew, G.L. Grun, D. Ledergerber, *J. Med. Chem.* 39 (1996) 834–841.
- (29) Y. Zhuang, R.W. Hartmann, *Arch. Pharm. Pharm. Med. Chem.* 332 (1999) 25–30.
- (30) Y. Zhuang, B.G. Wachall, R.W. Hartmann, *Bioorg. Med. Chem.* 8 (2000) 1245–1252.
- (31) B.G. Wachall, M. Hector, Y. Zhuang, R.W. Hartmann, *Bioorg. Med. Chem.* 7 (1999) 1913–1924.
- (32) C. Jagusch, M. Negri, U.E. Hille, Q. Hu, M. Bartels, K. Jahn-Hoffmann, M.A. Pinto-Bazurco Mendieta, B. Rodenwaldt, U. Müller-Vieira, D. Schmidt, T. Lauterbach, M. Recanatini, A. Cavalli, R.W. Hartmann, *Bioorg. Med. Chem.* 16 (2008) 1992–2010.
- (33) T.U. Hutschenreuter, P.B. Ehmer, R.W. Hartmann, *J. Enzyme Inhib. Med. Chem.* 19 (2004) 17–32.
- (34) Q. Hu, M. Negri, K. Jahn-Hoffmann, Y. Zhuang, S. Olgen, M. Bartels, U. Müller-Vieira, D. Schmidt, T. Lauterbach, R.W. Hartmann, *Bioorg. Med. Chem.* (submitted).
- (35) F. Leroux, T. Hutschenreuter, C. Charrière, R. Scopelliti, R.W. Hartmann, *Helvetica Chimica Acta.* 86 (2003) 2671–2686.
- (36) N. Miyaura, A. Suzuki, *Chem. Rev.* 95 (1995) 2457–2483.

- (37) Y. Tang, Y. Dong, J. Vennerstrom, *Synthesis*. 15 (2004) 2540–2544.
- (38) P.B. Ehmer, J. Jose, R.W. Hartmann, *J. Steroid Biochem. Mol. Biol.* 75 (2000) 57–63.
- (39) M.A.E. Pinto-Bazurco Mendieta, M. Negri, Q. Hu, U.E. Hille, C. Jagusch, K. Jahn-Hoffmann, U. Müller-Viera, D. Schmidt, *Arch. Pharm. Pharm. Med. Chem.* (in press).
- (40) P.B. Ehmer, M. Bureik, R. Bernhardt, U. Müller, R.W. Hartmann, *J. Steroid Biochem. Mol. Biol.* 81 (2002) 173–179.
- (41) G. Jones, P. Willett, R. C. Glen, A. R. Leach, R. Taylor, *J. Mol. Biol.* 267 (1997) 727–48.
- (42) S. Ulmschneider, U. Müller-Vieira, C.D. Klein, I. Antes, T. Lengauer, R. W. Hartmann, *J. Med. Chem.* 48 (2005) 1563–1575.
- (43) T.A.J. Halgren, *Comput. Chem* 20 (1999) 730–748.
- (44) P.J. Stevens, J.F. Devlin, C.F. Chabalowski, M.J. Frisch, *J. Phys. Chem.* 98 (1994) 11623–11627.
- (45) A.D. Becke, *J. Chem. Phys.* 98 (1993) 5648–5652.
- (46) G. Bottegoni, W. Rocchia, M. Recanatini, A. Cavalli, *Bioinformatics* 22 (2006) e58–65.
- (47) G. Bottegoni, A. Cavalli, M. Recanatini, *J. Chem. Inf. Model.* 46 (2006) 852–862.

3.1.4.7. Paper VII.

Role of Fluorine Substitution in Biphenyl Methylene Imidazole Type CYP17 Inhibitors for the Treatment of Prostate Carcinoma.

Qingzhong Hu, Matthias Negri, Sureyya Olgen, Rolf W. Hartmann.

Qingzhong Hu and Matthias Negri contributed equally to the work.

submitted to *ChemMedChem* 2010

Abstract.

It has been illuminated that the growth of most prostate carcinoma depends on androgen stimulation. Therefore the inhibition of CYP17 to block androgen biosynthesis is regarded as a promising therapy. Based on our previously identified lead compound **Ref 1**, a series of fluorine substituted biphenyl methylene imidazoles were designed, synthesized and evaluated as CYP17 inhibitors, to elucidate the influence of fluorine on in vitro and in vivo activity. It has been found that *meta*-F substitution on the C- ring improved the activity, whereas *ortho*- substitution reduced the potency. Docking studies which were performed with our human CYP17 homology model suggest multi-polar interactions between fluorine and Arg109, Lys231, His235 and Glu305. As expected, introduction of fluorine also prolonged the plasma half-life. The SARs obtained confirm the reliability of the protein model and result in compound **9** (IC₅₀ = 131 nM) as strong CYP17 inhibitor showing potent activity in the rat, a high bioavailability and a long plasma half-life (12.8 hours).

Introduction.

As the most common malignancy in male elders, prostate carcinoma also acts as a major cause of death.¹ It has been illuminated that the growth of up to 80 % of prostate carcinoma depends on androgen stimulation. Therefore, segregation of tumour cells from androgen will effectively prevent cancer cell proliferation. Since more than 90 % of testosterone is produced in testes, orchidectomy or treatment with gonadotropin-releasing hormone (GnRH) analogues² (chemical castration) are applied in clinic. As this therapy has no effect on the minor amount of androgen produced in the adrenals, androgen receptor antagonists are employed additionally. This is the current standard therapy for prostate carcinoma, the so called “combined androgen blockade” (CAB).³ However, CAB often leads to resistance which can be associated with androgen receptor mutations. The mutated androgen receptor recognizes antagonists and glucocorticoids as agonists, finally resulting in the collapse of CAB therapy.⁴

The shortcomings of CAB waken a more promising alternative: total blockage of androgen biosynthesis, which means inhibition of cytochrome P450-17 (17 α -hydroxylase-17, 20-lyase, CYP17). CYP17 is one of six CYP enzymes involved in steroid biosynthesis. Like all CYP enzymes, CYP17 consists of a heme and an apoprotein moiety. Although all potent inhibitors interfere with the heme, which is common to CYP enzymes, by complexing its central iron ion, it is nevertheless possible to selectively inhibit these enzymes as has been demonstrated with CYP19 (aromatase, estrogen synthase)⁵ and CYP11B2 (aldosterone synthase).⁶ While aromatase inhibitors are already in clinical use,^{5a} the first highly potent and selective CYP11B2 inhibitors have been identified just recently,⁶ some of which are extremely selective.

CYP17, located in both testicular and adrenal tissue,⁷ is the key enzyme catalyzing the conversion of pregnenolone and progesterone to dehydroepiandrosterone (DHEA) and androstenedione, respectively. DHEA can be transformed into androstenedione by 3 β -HSD, which is subsequently converted into the most potent androgen dihydrotestosterone (DHT) in androgen target cells through two enzymatic steps catalyzed by 17 β -HSD1 or 3 and steroid 5 α -reductase (5 α R). Thus, inhibition of CYP17 could annihilate the androgen production both in testes and in adrenals. Furthermore, targeting genetically stable human tissue instead of cancer cells would avoid the resistance caused by mutation.

Ketoconazole (Chart 1), an antimycotic agent showing non-selective inhibition of CYP17, is the first medication which has been used clinically in treatment of prostate carcinoma. Although withdrawn because of side-effects, Ketoconazole shows good curative effects,⁸ which demonstrates the feasibility of prostate carcinoma treatment via CYP17 inhibition. Since then, in mimicry of the physiological substrates, many steroidal CYP17 inhibitors were synthesized by others⁹ and our group,¹⁰ including Abiraterone (Chart 1), which has entered into phase II clinical trial recently. However, the affinity of steroidal compounds toward steroid receptors, which often results in side effects no matter acting as agonists or antagonists, prompted us to develop non-steroidal CYP17 inhibitors.^{11, 12}

Our group has reported about series of biphenyl methylene imidazoles as potent CYP17 inhibitors.¹² A promising lead compound 1-[1-(4'-fluoro-biphenyl-4-yl)-propyl]-1*H*-imidazole^{12g} (**Ref 1**, Chart 1) was identified in the optimization process. In the present investigation this compound was further modified to elevate potency, selectivity as well as pharmacokinetic properties. Since fluorine is known to be able to form multi-polar interactions with several amino acids^{13e-1} and due to its capability to enhance metabolic stability, the biphenyl core was substituted with additional fluorine atoms leading to compounds **1-22**. Exchanging the 1-imidazolyl group by a 5-imidazolyl moiety while maintaining 4-fluoro-phenyl as A- ring, compounds **23-26** were subsequently obtained. Furthermore, besides determination of inhibitory activities toward human CYP17 in vitro, selected compounds were examined for their potency to reduce plasma testosterone concentration and for their pharmacokinetic properties in rats. Moreover, computational investigations were performed: molecular docking studies using our homology model of human CYP17^{12e} to elucidate the enzyme-inhibitor interactions and quantum mechanical studies to explore the influence of fluorine substitution on potency and pharmacokinetic properties of this type of CYP17 inhibitors.

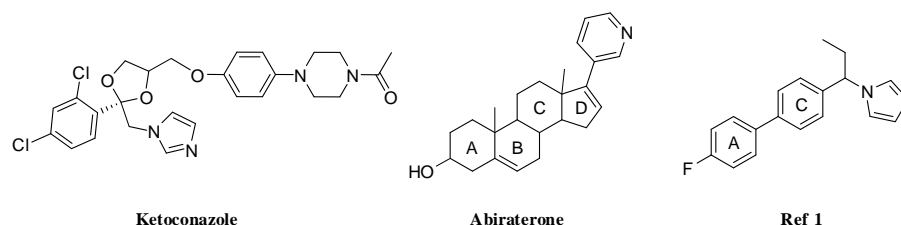


Chart 1. Typical CYP17 inhibitors

Drug design

Fluorine, as the most electronegative atom, has been widely employed to prevent undesired metabolism because of the strong C-F bonds. Besides the increase of metabolic stability, fluorine can also improve other pharmacokinetic properties by means of influencing pKa, elevating lipophilicity and reducing plasma protein binding.¹³ Recently, multi-polar interactions between fluorine and some amino acid residues, responsible for the enhanced binding potency, have also been reported.^{13e-1} Based on these findings, fluorophilicity and fluorophobicity in protein active site have been discussed,^{13c, d} and systemic fluorine scan was recommended in drug discovery and lead optimization.

We found that fluorine substituted at the *para*- position of the A- ring could significantly increase the inhibitory potency of biphenyl methylene imidazole type CYP17 inhibitors, resulting in compound **Ref 1** (IC₅₀ value 345 nM).^{12g} Besides the complexation of the heme iron, recognized as the main anchor point for non-steroidal CYP inhibitors (first notified for CYP19 inhibitors^{5b-c}), by a heterocyclic nitrogen, polar interactions between this fluorine atom and the guanidinium side chain of Arg109 and the amino side chain of Lys231 were observed for **Ref 1** and considered as important for binding affinity^{12g} (Fig. 1). The A- ring is presumably stabilized by a strong T-shaped arene quadrupole interaction with Phe114, a conformationally flexible residue responsible for dividing the CYP17 active site into two lobes. Furthermore, some more amino acid residues such as Asn, Arg or Gln were identified close to the A- or C- ring, which might provide the potential for additional fluorine substituents to form multi-polar interaction with H-X (where X = N, O, S)^{13h-1} and backbone C=O (in an orthogonal manner),^{13e-f} or even with the H-C_α.^{13c, 13g} Consequently, the following strategies to increase the inhibitory potency and the metabolic stability of **Ref 1** were applied: a) shifting the fluorine to other positions in the A- ring; b) additional introduction of fluorine atoms on the A- or C- ring in order to identify new interaction areas. Since these modifications change the molecular electrostatic potentials (MEP) of the compounds, the protein pocket surrounding of the C- ring was scrutinized with the aim to identify potential interaction areas influenced by MEP variations, especially the backbone π-systems of amino acids such as Gly301-Ala302.

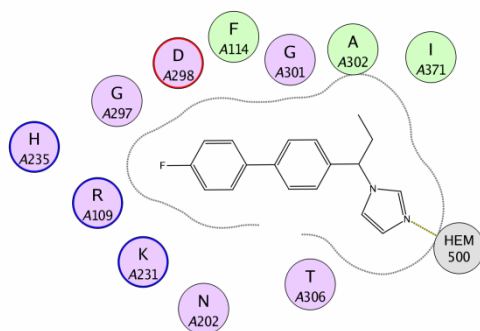
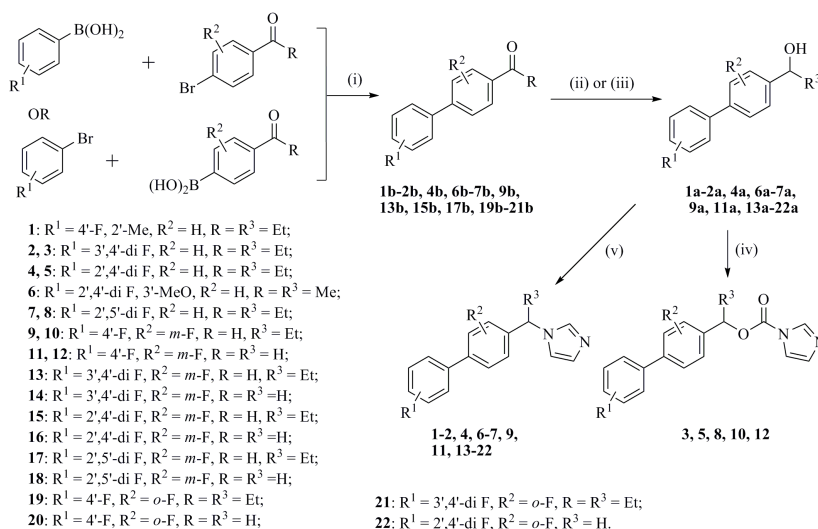


Figure 1. Amino acid residues surrounding **Ref 1**: Arg109 and Lys231 interact with the para- F on the A- ring. Some more amino acid residues around the A- ring or C- ring might form additional multi-polar interactions with further F substituents.

Results and Discussion

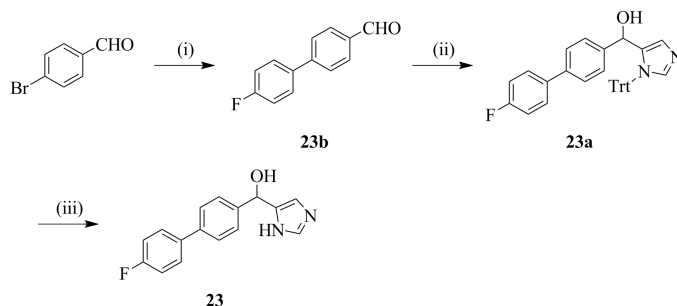
Chemistry. The syntheses of compounds **1-26** are shown in Schemes 1-3. For 1-imidazole analogues **1-22**, a general synthetic strategy was employed: ketone or aldehyde intermediates were obtained by means of Suzuki coupling (Method C) from the corresponding bromides and boronic acids. ¹⁴ Subsequently they were converted to the alcohols by reduction with NaBH₄ (Method D) or Grignard reaction (Method B). The alcohol intermediates reacted with 1, 1-carbonyl diimidazole (CDI) to give the racemic mixtures of the desired products, which were not separated into their enantiomers. Using different reaction conditions, such as solvent and reaction temperature, different products were obtained in this S_Nt reaction. After refluxing in NMP for 4 hours (Method A), ¹⁵ biphenyl methylene imidazoles were obtained; whereas boiling in THF for 4 days (Method E) gave imidazole-1-carboxylic acid biphenyl esters as major products. Distinguishing between these two products is easy as the chemical shifts of imidazole 2-H in biphenyl methylene imidazoles are around 7.6 ppm, whereas they are beyond 8.2 ppm in imidazole-1-carboxylic acid biphenyl esters. ¹⁵ Moreover, the proton chemical shift of CH is 5.1 ppm in the biphenyl methylene imidazoles, whereas in the imidazole-1-carboxylic acid biphenyl esters it is 5.9 ppm. Additionally, the strong carbonyl signal in the IR spectra contributes to the identification of the latter class of compounds. For the synthesis of the 5-imidazole analogues (**23-26**) trityl was employed as protecting group for imidazole. The alcohol intermediates, commercially available or obtained by reaction of imidazolyl lithium with aldehyde, underwent elimination of the H₂O group in acidic environment to give the corresponding isopropylidene product, which was subsequently saturated by hydrogenation of the double bond.

Scheme 1.



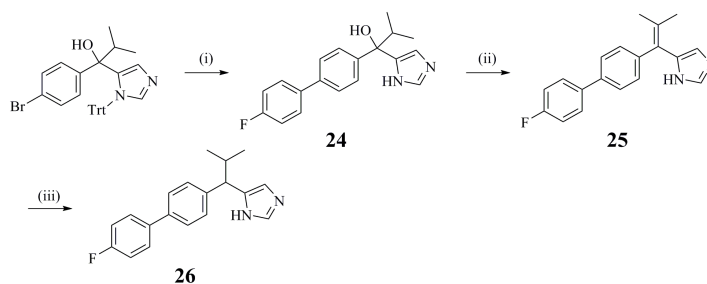
Reagents and conditions: (i) **Method C:** Pd(PPh₃)₄, Na₂CO₃, toluene, reflux, 6h; (ii) **Method D:** **1b-2b, 4b, 6b-7b, 9b, 13b, 15b, 17b, 19b-21b:** NaBH₄, MeOH; (iii) **Method B:** **9b, 13b, 15b, 17b:** EtMgBr, THF; (iv) **Method E:** **2a, 4a, 7a, 9a, 11a:** CDI, THF, reflux, 4 days; (v) **Method A:** **1a-22a:** CDI, NMP, reflux, 4h.

Scheme 2.



Reagents and conditions: (i) Method C: 4-fluoro boronic acid, Pd(PPh₃)₄, Na₂CO₃, toluene, reflux, 6h; (ii) a. imidazole, n-BuLi, TrtCl, THF, 0 °C, 2h; b. n-BuLi, tert-Bu-diMe-SiCl, THF, 0 °C, 2h; c. n-BuLi, 1b, THF, rt, 8h; (iii) pyridinium hydrochloride, MeOH, 60 °C, 4h.

Scheme 3.



Reagents and conditions: (i) a. Method C: 4-fluoro boronic acid, Pd(PPh₃)₄, Na₂CO₃, toluene, reflux, 6h; b. pyridinium hydrochloride, MeOH, 60 °C, 4h; (ii) HCl / *i*-PrOH, 80 °C, 2h; (iii) Pd(OH)₂, ethanol, THF, H₂, rt, 3h

In vitro activity. CYP17 inhibition of all compounds was evaluated using the 50,000 sediment after homogenation of *E.coli* expressing human CYP17 as well as cytochrome P450 reductase.^{12d} The assay was run with progesterone as substrate and NADPH as cofactor. Separation of substrate and product was accomplished by HPLC using UV detection.¹⁶ IC₅₀ values are presented in comparison to Ketoconazole and Abiraterone in Tables 1-2.

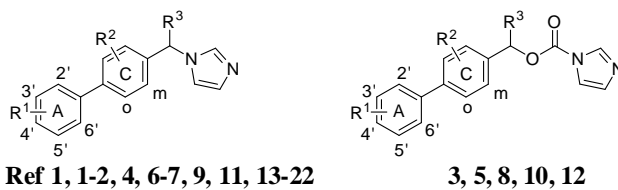
It is striking that in the series of 1-imidazole compounds (**1-22**), a sharp structure activity relationship is observed. The analogues can be divided into 3 classes regarding the fluorine substitution on the C- ring, i.e. without F, *meta*- F and *ortho*- F (positions relative to the A- ring, Table 1).

It can be seen that, in the class of compounds without fluorine on the C- ring, additional substitution at the A- ring by fluorine, methyl or methoxy (**1**, **2**, **4**, **6** and **7**), did not enhance the inhibitory activity compared to **Ref 1** (IC₅₀ = 345 nM). For example, extra fluorine substitution at *meta*- or *ortho*- position of the A- ring, resulting in 3',4'- di F (**2**) and 2',4'- di F (**4**) analogues, decreased activity somewhat (IC₅₀ = 803 and 985 nM, respectively). Interestingly, 2',5'- di F substitution (**7**) exhibited similar inhibitory potency (IC₅₀ = 956 nM) as seen with the 2',4'- di F analogue.

Importantly, the introduction of fluorine at the *meta*- position of the C- ring significantly increased the inhibitory potency. Compound **9** showed an IC₅₀ value of 131 nM, being 3 fold more potent than **Ref 1**. Similar improvements can be found for the other compounds in this class (**13**, **15** and **17**, IC₅₀ values around 350 nM) being 3 fold more potent than the corresponding compounds without F at the C- ring (**2**, **4** and **7**, respectively, IC₅₀ values around 900 nM). Moreover, it can be seen that the analogue with only one *para*- F at the A- ring (**9**) is more potent than other analogues with multi- F on the A- ring as mentioned above. A similar ranking of potency can be observed for multi- F analogues in this class of compounds too: the 3',4'-di F compound (**13**, IC₅₀ = 305 nM) being more potent than the others, e. g. the 2',5'-di F compound (**15**, IC₅₀ = 381 nM) and the 2',4'-di F compound (**17**, IC₅₀ = 364 nM).

On the contrary, *ortho*- F substitution at the C ring decreased activity. Compound **19** (IC₅₀ = 657 nM) was less potent than the corresponding analogues with *meta*- F (**9**, IC₅₀ = 131 nM) or without F (**Ref 1**, IC₅₀ = 345 nM). However, compound **19** exhibited stronger inhibition compared to compound 21 furnished with two fluorine substituents in 3',4'- position as expected.

Moreover, all imidazole-1-carboxylic acid biphenyl esters (**3**, **5**, **8**, **10** and **12**) were found to be inactive. This is probably due to the fact that these molecules are too large to fit into the binding pocket. Noteworthy is the importance of the ethyl substituent at the methylene bridge, as already reported,^{12g} i.e. that ethyl substitution results in more potent compounds compared to the corresponding non- or methyl substituted analogues.

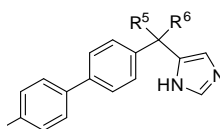
Table 1. Inhibition of CYP17 by compounds **1-22**

Compd.	R ¹	R ²	R ³	IC ₅₀ ^a	Compd.	R ¹	R ²	R ³	IC ₅₀ ^a	Compd.	R ¹	R ²	R ³	IC ₅₀ ^a
Ref 1	4'-F	H	Et	345	9	4'-F	<i>m</i> -F	Et	131	19	4'-F	<i>o</i> -F	Et	657
					10	4'-F	<i>m</i> -F	Et	4643					
					11	4'-F	<i>m</i> -F	H	2110	20	4'-F	<i>o</i> -F	H	2800
					12	4'-F	<i>m</i> -F	H	>5000					
1	4'-F, 2'-Me	H	Et	951										
2	3',4'-di F	H	Et	803	13	3',4'-di F	<i>m</i> -F	Et	305	21	3',4'-di F	<i>o</i> -F	Et	825
3	3',4'-di F	H	Et	>5000	14	3',4'-di F	<i>m</i> -F	H	>5000					
4	2',4'-di F	H	Et	985	15	2',4'-di F	<i>m</i> -F	Et	381					
5	2',4'-di F	H	Et	>5000	16	2',4'-di F	<i>m</i> -F	H	>5000	22	2',4'-di F	<i>o</i> -F	H	>5000
6	2',4'-di F, 3'-MeO	H	Me	>10000										
7	2',5'-di F	H	Et	956	17	2',5'-di F	<i>m</i> -F	Et	364					
8	2',5'-di F	H	Et	>5000	18	2',5'-di F	<i>m</i> -F	H	1640					
KTZ^b				2780						ABT^b				72

^a Concentration of inhibitors required to give 50 % inhibition. The mean values of at least three experiments are given in nM within ±10 % deviation

^b **KTZ**: Ketoconazole; **ABT**: Abiraterone.

Furthermore, 5-imidazole was employed instead of 1-imidazole leading to compounds **23-26** as shown in table 2. It is apparent that compounds with a hydroxy group substituted at the methylene bridge are inactive. Nonetheless, isopropyl substitution resulted in an active compound (**26**, IC₅₀ = 502 nM), which was, however, less potent compared to **Ref 1**. Surprisingly, the compound with an isopropylidene substitution (**25**) turned out to be very potent (IC₅₀ = 159 nM).

Table 2. Inhibition of CYP17 by compounds **23-26**.

No	R ⁵	R ⁶	IC ₅₀ ^a
23	OH	H	>>10000
24	OH	<i>i</i> -Pr	>5000
25	<i>i</i> -Propylidene		159
26	H	<i>i</i> -Pr	502
KTZ^b			2780
ABT^b			72

^a Concentration of inhibitors required to give 50 % inhibition. The mean values of at least three experiments are given in nM within ±10 % deviation.

^b **KTZ**: Ketoconazole; **ABT**: Abiraterone.

Finally, inhibition values of the most active compounds **9**, **13**, **15**, **17** and **25** toward the hepatic enzyme CYP3A4 were also determined, because of its important role in drug metabolism and drug-drug interaction. It turned out that the compounds tested showed only marginal inhibition (around 50 % at 10 μM), clearly lower than that shown by Ketoconazole (98 % at 10 μM).

Computational modelling studies.

Docking. Compounds **Ref 1**, **9**, **11**, **13**, **15**, **17** and **19**, both enantiomers if existing, were docked into the homology model of human CYP17^{12c} by means of two commercial docking softwares, GOLD_v4.0¹⁷ and FlexX 3.1.3,¹⁸ in order to elucidate their binding into the active site of the enzyme. The docking with GOLD was performed with both the scoring functions GOLDScore and ChEMScore, while FlexX was used with the FlexX-Pharm module, with the iron of the heme chosen as pharmacophoric constraint. A clustering with ACIAP¹⁹ of all the docking poses of the three procedures resulted in one main, statistical predominant binding mode (**BM1**)^{12c} and two minor representative clusters. Interestingly, each of the latter two clusters solely consisted of either the S- (**BM2**)^{12c} or the R- (**BM-ABT**)^{12h} enantiomers respectively (Fig. 2). This finding indicates that, together with the necessary perpendicular interaction angle between imidazole N and heme Fe to ensure sufficient coordination, the orientation of the hydrophobic pocket, which is occupied by the substituent on the methylene bridge, limits the pose distribution of different enantiomers. This geometrical restriction forces the S- enantiomers into **BM2** area and the R- enantiomers into **BM-ABT**. However, as the intersection of both areas, **BM1** is a better area for both enantiomers to bind to.

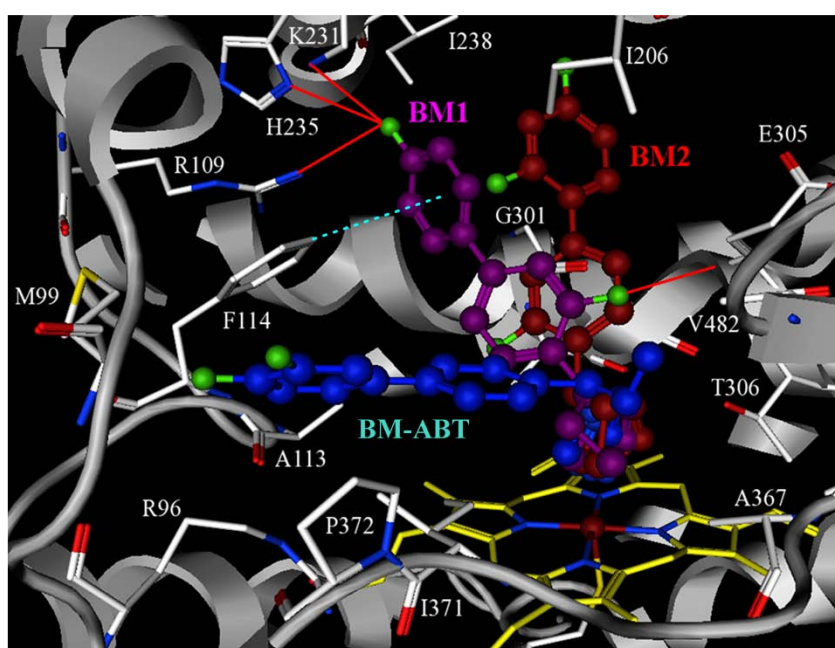


Figure 2. Presentation of the three main binding modes, exemplified by compounds **9** (magenta, **BM1**), **15** (red, **BM2**) and **13** (blue, **BM-ABT**). Heme, interacting residues and ribbon rendered tertiary structure of the active site are shown. Polar interactions are marked with red solid lines, whereas π - π stacking and metal complexation with cyan dotted lines. Figure was generated with MOE (<http://www.chemcomp.com>).

It can be observed for **BM1** that a conjugated scaffold orienting almost parallel to the I-helix is one of the key factors for high activity as previously described.^{12g} According to our docking studies this extended π -system obviously interacts not only with the π -system of the amino acid backbone in the I-helix (i.e. Gly301, Ala302, Gly303, Val304), but also with Phe114, which is oriented perpendicular toward the A- ring (Fig. 2 **BM1**) to form a quadrupole-quadrupole interaction. More importantly, fluorine in the molecule showed profound influence on the affinity for the enzyme. This can be explained by the obviously existing interactions of the para- F substituent with Arg109, Lys231 and His235 (Fig. 2). When the fluorines were shifted to other positions in the A- ring resulting in 2',5'-di F analogues, a decrease of activities can be observed. Obviously, the interactions mentioned above can no longer be maintained. These observations nicely validate the reliability of our protein model. Furthermore, the elevated activity of C- ring *meta*- F substituted compounds can be explained by a multi-polar interaction between F and the N-H group of Glu305 (Fig. 2) stabilizing the π - π interaction between the C- ring and the backbone π -system of Gly301-Ala302.

Additionally, a further flexible docking run was performed with GOLDv4.0-GOLDScore, with the side chains of Phe114, Arg109, Lys231, Asn202, Glu305, and Ile371 being set freely rotatable. Very similar results were observed as seen for the docking runs with the rigid side chains (data not shown).

MEP maps. To obtain an insight which physicochemical parameters might influence biological activity, the charge density distribution was considered and the molecular electrostatic potentials (MEPs) of selected compounds were determined. The geometry of these compounds (**Ref 1**, **2**, **9**, **13**, **15**, **17** and **25**) was optimized in the gas phase at the B3LYP/6-311++G** (d,p)²⁰ level of density functional theory (DFT) by means of Gaussian 03.²¹ MEPs of electron density were plotted for every compound with GaussView 3.09.²²

The introduction of a second fluorine or the shift of fluorine into another position on the A- ring always leads to a reduction of the A- ring electron density, which can be clearly seen in the different MEP maps of compounds **9**, **13**, **15**, **17** and **25** (Fig. 3A). This observation correlates with the different electron-withdrawing effects of the fluorine in *meta*- or *para*- position (σ values of +0.337 and +0.067, respectively). This reduction of electron density weakens the T-shaped interaction of the A- ring with Phe114, and consequently decreases the inhibitory potency of the compound.

The lower inhibitory potency of compounds with *ortho*- F substitution on the C- ring (**19** and **21**) might be due to the adverse effect that the fluorine exerts on the overall charge density of the biphenyl system by deforming the conjugated π - π system and by concentrating the electrons on the fluorine. However, for *meta*- F compounds (**9**, **13**, **15** and **17**) it seems that fluorine induces an increase in electron distribution on the imidazole ring, as visualized in the MEP maps of compounds **Ref 1** and **9** (Fig. 3C), which is linked with an augmented inhibitory potency of the compounds. An analogous phenomenon was observed for compound **25**, where the isopropylidene strengthened the π - π system and extended the conjugation over the whole molecule (Fig. 3B).

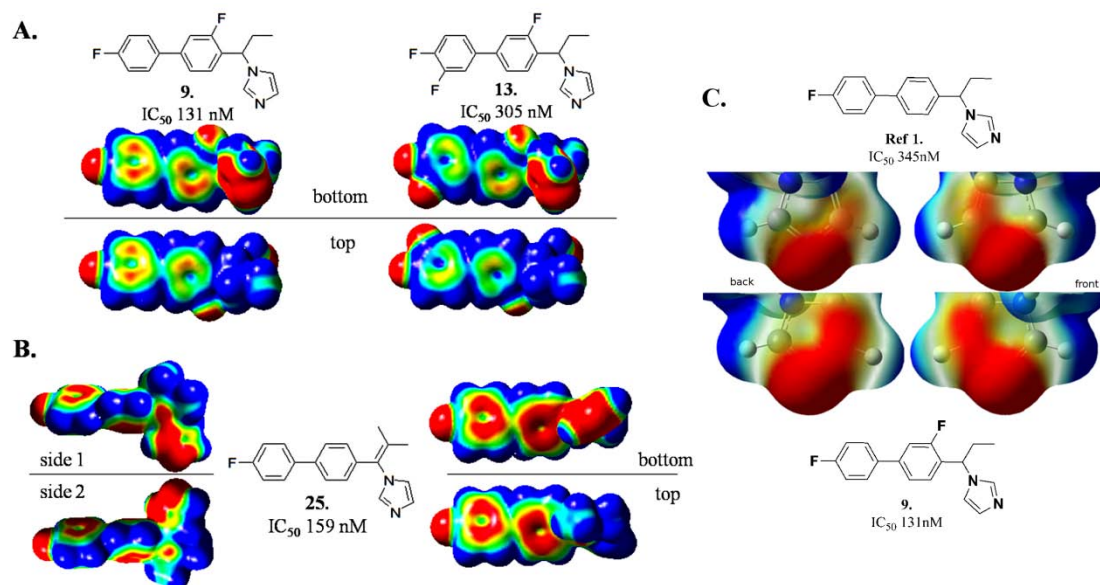


Figure 3. (A) Structure, CYP17 inhibitory activity and MEP maps (bottom and top view) of compounds **9** and **13**. For compounds **15** and **17**, nearly the same MEP maps (not shown) as for of compound **13** were observed. (B) MEP maps of compound **25**, highlighting in the side-views of the conjugated π - π system, enhanced by the isopropylidene substituent on the methylene bridge. The electrostatic potential surfaces shown in (A) and (B) were plotted with GaussView 3.0 in a range of -6 to +12 kcal/mol. (C) Transparent *color-coded* front and back view of the electrostatic potential maps of the imidazoles of both **Ref 1** and compound **9**, in a range of -15.7 to +0 kcal/mol, illustrative for the influence exerted on the electron distribution of the imidazole by fluorine substituents on the C- ring.

In vivo activity. The in vivo evaluation of the most potent compounds **9**, **13**, **15** and **17**, including the ability of reducing plasma testosterone concentration (Table 3) and the determination of pharmacokinetic properties (Table 4) was performed in male Wistar rats after oral application. Abiraterone which was administered as acetate to improve its oral absorption and **Ref 1** were used as reference compounds. The plasma concentrations of testosterone were determined using an ELISA assay and plasma drug concentrations were measured using LC-MS. In the case of Abiraterone acetate only the signals of free Abiraterone were monitored, as the acetate is inactive as CYP17 inhibitor. As can be seen from table 3 all compounds significantly reduced the plasma testosterone concentration. It is striking at each time point investigated that all non-steroidal compounds, which were less active in vitro, exhibited

higher activities in vivo than Abiraterone. After 24 hours, compound **9** and **Ref 1** still showed strong inhibitory activity, compounds **13** and **17** showed almost no inhibition, whereas compound **15** and Abiraterone exhibited an increase of testosterone levels above control at this time point, probably caused by feed-back stimulation. As expected this activity profile correlates to the pharmacokinetic properties of the compounds. Abiraterone exhibited a plasma half-life of only 1.6 hours, while the half-lives of other compounds are much longer (10 hours for **Ref 1** and 12.8 hours for **9**). Accordingly, the AUC values of the test compounds, except for compound **17**, are higher than for Abiraterone, indicating better bioavailability properties. Interestingly, the introduction of an additional fluorine into the C- ring of **Ref 1** prolongs plasma half-life (**9**), whereas introduction of further fluorine atoms into the A-ring reduces half-lives strongly (**13**, **15** and **17**, half-lives between 2 to 6 hours).

Table 3. Reduction of the plasma testosterone concentrations in rats by selected compounds ^a

Comp.	Relative plasma testosterone level (%) ^b					
	1h	2h	4h	6h	8h	24h
Control	171.7 ± 62.3	117.7 ± 48.0	141.2 ± 80.9	244.3 ± 126.4	188.6 ± 67.0	184.8 ± 82.2
9	23.4 ± 5.5 ^f	18.4 ± 4.2 ^f	16.9 ± 3.9 ^f	18.1 ± 5.2 ^f	21.1 ± 5.9 ^f	40.7 ± 11.9 ^e
13	21.9 ± 4.6 ^f	15.2 ± 3.2 ^f	14.9 ± 3.6 ^f	17.0 ± 4.5 ^f	19.5 ± 5.6 ^f	182.2 ± 86.9
15	52.0 ± 14.7 ^e	46.8 ± 13.2 ^e	46.5 ± 12.6 ^e	44.0 ± 13.1 ^e	49.7 ± 15.4 ^e	317.8 ± 76.9 ^e
17	30.6 ± 7.9 ^f	27.9 ± 11.3 ^e	74.5 ± 60.5	88.4 ± 68.8	62.4 ± 14.6	138.5 ± 61.9
Ref 1	16.5 ± 5.7 ^e	11.7 ± 5.0 ^e	13.9 ± 8.0 ^e	13.9 ± 7.1 ^e	13.4 ± 6.2 ^e	36.7 ± 27.4 ^e
ABT ^c	92.5 ± 43.1 ^d	44.0 ± 14.7 ^d	43.5 ± 12.4 ^d	43.3 ± 12.8 ^c	35.6 ± 9.7 ^d	476.0 ± 238.6

^a Compounds 9, 13, 15 and 17 were applied at a dose of 50 mg / kg body weight; Abiraterone was administrated as Abiraterone acetate (56 mg / kg body weight, equivalent to Abiraterone 50 mg / kg body weight). 5 to 6 intact adult male Wistar rats were employed for each treatment group; each sample was tested for 3 times.

^b The average plasma testosterone concentrations (1.97 ng / mL) at pre-treatment time points (-1, -0.5 and 0 h) were set to 100 %. The values shown are the relative levels compared to the pre-treatment value.

^c **ABT**: Abiraterone.

^d P < 0.05, ^e P < 0.01, ^f P < 0.001

Table 4. Pharmacokinetic properties of selected compounds ^a

Compounds	t _{1/2z} (h) ^b	t _{max} (h) ^b	C _{max} (ng / mL) ^b	AUC _{0-∞} (ng * h / mL) ^b
9	12.8	2.0	1036	24000
13	6.1	8.0	1106	17750
15	4.2	6.0	803	11100
17	2.2	1.0	145	650
Ref 1	10.0	6.0	3288	70729
Abiraterone	1.6	2.0	592	4015

^a Compounds 9, 13, 15 and 17 were applied at a dose of 50 mg / kg body weight; Abiraterone was administrated as Abiraterone acetate (56 mg / kg body weight, equivalent to Abiraterone 50 mg / kg body weight). 5 to 6 intact adult male Wistar rats were employed for each treatment group; each sample was tested for 3 times.

^b t_{1/2z}: terminal half-life; t_{max}: time of maximal concentration; C_{max}: maximal concentration; AUC_{0-∞}: area under the curve.

Conclusion

Herein, we reported the design, synthesis and bioactivity evaluation of a series of fluorine substituted biphenyl methylene imidazoles as CYP17 inhibitors. Fluorine substitution was found to show profound influence on the in vitro and in vivo activities, as well as the pharmacokinetic profiles.

It has been unveiled that fluorine in the *meta*- position of the C- ring increased the activity compared to the non-substituted analogues, whereas *ortho*- substitution reduced the potency. Compounds furnished with fluorine at the A- ring always followed the same activity ranking: 4'-F > 3',4'-di F > 2',5'-di F ≥ 2',4'-di F.

Although the compounds are racemates, it is not likely that one enantiomer would be much more potent than the other, because both S and R enantiomers predominately adapt **BMI** according to our docking studies.

Moreover, the biological data were well deciphered by docking studies and MEP mapping of selected compounds. The multi-polar interactions between the C- ring fluorine substituents and interacting amino acids

residues significantly increased the binding affinities compared to the parent compound. The charge distribution difference on both the A- and the C- ring indicates π - π stacking (i.e. with both Phe114 and Gly301-Ala302), hydrophobic and Van der Waals interactions as determinants for activity.

Furthermore, it could be demonstrated once again that fluorine substituted in an appropriate position, like in the C- ring, prolongs the plasma half life; in an unsuitable position, however, it decreases the $t_{1/2}$ value of the parent compound. This phenomenon might be due to a decrease in metabolic stability and is interesting for further investigations in the future.

Finally, after the modification compound **9** is identified as strong CYP17 inhibitor showing potent activity in vivo, a high bioavailability and a long plasma half-life. Thus, Compound **9** appears to be an optimal candidate which after further structural optimization could be the first non-steroidal CYP17 inhibitor to be applied clinically. CYP17 inhibitors should be superior to the presently used GnRH analogues as mentioned above due to the fact that they reduce not only testicular but also adrenal androgen formation. Nevertheless, PC treatment could be further optimized by combining CYP17 inhibitors with inhibitors of androgen activation to DHT, catalyzed by 17β -HSD1²³ and / or 17β -HSD3, as well as 5α -reductase.²⁴

Experimental Section

CYP17 preparation and assay

Human CYP17 was expressed in *E. coli* (coexpressing human CYP17 and cytochrome P450 reductase) and the assay was performed as previously described.^{12d, 16}

Inhibition of hepatic CYP enzymes

The recombinantly expressed enzymes from baculovirus-infected insect microsomes (Supersomes) were used and the manufacturer's instructions (www.gentest.com) were followed.

In vivo study

The in vivo tests were performed with intact adult male Wistar rats (Harlan Winkelmann, Germany), 5 to 6 for each treatment group. These rats were cannulated with silicone tubing via the right jugular vein. Compounds **9**, **13**, **15** and **17** were applied p.o. with doses of 50 mg / kg body weight, while Abiraterone was administrated as acetate 56 mg / kg body weight (equivalent to Abiraterone 50 mg / kg body weight). The concentrations of testosterone in the rat plasma were determined using the ELISA (EIA - 1559) from DRG Instruments according to the manufacturer's instructions. The plasma drug levels were measured by LC-MS. Non-compartmental pharmacokinetic analysis of concentration vs time data was performed for each compound on the mean plasma level using a validated computer program (PK solution 2 software; Summit Research Services, Montrose, USA). Plasma concentrations below the limit of detection were assigned a value of zero.

Chemistry Section

General

Melting points were determined on a Mettler FP1 melting point apparatus and are uncorrected. IR spectra were recorded neat on a Bruker Vector 33FT-infrared spectrometer. ¹H and ¹³C NMR spectra were measured on a Bruker DRX-500 (500 MHz). Chemical shifts are given in parts per million (ppm), and TMS was used as an internal standard for spectra obtained in CDCl₃. All coupling constants (*J*) are given in Hz. ESI (electrospray ionization) mass spectra were determined on a TSQ quantum (Thermo Electron Corporation) instrument. The purities of the final compounds were controlled by Surveyor®-LC-system. Purities were greater than 98 %. Column chromatography was performed using silica-gel 60 (50-200 μ m), and reaction progress was determined by TLC analysis on Alugram® SIL G/UV₂₅₄ (Macherey-Nagel). Boronic acids and bromoaryls used as starting materials were commercially obtained (CombiBlocks, Chempur, Aldrich, Acros etc).

Method A: CDI reaction in NMP

To a solution of the corresponding alcohol (1 eq) in NMP or acetonitrile (10 mL / mmol) was added CDI (5 eq). Then the solution was heated to reflux for 4 to 18 h. After cooling to ambient temperature, it was diluted with water (30 mL) and extracted with ethyl acetate (3 x 10 mL). The combined organic phases were washed with brine, dried over MgSO₄ and evaporated under reduced pressure. Then the desired product was purified by chromatography on silica gel.

1-[1-(4'-Fluoro-2'-methyl-biphenyl-4-yl)-propyl]-1H-imidazole (1). Synthesized according to Method A using **1a** (0.15 g, 0.61 mmol) and CDI (0.20 g, 1.23 mmol); yield: 0.06 g (32 %); colorless oil; R_f = 0.27 (DCM / MeOH,

95:5); δ_{H} (DMSO, 500 MHz) 0.98 (t, $J = 7.3$ Hz, 3H, CH₃), 2.23 (s, 3H, CH₃), 2.24-2.30 (m, 2H, CH₂), 5.07 (t, $J = 7.6$ Hz, 1H, CH), 6.90-6.93 (m, 1H), 6.95-6.97 (m, 1H), 7.01 (s, 1H), 7.11 (s, 1H), 7.14 (dd, $J = 6.0, 8.4$ Hz, 1H), 7.22-7.26 (m, 4H), 7.67 (s, 1H); MS (ESI): $m/z = 295$ [M⁺+H].

1-[1-(3',4'-Difluoro-biphenyl-4-yl)-propyl]-1H-imidazole (2). Synthesized according to Method A using **2a** (0.27 g, 1.09 mmol) and CDI (0.34 g, 2.06 mmol); yield: 0.09 g (27 %); colorless oil; $R_f = 0.29$ (DCM / MeOH, 95:5); δ_{H} (CDCl₃, 500 MHz) 0.98 (t, $J = 7.3$ Hz, 3H, CH₃), 2.23-2.31 (q, $J = 7.3, 7.6$ Hz, 2H, CH₂), 5.06 (t, $J = 7.6$ Hz, 1H, CH), 6.97-7.02 (m, 1H), 7.10-7.14 (m, 1H), 7.18-7.28 (m, 4H), 7.23-7.37 (m, 1H), 7.49 (m, 2H), 7.62-7.66 (m, 1H, Im-2H); MS (ESI): $m/z = 299$ [M⁺+H].

1-[1-(2',4'-Difluorobiphenyl-4-yl)propyl]-1H-imidazole (4). Synthesized according to Method A using **4a** (0.27 g, 1.09 mmol) and CDI (0.34 g, 2.06 mmol); yield: 0.12 g (36 %); colorless oil; $R_f = 0.34$ (DCM / MeOH, 95:5); δ_{H} (CDCl₃, 500 MHz) 0.85 (t, $J = 7.3$ Hz, 3H, CH₃), 2.12-2.18 (m, 2H, CH₂), 4.96 (t, $J = 7.6$ Hz, 1H, CH), 6.77-6.85 (m, 2H), 6.87-6.90 (m, 1H), 6.99-7.02 (m, 1H), 7.13-7.15 (m, 2H), 7.23-7.28 (m, 1H), 7.35-7.37 (m, 2H), 7.62-7.68 (m, 1H, Im-2H); MS (ESI): $m/z = 299$ [M⁺+H].

1-[1-(2',4'-Difluoro-3'-methoxybiphenyl-4-yl)ethyl]-1H-imidazole (6). Synthesized according to Method A using **6a** (0.30 g, 1.09 mmol) and CDI (0.34 g, 2.06 mmol); yield: 0.34 g (71 %); yellow oil; $R_f = 0.30$ (DCM / MeOH, 95:5); δ_{H} (CDCl₃, 500 MHz) 1.72-1.79 (d, $J = 7.5$ Hz, 3H, CH₃), 3.91 (s, 3H, OCH₃), 5.18-5.31 (q, $J = 7.5$ Hz, 1H, CH), 6.82-6.84 (m, 1H), 6.83-6.86 (m, 1H), 6.89-6.93 (m, 1H), 6.97-6.99 (m, 1H), 7.09-7.10 (m, 2H), 7.34-7.36 (m, 2H), 7.50-7.51 (m, 1H, Im-2H); MS (ESI): $m/z = 315$ [M⁺+H].

1-[1-(2',5'-Difluorobiphenyl-4-yl)propyl]-1H-imidazole (7). Synthesized according to Method A using **7b** (0.27 g, 1.09 mmol) and CDI (0.34 g, 2.06 mmol); yield: 0.13 g (41 %); colorless oil; $R_f = 0.38$ (DCM / MeOH, 95:5); δ_{H} (CDCl₃, 500 MHz) 0.98 (t, $J = 7.3$ Hz, 3H, CH₃), 2.26 (q, $J = 7.3, 7.6$ Hz, 2H, CH₂), 5.05 (t, $J = 7.6$ Hz, 1H, CH), 6.97-7.01 (m, 2H), 7.08-7.12 (m, 3H), 7.25-7.27 (m, 2H), 7.49-7.51 (m, 2H), 7.62-7.65 (m, 1H, Im-2H); MS (ESI): $m/z = 299$ [M⁺+H].

1-[1-(3,4'-difluorobiphenyl-4-yl)propyl]-1H-imidazole (9). Synthesized according to Method A using **9a** (0.38 g, 1.53 mmol) and CDI (0.47 g, 2.88 mmol); yield: 0.08 g (17 %); yellow oil; $R_f = 0.38$ (DCM / MeOH, 95:5); δ_{H} (CDCl₃, 500 MHz) 0.99 (t, $J = 7.3$ Hz, 3H, CH₃), 2.21-2.31 (m, 2H, CH₂), 5.38 (t, $J = 7.5$ Hz, 1H, CH), 7.01 (s, 1H), 7.08 (s, 1H), 7.10-7.14 (m, 2H), 7.19-7.25 (m, 2H), 7.27-7.29 (m, 1H), 7.40-7.51 (m, 2H), 7.64 (s, 1H, Im-2H); MS (ESI): $m/z = 299$ [M⁺+H].

1-[(3,4'-Difluorobiphenyl-4-yl)methyl]-1H-imidazole (11). Synthesized according to Method A using **11a** (0.28 g, 1.27 mmol) and CDI (0.41 g, 2.54 mmol); yield: 0.11 g (31 %); colorless oil; $R_f = 0.53$ (EtOAc / MeOH, 95:5); δ_{H} (CDCl₃, 500 MHz) 5.20 (s, 2H, CH₂), 6.98 (s, br, 1H), 7.10 (s, br, 1H), 7.11-7.16 (m, 3H), 7.26-7.31 (m, 2H), 7.50 (dd, $J = 5.4, 8.8$ Hz, 2H), 7.64 (s, br, 1H, Im-2H); MS (ESI): $m/z = 271$ [M⁺+H].

1-[1-(3,3',4'-Trifluorobiphenyl-4-yl)propyl]-1H-imidazole (13). Synthesized according to Method A using **13a** (0.40 g, 1.70 mmol) and CDI (0.53 g, 3.20 mmol); yield: 0.11 g (20 %); colorless oil; $R_f = 0.35$ (DCM / MeOH, 95:5); δ_{H} (CDCl₃, 500 MHz) 0.99 (t, $J = 7.3$ Hz, 3H, CH₃), 2.22-2.33 (m, 2H, CH₂), 5.39 (t, $J = 7.6$ Hz, 1H, CH), 7.01 (s, 1H), 7.09 (s, 1H), 7.20-7.29 (m, 5H), 7.31-7.35 (m, 1H), 7.64 (s, 1H, Im-2H); MS (ESI): $m/z = 317$ [M⁺+H].

1-[(3,3',4'-trifluorobiphenyl-4-yl)methyl]-1H-imidazole (14). Synthesized according to Method A using **14a** (0.35 g, 1.67 mmol) and CDI (0.53 g, 3.20 mmol); yield: 0.10 g (23 %); white powder: mp 60-61 °C; $R_f = 0.26$ (DCM / MeOH, 95:5); δ_{H} (CDCl₃, 500 MHz) 5.19 (s, 2H, CH₂), 6.97 (s, 1H), 7.10 (s, 1H), 7.11-7.14 (m, 2H), 7.20-7.28 (m, 3H), 7.31-7.35 (m, 1H), 7.59 (s, 1H, Im-2H); MS (ESI): $m/z = 289$ [M⁺+H].

1-[1-(2',3,4'-Trifluorobiphenyl-4-yl)propyl]-1H-imidazole (15). Synthesized according to Method A using **15a** (0.27 g, 1.14 mmol) and CDI (0.35 g, 2.10 mmol); yield: 0.09 g (24 %); colorless oil; $R_f = 0.37$ (DCM / MeOH, 95:5); δ_{H} (CDCl₃, 500 MHz) 0.99 (t, $J = 7.3$ Hz, 3H, CH₃), 2.23-2.32 (m, 2H, CH₂), 5.40 (t, $J = 7.6$ Hz, 1H, CH), 6.89-6.97 (m, 2H), 7.02 (s, 1H), 7.08 (s, 1H), 7.19-7.27 (m, 3H), 7.34-7.38 (m, 1H), 7.64 (s, 1H, Im-2H); MS (ESI): $m/z = 317$ [M⁺+H].

1-[(2',3,4'-Trifluorobiphenyl-4-yl)methyl]-1H-imidazole (16). Synthesized according to Method A using **16a** (0.18 g, 0.76 mmol) and CDI (0.24 g, 1.51 mmol); yield: 0.09 g (42 %); orange oil; $R_f = 0.52$ (EtOAc / MeOH, 95:5); δ_{H} (CDCl₃, 500 MHz) 5.20 (s, 2H, CH₂), 6.89-6.97 (m, 2H), 6.98 (s, br, 1H), 7.10 (s, br, 1H), 7.12 (dd, $J = 7.9, 8.2$ Hz, 1H), 7.24-7.27 (m, 2H), 7.36 (ddd, $J = 6.4, 8.5, 8.8$ Hz, 1H), 7.61 (s, br, 1H, Im-2H); MS (ESI): $m/z = 289$ [M⁺+H].

1-[1-(2',3,5'-Trifluorobiphenyl-4-yl)propyl]-1H-imidazole (17). Synthesized according to Method A using **17a** (0.40 g, 1.70 mmol) and CDI (0.53 g, 3.20 mmol); yield: 0.14 g (26 %); colorless oil; $R_f = 0.38$ (DCM / MeOH, 95:5); δ_{H} (CDCl₃, 500 MHz) 0.99 (t, $J = 7.3$ Hz, 3H, CH₃), 2.23-2.32 (m, 2H, CH₂), 5.40 (t, $J = 7.6$ Hz, 1H, CH),

7.00-7.04 (m, 2H), 7.08-7.14 (m, 2H), 7.20-7.24 (m, 1H), 7.26-7.30 (m, 2H), 7.64 (s, 1H, Im-2H); MS (ESI): $m/z = 317 [M^+ + H]$.

1-[(2',3,5'-Trifluorobiphenyl-4-yl)methyl]-1H-imidazole (18). Synthesized according to Method A using **18a** (0.17 g, 0.71 mmol) and CDI (0.23 g, 1.43 mmol); yield: 0.09 g (45 %); light yellow solid; mp 125-126 °C; $R_f = 0.48$ (EtOAc / MeOH, 95:5); δ_H (CDCl₃, 500 MHz) 5.21 (s, 2H, CH₂), 6.98 (s, br, 1H), 7.00-7.05 (m, 1H), 7.08-7.16 (m, 4H), 7.28-7.31 (m, 2H), 7.64 (s, br, 1H, Im-2H); MS (ESI): $m/z = 289 [M^+ + H]$.

1-[1-(2,4'-Difluorobiphenyl-4-yl)propyl]-1H-imidazole (19). Synthesized according to Method A using **19a** (0.31 g, 1.22 mmol) and CDI (0.40 g, 2.46 mmol); yield: 0.11 g (31 %); colorless oil; $R_f = 0.56$ (EtOAc / MeOH, 95:5); δ_H (CDCl₃, 500 MHz) 0.97 (t, $J = 7.3$ Hz, 3H), 2.21-2.27 (m, 2H), 5.04 (t, $J = 7.7$ Hz, 1H), 6.96-6.99 (m, 2H), 7.02 (dd, $J = 1.9, 7.9$ Hz, 1H), 7.11 (s, br, 1H), 7.12 (t, $J = 8.6$ Hz, 2H), 7.37 (t, $J = 7.9$ Hz, 1H), 7.47 (ddd, $J = 1.3, 5.4, 8.8$ Hz, 1H), 7.64 (s, br, 1H, Im-2H); MS (ESI): $m/z = 299 [M^+ + H]$.

1-(2,4'-Difluoro-biphenyl-4-ylmethyl)-1H-imidazole (20). Synthesized according to Method A using **20a** (0.10 g, 0.44 mmol) and CDI (0.40 g, 2.46 mmol); yield: 0.05 g (42 %); white solid; mp 93-94 °C; $R_f = 0.52$ (EtOAc / MeOH, 95:5); δ_H (CDCl₃, 500 MHz) 5.15 (s, 2H, CH₂), 6.90-6.98 (m, 3H), 7.11-7.13 (m, 2H), 7.25-7.27 (m, 3H), 7.36-7.39 (m, 1H), 7.60 (s, 1H, Im-2H); MS (ESI): $m/z = 271 [M^+ + H]$.

1-[1-(2,3,4'-Trifluorobiphenyl-4-yl)propyl]-1H-imidazole (21). Synthesized according to Method A using **21a** (0.28 g, 1.03 mmol) and CDI (0.34 g, 2.06 mmol); yield: 0.09 g (29 %); light brown oil; $R_f = 0.53$ (EtOAc / MeOH, 95:5); δ_H (CDCl₃, 500 MHz) 0.97 (t, $J = 7.4$ Hz, 3H), 2.20-2.28 (m, 2H), 5.04 (t, $J = 7.6$ Hz, 1H), 6.96-6.99 (m, 2H), 7.03 (dd, $J = 1.9, 7.9$ Hz, 1H), 7.11 (s, br, 1H), 7.18-7.23 (m, 2H), 7.31-7.34 (m, 1H), 7.35 (t, $J = 8.0$ Hz, 1H), 7.64 (s, br, 1H, Im-2H); MS (ESI): $m/z = 317 [M^+ + H]$.

1-(2,2',4'-Trifluoro-biphenyl-4-ylmethyl)-1H-imidazole (22). Synthesized according to Method A using **22a** (0.10 g, 0.39 mmol) and CDI (0.40 g, 2.46 mmol); yield: 0.06 g (54 %); white solid; mp 112-113 °C; $R_f = 0.47$ (EtOAc / MeOH, 95:5); δ_H (CDCl₃, 500 MHz) 5.21 (s, 2H, CH₂), 6.90-6.98 (m, 4H), 7.02 (d, $J = 7.8$ Hz, 1H), 7.16 (s, 1H), 7.33-7.35 (m, 2H), 7.85 (s, 1H, Im-2H); MS (ESI): $m/z = 289 [M^+ + H]$.

Method B: Grignard reaction

Under exclusion of air and moisture a 1.0 M EtMgBr (1.2 eq) solution in THF was added dropwise to a solution of the aldehyde or ketone (1 eq) in THF (12 mL / mmol). The mixture was stirred over night at rt. Then ethyl acetate (10 mL) and water (10 mL) were added and the organic phase was separated. The organic phase was extracted with water and brine, dried over Na₂SO₄, and evaporated under reduced pressure. The crude products were purified by flash chromatography on silica gel.

Method C: Suzuki-Coupling

The corresponding brominated aromatic compound (1 eq) was dissolved in toluene (7 mL / mmol), an aqueous 2.0 M Na₂CO₃ solution (3.2 mL / mmol) and an ethanolic solution (3.2 mL / mmol) of the corresponding boronic acid (1.5-2.0 eq) were added. The mixture was deoxygenated under reduced pressure and flushed with nitrogen. After repeating this cycle several times Pd(PPh₃)₄ (4 mol%) was added and the resulting suspension was heated to reflux for 8 h. After cooling down, ethyl acetate (10 mL) and water (10 mL) were added and the organic phase was separated. The water phase was extracted with ethyl acetate (2 x 10 mL). The combined organic phases were washed with brine, dried over Na₂SO₄, filtered over a short plug of celite® and evaporated under reduced pressure. The compounds were purified by flash chromatography on silica gel.

1-(4'-Fluorobiphenyl-4-yl)-1-(1H-imidazol-5-yl)-2-methylpropan-1-ol (24). Synthesized according to Method C using 1-(4-Bromophenyl)-2-methyl-1-(1-trityl-1H-imidazol-5-yl)propan-1-ol (0.50 g, 0.93 mmol) and 4-fluorophenyl boronic acid (0.23 mg, 1.63 mmol). After workup, the crude was stirred with pyridinium hydrochloride (0.17 g, 1.5 mmol) in MeOH (40 mL) at 60 °C for 4 hours. Then the reaction was quenched by adding saturated NaHCO₃ aq (10 mL). After 20 mL EtOAc were added, the phases separated. The water phase was extracted 2 times with EtOAc (20 mL), the combined organic extracts were dried over Na₂SO₄ and concentrated under reduced pressure. The crude product was purified by flash chromatography; yield: 0.21 g (73 %); colorless oil; $R_f = 0.17$ (EtOAc / MeOH, 95:5); δ_H (CDCl₃, 500 MHz) 0.82 (d, $J = 6.8$ Hz, 3H), 0.98 (d, $J = 6.8$ Hz, 3H), 2.63 (m, 1H), 7.01 (s, 1H), 7.10 (dd, $J = 8.7, 8.8$ Hz, 2H), 7.49 (d, $J = 8.5$ Hz, 2H), 7.53 (dd, $J = 5.4, 8.7$ Hz, 2H), 7.58 (s, 1H), 7.62 (d, $J = 8.3$ Hz, 2H); $m/z = 311 [M^+ + H]$.

Method D: Reduction with NaBH₄

To an ice-cooled solution of the corresponding aldehyde or ketone (1 eq) in methanol (5 mL / mmol) was added NaBH₄ (2 eq). Then the resulting mixture was heated to reflux for 30 minutes. After cooling to ambient temperature,

the solvent was distilled off under reduced pressure. Then water (10 mL) was added, and the resulting mixture was extracted with ethyl acetate (3 x 10 mL). The combined organic phases were washed with brine, dried over MgSO₄ and evaporated under reduced pressure. Then the desired product was purified by chromatography on silica gel.

Method E: CDI reaction in THF

To a solution of the corresponding alcohol (1 eq) in THF (10 mL / mmol) was added CDI (2 eq). Then the solution was heated to reflux at 70 °C for 4 days. After cooling to ambient temperature, the mixture was poured into water and extracted with CH₂Cl₂ (3 x 25 mL). The combined organic phases were washed with brine, dried over MgSO₄ and evaporated under reduced pressure. Then the desired product was purified by chromatography on silica gel.

Imidazole-1-carboxylic acid 1-(3',4'-difluoro-biphenyl-4-yl)-propyl ester (3). Synthesized according to Method E using **2a** (0.10 g, 0.42 mmol) and CDI (0.14 g, 0.83 mmol); yield: 0.09 g (37 %); white solid: mp 49-50 °C; $R_f = 0.29$ (DCM / MeOH, 95:5); δ_H (CDCl₃, 500 MHz) 1.01 (t, $J = 14.8$ Hz, 3H, CH₃), 2.01-2.21 (q, $J = 14.8$, 15.5 Hz, 2H, CH₂), 5.88 (t, $J = 15.5$ Hz, 1H, CH), 7.15 (s, 1H), 7.22-7.29 (m, 2H), 7.32-7.34 (m, 1H), 7.36-7.38 (m, 1H), 7.46 (d, $J = 8.2$ Hz, 2H), 7.54 (d, $J = 8.2$ Hz, 2H), 8.35 (s, 1H, Im-2H); MS (ESI): $m/z = 343$ [M⁺+H].

Imidazole-1-carboxylic acid 1-(2',4'-difluoro-biphenyl-4-yl)-propyl ester (5). Synthesized according to Method E using **4a** (0.21 g, 0.85 mmol) and CDI (0.28 g, 1.69 mmol); yield: 0.11 g (43 %); white solid: mp 76-77 °C; $R_f = 0.29$ (DCM / MeOH, 95:5); δ_H (CDCl₃, 500 MHz) 1.01 (t, $J = 14.8$ Hz, 3H, CH₃), 2.03-2.19 (q, $J = 14.8$, 15.5 Hz, 2H, CH₂), 5.87 (t, $J = 15.5$ Hz, 1H, CH), 6.89-7.06 (m, 2H), 7.09-7.11 (m, 1H), 7.36-7.40 (m, 1H), 7.45-7.48 (m, 3H), 7.52 (dd, $J = 1.6$, 1.9 Hz, 2H), 8.24 (s, 1H, Im-2H); MS (ESI): $m/z = 343$ [M⁺+H].

Imidazole-1-carboxylic acid 1-(2',5'-difluoro-biphenyl-4-yl)-propyl ester (8). Synthesized according to Method E using **7a** (0.12 g, 0.46 mmol) and CDI (0.15 g, 0.93 mmol); yield: 0.10 g (69 %); white solid: mp 77-78 °C; $R_f = 0.29$ (DCM / MeOH, 95:5); δ_H (CDCl₃, 500 MHz) 1.01 (t, $J = 14.8$ Hz, 3H, CH₃), 2.02-2.20 (q, $J = 14.8$, 15.5 Hz, 2H, CH₂), 5.88 (t, $J = 15.5$ Hz, 1H, CH), 6.93-7.02 (m, 1H), 7.09-7.15 (m, 3H), 7.46-7.48 (m, 3H), 7.52-7.55 (m, 2H), 8.23 (s, 1H, Im-2H); MS (ESI): $m/z = 343$ [M⁺+H].

Imidazole-1-carboxylic acid 1-(3,4'-difluoro-biphenyl-4-yl)-propyl ester (10). Synthesized according to Method E using **7a** (0.19 g, 0.75 mmol) and CDI (0.24 g, 1.50 mmol); yield: 0.10 g (69 %); colorless oil; $R_f = 0.29$ (DCM / MeOH, 95:5); δ_H (CDCl₃, 500 MHz) 1.01 (t, $J = 14.8$ Hz, 3H, CH₃), 2.02-2.20 (q, $J = 14.8$, 15.5 Hz, 2H, CH₂), 5.88 (t, $J = 15.5$ Hz, 1H, CH), 6.14 (s, 1H), 7.26-7.28 (m, 2H), 7.19-7.25 (m, 1H), 7.34-7.35 (m, 1H), 7.42-7.48 (m, 2H), 7.50-7.53 (m, 2H), 8.22 (s, 1H, Im-2H); MS (ESI): $m/z = 343$ [M⁺+H].

Imidazole-1-carboxylic acid 3,4'-difluoro-biphenyl-4-ylmethyl ester (12). Synthesized according to Method E using **11a** (0.26 g, 1.20 mmol) and CDI (0.39 g, 2.40 mmol); yield: 0.09 g (28 %); white solid: mp 220-221 °C; $R_f = 0.29$ (DCM / MeOH, 95:5); δ_H (CDCl₃, 500 MHz) 5.33 (s, 2H, CH₂), 7.07 (s, 1H), 7.12-7.15 (t, $J = 17.4$ Hz, 2H), 7.20 (s, 1H), 7.29 (d, $J = 11.0$ Hz, 1H), 7.33-7.35 (m, 2H), 7.49-7.52 (m, 2H), 8.32 (s, 1H, Im-2H); MS (ESI): $m/z = 315$ [M⁺+H].

(4'-Fluorobiphenyl-4-yl)(1H-imidazol-5-yl)methanol (23). A solution of **23a** (0.10 g, 0.20 mmol) in MeOH (5 mL) was stirred with pyridinium hydrochloride (35 mg, 0.30 mmol) at 60 °C for 4 hours. Then the reaction was quenched by adding saturated NaHCO₃ aq (10 mL), 20 mL EtOAc were added and the phases separated. The water phase was extracted 3 times with EtOAc (20 mL), the combined organic extracts were dried over Na₂SO₄, and concentrated under reduced pressure. The crude product was purified by flash chromatography; yield: 0.05 g (91 %); colorless oil; $R_f = 0.19$ (EtOAc / MeOH, 95:5); δ_H (CDCl₃ + *d*₆-DMSO, 500 MHz) 2.99 (s, 1H), 5.84 (s, 1H), 6.87 (s, 2H), 7.02-7.06 (m, 2H), 7.41-7.47 (m, 6H); $m/z = 269$ [M⁺+H].

5-(1-(4'-Fluorobiphenyl-4-yl)-2-methylprop-1-enyl)-1H-imidazole (25). Compound **24** (0.10 mg, 0.32 mol) was refluxed in an *i*-PrOH solution of HCl (10 mL, 3N) for 2 hours. Afterwards, the resulting solution was concentrated under reduced pressure and washed 3 times with Et₂O. No further purification was necessary; yield: 0.07 g (77 %); colorless oil; $R_f = 0.29$ (EtOAc / MeOH, 95:5); δ_H (CDCl₃, 500 MHz) 1.80 (s, 3H), 2.05 (s, 3H), 6.98 (s, 1H), 7.12 (dd, $J = 8.7$, 8.8 Hz, 2H), 7.19 (d, $J = 8.3$ Hz, 2H), 7.50 (d, $J = 8.3$ Hz, 2H), 7.54 (dd, $J = 5.3$, 8.7 Hz, 2H), 7.63 (s, 1H); $m/z = 293$ [M⁺+H].

5-(1-(4'-Fluorobiphenyl-4-yl)-2-methylpropyl)-1H-imidazole (26). Pearlman's catalyst (5 mg, 7.12 μmol) and **25** (50 mg, 0.17 mmol) were prepared in EtOH and THF (2:1, 5mL) under H₂ atmosphere. The mixture was left stirring for 3 hours, then the catalyst was filtered off 3 times and the solution concentrated under reduced pressure. The obtained solid was washed 3 times with Et₂O. No further purification was necessary; yield: 50 mg (100%); yield: 0.07 g (77 %); colorless oil; $R_f = 0.29$ (EtOAc / MeOH, 95:5); δ_H (CDCl₃, 500 MHz) 0.86 (d, $J = 6.6$ Hz, 3H, CH₃), 0.99 (d, $J = 6.6$ Hz, 3H, CH₃), 3.60 (d, $J = 9.4$ Hz, 1H, CH), 6.90 (s, 1H), 7.09 (dd, $J = 8.7$, 8.8 Hz, 2H), 7.36

(d, $J = 8.2$ Hz, 2H), 7.45 (d, $J = 8.2$ Hz, 2H), 7.51 (dd, $J = 5.4, 8.7$ Hz, 2H), 7.55 (s, 1H); $m/z = 295$ [$M^+ + H$].

Docking studies

Ligands. All molecular modeling studies were performed on Intel(R) P4 CPU 3.00GHz running Linux CentOS5.2. The structures of the inhibitors were built with SYBYL 8 (Sybyl, Tripos Inc., St. Louis, Missouri, USA) and energy-minimized in MMFF94s force-field²⁵ as implemented in Sybyl.

Docking. Molecular docking calculations were performed for various inhibitors of Table 1. Since the GOLD docking program allows flexible docking of the compounds, no conformational search was employed to the ligand structures. GOLD gave the best poses by a genetic algorithm (GA) search strategy. Ligands were docked in 50 independent genetic algorithm (GA) runs for each of the three GOLD-docking runs. Heme iron was chosen as active-site origin, while the radius was set equal to 19 Å. The automatic active-site detection was switched on. A distance constraint of a minimum of 1.9 and a maximum of 2.5 Å between the sp^2 -hybridised nitrogen of the imidazole and the iron was set. Additionally, the goldscore.p450_pdb parameters were used and some of the GOLDScore parameters were modified to improve the weight of hydrophobic interaction and of the coordination between iron and nitrogen. The genetic algorithm default parameters were set as suggested by the GOLD authors. On the other hand, the annealing parameters of fitness function were set at 3.5 Å for hydrogen bonding and 6.5 Å for Van der Waals interactions.

Analogously as for GOLD, no conformational search was performed prior docking with FlexX, since the ligands are docked according to an incremental fragment docking strategy. Standard parameter settings were used except for “base placement”, which was set on single interaction scan, and “chemical parameters”, in which the maximum overlap volume of the subroutine “clash handling” was set at a range of 3.6 Å. Additionally the “FlexX-Pharm” module was employed, setting the heme iron as an octahedral coordinating metal pharmacophore point. The very same iron atom was chosen as active site center and amino acid residues within 16 Å were considered as part of the active site.

All the poses resulting from three docking runs (GOLD-chemscore, GOLD-GOLDScore and FlexX) for each compound were clustered with ACIAP¹⁹ and the representative structure of each significant cluster was selected. After the docking simulations and cluster analysis were performed, the quality of the docked representative poses was evaluated based on visual inspection of the putative binding modes of the ligands. The latter were further evaluated by means of MOE (www.chemcompd.com) with its LigX module and evaluated by means of the various scoring functions (GOLDScore, CHEMScore and the empirical FlexX Score).

MEP. For each docked compound geometry optimization was performed employing the B3LYP hybrid functional²⁰ in combination with a 6-311++G (d,p) basis set using the package Gaussian03 (Gaussian, Inc., Pittsburgh, PA, 2003). The molecular electrostatic potential (MEP) maps were plotted using GaussView, version 3.0, the 3D molecular graphics package of Gaussian. These electrostatic potential surfaces were generated by mapping 6-311++G** electrostatic potentials onto surfaces of molecular electron density (isovalue = 0.004 electron/Å) and the ESP values on the surface color-coded ranging from -6 (red) to +12 (blue) kcal/mol.

Acknowledgement.

The authors thank Dr. Ursula Müller-Vieira and Maria-Christina Scherzberg for the IC_{50} determination, as well as Dr. Klaus Biemel for performing the in vivo test, and appreciate the help for synthesizing some compounds by Dr. Kerstin Jahn-Hoffmann, Dr. Mariano E. Pinto-Bazurco Mendieta and Dr. Marc Bartels.

Supporting Information Available.

The synthetic procedures and characterization of all intermediates as well as HPLC purities, ^{13}C -NMR and IR spectra of all final compounds. This material is available free of charge via the internet at <http://pubs.acs.org>.

References.

- (1) Jemal, A.; Siegel, R.; Ward, E.; Hao, Y.; Xu, J.; Murray, T.; Thun, M. J. Cancer statistics, 2008. *CA Cancer J. Clin.* **2008**, *58*, 71-96.4r
- (2) Huhtaniemi, I.; Nikula, H.; Parvinen, M.; Rannikko, S. Histological and functional changes of the testis tissue during GnRH agonist treatment of prostatic cancer. *Am. J. Clin. Oncol.* **1988**, *11*, Suppl. 1, S11-15.
- (3) Labrie, F.; Dupont, A.; Belanger, A.; Cusan, L.; Lacourciere, Y.; Monfette, G.; Laberge, J. G.; Emond, J. P.; Fazekas, A. T.; Raynaud, J. P.; Husson, J. M. New hormonal therapy in prostatic carcinoma: combined treatment with LHRH agonist and an antiandrogen. *Clin. Invest. Med.* **1982**, *5*, 267-275.
- (4) (a) Hara, T.; Miyazaki, J.; Araki, H.; Yamaoka, M.; Kanzaki, N.; Kusaka, M.; Miyamoto, M. Novel mutations of androgen receptor: a possible mechanism of bicalutamide withdrawal syndrome. *Cancer Res.* **2003**, *63*, 149-153. (b) Zhao, X. Y.; Malloy, P. J.; Krishnan, A. V.; Swami, S.; Navone, N. M.; Peehl, D. M.; Feldman, D. Glucocorticoids can promote androgen-independent growth of prostate cancer cells through a mutated androgen receptor. *Nature Medicine*, **2000**, *6*, 703-706.
- (5) (a) Herold, C. I.; Blackwell, K. L. Aromatase inhibitors for breast cancer: proven efficacy across the spectrum of disease. *Clin. Breast Cancer.* **2008**, *8*, 50-64. (b) Hartmann, R. W.; Bayer, H.; Grün, G. Aromatase inhibitors. Syntheses and structure-activity studies of novel pyridyl-substituted indanones, indans, and tetralins. *J. Med. Chem.* **1994**, *37*, 1275-81. (c) Leonetti, F.; Favia, A.; Rao, A.; Aliano, R.; Paluszczak, A.; Hartmann, R. W.; Carotti, A. Design, synthesis, and 3D QSAR of novel potent and selective aromatase inhibitors. *J. Med. Chem.* **2004**, *47*, 6792-6803. (d) Le Borgne, M.; Marchand, P.; Duflos, M.; Delevoye-Seiller, B.; Piessard-Robert, S.; Le Baut, G.; Hartmann, R. W.; Palzer, M. Synthesis and in vitro evaluation of 3-(1-Azolylmethyl)-1H-indoles and 3-(1-azoly1-1-phenylmethyl)-1H-indoles as inhibitors of P450 arom. *Arch. Pharm. (Weinheim, Ger.)* **1997**, *330*, 141-145. (e) Leze, M. P.; Le Borgne, M.; Pinson, P.; Paluszczak, A.; Duflos, M.; Le Baut, G.; Hartmann, R. W. Synthesis and biological evaluation of 5-[(aryl)(1H-imidazol-1-yl)methyl]-1H-indoles: potent and selective aromatase inhibitors. *Bioorg. Med. Chem. Lett.* **2006**, *16*, 1134-1137. (f) Gobbi, S.; Cavalli, A.; Rampa, A.; Belluti, F.; Piazza, L.; Paluszczak, A.; Hartmann, R. W.; Recanatini, M.; Bisi, A. Lead optimization providing a series of flavone derivatives as potent nonsteroidal inhibitors of the cytochrome P450 aromatase enzyme. *J. Med. Chem.* **2006**, *49*, 4777-4780. (g) Cavalli, A.; Bisi, A.; Bertucci, C.; Rosini, C.; Paluszczak, A.; Gobbi, S.; Giorgio, E.; Rampa, A.; Belluti, F.; Piazza, L.; Valenti, P.; Hartmann, R. W.; Recanatini, M. Enantioselective nonsteroidal aromatase inhibitors identified through a multidisciplinary medicinal chemistry approach. *J. Med. Chem.* **2005**, *48*, 7282-7289. (h) Castellano, S.; Stefancich, G.; Ragno, R.; Schewe, K.; Santoriello, M.; Caroli, A.; Hartmann, R. W.; Sbardella, G. CYP19 (aromatase): exploring the scaffold flexibility for novel selective inhibitors. *Bioorg. Med. Chem.* **2008**, *16*, 8349-8358.
- (6) (a) Lucas, S.; Heim, R.; Ries, C.; Schewe, K. E.; Birk, B.; Hartmann, R. W. In vivo active aldosterone synthase inhibitors with improved selectivity: lead optimization providing a series of pyridine substituted 3,4-dihydro-1H-quinolin-2-one derivatives. *J. Med. Chem.* **2008**, *51*, 8077-8087. (b) Lucas, S.; Heim, R.; Negri, M.; Antes, I.; Ries, C.; Schewe, K. E.; Bisi, A.; Gobbi, S.; Hartmann, R. W. Novel aldosterone synthase inhibitors with extended carbocyclic skeleton by a combined ligand-based and structure-based drug design approach. *J. Med. Chem.* **2008**, *51*, 6138-6149. (c) Heim, R.; Lucas, S.; Grombein, C. M.; Ries, C.; Schewe, K. E.; Negri, M.; Müller-Vieira, U.; Birk, B.; Hartmann, R. W. Overcoming undesirable CYP1A2 inhibition of pyridyl-naphthalene- type aldosterone synthase inhibitors: influence of heteroaryl derivatization on potency and selectivity. *J. Med. Chem.* **2008**, *51*, 5064-5074. (d) Voets, M.; Antes, I.; Scherer, C.; Müller-Vieira, U.; Biemel, K.; Marchais-Oberwinkler, S.; Hartmann, R. W. Synthesis and evaluation of heteroaryl-substituted dihydronaphthalenes and indenes: potent and selective inhibitors of aldosterone synthase (CYP11B2) for the treatment of congestive heart failure and myocardial fibrosis. *J. Med. Chem.* **2006**, *49*, 2222-2231. (e) Voets, M.; Antes, I.; Scherer, C.; Müller-Vieira, U.; Biemel, K.; Barassin, C.; Marchais-Oberwinkler, S.; Hartmann, R. W. Heteroaryl-substituted naphthalenes and structurally modified derivatives: selective inhibitors of CYP11B2 for the treatment of congestive heart failure and myocardial fibrosis. *J. Med. Chem.* **2005**, *48*, 6632-6642. (f) Ulmschneider, S.; Müller-Vieira, U.; Klein, C. D.; Antes, I.; Lengauer, T.; Hartmann, R. W. Synthesis and evaluation of (pyridylmethylene)tetrahydronaphthalenes/-indanes and structurally modified derivatives: potent and selective inhibitors of aldosterone synthase. *J. Med. Chem.* **2005**, *48*, 1563-1575. (g) Ulmschneider, S.; Müller-Vieira, U.; Mitrenga, M.; Hartmann, R. W.; Oberwinkler-Marchais, S.; Klein, C. D.; Bureik, M.; Bernhardt, R.; Antes, I.; Lengauer, T. Synthesis and evaluation of

- imidazolyl-methylene-tetrahydronaphthalenes and imidazolyl-methylene-indanes: potent inhibitors of aldosterone Synthase. *J. Med. Chem.* **2005**, *48*, 1796-1805.
- (7) Chung, B. C.; Picardo-Leonard, J.; Hanui, M.; Bienkowski, M.; Hall, P. F.; Shively, J. E.; Miller, W. L. Cytochrome P450c17(steroid 17 α -hydroxylase/C17,20-lyase): cloning of human adrenal and testis cDNA indicates the same gene is expressed in both tissues. *Proc. Natl. Acad. Sci. USA.* **1987**, *84*, 407-411.
- (8) (a) Harris, K. A.; Weinberg, V.; Bok, R. A.; Kakefuda, M.; Small, E. J. Low dose ketoconazole with replacement doses of hydrocortisone in patients with progressive androgen independent prostate cancer. *J. Urol.* **2002**, *168*, 542-545. (b) Eklund, J.; Kozloff, M.; Vlamakis, J.; Starr, A.; Mariott, M.; Gallot, L.; Jovanovic, B.; Schilder, L.; Robin, E.; Pins, M.; Bergan, R. C. Phase II study of mitoxantrone and ketoconazole for hormone-refractory prostate cancer. *Cancer* **2006**, *106*, 2459-2465.
- (9) (a) Potter, G. A.; Banie, S. E.; Jarman, M.; Rowlands, M. G. Novel steroidal inhibitors of human cytochrome P450 17, (17 α -hydroxylase- C_{17,20}-lyase): potential agents for the treatment of prostatic cancer. *J. Med. Chem.* **1995**, *38*, 2463-2471. (b) Burkhart, J. P.; Gates, C. A.; Laughlin, M. E.; Resvick, R. J.; Peet, N. P. Inhibition of steroid C17(20) lyase with C-17-heteroaryl steroids. *Bioorg. Med. Chem.* **1996**, *4*, 1411-1420. (c) Handratta, V. D.; Vasaitis, T. S.; Njar, V. C. O.; Gediya, L. K.; Kataria, R.; Chopra, P.; Newman, D. Jr.; Farquhar, R.; Guo, Z.; Qiu, Y.; Brodie, A. M. H. Novel C-17-heteroaryl steroidal CYP17 inhibitors/antiandrogens: Synthesis, in vitro biological activity, pharmacokinetics, and antitumor activity in the LAPC4 human prostate cancer xenograft model. *J. Med. Chem.* **2005**, *48*, 2972-2984. (d) Njar, V. C. O.; Kato, K.; Nnane, I. P.; Grigoryev, D. N.; Long, B. J.; Brodie, A. M. H. Novel 17-azolyl steroids, potent inhibitors of human cytochrome 17 α -hydroxylase-C17,20-lyase (P450 17 α): Potential agents for the treatment of prostate cancer. *J. Med. Chem.* **1998**, *41*, 902-912.
- (10) (a) Hartmann, R.W.; Hector, M.; Haidar, M.; Ehmer, P. B.; Reichert, W.; Jose, J. Synthesis and evaluation of novel steroidal oxime inhibitors of P450 17 (17 α -hydroxylase/C_{17,20}-lyase) and 5 α -reductase types 1 and 2. *J. Med. Chem.* **2000**, *43*, 4266-4277. (b) Hartmann, R.W.; Hector, M.; Wachall, B.G.; Paluszczak, A.; Palzer, M.; Huch, V.; Veith, M. Synthesis and evaluation of 17-aliphatic heterocycle-substituted steroidal inhibitors of 17 α -hydroxylase/C_{17,20}-lyase (P450 17). *J. Med. Chem.* **2000**, *43*, 4437-4445. (c) Njar, V. C. O.; Hector, M.; Hartmann, R.W. 20-Amino and 20, 21-aziridinyl pregnene steroids: development of potent inhibitors of 17 α -hydroxylase/C_{17,20}-lyase (P450 17). *Bioorg. Med. Chem.* **1996**, *4*, 1447-1453. (d) Haidar, S.; Ehmer, P. B.; Hartmann, R. W. Novel steroidal pyrimidyl inhibitors of P450 17 (17 α -hydroxylase/C17-20-lyase). *Arch. Pharm. (Weinheim, Ger.)* **2001**, *334*, 373-374.
- (11) (a) Wächter, G. A.; Hartmann, R. W.; Sergejew, T.; Grün, G. L.; Ledergerber, D. Tetrahydronaphthalenes: Influence of heterocyclic substituents on inhibition of steroidogenic enzymes P450 arom and P450 17. *J. Med. Chem.* **1996**, *39*, 834-841. (b) Chan, F. C. Y.; Potter, G. A.; Barrie, S. E.; Haynes, B. P.; Rowlands, M. G.; Houghton, G.; Jarman, M. 3- and 4-Pyridylalkyl adamantanecarboxylates: inhibitors of human cytochrome P450 17 α (17 α -hydroxylase/C17,20-lyase). Potential nonsteroidal agents for the treatment of prostatic cancer. *J. Med. Chem.* **1996**, *39*, 3319-3323.
- (12) (a) Wachall, B. G.; Hector, M.; Zhuang, Y.; Hartmann, R. W. Imidazole substituted biphenyls: a new class of highly potent and in vivo active inhibitors of P450 17 as potential therapeutics for treatment of prostate cancer. *Bioorg. Med. Chem.* **1999**, *7*, 1913-1924. (b) Zhuang, Y.; Wachall, B. G.; Hartmann, R. W. Novel imidazolyl and triazolyl substituted biphenyl compounds: synthesis and evaluation as nonsteroidal inhibitors of human 17 α -hydroxylase-C17, 20-lyase (P450 17). *Bioorg. Med. Chem.* **2000**, *8*, 1245-1252. (c) Leroux, F.; Hutschenreuter, T. U.; Charriere, C.; Scopelliti, R.; Hartmann, R. W. N-(4-biphenylmethyl)imidazoles as potential therapeutics for the treatment of prostate cancer: metabolic robustness due to fluorine substitution? *Helv. Chim. Acta* **2003**, *86*, 2671-2686. (d) Hutschenreuter, T. U.; Ehmer, P. E.; Hartmann, R. W. Synthesis of hydroxy derivatives of highly potent non-steroidal CYP 17 Inhibitors as potential metabolites and evaluation of their activity by a non cellular assay using recombinant human enzyme. *J. Enzyme Inhib. Med. Chem.* **2004**, *19*, 17-32. (e) Jagusch, C.; Negri, M.; Hille, U. E.; Hu, Q.; Bartels, M.; Jahn-Hoffmann, K.; Pinto-Bazurco Mendieta, M. A. E.; Rodenwaldt, B.; Müller-Vieira, U.; Schmidt, D.; Lauterbach, T.; Recanatini, M.; Cavalli, A.; Hartmann, R. W. Synthesis, biological evaluation and molecular modeling studies of methyleneimidazole substituted biaryls as inhibitors of human 17 α -hydroxylase-17,20-lyase (CYP17) – Part I: heterocyclic modifications of the core structure. *Bioorg. Med. Chem.* **2008**, *16*, 1992-2010. (f) Pinto-Bazurco Mendieta, M. A. E.; Negri, M.; Jagusch, C.; Hille, U. E.; Müller-Vieira, U.; Schmidt, D.; Hansen, K.; Hartmann, R. W. Synthesis, biological evaluation and molecular modelling studies of novel ACD- and ABD-ring steroidomimetics as inhibitors of CYP17. *Bioorg. Med. Chem. Lett.* **2008**, *18*, 267-73.

- (g) Hu, Q.; Negri, M.; Jahn-Hoffmann, K.; Zhuang, Y.; Olgen, S.; Bartels, M.; Müller-Vieira, U.; Lauterbach, T.; Hartmann, R. W. Synthesis, biological evaluation, and molecular modeling studies of methylene imidazole substituted biaryls as inhibitors of human 17 α -hydroxylase-17,20-lyase (CYP17)-Part II: Core rigidification and influence of substituents at the methylene bridge. *Bioorg. Med. Chem.* **2008**, *16*, 7715-7727. (h) Pinto-Bazurco Mendieta, M. A. E.; Negri, M.; Jagusch, C.; Müller-Vieira, U.; Lauterbach, T.; Hartmann, R. W. Synthesis, biological evaluation, and molecular modeling of abiraterone analogues: Novel CYP17 inhibitors for the treatment of prostate cancer. *J. Med. Chem.* **2008**, *51*, 5009-5018. (i) Hille, U. E.; Hu, Q.; Vock, C.; Negri, M.; Bartels, M.; Müller-Vieira, U.; Lauterbach, T.; Hartmann, R. W. Novel CYP17 inhibitors: Synthesis, biological evaluation, structure-activity relationships and modeling of methoxy- and hydroxy-substituted methyleneimidazolyl biphenyls. *Eur. J. Med. Chem.* **2009**, *44*, 2765-2775. (j) Pinto-Bazurco Mendieta, M. A. E.; Negri, M.; Hu, Q.; Hille, U. E.; Jagusch, C.; Jahn-Hoffmann, K.; Müller-Vieira, U.; Schmidt, D.; Lauterbach, T.; Hartmann, R. W. CYP17 inhibitors. Annulations of additional rings in methylene imidazole substituted biphenyls: synthesis, biological evaluation and molecular modeling. *Arch. Pharm. (Weinheim, Ger.)* **2008**, *341*, 597-609. (k) Hille, U. E.; Hu, Q.; Pinto-Bazurco Mendieta, M. A. E.; Bartels, M.; Vock, C. A.; Lauterbach, T.; Hartmann, R. W. Steroidogenic cytochrome P450 (CYP) enzymes as drug targets: Combining substructures of known CYP inhibitors leads to compounds with different inhibitory profile. *C. R. Chim.* **2009**, *12*, 1117-1126.
- (13) (a) Hagmann, W. K. The many roles for fluorine in medicinal chemistry. *J. Med. Chem.* **2008**, *51*, 4359-4369. (b) Böhm, H. J.; Banner, D.; Bendels, S.; Kansy, M.; Kuhn, B.; Müller, K.; Obst-Sander, U.; Stahl, M. Fluorine in medicinal chemistry. *ChemBioChem.* **2004**, *5*, 637-643. (c) Müller, K.; Faeh, C.; Diederich, F. Fluorine in pharmaceuticals: Looking beyond intuition. *Science.* **2007**, *317*, 1881-1886. (d) DiMaggio, S. and Sun, H. The strength of weak interactions: Aromatic fluorine in drug design. *Curr. Top. Med. Chem.* **2006**, *6*, 1473-1482. (e) Paulini, R.; Müller, K.; Diederich, F. Orthogonal multipolar interactions in structural chemistry and biology. *Angew. Chem., Int. Ed.* **2005**, *44*, 1788-1805. (f) Olsen, J. A.; Banner, D. W.; Seiler, P.; Sander, U. O.; D'Arcy, A.; Stihle, M.; Müller, K.; Diederich, F. A fluorine scan of thrombin inhibitors to map the fluorophilicity/ fluorophobicity of an enzyme active site: Evidence for C-F \cdots C=O interactions. *Angew. Chem., Int. Ed.* **2003**, *42*, 2507-2511. (g) Olsen, J. A.; Banner, D. W.; Seiler, P.; Wagner, B.; Tschopp, T.; Obst-Sander, U.; Kansy, M.; Müller, K.; Diederich, F. Fluorine interactions at the thrombin active site: Protein backbone fragments H-C α -C=O comprise a favorable C-F environment and interactions of C-F with electrophiles. *ChemBioChem*, **2004**, *5*, 666-675. (h) Hof, F.; Scofield, D. M.; Schweizer, W. B.; Diederich, F. A weak attractive interaction between organic fluorine and an amide group. *Angew. Chem., Int. Ed.* **2004**, *43*, 5056-5059. (i) Istvan, E. S.; Deisenhofer, J. Structural mechanism for statin inhibition of HMG-CoA reductase. *Science*, **2001**, *292*, 1160-1164. (j) Phillips, G.; Davey, D. D.; Eagen, K. A.; Koovakkat, S. K.; Liang, A.; Ng, H. P.; Pinkerton, M.; Trinh, L.; Whitlow, M.; Beatty, A. M.; Morrissey, M. M. Design, synthesis and activity of 2,6-diphenoxypyridine-derived factor Xa inhibitors. *J. Med. Chem.* **1999**, *42*, 1749-1756. (k) Parlow, J. J.; Stevens, A. M.; Stegeman, R. A.; Stallings, W. C.; Kurumbail, R.G.; South, M. S. Synthesis and Crystal Structures of Substituted Benzenes and Benzoquinones as Tissue Factor VIIa Inhibitors. *J. Med. Chem.* **2003**, *46*, 4297-4312. (l) Parlow, J. J.; Kurumbail, R. G.; Stegeman, R. A.; Stevens, A. M.; Stallings, W. C.; South, M. S. Design, Synthesis, and Crystal Structure of Selective 2-Pyridone Tissue Factor VIIa Inhibitors. *J. Med. Chem.* **2003**, *46*, 4696-4701.
- (14) Miyaura, N.; Suzuki, A. Palladium-catalyzed cross-coupling reaction of organoboron compounds. *Chem. Rev.* **1995**, *95*, 2457-2483.
- (15) Tang, Y.; Dong, Y.; Vennerstrom J. L. The reaction of carbonyldiimidazole with alcohols to form carbamates and N-alkylimidazole. *Synthesis* **2004**, *15*, 2540-2544.
- (16) Ehmer, P. B.; Jose, J.; Hartmann, R. W. Development of a simple and rapid assay for the evaluation of inhibitors of human 17 α -hydroxylase-C(17,20)-lyase (P450c17) by coexpression of P450c17 with NADPH-cytochrome-P450-reductase in Escherichia coli. *J. Steroid Biochem. Mol. Biol.* **2000**, *75*, 57-63.
- (17) a) Jones, G.; Willett, P.; Glen, R. C.; Leach, A. R.; Taylor, R. Development and validation of a genetic algorithm for flexible docking. *J. Mol. Biol.* **1997**, *267*, 727-748. b) Verdonk, M. L.; Cole, J. C.; Hartshorn, M. J.; Murray, C.W.; Taylor, R. D. Improved protein-ligand docking using GOLD. *Proteins* **2003**, *52*, 609-623.
- (18) a) Kramer, B.; Rarey, M.; Lengauer, T. Evaluation of the FlexX incremental construction algorithm for protein-ligand docking. *Proteins: Struct., Funct., and Gene.* **1999**, *37*, 228-241. b) FlexX trial Version 3.1.3; BioSolveIT GmbH, Sankt Augustin. <http://www.biosolveit.de/>

- (19) (a) Bottegoni, G.; Cavalli, A.; Recanatini, M. A comparative study on the application of hierarchical-agglomerative clustering approaches to organize outputs of reiterated docking runs. *J. Chem. Inf. Mod.* **2006**, *46*, 852-862. (b) Bottegoni, G.; Rocchia, W.; Recanatini, M.; Cavalli, A. ACIAP, autonomous hierarchical agglomerative cluster analysis based protocol to partition conformational datasets. *Bioinformatics* **2006**, *22*, 58-65.
- (20) a) Becke, A. D. Density-functional thermochemistry. III. The role of exact exchange. *J. Chem. Phys.* **1993**, *98*, 5648-5652; b) Stephens, P. J.; Devlin, F. J.; Chabalowski, C. F.; Frisch, M. J. Ab Initio calculation of vibrational absorption and circular dichroism spectra using density functional force fields. *J. Phys. Chem.* **1994**, *98*, 11623-11627.
- (21) Frisch, M. J.; Trucks, G. W.; Schlegel, H. B.; Scuseria, G. E.; Robb, M. A.; Cheeseman, J. R.; Montgomery, J. A., Jr.; Vreven, T.; Kudin, K. N.; Burant, J. C.; Millam, J. M.; Lyengar, S. S.; Tomasi, J.; Barone, V.; Mennucci, B.; Cossi, M.; Scalmani, G.; Rega, N.; Petersson, G. A.; Nakatsuji, H.; Hada, M.; Ehara, M.; Toyota, K.; Fukuda, R.; Hasegawa, J.; Ishida, M.; Nakajima, T.; Honda, Y.; Kitao, O.; Nakai, H.; Klene, M.; Li, X.; Knox, J. E.; Hratchian, H. P.; Cross, J. B.; Bakken, V.; Adamo, C.; Jaramillo, J.; Gomperts, R.; Stratmann, R. E.; Yazyev, O.; Austin, A. J.; Cammi, R.; Pomelli, C.; Ochterski, J. W.; Ayala, P. Y.; Morokuma, K.; Voth, G. A.; Salvador, P.; Dannenberg, J. J.; Zakrzewski, V. G.; Dapprich, S.; Daniels, A.D.; Strain, M. C.; Farkas, O.; Malick, D. K.; Rabuck, A. D.; Raghavachari, K.; Foresman, J. B.; Ortiz, J. V.; Cui, Q.; Baboul, A. G.; Clifford, S.; Cioslowski, J.; Stefanov, B. B.; Liu, G.; Liashenko, A.; Piskorz, P.; Komaromi, I.; Martin, R. L.; Fox, D. J.; Keith, T.; Al-Laham, M. A.; Peng, C. Y.; Nanayakkara, A.; Challacombe, M.; Gill, P. M. W.; Johnson, B.; Chen, W.; Wong, M. W.; Gonzalez, C.; Pople, J. A. Gaussian 03; Gaussian, Inc.: Pittsburgh, PA, 2004.
- (22) Dennington, I.; Roy, K. T.; Millam, J.; Eppinnett, K.; Howell, W. L.; Gilliland, R. GaussView, version 3.0; SemicheM Inc.: Shawnee Mission, KS, 2003.
- (23) (a) Bey, E.; Marchais-Oberwinkler, S.; Negri, M.; Kruchten, P.; Oster, A.; Klein, T.; Spadaro, A.; Werth, R.; Frotscher, M.; Birk, B.; Hartmann, R. W. New Insights into the SAR and binding modes of bis(hydroxyphenyl)thiophenes and -benzenes: influence of additional substituents on 17 β -hydroxysteroid dehydrogenase type 1 (17 β -HSD1) inhibitory activity and selectivity. *J. Med. Chem.* **2009**, *52*, 6724-6743. (b) Kruchten, P.; Werth, R.; Bey, E.; Oster, A.; Marchais-Oberwinkler, S.; Frotscher, M.; Hartmann, R. W. Selective inhibition of 17 β -hydroxysteroid dehydrogenase type 1 (17 β -HSD1) reduces estrogen responsive cell growth of T47-D breast cancer cells. *J. Steroid Biochem. Mol. Biol.* **2009**, *114*, 200-206. (c) Bey, E.; Marchais-Oberwinkler, S.; Werth, R.; Negri, M.; Al-Soud, Y. A.; Kruchten, P.; Oster, A.; Frotscher, M.; Birk, B.; Hartmann, R. W. Design, synthesis, biological evaluation and pharmacokinetics of bis(hydroxyphenyl) substituted azoles, thiophenes, benzenes, and aza-benzenes as potent and selective nonsteroidal inhibitors of 17 β -hydroxysteroid dehydrogenase type 1 (17 β -HSD1). *J. Med. Chem.* **2008**, *51*, 6725-6739. (d) Marchais-Oberwinkler, S.; Kruchten, P.; Frotscher, M.; Ziegler, E.; Neugebauer, A.; Bhoga, U.; Bey, E.; Müller-Vieira, U.; Messinger, J.; Thole, H.; Hartmann, R. W. Substituted 6-phenyl-2-naphthols. potent and selective nonsteroidal inhibitors of 17 β -hydroxysteroid dehydrogenase type 1 (17 β -HSD1): design, synthesis, biological evaluation, and pharmacokinetics. *J. Med. Chem.* **2008**, *51*, 4685-4698. (e) Frotscher, M.; Ziegler, E.; Marchais-Oberwinkler, S.; Kruchten, P.; Neugebauer, A.; Fetzer, L.; Scherer, C.; Müller-Vieira, U.; Messinger, J.; Thole, H.; Hartmann, R. W. Design, synthesis, and biological evaluation of (hydroxyphenyl)naphthalene and -quinoline derivatives: potent and selective nonsteroidal inhibitors of 17 β -hydroxysteroid dehydrogenase type 1 (17 β -HSD1) for the treatment of estrogen-dependent diseases. *J. Med. Chem.* **2008**, *51*, 2158-2169.
- (24) (a) Picard, F.; Schulz, T.; Hartmann, R. W. 5-Phenyl substituted 1-methyl-2-pyridones and 4-substituted biphenyl-4-carboxylic acids: synthesis and evaluation as inhibitors of steroid-5 α -reductase type 1 and 2. *Bioorg. Med. Chem.* **2002**, *10*, 437-448. (b) Baston, E.; Paluszczak, A.; Hartmann, R. W. 6-Substituted 1H-quinolin-2-ones and 2-methoxy-quinolines: synthesis and evaluation as inhibitors of steroid 5 α reductases types 1 and 2. *Eur. J. Med. Chem.* **2000**, *35*, 931-940. (c) Reichert, W.; Jose, J.; Hartmann, R. W. 5 α -Reductase in intact DU145 cells: evidence for isozyme I and evaluation of novel inhibitors. *Arch. Pharm. (Weinheim, Ger.)* **2000**, *333*, 201-204. (d) Picard, F.; Baston, E.; Reichert, W.; Hartmann, R. W. Synthesis of N-substituted piperidine-4-(benzylidene-4-carboxylic acids) and evaluation as inhibitors of steroid-5 α -reductase type 1 and 2. *Bioorg. Med. Chem.* **2000**, *8*, 1479-1487. (e) Baston, E.; Hartmann, R. W. N-substituted 4-(5-indolyl)benzoic acids. Synthesis and evaluation of steroid 5 α -reductase type I and II inhibitory activity. *Bioorg. Med. Chem. Lett.* **1999**, *9*, 1601-1606.

- (25) Halgren, T. A. MMFF VII. Characterization of MMFF94, MMFF94s, and other widely available force fields for conformational energies and for intermolecular interaction energies and geometries. *J. Comput. Chem.* **1999**, *20*, 730-748.

3.1.5. Conclusions and Outlook

In the first chapter of this doctoral thesis a good quality homology-based CYP17 model was built using, despite the low sequence identity (28.9%), a human CYP crystal structure as template (CYP2C9). This model shows a good geometrical profile and was used for docking studies performed with the softwares GOLD and FlexX. The model presents a polar SRS-1 and a hydrophobic SRS-5, which influences strongly the ligand binding (Fig. 26).

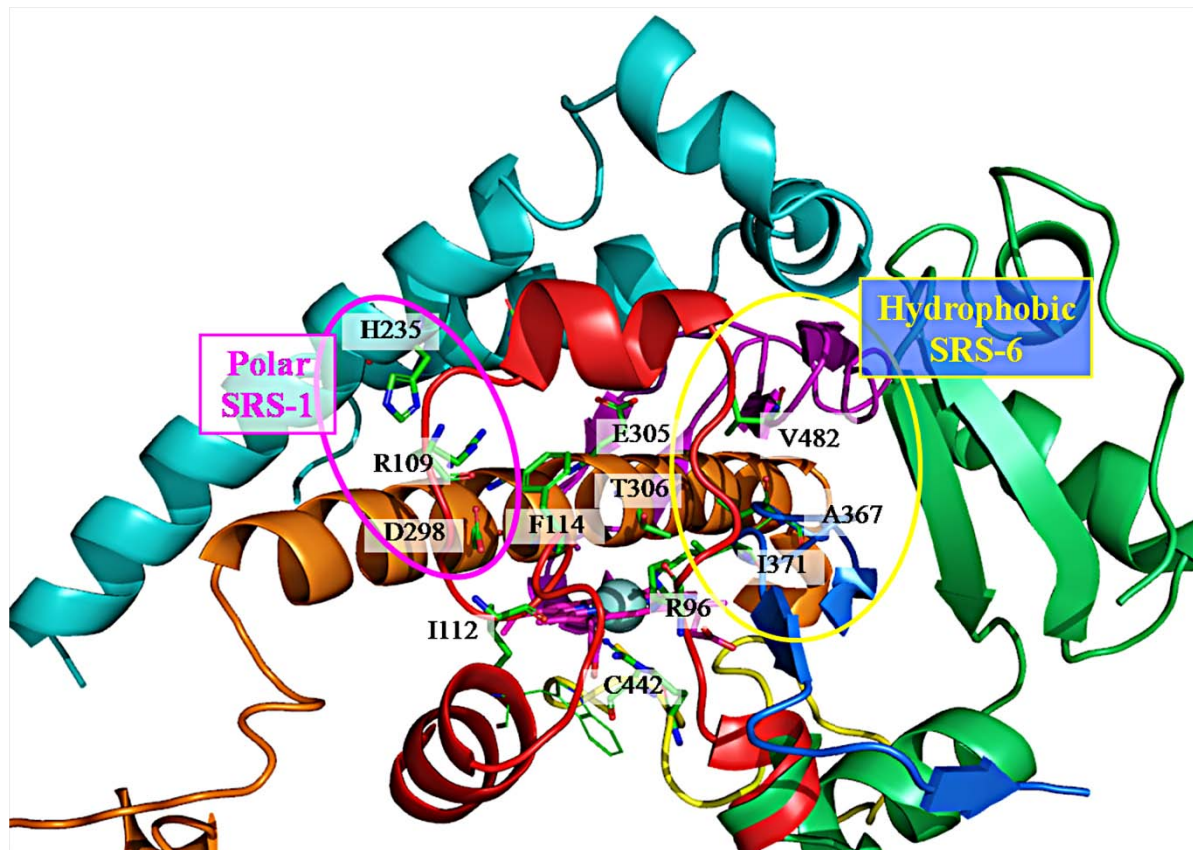


Figure 26. Active site of CYP17 rendered with FG-segment in cyan, BC-loop in red, I-helix orange, C-terminal loop violet and the β -domain in green. The SRS-1 (polar) and SRS-5 (hydrophobic) are circled in magenta and yellow, respectively, with the most important residues rendered as sticks and labelled.

Three different binding modes (Fig. 27) could be identified for the different classes of CYP17 inhibitors and the substrate pregnenolone (paper I-VII). In **BM1** the biaryl skeleton is oriented parallel to the I-helix pointing the A-ring next to the polar area SRS-1. In **BM2** the biaryl skeleton crosses the I-helix at the height of the I-helix kink (Gly301-Val304), pointing the A-ring toward the backbone of the F-helix. Only structures with a small substituent (R=H, F) in para position of the A-ring can occupy this pose. **BM3** resembles the preferred substrate binding mode (paper III), with the hydrophobic skeleton placed parallel to the heme-plane, pointing the A-ring toward the BC-loop.

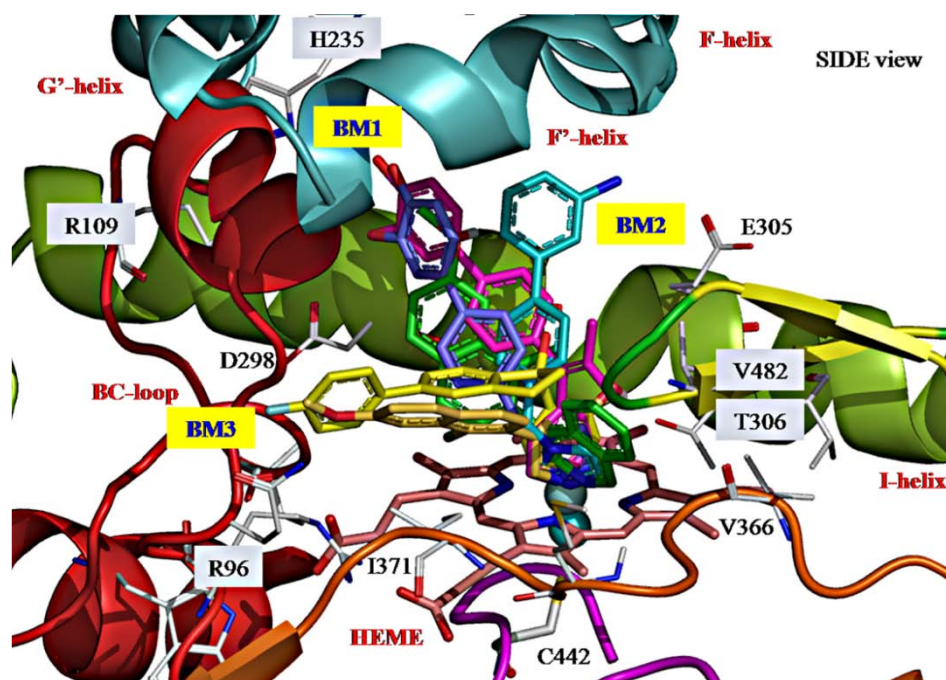


Figure 27. Docking complex of CYP17 with the three main binding modes (BM1-BM3), observed for different classes of CYP17 inhibitors. FG-segment and BC-loop are colored like in Fig. 26 in cyan and red, respectively, whereas I-helix and hydrophobic β 1-4 sheet are shown in green and orange, respectively.

Despite a spurious correlation between the IC_{50} values and the scoring functions of the docking software (data not shown), the model could explain the differences in the binding affinities of our *in-house* CYP17 inhibitors (papers **I-VII**) for the various binding modes. These binding modes were partially substantiated by the MEP investigations performed for some classes of inhibitors, confirming the quality of the homology model and the trustworthiness of the docking modes. Thus the CYP17 homology model became a precious tool in designing new inhibitors, especially for the choice of substituents on the A-ring and on the methylene-linker characterizing all bi-aryl based inhibitors.

In order to validate the binding modes identified for the classes of CYP17 inhibitors presented in papers **I-VII** a series of molecular dynamic studies should be performed. Moreover, snapshots of the stable parts of the dynamics should be used for free energy and, especially, free binding affinity calculations by means of MM-PBSA methods. This combination should lead to a reliable interpretation of the binding of the already developed inhibitor classes and furthermore fasten the rational drug design of a new generation of CYP17 inhibitors with an increased molecular complexity and a better potency and selectivity profile.

MD simulations conducted on a CYP17-pregnenolone complex should also be performed to gain insights in the binding mode of the substrate and in the entrance and egress pathways followed by pregnenolone approaching to the heme and the active site. These studies should envisage important contributions to the kinetic mechanism occurring for CYP17, especially when combined to QMMM studies focused on the electron transfer and especially the hydroxylation and subsequent lyase reaction.

3.2 Estrogen-dependent breast cancer (BC) - selective CYP19 inhibition

3.2.1. Molecular docking of non-steroidal aromatase inhibitors

In order to rationalize the different aromatase inhibitory potencies observed for a series of imidazolylmethylenebenzophenones in paper VII representative compounds were docked in the homology model (PDB entry 1TQA) built by Favia et al.¹²⁶ by means of GOLD software. In particular, we investigated the insertion of the imidazolylmethylene-group and the presence of additional substituents on the benzophenone core.

The two most potent compounds **1b** and **1d** (paper VII) shared a similar binding mode, showing a good complexation between the sp^2 -hybridized nitrogen of the imidazoles and the heme iron, and being involved in a H-bond network with Asp309 and Ser478 (Fig. 28). Moreover, the docking poses of these highly flexible AI envisaged the capability of aromatase, in the form of the homology model 1tqa, to host sterically more hindered substituents, like the additional 4'-Phe group (**1d**), close to the C-terminal loop, stabilized by π - π stackings with His475 and His480.

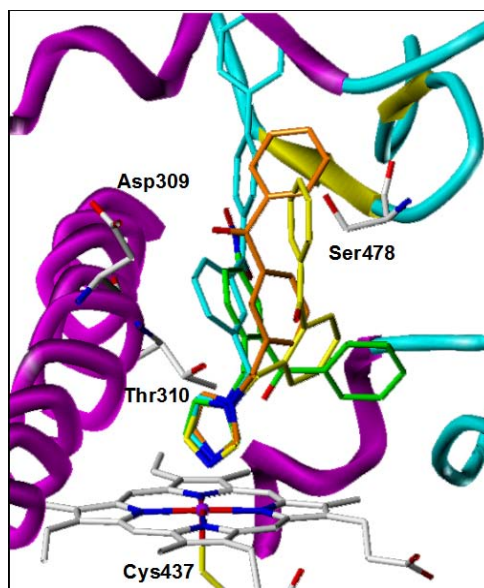


Figure 28. Docking complexes between aromatase and **1a** (yellow), **1b** (orange), **1d** (cyan), and **3** (green). The heme iron atom at the bottom of the picture is depicted as a violet ball. Critical residues of the aromatase active site are rendered as sticks.

3.2.2. Articles published in CYP19 project – paper VIII

Imidazolylmethylbenzophenones: a novel class of potent and selective aromatase inhibitors

Silvia Gobbi, Andrea Cavalli, Matthias Negri, Katarzyna E. Schewe, Federica Belluti, Lorna Piazzzi, Rolf W. Hartmann, Maurizio Recanatini, Alessandra Bisi

This article is protected by copyrights of ‘Journal of Medicinal Chemistry’

J. Med. Chem. **2007**, 50, 3420–3422.

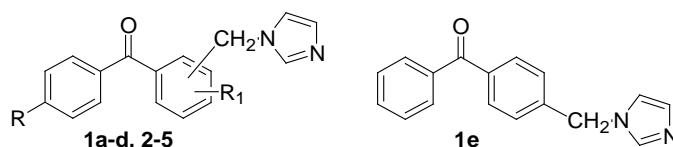
Abstract

Suppression of tumor and plasma estrogen levels by inhibition of aromatase is one of the most effective treatments for postmenopausal breast cancer patients. Starting from an easy-synthetically accessible benzophenone scaffold, a new class of potent and selective aromatase inhibitors was synthesized. Compounds **1b** and **1d** proved to be among the most potent inhibitors described so far.

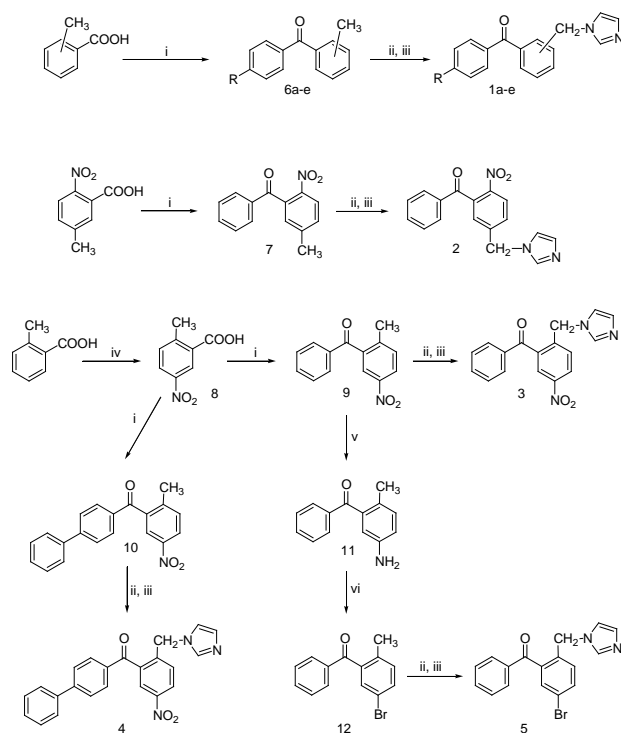
Estrogens are known to be implicated in breast cancer occurrence and development, and different strategies have been devised in order to control or block the progression of hormone-dependent breast cancer. The action of estrogens on their receptor can be blocked by the use of selective estrogen receptor modulators (SERMs), like tamoxifen. These compounds have been widely used as first line therapy in post-menopausal women with advanced breast cancer, but they are known to possess proestrogenic effects particularly on the endometrium and vascular system, and this partial agonism has been associated with possible development of tumors.¹ A different approach comes from the reduction of hormone levels by inhibition of cytochrome P450 aromatase (CYP19),² a key enzyme involved in the synthesis of estrogens, promoting the aromatization of the A ring of androgen precursors. Third generation aromatase inhibitors (AIs), such as letrozole, anastrozole and exemestane, are now considered a valid alternative to tamoxifene as first line treatment of advanced breast cancer.³ The search for potent and selective aromatase inhibitors still remains an attractive subject, since some interesting compounds have recently been developed by different groups working in the field.⁴⁻⁷ In addition, in a previous paper, we described some xanthenone-based molecules as potent inhibitors.⁸

In this letter, we report a new class of potent and selective inhibitors of aromatase, characterized by a rather flexible imidazolylmethylbenzophenone scaffold, which offers the advantage of a large synthetic accessibility. Moreover, these compounds could allow us to establish whether the conformationally constrained scaffold of the previously synthesized series of molecules is an essential element for optimal interaction with the enzyme and to determine the best positioning on this scaffold of the imidazole nitrogen that coordinates the iron atom of the heme group. To this aim, the position of the imidazole ring on the benzophenone moiety was varied, substituents were introduced on the phenyl ring carrying the imidazole, since the same pattern of substitution was also present in the previous series, and an additional benzene was placed on the other phenyl ring in order to explore the spatial requirements of that part of the molecule. The structures of the new compounds are reported in Chart 1.

Chart 1. Structures of the studied compounds



The synthesis was performed, according to Scheme 1, via Friedel-Craft acylation of benzene or biphenyl with the appropriately substituted benzoyl chloride to give **6a-d**, **7**, **9** and **10**, followed by bromination of the methyl group with NBS and subsequent substitution with imidazole to provide compounds **1a-d** and **2-4**. 2-methyl-5-nitrobenzoic acid **8**, which was not commercially available, was prepared via nitration of o-toluic acid. For the synthesis of compound **5**, 2-methyl-5-nitrobenzophenone **9** was reduced with H₂ and Pd/CaCO₃ to give 2-methyl-5-aminobenzophenone **11** and the amino group was substituted by a bromine atom to give **12** via the formation of the diazonium salt followed by addition of CuBr. This intermediate was then reacted as reported above to provide the final compound.



Scheme 1. Syntheses of the new compounds. **Reagents and conditions:** i) SOCl₂, reflux then AlCl₃ or trifluoromethanesulfonic acid, benzene or biphenyl, rt; ii) NBS, benzoyl peroxide, CCl₄, reflux; iii) imidazole, CH₃CN, N₂, reflux; iv) KNO₃, H₂SO₄, 0 °C; v) THF, H₂, Pd/CaCO₃, rt; vi) HBr, NaNO₂, 0 °C, then hot CuBr solution, rt.

The new compounds were tested for inhibition of aromatase using human placental microsomes incubated with 18[³H]androstenedione and measuring the tritiated water formed during the aromatisation of the substrate, as previously described.⁹ The inhibitory activity of the compounds towards 17β-hydroxylase/17,20-lyase (CYP17), another cytochrome P450 involved in the synthesis of androgens, was also assessed in order to evaluate their selectivity towards related enzymes. For the CYP17 inhibition tests *E.coli* cells overexpressing human CYP17 and P450 reductase were used.¹⁰ Another benzophenone derivative (**1e**),¹¹ previously reported in the literature as part of a large series of azole compounds tested for inhibition of aromatase, was also included in the evaluation and tested in our assays.

The results reported in Table 1 showed that all tested compounds were highly selective toward aromatase with respect to liase and some of them exhibited activity in the low nanomolar range. Interestingly, despite an increase in conformational flexibility, this series of molecules turned out to be more potent than the conformationally constrained series of compounds previously reported.⁸ It can promptly be observed that the position of the imidazole side chain is of crucial importance for the activity, since moving it from position 2 (compound **1a**) to 3 (**1b**) on the benzophenone nucleus led to a hundred-fold increase in potency. Compound **1e**, in which the imidazolylmethyl chain is in position 4, whose previously reported IC₅₀ value was 10 nM,¹¹ proved to be significantly less active when tested in our assay (IC₅₀ = 252 nM), showing activity comparable to the ortho-derivative **1a**. The introduction of a nitro group in both **1b** and **1a**, leading to compounds **2** and **3** respectively, was of no significant influence for the most active one **1b**, but highly beneficial for **1a**, since it increased its potency of more than one log unit. Looking at this result in view of the possible binding mode of these molecules at the enzyme active site (see below) and

assuming that the coordination of the heme iron by the imidazole moiety would be the primary interaction, it could be reasoned that, while the ketone in compound **1b** could be located at the optimal distance from the imidazole moiety in order to properly interact via H-bond with the enzyme, this is not possible for **1a**. If this is the case, the nitro group is only critical for compound **3**, as its position relative to the imidazole could be the appropriate one in order to give the molecule the possibility to establish a correct H-bond interaction with the enzyme.

Table 1. Biological activities of the new compounds towards CYP19 and CYP17.

compound	R	R ₁	CH ₂ imid position	CYP19 ^a IC ₅₀ nM ^c	CYP17 ^b % inhib. at 2.5 μM
1a	-	-	2	560	-
1b	-	-	3	7.3	-
1c	Ph	-	2	260	24
1d	Ph	-	3	5.3	NT
1e	-	-	4	252	NT
2	-	6-NO ₂	3	31	-
3	-	5-NO ₂	2	25.9	-
4	Ph	5-NO ₂	2	17.7	17
5	-	5-Br	2	400	15
Fadrozole				52	-

^aSubstrate 1β[³H]androstenedione 500 nM; ^bSubstrate progesterone 25 μM. ^cThe given values are mean values of at least three experiments. The deviations were within ± 5%. NT=not tested. “-“=no activity detected.

A further evidence to support this hypothesis came from the introduction on the structure of **1a** of a bromine atom which, unlike the nitro group, is devoid of H-bond potential, leading to compound **5**: the potency did not improve by the introduction of this substituent. Activity seemed to be slightly influenced by the presence of an additional phenyl ring in position 4'. For compounds **1a**, **1b**, and **3** the introduction of this additional substituent (compounds **1c**, **1d** and **4** respectively) led to an increase in potency which, though small, still showed that a bulky group in that position could be beneficial. In particular, compound **1d** proved to be among the most potent inhibitors synthesized so far (IC₅₀ = 5.3 nM).

To further investigate the SAR of the present series of derivatives and to additionally validate the previously postulated ‘H-bonding hypothesis’,⁸ docking experiments were also performed, using the recently developed homology-built aromatase model (PDB code 1TQA).¹² In Figure 1, the putative binding modes of compounds **1a** (yellow), **1b** (orange), **1d** (cyan), and **3** (green) as outcome of docking simulations and cluster analysis^{13,14} are reported. Docking simulations were carried out constraining ligands to properly coordinate the heme iron atom, while leaving the rest of the molecules free to move (see Supporting Information). It clearly arose that the meta (**1b**) and the ortho (**1a**) derivatives interacted with the target in a quite different way. In details, the carbonyl oxygen atom of **1b** was positioned at ~ 3-4 Å from the carboxyl group of Asp309 of the I-helix and ~ 5-6 Å from the hydroxyl group of Ser478 of the C-terminal loop. Both residues could reasonably interact by means of H-bond with **1b** carbonyl group, thus accounting for the higher activity of this compound relative to **1a**, in which the same moiety is not properly oriented to establish similar interactions. A comment is required on Asp309 that in this study was treated as ionized. While in this form it obviously cannot interact by means of H-bond, it is widely accepted that during the aromatization Asp309 can be protonated, and therefore able to favorably interact with our compound.¹⁵

Concerning Ser478, both ligand-^{16,17} and target-based¹⁸⁻²⁰ computational studies point to this residue as a fundamental amino acid for the interaction with nonsteroidal aromatase inhibitors belonging to different classes. Also mutagenesis experiments show that this residue is one of the amino acids located in the aromatase active site and involved in the interaction with ligands.²¹ The proposed binding mode (Figure 1) well confirmed the difference in potency between the meta- (**1b**, IC₅₀ = 7.3 nM) and the ortho-derivative (**1a**, IC₅₀ = 560 nM).

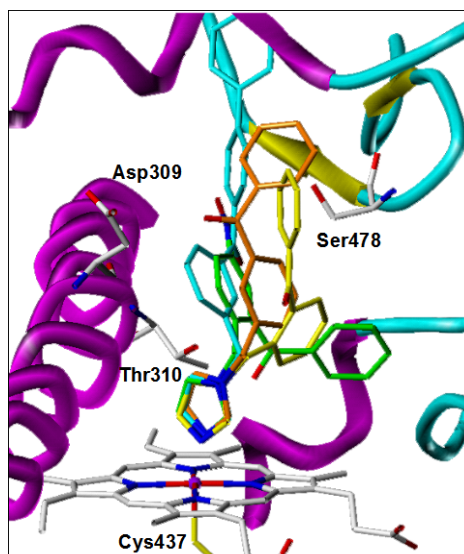


Figure 1. Docking complexes between aromatase and **1a** (yellow), **1b** (orange), **1d** (cyan), and **3** (green) as outcome of docking simulations carried out with GOLD and cluster analysis performed with ACIAP. The heme iron atom at the bottom of the picture is depicted as a violet ball. Moreover, some aromatase active site amino acids are also explicitly indicated.

In Figure 1, the putative binding mode of **3**, carrying a NO₂ group in para position with respect to the methylimidazole chain, is also reported. Docking simulations clearly pointed out the possibility for this additional group to establish H-bond interactions with Ser478, thus accounting for the significantly increased potency (IC₅₀ = 25.9 nM) with respect to the parent compound **1a**. Furthermore, to investigate the effects of the introduction of bulky substituents on the benzophenone scaffold, docking simulations were also performed with **1d**, namely the meta derivative with an additional phenyl ring in position 4'. A pose representative of a statistically populated cluster is reported in Figure 1. This binding mode showed that aromatase can accommodate sterically hindered ligands in this region of its active site, as **1d** proved to be the most potent aromatase inhibitor that we reported so far, with an IC₅₀ value of 5.3 nM.

In conclusion, a new class of highly potent and selective aromatase inhibitors was synthesized, which combine remarkable activity (in the low nanomolar range) with higher accessibility via straightforward synthetic procedures when compared to the conformationally constrained xanthone-derivatives.⁸ Compound **1d** turned out to be our most potent aromatase inhibitor, comparable to currently marketed drugs. Docking simulations in combination with cluster analysis were also carried out, providing a fairly good explanation for the binding mode of the present series of new inhibitors at the aromatase active site.

Acknowledgement. This work was supported by grants from MIUR-COFIN2004 (Rome, Italy).

Supporting Information Available: Full experimental procedures of both synthesis and computational studies, elemental analyses of target compounds. This material is available free of charge via the Internet at <http://pubs.acs.org>.

References.

- (1) Howell, A. New developments in the treatment of postmenopausal breast cancer. *Trends Endocrinol. Metab.* **2005**, *16*, 420-428.
- (2) Brueggemeier, R. W.; Hackett, J. C.; Diaz-Cruz, E. S. Aromatase inhibitors in the treatment of breast cancer. *Endocr. Rev.* **2005**, *26*, 331-345.
- (3) Mouridsen, H.; Gershonovich, M.; Sun, Y.; Perez-Carrion, R.; Boni, C.; Monnier, A.; Apffelstaedt, J.; Smith, R.; Sleeboom, H. P. et al. Phase III study of letrozole versus tamoxifen as first-line therapy of advanced breast cancer in postmenopausal women: analysis of survival and update of efficacy from the International Letrozole Breast Cancer Group. *J. Clin. Oncol.* **2003**, *21*, 2101-2109.

- (4) Saberi, M. R.; Vinh, T. K.; Yee, S. W.; Griffiths, B. J. N.; Evans, P. J.; Simons, C. Potent CYP19 (aromatase) 1-[(benzofuran-2-yl)(phenylmethyl)pyridine, -imidazole, and -triazole inhibitors: synthesis and biological evaluation. *J. Med. Chem.* **2006**, *49*, 1016-1022.
- (5) Su, B.; Diaz-Cruz, E. S.; Landini, S.; Brueggemeier, R. W. Novel sulfonanilide analogues suppress aromatase expression and activity in breast cancer cells independent of COX-2 inhibition. *J. Med. Chem.* **2006**, *49*, 1413-1419.
- (6) L  z  , M. P.; Le Borgne, M.; Pinson, P.; Paluszczak, A.; Duflos, M.; Le Baut, G.; Hartmann, R. W. Synthesis and biological evaluation of 5-[(aryl)(1H-imidazol-1-yl)methyl]-1H-indoles: potent and selective aromatase inhibitors. *Bioorg. Med. Chem. Lett.* **2006**, *16*, 1134-1137.
- (7) Gobbi, S.; Cavalli, A.; Rampa, A.; Belluti, F.; Piazzzi, L.; Paluszczak, A.; Hartmann, R. W.; Recanatini, M.; Bisi, A. Lead optimization providing a series of flavone derivatives as potent nonsteroidal inhibitors of the cytochrome P450 aromatase enzyme. *J. Med. Chem.* **2006**, *49*, 4777-4780.
- (8) Recanatini, M.; Bisi, A.; Cavalli, A.; Belluti, F.; Gobbi, S.; Rampa, A.; Valenti, P.; Palzer, M.; Paluszczak, A.; Hartmann, R. W. A new class of nonsteroidal aromatase inhibitors: design and synthesis of chromone and xanthone derivatives and inhibition of the P450 enzymes aromatase and 17 alpha-hydroxylase/C17,20-lyase. *J. Med. Chem.* **2001**, *44*, 672-680.
- (9) Thompson, E. A., Jr.; Siiteri, P. K. Utilization of oxygen and reduced nicotinamide adenine dinucleotide phosphate by human placental microsomes during aromatization of androstenedione. *J. Biol. Chem.* **1974**, *249*, 5364-5372.
- (10) Hutschenreuter, T. U.; Ehmer, P. B.; Hartmann, R. W. Synthesis of hydroxy derivatives of highly potent non-steroidal CYP 17 inhibitors as potential metabolites and evaluation of their activity by a non cellular assay using recombinant human enzyme. *J. Enzyme Inhib. Med. Chem.* **2004**, *19*, 17-32.
- (11) Lang, M.; Batzl, C.; Furet, P.; Bowman, R.; Hausler, A.; Bhatnagar, A. S. Structure-activity relationships and binding model of novel aromatase inhibitors. *J. Steroid Biochem. Molec. Biol.* **1993**, *44*, 421-428.
- (12) Favia, A. D.; Cavalli, A.; Masetti, M.; Carotti, A.; Recanatini, M. Three-dimensional model of the human aromatase enzyme and density functional parameterization of the iron-containing protoporphyrin IX for molecular dynamics study of heme-cysteinato cytochromes. *Proteins* **2006**, *62*, 1074-1087.
- (13) Bottegoni, G.; Cavalli, A.; Recanatini, M. A comparative study on the application of hierarchical-agglomerative clustering approaches to organize outputs of reiterated docking runs. *J. Chem. Inf. Model.* **2006**, *46*, 852-862.
- (14) Bottegoni, G.; Rocchia, W.; Recanatini, M.; Cavalli, A. ACIAP, Autonomous hierarchical agglomerative Cluster Analysis based Protocol to partition conformational datasets. *Bioinformatics* **2006**, *22*, e58-e65
- (15) Recanatini, M.; Cavalli, A.; Valenti, P. Nonsteroidal aromatase inhibitors: recent advances. *Med. Res. Rev.* **2002**, *22*, 282-304.
- (16) Recanatini, M.; Cavalli, A. Comparative Molecular Field Analysis of non-steroidal aromatase inhibitors: an extended model for two different structural classes. *Bioorg. Med. Chem.* **1998**, *6*, 377-388.
- (17) Cavalli, A.; Bisi, A.; Bertucci, C.; Rosini, C.; Paluszczak, A.; Gobbi, S.; Giorgio, E.; Rampa, A.; Belluti, F.; Piazzzi, L.; Valenti, P.; Hartmann, R.W.; Recanatini, M. Enantioselective nonsteroidal aromatase inhibitors identified through a multidisciplinary medicinal chemistry approach. *J. Med. Chem.* **2005**, *48*, 7282-7289.
- (18) Graham-Lorence, S.; Amarneh, B.; White, R. E.; Peterson, J. A.; Simpson, E. R. A three-dimensional model of aromatase cytochrome P450. *Protein Sci.* **1995**, *4*, 1065-1080.
- (19) Koymans, L. M.; Moereels, H.; Van den Bossche, H. A molecular model for the interaction between vorozole and other non-steroidal inhibitors and human cytochrome P450 19 (P450 aromatase). *J. Steroid Biochem. Mol. Biol.* **1995**, *53*, 191-197.
- (20) Cavalli, A.; Greco, G.; Novellino, E.; Recanatini, M. Linking CoMFA and protein homology models of enzyme-inhibitor interactions: an application to non-steroidal aromatase inhibitors. *Bioorg. Med. Chem.* **2000**, *8*, 2771-2780, and references therein.
- (21) Kao, Y. C.; Korzekwa, K. R.; Laughton, C. A.; Chen, S. Evaluation of the mechanism of aromatase cytochrome P450. A site-directed mutagenesis study. *Eur. J. Biochem.* **2001**, *268*, 243-251.

3.2.3. Conclusions and Outlook

The combination of docking simulations and ligand cluster analysis performed in paper **VIII** provided a fairly good explanation for the binding mode of the present series of new inhibitors at the aromatase active site. It represented a valid starting point for further drug design studies, especially focused on the position of the nitro group and the insertion of the methyleneimidazolyl group. First compounds were obtained in ongoing drug design showing aromatase inhibition values close to the best values reported so far in literature (data not shown; soon to be published).

Recently the crystal structure of aromatase was solved (PDB entry 3eqm), co-crystallized with androstenedione. In order to validate the identified docking poses for the imidazolylmethylenebenzophenones obtained with the aromatase homology model 1tqa, new docking studies using the aromatase x-ray 3eqm should be performed. Furthermore, molecular dynamic studies conducted on the docked poses of compounds 1b and 1d (paper **VIII**) would be advisable, with the aim to investigate induced-fit motions which could improve further drug design.

3.3 Estrogen-dependent endometriosis – selective 17 β -HSD1 inhibition

3.3.1. X-ray Analysis

In paper **XI** a structural analysis was performed of the 18 crystal structures of 17 β -HSD1 (Table 1) available in the PDB Brookhaven database.¹²⁹ Superimposition of all crystal structures gave a mean backbone root mean-square distance (RMSD) value of ca. 0.55 Å (ca. 1.5 Å if all atoms are considered). This highlights the rigid functional three-dimensional structure typical of the short-chain dehydrogenases/reductases (SDR), consisting of a rigid β - α - β fold with a core of parallel β -strands fanning across the center and α -helices draped on the outside.^{85a} Moreover, the tertiary structure resulted in a rigid cofactor binding site (COF) at the N-terminus, comprising Rossman fold and GXXXGXXG motif (where G is glycine and X is any other amino acid), plus the YXXXXK (where Y is Tyr155 and K is Lys159) sequence that participates in catalysis, and a structurally variable substrate binding site (SUB) at the C-terminus.

Table 1. Summary of the 17 (18) crystal structures of 17 β -HSD.

PDB-ID	Amino acid number	Complex ligand ^a	Res. (Å)	Chain	backbone cluster of entry-loop ^b (loop helix residues)	mutants	active site volume (Å ³) of ternary complex calculated with castP	
							COF	SUB
1A27	285	EST, NAP	1.90	A	cl2	--	1855	
							1232 / 66%	623 / 34%
1BHS	284	--	2.20	A	cl1 A191-E194	--	2214	
1DHT	284	DHT	2.24	A	cl1 M193-V196	--	1944	
1EQU	284	EQI, NAP	3.00	A/B	cl2 (_A) / cl1 (_B) M193-V196	--	1606 / 67%	797 / 33%
1FDS	282	EST	1.70	A	--	--	2323	
1FDT_A	285	EST, NAP	2.20	A	cl2	--	2000	
							1255 / 63%	745 / 37%
1FDT_B	285	EST, NAP	2.20	A	cl2	--	2259	
							1583 / 70%	676 / 30%
1FDU	281	EST, NAP	2.70	A-D	cl2 (_C) M193-K195	H221L	C: 1645	
1FDV	285	NAD	3.10	A-D	cl2 (_A, _C) E194-V196	H221L	A: 1892 / C: 2051	
1FDW	279	EST	2.70	A	--	H221Q	2301	
115R	285	HYC	1.60	A	cl3	--	2755	
110L	284	EST	2.30	A	cl1 A191-V196	--	2296	
1JTV	278	TES	1.54	A	--	--	1855	
1QYV	276	NAP	1.81	A	--	--	2906	
1QYW	276	5SD, AP2	1.63	A	--	--	1858	
1QYX	277	ASD, AP2	1.89	A	--	--	1888	
3DHE	284	AND	2.30	A	cl1 M193-V196	--	2152	
3DEY	277	DHT	1.70	A	-	--		

Detailed informations are given regarding ^a complexed ligands (EST estradiol, NAP nicotinamide-adenine-dinucleotide phosphate (NADP⁺), DHT dihydrotestosterone, EQI equilin, NAD nicotinamide-adenine-dinucleotide (NAD⁺), HYC O⁵'-[9-(3,17 β -dihydroxy-1,3,5(10)-estratrien-16 β -yl)-nonanoyl] adenosine, TES testosterone, 5SD 5 α -androstane-3,17-dione, ASD 4-androstene-3,17-dione, AP2 2'-monophosphoadenosine 5'-diphosphoribose, AND 3 β -hydroxy-5-androstene-17-one), number of chains, ^b β FuG'-loop backbone clusters (cl1 loop close to the α G'-helix, cl2 loop placed in front of the nicotinamide moiety of the cofactor, cl3 loop shifted towards the cofactor), mutants and active site volumes calculated with castP.¹³⁰

The only highly flexible part is the $\beta F\alpha G'$ loop, strongly modulating shape and volume of the active site (including both COF and SUB), and the C-terminal helix. It delimits the SUB and is probably involved in entrance and exit mechanisms of small molecules as well as in the enzymatic catalysis.

Several different conformations of the long, flexible $\beta F\alpha G'$ loop were identified, with the loop occurring either as a disordered coil or presenting a turn-helix-turn motif. Moreover, high b-factor values characterize the loop residues and in seven crystal structures the loop is not fully resolved. The multiplicity of conformations suggests various enzyme substates for 17 β -HSD1, subjected to fast dynamic motions and secondary structure rearrangements with direct implication of the loop residues Thr190-Leu197 in the catalytic cycle.

Then, only the eleven full-length crystal structures of 17 β -HSD1 were superimposed. Clustering according to the backbone RMSD (ca. 3 Å) of the five loop residues Phe192-Val196 neglected active site volume changes and its output was limited to ascribe the presence of gates in the three identified clusters cl1, cl2 and cl3 (Fig. 29; representative structures: 1IOL, 1A27 and 1I5R, respectively).

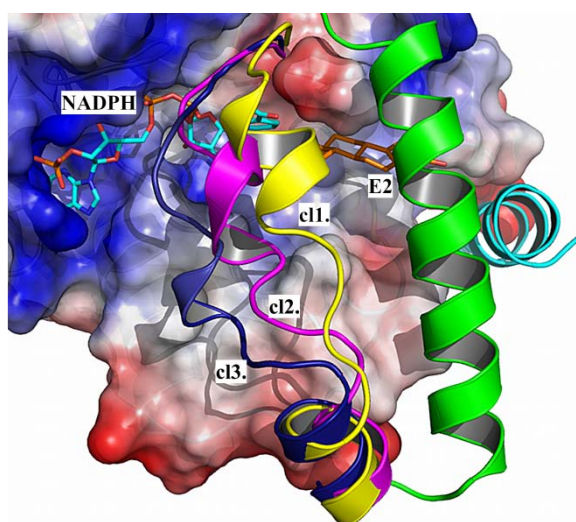


Figure 29. Representative structures of the three $\beta F\alpha G'$ -loop conformations **cl1** (yellow, PDB entry 1iol), **cl2** (magenta, 1a27) and **cl3** (blue, 1i5r), clustered according to the backbone RMSD of the five residues Phe192-Val196. Moreover, $\alpha G'$ -helix (green) and C-terminal helix (cyan) are rendered in cartoon, NADPH and E2 in sticks and the rest of the enzyme (active site) as electrostatic surface.

Thus, clustering according to the all-atom RMSD (ca. 6 Å) of the same loop residues led to the identification of five clusters, with Phe192 and Met193 showing the largest influence on shape and volume variations. Phe192, in particular, emerged as an important marker for the conformational variations, since its side chain presents the largest RMSD deviation (ca. 10 Å) and it rotates for about 200 degrees around the loop axis (Fig. 30). The two extremes in the orientation of the side chain of Phe192 corresponded to the major changes of the active site volumes of all wild type enzyme (E)-NADPH-estradiol (E2) complexes, where the ratio volume SUB/volume COF changes from 30:70 of 1fdtB to 37:63 of 1fdtA (Table 1).

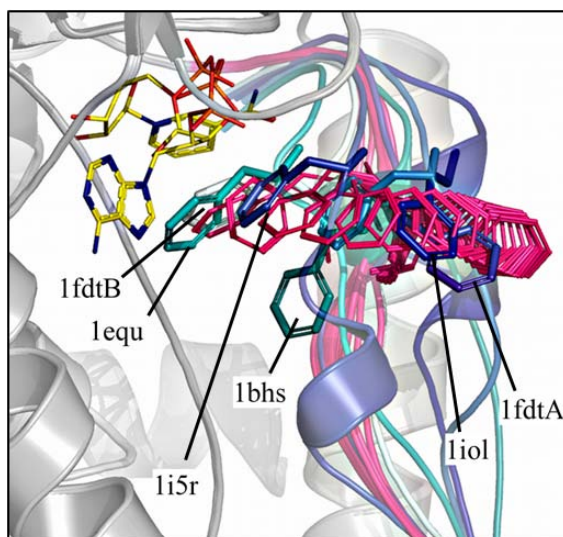


Figure 30. Different orientations of Phe192 for the 5 clusters obtained by all-atom RMSD classification of the five loop residues (rendered in sticks, color-coded blue-violet) and for the 17 intermediate positions (rendered in lines, magenta) obtained by simulating the transition from 1fdtA to 1fdtB, the two extremes in the Phe192 rotation, using the Yale Morph Server.¹³¹

3.3.2. Rapid equilibrium random bi-bi kinetic cycle – a hypothesis.

The kinetic mechanism for 17 β -HSD1 is not fully clarified, although, it had been reported in literature to follow a rapid equilibrium random bi-bi mechanism.^{132a} This is a peculiarity of 17 β -HSD1, like the long β F α G'-loop, with respect to the other HSD family members, which follow a sequential ordered bi-bi kinetic mechanism.^{87, 132b}

Inspired by a recent work of Cooper et al.,¹³³ which elucidated the complete kinetic mechanism for the rat liver 3 α -HSD taking into account the different enzyme crystal structures, in paper **XI** enzyme conformations were assigned to each of the five steps of which the random bi-bi kinetic mechanism consists (Fig. 31). Furthermore, the kinetic cycle was hypothesized and the specific role played by the flexible loop was elucidated for each reaction step (Fig. 32).

Supported by X-ray analysis and biochemical and thermodynamic data,^{84, 132b, 134} NADPH was assumed to enter and bind first, inducing a conformational rearrangement of the β F α G'-loop.

The hypothesized random bi-bi kinetic cycle was validated through a set of molecular dynamic (MD) simulations performed on apoform (2 MDs), binary (E-NADPH; 3MDs) and ternary complexes (E-NADPH-E1; 3 MDs). The eight MD simulations were designed based on four crystal structures (1fdtA, 1i5r, 1fdtB and 1bhs), in order to cover the conformational ensemble of the flexible β F α G'-loop. In fact, the enzyme was investigated in its opened-state (1fdtA) - characterized by a fused COF and SUB and by Phe192 turned outwards, in a semi-opened (occluded) state (1i5r) - with the loop shifted towards the COF and Phe192 more buried than in 1fdtA, and in its closed-state (1fdtB) - which mimics the ternary complex at the catalytic moment and presents a closed SUB and Phe192 pointing inwards perpendicular to the catalytic Tyr155.

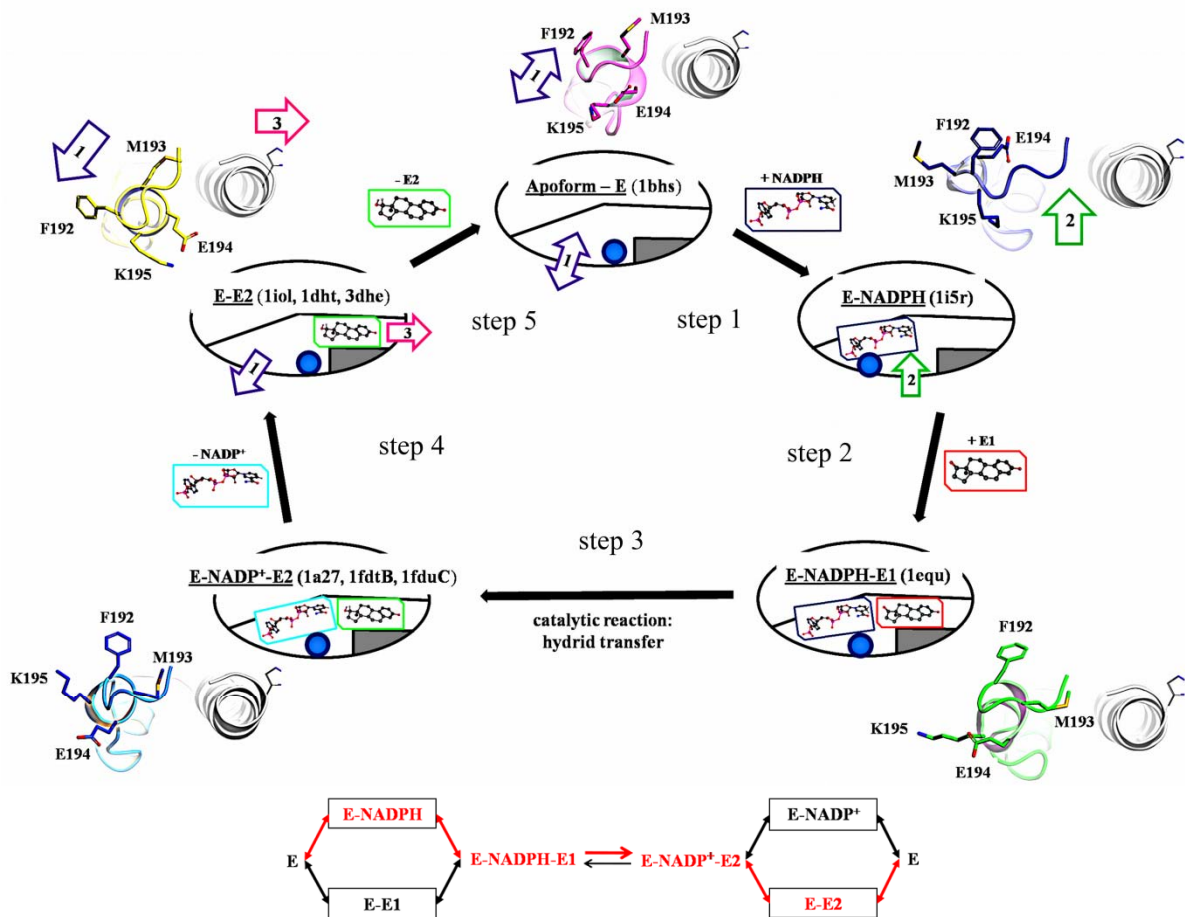


Figure 31. Random bi-bi kinetic mechanism of the catalytic cycle of 17 β -HSD1 (in red the herein proposed path). To each of the five steps one or more crystal structures were assigned. Side chains of the β F α G'-loop residues Phe192, Met193, Glu194 and Lys195 are rendered as sticks and the orientation of the loop (blue circle) with respect to the α G'-helix (gray triangle and rendered as cartoon) is represented. Arrows 1-3 indicate the entrance and egress gates.

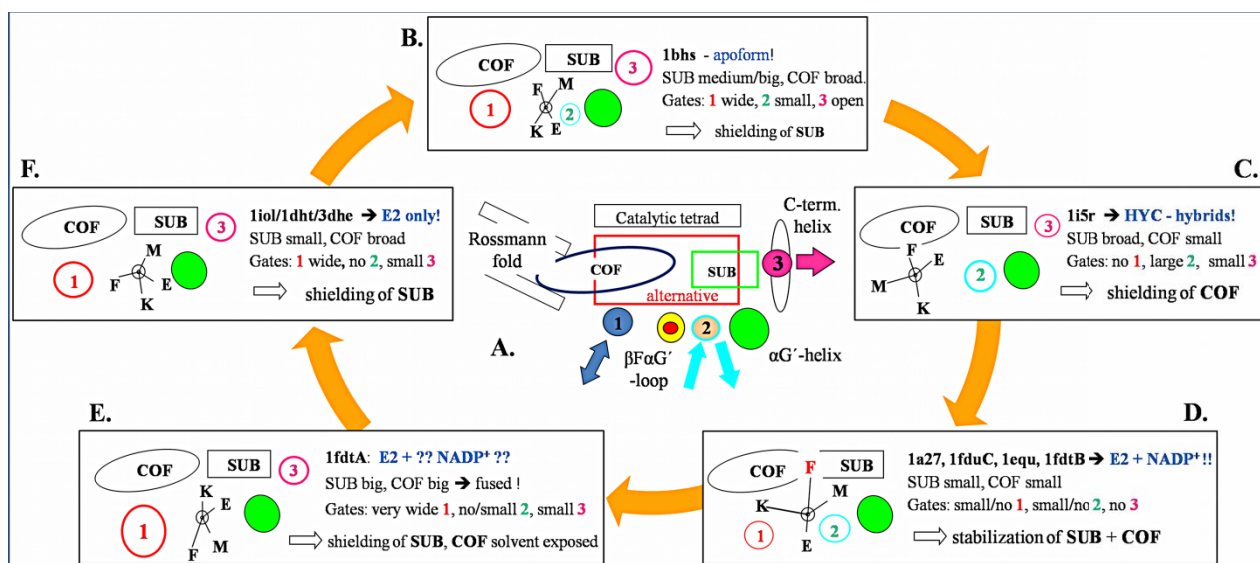


Figure 32. Schematic representation of the catalytic cycle, with detailed informations about the role of the loop in the various steps.

The different final complexes obtained from these eight dynamic simulations substantiated the importance of the presence of a ligand in either the SUB (E1) or the COF (NADPH) in order to stabilize the enzyme. Occupying one or both binding pockets influenced the motions of the flexible loop and induced concerted conformational changes of α G-helix and C-terminal helix. Moreover, the MDs of the ternary complexes, especially the one performed using the closed (1fdtB) and the occluded (1i5r) enzyme substates, highlighted the importance of the residues Ser142/Tyr155 and His221/Glu282, involved in the hydrogen bond network anchoring E1 in the SUB and in the hydride transfer (Fig. 33).

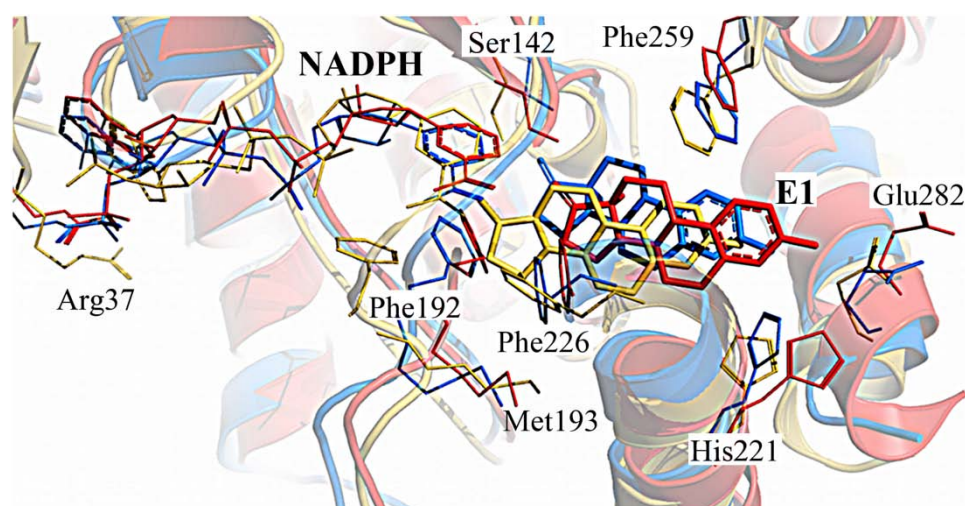


Figure 33. Overlay of the representative clusters of complex E(1fdtB)-NADPH-E1 (initial position - yellow, stable segment of MD – blue, final complex after 17 ns of MD – red).

Molecular mechanics Poisson-Boltzmann surface area (MM-PBSA) methods,¹³⁵ in combination with normal mode analysis, were exploited to calculate the absolute free energies (ΔG) and free binding energies ($\Delta\Delta G_{\text{bind}}$) of the complexes, leading to the determination of the most probable conformations to which E1 and NADPH bind in the 5 steps of the catalytic cycle. Furthermore, these methods validated the binding mode of E1 at the catalytic moment and supported the closed substate of the enzyme as the one occurring at the catalytic moment. Additionally, insights into the high adaptability of the loop at the different steps were ensured, in particular with regard to its importance in stabilizing the cofactor and substrate. Mutagenesis experiments for selected loop residues would give a final proof to our findings.

3.3.3. Validating the binding mode of bis(hydroxyphenyl)-arenes: docking and MDs

Starting point in the investigation of the binding mode of a series of bis(hydroxyphenyl)-arenes were docking simulations performed on a closed state crystal structure of 17 β -HSD1 (1fdtB).¹³⁶ These inhibitors were based on a (*m*-hydroxyphenyl)-X-(*p*-hydroxyphenyl) core, with X being a heterocycle (chart 1). From these studies resulted that the inhibitors bind into the SUB, mimicking the substrate, and forming hydrogen bonds with Ser142/Tyr155 and His221/Glu282. However, no correlation between the inhibitory potency of the compounds and the scoring functions could be found. It became also not clear why the different central heterocycles led to different inhibitions.

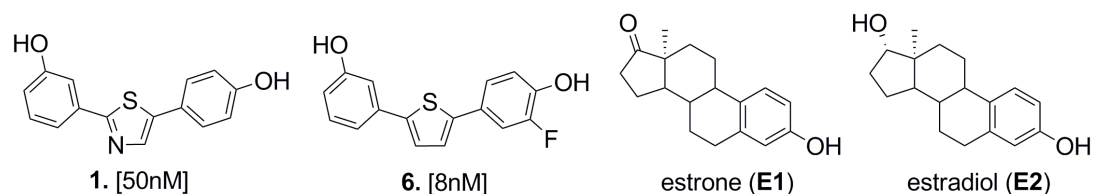


Chart 1. Structures and inhibitory activity of two non-steroidal 17β -HSD1 inhibitors, compound **1** and **6**, of the series of the bis(hydroxyphenyl)-arenes, as well as of the substrate estrone (E1) and the product estradiol (E2).

Based on the crystal structure analysis (see 3.3.1.) an ensemble of 3D-structures of the enzyme was identified and used for new docking studies (paper IX-X). These resulted again in a steroidal, but mostly in an alternative binding mode for the class of bis(hydroxyphenyl)-arenes. The latter mode (Fig. 34) was found only for crystal structures with space below the cofactor (i.e. 1fdtA), presenting the inhibitor bound with the *m*-hydroxyphenyl-X moiety to the phosphor-nicotinamide moiety of NADPH. Thus, a synergistic interaction with the cofactor could be observed instead of a competition between inhibitor and NADPH for the COF. The inhibitor was flanked on its sides by Tyr155 and the flexible loop, while its *p*-hydroxyphenyl ring occupied the SUB.

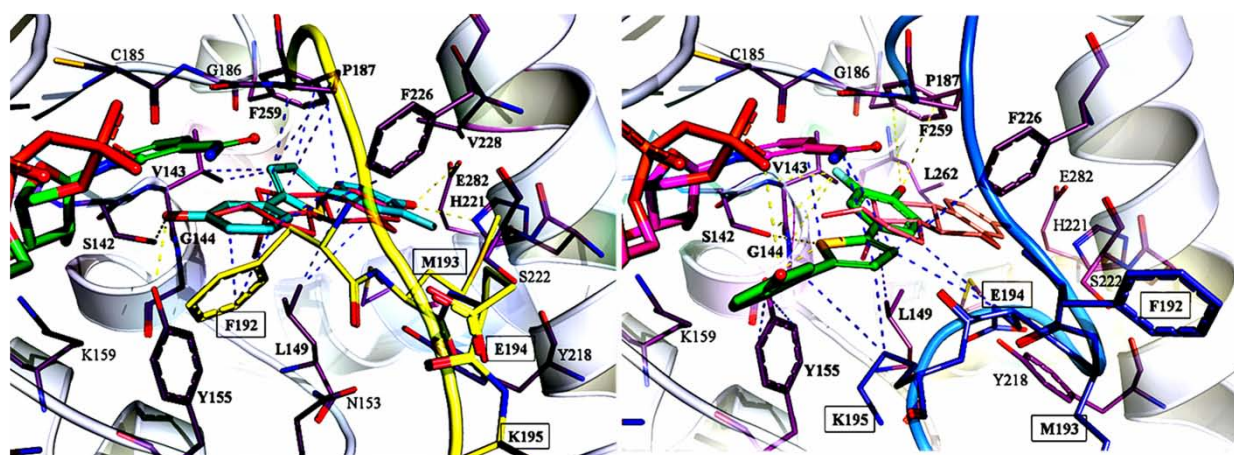


Figure 34. Docking poses of compound **6** and estrone (rosa) in the closed (left, PDB entry 1fdtB, yellow) and in the opened state of the enzyme (right, PDB entry 1fdtA, blue), leading to the steroidal (cyan, left) and the alternative binding mode (green, right), respectively.

In order to validate the identified binding modes, four MD simulations were performed on ternary complexes with compound **1** (chart 1; **1** shows the same binding mode as **6** in Fig 34), a very potent representative of the bis(hydroxyphenyl)-arenes (50 nM IC_{50}). Two MDs were conducted with **1** in the alternative binding mode, respectively for the open (1fdtA) and the semi-open (1i5r) enzyme forms, while the other two MDs for the close state (1fdtB) of 17β -HSD1, with compound **1** in the steroidal binding mode. Interestingly the first two dynamic simulations ended with compound **1** close to its starting position (Fig. 35a), maintaining the hydrogen bond between its *m*-OH group and the phosphate close to the nicotinamide ring and the π - π stacking with the nicotinamide moiety. Moreover, a clear adaptation of the enzyme to the inhibitor could be observed and free energies values (ΔG and $\Delta\Delta G_{bind}$) in good agreement with the inhibitory potency (i.e. ΔG of -8.44 and -29.84 kcal/mol for 1fdtA and 1i5r, respectively) could be calculated with MM-PBSA-methods.

On the contrary, for the two MD simulations with compound **1** placed in the SUB, the stable part of the simulation resulted with the inhibitor pushed away from its starting pose, ending either perpendicular to the estradiol plane or lying completely out of the SUB (Fig. 35b). These observations, bad ΔG values (-1.53 and +3.13 kcal/mol) and the long MD runs necessary for complex stability in terms of RMSD, led to consider the steroidal binding mode as a minor one for this class of inhibitors, more likely as a transition step on the egress pathway.

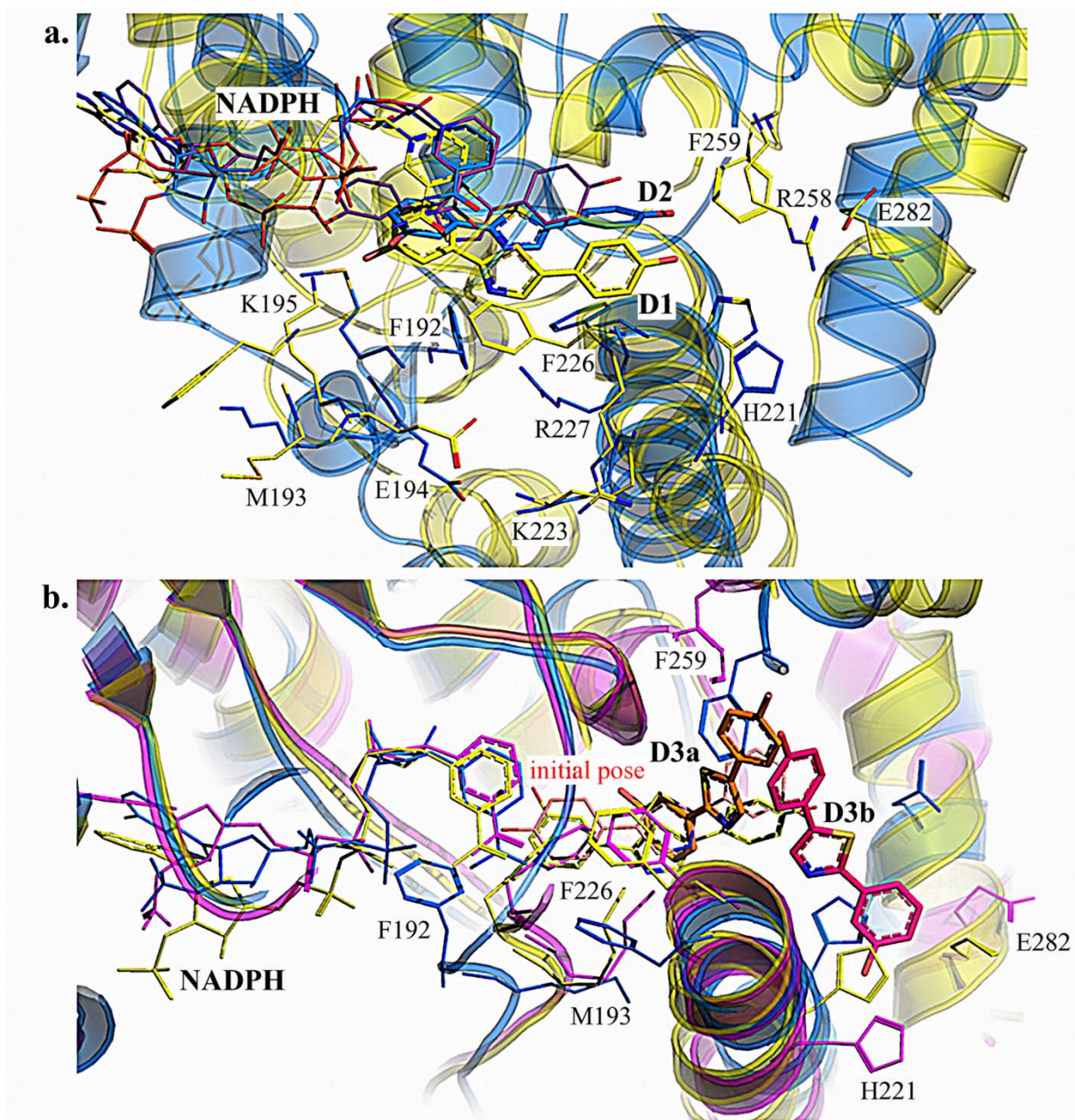


Figure 35. Analysis of the MD simulations performed on the four E-NADPH-compound **1** complexes. **a.**) Overlay of initial (violet) and final poses of compound **1** in the alternative binding mode (yellow - 1fdtA (D1), blue – 1i5r (D2)). **b.**) Overlay in the steroidal binding mode (1fdtB), with the final poses of compound **1** rendered as sticks (yellow/orange D3a and magenta D3b; starting conformations of amino acids are colored blue).

3.3.4. Validating the binding mode of bis(hydroxyphenyl)-arenes: “semi-QMAR”

Since docking studies could not elucidate the reason for the different inhibitory activities observed among the bis(hydroxyphenyl)-arene series due to the presence of different central heterorings, a ligand-based approach was followed in paper IX. Quantum chemical investigations were performed on a set of representative compounds by means of Gaussian03 software¹³⁷ and the molecular electrostatic potentials were plotted on the electron densities of the five compounds with GaussView 3.0.¹³⁸ For a better comparison the MEP maps were divided into three different regions, each corresponding to one aromatic ring of the compounds.

Trying to establish a semi-quantitative MEP-activity relationship (“semi-QMAR”), optimal ESP ranges for area I, II and III for high inhibition activity were identified: for region I ESP from -1.7 to $-1.2 \cdot 10^{-2}$, for region II -1.6 to $-0.9 \cdot 10^{-2}$ and for region III -1.2 to $-0.5 \cdot 10^{-2}$ Hartree. Similarly, the optimal Δ values of ESP for each region were determined: 0.5, 0.7 and 0.7 Hartree, respectively. The shift of a certain ESP distribution range on the scale or the change of the Δ value results in a decrease of inhibitory activity (Fig 36).

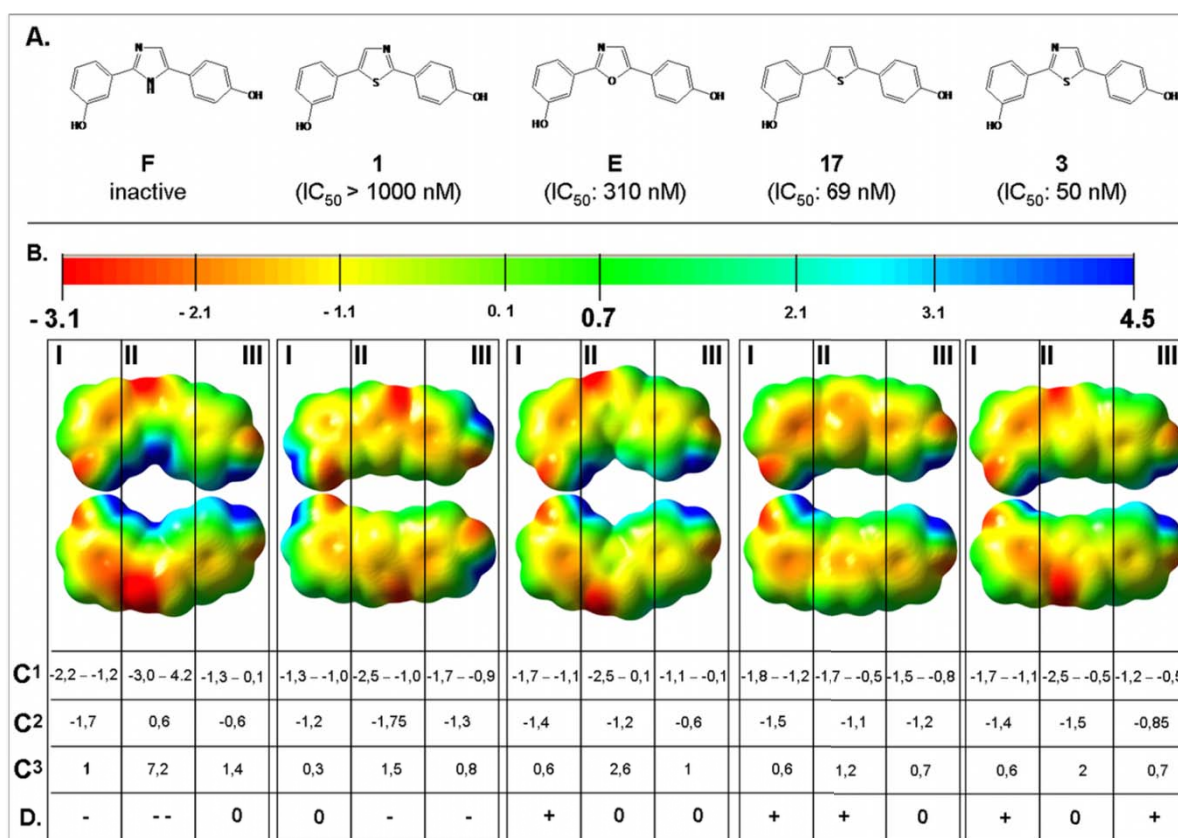


Figure 36. (A) Structure and 17 β -HSD1 inhibitory activity of compounds 1-5 ordered by increasing activity; (B) MEP maps, dorsal and ventral view; (C¹) ESP distribution range (Hartree; $\cdot 10^{-2}$); (C²) mean value of distribution range (Hartree, $\cdot 10^{-2}$); (C³) Δ of ESP; (D) “semi-QMAR”. MEP surfaces were plotted with GaussView 3.0.

The high importance of the location of the heteroatoms on the central aromatic ring on the MEP maps was well demonstrated with the two 1,3-thiazoles 1 and 4 (Fig. 36), which only differ by the position of the nitrogen in the thiazole moiety. The change of the position of the nitrogen in the thiazole ring has a decisive influence on the electronic distribution in each area, as the IC₅₀

values of **1** and **4** demonstrated (50 nM vs 1000 nM, respectively). Furthermore, a complementarity between the MEP of nicotinamide ring of the cofactor and the *m*-hydroxyphenyl ring (region I) of these compounds was observed, suggesting π - π stackings between cofactor and inhibitor (Fig. 37).

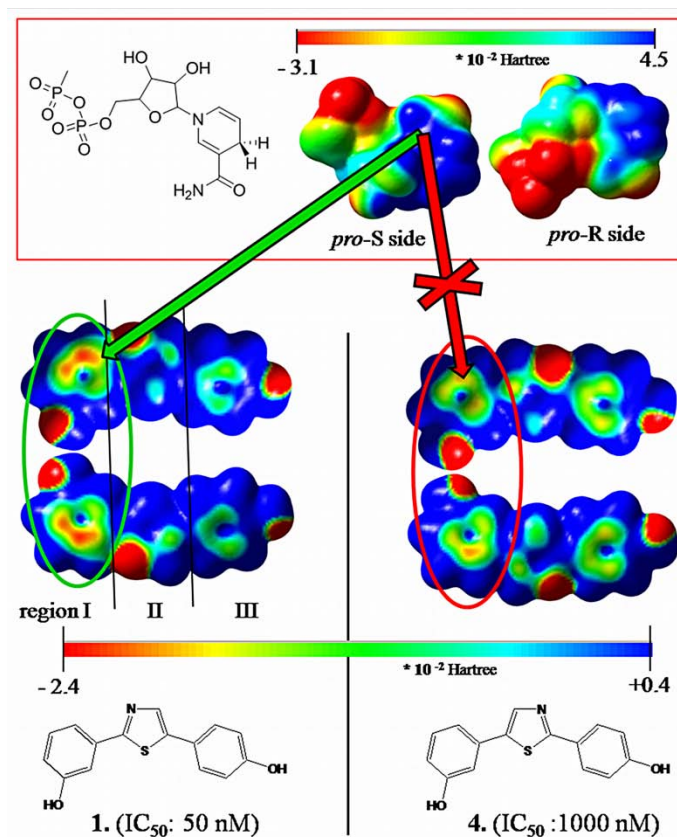


Figure 37. Differences in the MEP maps of compounds **1** and **4** in region I (*m*-hydroxyphenyl ring) and III (*p*-hydroxyphenyl ring) and the complementarity to the nicotinamide moiety of NADPH. MEP are color-coded in a range of 2.5 (red) to -15 kcal/mol (blue).

In order to verify complementarity of the MEPs and the electrostatic nature of the binding, a set of 5 ternary complexes formed by the catalytic residues (Asn114, Ser142, Tyr155 and Lys159), NADPH and compounds **1** to **5** (Fig. 36), respectively, was created and one binary complex catalytic residues-NADPH.

For compound **1** the MEP maps for binary and ternary complex had been calculated (Fig.36a). Comparing their MEP maps, changes in the color scale for the area corresponding to the nicotinamide ring could be observed. They varied from red in the binary complex, standing for a negative ESP and a reactive area, to green/yellow in the ternary complex, indicating a neutral, less reactive area. Thus, compound **1** seemed to neutralize the electrostatic potential distribution of the nicotinamide ring (Fig. 38a) as a consequence of the electron rearrangement occurring after the π - π interaction between ligand and nicotinamide moiety. This *ab initio* approach resulted in an overall good correlation with the biological data (Fig. 38b), explicated by a correlation factor r of 0.92. However, this correlation is depleted of part of its statistical significance due to the reduced number of data points considered.

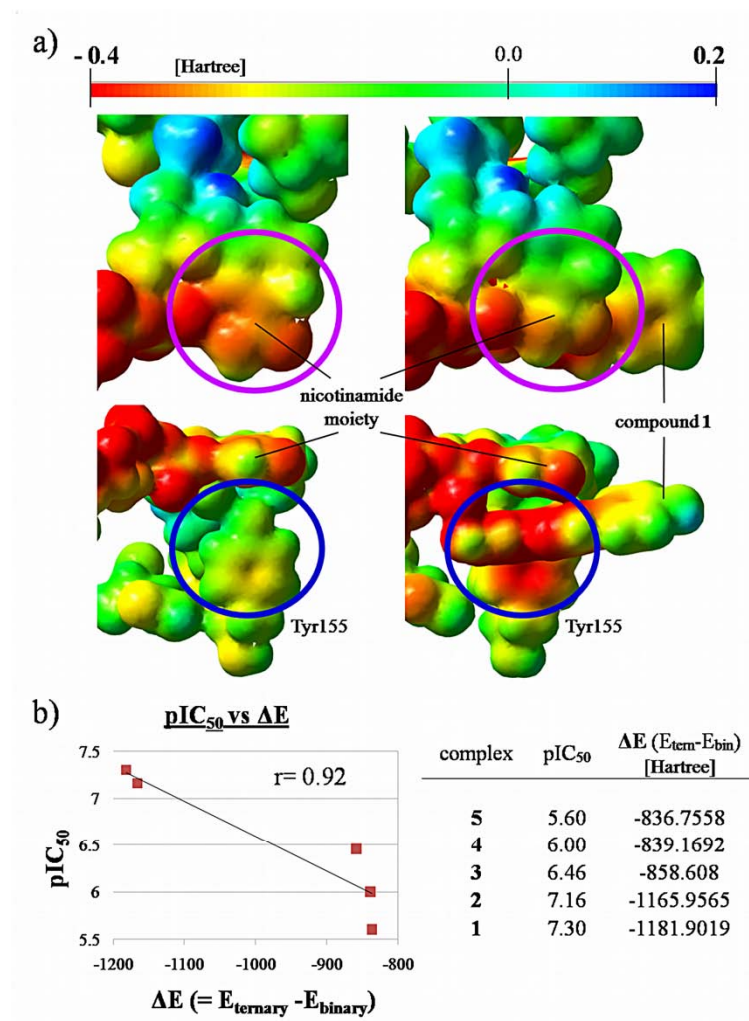


Figure 38. a) Differences of the electrostatic potential distribution for binary and ternary complex, enzyme-NADPH-1 and enzyme-NADPH, respectively, and b) correlation between the pIC₅₀ values of compounds 1-5 and the energy difference between the two complexes (ΔE).

3.3.5. Articles published in 17 β -HSD1 project – paper IX-XI

3.3.5.1. Paper IX.

Design, synthesis, biological evaluation and pharmacokinetics of bis(hydroxyphenyl) substituted azoles, thiophenes, benzenes and aza-benzenes as potent and selective non-steroidal inhibitors of 17 β -hydroxysteroid dehydrogenase type 1 (17 β -HSD1)

Emmanuel Bey, Sandrine Marchais-Oberwinkler, Ruth Werth, Matthias Negri, Yaseen A. Al-Soud, Patricia Kruchten, Alexander Oster, Martin Frotscher, Barbara Birk and Rolf W. Hartmann

This article is protected by copyrights of ‘Journal of Medicinal Chemistry.’

J. Med. Chem. **2008**, 51, 6725-6739

Abstract

17 β -Estradiol (E2), the most potent female sex hormone, stimulates the growth of mammary tumours and endometriosis via activation of the estrogen receptor α (ER α). 17 β -Hydroxysteroid dehydrogenase type 1 (17 β -HSD1), which is responsible for the catalytic reduction of the weakly active estrogen estrone (E1) into E2, is therefore discussed as a novel drug target. Recently, we have discovered a 2,5-bis(hydroxyphenyl) oxazole to be a potent inhibitor of 17 β -HSD1. In this paper, further structural optimizations were performed: 39 bis(hydroxyphenyl) azoles, thiophenes, benzenes and aza-benzenes were synthesized and their biological properties were evaluated. The most promising compounds of this study show enhanced IC₅₀ values in the low nanomolar range, a high selectivity toward 17 β -HSD2, a low binding affinity to ER α , a good metabolic stability in rat liver microsomes and a reasonable pharmacokinetic profile after peroral application. Calculation of the molecular electrostatic potentials revealed a correlation between 17 β -HSD1 inhibition and the electron density distribution.

Introduction

Estrogens, the most potent one being 17 β -estradiol (E2), act as female sex hormones and are predominantly produced before menopause by the ovaries. They unfold their activity by stimulation of the estrogen receptors (ERs) α and β . Besides their physiological effects, they are, however, also involved in the initiation and progression of estrogen-dependent diseases like mammary tumor¹ and endometriosis.² Presently, the three main endocrine therapies for the treatment of breast cancer are:^{3,4} inhibition of estrogen biosynthesis by aromatase inhibitors or GnRH agonists or antagonists and interference with the estrogen action at the receptor level by selective estrogen receptor modulators (SERMs) or pure antiestrogens.⁵ Besides specific disadvantages of each therapeutic concept, all of these strategies have in common that they reduce estrogen levels systemically leading to the corresponding side effects.

A softer approach could be inhibition of the enzyme involved in the last step of the E2 biosynthesis: 17 β -hydroxysteroid dehydrogenase (17 β -HSD) which is able to convert estrone (E1) into E2. There are three subtypes (1, 7 and 12) described, the most important of which is 17 β -HSD1. The primary function of 17 β -HSD7 and 17 β -HSD12 is supposed to be in the cholesterol synthesis⁶ and in the regulation of the lipid biosynthesis,⁷ respectively. Moreover, Day et al.⁸ showed that 17 β -HSD12, although highly expressed in breast cancer cell lines, is inefficient in E2 formation.

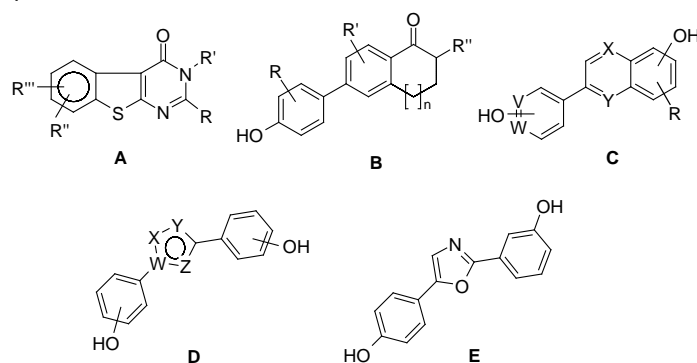
17 β -HSD1 is NAD(P)H-dependent and intracellularly converts the weak estrogen E1 into the strong estrogen E2. As it is often over-expressed in breast cancer cells⁹⁻¹² and endometriosis,¹³ 17 β -HSD1 is regarded as a promising novel target for the treatment of estrogen-dependent diseases. Appropriate inhibitors of this enzyme should exhibit less side effects compared to the current treatments as they should selectively reduce the concentration of active E2 in the diseased tissues.¹⁴

As a biological counterpart, 17 β -hydroxysteroid dehydrogenase type 2 (17 β -HSD2) catalyses the deactivation of E2 into E1. It protects the cell from excessively high concentrations of active estrogens¹⁵ and should therefore not be affected by inhibitors of 17 β -HSD1. In addition 17 β -HSD1 inhibitors should not show affinity to the ERs to avoid intrinsic estrogenic effects.

17 β -HSD1 was crystallized with different steroidal ligands.¹⁶⁻²⁴ The published X-ray structures provide insight into the active site, a narrow hydrophobic tunnel with polar contacts at each end. On one side His221/Glu282 are located, on the other Ser142/Tyr155 (two members of the catalytic tetrad).²⁵ Surprisingly, close to the hydrophobic B/C region of the steroid two polar amino acids, Tyr218 and Ser222, can be found which do not interact with E2.

Several steroidal and non-steroidal inhibitors of 17 β -HSD1 have been described. The first report on steroidal compounds by Penning²⁶ was as early as 1996. In the last few years several articles of other groups followed.²⁷ Regarding the non-steroidal inhibitors, only four compound classes have been described so far, all of them very recently: thienopyrimidinones **A**,^{28,29} biphenyl ethanones **B**,³⁰ and from our group 6-(hydroxyphenyl) naphthols **C**^{31,32} and bis(hydroxyphenyl) azoles **D**³³ (Chart 1).

Chart 1: Non-steroidal 17 β -HSD1 inhibitors

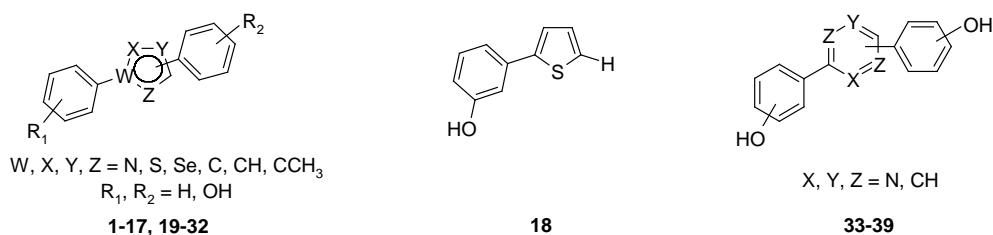


The most promising compound in the latter series was the 2,5-bis(hydroxyphenyl) oxazole **E** with an IC₅₀ of 310 nM and a selectivity factor of 56 against 17 β -HSD2. In general it was discovered that the inhibitory activity of these compounds depends on the existence of hydroxy rather than methoxy groups on the phenyl substituents and on the OH substitution pattern, *meta-para* and *para-meta* substituted compounds being more active than *para-para* substituted ones. Furthermore it became apparent that inhibition also depends on the nature of the heterocycle. Hydrogen bond donor functions turned out to be inappropriate, whereas in several compounds H-bond acceptor atoms were favorable. This finding led to the hypothesis that active compounds are capable of interacting with Tyr218 or Ser222 via H-bonds.³³

In order to enhance activity and selectivity and to get a better insight into the interaction of these compounds with the active site of 17 β -HSD1, the significance of the OH groups will be further evaluated and other five-membered heterocycles, especially sulfur containing ones, will be investigated. Furthermore it will be evaluated, whether six-membered rings are also appropriate to connect the two hydroxyphenyl moieties.

In the following we describe the synthesis of 39 bis(hydroxyphenyl) azoles, thiophenes, benzenes and aza-benzenes (Chart 2) as well as the determination of their 17 β -HSD1 inhibitory activity and selectivity toward 17 β -HSD2, ER α and ER β . Furthermore, cell permeability using CaCo-2 cells, metabolic stability in rat liver microsomes, inhibition of the most important hepatic CYP enzymes and pharmacokinetic properties in the rat of selected compounds are determined. For a better understanding of the SARs molecular electrostatic potentials (MEPs) were calculated.

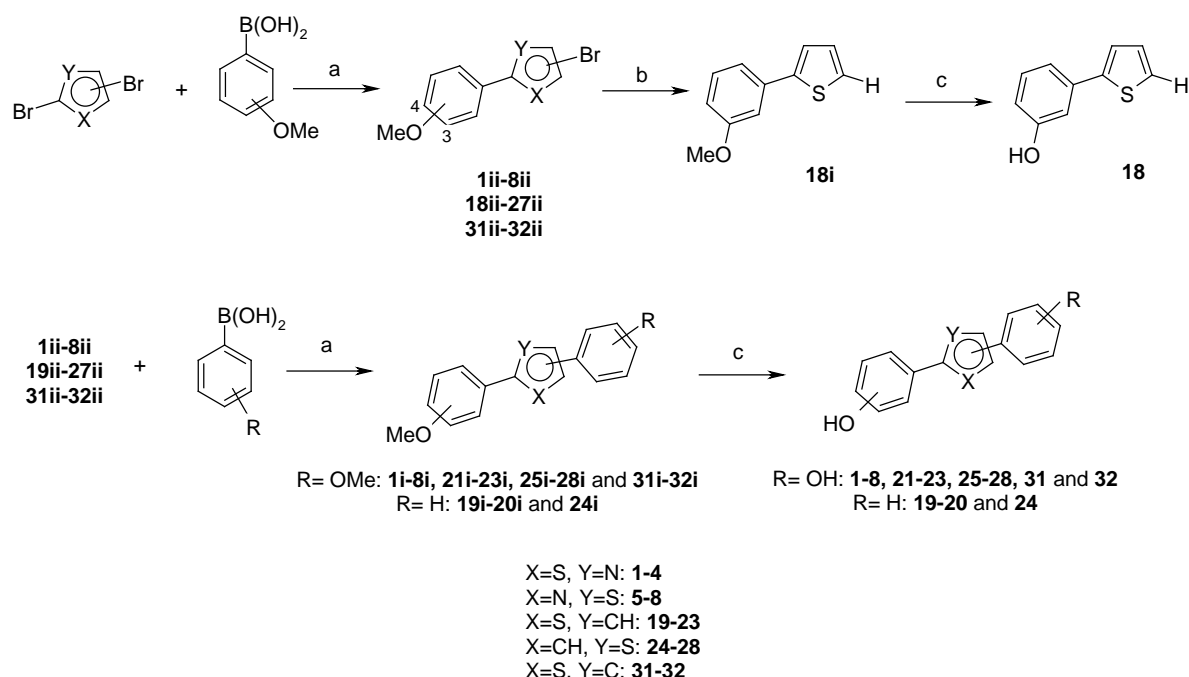
Chart 2: Title compounds



Chemistry

Starting from the commercially available dibrominated heterocycles and methoxylated benzene boronic acids, compounds **1** to **8**, **19** to **28**, **31** and **32** were prepared via two successive Suzuki reactions³⁴ followed by a demethylation step using borontribromide³⁵ as reagent. The Suzuki cross-coupling was carried out using three different methods. Intermediates **1ii** to **8ii**, **18ii** to **27ii** and **1i** to **8i** were prepared following Method A (aq. sodium carbonate, toluene, Pd(PPh₃)₄, reflux, 4 h) and compounds **31ii**, **32ii**, **19i** to **28i**, **31i** and **32i** were synthesized using Method B (sodium carbonate, THF/water (1:1), Pd(PPh₃)₄, reflux, 20 h). During the first cross coupling reaction leading to the mono(methoxyphenyl) substituted derivatives **1ii-8ii**, **18ii-27ii**, **31ii**, **32ii** no disubstituted compounds were obtained indicating that the (methoxyphenyl)bromo azoles and thiophenes are less reactive than their dibromo aryl precursors. The bromo intermediate **18ii** was treated with *n*-BuLi in anhydrous THF and subsequently hydrolyzed with water to yield the mono methoxylated thiophene **18i**. The methoxy groups of **1i** to **8i**, **18i** to **28i**, **31i** and **32i** were cleaved with boron tribromide (Method E: BBr₃, CH₂Cl₂, -78 °C to rt, 18 h, Scheme 1).

Scheme 1^a: Synthesis of compounds **1** to **8**, **18** to **28**, **31** and **32**

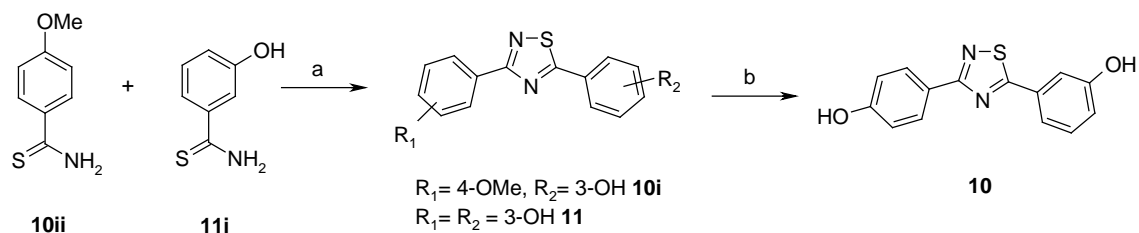


^a**Reagents and conditions:** a. for compounds **1ii** to **8ii**, **18ii** to **27ii** and **1i** to **8i**: Method A: aq. Na₂CO₃, toluene, Pd(PPh₃)₄, reflux, 4 h; for compounds **31ii**, **31i**, **32ii**, **32i** and **19i** to **28i**: Method B: Na₂CO₃, THF/water (1:1), Pd(PPh₃)₄, reflux, 20 h; b. 1. *n*-BuLi, THF dry, -78 °C, 15 min, 2. water; c. Method E: BBr₃, CH₂Cl₂, -78 °C to rt, 18 h.

The 1,3,4-thiadiazole **9** was prepared in a three step synthetic pathway based on the method described by Gierczyk and Zalas.³⁶ The 3-methoxybenzoyl chloride was treated with hydrazine monohydrate to give the resulting 3-methoxy-*N'*-(3-methoxybenzoyl)benzohydrazide, which was cyclized into the corresponding thiadiazole using Lawesson reagent in DME under microwave assisted conditions. In a last step, the methoxy substituents were cleaved with boron tribromide (Method E: BBr₃, CH₂Cl₂, -78 °C to rt, 18 h).

The synthesis of the 1,2,4-thiadiazoles **10** and **11** is shown in Scheme 2. The commercially available 4-methoxybenzoyl chloride and 3-hydroxybenzoyl chloride were converted into the thioamide intermediates **10ii** and **11i**, respectively, using aqueous ammonium sulfide under microwave assisted reaction.³⁷ These thioamides were submitted to strong acidic conditions resulting in a mixture of the thiadiazoles **10i** and **11** which were separated by column chromatography. The bis(methoxyphenyl) compound could not be isolated. Compound **10i** was demethylated with boron tribromide (Method E: BBr₃, CH₂Cl₂, -78 °C to rt, 18 h, Scheme 2).

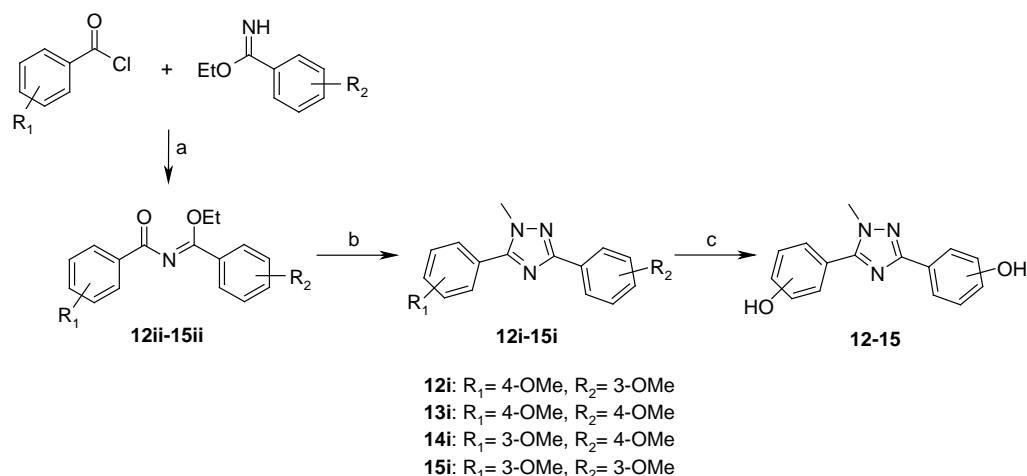
Scheme 2^a: Synthesis of compounds **10** and **11**



^a**Reagents and conditions:** a. conc. HCl, 38 °C, 8 h; b. Method E: BBr₃, CH₂Cl₂, -78 °C to rt, 18 h.

The synthesis of compounds **12** to **15** is presented in Scheme 3. The dimethoxylated-1,2,4-triazoles **12i** to **15i** were synthesized by reaction of the *N*-acylimidates³⁸ **12ii** to **15ii** with methylhydrazine (Method D: MeNHNH₂, CH₂Cl₂, 30-40 °C, 4 h). The methoxy groups of compounds **12i** to **15i** were cleaved with borontrifluoride dimethyl sulfide complex³⁵ (Method F: BF₃·SMe₂, CH₂Cl₂, rt, 20 h, Scheme 3).

Scheme 3^a: Synthesis of compounds **12** to **15**



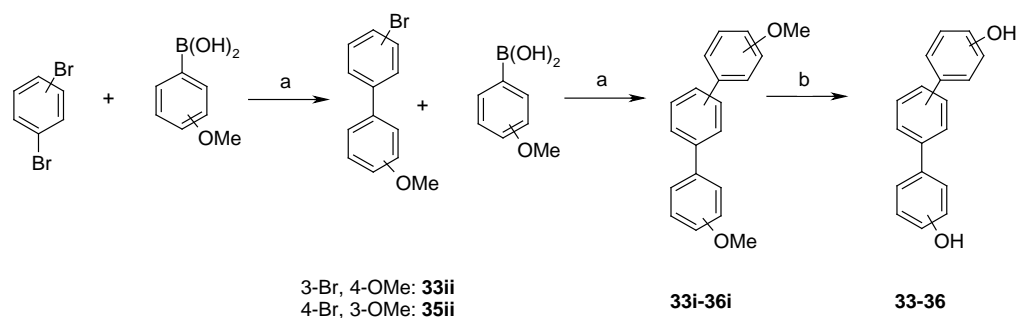
^a**Reagents and conditions:** a. CH₂Cl₂, NEt₃, 30-40 °C, 6 h; b. Method D: MeNHNH₂, CH₂Cl₂, 30-40 °C, 4 h; c. Method F: BF₃·SMe₂, CH₂Cl₂, rt, 20 h.

Compound **16** was prepared according to Sharpless³⁹ using 3-azidophenol and 3-hydroxyphenyl acetylene. Compounds **17**, **29**, **30**, **37** and **38** were obtained, under microwave assisted conditions, in a one pot synthesis (Method C: DME/EtOH/water (1:1:1), Cs₂CO₃, Pd(PPh₃)₄, MW (150 W, 150 °C, 15 bar, 15 min)) with benzene boronic acid for **17**, hydroxylated benzene boronic acid for **29**, **30**, **37** and **38** and the corresponding dibrominated heterocycle.

The synthesis of compounds **33** to **36** is depicted in Scheme 4. Starting from the commercially available dibrominated benzene and methoxylated benzene boronic acids, compounds **33** to **36** were prepared via two successive Suzuki reactions following the conditions of Method A. In the first reaction only the mono substituted compounds **33ii** and **35ii** were obtained due to the fact that the (methoxyphenyl)bromobenzenes are less reactive than the dibromobenzenes. Consequently, longer reaction times were required for the second cross coupling reaction (20 versus 4 h). The methoxy groups of compounds **33i-36i** were cleaved using boron tribromide (Method E: BBr₃, CH₂Cl₂, -78 °C to rt, 18 h, Scheme 4).

1,2,4,5-Tetrazine **39** was synthesized following the procedure described by Guither et al.⁴⁰ Briefly, 3-hydroxybenzothioamide was refluxed with hydrazine monohydrate and sulfur. Treatment with sodium nitrite led to cyclization resulting in 3,3'-(1,2,4,5-tetrazine-3,6-diyl)diphenol **39**.

Scheme 4^a: Synthesis of compounds 33 to 36



^aReagents and conditions: a. Method A: Na₂CO₃ 10 % in water, toluene, Pd(PPh₃)₄, reflux, 4 h; b. Method E: BBr₃, CH₂Cl₂, -78 °C to rt, 18 h.

Biological results

Activity: inhibition of human 17 β -HSD1

Placental enzyme was partially purified following a described procedure.⁴¹ Tritiated E1 was incubated with 17 β -HSD1, cofactor and inhibitor. The amount of labelled E2 formed was quantified by HPLC. Compounds showing less than 10 % inhibition at 1 μ M were considered to be inactive.

The inhibition values of the test compounds are shown in Table 1. It becomes apparent that eleven compounds are more active than the previously described oxazole **E**³³ (IC₅₀ = 310 nM).

All methoxy compounds (data not shown) and *para-para* dihydroxylated derivatives are inactive except phenylene **34** which is a weak inhibitor (IC₅₀ > 1000 nM). The shift of one hydroxy substituent from the *para*- into the *meta*- position leads to highly active compounds except for thiazoles **1**, **7** (IC₅₀ values > 1000 nM) and **5** (IC₅₀ > 5000 nM) which have a weak inhibitory activity and triazoles **12** and **14** which are inactive. Moving the second OH substituent also in *meta* position (*meta-meta* derivatives) results in potent compounds except for triazole **16** which is a weak inhibitor (IC₅₀ > 5000 nM) and selenophene **30** and triazole **15** which are inactive.

The exchange of the *para*-OH group of the highly active thiophene **22** (IC₅₀ = 69 nM) with hydrogen reduces activity (compound **19**, IC₅₀ = 342 nM). More dramatically, the replacement of the *meta*-OH function of compound **22** with hydrogen results in the inactive compound **20**. Similarly, the exchange of the *meta*-hydroxyphenyl moiety as well as the two hydroxy groups of **22** with hydrogens leads to the inactive compounds **17** and **18**. This exemplifies the importance of the existence of two OH substituents and their positions at the phenyl moieties with at least one being in the *meta* position.

The synthesized thiazoles **1** to **8** show lower activities than the thiophene analogues **17** to **28** except compound **3** (IC₅₀ = 50 nM) which exhibits similar inhibition as **22** (IC₅₀ = 69 nM) and **27** (IC₅₀ = 77 nM). The introduction of a second nitrogen (compounds **9** to **11**) in the heterocyclic scaffold of these potent inhibitors does not strongly reduce activity (**9**, IC₅₀ = 336 nM; **11**, IC₅₀ = 169 nM). For *meta-meta* disubstituted compounds the introduction of nitrogen in compound **4** decreases activity slightly (**9**, IC₅₀ = 336 vs 243 nM), whereas introduction in compound **8** increases activity (**11**, IC₅₀ = 169 vs 455 nM), as it is observed for the *meta-para* disubstituted compound **7** (**10**, IC₅₀ = 413 vs >1000 nM).

Moving the hydroxyphenyl moiety of the highly active thiophene **22** (IC₅₀ = 69 nM) from position 5 to the 3 position decreases activity dramatically (**32**, IC₅₀ > 1000 nM). Exchange of the sulfur atom of the potent thiophene **23** (IC₅₀ = 173 nM) with selenium results in the inactive compound **30**.

In case of the six-membered rings, benzene and some of its aza-analogues were investigated. The 1,3-bis(hydroxyphenyl) substituted phenylenes were not active, whereas the 1,4-disubstituted compounds showed some activity, the most active benzene compound being the *meta-meta* derivative **35** (IC₅₀ = 173 nM). The introduction of one or more nitrogens into the central benzene ring of **35** (compounds **37** to **39**) results in an increase (pyridine **37**, IC₅₀ = 101 nM), no change (tetrazine **39**, IC₅₀ = 201 nM) and a decrease of inhibitory activity (pyrazine **38**, IC₅₀ = 1000 nM).

Furthermore in Table 1, the angles between the two phenyl moieties are presented as a structural parameter. No correlation to the activities of the corresponding compounds can be observed.

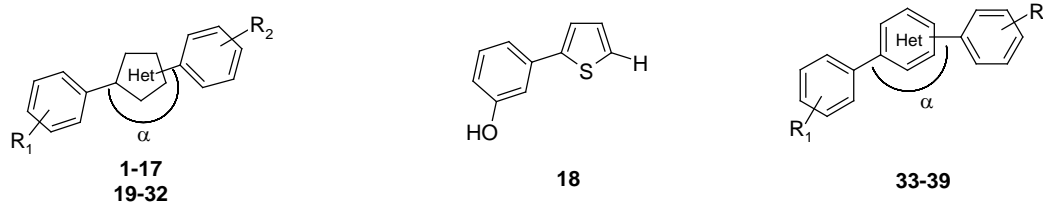
Selectivity: inhibition of human 17 β -HSD2 and affinities for ER α and ER β

Since 17 β -HSD2 catalyzes the inactivation of E2 to E1, inhibitory activity toward this enzyme must be avoided. The 17 β -HSD2 inhibition was determined using an assay similar to the 17 β -HSD1 test. Placental microsomes were incubated with tritiated E2 in the presence of NAD⁺ and inhibitor. Separation and quantification of labelled product (E1) was performed by HPLC using radio detection. A selection of the most potent 17 β -HSD1 inhibitors was tested for inhibition of 17 β -HSD2. IC₅₀ values and selectivity factors (IC₅₀HSD2 / IC₅₀ HSD1) are presented in Table 1.

It is striking that most *meta-meta* bis(hydroxyphenyl) substituted inhibitors present only poor selectivity except for compounds **37** and **39** which show high selectivity factors of 34 and 25, respectively. The *meta-para/para-meta* disubstituted inhibitors mostly show higher selectivity with compound **3** exhibiting the highest selectivity factor of 80.

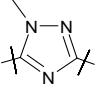
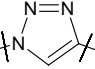
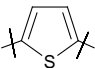
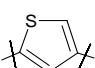
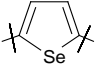
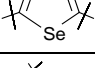
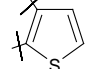
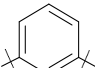
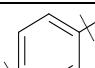
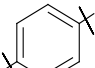
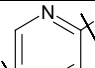
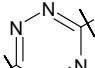
A further prerequisite for 17 β -HSD1 inhibitors to be used as potential drugs is that these compounds do not show affinity for ER α and ER β , or only a marginal one, since binding to these receptors could counteract the therapeutic efficacy. The binding affinities of selected compounds were determined using recombinant human protein in a competition assay applying [³H]-E2 and hydroxyapatite (Table 2). All tested compounds show very marginal or marginal affinity to the ERs.

Table 1: Inhibition of human 17 β -HSD1 and 17 β -HSD2 by compounds **1-39**, O-O distances and phenyl-het-phenyl angles



compound	Het	R ₁	R ₂	d(Å) ^a	α^b	IC ₅₀ (nM) ^c		selectivity factor ^f
						17 β -HSD1 ^d	17 β -HSD2 ^e	
1		4-OH	3-OH	11.9 < d < 12.7		>1000	nt	
2		4-OH	4-OH	13.6	153	ni	nt	
3		3-OH	4-OH	11.9 < d < 12.7		50	4004	80
4		3-OH	3-OH	10.1 < d < 11.7		243	2500	10
5		4-OH	3-OH	10.5 < d < 12.0		>5000	nt	
6		4-OH	4-OH	12.5	130	ni	nt	
7		3-OH	4-OH	10.5 < d < 12.0		>1000	nt	
8		3-OH	3-OH	9.0 < d < 11.2		455	2220	5
9		3-OH	3-OH	9.9 < d < 11.5		157	336	nt
10		3-OH	4-OH	9.7 < d < 11.9	128	413	2194	5
11		3-OH	3-OH	8.5 < d < 11.2		169	602	3

Table 1 continued

compound	Het	R ₁	R ₂	d(Å) ^a	α ^b	IC ₅₀ (nM) ^c		selectivity factor ^f
						17β-HSD1 ^d	17β-HSD2 ^e	
12		4-OH	3-OH	10.2 < d < 11.9		ni	nt	
13		4-OH	4-OH	12.4	145	ni	nt	
14		3-OH	4-OH	10.2 < d < 11.9		ni	nt	
15		3-OH	3-OH	8.7 < d < 11.4		ni	nt	
16			3-OH	3-OH		8.7 < d < 11.2	147	>5000
17		H	H			ni	nt	
18						ni	nt	
19		3-OH	H		147	342	2337	7
20		4-OH	H			ni	nt	
21		4-OH	4-OH	13.5		ni	nt	
22		3-OH	4-OH	11.8 < d < 12.8		69	1953	28
23		3-OH	3-OH	9.8 < d < 11.8		173	745	4
24		3-OH	H			>5000	nt	
25		4-OH	3-OH	10.4 < d < 12.0	136	151	1690	11
26		4-OH	4-OH	12.3		ni	nt	
27		3-OH	4-OH	10.4 < d < 12.0		77	1271	16
28		3-OH	3-OH	8.5 < d < 11.4		185	559	3
29			4-OH	4-OH		13.8	162	ni
30		3-OH	3-OH	10.4 < d < 11.3	ni	nt		
31		4-OH	4-OH	8.1	69	ni	nt	
32		3-OH	4-OH	6.2 < d < 8.9		>1000	nt	
33		4-OH	3-OH	9.3 < d < 12.1	120	>1000	nt	
34		4-OH	4-OH	12.3		>1000	nt	
35		3-OH	3-OH	11.4 < d < 12.4	180	173	2259	13
36		3-OH	4-OH	13.1		471	4509	9
37		3-OH	3-OH	11.6 < d < 12.3	180	101	3399	34
38		3-OH	3-OH	11.4 < d < 12.2	180	1000	5502	5
39		3-OH	3-OH	11.3 < d < 12.2	180	201	5102	25

^aO-O distance between the hydroxy substituents, for E2 d= 11.0 Å; ^bAngle between the two phenyl moieties in °; ^cMean values of three determinations, standard deviation less than 12 % except **3**: 18 % for 17β-HSD1; ^dHuman placental, cytosolic fraction, substrate [³H]-E1 + E1 [500 nM], cofactor NADH [500 μM]; ^eHuman placental, microsomal fraction, substrate [³H]-E2 + E2 [500 nM], cofactor NAD⁺ [1500 μM]; ^fIC₅₀ (17β-HSD2)/ IC₅₀ (17β-HSD1); ni: no inhibition, nt: not tested.

Table 2: Binding affinities for the human estrogen receptors α and β of selected compounds

compound	RBA ^a (%)	
	ER α ^b	ER β ^b
3	<0.01	0.01 < RBA < 0.1
22	0.1 < RBA < 1	1.5
25	0.01 < RBA < 0.1	0.1 < RBA < 1
27	0.01 < RBA < 0.1	0.1 < RBA < 1
35	<0.001	0.01 < RBA < 0.1
37	0.01 < RBA < 0.1	<0.01

^aRBA (relative binding affinity), E2: 100 %, mean values of three determinations, standard deviations less than 10 %; ^bHuman recombinant protein, incubation with 10 nM [³H]-E2 and inhibitor for 1 h.

Further biological evaluation

The intrinsic estrogenic activity of a representative compound of each class was determined using the ER-positive mammary tumor T-47D cell line. No agonistic, i.e. no stimulatory effect was observed after application of the inhibitors even at a concentration 1000 fold higher than E2 (data not shown).

A selection of active and selective compounds was investigated for permeation of CaCo-2 cells. These cells exhibit morphological and physiological properties of the human small intestine⁴² and are a generally accepted model for the prediction of peroral absorption. Depending on the P_{app} data obtained, compounds can be classified as low ($P_{app} (\cdot 10^{-6} \text{ cm/sec}) < 1$), medium ($1 < P_{app} < 10$) or highly permeable ($P_{app} > 10$). Thiazole **3** shows medium cell permeation while thiophenes **22**, **25** and phenylene **35** exhibit high cell permeability (Table 3).

Table 3: CaCo-2 cell permeation of highly active 17 β -HSD1 inhibitors

compound	$P_{app} (\cdot 10^{-6} \text{ cm/s})^{a,b}$	classification
3	7.8	medium
22	22.0	high
25	14.4	high
35	12.5	high
atenolol	0.1	low
testosterone	9.4	medium
ketoprofene	25.7	high

^aPermeability of reference compounds similar to the values described [atenolol,⁷¹ testosterone,⁶⁷ ketoprofene⁷²]; ^b P_{app} : apparent permeability coefficient, mean values of three determinations, standard deviations less than 10 %.

A representative compound of the thiazole, thiophene and phenylene class (compounds **4**, **25** and **35**) was evaluated for their phase 1 metabolic stability using rat liver microsomes. Samples were taken at defined time points and the remaining percentage of parent compound was determined by LC-MS/MS. Half-life and intrinsic clearance were evaluated and compared to the two reference compounds diazepam and diphenhydramine (Table 4). All tested compounds show longer half lives than the antihistaminic drug diphenhydramine (values in the range between 12.6 and 22.7 min vs 6.8 min).

The same compounds (**4**, **25** and **35**) were further investigated for inhibition of the six most important human hepatic enzymes: CYP1A2, 2B6, 2C9, 2C19, 2D6 and 3A4. All compounds show very low inhibition of CYP1A2, 2B6, 2C19 and 2D6 ($IC_{50} > 4 \mu\text{M}$). In case of CYP2C9 and CYP3A4 (**4**: 2.1 and 0.8, **25**: 0.8 and 1.9, **35**: 1.9 and 2.1 μM , respectively) inhibition was higher, but still clearly below the IC_{50} values of 17 β -HSD1 inhibition. These results indicate a low risk of drug-drug interaction caused by CYP-inhibition.

Table 4: Half-lives and intrinsic clearances of compounds **4**, **25** and **35** in rat liver microsomes^a

compound	half-life (min)	CL _{int} ^b (μL /min /mg protein)
4	12.6	367.2
25	18.6	248.5
35	22.7	203.4
diazepam ^c	40.8	113.3
diphenhydramine ^c	6.8	679.6

^a0.33 mg/mL protein, NADP⁺-regenerating system, [inhibitor]: 1 μM, incubation at 37 °C, samples taken at 0, 15, 30 and 60 min, determination of parent compound by MS; ^bCL_{int}: intrinsic body clearance; ^cvalues of reference compounds similar to described values.

The pharmacokinetic profiles of the most active and selectiveazole compound **3** and one of the six-membered ring compounds (**39**) were determined in rats after oral administration in a cassette. The most potent six-membered ring compound **37** was not chosen as it was unstable in buffer over 24 h. Each group consisted of 4 male rats and the compounds were administered in doses of 10 mg/kg. Plasma samples were collected over 24 h and plasma concentrations were determined by HPLC-MS/MS. The pharmacokinetic parameters are presented in Table 5. Maximal plasma concentration (C_{max}) and AUC value are much higher for compound **39** compared to compound **3**.

Table 5: Pharmacokinetic parameters of compound **3** and **39** in male rats after oral application of 10 mg/kg

parameters	compound	
	3	39
C _{max obs} (ng/mL) ^a	7.8	106.0
C _z (ng/mL) ^b	6.6	54.0
t _{max obs} (h) ^c	8.0	3.0
t _z (h) ^d	10.0	10.0
t _{1/2z} (h) ^e	1.5	1.2
AUC _{0-tz} (ng/mL) ^f	99.2	1204.0

^aC_{max obs}: maximal measured concentration; ^bC_z: last analytical quantifiable concentration; ^ct_{max obs}: time to reach the maximum measured concentration; ^dt_z: time of the last sample which has an analytically quantifiable concentration; ^et_{1/2z}: half-life of the terminal slope of a concentration time curve; ^fAUC_{0-tz}: area under the concentration time curve up to the time t_z of the last sample.

Computational Chemistry

To obtain an insight which physicochemical parameter might influence biological activity, the charge density distribution was considered and the molecular electrostatic potentials (MEPs) of selected compounds were determined. The geometry of the compounds had been fully optimized in the gas phase at the B3LYP/6-311++G (d,p) level of density functional theory (DFT). MEPs were plotted for every compound on its electron density with GaussView 3.09. The electrostatic potential distribution of the charge density is presented by a color code ranging from $-3.1 \cdot 10^{-2}$ to $4.5 \cdot 10^{-2}$ Hartree (Figures 1 and 2 and Supporting Information). For better comparison, the MEPs of different compounds were divided into 3 regions corresponding to each aromatic system.

In Figure 1, the MEPS of five-membered heterocyclic compounds are arranged based on their increasing inhibitory potency. While the positions of the hydroxyphenyl moieties are fixed, the nature of the heterocycle is varied. It becomes apparent that the heterocycle influences the ESP distribution of the whole molecule. In order to rationalise these MEPs, the ESP distribution ranges (C¹), the mean values of the distribution ranges (C²) and the Δ of ESP (C³) were analyzed: negative ESP values (red/orange/yellow) in region I and II and less negative to almost neutral ESP values (green/yellow) in region III are obviously an important factor for high inhibitory potency. Trying to establish a semi-quantitative MEP-activity relationship ("semi-QMAR") optimal ESP ranges for areas I, II and III for potent inhibition were identified (hydrogens and the OH groups were not considered): for region I ESP from -1.7 to $-1.2 \cdot 10^{-2}$, for region II -1.6 to $-0.9 \cdot 10^{-2}$ and for region III -1.2 to $-0.5 \cdot 10^{-2}$ Hartree. Similarly, the optimal Δ values of ESP for each region were determined: 0.5, 0.7 and 0.7 Hartree, respectively. Both the shift of a certain ESP distribution range on the scale and the change of the value result in a decrease of inhibitory activity. The

combination of these two criteria is substantiated with +, – and 0 in Figure 1.D indicating favorable, unfavorable and neutral impact on activity.

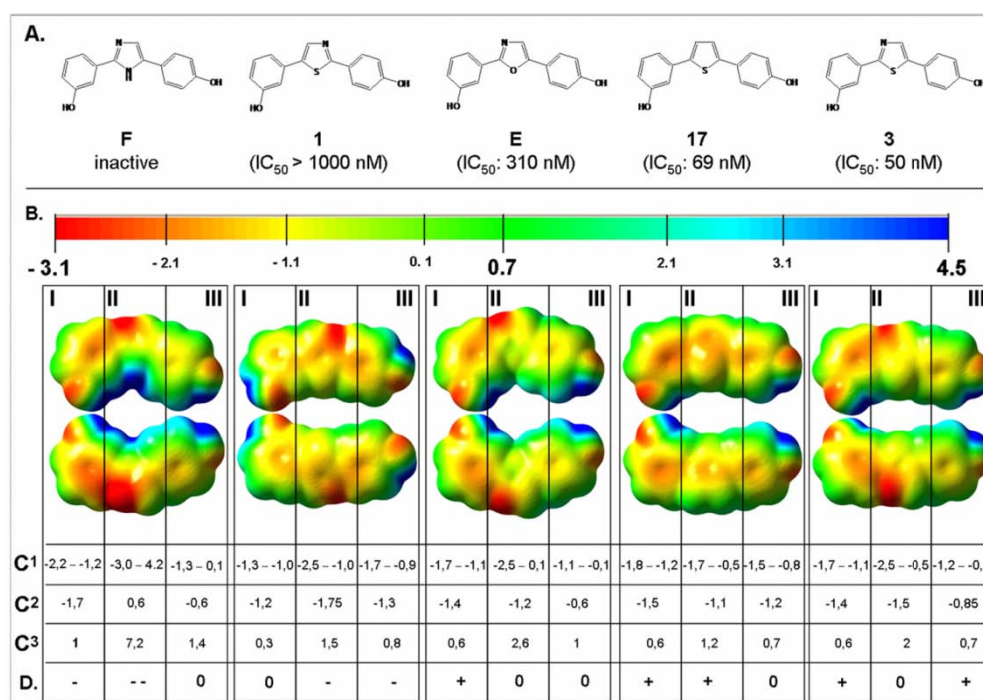


Figure 1. (A) Structure and 17 β -HSD1 inhibitory activity of **F**,³³ **E**,³³ and compounds **1**, **3**, **17** ordered by increasing activity; (B) MEP maps, dorsal and ventral view; (C¹) ESP distribution range (Hartree; $\cdot 10^{-2}$); (C²) mean value of distribution range (Hartree; $\cdot 10^{-2}$); (C³) Δ of ESP; (D) “semi-QMAR”. MEP surfaces were plotted with GaussView 3.09.

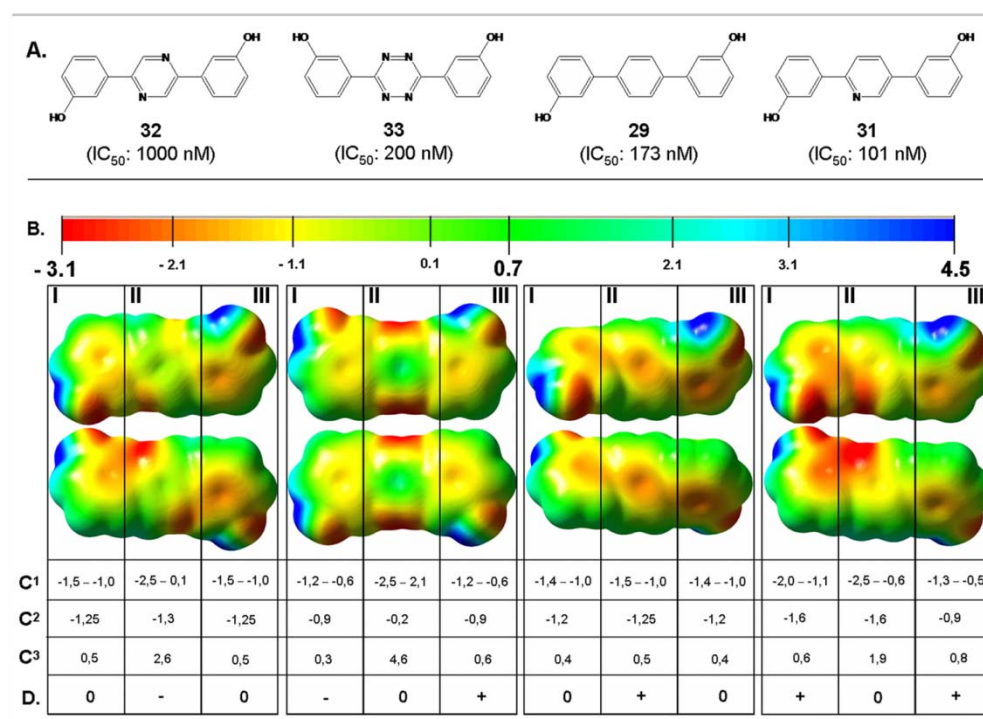


Figure 2. (A) Structure and 17 β -HSD1 inhibitory activity of compounds **29** and **31** to **33** ordered by increasing activity; (B) MEP maps, dorsal and ventral view; (C¹) ESP distribution range (Hartree; $\cdot 10^{-2}$); (C²) mean value of distribution range (Hartree; $\cdot 10^{-2}$); (C³) Δ of ESP; (D) “semi-QMAR”. MEP surfaces were plotted with GaussView 3.09.

Compound **F**³³ exhibits a polarization between top and bottom sides of the molecule: the vertex-side (NH) has positive ESP values, while on the opposite side (N-C) negative to neutral values are predominant. This polarisation ($\Delta = 7.2 \cdot 10^{-2}$ Hartree) results in an inactive compound, indicating that the ESP of the central heterocycle is crucial for 17 β -HSD1 inhibitory activity.

A good example for the change in activity is well demonstrated by the ESP distribution in region III for thiazoles **1** and **3** (Figure 1 **C**¹ and **C**²). The dramatic loss of activity of compound **1** ($IC_{50} > 1000$ nM) in comparison to **3** ($IC_{50} = 50$ nM) is due to a non optimal electron density distribution.

The MEP maps of the six-membered ring compounds are depicted in Figure 2. A similar charge density distribution was observed except for the only planar compound of this series, tetrazine **33**, which showed no polarization between top and bottom side of the molecule. It remains to be clarified whether this is the reason for the reasonable activity of compound **33**.

Discussion and conclusion

The present paper shows that compound **E** from a previous study³³ could be optimized. The most active and selective thiazole **3** shows an IC_{50} value of 50 nM and a selectivity factor of 80 (compound **E**, $IC_{50} = 310$ nM, selectivity factor: 56).

The biological results obtained confirm similar findings described in our previous article:³³ the OH substitution pattern of our compounds is decisive for inhibitory activity. Comparison of the mono hydroxylated thiophenes **19** and **20** (*meta*- and *para*-, respectively) shows that the *meta*-hydroxy group is crucial for activity. The inactivity of compound **18** indicates that the phenyl moiety of the *meta*-hydroxyphenyl thiophene **19** is also important for potency. The replacement of the *meta*-hydroxy group of **19** with hydrogen leading to the inactive compound **17** demonstrates the importance of the hydrogen bond interaction for activity.

As observed for the previously described bis(hydroxyphenyl) derivatives,³³ the distance between the two oxygens obviously has to be close to the value observed for the substrate ($d = 11$ Å). The *para-para* disubstituted compounds show distances longer than 12.5 Å. They are all inactive. Concerning the *meta-para* and *meta-meta* disubstituted compounds, which have O-O distances between 8.5 and 12.8 Å, medium to high inhibitory activities are observed for most compounds. They could be able to establish hydrogen bond interactions with His221/Glu282 and Ser142/Tyr155. However, the inactivity of thiazoles **1**, **5**, **7** and triazoles **12** to **16**, which are all *meta-para* and *meta-meta* disubstituted, indicates that this distance is not the only decisive criterion for activity. The heterocycle also influences the inhibitory potencies of the compounds.

In the five-membered ring series, the potency of 1,2,3-triazoles described previously³³ led us to further investigate this class of compounds. The inactivity of compounds **12** to **15** shows that either the nitrogen distribution in the ring or the methyl group are not tolerated by the enzyme. The replacement of the N-Me moiety of **14** with sulfur (compound **10**) leading to a fairly potent compound indicates that S in this position has a positive influence. To further investigate the role of the nitrogen in the ring, thiazoles **1** to **8** and thiophenes **21** to **28**, **31** and **32** were investigated. The fact that thiazole **3** and thiophene **22** exhibit almost identical potencies shows that the nitrogen does not contribute to binding, i.e. that there is obviously no hydrogen bond interaction.

In this report, we could also show that six-membered rings are appropriate for the design of highly active 17 β -HSD1 inhibitors. Comparison of the almost equipotent phenylene **35**, pyridine **37** and tetrazine **39** confirms the hypothesis that nitrogens are tolerated in the ring but do not contribute to a specific interaction.

The role of the angle between the two hydroxyphenyl moieties was also investigated in order to find out whether there is a correlation between this parameter and the inhibitory potency. The broad range of angles calculated (128° for **11** to 180° for **37**, two highly active compounds) could not be correlated with high or low inhibitory potency indicating that the enzyme presents some flexibility for ligand binding. Interestingly, for smaller angles between the two hydroxyphenyl groups, as in case of compounds **10** and **11** (N atom at the vertex), the *meta-meta* substitution results in a higher activity, while for larger angles, in presence of a sulfur atom at the vertex of the five-membered heterocycle (2,5-disubstituted thiazoles and 2,5-disubstituted thiophenes), the optimal substitution pattern is *meta-para/para-meta*. This phenomenon will be further investigated.

Our finding that there exists a correlation between the MEPs and the biological activities of the compounds (semi-QMAR) might be exploited for further structure optimization underlining the relevance of this descriptor for biological activity. Furthermore, the MEPs could be used to investigate how these inhibitors approach and bind to the enzyme as it is described for genistein and the estrogen receptor.⁴³

Interestingly the exchange of a CH in the thiophene **22** by a N leading to the thiazole **3** increases selectivity toward 17 β -HSD2 dramatically (IC₅₀ 17 β -HSD2 / IC₅₀ 17 β -HSD1, 28 vs 80). In general, the most potent compounds exhibit a really low affinity for the ER α and ER β and show no stimulation of cell proliferation (agonistic effect) in the ER-positive T-47D cell line. It is worth mentioning that **3** in spite of its good CaCo-2 permeability shows a really low bioavailability compared to **39**. Glucuronidation and/or sulfation might be responsible for the low plasma levels of the parent compounds.

In the present report, we described the synthesis of bis(hydroxyphenyl) azoles, thiophenes, benzenes, azabenzene and the evaluation of their biological properties. The most promising compounds of this study, **3**, **22** and **39**, show a high selectivity toward 17 β -HSD2, a low binding affinity to the ER α , a high CaCo-2 permeability and a reasonable pharmacokinetic profile after peroral application. These new compounds should be useful tools to further investigate *in vivo* 17 β -HSD1 as a target for the treatment of estrogen-dependent diseases.

Experimental section

Chemical methods

Chemical names follow IUPAC nomenclature. Starting materials were purchased from Aldrich, Acros, Lancaster, Roth, Merck or Fluka and were used without purification.

Column chromatography (CC) was performed on silica gel (70-200 μ m) coated with silica, preparative thin layer chromatography (TLC) on 1 mm SIL G-100 UV₂₅₄ glass plates (Macherey-Nagel) and reaction progress was monitored by TLC on Alugram SIL G UV₂₅₄ (Macherey-Nagel).

Melting points were measured on a Mettler FP1 melting point apparatus and are uncorrected.

IR spectra were recorded on a Bruker Vector 33 spectrometer (neat sample).

¹H-NMR and ¹³C-NMR spectra were measured on a Bruker AM500 spectrometer (500 MHz) at 300 K. Chemical shifts are reported in δ (parts per million: ppm), by reference to the hydrogenated residues of deuteriated solvent as internal standard (CDCl₃: δ = 7.24 ppm (¹H NMR) and δ = 77 ppm (¹³C NMR), CD₃OD: δ = 3.35 ppm (¹H NMR) and δ = 49.3 ppm (¹³C NMR), CD₃COCD₃: δ = 2.05 ppm (¹H NMR) and δ = 29.9 ppm (¹³C NMR), CD₃SOCD₃: δ = 2.50 ppm (¹H NMR) and δ = 39.5 ppm (¹³C NMR). Signals are described as s, d, t, dd, m, dt for singlet, doublet, triplet, doublet of doublets, multiplet and doublet of triplets, respectively. All coupling constants (*J*) are given in hertz (Hz).

Mass spectra (ESI) were recorded on a TSQ Quantum (Thermo/Fischer) instrument. Elemental analyses were performed at the Department of Instrumental Analysis and Bioanalysis, Saarland University.

5-Bromo-2-(4-methoxyphenyl)-1,3-thiazole (**1ii**),⁴⁴ 4-methoxythiobenzamide (**10ii**),⁴⁵ 3-bromo-2-(4-methoxyphenyl)thiophene (**31ii**),⁴⁶ 3-bromo-4'-methoxybiphenyl (**33ii**),⁴⁷ 4'-bromo-3-methoxybiphenyl (**35ii**),⁴⁸ 2-(4-methoxyphenyl)-5-(3-methoxyphenyl)-1,3-thiazole (**1i**),⁴⁹ 2,5-bis(4-methoxyphenyl)-1,3-thiazole (**2i**),⁵⁰ 2,4-bis(4-methoxyphenyl)-1,3-thiazole (**6i**),³⁵ 3-hydroxythiobenzamide (**11i**),¹⁶ 2,5-bis(4-methoxyphenyl)thiophene (**21i**),⁵¹ 2,4-bis(4-methoxyphenyl)thiophene (**26i**),⁵² 2,3-bis(4-methoxyphenyl)thiophene (**31i**),⁵³ 3,4"-dimethoxy-1,1':3',1"-terphenyl (**33i**),⁵⁴ 4,4"-dimethoxy-1,1':3',1"-terphenyl (**34i**),⁵⁴ 4,4'-(1,3-thiazole-2,5-diyl)diphenol (**2**),⁵⁵ 4,4'-(1,3-thiazole-2,4-diyl)diphenol (**6**),³⁵ 3,3'-(1,2,4-thiadiazole-3,5-diyl)diphenol (**11**),⁵⁶ 3,3'-(1*H*-1,2,3-triazole-1,4-diyl)diphenol (**16**),⁵⁷ 2,5-diphenylthiophene (**17**),⁵⁸ 4,4'-thiene-2,5-diyl diphenol (**21**),⁵¹ 4,4'-thiene-2,4-diyl diphenol (**26**),⁵⁵ 1,1':3',1"-terphenyl-3,4"-diol (**33**),⁵⁹ 1,1':3',1"-terphenyl-4,4"-diol (**34**),⁶⁰ 1,1':4',1"-terphenyl-3,3"-diol (**35**),⁵⁹ 1,1':4',1"-terphenyl-3,4"-diol (**36**),⁵⁹ 3,3'-pyrazine-2,5-diyl diphenol (**38**),⁶¹ 3,3'-(1,2,4,5-tetrazine-3,6-diyl)diphenol (**39**)⁴⁰ were prepared following described procedures.

General procedure for Suzuki coupling

Method A:

A mixture of arylbromide (1 eq), methoxybenzene boronic acid (1 eq), sodium carbonate (2 eq) and tetrakis(triphenylphosphine) palladium (0.005 eq) in an oxygen free toluene/water (1:1) solution was stirred at 100 °C for 4 h under nitrogen. The reaction mixture was cooled to rt. The aqueous layer was extracted with ethyl acetate. The combined organic layers were washed with brine, dried over magnesium sulfate, filtered and concentrated to dryness. The product was purified by CC.

Method B:

A mixture of arylbromide (1 eq), methoxybenzene boronic acid (1.2 eq), sodium carbonate (2 eq) and tetrakis(triphenylphosphine) palladium (0.005 eq) in an oxygen free tetrahydrofuran/water (1:1) solution was

stirred at 100 °C for 20 h under nitrogen. The reaction mixture was cooled to rt. The aqueous layer was extracted with ethyl acetate. The combined organic layers were washed with brine, dried over magnesium sulfate, filtered and concentrated to dryness. The product was purified by CC.

Method C:

A mixture of aryl dibromide (1 eq), methoxybenzene boronic acid (2.4 eq), caesium carbonate (4 eq) and tetrakis(triphenylphosphine) palladium (0.001 eq) was suspended in an oxygen free DME/EtOH/water (1:1:1) solution. The reaction mixture was exposed to microwave irradiation (15 min, 150 W, 150 °C, 15 bar). After reaching rt, water was added and the aqueous layer was extracted with ethyl acetate. The combined organic layers were washed with brine, dried over magnesium sulfate, filtered and concentrated to dryness. The product was purified by preparative TLC.

Method D: General procedure for synthesis of 1,2,4-triazoles:

A solution of acyl chloride (1 eq) in dichloromethane was added dropwise to a mixture of ethyl imino ester (1 eq) and dry triethylamine (1 eq) in 20 mL dichloromethane and heated to 30-35 °C for 6 h. After cooling to rt, the mixture was poured into 3 % NaHCO₃ solution (25 mL). The layers were separated and the organic layer was washed with water, dried over sodium sulfate and evaporated to dryness under reduced pressure. The resulting *N*-acylimino esters **12ii** to **15ii** were heated to 30-35°C with methyl hydrazine (2 eq) in CH₂Cl₂ for 4 h. The solvent was removed under reduced pressure and the 1,2,4-triazoles **12i** to **15i** were crystallized from CH₂Cl₂/ Et₂O.

General procedure for ether cleavage

Method E:

To a solution of methoxybenzene derivative (1 eq) in dry dichloromethane at -78 °C (dry ice/acetone bath), boron tribromide in dichloromethane (1 M, 3 eq per methoxy function) was added dropwise. The reaction mixture was stirred for 20 h at rt under nitrogen. Water was added to quench the reaction, and the aqueous layer was extracted with ethyl acetate. The combined organic layers were washed with brine, dried over sodium sulfate, evaporated to dryness under reduced pressure and purified by preparative TLC.

Method F:

To a solution of bis(methoxyphenyl) derivative (1 eq) in dry dichloromethane, borontrifluoride dimethyl sulfide complex (75 eq) was added dropwise at rt. The reaction mixture was stirred for 20 h. Water was added to quench the reaction and the aqueous layer was extracted with ethyl acetate. The combined organic layers were washed with brine, dried over sodium sulfate, evaporated to dryness under reduced pressure and purified by preparative TLC.

3-[2-(4-Hydroxyphenyl)-1,3-thiazol-5-yl]phenol (1). The title compound was prepared by reaction of 5-(3-methoxyphenyl)-2-(4-methoxyphenyl)-1,3-thiazole (**1i**) (40 mg, 0.13 mmol) and boron tribromide (0.81 mmol) according to method E. The product was purified by preparative TLC (hexane/ethyl acetate 5:5); yield: 77 % (28 mg); MS (ESI): 270 (M+H)⁺; Anal. (C₁₅H₁₁NO₂S) C, H, N.

5-Bromo-2-(3-methoxyphenyl)-1,3-thiazole (3ii). The title compound was prepared by reaction of 2,5-dibromo-1,3-thiazole (500 mg, 2.06 mmol), 3-methoxybenzeneboronic acid (376 mg, 2.47 mmol), sodium carbonate (437 mg, 4.12 mmol) and tetrakis(triphenylphosphine) palladium (11 mg, 10 μmol) according to method A. The product was purified by CC (dichloromethane/methanol 95:5); yield: 50 % (278 mg).

2-(3-Methoxyphenyl)-5-(4-methoxyphenyl)-1,3-thiazole (3i). The title compound was prepared by reaction of 5-bromo-2-(3-methoxyphenyl)-1,3-thiazole (**3ii**) (250 mg, 0.93 mmol), 4-methoxybenzeneboronic acid (170 mg, 1.11 mmol), sodium carbonate (197 mg, 1.86 mmol) and tetrakis(triphenylphosphine) palladium (5.4 mg, 4.6 μmol) according to method A. The product was purified by CC (hexane/ethyl acetate 9:1); yield: 58 % (160 mg).

3-[5-(4-Hydroxyphenyl)-1,3-thiazol-2-yl]phenol (3). The title compound was prepared by reaction of 2-(3-methoxyphenyl)-5-(4-methoxyphenyl)-1,3-thiazole (**3i**) (40 mg, 0.13 mmol) and boron tribromide (0.81 mmol) according to method E. The product was purified by preparative TLC (hexane/ethyl acetate 5:5); yield: 80 % (50 mg); MS (ESI): 270 (M+H)⁺; Anal. (C₁₅H₁₁NO₂S) C, H, N.

2,5-Bis(3-methoxyphenyl)-1,3-thiazole (4i). The title compound was prepared by reaction of 5-bromo-2-(3-methoxyphenyl)-1,3-thiazole (**3ii**) (250 mg, 0.93 mmol), 3-methoxybenzeneboronic acid (170 mg, 1.11 mmol), sodium carbonate (197 mg, 1.86 mmol) and tetrakis(triphenylphosphine) palladium (5.4 mg, 4.6 μmol) according to method A. The product was purified by CC (hexane/ethyl acetate 9:1); yield: 40 % (111 mg).

3,3'-(1,3-Thiazole-2,5-diyl)diphenol (4). The title compound was prepared by reaction of 2,5-bis(3-methoxyphenyl)-1,3-thiazole (**4i**) (100 mg, 0.36 mmol) and boron tribromide (2.02 mmol) according to method E.

The product was purified by preparative TLC (hexane/ethyl acetate 5:5); yield: 85 % (82 mg); MS (ESI): 270 (M+H)⁺; Anal. (C₁₅H₁₁NO₂S) C, H, N.

4-Bromo-2-(4-methoxyphenyl)-1,3-thiazole (5ii). The title compound was prepared by reaction of 2,4-dibromo-1,3-thiazole (500 mg, 2.06 mmol), 4-methoxybenzeneboronic acid (376 mg, 2.47 mmol), sodium carbonate (437 mg, 4.12 mmol) and tetrakis(triphenylphosphine) palladium (11 mg, 10 μmol) according to method A. The product was purified by CC (hexane/ethyl acetate 9:1); yield: 55 % (305 mg).

2-(4-Methoxyphenyl)-4-(3-methoxyphenyl)-1,3-thiazole (5i). The title compound was prepared by reaction of 4-bromo-2-(4-methoxyphenyl)-1,3-thiazole (5ii) (250 mg, 0.93 mmol), 3-methoxybenzeneboronic acid (170 mg, 1.11 mmol), sodium carbonate (197 mg, 1.86 mmol) and tetrakis(triphenylphosphine) palladium (5.4 mg, 4.6 μmol) according to method A. The product was purified by CC (hexane/ethyl acetate 9:1); yield: 52 % (143 mg).

3-[2-(4-Hydroxyphenyl)-1,3-thiazol-4-yl]phenol (5). The title compound was prepared by reaction of 2-(4-methoxyphenyl)-4-(3-methoxyphenyl)-1,3-thiazole (5i) (70 mg, 0.24 mmol) and boron tribromide (1.44 mmol) according to method E. The product was purified by preparative TLC (hexane/ethyl acetate 5:5); yield: 78 % (50 mg); MS (ESI): 268 (M-H)⁻; Anal. (C₁₅H₁₁NO₂S) C, H, N.

4-Bromo-2-(3-methoxyphenyl)-1,3-thiazole (7ii). The title compound was prepared by reaction of 2,4-dibromo-1,3-thiazole (500 mg, 2.06 mmol), 3-methoxybenzeneboronic acid (376 mg, 2.47 mmol), sodium carbonate (437 mg, 4.12 mmol) and tetrakis(triphenylphosphine) palladium (11 mg, 10 μmol) according to method A. The product was purified by CC (hexane/ethyl acetate 9:1); yield: 50 % (270 mg).

2-(3-Methoxyphenyl)-4-(4-methoxyphenyl)-1,3-thiazole (7i). The title compound was prepared by reaction of 4-bromo-2-(3-methoxyphenyl)-1,3-thiazole (7ii) (250 mg, 0.93 mmol), 4-methoxybenzeneboronic acid (170 mg, 1.11 mmol), sodium carbonate (197 mg, 1.86 mmol) and tetrakis(triphenylphosphine) palladium (5.4 mg, 4.6 μmol) according to method A. The product was purified by CC (hexane/ethyl acetate 9:1); yield: 79 % (218 mg).

3-[4-(4-Hydroxyphenyl)-1,3-thiazol-2-yl]phenol (7). The title compound was prepared by reaction of 2-(3-methoxyphenyl)-4-(4-methoxyphenyl)-1,3-thiazole (7i) (70 mg, 0.24 mmol) and boron tribromide (1.44 mmol) according to method E. The product was purified by preparative TLC (hexane/ethyl acetate 5:5); yield: 80 % (52 mg); MS (ESI): 268 (M-H)⁻; Anal. (C₁₅H₁₁NO₂S) C, H, N.

2,4-Bis(3-methoxyphenyl)-1,3-thiazole (8i). The title compound was prepared by reaction of 4-bromo-2-(3-methoxyphenyl)-1,3-thiazole (7ii) (250 mg, 0.93 mmol), 3-methoxybenzeneboronic acid (170 mg, 1.11 mmol), sodium carbonate (197 mg, 1.86 mmol) and tetrakis(triphenylphosphine) palladium (5.4 mg, 4.6 μmol) according to method A. The product was purified by CC (hexane/ethyl acetate 9:1); yield: 18 % (50 mg).

3,3'-(1,3-Thiazol-2,4-diyl)diphenol (8). The title compound was prepared by reaction of 2,4-bis(3-methoxyphenyl)-1,3-thiazole (8i) (70 mg, 0.24 mmol) and boron tribromide (1.44 mmol) according to method E. The product was purified by preparative TLC (hexane/ethyl acetate 5:5); yield: 78 % (50 mg); MS (ESI): 268 (M-H)⁻; Anal. (C₁₅H₁₁NO₂S) C, H, N.

3,3'-(1,2,4-Thiadiazol-2,5-diyl)diphenol (9). A solution of 3-hydroxythiobenzamide (100 mg, 0.17 mmol, 2 eq) in DMSO (10 ml) was stirred for 5 h at rt with 3 ml concentrated chlorhydric acid. The crude mixture was poured into water and the resulting precipitate was filtered, washed with water and dried overnight in a desiccator; yield: 92 % (41 mg); MS (ESI): 269 (M-H)⁻. Anal. (C₁₄H₁₀N₂O₂S) C, H, N.

3-[3-(4-Methoxyphenyl)-1,2,4-thiadiazol-5-yl]phenol (10i). A solution of 4-methoxythiobenzamide (10ii) (318 mg, 1.90 mmol, 1 eq) in DMSO was heated for 8 h at 38 °C with 3-hydroxythiobenzamide (11i) (290 mg, 1.90 mmol, 1 eq) and concentrated hydrochloric acid (193 μL, 1.90 mmol, 1 eq). After cooling to rt, the crude mixture was poured into water and the resulting precipitate was collected by filtration. The mixture of 10i and 11 was separated by CC (hexane/ethyl acetate 8:2); yield: 30 % (70 mg) for 10i and 42 % (215 mg) for 11.

3-[3-(4-Hydroxyphenyl)-1,2,4-thiadiazol-5-yl]phenol (10). The title compound was prepared by reaction of 3-[3-(4-methoxyphenyl)-[1,2,4]-thiadiazol-5-yl]-phenol (10i) (150 mg, 0.53 mmol) and boron tribromide (1.59 mmol) according to method E. The product was purified by preparative TLC (hexane/ethyl acetate 5:5); yield: 91 % (130 mg); MS (ESI): 271 (M+H)⁺; Anal. (C₁₄H₁₀N₂O₂S) C, H, N.

3-(3-Methoxyphenyl)-5-(4-methoxyphenyl)-1-methyl-1H-1,2,4-triazole (12i). The title compound was prepared from *para*-anisoyl chloride (170 mg, 1.0 mmol), ethyl 3-methoxybenzimidate (179 mg, 1.0 mmol) and methyl hydrazine (92 mg, 2.0 mmol) according to method D; yield: 85 % (250 mg); m.p. 108-110 °C (CH₂Cl₂/Et₂O); MS (ESI): 296 (M+H)⁺.

3-[5-(4-Hydroxyphenyl)-1-methyl-1H-1,2,4-triazol-3-yl]phenol (12). The title compound was prepared by reaction of 3-(3-methoxyphenyl)-5-(4-methoxyphenyl)-1-methyl-1H-1,2,4-triazole (12i) (100 mg, 0.37 mmol) and

borontrifluoride dimethyl sulfide complex (27.75 mmol) according to method F. The product was purified by preparative TLC (ethyl acetate); yield: 46 % (42 mg); MS (ESI): 268 (M+H)⁺.

3,5-Bis(4-methoxyphenyl)-1-methyl-1H-1,2,4-triazole (13i). The title compound was prepared from *para*-anisoyl chloride (170 mg, 1.0 mmol), ethyl 4-methoxybenzimidate (179 mg, 1.0 mmol) and methyl hydrazine (92 mg, 2.0 mmol) according to method D; yield: 78 % (230 mg); m.p. 141-143 °C (CH₂Cl₂/ Et₂O); MS (ESI): 296 (M+H)⁺.

4-[5-(4-Hydroxyphenyl)-1-methyl-1H-1,2,4-triazol-3-yl]phenol (13). The title compound was prepared by reaction of 3,5-bis(4-methoxyphenyl)-1-methyl-1H-1,2,4-triazole (13i) (100 mg, 0.37 mmol) and borontrifluoride dimethyl sulfide complex (27.7 mmol) according to method F. The product was purified by preparative TLC (ethyl acetate); yield: 63 % (57 mg); MS (ESI): 268 (M+H)⁺.

3-(4-Methoxyphenyl)-5-(3-methoxyphenyl)-1-methyl-1H-1,2,4-triazole (14i). The title compound was prepared from *meta*-anisoyl chloride (170 mg, 1.0 mmol), ethyl 4-methoxybenzimidate (179 mg, 1.0 mmol) and methyl hydrazine (92 mg, 2.0 mmol) according to method D; yield: 77 % (227 mg); m.p. 114-116 °C (CH₂Cl₂/ Et₂O); MS (ESI): 296 (M+H)⁺.

4-[5-(3-Hydroxyphenyl)-1-methyl-1H-1,2,4-triazol-3-yl]phenol (14). The title compound was prepared by reaction of 3-(4-methoxyphenyl)-5-(3-methoxyphenyl)-1-methyl-1H-1,2,4-triazole (14i) (100 mg, 0.37 mmol) and borontrifluoride dimethyl sulfide complex (27.7 mmol) according to method F. The product was purified by preparative TLC (ethyl acetate); yield: 53 % (48 mg); MS (ESI): 268 (M+H)⁺.

3,5-Bis(3-methoxyphenyl)-1-methyl-1H-1,2,4-triazole (15i). The title compound was prepared from *meta*-anisoyl chloride (170 mg, 1.0 mmol), ethyl 3-methoxybenzimidate (179 mg, 1.0 mmol) and methyl hydrazine (92 mg, 2.0 mmol) according to method D; yield: 67 % (198 mg); m.p. 67-69 °C (CH₂Cl₂/ Et₂O); MS (ESI): 296 (M+H)⁺.

3-[5-(3-Hydroxyphenyl)-1-methyl-1H-1,2,4-triazol-3-yl]phenol (15). The title compound was prepared by reaction of 3,5-bis(3-methoxyphenyl)-1-methyl-1H-1,2,4-triazole (15i) (100 mg, 0.37 mmol) and borontrifluoride dimethyl sulfide complex (27.7 mmol) according to method F. The product was purified by preparative TLC (ethyl acetate); yield: 64 % (58 mg); MS (ESI): 268 (M+H)⁺.

2-Bromo-5-(3-methoxyphenyl)thiophene (18ii). The title compound was prepared by reaction of 2,5-dibromothiophene (465 μL, 4.13 mmol), 3-methoxybenzeneboronic acid (753 mg, 4.95 mmol), sodium carbonate (876 mg, 8.26 mmol) and tetrakis(triphenylphosphine) palladium (24 mg, 20 μmol) according to method A. The product was purified by CC (hexane/ethyl acetate 9:1); yield: 41 % (445 mg).

2-(3-Methoxyphenyl)thiophene (18i). To a solution of 2-bromo-5-(3-methoxyphenyl)thiophene (18ii) (100 mg, 0.37 mmol, 1 eq) in dry THF cooled to -78 °C for 5 min, *n*-BuLi (1.6 M in hexane, 0.28 mL, 0.44 mmol, 1.2 eq) was added dropwise and stirred for 15 min at -78 °C. The crude mixture was carefully hydrolyzed by addition of water (10 ml) and layers were separated. The aqueous layer was extracted with ethyl acetate. The combined organic layers were washed with brine, dried over magnesium sulfate and evaporated to dryness under reduced pressure; yield: 98 % (69 mg).

3-(2-Thienyl)phenol (18). The title compound was prepared by reaction of 2-(3-methoxyphenyl)thiophene (18i) (80 mg, 0.42 mmol) and boron tribromide (1.26 mmol) according to method E. The product was purified by preparative TLC (hexane/ethyl acetate 7:3); yield: 85 % (63 mg); MS (ESI): 177 (M+H)⁺; Anal. (C₁₀H₈OS) C, H, N.

2-(3-Methoxyphenyl)-5-phenylthiophene (19i). The title compound was prepared by reaction of 2-bromo-5-(3-methoxyphenyl)thiophene (18ii) (400 mg, 1.52 mmol), benzeneboronic acid (223 mg, 1.82 mmol), sodium carbonate (322 mg, 3.04 mmol) and tetrakis(triphenylphosphine) palladium (8.8 mg, 7.6 μmol) according to method B. The product was purified by CC (hexane/ethyl acetate 7:3); yield: 70 % (283 mg).

3-(5-Phenyl-2-thienyl)phenol (19). The title compound was prepared by reaction of 2-(3-methoxyphenyl)-5-phenylthiophene (19i) (100 mg, 0.37 mmol) and boron tribromide (2.22 mmol) according to method E. The product was purified by preparative TLC (hexane/ethyl acetate 5:5); yield: 81 % (75 mg); MS (ESI): 253 (M+H)⁺; Anal. (C₁₆H₁₂OS) C, H, N.

2-Bromo-5-(4-methoxyphenyl)thiophene (20ii). The title compound was prepared by reaction of 2,5-dibromothiophene (V= 465 μL, 4.13 mmol), 4-methoxybenzeneboronic acid (753 mg, 4.95 mmol), sodium carbonate (876 mg, 8.26 mmol) and tetrakis(triphenylphosphine) palladium (24 mg, 20 μmol) according to method A. The product was purified by CC (hexane/ethyl acetate 9:1); yield: 75 % (815 mg).

2-(4-Methoxyphenyl)-5-phenylthiophene (20i). The title compound was prepared by reaction of 2-bromo-5-(4-methoxyphenyl)thiophene (20ii) (400 mg, 1.52 mmol), benzeneboronic acid (223 mg, 1.82 mmol), sodium

carbonate (322 mg, 3.04 mmol) and tetrakis(triphenylphosphine) palladium (8.8 mg, 7.6 μ mol) according to method B. The product was purified by CC (hexane/ethyl acetate 7:3); yield: 75 % (303 mg).

4-(5-Phenyl-2-thienyl)phenol (20). The title compound was prepared by reaction of 2-(4-methoxyphenyl)-5-phenylthiophene (**20i**) (100 mg, 0.37 mmol) and boron tribromide (2.22 mmol) according to method E. The product was purified by preparative TLC (dichloromethane/methanol 99:1); yield: 95 % (89 mg); MS (ESI): 253 (M+H)⁺; Anal. (C₁₆H₁₂OS) C, H, N.

2-(3-Methoxyphenyl)-5-(4-methoxyphenyl)thiophene (22i). The title compound was prepared by reaction of 2-bromo-5-(3-methoxyphenyl)thiophene (**18ii**) (150 mg, 0.57 mmol), 4-methoxybenzeneboronic acid (223 mg, 0.68 mmol), sodium carbonate (120 mg, 1.14 mmol) and tetrakis(triphenylphosphine) palladium (3.2 mg, 2.8 μ mol) according to method B. The product was purified by CC (hexane/ethyl acetate 9:1); yield: 75 % (126 mg).

3-[5-(4-Hydroxyphenyl)-2-thienyl]phenol (22). The title compound was prepared by reaction of 2-(3-methoxyphenyl)-5-(4-methoxyphenyl)thiophene (**22i**) (150 mg, 0.51 mmol) and boron tribromide (3.06 mmol) according to method E. The product was purified by preparative TLC (hexane/ethyl acetate 5:5); yield: 93 % (127 mg); MS (ESI): 269 (M+H)⁺; Anal. (C₁₆H₁₂O₂S) C, H, N.

2,5-Bis(3-methoxyphenyl)thiophene (23i). The title compound was prepared by reaction of 2-bromo-5-(3-methoxyphenyl)thiophene (**18ii**) (150 mg, 0.57 mmol), 3-methoxybenzeneboronic acid (223 mg, 0.68 mmol), sodium carbonate (120 mg, 1.14 mmol) and tetrakis(triphenylphosphine) palladium (3.2 mg, 2.8 μ mol) according to method B. The product was purified by CC (hexane/ethyl acetate 9:1); yield: 78 % (132 mg).

3,3'-Thiene-2,5-diylidiphenol (23). The title compound was prepared by reaction of 2,5-bis(3-methoxyphenyl)thiophene (**23i**) (150 mg, 0.51 mmol) and boron tribromide (3.06 mmol) according to method E. The product was purified by preparative TLC (hexane/ethyl acetate 5:5); yield: 95 % (130 mg); MS (ESI): 269 (M+H)⁺; Anal. (C₁₆H₁₂O₂S) C, H, N.

4-Bromo-2-(3-methoxyphenyl)thiophene (24ii). The title compound was prepared by reaction of 2,4-dibromothiophene (1.00 g, 4.13 mmol), 3-methoxybenzeneboronic acid (753 mg, 4.95 mmol), sodium carbonate (876 mg, 8.26 mmol) and tetrakis(triphenylphosphine) palladium (24 mg, 20 μ mol) according to method A. The product was purified by CC (hexane/ethyl acetate 9:1); yield: 72 % (782 mg).

2-(3-Methoxyphenyl)-4-phenylthiophene (24i). The title compound was prepared by reaction of 4-bromo-2-(3-methoxyphenyl)thiophene (**24ii**) (250 mg, 0.93 mmol), benzeneboronic acid (137 mg, 1.12 mmol), sodium carbonate (197 mg, 1.86 mmol) and tetrakis(triphenylphosphine) palladium (6 mg, 4.64 μ mol) according to method B. The product was purified by CC (petroleum ether/ethyl acetate 7:3); yield: 91% (225 mg).

3-(4-Phenyl-2-thienyl)phenol (24). The title compound was prepared by reaction of 2-(3-methoxyphenyl)-4-phenylthiophene (**24i**) (225 mg, 0.85 mmol) and boron tribromide (3.6 mmol) according to method E. The product was purified by preparative TLC (dichloromethane/methanol 99:1); yield: 69 % (147 mg); MS (ESI): 253 (M+H)⁺.

4-Bromo-2-(4-methoxyphenyl)thiophene (25ii). The title compound was prepared by reaction of 2,4-dibromothiophene (1.00 g, 4.13 mmol), 4-methoxybenzeneboronic acid (753 mg, 4.95 mmol), sodium carbonate (876 mg, 8.26 mmol) and tetrakis(triphenylphosphine) palladium (24 mg, 20 μ mol) according to method A. The product was purified by CC (hexane/ethyl acetate 9:1); yield: 78 % (847 mg).

2-(4-Methoxyphenyl)-4-(3-methoxyphenyl)thiophene (25i). The title compound was prepared by reaction of 4-bromo-2-(4-methoxyphenyl)thiophene (**25ii**) (150 mg, 0.57 mmol), 3-methoxybenzeneboronic acid (223 mg, 0.68 mmol), sodium carbonate (120 mg, 1.14 mmol) and tetrakis(triphenylphosphine) palladium (3.2 mg, 2.8 μ mol) according to method B. The product was purified by CC (hexane/ethyl acetate 9:1); yield: 70 % (118 mg).

3-[5-(4-Hydroxyphenyl)-3-thienyl]phenol (25). The title compound was prepared by reaction of 2-(4-methoxyphenyl)-4-(3-methoxyphenyl)thiophene (**25i**) (150 mg, 0.51 mmol) and boron tribromide (3.06 mmol) according to method E. The product was purified by preparative TLC (hexane/ethyl acetate 5:5); yield: 80 % (109 mg); MS (ESI): 267 (M-H)⁻; Anal. (C₁₆H₁₂O₂S) C, H, N.

2-(3-Methoxyphenyl)-4-(4-methoxyphenyl)thiophene (27i). The title compound was prepared by reaction of 4-bromo-2-(3-methoxyphenyl)thiophene (**24ii**) (150 mg, 0.57 mmol), 4-methoxybenzeneboronic acid (223 mg, 0.68 mmol), sodium carbonate (120 mg, 1.14 mmol) and tetrakis(triphenylphosphine) palladium (3.2 mg, 2.8 μ mol) according to method B. The product was purified by CC (hexane/ethyl acetate 9:1); yield: 70 % (118 mg).

3-[4-(4-Hydroxyphenyl)-2-thienyl]phenol (27). The title compound was prepared by reaction of 2-(3-methoxyphenyl)-4-(4-methoxyphenyl)thiophene (**27i**) (150 mg, 0.51 mmol) and boron tribromide solution (3.06 mmol) according to method E. The product was purified by preparative TLC (hexane/ethyl acetate 5:5); yield: 85 % (116 mg); MS (ESI): 267 (M-H)⁻; Anal. (C₁₆H₁₂O₂S) C, H, N.

2,4-Bis(3-methoxyphenyl)thiophene (28i). The title compound was prepared by reaction of 4-bromo-2-(3-methoxyphenyl)thiophene (**24ii**) (150 mg, 0.57 mmol), 3-methoxybenzeneboronic acid (223 mg, 0.68 mmol), sodium carbonate (120 mg, 1.14 mmol) and tetrakis(triphenylphosphine) palladium (3.2 mg, 2.8 μ mol) according to method B. The product was purified by CC (hexane/ethyl acetate 9:1); yield: 72 % (121 mg).

3,3'-Thiene-2,4-diyl)diphenol (28). The title compound was prepared by reaction of 2,4-bis(3-methoxyphenyl)thiophene (**28i**) (150 mg, 0.51 mmol) and boron tribromide (3.06 mmol) according to method E. The product was purified by preparative TLC (hexane/ethyl acetate 5:5); yield: 88 % (120 mg); MS (ESI): 267 (M-H)⁻; Anal. (C₁₆H₁₂O₂S) C, H, N.

4,4'-(Seleniene-2,5-diyl)diphenol (29). The title compound was prepared by reaction of 2,5-dibromoselenophene (150 mg, 0.52 mmol), 4-hydroxybenzeneboronic acid (172 mg, 1.25 mmol), caesium carbonate (679 mg, 2.08 mmol) and tetrakis(triphenylphosphine) palladium (6.0 mg, 5.2 μ mol) according to method C. The product was purified by preparative TLC (hexane/ethyl acetate 6:4); yield: 49 % (81 mg); MS (ESI): 317 (M+H)⁺; Anal. (C₁₆H₁₂O₂Se) C, H, N.

3,3'-(Seleniene-2,5-diyl)diphenol (30). The title compound was prepared by reaction of 2,5-dibromoselenophene (150 mg, 0.52 mmol), 3-hydroxybenzeneboronic acid (172 mg, 1.25 mmol), caesium carbonate (679 mg, 2.08 mmol) and tetrakis(triphenylphosphine) palladium (6.0 mg, 5.2 μ mol) according to method C. The product was purified by preparative TLC (hexane/ethyl acetate 6:4); yield: 42 % (69 mg); MS (ESI): 317 (M+H)⁺; Anal. (C₁₆H₁₂O₂Se) C, H, N.

3-Bromo-2-(4-methoxyphenyl)thiophene (31ii). The title compound was prepared by reaction of 2,3-dibromothiophene (234 μ L, 2.1 mmol), 4-methoxybenzeneboronic acid (383 mg, 2.52 mmol), sodium carbonate (403 mg, 4.2 mmol) and tetrakis(triphenylphosphine) palladium (12 mg, 10 μ mol) according to method B. The product was purified by CC (hexane); yield: 70 % (387 mg).

4,4'-(Thiene-2,3-diyl)diphenol (31). The title compound was prepared by reaction of 2,3-bis(4-methoxyphenyl)thiophene (**31i**) (150 mg, 0.51 mmol) and boron tribromide (3.06 mmol) according to method E. The product was purified by preparative TLC (hexane/ethyl acetate 5:5); yield: 70 % (95 mg); MS (ESI): 269 (M+H)⁺; Anal. (C₁₆H₁₂O₂S) C, H, N.

3-Bromo-2-(3-methoxyphenyl)thiophene (32ii). The title compound was prepared by reaction of 2,3-dibromothiophene (234 μ L, 2.1 mmol), 3-methoxybenzeneboronic acid (383 mg, 2.52 mmol), sodium carbonate (403 mg, 4.2 mmol) and tetrakis(triphenylphosphine) palladium (12 mg, 10 μ mol) according to method B. The product was purified by CC (hexane); yield: 58 % (320 mg).

2-(3-Methoxyphenyl)-3-(4-methoxyphenyl)-thiophene (32i). The title compound was prepared by reaction of 3-bromo-2-(3-methoxyphenyl)thiophene (**32ii**) (150 mg, 0.57 mmol), 4-methoxybenzeneboronic acid (223 mg, 0.68 mmol), sodium carbonate (120 mg, 1.14 mmol) and tetrakis(triphenylphosphine) palladium (3.2 mg, 2.8 μ mol) according to method B. The product was purified by CC (hexane/ethyl acetate 7:3); yield 40 % (68 mg).

3-[3-(4-Hydroxyphenyl)-2-thienyl]phenol (32). The title compound was prepared by reaction of 2-(3-methoxyphenyl)-3-(4-methoxyphenyl)thiophene (**32i**) (150 mg, 0.51 mmol) and boron tribromide (3.06 mmol) according to method E. The product was purified by preparative TLC (hexane/ethyl acetate 5:5); yield: 56 % (77 mg); MS (ESI): 269 (M+H)⁺; Anal. (C₁₆H₁₂O₂S) C, H, N.

3,3''-Dimethoxy-1,1':4,1''-terphenyl (35i). The title compound was prepared by reaction of 4'-bromo-3-methoxybiphenyl (**35ii**) (500 mg, 1.90 mmol), 3-methoxybenzeneboronic acid (346 mg, 2.28 mmol), sodium carbonate (403 mg, 3.80 mmol) and tetrakis(triphenylphosphine) palladium (11 mg, 9.5 μ mol) according to an adaptation of method A (heating the mixture 20 h instead of 4 h). The product was purified by CC (hexane/ethyl acetate 95:5); yield: 14 % (77 mg).

3,4''-Dimethoxy-1,1':4,1''-terphenyl (36i). The title compound was prepared by reaction of 4'-bromo-3-methoxybiphenyl (**35ii**) (500 mg, 1.90 mmol), 4-methoxybenzeneboronic acid (346 mg, 2.28 mmol), sodium carbonate (403 mg, 3.80 mmol) and tetrakis(triphenylphosphine) palladium (11 mg, 9.5 μ mol) according to an adaptation of method A (heating the mixture 20 h instead of 4 h). The product was purified by CC (hexane/ethyl acetate 95:5); yield: 90 % (496 mg).

3,3'-Pyridine-2,5-diyl)diphenol (37). The title compound was prepared by reaction of 2,5-dibromo pyridine (150 mg, 0.63 mmol), 3-hydroxybenzeneboronic acid (231 mg, 1.52 mmol), caesium carbonate (821 mg, 2.52 mmol) and tetrakis(triphenylphosphine) palladium (7.3 mg, 6.3 μ mol) according to method C. The product was purified by preparative TLC (dichloromethane/methanol 98:2); yield: 67 % (111 mg); MS (ESI): 262 (M-H)⁻; Anal. (C₁₇H₁₃NO₂) C, H, N.

Biological Methods

[2, 4, 6, 7-³H]-E2 and [2, 4, 6, 7-³H]-E1 were bought from Perkin Elmer, Boston. Quickszint Flow 302 scintillator fluid was bought from Zinsser Analytic, Frankfurt.

17 β -HSD1 and 17 β -HSD2 were obtained from human placenta according to previously described procedures.^{22,62} Fresh human placenta was homogenized and centrifuged. The pellet fraction contains the microsomal 17 β -HSD2, while 17 β -HSD1 was obtained after precipitation with ammonium sulfate from the cytosolic fraction.

Inhibition of 17 β -HSD1

Inhibitory activities were evaluated by a well established method with minor modifications.^{41, 63, 64} Briefly, the enzyme preparation was incubated with NADH [500 μ M] in the presence of potential inhibitors at 37 °C in a phosphate buffer (50 mM) supplemented with 20 % of glycerol and EDTA 1mM. Inhibitor stock solutions were prepared in DMSO. Final concentration of DMSO was adjusted to 1 % in all samples. The enzymatic reaction was started by addition of a mixture of unlabelled- and [2, 4, 6, 7-³H]- E1 (final concentration: 500 nM, 0.15 μ Ci). After 10 min, the incubation was stopped with HgCl₂ and the mixture was extracted with ether. After evaporation, the steroids were dissolved in acetonitrile. E1 and E2 were separated using acetonitrile/water (45:55) as mobile phase in a C18 rp chromatography column (Nucleodur C18 Gravity, 3 μ m, Macherey-Nagel, Düren) connected to a HPLC-system (Agilent 1100 Series, Agilent Technologies, Waldbronn). Detection and quantification of the steroids were performed using a radioflow detector (Berthold Technologies, Bad Wildbad). The conversion rate was calculated according to following equation: $\%conversion = \frac{\%E2}{\%E2 + \%E1} \cdot 100$. Each value was calculated from at least three independent experiments.

Inhibition of 17 β -HSD2

The 17 β -HSD2 inhibition assay was performed similarly to the 17 β -HSD1 procedure. The microsomal fraction was incubated with NAD⁺ [1500 μ M], test compound and a mixture of unlabelled- and [2, 4, 6, 7-³H]-E2 (final concentration: 500 nM, 0.11 μ Ci) for 20 min at 37 °C. Further treatment of the samples and HPLC separation was carried out as mentioned above.

ER affinity

The binding affinity of select compounds to the ER α and ER β was determined according to Zimmermann et al.⁶⁵ Briefly, 0.25 pmol of ER α or ER β , respectively, were incubated with [2, 4, 6, 7-³H]-E2 (10 nM) and test compound for 1 h at rt. The potential inhibitors were dissolved in DMSO (5 % final concentration). Non-specific-binding was performed with diethylstilbestrol (10 μ M). After incubation, ligand-receptor complexes were selectively bound to hydroxyapatite (5 g/ 60 mL TE-buffer). The formed complex was separated, washed and resuspended in ethanol. For radiodetection, scintillator cocktail (Quickszint 212, Zinsser Analytic, Frankfurt) was added and samples were measured in a liquid scintillation counter (Rack Beta Primo 1209, Wallac, Turku). For determination of the relative binding affinity (RBA), inhibitor and E2 concentrations required to displace 50 % of the receptor bound labelled E2 were determined. RBA values were calculated according to the following equation:

$$RBA[\%] = \frac{IC_{50}(E2)}{IC_{50}(compound)} \cdot 100. \text{ The RBA value for E2 was arbitrarily set at 100 \% .}$$

Evaluation of the estrogenic activity using T-47D cells

Phenol red-free medium was supplemented with sodium bicarbonate (2 g/L), streptomycin (100 μ g/mL), insuline zinc salt (10 μ g/mL), sodium pyruvate (1 mM), L-glutamine (2 mM), penicillin (100 U/mL) and DCC-FCS 5% (v/v). RPMI 1640 (without phenol red) was used for the experiments. Cells were grown for 48 h in phenol red-free medium. Compounds **4**, **10**, **22**, **25**, **35** and **36** were added at a final concentration of 100 nM. Inhibitors and E2 were diluted in ethanol (final ethanol concentration was adjusted to 1 %). As a positive control E2 was added at a final concentration of 0.1 nM. Ethanol was used as negative control. Medium was changed every two to three days and supplemented with the respective additive. After eight days of incubation, the cell viability was evaluated measuring the reduction of 3-(4,5-dimethylthiazol-2-yl)-2,5-diphenyl-tetrazoliumbromide (MTT). The cleavage of MTT to a blue formazan by mitochondrial succinat-dehydrogenase was quantified spectrophotometrically at 590 nm as

described by Denizot and Lang⁶⁶ with minor modifications. The control proliferation was arbitrarily set at 1 and the stimulation induced by the inhibitor was calculated according to following equation:

$$\% \text{ stimulation} = \frac{[\text{proliferation}(\text{compound} - \text{induced}) - 1]}{[\text{proliferation}(E2 - \text{induced}) - 1]} \cdot 100\% .$$

Each value is calculated as a mean value of at least three independent experiments

Caco-2 transport experiments

Caco-2 cell culture and transport experiments were performed according to Yee⁶⁷ with small modifications. Cell culture time was reduced from 21 to 10 days by increasing seeding density from $6.3 \cdot 10^4$ to $1.65 \cdot 10^5$ cells per well. Four reference compounds (atenolol, testosterone, ketoprofene, erythromycin) were used in each assay for validation. The compounds were applied to the cells as a mixture (cassette dosing) to increase the throughput. The initial concentration of the compounds in the donor compartment was 50 μM (0.2 M MES, pH: 6.5, containing either 1 % ethanol or DMSO). Samples were taken from the acceptor side after 0 min, 60, 120 and 180 min and from the donor side after 0 and 180 min. Each experiment was run in triplicate. The integrity of the monolayers was checked by measuring the transepithelial electrical resistance (TEER) before the transport experiments and by measuring lucifer yellow permeability after each assay. All samples of the CaCo-2 transport experiments were analyzed by LC/MS/MS after dilution with buffer of the opposite transwell chamber (1:1, containing 2 % acetic acid). The apparent permeability coefficients (P_{app}) were calculated using equation $P_{\text{app}} = \frac{dQ}{dtAc_0}$, where $\frac{dQ}{dt}$ is the appearance rate of mass in the acceptor compartment, A the surface area of the transwell membrane, and c_0 the initial concentration in the donor compartment.

Metabolic stability assay

The assay was performed with liver microsomes from male Sprague Dawley rats (BD Gentest, USA). Stock solutions (10 mM in acetonitrile) were diluted to give working solutions in 20 % acetonitrile. The incubation solutions consisted of a microsomal suspension of 0.33 mg/mL of protein in phosphate buffer 100 mM pH 7.4 and 90 μL NADP⁺-regenerating system (NADP⁺ 1 mM, glucose-6-phosphate 5 mM, glucose-6-phosphate dehydrogenase 5 U/mL, MgCl₂ 5 mM).

The reaction was initiated by the addition of test compound (final concentration 1 μM) to the pre-incubated microsomes/buffer mix at 37 °C. The samples were removed from the incubations after 0, 15, 30, and 60 min and processed for acetonitrile precipitation. The samples were analyzed by LC-MS/MS. Two control groups were run in parallel: positive controls (PC; n= 1) using 7-ethoxycoumarin as reference compound to prove the quality of the microsomal enzymatic activity and negative controls (NC; n= 1), using boiled microsomes (boiling water bath, 25 min) without regenerating system to ensure that the potential apparent loss of parent compound in the assay incubation is due to metabolism. The amount of compound in the samples was expressed in percentage of remaining compound compared to time point zero (= 100 %). These percentages were plotted against the corresponding time points and the half-life time was derived by a standard fit of the data.

Intrinsic clearance (Cl_{int}) estimates were determined using the rate of parent disappearance. The slope (-k) of the linear regression from log [test compound] versus time plot was determined as well as the elimination rate constant: $k = \ln 2/t_{1/2}$. The equation expressing the microsomal Cl_{int} can be derived: $Cl_{\text{int}} = k \cdot V \cdot f_u$ [$\mu\text{L}/\text{min}/\text{mg}$ protein], where f_u is the unbound fraction. V gives a term for the volume of the incubation expressed in $\mu\text{L} / \text{mg}$ protein. As f_u is not known for the tested compound, the calculation was performed with $f_u = 1$ ($V = \text{incubation volume } [\mu\text{L}]/\text{microsomal protein}[\text{mg}] = 6667$).

Inhibition of human hepatic CYPs

The commercially available P450 inhibition kits from BD GentestTM (Heidelberg, Germany) were used according to the instructions of the manufacturer. Compounds **4**, **25** and **35** were tested for inhibition of the following enzymes: CYP1A2, 2B6, 2C9, 2C19, 2D6 and 3A4. Inhibitory potencies were determined as IC₅₀-values.

In-Vivo Pharmacokinetics

Male Wistar rats weighing 300-330 g (Janvier France) were housed in a temperature- controlled room (20-22 °C) and maintained in a 12h light/12h dark cycle. Food and water were available *ad libitum*. They were anesthetized

with a ketamine (135 mg/kg)/ xylyzine (10 mg/kg) mixture and cannulated with silicone tubing via the right jugular vein and attached to the skull with dental cement.⁶⁸ Prior to the first blood sampling, animals were connected to a counterbalanced system and tubing to perform blood sampling in the freely moving rat.

Compounds **3** and **39** were applied orally in a cassette dosing in 4 rats at the dose of 10 mg/kg body weight by using a feeding needle. The compounds were dissolved in a mixture labrasol/water (1:1) and given at a volume of 5mL/kg. Blood samples (0.2 mL) were taken at 0, 1, 2, 3, 4, 6, 8, 10 and 24 h postdose and collected in heparinised tubes. They were centrifuged at 3000g for 10 min, and plasma was harvested and kept at -20 °C until analyzed.

HPLC-MS/MS analysis and quantification of the samples was carried out on a Surveyor-HPLC-system coupled with a TSQ Quantum (Thermo/Fisher) triple quadrupole mass spectrometer equipped with an electrospray interface (ESI).

Computational chemistry

Distance and angle calculations

All distances and angles were calculated after energy minimisation using Hyperchem v. 6.0.

MEP

For selected compounds *ab initio* geometry optimisations were performed gas phase at the B3LYP/6-311**G (d,p) level of density functional theory (DFT) by means of the Gaussian03 software and the molecular electrostatics potential map (MEP) was plotted using GaussView 3.09, the 3D molecular graphics package of Gaussian.⁶⁹ These electrostatic potential surfaces were generated by mapping 6-311G** electrostatic potentials onto surfaces of molecular electron density (isovalue = 0.002e/Å). The MEP maps are color coded, where red stands for negative values ($3.1 \cdot 10^{-2}$ Hartree) and blue for positive ones ($4.5 \cdot 10^{-2}$ Hartree).⁷⁰

Acknowledgments. We are grateful to the Deutsche Forschungsgemeinschaft (HA1315/8-1) for financial support. We thank Dr. Christiane Scherer for performing the CaCo-2 cell test, Anja Paluszczak and Beate Geiger for their help in performing the enzyme inhibition tests (17 β -HSD1, 17 β -HSD2, ER α and ER β), and Dr. Ursula Müller-Viera, Pharmacelsus CRO Saarbrücken Germany, for the stability tests with rat liver microsomes. Patricia Kruchten is grateful to the European Postgraduate School 532 (DFG) for a scholarship. Dr. Yaseen A. Al-Soud is grateful to the Alexander von Humboldt Foundation (AvH) for a fellowship.

Supporting information. Spectroscopic data of all compounds (¹H-NMR, ¹³C-NMR, IR), purity data of final compounds and MEP maps of compounds **7**, **10**, **14**, **27** and **G**. This material is available free of charge via internet at <http://pubs.acs.org>

References

- (1) Travis, R. C.; Key, T. J. Oestrogen exposure and breast cancer risk. *Breast Cancer Res.* **2003**, *5*, 239-247.
- (2) Dizerega, G. S.; Barber, D. L.; Hodgen, G. D. Endometriosis: role of ovarian steroids in initiation, maintenance and suppression. *Fertil. Steril.* **1980**, *33*, 649-653.
- (3) Miller, W. R.; Bartlett, J. M.; Canney, P.; Verrill, M. Hormonal therapy for postmenopausal breast cancer: the science of sequencing. *Breast Cancer Res. Treat.* **2007**, *103*, 149-160.
- (4) Bush, N. J. Advances in hormonal therapy for breast cancer. *Semin. Oncol. Nurs.* **2007**, *23*, 46-54.
- (5) Adamo, V.; Iorfida, M.; Montalto, E.; Festa, V.; Garipoli, C.; Scimone, A.; Zanghi, M.; Caristi, N. Overview and new strategies in metastatic breast cancer (MBC) for treatment of tamoxifen-resistant patients. *Ann. Oncol.* **2007**, *18 Suppl 6*, vi53-57.
- (6) Ohnesorg, T.; Keller, B.; Hrabe de Angelis, M.; Adamski, J. Transcriptional regulation of human and murine 17beta-hydroxysteroid dehydrogenase type-7 confers its participation in cholesterol biosynthesis. *J. Mol. Endocrinol.* **2006**, *37*, 185-197.
- (7) Sakurai, N.; Miki, Y.; Suzuki, T.; Watanabe, K.; Narita, T.; Ando, K.; Yung, T. M.; Aoki, D.; Sasano, H.; Handa, H. Systemic distribution and tissue localizations of human 17beta-hydroxysteroid dehydrogenase type 12. *J. Steroid Biochem. Mol. Biol.* **2006**, *99*, 174-181.
- (8) Day, J. M.; Foster, P. A.; Tutill, H. J.; Parsons, M. F.; Newman, S. P.; Chander, S. K.; Allan, G. M.; Lawrence, H. R.; Vicker, N.; Potter, B. V.; Reed, M. J.; Purohit, A. 17beta-hydroxysteroid dehydrogenase Type 1, and not Type 12, is a target for endocrine therapy of hormone-dependent breast cancer. *Int. J. Cancer* **2008**, *122*, 1931-1940.

- (9) Gunnarsson, C.; Hellqvist, E.; Stål, O. 17beta-Hydroxysteroid dehydrogenases involved in local oestrogen synthesis have prognostic significance in breast cancer. *Br. J. Cancer* **2005**, *92*, 547-552.
- (10) Gunnarsson, C.; Olsson, B. M.; Stål, O. Abnormal expression of 17beta-hydroxysteroid dehydrogenases in breast cancer predicts late recurrence. *Cancer Res.* **2001**, *61*, 8448-8451.
- (11) Miyoshi, Y.; Ando, A.; Shiba, E.; Taguchi, T.; Tamaki, Y.; Noguchi, S. Involvement of up-regulation of 17beta-hydroxysteroid dehydrogenase type 1 in maintenance of intratumoral high estradiol levels in postmenopausal breast cancers. *Int. J. Cancer* **2001**, *94*, 685-689.
- (12) Suzuki, T.; Moriya, T.; Ariga, N.; Kaneko, C.; Kanazawa, M.; Sasano, H. 17Beta-hydroxysteroid dehydrogenase type 1 and type 2 in human breast carcinoma: a correlation to clinicopathological parameters. *Br. J. Cancer* **2000**, *82*, 518-523.
- (13) Šmuc, T.; Pucelj Ribič, M.; Šinkovec, J.; Husen, B.; Thole, H.; Lanisnik Rižner, T. Expression analysis of the genes involved in estradiol and progesterone action in human ovarian endometriosis. *Gynecol. Endocrinol.* **2007**, *23*, 105-111.
- (14) Labrie, F. Intracrinology. *Mol. Cell. Endocrinol.* **1991**, *78*, C113-C118.
- (15) Vihko, P.; Härkönen, P.; Soronen, P.; Törn, S.; Herrala, A.; Kurkela, R.; Pulkka, A.; Oduwale, O.; Isomaa, V. 17beta-hydroxysteroid dehydrogenases- their role in pathophysiology. *Mol. Cell. Endocrinol.* **2004**, *215*, 83-88.
- (16) Azzi, A.; Rehse, P. H.; Zhu, D. W.; Campbell, R. L.; Labrie, F.; Lin, S.-X. Crystal structure of human estrogenic 17beta-hydroxysteroid dehydrogenase complexed with 17 beta-estradiol. *Nat. Struct. Biol.* **1996**, *3*, 665-668.
- (17) Breton, R.; Housset, D.; Mazza, C.; Fontecilla-Camps, J. C. The structure of a complex of human 17beta-hydroxysteroid dehydrogenase with estradiol and NADP⁺ identifies two principal targets for the design of inhibitors. *Structure* **1996**, *4*, 905-915.
- (18) Gangloff, A.; Shi, R.; Nahoum, V.; Lin, S.-X. Pseudo-symmetry of C19 steroids, alternative binding orientations, and multispecificity in human estrogenic 17beta-hydroxysteroid dehydrogenase. *FASEB J.* **2003**, *17*, 274-276.
- (19) Ghosh, D.; Pletnev, V. Z.; Zhu, D. W.; Wawrzak, Z.; Duax, W. L.; Pangborn, W.; Labrie, F.; Lin, S.-X. Structure of human estrogenic 17beta- hydroxysteroid dehydrogenase at 2.20 Å resolution. *Structure* **1995**, *3*, 503-513.
- (20) Han, Q.; Campbell, R. L.; Gangloff, A.; Huang, Y. W.; Lin, S.-X. Dehydroepiandrosterone and dihydrotestosterone recognition by human estrogenic 17beta-hydroxysteroid dehydrogenase. C-18/C-19 steroid discrimination and enzyme-induced strain. *J. Biol. Chem.* **2000**, *275*, 1105-1111.
- (21) Mazza, C.; Breton, R.; Housset, D.; Fontecilla-Camps, J. C. Unusual charge stabilization of NADP⁺ in 17beta-hydroxysteroid dehydrogenase. *J. Biol. Chem.* **1998**, *273*, 8145-8152.
- (22) Qiu, W.; Campbell, R. L.; Gangloff, A.; Dupuis, P.; Boivin, R. P.; Tremblay, M. R.; Poirier, D.; Lin, S.-X. A concerted, rational design of type 1 17beta-hydroxysteroid dehydrogenase inhibitors: estradiol-adenosine hybrids with high affinity. *FASEB J.* **2002**, *16*, 1829-1831.
- (23) Sawicki, M. W.; Erman, M.; Puranen, T.; Vihko, P.; Ghosh, D. Structure of the ternary complex of human 17beta-hydroxysteroid dehydrogenase type 1 with 3-hydroxyestra-1,3,5,7-tetraen-17-one (equilin) and NADP⁺. *Proc. Natl. Acad. Sci. U.S.A.* **1999**, *96*, 840-845.
- (24) Shi, R.; Lin, S.-X. Cofactor hydrogen bonding onto the protein main chain is conserved in the short chain dehydrogenase/reductase family and contributes to nicotinamide orientation. *J. Biol. Chem.* **2004**, *279*, 16778-16785.
- (25) Filling, C.; Berndt, K. D.; Benach, J.; Knapp, S.; Prozorovski, T.; Nordling, E.; Ladenstein, R.; Jornvall, H.; Oppermann, U. Critical residues for structure and catalysis in short-chain dehydrogenases/reductases. *J. Biol. Chem.* **2002**, *277*, 25677-25684.
- (26) Penning, T. M. 17beta-hydroxysteroid dehydrogenase: inhibitors and inhibitor design. *Endocr. Relat. Cancer* **1996**, *3*, 41-56.
- (27) Brožic, P.; Lanišnik Rižner, T.; Gobec, S. Inhibitors of 17beta-hydroxysteroid dehydrogenase type 1. *Curr. Med. Chem.* **2008**, *15*, 137-150 and references therein cited.
- (28) Messinger, J.; Hirvelä, L.; Husen, B.; Kangas, L.; Koskimies, P.; Pentikäinen, O.; Saarenketo, P.; Thole, H. New inhibitors of 17beta-hydroxysteroid dehydrogenase type 1. *Mol. Cell. Endocrinol.* **2006**, *248*, 192-198.

- (29) Karkola, S.; Lilienkampf, A.; Wähälä, K. A 3D QSAR model of 17 β -HSD1 inhibitors based on a thieno[2,3-d]pyrimidin-4(3H)-one core applying molecular dynamics simulations and ligand-protein docking. *ChemMedChem* **2008**, *3*, 461-472.
- (30) Allan, G. M.; Vicker, N.; Lawrence, H. R.; Tutill, H. J.; Day, J. M.; Huchet, M.; Ferrandis, E.; Reed, M. J.; Purohit, A.; Potter, B. V. Novel inhibitors of 17 β -hydroxysteroid dehydrogenase type 1: templates for design. *Bioorg. Med. Chem.* **2008**, *16*, 4438-4456.
- (31) Frotscher, M.; Ziegler, E.; Marchais-Oberwinkler, S.; Kruchten, P.; Neugebauer, A.; Fetzner, L.; Scherer, C.; Müller-Vieira, U.; Messinger, J.; Thole, H.; Hartmann, R. W. Design, synthesis and biological evaluation of (hydroxyphenyl)-naphthalene and quinoline derivatives: potent and selective non steroidal inhibitors of 17 β -hydroxysteroid dehydrogenase type 1 (17 β -HSD1) for the treatment of estrogen-dependent diseases. *J. Med. Chem.* **2008**, *51*, 2158-2169.
- (32) Marchais-Oberwinkler, S.; Kruchten, P.; Frotscher, M.; Ziegler, E.; Neugebauer, A.; Bhoga, U. D.; Bey, E.; Müller-Vieira, U.; Messinger, J.; Thole, H.; Hartmann, R. W. Substituted 6-phenyl-2-naphthols. Potent and selective non-steroidal inhibitors of 17 β -hydroxysteroid dehydrogenase type 1 (17 β -HSD1): design, synthesis, biological evaluation and pharmacokinetics. *J. Med. Chem.* **2008**, *51*, 4685-4698.
- (33) Bey, E.; Marchais-Oberwinkler, S.; Kruchten, P.; Frotscher, M.; Werth, R.; Oster, A.; Algül, O.; Neugebauer, A.; Hartmann, R. W. Design, synthesis and biological evaluation of bis(hydroxyphenyl) azoles as potent and selective non-steroidal inhibitors of 17 β -hydroxysteroid dehydrogenase type 1 (17 β -HSD1) for the treatment of estrogen-dependent diseases. *Bioorg. Med. Chem.* **2008**, *16*, 6423-6435.
- (34) Miyaura, N.; Suzuki, A. The palladium catalysed cross-coupling reaction of phenylboronic acid with haloarenes in the presence of bases. *Synth. commun.* **1995**, *11*, 513-519.
- (35) Fink, B. E.; Mortensen, D. S.; Stauffer, S. R.; Aron, Z. D.; Katzenellenbogen, J. A. Novel structural templates for estrogen-receptor ligands and prospects for combinatorial synthesis of estrogens. *Chem. Biol.* **1999**, *6*, 205-219.
- (36) Gierczyk, B.; Zalas, M. Synthesis of substituted 1,3,4-thiadiazoles using Lawesson reagents. *Org. Prep. proc. int.* **2005**, *37*, 213-222.
- (37) Bagley, M. C.; Chapaneri, K.; Glover, C.; Merrit, E. A. Simple microwave-assisted method for the synthesis of primary thioamides from nitriles. *Synlett* **2004**, *14*, 2615-2617.
- (38) Kelarev, V. I.; Silin, M. A.; Kobrakov, K. I.; Rybina, I. I.; Korolev, V. K. Synthesis of 1,3,5-trisubstituted 1H-1,2,4-triazoles containing hetaryl fragments. *Chem. Heterocycl. Comp.* **2003**, *39*, 736-743.
- (39) Kolb, H. C.; Finn, M. G.; Sharpless, K. B. Click chemistry: Diverse chemical function from a few good reactions. *Angew. Chem., Int. Ed.* **2001**, *40*, 2004-2021.
- (40) Guither, W. D.; Coburn, M. D.; Castle, R. N. 3,6-Bis-substituted s-tetrazines. *Heterocycles* **1979**, *12*, 745-749.
- (41) Lin, S.-X.; Yang, F.; Jin, J. Z.; Breton, R.; Zhu, D. W.; Luu-The, V.; Labrie, F. Subunit identity of the dimeric 17 β -hydroxysteroid dehydrogenase from human placenta. *J. Biol. Chem.* **1992**, *267*, 16182-16187.
- (42) Hidalgo, I. J. Assessing the absorption of new pharmaceuticals. *Curr. Top. Med. Chem.* **2001**, *1*, 385-401.
- (43) Yearley, E. J.; Zhurova, E. A.; Zhurov, V. V.; Pinkerton, A. A. Binding of genistein to the estrogen receptor based on an experimental electron density study. *J. Am. Chem. Soc.* **2007**, *129*, 15013-15021.
- (44) White, E. H.; Bursey, M. M.; Roswel, D. F.; Hill, J. H. M. Chemiluminescence of some monoacylhydrazides. *J. Org. Chem.* **1967**, *32*, 1198-1202.
- (45) Manaka, A.; Sato, M. Synthesis of aromatic thioamide from nitrile without handling of hydrogen sulfide. *Synth. commun.* **2005**, *11*, 761-764.
- (46) Ando, K.; Kato, T.; Kawai, A.; Nonomura, T. Preparation of heterocyclyl sulfonylbenzene compounds as anti-inflammatory/analgesic agents. WO9964415A1, **1999**.
- (47) Uozumi, Y.; Kikuchi, M. Controlled monoarylation of dibromoarenes in water with a polymeric palladium catalyst. *Synlett* **2005**, *11*, 1775-1778.
- (48) Ewing, W. R.; Becker, M. R.; Pauls, H. W.; Cheney, D. L.; Mason, J. S.; Spada, A. P.; Choi-Sledeski, Mi., Y. Preparation of substituted (sulfinic acid, sulfonic acid, sulfonylamino or sulfynylamino) N-[(aminoiminomethyl)phenylalkyl]azaheterocyclamide compounds as factor Xa inhibitors. WO9640679A1, **1996**.
- (49) Vachal, P.; Toth, L. M. General facile synthesis of 2,5-diarylheteropentalenes. *Tetrahedron Lett.* **2004**, *45*, 7157-7161.

- (50) Yokooji, A.; Okazawa, T.; Satoh, T.; Miura, M.; Nomura, M. Palladium-catalyzed direct arylation of thiazoles with aryl bromides. *Tetrahedron* **2003**, *59*, 5685-5689.
- (51) Chandra, R.; Kung, M.-P.; Kung, H. F. Design, synthesis, and structure-activity relationship of novel thiophene derivatives for beta-amyloid plaque imaging. *Bioorg. Med. Chem. Lett.* **2006**, *16*, 1350-1352.
- (52) Sone, T.; Sato, K.; Umetsu, Y.; Yoshino, A.; Takahashi, K. Acid-catalyzed reactions of thiophene nuclei. VIII. Synthesis of unsymmetrical 2,3-diaryl- and 2,4-diarylthiophenes starting from 2,5-dichlorothiophene. *Bull. Chem. Soc. Jpn.* **1994**, *67*, 2187-2194.
- (53) Nakano, M.; Satoh, T.; Miura, M. Palladium-catalyzed selective 2,3-diarylation of alpha, alpha-disubstituted 3-thiophenemethanols via cleavage of C-H and C-C bonds. *J. Org. Chem.* **2006**, *71*, 8309-8311.
- (54) Liu, L.; Zhang, Y.; Xin, B. Synthesis of biaryls and polyaryls by ligand-free Suzuki reaction in aqueous phase. *J. Org. Chem.* **2006**, *71*, 3994-3997.
- (55) Demerseman, P.; Buu-Hoi, N. P.; Royer, R. Thiophene derivatives of biological interest. VII. The synthesis of 2,4-diarylthiophenes and 2,4-diarylselenophenes from anils of alkyl aryl ketones. *J. Chem. Soc.* **1954**, 2720-2722.
- (56) Lebrini, M.; Bentiss, F.; Lagrenee, M. Rapid synthesis of 2,5-disubstituted 1,3,4-thiadiazoles under microwave irradiation. *J. Het. Chem.* **2005**, *42*, 991-994.
- (57) Pirali, T.; Gatti, S.; Di Brisco, R.; Tacchi, S.; Zaninetti, R.; Brunelli, E.; Massarotti, A.; Sorba, G.; Canonico, P. L.; Moro, L.; Genazzani, A. A.; Tron, G. C.; Billington, R. A. Estrogenic analogues synthesized by click chemistry. *ChemMedChem* **2007**, *2*, 437-440.
- (58) Yas'ko, S. V.; Korchevin, N. A.; Gusarova, N. K.; Kazantseva, T. I.; Chernysheva, N. A.; Klyba, L. V.; Trofimov, B. A. Microwave induced synthesis of diphenylthiophenes from elemental sulfur and styrene. *Chem. Het. Comp.* **2006**, *42*, 1486-1487.
- (59) Lahti, P. M.; Ichimura, A. S. Semiempirical study of electron exchange interaction in organic high-spin pi-systems. Classifying structural effects in organic magnetic molecules. *J. Org. Chem.* **1991**, *56*, 3030-3042.
- (60) Tagat, J. R.; McCombie, S. W.; Barton, B. E.; Jackson, J.; Shortall, J. Synthetic inhibitors of interleukin-6. II. 3,5-Diarylpyridines and m-terphenyls. *Bioorg. Med. Chem. Lett.* **1995**, *5*, 2143-2146.
- (61) Muller, G.; Amiard, G.; Mathieu, J. Dihydropyrazines and pyrazines obtained by condensation of some phenacylamines. *Bull. Soc. Chim. Fr.* **1949**, 533-535.
- (62) Zhu, D. W.; Lee, X.; Breton, R.; Ghosh, D.; Pangborn, W.; Duax, W. L.; Lin, S.-X. Crystallization and preliminary X-ray diffraction analysis of the complex of human placental 17beta-hydroxysteroid dehydrogenase with NADP⁺. *J. Mol. Biol.* **1993**, *234*, 242-244.
- (63) Sam, K. M.; Auger, S.; Luu-The, V.; Poirier, D. Steroidal spiro-gamma-lactones that inhibit 17beta-hydroxysteroid dehydrogenase activity in human placental microsomes. *J. Med. Chem.* **1995**, *38*, 4518-4528.
- (64) Sam, K. M.; Boivin, R. P.; Tremblay, M. R.; Auger, S.; Poirier, D. C16 and C17 derivatives of estradiol as inhibitors of 17beta-hydroxysteroid dehydrogenase type 1: chemical synthesis and structure-activity relationships. *Drug. Des. Discov.* **1998**, *15*, 157-180.
- (65) Zimmermann, J.; Liebl, R.; von Angerer, E. 2,5-Diphenylfuran-based pure antiestrogens with selectivity for the estrogen receptor alpha. *J. Steroid Biochem. Mol. Biol.* **2005**, *94*, 57-66.
- (66) Denizot, F.; Lang, R. Rapid colorimetric assay for cell growth and survival. Modifications to the tetrazolium dye procedure giving improved sensitivity and reliability. *J. Immunol. Methods* **1986**, *89*, 271-277.
- (67) Yee, S. In vitro permeability across Caco-2 cells (colonic) can predict in vivo (small intestinal) absorption in man - fact or myth. *Pharm. Res.* **1997**, *14*, 763-766.
- (68) Van Dongen, J. J.; Remie, R.; Rensema, J. W.; Van Wunnik, G. H. J. Manual of microsurgery on the laboratory rat. In Huston, J. P., Ed., Ed. 1990; p 159.
- (69) Dennington, I.; Roy, K. T.; Millam, J.; Eppinnett, K.; Howell, W. L.; Gilliland, R. *GaussView*, 3.0; Semicem Inc., Shawnee Mission: 2003.
- (70) Petti, M. A.; Shepodd, T. J.; Barrans, R. E.; Dougherty, D. A. "Hydrophobic" binding of water-soluble guests by high-symmetry, chiral hosts. An electron-rich receptor site with a general affinity for quaternary ammonium compounds and electron-deficient pi-systems. *J. Am. Chem. Soc.* **1988**, *110*, 6825-6840.
- (71) Tannergren, C.; Langguth, P.; Hoffmann, K. J. Compound mixtures in CaCo-2 cell permeability screens as a means to increase screening capacity. *Pharmazie* **2001**, *56*, 337-342.

- (72) Laitinen, L.; Kangas, H.; Kaukonen, A. M.; Hakala, K.; Kotiaho, T.; Kostainen, R.; Hirvonen, J. N-in-one permeability studies of heterogeneous sets of compounds across Caco-2 cell monolayers. *Pharm. Res.* **2003**, *20*, 187-197.

3.3.5.2. Paper X.

New Insights into the SAR and Binding Modes of Bis(hydroxyphenyl)thiophenes and -benzenes: Influence of Additional Substituents on 17 β -Hydroxysteroid Dehydrogenase Type 1 (17 β -HSD1) Inhibitory Activity and Selectivity

Emmanuel Bey, Sandrine Marchais-Oberwinkler, Ruth Werth, Matthias Negri, Yaseen A. Al-Soud, Patricia Kruchten, Alexander Oster, Martin Frotscher, Barbara Birk and Rolf W. Hartmann

This article is protected by copyrights of 'Journal of Medicinal Chemistry.'

J. Med. Chem. **2008**, 51, 6725-6739

Abstract

17 β -hydroxysteroid dehydrogenase type 1 (17 β -HSD1) is responsible for the catalytic reduction of weakly active E1 to highly potent E2. E2 stimulates the proliferation of hormone-dependent diseases via activation of the estrogen receptor α (ER α). Due to the overexpression of 17 β -HSD1 in mammary tumors, this enzyme should be an attractive target for the treatment of estrogen-dependent pathologies. Recently, we have reported on a series of potent 17 β -HSD1 inhibitors: bis(hydroxyphenyl) azoles, thiophenes and benzenes. In this paper, different substituents were introduced into the core structure and the biological properties of the corresponding inhibitors were evaluated. Computational methods and analysis of different X-rays of 17 β -HSD1 lead to identification of two different binding modes for these inhibitors. The fluorine compound **23** exhibits an IC₅₀ value of 8 nM and is the most potent non-steroidal inhibitor described so far. It also shows a high selectivity (17 β -HSD2, ER α) and excellent pharmacokinetic properties after peroral application to rats.

Introduction.

Estrogens are involved in the regulation of the female reproduction system. However, it is also well known that 17 β -estradiol (E2), the natural ligand of the estrogen receptors (ERs) α and β , plays a critical role in the development of several estrogen-dependent pathologies like breast cancer¹ and endometriosis.²

Until now, hormone-dependent breast cancers are treated using three different endocrine therapies:^{3,4} aromatase inhibitors and GnRH analogues disrupt the estrogen biosynthesis while selective estrogen receptor modulators (SERMs) or pure antiestrogens⁵ prevent E2 to unfold its action at the receptor level. Besides specific disadvantages of each therapeutic approach, all of these strategies have in common a rather radical reduction of estrogen levels in the whole body leading to significant side effects.

A softer approach could be the inhibition of an enzyme of the 17 β -hydroxysteroid dehydrogenase (17 β -HSD) family, especially one which is responsible for the E2 formation from estrone (E1). Until now, three subtypes (1, 7 and 12) are able to catalyze this reaction, the most important being 17 β -HSD1. The primary physiological role of 17 β -HSD7 and 17 β -HSD12 is supposed to be in the cholesterol synthesis^{6,7} and in the regulation of the lipid biosynthesis,⁸ respectively. In addition, Day et al.⁹ recently, showed that 17 β -HSD12, although highly expressed in breast cancer cell lines, is inefficient in E2 formation.

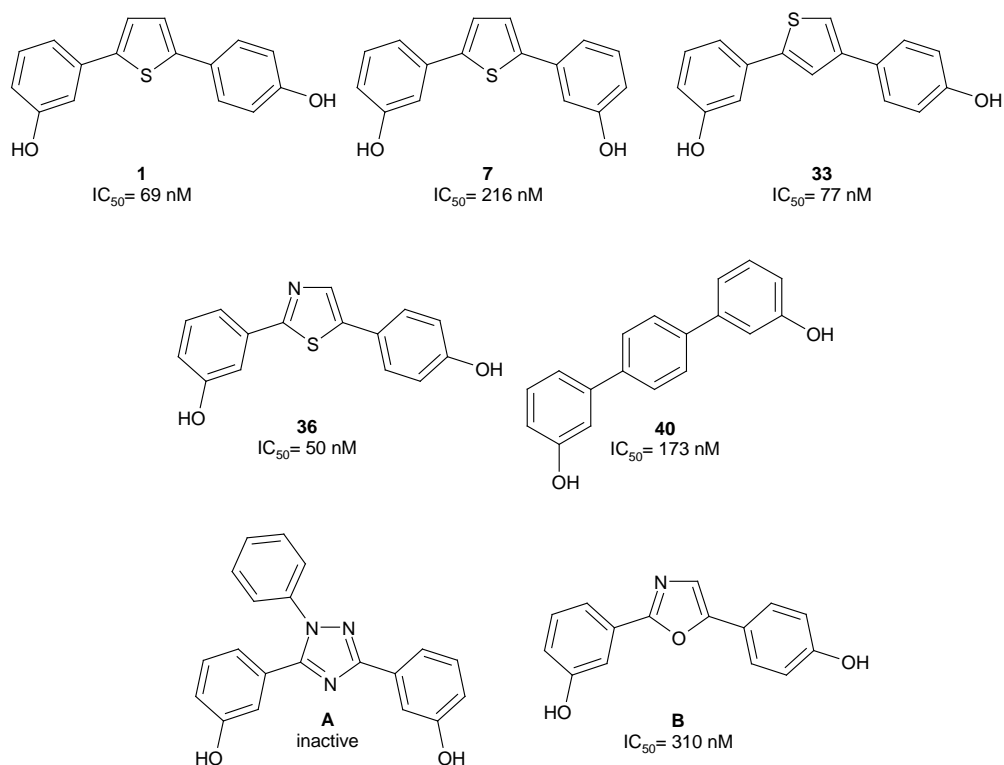
17 β -HSD1, which is responsible for the intracellular NAD(P)H-dependent conversion of the weak E1 into the highly potent estrogen E2, is often overexpressed in breast cancer cells¹⁰⁻¹³ and endometriosis.¹⁴ Inhibition of this enzyme is therefore regarded as a promising novel target for the treatment of estrogen-dependent diseases.

Recently, two groups^{9,15,16} reported about the *in-vivo* efficacy of 17 β -HSD1 inhibitors to reduce E1 induced tumour growth using two different mouse models and indicating that the 17 β -HSD1 enzyme is a suitable target for the treatment of breast cancer.

In order to not counteract the therapeutic efficacy of 17 β -HSD1 inhibitors, it is very important that the compounds are selective toward 17 β -HSD2, the enzyme which catalyzes the deactivation of E2 into E1. Additionally, to avoid intrinsic estrogenic effects, the inhibitors should not show affinity to the estrogen receptor α and β .

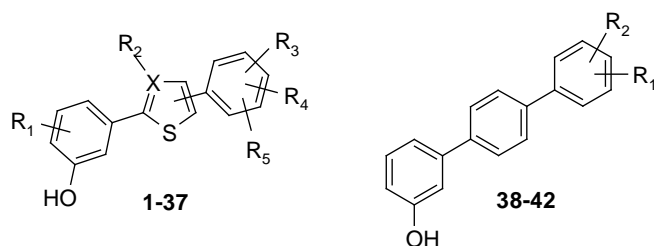
During the last decade, several groups reported on 17 β -HSD1 inhibitors, most of them having steroidal structures.¹⁷⁻²⁰ Recently non-steroidal cores have been published too. Until today four classes of compounds are described: thienopyrimidinones,^{21,22} biphenyl ethanones²³ and from our group (hydroxyphenyl)naphthalenes²⁴⁻²⁶ and bis(hydroxyphenyl)azoles, thiophenes, benzenes and aza-benzenes.²⁷⁻³² The most promising compounds of the later series are thiophenes **1**, **7** and **33**, thiazole **36** and phenylene **41** exhibiting IC₅₀ values toward 17 β -HSD1 in the nanomolar range and high selectivity toward 17 β -HSD2 and the ERs (Chart 1).

Chart 1: Described bis(hydroxyphenyl)azoles, thiophenes, benzenes and aza-benzenes



In the following, we will report on structural optimizations which led to the discovery of new highly potent and selective 17 β -HSD1 inhibitors (Chart 2).

Chart 2: Title compounds



Design

Up to now, several crystal structures of human 17 β -HSD1 were resolved: as apoenzyme (i.e. PDB code: 1BHS³³), as binary complex (enzyme-E2, i.e. PDB code: 1IOL³⁴) or as ternary complex (enzyme-E2-NADP⁺: i.e. PDB code 1FDT;³⁵ 1A27;³⁶ enzyme-HYC (hybride inhibitor): PDB code: 1I5R³⁷).

The analysis of the ternary complexes available from 17 β -HSD1 provides useful knowledge about the architecture of the enzyme and important hints for structure based drug design: a substrate binding site (SUB) and a cofactor binding pocket (COF) are present as well as the most important amino acids responsible for substrate and cofactor anchoring. The SUB is a narrow hydrophobic tunnel containing two polar regions at each end: His221/Glu282 on the one side and Ser142/Tyr155 on the other side, corresponding to the binding oxygens in 3- and 17-hydroxy group of E2. Additionally a flexible loop can be identified which is not well resolved in almost all the structures.

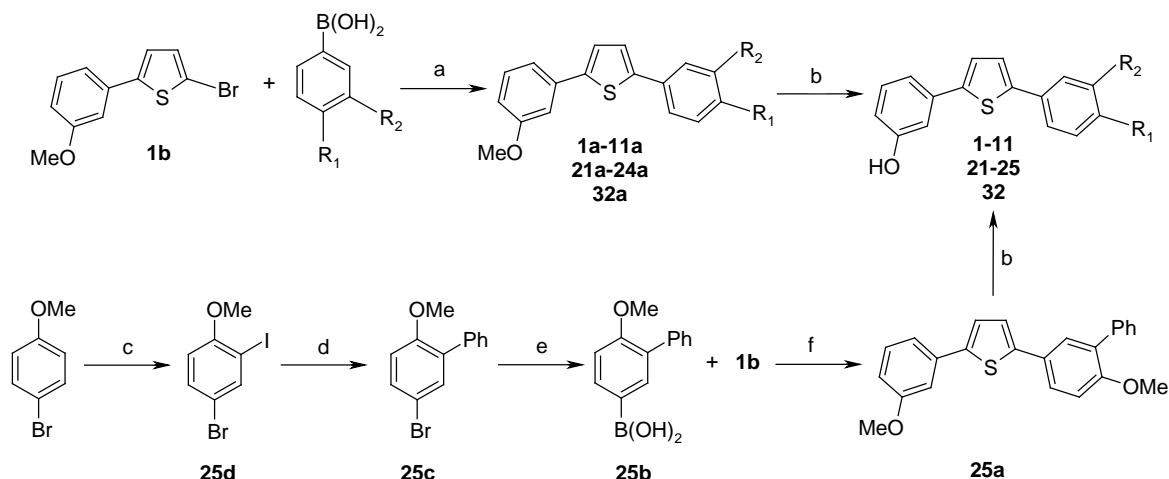
From previous results obtained in the class of bis(hydroxyphenyl)azoles, thiophenes, benzenes and aza-benzenes,^{27,28} a SAR study highlighted four structural features which are important for high 17 β -HSD1 inhibitory activity: 1. one hydroxyphenyl moiety on the core structure is not sufficient for a high potency, 2. only the *meta-para* and *meta-meta* dihydroxy substitution pattern (O-O distance in the same range as observed for the steroid, $d = 11$ Å) are active, 3. the presence of the *meta*-hydroxy group is more important for inhibitory activity than the *para*-, 4. only central aromatic rings without hydrogen bond donor function like thiophene, thiazole, benzene exhibit inhibitory activity. It was also shown that a correlation seems to exist between the activity of the compounds and the electrostatic potential distribution of the molecules:²⁸ to be active the ESP values of the different regions of the inhibitor have to be in an appropriate range.

In the present report, we will present the structure optimization of this class of compounds leading to an increase in activity and in selectivity of these inhibitors. First, the influence of the bioisosteric exchange of one OH group on the enzyme activity will be determined. Secondly, the space availability around the inhibitors and the nature of the most appropriate substituents will be investigated by substitutions, either on the heterocycle, or on the hydroxyphenyl moieties. The nature of the substituents will be varied in order to investigate the possible interactions between the inhibitor and the enzyme. Thirdly, computational studies (docking studies and ESP calculations) will be performed in order to identify the most plausible binding mode for this class of compounds. Furthermore the selectivity toward 17 β -HSD2 and the ERs α and β will be determined as well as the potency of the compounds in T-47D cells and inhibition of the two most important hepatic CYP enzymes. Finally, the pharmacokinetic profile of the two most promising candidates will be evaluated in rats after oral administration.

Chemistry

The synthesis of compounds **1** to **11**, **21** to **25** and **32** is presented in Scheme 1. Starting from the mono-brominated key intermediate **1b** and the appropriate commercially available boronic acids, the preparation of compounds **1a** to **11a**, **21a** to **25a** and **32a** was accomplished via Suzuki cross coupling reaction³⁸ under microwave assisted conditions (Method A: Cs₂CO₃, DME/EtOH/water (1:1:1), Pd(PPh₃)₄, MW (150 W, 150 °C, 15 bars), 15 min). The resulting disubstituted thiophenes were subsequently submitted to ether cleavage with borontribromide²⁸ (Method C: BBr₃, CH₂Cl₂, -78 °C to rt, 18 h) leading to compounds **1** to **11**, **21** to **25** and **32** (Scheme 1). In case of intermediate **25a**, the boronic acid **25b** was prepared in a three step synthesis pathway: first, an iodine substituent was selectively introduced in position 2 of the *para*-bromoanisole (compound **25d**) using (diacetoxyiodo) benzene.³⁹ Then, a selective Suzuki reaction on the iodo-position of **25d** under Method B (Na₂CO₃, toluene/water (1:1), Pd(PPh₃)₄, reflux, 20 h) led to the intermediate **25c** and the corresponding boronic acid **25b** was prepared using *n*-butyl lithium and triethyl borate followed by hydrolysis with diluted hydrochloric acid.

Scheme 1^a: Synthesis of compounds **1** to **11**, **21** to **25** and **32**



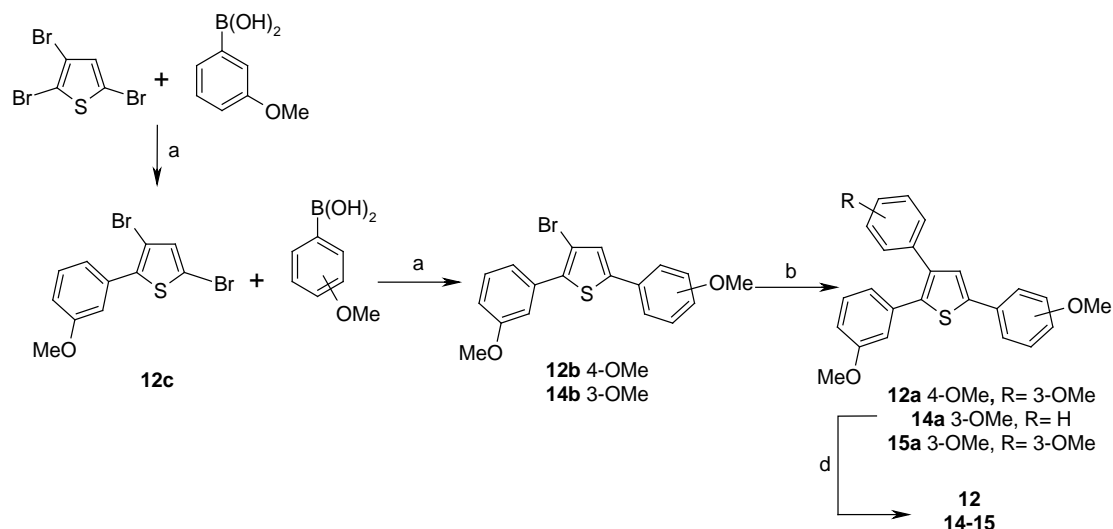
cmpd	R ₁	R ₂	cmpd	R ₁	R ₂
1	OH	H	9	H	
2	H	H	10	H	
3	F	H	11	H	
4	NH ₂	H	21	OH	CH ₃
5	SH	H	22	OH	OH
6	CN	H	23	OH	F
7	H	OH	24	OH	CF ₃
8	H	F	25	OH	Ph
			32	F	F

^a**Reagents and conditions:** (a) Method A: Cs₂CO₃, DME/EtOH/water (1:1:1), Pd(PPh₃)₄, MW (150 W, 150 °C, 15 bars), 15 min; (b) BBr₃, CH₂Cl₂, -78 °C to rt, 18 h; (c) PhI(OAc)₂, I₂, AcOEt, 60 °C, 5 h; (d) Ph-B(OH)₂, Method B: Na₂CO₃, toluene/water (1:1), Pd(PPh₃)₄, reflux, 20 h; (e) 1. *n*-BuLi, dry THF, 5 min, -78 °C, 2. B(OEt)₃, 2 h -78°C to rt, 3. HCl 1N, rt; (f) Method B: Na₂CO₃, toluene/water (1:1), Pd(PPh₃)₄, reflux, 20 h.

The preparation of compounds **31** and **33** to **42** is similar to the synthetic pathway presented in Scheme 1 for compounds **1** to **11**. The first Suzuki coupling was carried out according to Method B with the corresponding dibrominated heterocycle and the methoxylated benzene boronic acid. The resulting mono substituted compounds **31b** and **33b** to **42b** were submitted to a second cross coupling reaction under microwave assisted conditions following Method A. The compounds were subsequently demethylated with boron tribromide to yield compounds **31** and **33** to **42**.

The synthesis of compounds **12**, **14** and **15** is depicted in Scheme 2. The key intermediate mono methoxylated dibromothiophene **12c** was prepared following two successive Suzuki coupling reactions according to Method B (Na₂CO₃, toluene/water (1:1), Pd(PPh₃)₄, reflux, 4 h) from 2,3,5-tribromothiophene and methoxybenzene boronic acid. The reaction time of both cross couplings was carefully controlled (restricted to 4 h) in order to get a selective bromine replacement each time. Intermediates **12a**, **14a**, and **15a** were obtained via a third Suzuki coupling using Method B. The methoxy substituents were cleaved in a last step, using boron tribromide (Method C: BBr₃, CH₂Cl₂, -78 °C to rt, 18 h).

Scheme 2^a: Synthesis of compounds **12**, **14** and **15**

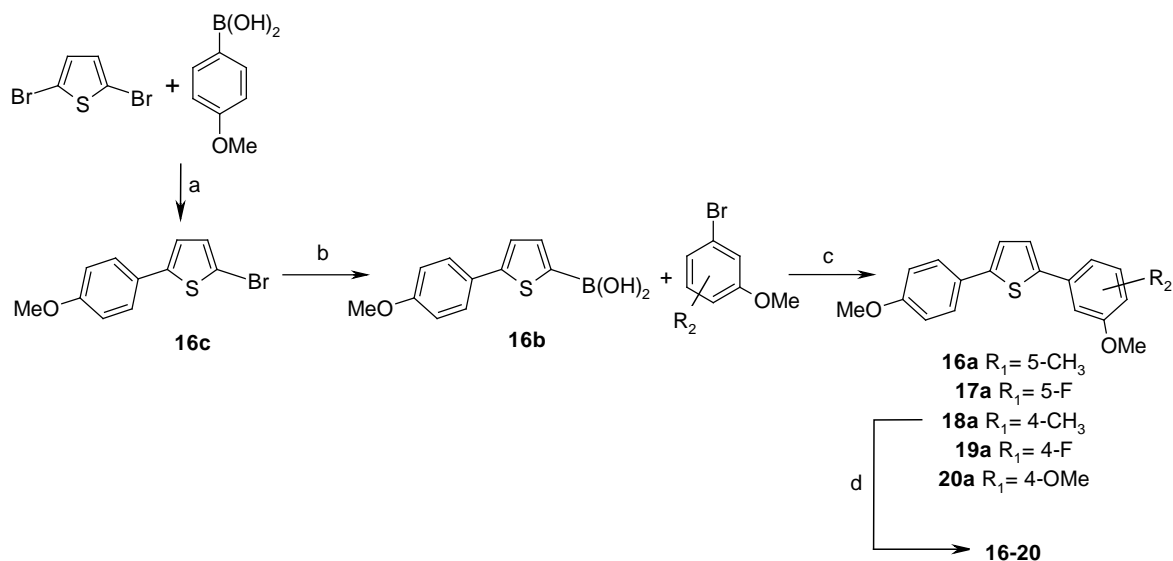


^a**Reagents and conditions:** (a) Method B: Na₂CO₃, toluene/water (1:1), Pd(PPh₃)₄, reflux, 4 h; (h) boronic acid, Method B: Na₂CO₃, toluene/water (1:1), Pd(PPh₃)₄, reflux, 20 h; (d) BBr₃, CH₂Cl₂, -78 °C to rt, 18 h.

Compound **13** was synthesized under microwave assisted conditions in a one pot reaction using 2,5-dibromo-3-methylthiophene and 3-hydroxyphenyl boronic acid following Method A (Cs₂CO₃, DME/EtOH/water (1:1:1), Pd(PPh₃)₄, MW (150 W, 150 °C, 15 bars)) for 15 min.

The synthesis of the molecules bearing an additional substituent on the *meta*-hydroxyphenyl moiety of thiophene **1** (compounds **16** to **20**) is shown in Scheme 3. Intermediate **16c** was prepared via Suzuki reaction from the *para*-methoxylated benzene boronic acid and the 2,5-dibromothiophene following Method B heating the reaction 4 h instead of 20 h in order to avoid any dicoupling reaction. Treatment of **16c** with *n*-butyl lithium and triethyl borate afforded after hydrolysis with diluted hydrochloric acid the corresponding boronic acid **16b**. The resulting compound was subjected to an additional cross coupling reaction which was carried out with the appropriate bromine derivative following Method A for compounds **17a** to **20a** and Method B for compound **16a**. The hydrolysis of the methoxy groups with boron tribromide (Method C) led to compounds **16** to **20**.

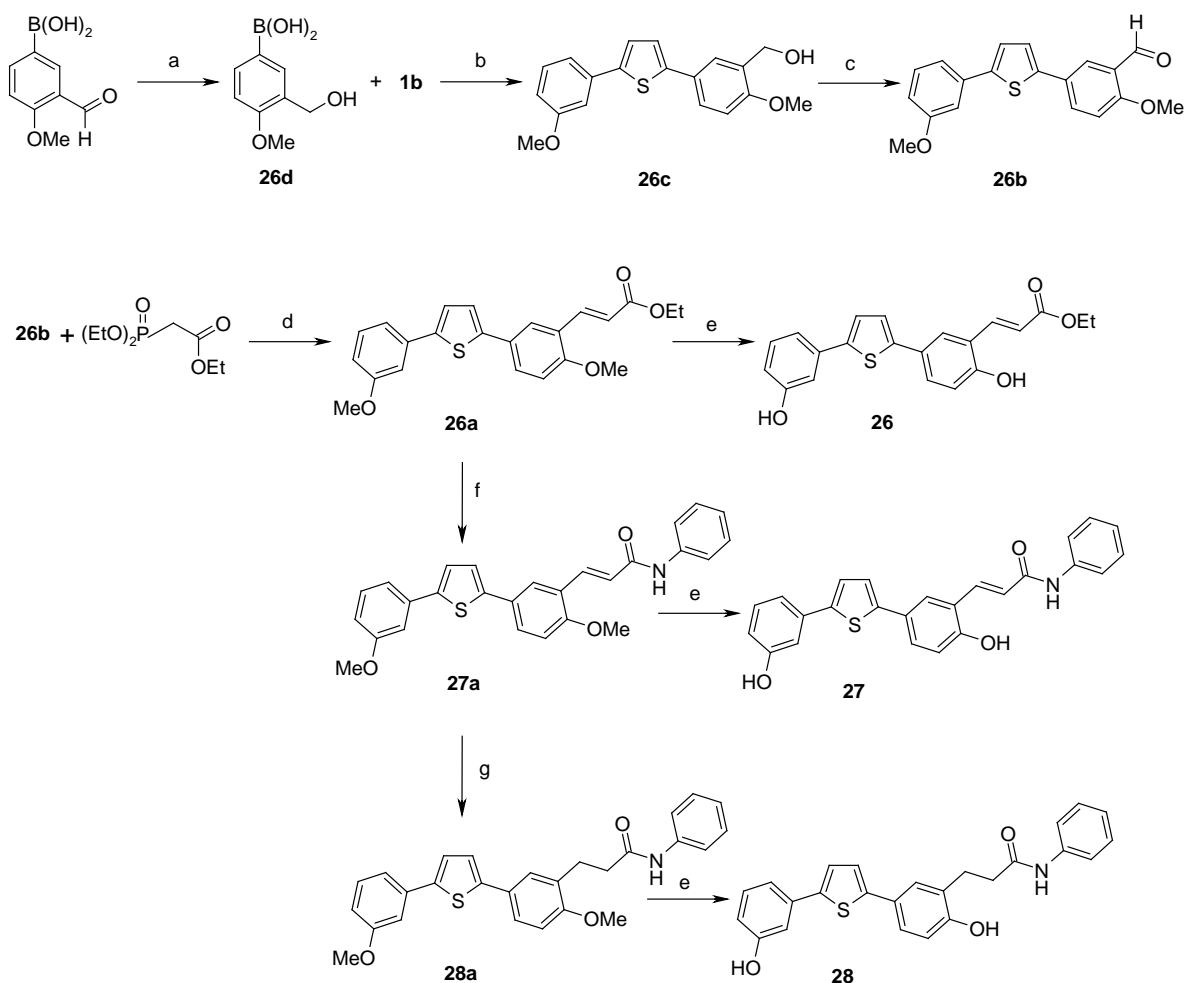
Scheme 3^a: Synthesis of compounds **16** to **20**



^a**Reagents and conditions:** (a) Method B: Na₂CO₃, toluene/water (1:1), Pd(PPh₃)₄, reflux, 4 h; (b) 1.*n*-BuLi, anhydrous THF, -78 °C, 15 min, 2. B(OEt)₃, THF, -78 °C to rt, 2 h, 3. HCl 1N; (c) Method A for **17a-20a** (Cs₂CO₃, DME/EtOH/water (1:1:1), Pd(PPh₃)₄, MW (150 W, 150 °C, 15 bars), 15 min); Method B for **16a** (Na₂CO₃, toluene/water (1:1), Pd(PPh₃)₄, reflux, 20 h); (d) BBr₃, CH₂Cl₂, -78 °C to rt, 18 h.

The synthesis of compounds **26** to **28** substituted in *ortho*-position of the *para*-OH group is depicted in Scheme 4. The preparation of the key intermediate **26b** started from the commercially available 3-formyl-4-methoxyphenyl boronic acid. Reduction of the aldehyde function using sodium borohydride followed by a cross coupling reaction with **1b** under microwave irradiation according to Method A (Cs₂CO₃, DME/EtOH/water (1:1:1), Pd(PPh₃)₄, MW (150 W, 150 °C, 15 bars), 15 min) afforded the disubstituted thiophene **26c**. The alcohol function of **26c** was subsequently oxidized with pyridinium chlorochromate to yield to the key aldehyde **26b**. It was subjected to the Horner-Wadsworth-Emmons conditions⁴⁰ to introduce the acrylic ester moiety (intermediate **26a**). Hydrolysis of the ester function using lithium hydroxide,²⁵ amide bond formation with aniline, EDCI and HOBt⁴¹ afforded compound **27a**. The catalytic double bond hydrogenation of **27a** was performed using Perlman's catalyst.⁴² The ether functions of **26a**, **27a** and **28a** were deprotected using boron tribromide (Method C) to give the desired compounds **26** to **28**.

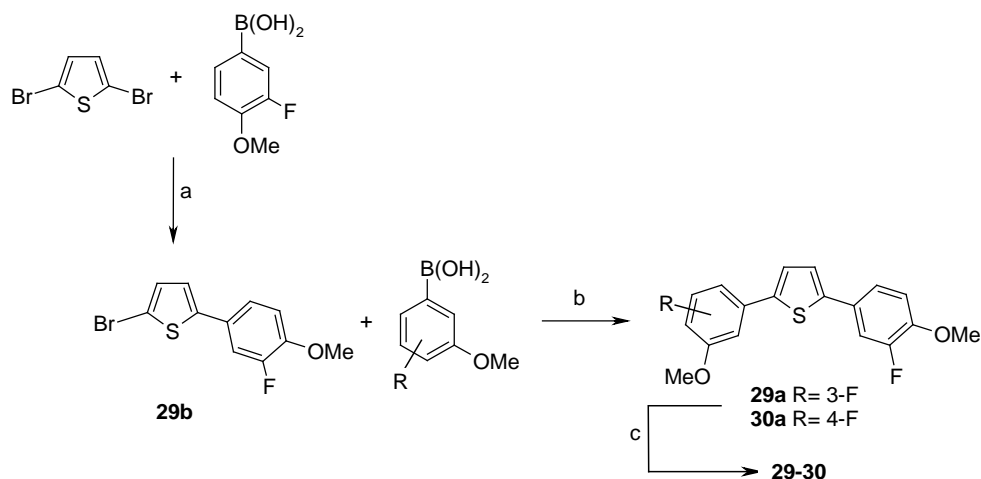
Scheme 4^a: Synthesis of compounds **26** to **28**



^a**Reagents and conditions:** (a) NaBH₄, THF/EtOH (1:1), 0 °C to rt, 2 h; (b) Method A: Cs₂CO₃, DME/EtOH/water (1:1:1), Pd(PPh₃)₄, MW (150 W, 150 °C, 15 bars), 15 min; (c) PCC, CH₂Cl₂, rt, 30 min; (d) NaH, THF dry, rt, 4 h; (e) BBr₃, CH₂Cl₂, -78 °C to rt, 18 h; (f) 1. LiOH, THF/H₂O (2:1), reflux, 20 h, 2. aniline, EDCI, HOBt, CH₂Cl₂, reflux, 20 h; (g) Pd(OH)₂, THF/EtOH (1:1), H₂, rt, 20 h.

The synthesis of the difluorinated thiophenes **29** and **30** is presented in Scheme 5. These compounds were obtained after two successive cross coupling reactions: in a first step 2,5-dibromothiophene reacted with 3-fluoro-4-methoxyphenyl boronic acid following Method B (Na₂CO₃, toluene/water (1:1), Pd(PPh₃)₄, reflux, 20 h). In a second step, the resulting mono substituted thiophene **29b** was subsequently submitted to a second cross coupling reaction under microwave irradiation (Method A: Cs₂CO₃, DME/EtOH/water (1:1:1), Pd(PPh₃)₄, MW (150 W, 150 °C, 15 bars), 15 min) to yield the intermediates **29a** and **30a**. Ether cleavage with boron tribromide led to the final compounds **29** and **30**.

Scheme 5^a: Synthesis of compounds **29** to **30**



^aReagents and conditions: (a) Method B: Na₂CO₃, toluene/water (1:1), Pd(PPh₃)₄, reflux, 20 h; (b) Method A: Cs₂CO₃, DME/EtOH/water (1:1:1), Pd(PPh₃)₄, MW (150 W, 150 °C, 15 bars), 15 min; (c) BBr₃, CH₂Cl₂, -78 °C to rt, 18 h.

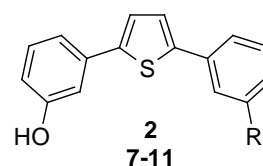
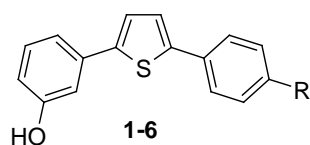
Biological Results

Activity: inhibition of human 17β-HSD1

Placental enzyme was partially purified following a described procedure.^{27,28} Tritiated E1 was incubated with 17β-HSD1, cofactor and inhibitor. After HPLC separation of substrate and product, the amount of labelled E2 formed was quantified. The inhibition values of the test compounds are shown in Tables 1 to 5. Thiophenes **1**, **2**, **7** and **33**, thiazole **36** and phenylenes **38** and **41**, identified in our previous article,²⁸ were used as reference compounds.

It was first investigated whether one of the two hydrophenyl moieties could be exchanged by another functional group having similar properties. Recent results²⁸ showed that the *meta*-hydroxy group is highly important for activity and was therefore maintained in the core structure. The exchange of the *para*-hydroxy group on the *meta-para* disubstituted thiophene (**1**, IC₅₀= 69 nM) by a bioisosteric function (F, NH₂, SH) resulted in moderate (**3**, IC₅₀= 717 nM) or weak inhibitors (**4** and **5**, IC₅₀> 5000 nM) of 17β-HSD1 (Table 1). Moving the F atom from the *para*- (compound **3**) to the *meta*-position (compound **8**) led to a small increase in activity (**8**, IC₅₀= 535 nM vs. **3**, IC₅₀= 717 nM). Replacement of the *meta*-fluorine for a methylsulfonamide moiety (**9**) did not improve the activity (**9**, IC₅₀= 523 nM vs. **8**, IC₅₀= 535 nM), while a compound bearing a bulky substituent like tolylsulfonamide (**11**, IC₅₀= 350 nM) showed comparable activity to the mono hydroxylated thiophene (**2**, IC₅₀= 342 nM) indicating that there is some space in this region of the enzyme for substitution but it is unlikely that specific interactions between the tolylsulfonamide moiety and amino acids of the active site take place. The insertion of a C1-linker between the phenyl moiety and the methylsulfonamide group was detrimental for the activity (**9**, IC₅₀= 523 nM vs. **10**, IC₅₀> 1000 nM). It can be therefore concluded that the two hydroxy functions are necessary for high activity and the *para*-hydroxy group can not be replaced by a bioisosteric group.

Table 1: Effect of the exchange of one OH substituent for other functional groups on human 17 β -HSD1 and 17 β -HSD2 inhibitory activities.



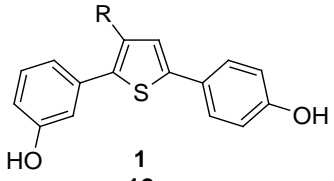
cmpd	R	IC ₅₀ (nM) ^a		selectivity factor ^d	cmpd	R	IC ₅₀ (nM) ^a		selectivity factor ^d
		17 β -HSD1 ^b	17 β -HSD2 ^c				17 β -HSD1 ^b	17 β -HSD2 ^c	
1	OH	69	1950	28	7	OH	173	745	4
2	H	342	2337	7	2	H	342	2337	7
3	F	717	3655	5	8	F	535	1824	3
4	NH ₂	>5000	nt		9		523	1575	3
5	SH	>5000	nt		10		>1000	nt	
6	CN	>1000	nt		11		350	276	1

^aMean values of three determinations, standard deviation less than 10 %; ^bHuman placenta, cytosolic fraction, substrate ³H-E1 + E1 [500 nM], cofactor NADH [500 μ M], ^cHuman placenta, microsomal fraction, substrate ³H-E2 + E2 [500 nM], cofactor NAD⁺ [1500 μ M], ^dIC₅₀ (17 β -HSD2)/ IC₅₀ (17 β -HSD1); ni: no inhibition, nt: not tested

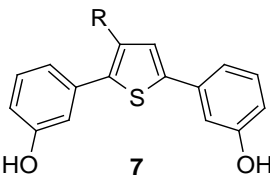
In order to improve the activity and the selectivity of our inhibitors, substituents capable to establish further interactions with the enzyme were added either on the heterocycle or on the hydroxyphenyl moieties. Additional functional groups were introduced in both of the *meta-para* 2,5-bis(hydroxyphenyl)thiophene **1** (IC₅₀ = 69 nM) and the *meta-meta* 2,5-disubstituted derivative **7** (IC₅₀ = 173 nM).

Concerning substitution on the heterocycle, two kinds of hydrophobic substituents (Me, Ph) were introduced in position 3 on the thiophene ring to investigate the space availability around the core (Table 2). The *meta-meta* thiophenes bearing a methyl (compound **13**) or phenyl (compound **14**) as well as the *meta-para* thiophene bearing a hydroxyphenyl substituent (compound **12**) showed a reduction of activity compared to the reference compound **7** (IC₅₀ = 216 nM vs. IC₅₀ > 1000 nM, 567 nM and 493 nM for **12**, **13** and **14**, respectively). It is striking that only in case of the *meta-meta* disubstituted series the insertion of a polar *meta*-hydroxyphenyl substituent leads to an increase in activity (**15**, IC₅₀ = 119 nM vs. **12**, IC₅₀ > 1000 nM). This exemplifies that there is space available for further substitution around the heterocycle only in case of the *meta-meta* bis(hydroxyphenyl) substitution pattern and that the third *meta*-OH group is certainly at an appropriate distance to establish supplementary hydrogen bond interactions with the active site.

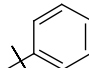
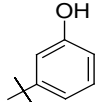
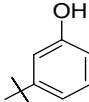
Table 2: Inhibition of human 17 β -HSD1 and 17 β -HSD2 by compounds bearing a supplementary substituent on the thiophene core structure



1
12



7
13-15

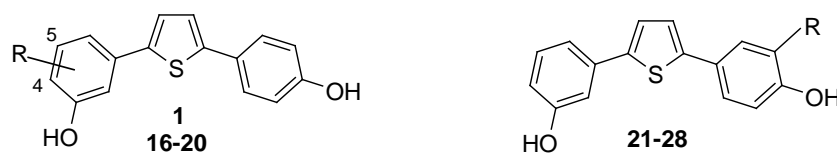
cmpd	R	IC ₅₀ (nM) ^a		selectivity factor ^d	cmpd	R	IC ₅₀ (nM) ^a		selectivity factor ^d
		17 β -HSD1 ^b	17 β -HSD2 ^c				17 β -HSD1 ^b	17 β -HSD2 ^c	
1	H	69	1950	28	7	H	173	745	4
					13	CH ₃	567	856	1
					14		493 ^e	nt	
12		>1000	nt		15		119	188	2

^aMean values of three determinations, standard deviation less than 10 %; ^bHuman placenta, cytosolic fraction, substrate ³H-E1 + E1 [500 nM], cofactor NADH [500 μ M]; ^cHuman placenta, microsomal fraction, substrate ³H-E2 + E2 [500 nM], cofactor NAD⁺ [1500 μ M]; ^dIC₅₀ (17 β -HSD2)/ IC₅₀ (17 β -HSD1); ^epredicted value, obtained with the LOGIT transformed; ni: no inhibition, nt: not tested

Concerning the substitution of the hydroxyphenyl rings, different groups were introduced either on the *meta*-hydroxyphenyl ring (compounds **16** to **20**) or on the *para*-hydroxyphenyl moiety (compounds **21** to **28**, Table 3). The synthesis of compounds bearing *ortho*-(to the heterocycle)-substituents at the hydroxyphenyl moieties was not considered, as the conformational constraints induced by the *ortho*-effect will not allow the compound to adopt a planar geometry. Planarity of our structures was considered as necessary to mimic the steroidal substrate.^{27,28}

Introduction of a substituent in position 5 on the *meta*-hydroxyphenyl moiety resulted in case of a methyl group in a reduction of activity (**16**, IC₅₀= 629 nM vs. **1**, IC₅₀= 69 nM). The introduction of a fluorine atom led to a slight increase in activity in comparison to the unsubstituted compound **1** (**17**, IC₅₀= 42 nM vs. **1**, IC₅₀= 69 nM). Moving these functional groups to position 4 gave a highly active fluorinated compound **19** (IC₅₀= 113 nM) and a very weak methylated inhibitor **18** (IC₅₀> 5000 nM). Substituents have also been introduced in position 5 on the *para*-hydroxyphenyl ring: a polar group like hydroxy (compound **22**) or a bulky substituent like the phenyl (compound **25**) in *ortho*- of the *para*-OH induced a decrease in activity compared to thiophene compound **1** (IC₅₀= 69 nM vs. IC₅₀= 402 nM and >5000 nM for **22** and **25**, respectively). The introduction of a fluorine substituent into the same position led to the highly potent compound **23** (IC₅₀= 8 nM) while substituents like methyl or trifluoromethyl showed similar or slightly better activities compared to the reference compound **1** (IC₅₀= 69 nM vs. IC₅₀= 46 nM and 38 nM for **21** and **24**, respectively). Other functional groups showing a higher flexibility like ethylacrylate (compound **26**), phenylacrylamide (compound **27**) or phenylpropanamide (compound **28**) were also synthesized and the resulting compounds **26**, **27** and **28** turned out to have weaker inhibitory activity compared to the unsubstituted thiophene **1** (IC₅₀= 69 nM vs. 130, 427 and 620 nM for **26**, **27** and **28**, respectively). The low activity of the unconjugated compound **28** indicates that an overall distributed electronic density is an important parameter for activity. These results indicate that there is space available in this area for substituents but the nature of the substituents is probably not yet optimal (Table 3).

Table 3: Effect of a supplementary substituent on the hydroxyphenyl moieties on the inhibition of the human 17 β -HSD1 and 17 β -HSD2

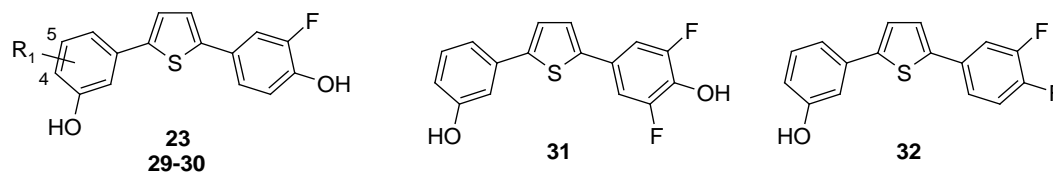


cmpd	R	IC ₅₀ (nM) ^a		selectivity factor ^d
		17 β -HSD1 ^b	17 β -HSD2 ^c	
1	H	69	1950	28
16	5-CH ₃	629	2584	4
17	5-F	42	463	11
18	4-CH ₃	>5000	nt	
19	4-F	113	183	2
20	4-OH	>5000	nt	
21	CH ₃	46	1971	49
22	OH	402	1636	4
23	F	8	940	118
24	CF ₃	38	97	3
25	Ph	>5000	nt	
26		130	502	4
27		427	468	1
28		620	982	2

^aMean values of three determinations, standard deviation less than 15 %; ^bHuman placenta, cytosolic fraction, substrate ³H-E1 + E1 [500 nM], cofactor NADH [500 μ M], ^cHuman placenta, microsomal fraction, substrate ³H-E2 + E2 [500 nM], cofactor NAD⁺ [1500 μ M], ^dIC₅₀ (17 β -HSD2)/ IC₅₀ (17 β -HSD1); ni: no inhibition, nt: not tested

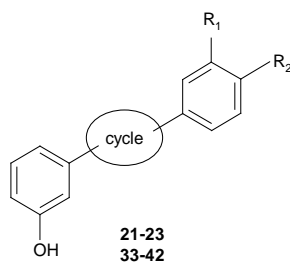
The influence of the introduction of a second fluorine on the highly active thiophene **23** (IC₅₀= 8 nM), either one F on each hydroxyphenyl ring or two F on the same hydroxyphenyl moiety, was also examined (Table 4). When the two F were located on each hydroxyphenyl moieties, the 4-substituted fluoro derivative (compound **30**) is slightly more potent than the one with the fluorine in 5-position (**29**, IC₅₀= 29 nM, vs. **30** IC₅₀= 17 nM). A small decrease in activity was observed when the two fluorine substituents were present at the same hydroxyphenyl ring (compound **31**, IC₅₀= 56 nM). The exchange of the *para*-OH function of **23** by a fluorine atom (compound **32**) confirmed the essential role of this *para*-hydroxy moiety as previously observed.

Methyl and fluorine substituents have been identified as functional groups able to increase the inhibitory activity of the 2,5-bis(hydroxyphenyl) thiophene **1**. Previously²⁸ we reported that other central core structures like 2,4-thiophene, 2,5-thiazole and 1,4-benzene lead to highly active compounds. The influence of an additional methyl or fluorine substituent at these structures was therefore also investigated (Table 5). Introduction of CH₃ or F into the *para*-hydroxyphenyl ring of **33**, **36** and **38** resulting in compounds **34**, **35**, **37**, **39** and **40** led to similarly active derivatives in case of **34** and **35** (IC₅₀= 64 nM vs. **21**, IC₅₀= 46 nM). A decrease in inhibitory activity in the thiazole and in the benzene classes of compounds was observed compared to the thiophene family (**37**, IC₅₀= 143 nM vs. **21**, IC₅₀= 46 nM; **40** and **41**, IC₅₀= 123 nM and 51 nM, respectively vs. **23**, IC₅₀= 8 nM). Amongst the investigated molecules, introduction of a methyl or fluorine substituent led only in the class of the bis(hydroxyphenyl) thiophenes to an increase in activity.

Table 4: Effect of two additional fluorine atoms on the 17 β -HSD1 and 17 β -HSD2 inhibitory activity

cmpd	R ₁	IC ₅₀ (nM) ^a		selectivity factor ^d
		17 β -HSD1 ^b	17 β -HSD2 ^c	
23	H	8	940	118
29	5-F	29	227	8
30	4-F	17	218	13
31		56	312	6
32		780	2640	3

^aMean values of three determinations, standard deviation less than 10 %; ^bHuman placenta, cytosolic fraction, substrate ³H-E1 + E1 [500 nM], cofactor NADH [500 μ M], ^cHuman placenta, microsomal fraction, substrate ³H-E2 + E2 [500 nM], cofactor NAD⁺ [1500 μ M], ^dIC₅₀ (17 β -HSD2)/ IC₅₀ (17 β -HSD1); nt: not tested.

Table 5: Influence of the core and a supplementary substituent on the inhibition of the human 17 β -HSD1 and 17 β -HSD2

cmpd	cycle	R ₁	R ₂	IC ₅₀ (nM) ^a		selectivity factor ^d
				17 β -HSD1 ^b	17 β -HSD2 ^c	
21		CH ₃	OH	46	1971	49
23		F	OH	8	940	118
33		H	OH	77	1270	16
34		CH ₃	OH	64	869	14
35		F	OH	64	510	8
36		H	OH	50	4000	80
37		CH ₃	OH	143	2023	14
38		H	OH	471	4509	10
39		CH ₃	OH	171	1248	7
40		F	OH	123	872	7
41		OH	H	173	2259	21
42		OH	F	51	253	5

^aMean values of three determinations, standard deviation less than 13 %; ^bHuman placenta, cytosolic fraction, substrate ³H-E1 + E1 [500 nM], cofactor NADH [500 μ M], ^cHuman placenta, microsomal fraction, substrate ³H-E2 + E2 [500 nM], cofactor NAD⁺ [1500 μ M], ^dIC₅₀ (17 β -HSD2)/ IC₅₀ (17 β -HSD1); ni: no inhibition, nt: not tested

Selectivity: inhibition of 17 β -HSD2 and affinities to the estrogen receptors α and β

In order to gain insight into the selectivity of the most active compounds, inhibition of 17 β -HSD2 and the relative binding affinities to the estrogen receptors α and β were determined.

Since 17 β -HSD2 catalyzes the inactivation of E2 into E1, inhibitory activity toward this enzyme must be avoided. The 17 β -HSD2 inhibition was determined using an assay similar to the 17 β -HSD1 test. Placental microsomes were incubated with tritiated E2 in the presence of NAD⁺ and inhibitor. Separation and quantification of labelled product (E1) was performed by HPLC using radio detection. A selection of the most potent 17 β -HSD1 inhibitors was tested for inhibition of 17 β -HSD2. IC₅₀ values and selectivity factors (IC₅₀ HSD2 / IC₅₀ HSD1) are presented in Tables 1 to 5.

Mono-hydroxylated compounds (Table 1) exhibited a poor selectivity regarding 17 β -HSD2, the most selective one being compound **5** with a selectivity factor of 5. This finding suggests that the *para*-OH is important for activity as well as for selectivity (selectivity of the *para-meta* derivative **1**: 28). Introduction of further substituents (Tables 2 to 5) into the highly active bis(hydroxyphenyl) scaffold induced a loss of selectivity against 17 β -HSD2 except in case of compounds **21** and **23**, which exhibit excellent selectivity factors of 49 and 118, respectively.

A further prerequisite for 17 β -HSD1 inhibitors to be used as potential drugs is that they do not show affinity for ER α and ER β , since binding to these receptors could counteract the therapeutic concept of selective 17 β -HSD1 inhibition. The binding affinities of the most selective compounds of this study were determined using recombinant human protein in a competition assay applying [³H]-E2 and hydroxyapatite (Table 6). All tested compounds show very marginal to marginal affinity to the ERs except compound **23**, which binds weakly to ER β (RBA= 1 %). Compound **21** was evaluated for estrogenic effects on the ER-positive, mammary tumor T47D cell line. No agonistic, i.e. stimulatory effect was observed after application of compound **21** even at a concentration 1000 fold higher compared to E2.

Table 6: Binding affinities for the human estrogen receptors α and β of selected compounds

cmpd	RBA ^a (%)	
	ER α ^b	ER β ^b
1	0.1 < RBA < 1	1.5
17	0.1 < RBA < 1	0.1 < RBA < 1
21	< 0.01	< 0.01
23	0.01 < RBA < 0.1	1
30	0.1	0.01 < RBA < 0.1
34	0.01 < RBA < 0.1	0.01 < RBA < 0.1
37	0.01 < RBA < 0.1	< 0.01

^aRBA (relative binding affinity), E2: 100 %, mean values of three determinations, standard deviations less than 10 %; ^bHuman recombinant protein, incubation with 10 nM ³H-E2 and inhibitor for 1 h.

Further biological evaluations

Additionally, the intracellular potency of compounds **21**, **23** and **37** on E2 formation was evaluated using a cell line which expresses both 17 β -HSD1 and 17 β -HSD2 (T47D cells). The compounds inhibited the formation of E2 after incubation with labelled E1 showing IC₅₀ values of 426 nM, 282 nM and 362 nM for **21**, **23** and **37**, respectively. These results indicate that the compounds are able to permeate the cell membrane and inhibit the transformation of E1 into E2.

The same compounds (**21**, **23** and **37**) were further investigated for inhibition of three human hepatic enzymes: CYP3A4, CYP2D6 and CYP2C19. The three compounds showed very little to weak inhibition of the hepatic CYP enzymes (10 > IC₅₀ > 1.50 μ M) except for CYP3A4 (IC₅₀= 0.50 and 0.82 μ M for **21** and **23**, respectively) and CYP2C19 (IC₅₀= 0.94 μ M for **21**) for which an enhanced inhibition was observed.

The relatively high inhibition of CYP3A4 by **21** and **23** has to be taken into consideration for the further optimization process but should not have an impact on the proof of concept *in vitro*.

The pharmacokinetic profiles of the two most active and selective compounds of this study (**21** and **23**) were determined in rats after oral administration in a cassette dosing approach. Each group consisted of 4 male rats and the compounds were administered in doses of 10 mg/kg. Plasma samples were collected over 24 h and plasma concentrations were determined by HPLC-MS/MS. The pharmacokinetic parameters are presented in Table 7. The maximal concentration ($C_{\max \text{ obs}}$) as well as the AUC-value is higher for compound **23** ($C_{\max} = 1388.2$ ng/mL, AUC = 19407 ng/mL) than for compound **21** ($C_{\max} = 905.0$ ng/mL, AUC = 12275 ng/mL). The maximal plasma concentration ($t_{\max \text{ obs}}$) for compounds **21** and **23** was reached after 4.0 and 8.0 h, respectively. These data show that both compounds exhibit excellent pharmacokinetic properties in the rat and might therefore be good candidates for further experiments in disease-oriented rat models.

Table 7: Pharmacokinetic parameters of compounds **21** and **23** in male rats after oral application (10 mg/kg)

parameters ^a	compd	
	21	23
$C_{\max \text{ obs}}$ (ng/mL)	905.0	1388.2
C_z (ng/mL)	43.3	24.9
$t_{\max \text{ obs}}$ (h)	4.0	8.0
t_z (h)	24.0	24.0
$t_{1/2z}$ (h)	3.8	2.7
AUC _{0-∞} (ng/mL)	12275	19407

^a $C_{\max \text{ obs}}$, maximal measured concentration; C_z , last analytical quantifiable concentration; $t_{\max \text{ obs}}$, time to reach the maximum measured concentration; t_z , time of the last sample which has an analytical quantifiable concentration; $t_{1/2z}$, half-life of the terminal slope of a concentration time curve; AUC_{0-∞}, area under the concentration- time curve extrapolated to infinity.

Computational chemistry

Molecular modelling

From the biological results it became apparent that introduction of a fluorine atom in *ortho*-position to the *para*-OH phenyl thiophene (compound **23**) led to a significant increase in the 17 β -HSD1 inhibitory activity. To get an insight into the binding mode of this compound and to better understand the favourable interactions achieved by this inhibitor in the active site, computational studies were performed by means of the docking software GOLDv3.2 and Autodock 4.1.

The choice of the 3D-structure of the enzyme, i.e. crystal structure, as well as the oxidation state of the cofactor i.e. NADPH or NADP⁺, used for the docking studies are crucial for obtaining reliable results.

We focused on X-ray structures of 17 β -HSD1 having a high resolution and showing a ternary complex (to get closer to the *in vivo* conditions). Three structures fulfilled these criteria: 1FDT and 1A27 both describing the ternary complex: enzyme-E2-NADP⁺ and 1I5R, describing the binary complex: enzyme-steroidal hybrid inhibitor (HYC), the latter being an adenosine moiety linked to an E2 core via a C9-linker. These three crystal structures differ mainly in the location of the amino acids belonging to the flexible loop α G β F (Pro187-Pro200). Since this loop borders both the SUB and the COF, its conformational variations strongly influence the size of both binding cavities. It is therefore important to take care of the position of this loop in the structures used for the docking studies.

In the X-ray structure 1FDT, the residues 187-200 are not well resolved, but two plausible conformations for the loop (noted 1FDT-A and 1FDT-B) have been described.³⁵ The backbones of these two loops are similar (RMSD of ~ 1 Å), while the main difference is given by the orientation of the side chains, mainly concerning the four amino acids Phe192, Met193, Glu194 and Lys195. In 1FDT-A, Phe192 and Met193 are turned toward the outer part of the enzyme while Glu194 and Lys195 are oriented toward the substrate and the cofactor (extending the substrate binding site = open conformation). On the other hand, in 1FDT-B these two pairs of residues show a reversed orientation limiting length and volume of the steroid binding site compared to 1FDT-A (= closed conformation). Although others²² have only considered 1FDT-B, we decided to investigate both conformations of this loop.

Interestingly, the flexible loop in 1A27 shows a comparable geometry as observed in 1FDT-B, with Phe192 and Met193 oriented toward the nicotinamide moiety, also restricting the space in the substrate binding site. In case of

115R, the loop is shifted in direction of the cofactor, resulting in a different conformation compared to both 1FDT-A and 1FDT-B. Although, like for 1FDT-A, it extends the SUB.

The docking studies were performed with NADPH as cofactor, as it is described that NADPH is present in a 500 fold higher concentration than its oxidized form NADP^+ in living cells.^{43,44}

Compound **23** was docked with NADPH into four different X-ray structures: 1FDT-A, 1FDT-B, 1A27 and 115R. Two different binding modes were observed for compound **23**: in case of 1FDT-B and 1A27, the inhibitor is located exclusively in the steroid binding site (Figure 1) adopting a similar orientation as previously described for the bis(hydroxyphenyl) oxazole **B**²⁷ (chart 1) while for 1FDT-A and 115R, the inhibitor is located in between the steroid and the cofactor binding sites, interacting with the nicotinamide moiety. In the following, this binding mode will be named as alternative binding mode (Figure 2).

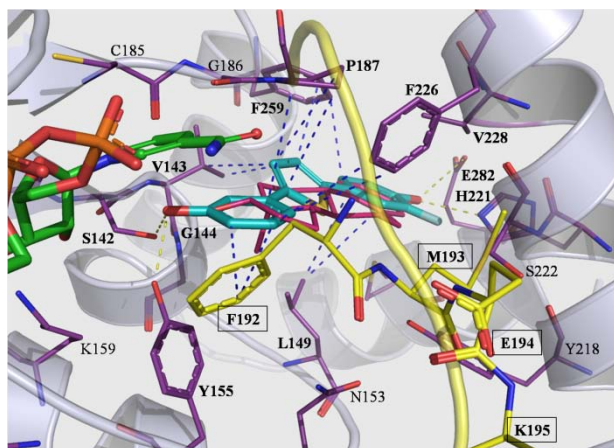


Figure 1. Docking complex between 17 β -HSD1 (X-ray 1FDT-B) and compound **23** (blue; SUB binding mode). NADPH, interacting residues and ribbon rendered tertiary structure of the active site are shown. Residues of the flexible loop are rendered in sticks and colored in yellow. Hydrogen bonds and π - π stackings (and hydrophobic interactions) are drawn in yellow and blue dashed lines, respectively. For comparison, E2 is depicted in magenta lines. Figures were generated with Pymol (<http://www.pymol.org>).

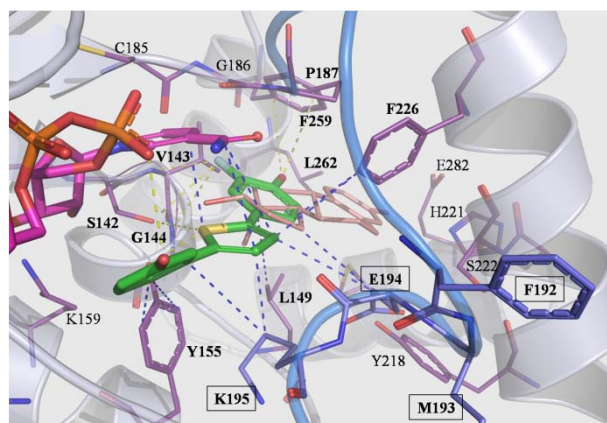


Figure 2. Docking complex between 17 β -HSD1 (X-ray 1FDT-A) and compound **23** (green; alternative binding mode). NADPH, interacting residues and ribbon rendered tertiary structure of the active site are shown. Residues of the flexible loop are rendered in sticks and colored in blue. Hydrogen bonds and π - π stackings (and hydrophobic interactions) are drawn in yellow and blue dashed lines, respectively. For comparison, E2 is depicted in magenta lines.

In case of the steroidal binding mode (1FDT-B and 1A27, Figure 1) the following specific interactions can be observed: hydrogen bond interactions between the *meta*-hydroxy group of **23** and Ser142/Tyr155 ($d_{\text{O-O}} = 2.6 \text{ \AA}$ for both amino acids) and between the *para*-OH group and His221/Glu282 ($d_{\text{O-N}} = 2.8 \text{ \AA}$ and $d_{\text{O-O}} = 3.8 \text{ \AA}$, Figure 1). Additionally, hydrophobic interactions and π - π stackings (Phe226, Phe259) are also involved.

In the alternative binding mode obtained using 1FDT-A and 1I5R (Figure 2), compound **23** is also stabilized by hydrogen bond interactions: the *meta*-OH group forms a strong H-bond with the phosphate group of the cofactor ($d_{\text{O}\cdots\text{O}} = 2.9 \text{ \AA}$). The fluorine atom could establish halogen bonds with the backbone $-\text{NH}-$ of Val143 and Gly144 ($d_{\text{F}\cdots\text{N}} = 3.2 \text{ \AA}$ and 3.8 \AA , respectively), in addition to a halogen bond with the OH-group of Ser142 ($d_{\text{F}\cdots\text{O}} = 3.5 \text{ \AA}$) which is involved in the catalytic process. Further, the *para*-OH points perpendicular toward Phe259 ($d_{\text{O}\cdots\text{centroid}} = 4.5 \text{ \AA}$) indicating a possible OH- π interaction. This could explain the importance of this group observed in the SARs. Moreover, strong π - π stacking interactions seem to stabilize the inhibitor in this binding mode: between the *meta*-OHphenyl-thiophene moiety and the nicotinamide part of the cofactor (parallel-displaced configuration; distance between the two ring centers, 4.3 \AA) and between the *para*-OH-phenyl-thiophene moiety and Phe226 (T-shape conformation; closest C-C contact distance 3.7 \AA). Moreover, electrostatic interactions between the sulfur atom of the heterocycle with the surrounding amino acids like Tyr155 and Ser142 might also play a role as described.⁴⁵

The results presented so far suggest that both binding modes have to be considered as possible for this class of inhibitors. They depend mainly on the orientation of the flexible loop. There is only one conformation of the loop leading to a steroidal binding mode (1FDT-B/1A27). In case of 1FDT-A/1I5R the pose showing the alternative binding mode is obtained using two X-ray structures having two different conformations of the loop. Unfortunately, due to the almost identical scoring function values observed for both poses with the docking programs (Gold and Autodock), it was not possible to determine which model (1FDT-A/1I5R or 1FDT-B/1A27) is the most appropriate to describe the interactions between the inhibitor and the enzyme and therefore which is the most plausible binding mode.

Comparing both poses obtained by docking of **23** in 1FDT-A and 1FDT-B shows that there is a common area in the neighbourhood of the catalytic tetrad which corresponds to the D-ring of the enzyme-substrate complex (Figure in Supporting Information).

Molecular Electrostatic Potential (MEP)

Recently we reported on the influence of the electronic density (MEP maps, “semi-QMAR”) on the potency of the inhibitors in this class of compounds.²⁸ The 3D-structures of the inhibitors were virtually divided into three areas and a given optimal range of ESP values (in Hartree) was determined for each region (-1.7 to -1.2×10^{-2} for I, -1.6 to -0.9×10^{-2} for II and -1.2 to -0.5×10^{-2} for III). The MEPs of compound **23** were calculated as shown in Figure 3. The molecular ESP distribution observed (-1.8 to -1.2×10^{-2} for I, -1.6 to -0.8×10^{-2} for II and -1.1 to -0.4×10^{-2} for III) fitted well to the optimal ranges identified previously, confirming the correlation between the ESP range and the potency of the compounds. The MEP maps of the natural substrate E1 and of E2 were also calculated (Figure 3) and compared to the one of **23**. The finding that the ESP distribution of **23** and E2/E1 is very different might be an indication that compound **23** does not bind in the same way as the steroid.

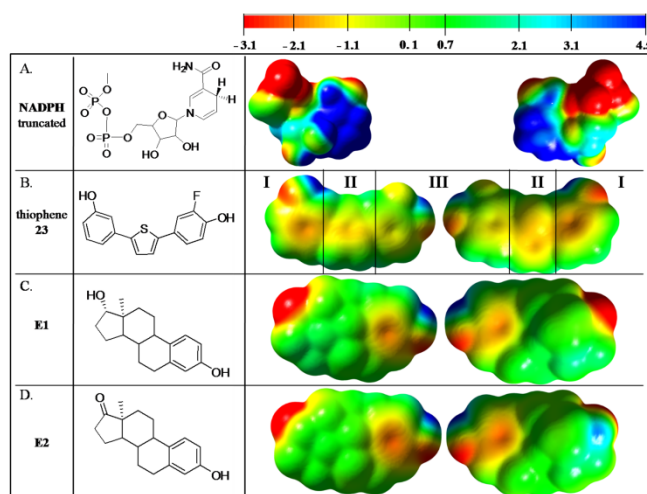


Figure 3. Structures and MEP maps of both ventral (steroidal α -side) and dorsal (steroidal β -side) views of truncated NADPH (A), thiophene **23** (B), E1 (C) and E2 (D). MEP surfaces were plotted with GaussView 3.09.

According to the alternative binding mode, the *meta*-hydroxyphenyl thiophene part of **23** overlaps with the nicotinamide part of the cofactor and forms stabilizing π - π interactions. The ESP distribution of these two entities should therefore show complementarity. To get an insight into this, the MEP map of a truncated NADPH –the counterpart of the *meta*-OHphenyl-thiophene moiety- was calculated by *ab initio* methods. As can be seen in Figure 3 a certain complementarity was observed. The NADPH MEP maps give the explanation for the observation²⁸ that a strong polarization between the vertex and the base of the central ring of the inhibitors is negative for binding. Positive ESP values on the vertex side lead to repulsion effects with the nicotinamide and therefore reduce the inhibitory activity. This finding indicates that this class of compound might bind according to the alternative binding mode (Figure 2). However, this hypothesis needs to be further investigated.

Discussion and Conclusion

Structural optimizations of compound **1** led to the discovery of new substituted 2,5-bis(hydroxyphenyl)thiophene derivatives: the fluorinated **23** and the methylated **21** being the most active and selective inhibitors identified.

From a previous work in this class of compounds²⁸ it was demonstrated that removal of one of the two hydroxyphenyl moieties is detrimental for the activity. In this paper it was shown that replacement of the *para*-OH function by a bioisoteric group like F, NH₂, SH, CN leads to a reduction of activity. The lack of hydrogen donating properties of the fluoro and cyano substituents might not be the only reason for this decrease in activity as the amino and the thiol derivatives are also less active than the parent compound **1**. Interestingly, the omission of a C1-linker between the methylsulfonamide moiety and the phenyl ring (compound **9**) resulted in an increase of potency. Deprivation of electrons from the phenyl ring, obviously is necessary for good inhibition. The relatively high activity observed for compound **11** (IC₅₀= 350 nM) especially compared to compound **9** (IC₅₀= 523 nM) demonstrates that in the protein there is some space available in this position for a bulky substituent. Furthermore, the tolyl group might also be involved in the stabilization of the inhibitor in the binding site, establishing π - π stacking interactions with appropriate amino acid residues present in this region.

With the aim to increase the activity and the selectivity in this class of compounds, substituents were introduced on the 2,5-bis(hydroxyphenyl)thiophenes **1** and **7**. This was successful for compound **15** (IC₅₀= 119 nM vs. **7**, IC₅₀= 216 nM). Apparently, the formation of an additional hydrogen bond is responsible for this increase in inhibitory activity, while a pure π - π stacking interaction as supposed for compound **14** is not sufficient. The 2,5-disubstituted thiophenes **12** and **15** differ only in the position of one hydroxy group (*para*: compound **12**, *meta*: compound **15**). The fact that compound **15** shows a much higher activity (IC₅₀= 119 nM vs. **12**, IC₅₀> 1000 nM) indicates that only in case of **15** the geometry of the OH groups is acceptable for a reasonable interaction. It demonstrates, as observed already,^{24,27} a sharp SAR and a reduced flexibility in this region of the active site.

The trisubstituted compound **14** bearing a phenyl substituent at the thiophene differs from the triazole **A**³² (Chart 2) only in the nature of the heterocycle. The following comparisons highlight the importance of the heterocycle for the potency of the molecules: inactive compound **A** vs. thiophene **14** (IC₅₀= 493 nM), thiophene **21** (IC₅₀= 46 nM) vs. thiazole **37** (IC₅₀= 143 nM) and thiophene **23** (IC₅₀= 8 nM) vs. benzene **40** (IC₅₀= 123 nM). It becomes apparent that the thiophene ring is the most appropriate heterocycle for high inhibitory activity. Provided that all compounds bind according to the same binding mode, there are different explanations for these results: 1. The presence and the position of one or several nitrogens in the heterocycle modulate the MEP distribution of the compound and in particular the electronic distribution of the *meta*-hydroxyphenyl moiety²⁸ – in case of the compounds under consideration resulting to inadequate electronic properties for binding, 2. Similarly the replacement of the sulfur leads to an inadequate repartition of the electron density in the heterocycle 3. A reduced flexibility in the binding site is responsible that the enzyme can not adjust its geometry to the different hydroxyphenyl moieties (depending on the heterocycle, the angles between the phenyl-OHs are different).

A high increase in activity and selectivity could be reached by introduction of substituents into the hydroxyphenyl moiety, especially when the substituent is located *ortho*- of the *para*-hydroxyphenyl group (compounds **21** to **24**). Not all substituents are equally well tolerated: there is no space available for a phenyl group (compound **25**). An additional OH group (compound **22**) is obviously not able to establish specific interactions while small lipophilic substituents (methyl, **21**; fluorine, **23** and trifluoromethyl, **24**) are enhancing the activity. There is enough space in this region of the enzyme to introduce a flexible chain (**26**) but conjugation seems to be necessary to achieve a higher activity as already observed with the tolylsulfonamide substituent (compound **11**).

The positive influence of the fluorine atom has often been demonstrated in medicinal chemistry⁴⁶⁻⁴⁸ and was also proven in this study with compound **23** (IC₅₀ = 8 nM). The position of the fluorine is decisive for an increase in activity: it has to be in *meta*-position (**17** and **23**). Highest activity was achieved in *ortho*- of the hydroxy group (compound **23**). This indicates that either direct interactions of the fluorine with amino acid residues in this region of the active site or the increase of acidity of the neighbouring OH groups might be responsible for this effect.

Introduction of a second fluorine atom into this fluorohydroxyphenyl ring (compound **31**) does not enhance the activity suggesting that the effects of the fluorine are not additive. A second fluorine was also added to the other hydroxyphenyl moiety (in *ortho*- and *meta*- of the *meta*-OH group) leading to compounds **29** and **30**. However, no enhancement of the activity compared to the monofluorinated **23** was observed indicating that there are no specific interactions of the second fluoro substituent.

A close look at the X-ray structures of 17 β -HSD1 crystallized in presence of different steroidal ligands showed that the flexible loop (amino acids 187-200) can adopt different geometries depending on the nature of the ligand and on the absence or presence of the cofactor in the catalytic region. It indicates that some parts of the enzyme can adapt their geometry to the molecule present in the active site in order to stabilize it. However, other parts are rigid, explaining the sharp SAR observed in this paper and previously.^{27,28}

Two plausible conformations of the loop in the ternary complex enzyme-E2-NADP⁺, PDB code: 1FDT, have been described (1FDT-A, 1FDT-B). We have shown that both can be used for docking studies. In case of 1FDT-A the substrate binding pocket is extended, enhancing the volume of the active site. It is therefore a good model to evaluate an alternative binding mode for inhibitors which are larger than the steroid. A binding mode as observed for steroids in the X-ray structures was found when the loop closes the SUB (1FDT-B). Surprisingly, when the inhibitors were docked to the protein with the loop in the open conformation, they interact with the nicotinamide part of the cofactor. MEP calculations showed a certain complementarity between the electronic density of **23** and of the nicotinamide moiety of the cofactor indicating that this alternative binding mode is not only plausible, it might be the one which is more likely.

Up to now, designing compounds as potential 17 β -HSD1 inhibitors, several groups^{37,49-51} tried to mimic the cofactor. Our finding of the above mentioned alternative binding mode makes another strategy very promising: the cofactor, which is likely to be present in the active site when the inhibitor is entering, could be used as partner to achieve additional interactions rather than trying to displace it.

The most potent 17 β -HSD1 inhibitors **21** and **23** exhibit a higher selectivity toward 17 β -HSD2 compared to parent compound, (selectivity factors 49 and 118, respectively vs. 28 for **1**). This indicates that the amino acids close to the CH₃ or F substituents must have different properties in the two 17 β -HSD enzymes, which could be further exploited to increase selectivity.

The most potent inhibitors show only marginal to very little affinity to the ER α and no stimulation of cell proliferation (agonistic effect) in the ER-positive T47D cell line could be observed. The weak affinity of compound **23** for ER β may not be critical as it is reported that ER β exhibits anti-proliferative effects in breast cancer cells.⁵²

Compound **23** might be used in an appropriate animal model to prove the concept of 17 β -HSD1 inhibition with non-steroidal inhibitors. This compound shows a good pharmacokinetic profile in rats.

In this paper, we described the synthesis of substituted bis(hydroxyphenyl)thiophenes, thiazoles and benzenes as inhibitors of 17 β -HSD1 and the evaluation of their biological properties. The most promising compounds of this study, **21** and **23**, exhibit high selectivity toward 17 β -HSD2, marginal binding to ER α and excellent pharmacokinetic profiles in rats after peroral application. These new compounds provide useful tools to validate 17 β -HSD1 as a target for the treatment of estrogen-dependent diseases.

Experimental section

Chemical methods

Chemical names follow IUPAC nomenclature. Starting materials were purchased from Aldrich, Acros, Lancaster, Roth, Merck or Fluka and were used without purification.

Column chromatography (CC) was performed on silica gel (70–200 μm) coated with silica, preparative thin layer chromatography (TLC) on 1 mm SIL G-100 UV₂₅₄ glass plates (Macherey-Nagel) and reaction progress was monitored by TLC on Alugram SIL G UV₂₅₄ (Macherey-Nagel).

IR spectra were recorded on a Bruker Vector 33 spectrometer (neat sample).

¹H-NMR and ¹³C-NMR spectra were measured on a Bruker AM500 spectrometer (500 MHz) at 300 K. Chemical shifts are reported in δ (parts per million: ppm), by reference to the hydrogenated residues of deuterated solvent as internal standard (CDCl₃: δ = 7.24 ppm (¹H NMR) and δ = 77 ppm (¹³C NMR), CD₃OD: δ = 3.35 ppm (¹H NMR) and δ = 49.3 ppm (¹³C NMR), CD₃COCD₃: δ = 2.05 ppm (¹H NMR) and δ = 29.9 ppm (¹³C NMR), CD₃SOCD₃: δ = 2.50 ppm (¹H NMR) and δ = 39.5 ppm (¹³C NMR)). Signals are described as s, d, t, q, dd, m, dt for singlet, doublet, triplet, quadruplet, doublet of doublets, multiplet and doublet of triplets, respectively. All coupling constants (*J*) are given in hertz (Hz).

Mass spectra (ESI) were recorded on a TSQ Quantum (ThermoFischer) instrument. Elemental analyses (C, H, N) were performed at the Department of Instrumental Analysis and Bioanalysis, Saarland University. The purity of the compounds, which in all cases was higher than 95 %, was determined using 2 different methods: elemental analysis for compounds **3** to **6**, **8** to **32**, **34** and **37** and LC/MS for compounds **35**, **39**, **41** and **42**.

Compounds 2-bromo-5-(3-methoxyphenyl)thiophene (**1b**)²⁸, 2-(3-methoxyphenyl)-5-(4-methoxyphenyl)-thiophene (**1a**)²⁸, 3-[5-(4-hydroxyphenyl)-2-thienyl]phenol (**1**)²⁸, 2-(3-methoxyphenyl)-5-phenylthiophene (**2a**)²⁸, 3-(5-phenyl-2-thienyl)phenol (**2**)²⁸, 2,5-bis(3-methoxyphenyl)thiophene (**7a**)²⁸, 3,3'-thiene-2,5-diylidiphenol (**7**)²⁸, 2-bromo-5-(4-methoxyphenyl)thiophene (**16c**)²⁸, 4-bromo-2-iodo-1-methoxy-benzene (**25d**)⁵³, 5-bromo-2-methoxybiphenyl (**25c**)⁵⁴, [6-methoxy-1,1'-biphenyl-3-yl]boronic acid (**25b**)⁵⁴, [3-(hydroxymethyl)-4-methoxyphenyl]-boronic acid (**26d**)⁵⁵, 4-bromo-2-(3-methoxyphenyl)thiophene (**33b**)²⁸, 2-(3-methoxyphenyl)-4-(4-methoxyphenyl)thiophene (**33a**)²⁸, 3-[4-(4-hydroxyphenyl)-2-thienyl]phenol (**29**)²⁸, 5-bromo-2-(3-methoxyphenyl)-1,3-thiazole (**36b**)²⁸, 2-(3-methoxyphenyl)-5-(4-methoxyphenyl)-1,3-thiazole (**36a**)²⁸, 3-[5-(4-hydroxyphenyl)-1,3-thiazol-2-yl]phenol (**36**)²⁸, 4'-bromo-3-methoxybiphenyl (**38b**)²⁸, 3,4"-dimethoxy-1,1':4',1"-terphenyl (**38a**)²⁸, 1,1':4',1"-terphenyl-3,4"-diol (**38**)²⁸, 3,3"-dimethoxy-1,1':4',1"-terphenyl (**40a**)²⁸ and 1,1':4',1"-terphenyl-3,3"-diol (**40**)²⁸ were prepared following described procedures.

General procedure for Suzuki coupling

Method A

A mixture of aryl bromide (1 eq), aryl boronic acid (1.2 eq), caesium carbonate (2.2 eq) and tetrakis(triphenylphosphine) palladium (0.01 eq) was suspended in an oxygen free DME/EtOH/water (1:1:1) solution. The reaction mixture was exposed to microwave irradiation (15 min, 150 W, 150 °C, 15 bars). After cooling to rt, water was added and the aqueous layer was extracted with ethyl acetate. The combined organic layers were washed with brine, dried over magnesium sulfate, filtered and concentrated to dryness. The product was purified by column chromatography (CC).

Method B:

A mixture of arylbromide (1 eq), aryl boronic acid (1 eq), sodium carbonate (2 eq) and tetrakis(triphenylphosphine) palladium (0.05 eq) in an oxygen free toluene/water (1:1) solution was stirred at 100 °C for 20 h under nitrogen atmosphere. The reaction mixture was cooled to rt. The aqueous layer was extracted with ethyl acetate. The combined organic layers were washed with brine, dried over magnesium sulfate, filtered and concentrated to dryness. The product was purified by CC.

General procedure for ether cleavage

Method C:

To a solution of methoxyphenyl derivative (1 eq) in dry dichloromethane at -78 °C (dry ice/acetone bath), boron tribromide in dichloromethane (1 M, 3 eq per methoxy function) was added dropwise. The reaction mixture was stirred for 20 h at rt under nitrogen atmosphere. Water was added to quench the reaction, and the aqueous layer was extracted with ethyl acetate. The combined organic layers were washed with brine, dried over sodium sulfate, filtered and concentrated to dryness. The product was purified by preparative thin layer chromatography (TLC).

2-(4-Fluorophenyl)-5-(3-methoxyphenyl)thiophene (3a). The title compound was prepared by reaction of 2-bromo-5-(3-methoxyphenyl)thiophene (**1b**) (150 mg, 0.56 mmol), 4-fluorophenylboronic acid (94 mg, 0.67 mmol), caesium carbonate (383 mg, 1.24 mmol) and tetrakis(triphenylphosphine) palladium (6.4 mg, 5.6 μmol) according to method A. The product was purified by CC (hexane/ethyl acetate 9:1); yield: 75 % (120 mg).

3-[5-(4-Fluorophenyl)-2-thienyl]phenol (3). The title compound was prepared by reaction of 2-(4-fluorophenyl)-5-(3-methoxyphenyl)thiophene (**3a**) (80 mg, 0.28 mmol) and boron tribromide (0.84 mmol) according to method C. The product was purified by preparative TLC (hexane/ethyl acetate 1:1); yield: 68 % (52 mg); MS (ESI): 270 (M+H)⁺; Anal. (C₁₆H₁₁FOS) C, H, N.

4-[5-(3-Methoxyphenyl)-2-thienyl]aniline (4a). The title compound was prepared by reaction of 2-bromo-5-(3-methoxyphenyl)thiophene (**1b**) (150 mg, 0.56 mmol), 4-aminophenylboronic acid (92 mg, 0.67 mmol), caesium carbonate (383 mg, 1.24 mmol) and tetrakis(triphenylphosphine) palladium (6.4 mg, 5.6 μmol) according to method A. The product was purified by CC (hexane/ethyl acetate 7:3); yield: 63 % (100 mg).

3-[5-(4-Aminophenyl)-2-thienyl]phenol (4). The title compound was prepared by reaction of 4-[5-(3-methoxyphenyl)-2-thienyl]aniline (**4a**) (100 mg, 0.37 mmol) and boron tribromide (1.11 mmol) according to method C. The product was purified by preparative TLC (hexane/ethyl acetate 1:1); yield: 82 % (82 mg); MS (ESI): 268 (M+H)⁺; Anal. (C₁₆H₁₃NOS) C, H, N.

4-[5-(3-Methoxyphenyl)-2-thienyl]benzenethiol (5a). The title compound was prepared by reaction of 2-bromo-5-(3-methoxyphenyl)thiophene (**1b**) (250 mg, 0.93 mmol), 4-mercaptophenylboronic acid (172 mg, 1.12 mmol), caesium carbonate (636 mg, 2.05 mmol) and tetrakis(triphenylphosphine) palladium (10.8 mg, 9.3 μmol) according to method A. The product was purified by CC (hexane/ethyl acetate 7:3); yield: 61 % (160 mg).

3-[5-(4-Sulfanyphenyl)-2-thienyl]phenol (5). The title compound was prepared by reaction of 4-[5-(3-methoxyphenyl)-2-thienyl]benzenethiol (**5a**) (150 mg, 0.50 mmol) and boron tribromide (1.50 mmol) according to method C. The product was purified by preparative TLC (hexane/ethyl acetate 1:1); yield: 81 % (115 mg); MS (ESI): 285 (M+H)⁺; Anal. (C₁₆H₁₂OS₂) C, H, N.

4-[5-(3-Methoxyphenyl)-2-thienyl]benzonitrile (6a). The title compound was prepared by reaction by reaction of 2-bromo-5-(3-methoxyphenyl)thiophene (**1b**) (200 mg, 0.74 mmol), 4-cyanophenylboronic acid (131 mg, 0.89 mmol), caesium carbonate (508 mg, 1.64 mmol) and tetrakis(triphenylphosphine) palladium (8.5 mg, 7.4 μmol) according to method A. The product was purified by CC (hexane/ethyl acetate 7:3); yield: 27 % (60 mg).

4-[5-(3-Hydroxyphenyl)-2-thienyl]benzonitrile (6). The title compound was prepared by reaction of 4-[5-(3-methoxyphenyl)-2-thienyl]benzonitrile (**6a**) (42 mg, 0.14 mmol) and boron tribromide (0.42 mmol) according to method C. The product was purified by preparative TLC (hexane/ethyl acetate 6:4); yield: 62 % (25 mg); MS (APCI): 277 (M)⁺; Anal. (C₁₇H₁₁NOS) C, H, N.

2-(3-Fluorophenyl)-5-(3-methoxyphenyl)thiophene (8a). The title compound was prepared by reaction of 2-bromo-5-(3-methoxyphenyl)thiophene (**1b**) (150 mg, 0.56 mmol), 3-fluorophenylboronic acid (94 mg, 0.67 mmol), caesium carbonate (381 mg, 1.22 mmol) and tetrakis(triphenylphosphine) palladium (6.5 mg, 5.6 μmol) according to method A. The product was purified by CC (hexane/ethyl acetate 9:1); yield: 82 % (130 mg).

3-[5-(3-Fluorophenyl)-2-thienyl]phenol (8). The title compound was prepared by reaction of 2-(3-fluorophenyl)-5-(3-methoxyphenyl)thiophene (**8a**) (130 mg, 0.45 mmol) and boron tribromide (1.35 mmol) according to method C. The product was purified by preparative TLC (dichloromethane/methanol 99:1); yield: 66 % (82 mg); MS (ESI): 271 (M+H)⁺; Anal. (C₁₆H₁₁FOS) C, H, N.

N-(3-[5-(3-Methoxyphenyl)-2-thienyl]phenyl)methanesulfonamide (9a). The title compound was prepared by reaction of 2-bromo-5-(3-methoxyphenyl)thiophene (**1b**) (160 mg, 0.60 mmol), 3-methylsulfonylaminophenylboronic acid (155 mg, 0.72 mmol), caesium carbonate (410 mg, 1.32 mmol) and tetrakis(triphenylphosphine) palladium (6.9 mg, 6.0 μmol) according to method A. The product was purified by CC (petroleum ether/ethyl acetate 6:4); yield: 75 % (150 mg).

N-(3-[5-(3-Hydroxyphenyl)-2-thienyl]phenyl)methanesulfonamide (9). The title compound was prepared by reaction of N-(3-[5-(3-methoxyphenyl)-2-thienyl]phenyl)methanesulfonamide (**9a**) (150 mg, 0.44 mmol) and boron tribromide (1.32 mmol) according to method C. The product was purified by preparative TLC (hexane/ethyl acetate 1:1); yield: 61 % (92 mg); MS (ESI): 346 (M+H)⁺; Anal. (C₁₇H₁₅NO₃S₂) C, H, N

N-(3-[5-(3-Methoxyphenyl)-2-thienyl]benzyl)methanesulfonamide (10a). The title compound was prepared by reaction of 2-bromo-5-(3-methoxyphenyl)thiophene (**1b**) (150 mg, 0.56 mmol), 3-[(methylsulfonylamino)methyl]-benzeneboronic acid (153 mg, 0.67 mmol), caesium carbonate (382 mg, 1.23 mmol) and tetrakis(triphenylphosphine) palladium (6.5 mg, 5.6 μmol) according to method A. The product was purified by CC (petroleum ether/ethyl acetate 8:2); yield: 58 % (122 mg).

N-(3-[5-(3-Hydroxyphenyl)-2-thienyl]benzyl)methanesulfonamide (10). The title compound was prepared by reaction of N-(3-[5-(3-methoxyphenyl)-2-thienyl]benzyl)methanesulfonamide (**10a**) (122 mg, 0.37 mmol) and boron tribromide (1.11 mmol) according to method C. The product was purified by preparative TLC (hexane/ethyl acetate 1:1); yield: 33 % (44 mg); MS (ESI): 360 (M+H)⁺; Anal. (C₁₈H₁₇NO₃S₂) C, H, N.

***N*-(3-[5-(3-Methoxyphenyl)-2-thienyl]phenyl)-4-methylbenzenesulfonamide (11a).** The title compound was prepared by reaction of 2-bromo-5-(3-methoxyphenyl)thiophene (**1b**) (150 mg, 0.56 mmol), [3-[[4-methylphenyl)sulfonyl]amino]phenyl]-boronic acid (195 mg, 0.67 mmol), caesium carbonate (383 mg, 1.23 mmol) and tetrakis(triphenylphosphine) palladium (6.5 mg, 5.6 μ mol) according to method A. The product was purified by CC (petroleum ether/ethyl acetate 9:1); yield: 88 % (214 mg).

***N*-(3-[5-(3-Hydroxyphenyl)-2-thienyl]phenyl)-4-methylbenzenesulfonamide (11).** The title compound was prepared by reaction of *N*-(3-[5-(3-methoxyphenyl)-2-thienyl]phenyl)-4-methylbenzenesulfonamide (**11a**) (214 mg, 0.49 mmol) and boron tribromide (1.47 mmol) according to method C. The product was purified by preparative TLC (hexane/ethyl acetate 1:1); yield: 75 % (156 mg); MS (APCI): 421 (M)⁺; Anal. (C₂₃H₁₉NO₃S₂) C, H, N.

3,5-Dibromo-2-(3-methoxyphenyl)thiophene (12c). The title compound was prepared by reaction of 2,3,5-tribromothiophene (100 mg, 0.31 mmol), 3-methoxybenzeneboronic acid (46 mg, 0.31 mmol), sodium carbonate (67 mg, 0.62 mmol) and tetrakis(triphenylphosphine) palladium (17.9 mg, 15.5 μ mol) according to method B heating the reaction 4 h instead of 20 h. The product was purified by CC (petroleum ether/ethyl acetate 9:1); yield: 23 % (25 mg).

3-Bromo-2-(3-methoxyphenyl)-5-(4-methoxyphenyl)thiophene (12b). The title compound was prepared by reaction of 3,5-dibromo-2-(3-methoxyphenyl)thiophene (**12c**) (500 mg, 1.43 mmol), 4-methoxybenzeneboronic acid (268 mg, 1.72 mmol), sodium carbonate (333 mg, 3.15 mmol) and tetrakis(triphenylphosphine) palladium (82.6 mg, 71.5 μ mol) according to method B. The product was purified by CC (petroleum ether/ethyl acetate 9:1); yield: 52 % (278 mg).

2,3-Bis(3-methoxyphenyl)-5-(4-methoxyphenyl)thiophene (12a). The title compound was prepared by reaction of 3-bromo-2-(3-methoxyphenyl)-5-(4-methoxyphenyl)thiophene (**12b**) (250 mg, 0.67 mmol), 3-methoxybenzeneboronic acid (124 mg, 0.80 mmol), sodium carbonate (142 mg, 1.34 mmol) and tetrakis(triphenylphosphine) palladium (38.7 mg, 33.5 μ mol) according to method B. The product was purified by CC (petroleum ether/ethyl acetate 9:1); yield: 72 % (194 mg).

3,3'-[5-(4-Hydroxyphenyl)thiense-2,3-diyl]diphenol (12). The title compound was prepared by reaction of 2,3-bis(3-methoxyphenyl)-5-(4-methoxyphenyl)thiophene (**12a**) (100 mg, 0.24 mmol) and boron tribromide (2.16 mmol) according to method C. The product was purified by preparative TLC (hexane/ethyl acetate 1:1); yield: 92 % (79 mg); MS (ESI): 359 (M-H)⁺; Anal. (C₂₂H₁₆O₃S) C, H, N.

3,3'-(3-Methylthiense-2,5-diyl)diphenol (13). The title compound was prepared by reaction of 2,5-dibromo-3-methylthiophene (150 mg, 0.58 mmol), 3-hydroxybenzeneboronic acid (179 mg, 1.27 mmol), caesium carbonate (868 mg, 2.79 mmol) and tetrakis(triphenylphosphine) palladium (6.7 mg, 5.8 μ mol) according to method A. The product was purified by CC (hexane/ethyl acetate 4:6); yield: 45 % (73 mg); MS (ESI): 281 (M-H)⁺; Anal. (C₁₇H₁₄O₂S) C, H, N.

3-Bromo-2,5-bis(3-methoxyphenyl)thiophene (14b). The title compound was prepared by reaction of 3,5-dibromo-2-(3-methoxyphenyl)thiophene (**12c**) (250 mg, 0.72 mmol), 3-methoxybenzeneboronic acid (134 mg, 0.86 mmol), sodium carbonate (148 mg, 1.44 mmol) and tetrakis(triphenylphosphine) palladium (41.6 mg, 36.0 μ mol) according to method B. The product was purified by CC (petroleum ether/ethyl acetate 9:1); yield: 72 % (194 mg).

2,5-Bis(3-methoxyphenyl)-3-phenylthiophene (14a). The title compound was prepared by reaction of 3-bromo-2,5-bis(3-methoxyphenyl)thiophene (**14b**) (102 mg, 0.27 mmol), benzeneboronic acid (38 mg, 0.27 mmol), sodium carbonate (58 mg, 0.54 mmol) and tetrakis(triphenylphosphine) palladium (15.6 mg, 13.5 μ mol) according to method B. The product was purified by CC (petroleum ether/ethyl acetate 9:1); yield: 54 % (51 mg).

3,3'-(3-Phenylthiense-2,5-diyl)diphenol (14). The title compound was prepared by reaction of 2,5-bis(3-methoxyphenyl)-3-phenylthiophene (**14a**) (50 mg, 0.13 mmol) and boron tribromide (0.78 mmol) according to method C. The product was purified by preparative TLC (hexane/ethyl acetate 1:1); yield: 53 % (49 mg); MS (ESI): 345 (M+H)⁺; Anal. (C₂₂H₁₆O₂S) C, H, N.

2,3,5-Tris(3-methoxyphenyl)thiophene (15a). The title compound was prepared by reaction of 3-bromo-2,5-bis(3-methoxyphenyl)thiophene (**14b**) (102 mg, 0.27 mmol), 3-methoxybenzene boronic acid (42 mg, 0.27 mmol), sodium carbonate (58 mg, 0.54 mmol) and tetrakis(triphenylphosphine) palladium (15.6 mg, 13.5 μ mol) according to method B. The product was purified by CC (petroleum ether/ethyl acetate 9:1); yield: 34 % (37 mg).

3,3',3''-Thiense-2,3,5-triyltriphenol (15). The title compound was prepared by reaction of 2,3,5-tris(3-methoxyphenyl)thiophene (**15a**) (37 mg, 0.09 mmol) and boron tribromide (0.81 mmol) according to method C. The product was purified by preparative TLC (hexane/ethyl acetate 1:1); yield: 67 % (21 mg); MS (ESI): 361 (M+H)⁺; Anal. (C₂₂H₁₆O₃S) C, H, N.

5-(4-Methoxyphenyl)-2-(boronic acid)thiophene (16b). To a solution of 2-bromo-5-(4-methoxyphenyl)thiophene (**16c**) (100 mg, 0.37 mmol, 1 eq) in anhydrous THF cooled to -78 °C for 5 min, *n*-BuLi (1.6 M in hexane, 0.28 mL, 0.44 mmol, 1.2 eq) was added dropwise and stirred at -78 °C. After 15 min, triethyl borate (0.37 mL, 2.22 mmol, 6 eq) was added at -78 °C and the mixture was stirred for 2 h. After warming to rt, the crude material was acidified with 20 mL of a 1N hydrochloric acid solution. The aqueous layer was washed with ethyl acetate. The combined organic layers were dried over sodium sulfate, filtered and evaporated under reduced pressure. The title compound was not characterized and used without further purification.

2-(3-Methoxyphenyl-5-methylphenyl)-5-(4-methoxyphenyl)thiophene (16a). The title compound was prepared by reaction of 1-bromo-3-methoxy-5-methylbenzene (150 mg, 0.74 mmol), [5-(4-methoxyphenyl)-2-thienyl]-boronic acid (**16b**) (206 mg, 0.88 mmol), sodium carbonate (181 mg, 1.76 mmol) and tetrakis(triphenylphosphine) palladium (42.7 mg, 37.0 μmol) according to method B. The product was purified by CC (hexane/ethyl acetate 7:3); yield: 22 % (50 mg).

3-[5-(4-Hydroxyphenyl)-2-thienyl]-5-methylphenol (16). The title compound was prepared by reaction of 2-(3-methoxyphenyl-5-methylphenyl)-5-(4-methoxyphenyl)thiophene (**16a**) (50 mg, 0.16 mmol) and boron tribromide (0.96 mmol) according to method C. The product was purified by preparative TLC (hexane/ethyl acetate 1:1); yield: 90 % (41 mg); MS (ESI): 281 (M-H)⁺; Anal. (C₁₇H₁₄O₂S) C, H, N.

2-(3-Fluoro-5-methoxyphenyl)-5-(4-methoxyphenyl)thiophene (17a). The title compound was prepared by reaction of 2-bromo-5-(4-methoxyphenyl)thiophene (**16c**) (200 mg, 0.75 mmol), 3-fluoro-5-methoxybenzeneboronic acid (152 mg, 0.89 mmol), caesium carbonate (513 mg, 1.65 mmol) and tetrakis(triphenylphosphine) palladium (8.7 mg, 7.5 μmol) according to method A. The product was purified by CC (hexane/ethyl acetate 7:3); yield: 43 % (122 mg).

3-Fluoro-5-[5-(4-hydroxyphenyl)-2-thienyl]phenol (17). The title compound was prepared by reaction of 2-(3-fluoro-5-methoxyphenyl)-5-(4-methoxyphenyl)thiophene (**17a**) (100 mg, 0.32 mmol) and boron tribromide (1.92 mmol) according to method C. The product was purified by preparative TLC (hexane/ethyl acetate 7:3); yield: 88 % (80 mg); MS (APCI): 286 M⁺; Anal. (C₁₆H₁₁FO₂S) C, H, N.

5-[5-(4-Methoxyphenyl)-2-thienyl]-2-methylphenol (18a). The title compound was prepared by reaction of 5-bromo-2-methylphenol (250 mg, 1.34 mmol), [5-(4-methoxyphenyl)-2-thienyl]-boronic acid (**16b**) (690 mg, 2.95 mmol), caesium carbonate (914 mg, 2.94 mmol) and tetrakis(triphenylphosphine) palladium (15.5 mg, 13.4 μmol) according to method A. The product was purified by CC (hexane/ethyl acetate 7:3); yield: 47 % (193 mg).

5-[5-(4-Hydroxyphenyl)-2-thienyl]-2-methylphenol (18). The title compound was prepared by reaction of 5-[5-(4-methoxyphenyl)-2-thienyl]-2-methylphenol (**18a**) (161 mg, 0.54 mmol) and boron tribromide (3.24 mmol) according to method C. The product was purified by preparative TLC (hexane/ethyl acetate 7:3); yield: 27 % (42 mg); MS (ESI): 283 (M+H)⁺; Anal. (C₁₇H₁₄O₂S) C, H, N.

2-(4-Fluoro-3-methoxyphenyl)-5-(4-methoxyphenyl)thiophene (19a). The title compound was prepared by reaction of 2-bromo-5-(4-methoxyphenyl)thiophene (**16c**) (200 mg, 0.75 mmol), 4-fluoro-3-methoxybenzeneboronic acid (152 mg, 0.89 mmol), caesium carbonate (553 mg, 1.78 mmol) and tetrakis(triphenylphosphine) palladium (8.7 mg, 7.5 μmol) according to method A. The product was purified by CC (hexane/ethyl acetate 7:3); yield: 49 % (149 mg).

2-Fluoro-5-[5-(4-hydroxyphenyl)-2-thienyl]phenol (19). The title compound was prepared by reaction of 2-(4-fluoro-3-methoxyphenyl)-5-(4-methoxyphenyl)thiophene (**19a**) (100 mg, 0.32 mmol) and boron tribromide (1.92 mmol) according to method C. The product was purified by preparative TLC (hexane/ethyl acetate 7:3); yield: 88 % (80 mg); MS (ESI): 287 (M+H)⁺; Anal. (C₁₆H₁₁FO₂S) C, H, N.

2-(3,4-Dimethoxyphenyl)-5-(4-methoxyphenyl)thiophene (20a). The title compound was prepared by reaction of 2-bromo-5-(4-methoxyphenyl)thiophene (**16c**) (195 mg, 0.73 mmol), 3,4-dimethoxybenzene boronic acid (160 mg, 0.88 mmol), caesium carbonate (500 mg, 1.61 mmol) and tetrakis(triphenylphosphine) palladium (8.4 mg, 7.3 μmol) according to method A. The product was purified by CC (dichloromethane/methanol 99:1); yield: 46 % (119 mg).

4-[5-(4-Hydroxyphenyl)-2-thienyl]benzene-1,2-diol (20). The title compound was prepared by reaction of 2-(3,4-dimethoxyphenyl)-5-(4-methoxyphenyl)thiophene (**20a**) (100 mg, 0.31 mmol) and boron tribromide (2.79 mmol) according to method C. The product was purified by preparative TLC (hexane/ethyl acetate 1:1); yield: 17 % (49 mg); MS (ESI): 285 (M+H)⁺; Anal. (C₁₆H₁₂O₃S) C, H, N.

2-(4-Methoxy-3-methylphenyl)-5-(3-methoxyphenyl)thiophene (21a). The title compound was prepared by reaction of 2-bromo-5-(3-methoxyphenyl)thiophene (**1b**) (250 mg, 0.92 mmol), 3-methyl-4-methoxybenzeneboronic acid (152.8 mg, 0.92 mmol), sodium carbonate (243 mg, 2.36 mmol) and tetrakis(triphenylphosphine) palladium

(53.1 mg, 46.0 μ mol) according to method B. The product was purified by CC (hexane/ethyl acetate 7:3); yield: 54 % (154 mg).

4-[5-(3-Hydroxyphenyl)-2-thienyl]-2-methylphenol (21). The title compound was prepared by reaction of 2-(4-methoxy-3-methylphenyl)-5-(3-methoxyphenyl)thiophene (**21a**) (100 mg, 0.32 mmol) and boron tribromide (1.92 mmol) according to method C. The product was purified by preparative TLC (hexane/ethyl acetate 6:4); yield: 79 % (72 mg); MS (ESI): 281 (M-H)⁺; Anal. (C₁₇H₁₄O₂S) C, H, N.

2-(3,4-Dimethoxyphenyl)-5-(3-methoxyphenyl)thiophene (22a). The title compound was prepared by reaction of 2-bromo-5-(3-methoxyphenyl)thiophene (**1b**) (206 mg, 1.14 mmol), 3,4-dimethoxybenzeneboronic acid (247 mg, 1.36 mmol), caesium carbonate (779 mg, 2.51 mmol) and tetrakis(triphenylphosphine) palladium (13.2 mg, 11.4 μ mol) according to method A. The product was purified by CC (dichloromethane/methanol 99:1); yield: 34 % (126 mg).

4-[5-(3-Hydroxyphenyl)-2-thienyl]benzene-1,2-diol (22). The title compound was prepared by reaction of 2-(3,4-dimethoxyphenyl)-5-(3-methoxyphenyl)thiophene (**22a**) (100 mg, 0.32 mmol) and boron tribromide (2.88 mmol) according to method C. The product was purified by preparative TLC (hexane/ethyl acetate 6:4); yield: 61 % (56 mg); MS (ESI): 283 (M-H)⁺; Anal. (C₁₆H₁₂O₃S) C, H, N.

2-(3-Fluoro-4-methoxyphenyl)-5-(3-methoxyphenyl)thiophene (23a). The title compound was prepared by reaction of 2-bromo-5-(3-methoxyphenyl)thiophene (**1b**) (370 mg, 1.37 mmol), 3-fluoro-4-methoxybenzeneboronic acid (255 mg, 1.50 mmol), caesium carbonate (717 mg, 3.01 mmol) and tetrakis(triphenylphosphine) palladium (15.8 mg, 13.7 μ mol) according to method A. The product was purified by CC (hexane/ethyl acetate 7:3); yield: 98 % (421 mg).

2-Fluoro-4-[5-(3-hydroxyphenyl)-2-thienyl]phenol (23). The title compound was prepared by reaction of 2-(3-fluoro-4-methoxyphenyl)-5-(3-methoxyphenyl)thiophene (**23a**) (240 mg, 0.76 mmol) and boron tribromide (4.56 mmol) according to method C. The product was purified by preparative TLC (hexane/ethyl acetate 1:1); yield: 90 % (195 mg); MS (ESI): 285 (M-H)⁺; Anal. (C₁₆H₁₁FO₂S) C, H, N.

2-(3-Methoxyphenyl)-5-[4-methoxy-3-(trifluoromethyl)phenyl]thiophene (24a). The title compound was prepared by reaction of 2-bromo-5-(3-methoxyphenyl)thiophene (**1b**) (408 mg, 1.51 mmol), 3-trifluoromethyl-4-methoxybenzeneboronic acid (398 mg, 1.81 mmol), caesium carbonate (1033 mg, 3.32 mmol) and tetrakis(triphenylphosphine) palladium (17.5 mg, 15.1 μ mol) according to method A. The product was purified by CC (hexane/ethyl acetate 7:3); yield: 75 % (412 mg).

4-[5-(3-Hydroxyphenyl)-2-thienyl]-2-(trifluoromethyl)phenol (24). The title compound was prepared by reaction of 2-(3-methoxyphenyl)-5-[4-methoxy-3-(trifluoromethyl)phenyl]thiophene (**24a**) (300 mg, 0.82 mmol) and boron tribromide (4.95 mmol) according to method C. The product was purified by preparative TLC (hexane/ethyl acetate 1:1); yield: 98 % (272 mg); MS (ESI): 285 (M-H)⁺; Anal. (C₁₇H₁₁F₃O₂S) C, H, N.

2-(6-Methoxybiphenyl-3-yl)-5-(3-methoxyphenyl)thiophene (25a). The title compound was prepared by reaction of 2-bromo-5-(3-methoxyphenyl)thiophene (**1b**) (287 mg, 1.07 mmol), [6-methoxy-1,1'-biphenyl-3-yl]boronic acid (**25b**) (338 mg, 1.29 mmol), sodium carbonate (250 mg, 2.35 mmol) and tetrakis(triphenylphosphine) palladium (61.8 mg, 53.5 μ mol) according to method B. The product was purified by CC (hexane/ethyl acetate 7:3); yield: 35 % (135 mg).

5-[5-(3-Hydroxyphenyl)-2-thienyl]biphenyl-2-ol (25). The title compound was prepared by reaction of 2-(6-methoxybiphenyl-3-yl)-5-(3-methoxyphenyl)thiophene (**25a**) (100 mg, 0.26 mmol) and boron tribromide (1.56 mmol) according to method C. The product was purified by preparative TLC (hexane/ethyl acetate 1:1); yield: 88 % (81 mg); MS (ESI): 343 (M-H)⁺; Anal. (C₂₂H₁₆O₂S) C, H, N.

[2-Methoxy-5-[5-(3-methoxyphenyl)-2-thienyl]phenyl]methanol (26c). The title compound was prepared by reaction of 2-bromo-5-(3-methoxyphenyl)thiophene (**1b**) (408 mg, 1.51 mmol), [3-(hydroxymethyl)-4-methoxyphenyl]-boronic acid (**26d**) (329 mg, 1.81 mmol), caesium carbonate (1032 mg, 3.32 mmol) and tetrakis(triphenylphosphine) palladium (17.5 mg, 15.1 μ mol) according to method A. The product was purified by CC (hexane/ethyl acetate 8:2); yield: 12 % (59 mg).

2-Methoxy-5-[5-(3-methoxyphenyl)-2-thienyl]benzaldehyde (26b). To a solution of [2-methoxy-5-[5-(3-methoxyphenyl)-2-thienyl]phenyl]methanol (**26c**) (100 mg, 0.31 mmol, 1 eq) in dichloromethane, pyridium chlorochromate (66 mg, 0.31 mmol, 1 eq) was added in small portions over 5 min and stirred at rt. After 30 min, the reaction was quenched with water. The resulting organic layer was dried over sodium sulfate, filtered and concentrated to dryness. The title compound was not characterized and used in the next step without purification.

Ethyl (2E)-3-[2-Methoxy-5-[5-(3-methoxyphenyl)-2-thienyl]phenyl]acrylate (26a). To a solution of sodium hydride (10.4 mg, 0.43 mmol, 1 eq) in anhydrous THF triethyl phosphonoacetate (93 μ L, 0.46 mmol, 1.1 eq) was

added dropwise and stirred at rt. After 15 min, 2-methoxy-5-[5-(3-methoxyphenyl)-2-thienyl]benzaldehyde (**26b**) (100 mg, 0.31 mmol, 0.6 eq) was added and stirred for 4 h at rt. To quench the reaction water was added and the resulting organic layer was washed with brine, dried over sodium sulfate, filtered, evaporated and purified by CC (hexane/ethyl acetate 7:3); yield: 98 % (120 mg).

Ethyl (2E)-3-[2-hydroxy-5-[5-(3-hydroxyphenyl)-2-thienyl]phenyl]acrylate (26). The title compound was prepared by reaction of ethyl (2E)-3-[2-methoxy-5-[5-(3-methoxyphenyl)-2-thienyl]phenyl]acrylate (**26a**) (60 mg, 0.15 mmol) and boron tribromide (0.90 mmol) according to method C. The product was purified by preparative TLC (hexane/ethyl acetate 1:1); yield: 17 % (10 mg); MS (APCI): 366 (M)⁺; Anal. (C₂₁H₁₈O₄S) C, H, N.

(2E)-3-[2-Methoxy-5-[5-(3-methoxyphenyl)-2-thienyl]phenyl]-N-phenylacrylamide (27a). Ethyl (2E)-3-[2-methoxy-5-[5-(3-methoxyphenyl)-2-thienyl]phenyl]acrylate (**26a**) (720 mg, 2.22 mmol, 1 eq) in a solution of THF/water (2:1), was refluxed for 20 h together with lithium hydroxide (320 mg, 13.33 mmol, 6 eq). After cooling to rt, ether was added, the aqueous layer was acidified with hydrochloric acid 1N and washed with dichloromethane. The combined organic layers were dried over sodium sulfate, filtered and evaporated under reduced pressure. The resulting carboxylic acid was solubilized in dichloromethane (180 mg, 0.53 mmol, 1 eq) and refluxed for 20 h with EDCI (102 mg, 0.53 mmol, 1 eq) and HOBt (72 mg, 0.53 mmol, 1 eq). After cooling to rt, the organic layer was washed with a 1.5 M sodium hydrogenocarbonate solution, brine, dried over sodium sulfate, evaporated under reduced pressure and purified by CC (hexane/ethyl acetate 7:3); yield: 51 % (120 mg); MS (ESI): 442 (M+H)⁺.

(2E)-3-[2-Hydroxy-5-[5-(3-hydroxyphenyl)-2-thienyl]phenyl]-N-phenylacrylamide (27).

The title compound was prepared by reaction of (2E)-3-[2-methoxy-5-[5-(3-methoxyphenyl)-2-thienyl]phenyl]-N-phenylacrylamide (**27a**) (55 mg, 0.13 mmol) and boron tribromide (0.78 mmol) according to method C. The product was purified by preparative TLC (hexane/ethyl acetate 4:6); yield: 31 % (17 mg); MS (ESI): 414 (M+H)⁺; Anal. (C₂₅H₁₉NO₃S) C, H, N.

3-[2-Methoxy-5-[5-(3-methoxyphenyl)-2-thienyl]phenyl]-N-phenylpropanamide (28a). (2E)-3-[2-Methoxy-5-[5-(3-methoxyphenyl)-2-thienyl]phenyl]-N-phenylacrylamide (**27a**) (50 mg, 0.11 mmol, 1 eq) was solubilized in a mixture of THF/EtOH (1:1). After addition of palladium hydroxide (1.7 mg, 0.01 mmol, 0.1 eq) the reaction was stirred at rt under nitrogen atmosphere for 20 h. The crude mixture was filtered and the organic layer was evaporated under reduced pressure; yield: quantitative.

3-[2-Hydroxy-5-[5-(3-hydroxyphenyl)-2-thienyl]phenyl]-N-phenylpropanamide (28). The title compound was prepared by reaction of 3-[2-methoxy-5-[5-(3-methoxyphenyl)-2-thienyl]phenyl]-N-phenylpropanamide (**28a**) (55 mg, 0.13 mmol) and boron tribromide (0.78 mmol) according to method C. The product was purified by preparative TLC (hexane/ethyl acetate 1:1); yield: 20 % (10 mg); MS (ESI): 416 (M+H)⁺; Anal. (C₂₅H₂₁NO₃S) C, H, N.

2-Bromo-5-(3-fluoro-4-methoxyphenyl)thiophene (29b). The title compound was prepared by reaction of 2,5-dibromothiophene (500 mg, 2.10 mmol), 3-fluoro-4-methoxybenzeneboronic acid (357 mg, 2.10 mmol), sodium carbonate (432 mg, 4.20 mmol) and tetrakis(triphenylphosphine) palladium (121 mg, 1.05 mmol) according to method B. The product was purified by CC (hexane/ethyl acetate 95:5); yield: 85 % (427 mg).

2-(3-Fluoro-4-methoxyphenyl)-5-(3-fluoro-5-methoxyphenyl)thiophene (29a). The title compound was prepared by reaction of 2-bromo-5-(3-fluoro-4-methoxyphenyl)thiophene (**29b**) (100 mg, 0.41 mmol), 3-fluoro-5-methoxybenzeneboronic acid (85 mg, 0.50 mmol), caesium carbonate (280 mg, 0.90 mmol) and tetrakis(triphenylphosphine) palladium (4.7 mg, 4.1 μmol) according to method A. The product was purified by CC (hexane/ethyl acetate 9:1); yield: 82 % (113 mg).

2-Fluoro-4-[5-(3-fluoro-5-hydroxyphenyl)thien-2-yl]phenol (29). The title compound was prepared by reaction of 2-(3-fluoro-4-methoxyphenyl)-5-(3-fluoro-5-methoxyphenyl)thiophene (**30a**) (100 mg, 0.30 mmol) and boron tribromide (1.80 mmol) according to method C. The product was purified by preparative TLC (hexane/ethyl acetate 6:4); yield: 38 % (35 mg); MS (APCI): 304 (M)⁺; Anal. (C₁₆H₁₀F₂O₂S) C, H, N.

2-(3-Fluoro-4-methoxyphenyl)-5-(4-fluoro-3-methoxyphenyl)thiophene (30a). The title compound was prepared by reaction of 2-bromo-5-(3-fluoro-4-methoxyphenyl)thiophene (**29b**) (100 mg, 0.41 mmol), 4-fluoro-3-methoxybenzeneboronic acid (85 mg, 0.50 mmol), caesium carbonate (279 mg, 0.90 mmol) and tetrakis(triphenylphosphine) palladium (4.7 mg, 4.1 μmol) according to method A. The product was purified by CC (hexane/ethyl acetate 9:1); yield: 72 % (100 mg).

2-Fluoro-4-[5-(4-fluoro-3-hydroxyphenyl)thien-2-yl]phenol (30). The title compound was prepared by reaction of 2-(3-fluoro-4-methoxyphenyl)-5-(3-fluoro-5-methoxyphenyl)thiophene (**30a**) (100 mg, 0.30 mmol) and boron tribromide (1.80 mmol) according to method C. The product was purified by preparative TLC (hexane/ethyl acetate 6:4); yield: 75 % (69 mg); MS (APCI): 304 (M)⁺; Anal. (C₁₆H₁₀F₂O₂S) C, H, N.

2-(3,5-Difluoro-4-methoxyphenyl)-5-(3-methoxyphenyl)thiophene (31a). The title compound was prepared by reaction of 2-bromo-5-(3-methoxyphenyl)thiophene (**1b**) (430 mg, 1.60 mmol), 3,5-difluoro-4-methoxybenzeneboronic acid (357 mg, 1.92 mmol), caesium carbonate (1094 mg, 3.52 mmol) and tetrakis(triphenylphosphine) palladium (18.5 mg, 16.0 μ mol) according to method A. The product was purified by CC (petroleum ether/ethyl acetate 9:1); yield: 42 % (223 mg).

2,6-Difluoro-4-[5-(3-hydroxyphenyl)-2-thienyl]phenol (31). The title compound was prepared by reaction of 2-(3,5-difluoro-4-methoxyphenyl)-5-(3-methoxyphenyl)thiophene (**31a**) (220 mg, 0.62 mmol) and boron tribromide (3.72 mmol) according to method C. The product was purified by preparative TLC (hexane/ethyl acetate 5:5); yield: 10 % (18 mg); MS (ESI): 305 (M+H)⁺; Anal. (C₁₆H₁₀F₂O₂S) C, H, N.

2-(3,4-Difluorophenyl)-5-(3-methoxyphenyl)thiophene (32a). The title compound was prepared by reaction of 2-bromo-5-(3-methoxyphenyl)thiophene (**1b**) (150 mg, 0.56 mmol), 3,4-difluorobenzeneboronic acid (105 mg, 0.67 mmol), caesium carbonate (383 mg, 1.23 mmol) and tetrakis(triphenylphosphine) palladium (6.5 mg, 5.6 μ mol) according to method A. The product was purified by CC (hexane/ethyl acetate 9:1); yield: 90 % (152 mg).

3-[5-(3,4-Difluorophenyl)-2-thienyl]phenol (32). The title compound was prepared by reaction of 2-(3,4-difluorophenyl)-5-(3-methoxyphenyl)thiophene (**32a**) (120 mg, 0.40 mmol) and boron tribromide (1.20 mmol) according to method C. The product was purified by CC (dichloromethane/methanol 99:1); yield: 85 % (98 mg); MS (ESI): 289 (M+H)⁺; Anal. (C₁₆H₉F₂OS) C, H, N.

4-(4-Methoxy-3-methylphenyl)-2-(3-methoxyphenyl)thiophene (34a). The title compound was prepared by reaction of 4-bromo-2-(3-methoxyphenyl)thiophene (**33b**) (400 mg, 1.49 mmol), 3-methyl-4-methoxybenzeneboronic acid (296 mg, 1.79 mmol), caesium carbonate (1019 mg, 3.27 mmol) and tetrakis(triphenylphosphine) palladium (17.2 mg, 14.9 μ mol) according to method A. The product was purified by CC (hexane/ethyl acetate 7:3); yield: 69 % (320 mg).

4-[5-(3-Hydroxyphenyl)-3-thienyl]-2-methylphenol (34). The title compound was prepared by reaction of 4-(4-methoxy-3-methylphenyl)-2-(3-methoxyphenyl)thiophene (**34a**) (180 mg, 0.58 mmol) and boron tribromide (3.48 mmol) according to method C. The product was purified by preparative TLC (hexane/ethyl acetate 1:1); yield: 54 % (88 mg); MS (ESI): 281 (M-H)⁺; Anal. (C₁₇H₁₄O₂S) C, H, N.

4-(3-Fluoro-4-methoxyphenyl)-2-(3-methoxyphenyl)thiophene (35a). The title compound was prepared by reaction of 4-bromo-2-(3-methoxyphenyl)thiophene (**33b**) (400 mg, 1.49 mmol), 3-fluoro-4-methoxybenzeneboronic acid (303 mg, 1.78 mmol), caesium carbonate (1019 mg, 3.30 mmol) and tetrakis(triphenylphosphine) palladium (17.2 mg, 14.9 μ mol) according to method A. The product was purified by CC (petroleum ether/ethyl acetate 9:1); yield: 80 % (403 mg).

2-Fluoro-4-[5-(3-hydroxyphenyl)-3-thienyl]phenol (35). The title compound was prepared by reaction of 4-(3-fluoro-4-methoxyphenyl)-2-(3-methoxyphenyl)thiophene (**35a**) (400 mg, 1.27 mmol) and boron tribromide (7.63 mmol) according to method C. The product was purified by CC (dichloromethane/methanol 98:2); yield: 22 % (88 mg); MS (ESI): 287 (M-H)⁺

4-(4-Methoxy-3-methylphenyl)-2-(3-methoxyphenyl)-1,3-thiazole (37a). The title compound was prepared by reaction of 5-bromo-2-(3-methoxyphenyl)-1,3-thiazole (**36b**) (402 mg, 1.49 mmol), 3-methyl-4-methoxybenzeneboronic acid (247 mg, 1.79 mmol), caesium carbonate (1019 mg, 3.27 mmol) and tetrakis(triphenylphosphine) palladium (17.2 mg, 14.9 μ mol) according to method A. The product was purified by CC (hexane/ethyl acetate 7:3); yield: 69 % (320 mg).

4-[2-(3-Hydroxyphenyl)-1,3-thiazol-5-yl]-2-methylphenol (37). The title compound was prepared by reaction of 4-(4-methoxy-3-methylphenyl)-2-(3-methoxyphenyl)-1,3-thiazole (**37a**) (80 mg, 0.26 mmol) and boron tribromide (1.56 mmol) according to method C. The product was purified by preparative TLC (hexane/ethyl acetate 3:7); yield: 16 % (11 mg), MS (ESI): 274 (M+H)⁺; Anal. (C₁₆H₁₃NO₂S) C, H, N.

3,4''-Dimethoxy-4-methyl-1,1':4',1''-terphenyl (39a). The title compound was prepared by reaction of 4'-bromo-3-methoxybiphenyl (**38b**) (230 mg, 0.87 mmol), 4-methoxy-3-methylbenzeneboronic acid (172 mg, 1.04 mmol), caesium carbonate (595 mg, 1.91 mmol) and tetrakis(triphenylphosphine) palladium (10.1 mg, 8.7 μ mol) according to method A. The product was purified by CC (hexane/ethyl acetate 98:2); yield: 53 % (140 mg).

4-Methyl-1,1':4',1''-terphenyl-3,4''-diol (39). The title compound was prepared by reaction of 3,3''-dimethoxy-4-methyl-1,1':4',1''-terphenyl (**41a**) (120 mg, 0.39 mmol) and boron tribromide (2.34 mmol) according to method C. The product was purified by preparative TLC (dichloromethane/methanol 97:3); yield: 38 % (42 mg); MS (ESI): 277 (M+H)⁺.

3-Fluoro-3'',4-dimethoxy-1,1':4',1''-terphenyl (40a). The title compound was prepared by reaction of 4'-bromo-3-methoxybiphenyl (**38b**) (175 mg, 0.67 mmol), 3-fluoro-4-methoxybenzeneboronic acid (136.7 mg, 0.88

mmol), caesium carbonate (457 mg, 1.47 mmol) and tetrakis(triphenylphosphine) palladium (7.7 mg, 6.7 μ mol) according to method A. The product was purified by CC (hexane/ethyl acetate 98:2); yield: 58 % (117 mg).

3'-Fluoro-1,1':4',1''-terphenyl-3,4''-diol (40). The title compound was prepared by reaction of 3-fluoro-3'',4-dimethoxy-1,1':4',1''-terphenyl (**40a**) (115 mg, 0.37 mmol) and boron tribromide (2.22 mmol) according to method C. The product was purified by preparative TLC (dichloromethane/methanol 99:1); yield: 62 % (65 mg); MS (ESI): 281 (M+H)⁺.

4-Fluoro-3,3''-dimethoxy-1,1':4',1''-terphenyl (42a). The title compound was prepared by reaction of 4'-bromo-3-methoxybiphenyl (**38b**) (200 mg, 0.76 mmol), 4-fluoro-3-methoxybenzeneboronic acid (154 mg, 0.91 mmol), caesium carbonate (520 mg, 1.67 mmol) and tetrakis(triphenylphosphine) palladium (8.8 mg, 7.6 μ mol) according to method A. The product was purified by CC (hexane/ethyl acetate 9:1); yield: 75 % (175 mg).

4-Fluoro-1,1':4',1''-terphenyl-3,3''-diol (42). The title compound was prepared by reaction of 4-fluoro-3,3''-dimethoxy-1,1':4',1''-terphenyl (**42a**) (175 mg, 0.57 mmol) and boron tribromide solution (3.42 mmol) according to method C. The product was purified by preparative TLC (hexane/ethyl acetate 1:1); yield: 63 % (100 mg); MS (ESI): 281 (M+H)⁺.

Biological Methods

[2, 4, 6, 7-³H]-E2 and [2, 4, 6, 7-³H]-E1 were bought from Perkin Elmer, Boston. Quickszint Flow 302 scintillator fluid was bought from Zinsser Analytic, Frankfurt.

17 β -HSD1 and 17 β -HSD2 were obtained from human placenta according to previously described procedures.^{31,37,56} Fresh human placenta was homogenized and centrifuged. The pellet fraction contains the microsomal 17 β -HSD2, while 17 β -HSD1 was obtained after precipitation with ammonium sulfate from the cytosolic fraction.

Inhibition of 17 β -HSD1

Inhibitory activities were evaluated by a well established method with minor modifications.⁵⁷⁻⁵⁹ Briefly, the enzyme preparation was incubated with NADH [500 μ M] in the presence of potential inhibitors at 37 °C in a phosphate buffer (50 mM) supplemented with 20 % of glycerol and EDTA (1mM). Inhibitor stock solutions were prepared in DMSO. Final concentration of DMSO was adjusted to 1 % in all samples. The enzymatic reaction was started by addition of a mixture of unlabelled- and [2, 4, 6, 7-³H]- E1 (final concentration: 500 nM, 0.15 μ Ci). After 10 min, the incubation was stopped with HgCl₂ and the mixture was extracted with ether. After evaporation, the steroids were dissolved in acetonitrile. E1 and E2 were separated using acetonitrile/water (45:55) as mobile phase in a C18 rp chromatography column (Nucleodur C18 Gravity, 3 μ m, Macherey-Nagel, Düren) connected to a HPLC-system (Agilent 1100 Series, Agilent Technologies, Waldbronn). Detection and quantification of the steroids were performed using a radioflow detector (Berthold Technologies, Bad Wildbad). The conversion rate was calculated according to following equation: $\%conversion = \frac{\%E2}{\%E2 + \%E1} \cdot 100$. Each value was calculated from at least three

independent experiments.

Inhibition of 17 β -HSD2

The 17 β -HSD2 inhibition assay was performed similarly to the 17 β -HSD1 procedure. The microsomal fraction was incubated with NAD⁺ [1500 μ M], test compound and a mixture of unlabelled- and [2, 4, 6, 7-³H]-E2 (final concentration: 500 nM, 0.11 μ Ci) for 20 min at 37 °C. Further treatment of the samples and HPLC separation was carried out as mentioned above.

ER affinity

The binding affinity of selected compounds to the ER α and ER β was determined according to Zimmermann et al.⁶⁰ Briefly, 0.25 pmol of ER α or ER β , respectively, were incubated with [2, 4, 6, 7-³H]-E2 (10 nM) and test compound for 1 h at rt. The potential inhibitors were dissolved in DMSO (5 % final concentration). Non-specific-binding was performed with diethylstilbestrol (10 μ M). After incubation, ligand-receptor complexes were selectively bound to hydroxyapatite (5 g/ 60 mL TE-buffer). The formed complex was separated, washed and resuspended in ethanol. For radiodetection, scintillator cocktail (Quickszint 212, Zinsser Analytic, Frankfurt) was added and samples were measured in a liquid scintillation counter (Rack Beta Primo 1209, Wallac, Turku). For determination of the relative binding affinity (RBA), inhibitor and E2 concentrations required to displace 50 % of

the receptor bound labelled E2 were determined. RBA values were calculated according to the following equation:

$$RBA[\%] = \frac{IC_{50}(E2)}{IC_{50}(compound)} \cdot 100. \text{ The RBA value for E2 was arbitrarily set at } 100 \%$$

Evaluation of the estrogenic activity using T-47D cells

Phenol red-free medium was supplemented with sodium bicarbonate (2 g/L), streptomycin (100 µg/mL), insuline zinc salt (10 µg/mL), sodium pyruvate (1 mM), L-glutamine (2 mM), penicillin (100 U/mL) and DCC-FCS 5% (v/v). RPMI 1640 (without phenol red) was used for the experiments. Cells were grown for 48 h in phenol red-free medium. Compound **21** was added at a final concentration of 100 nM. Inhibitors and E2 were diluted in ethanol (final ethanol concentration was adjusted to 1%). As a positive control E2 was added at a final concentration of 0.1 nM. Ethanol was used as negative control. Medium was changed every two to three days and supplemented with the respective additive. After eight days of incubation, the cell viability was evaluated measuring the reduction of 3-(4,5-dimethylthiazol-2-yl)-2,5-diphenyl-tetrazoliumbromide (MTT). The cleavage of MTT to a blue formazan by mitochondrial succinat-dehydrogenase was quantified spectrophotometrically at 590 nm as described by Denizot and Lang⁶¹ with minor modifications. The control proliferation was arbitrarily set at 1 and the stimulation induced by the inhibitor was calculated according to following equation: $\% \text{ stimulation} = \frac{[\text{proliferation}(\text{compound} - \text{induced}) - 1]}{[\text{proliferation}(E2 - \text{induced}) - 1]} \cdot 100\%$. Each value is calculated as a mean value of at least three independent experiments

Inhibition of human hepatic CYPs

The commercially available P450 inhibition kits from BD GentestTM (Heidelberg, Germany) were used according to the instructions of the manufacturer. Compounds **21**, **23** and **37** were tested for inhibition of the following enzymes: CYP3A4, 2D6 and 2C19. Inhibitory potencies were determined as IC₅₀ values.

In-Vivo Pharmacokinetics

Male Wistar rats weighing 300-330 g (Janvier France) were housed in a temperature- controlled room (20-22 °C) and maintained in a 12 h light/12 h dark cycle. Food and water were available *ad libitum*. They were anesthetized with a ketamine (135 mg/kg)/ xylazine (10 mg/kg) mixture and cannulated with silicone tubing via the right jugular vein and attached to the skull with dental cement. Prior to the first blood sampling, animals were connected to a counterbalanced system and tubing to perform blood sampling in the freely moving rat.

Compounds **21** and **23** were applied orally in a cassette dosing in 4 rats at the dose of 10 mg/kg body weight by using a feeding needle. The compounds were dissolved in a mixture labrasol/water (1:1) and given at a volume of 5mL/kg. Blood samples (0.2 mL) were taken at 0, 1, 2, 3, 4, 6, 8, 10 and 24 h postdose and collected in heparinised tubes. They were centrifuged at 3000g for 10 min, and plasma was harvested and kept at -20 °C until analyzed.

HPLC-MS/MS analysis and quantification of the samples was carried out on a Surveyor-HPLC-system coupled with a TSQ Quantum (Thermo/Fisher) triple quadrupole mass spectrometer equipped with an electrospray interface (ESI).

Computational Chemistry

Molecular Modelling

All molecular modelling studies were performed on Intel(R) P4 CPU 3.00 GHz running Linux CentOS 5.2. The X-ray structures of 17β-HSD1 (PDB-ID: 1A27, 1FDT and 1I5R) were obtained from the Protein Databank⁶² and further prepared using the BIOPOLYMER module of SYBYL v8.0 (Sybyl, Tripos Inc., St. Louis, Missouri, USA). Water molecules, E2 (or HYC for 1I5R) and sulfate ions were stripped from the PDB files and missing protein atoms were added and correct atom types set. Finally hydrogen atoms and neutral end groups were added. All basic and acidic residues were considered protonated and deprotonated, respectively. Since almost all histidines are oriented toward the outer part of the enzyme, accessible for the surface, they were considered as protonated (HIP) after a prediction run made by MolProbity.⁶³ For 1I5R the cofactor NADPH was merged into the enzyme after an accurate overlay with the hybrid inhibitor HYC and the X-rays 1A27 and 1FDT. Further, every crystal structure was minimized for 500 steps with the steepest descent minimizer as implemented in SYBYL with the backbone atoms

kept at fixed positions in order to fix close contacts, followed by 2000 steps conjugate gradient minimization requested for an overall better starting structure.

Inhibitor **23** was built with SYBYL and energy-minimized in MMFF94s force-field as implemented in Sybyl. Subsequently an *ab-initio* geometry optimizations was performed in gas phase at the B3LYP/6-311++G (d,p) level of density functional theory (DFT) by means of the Gaussian03 software,^{64,65} in order to obtain the RESP charges of compound **23**.

Two different softwares were used for docking studies: GOLDv3.2⁶⁶ and Autodock4,^{67,68} using the graphical user interface AutoDockTools (ADT 1.5.2). Since both allow flexible docking of ligands, no conformational search was employed to the ligand structure. For both programs the compound **23** was docked in 50 independent genetic algorithm (GA) runs.

GOLDv3.2: Active-site origin was set at the center of the steroid binding site, while the radius was set equal to 13 Å. The automatic active-site detection was switched on. Further, a slightly modified GOLDScore fitness function (increased scaling for hydrophobic contacts) was used and genetic algorithm default parameters were set as suggested by the GOLD authors.

Autodock4: The docking area has been defined by a box, centered on the mass center of the CD-rings of the cocrystallized E2. Grids points of 60 × 70 × 74 with 0.375 Å spacing were calculated around the docking area for all the ligand atom types using AutoGrid4. The Lamarckian genetic algorithm local search (GALS) method was used. Each docking run was performed with a population size of 200. A mutation rate of 0.02 and a crossover rate of 0.8 were used to generate new docking trials for subsequent generations. The GALS method evaluates a population of possible docking solutions and propagates the most successful individuals from each generation into the next one.

Both programs performed in a similar way, supporting the herein suggested binding modes. The quality of the docked poses was evaluated based mainly on visual inspection of the putative binding modes of the ligand, and secondly on the scoring functions, which give a good measure to discriminate between the found binding modes for one single X-ray conformation, but do not help us to compare the poses of different X-rays.

MEP

For selected compounds *ab-initio* geometry optimisations were performed gas phase at the B3LYP/6-311++G (d,p) level of density functional theory (DFT) by means of the Gaussian03 software and the molecular electrostatics potential map (MEP) was plotted using GaussView3, the 3D molecular graphics package of Gaussian.⁶⁹ These electrostatic potential surfaces were generated by mapping 6-311++G electrostatic potentials onto surfaces of molecular electron density (isovalue = 0.0002e/Å). The MEP maps are color coded, where red stands for negative values ($3.1 \cdot 10^{-2}$ Hartree) and blue for positive ones ($4.5 \cdot 10^{-2}$ Hartree).

Acknowledgments. We are grateful to the Deutsche Forschungsgemeinschaft (HA1315/8-1) for financial support. We thank Anja Paluszczak, Beate Geiger and Jannine Ludwig for their help in performing the enzyme inhibition tests (17β-HSD1, 17β-HSD2, ERα and ERβ) and Dr. Ursüller M -Viera, Pharmacelsus CRO Saarbrücken Germany, for the hepatic CYP inhibition tests. Patricia Kruchten is grateful to the European Postgraduate School 532 (DFG) for a scholarship.

Supporting Information Available. NMR spectroscopic data for all compounds, elemental analysis results of compounds **3** to **6**, **8** to **32**, **34** and **37**, purity determination of compounds **35**, **39**, **41** and **42** using LC/MS and overlay of the binding poses of compound **23** obtained with the two 1FDT X-rays. This material is available free of charge via the internet at <http://pubs.acs.org>.

References

- (1) Travis, R. C.; Key, T. J. Oestrogen exposure and breast cancer risk. *Breast Cancer Res.* **2003**, *5*, 239-247.
- (2) Dizerega, G. S.; Barber, D. L.; Hodgen, G. D. Endometriosis: role of ovarian steroids in initiation, maintenance and suppression. *Fertil. Steril.* **1980**, *33*, 649-653.
- (3) Miller, W. R.; Bartlett, J. M.; Canney, P.; Verrill, M. Hormonal therapy for postmenopausal breast cancer: the science of sequencing. *Breast Cancer Res. Treat.* **2007**, *103*, 149-160.
- (4) Bush, N. J. Advances in hormonal therapy for breast cancer. *Semin. Oncol. Nurs.* **2007**, *23*, 46-54.
- (5) Adamo, V.; Iorfida, M.; Montalto, E.; Festa, V.; Garipoli, C.; Scimone, A.; Zanghi, M.; Caristi, N. Overview and new strategies in metastatic breast cancer (MBC) for treatment of tamoxifen-resistant patients. *Ann. Oncol.* **2007**, *18 Suppl 6*, vi53-57.

- (6) Ohnesorg, T.; Keller, B.; Hrabe de Angelis, M.; Adamski, J. Transcriptional regulation of human and murine 17beta-hydroxysteroid dehydrogenase type-7 confers its participation in cholesterol biosynthesis. *J. Mol. Endocrinol.* **2006**, *37*, 185-197.
- (7) Shehu, A.; Mao, J.; Gibori, G. B.; Halperin, J.; Le, J.; Devi, Y. S.; Merrill, B.; Kiyokawa, H.; Gibori, G. Prolactin receptor-associated protein/17beta-hydroxysteroid dehydrogenase type 7 gene (Hsd17b7) plays a crucial role in embryonic development and fetal survival. *Mol. Endocrinol.* **2008**, *22*, 2268-2277.
- (8) Sakurai, N.; Miki, Y.; Suzuki, T.; Watanabe, K.; Narita, T.; Ando, K.; Yung, T. M.; Aoki, D.; Sasano, H.; Handa, H. Systemic distribution and tissue localizations of human 17beta-hydroxysteroid dehydrogenase type 12. *J. Steroid Biochem. Mol. Biol.* **2006**, *99*, 174-181.
- (9) Day, J. M.; Foster, P. A.; Tutill, H. J.; Parsons, M. F.; Newman, S. P.; Chander, S. K.; Allan, G. M.; Lawrence, H. R.; Vicker, N.; Potter, B. V.; Reed, M. J.; Purohit, A. 17beta-Hydroxysteroid dehydrogenase type 1, and not type 12, is a target for endocrine therapy of hormone-dependent breast cancer. *Int. J. Cancer* **2008**, *122*, 1931-1940.
- (10) Gunnarsson, C.; Hellqvist, E.; Stål, O. 17beta-Hydroxysteroid dehydrogenases involved in local oestrogen synthesis have prognostic significance in breast cancer. *Br. J. Cancer* **2005**, *92*, 547-552.
- (11) Gunnarsson, C.; Olsson, B. M.; Stål, O. Abnormal expression of 17beta-hydroxysteroid dehydrogenases in breast cancer predicts late recurrence. *Cancer Res.* **2001**, *61*, 8448-8451.
- (12) Miyoshi, Y.; Ando, A.; Shiba, E.; Taguchi, T.; Tamaki, Y.; Noguchi, S. Involvement of up-regulation of 17beta-hydroxysteroid dehydrogenase type 1 in maintenance of intratumoral high estradiol levels in postmenopausal breast cancers. *Int. J. Cancer* **2001**, *94*, 685-689.
- (13) Suzuki, T.; Moriya, T.; Ariga, N.; Kaneko, C.; Kanazawa, M.; Sasano, H. 17Beta-hydroxysteroid dehydrogenase type 1 and type 2 in human breast carcinoma: a correlation to clinicopathological parameters. *Br. J. Cancer* **2000**, *82*, 518-523.
- (14) Šmuc, T.; Pucelj Ribič, M.; Šinkovec, J.; Husen, B.; Thole, H.; Lanišnik Rižner, T. Expression analysis of the genes involved in estradiol and progesterone action in human ovarian endometriosis. *Gynecol. Endocrinol.* **2007**, *23*, 105-111.
- (15) Husen, B.; Huhtinen, K.; Poutanen, M.; Kangas, L.; Messinger, J.; Thole, H. Evaluation of inhibitors for 17beta-hydroxysteroid dehydrogenase type 1 in vivo in immunodeficient mice inoculated with MCF-7 cells stably expressing the recombinant human enzyme. *Mol. Cell. Endocrinol.* **2006**, *248*, 109-113.
- (16) Husen, B.; Huhtinen, K.; Saloniemi, T.; Messinger, J.; Thole, H.; Poutanen, M. Human hydroxysteroid (17-beta) dehydrogenase 1 expression enhances estrogen sensitivity of MCF-7 breast cancer cell xenografts. *Endocrinology* **2006**, *147*, 5333-5339.
- (17) Penning, T. M. 17beta-hydroxysteroid dehydrogenase: inhibitors and inhibitor design. *Endocr. Relat. Cancer* **1996**, *3*, 41-56.
- (18) Poirier, D. Inhibitors of 17 beta-hydroxysteroid dehydrogenases. *Curr. Med. Chem.* **2003**, *10*, 453-477.
- (19) Brožic, P.; Lanišnik Rižner, T.; Gobec, S. Inhibitors of 17beta-hydroxysteroid dehydrogenase type 1. *Curr. Med. Chem.* **2008**, *15*, 137-150 and references therein cited.
- (20) Poirier, D. Advances in development of inhibitors of 17beta hydroxysteroid dehydrogenases. *Anticancer Agents Med. Chem.* **2009**, *9*, 642-660.
- (21) Messinger, J.; Hirvelä, L.; Husen, B.; Kangas, L.; Koskimies, P.; Pentikäinen, O.; Saarenketo, P.; Thole, H. New inhibitors of 17beta-hydroxysteroid dehydrogenase type 1. *Mol. Cell. Endocrinol.* **2006**, *248*, 192-198.
- (22) Karkola, S.; Lilienkamp, A.; Wähälä, K. A 3D QSAR model of 17beta-HSD1 inhibitors based on a thieno[2,3-d]pyrimidin-4(3H)-one core applying molecular dynamics simulations and ligand-protein docking. *ChemMedChem* **2008**, *3*, 461-472.
- (23) Allan, G. M.; Vicker, N.; Lawrence, H. R.; Tutill, H. J.; Day, J. M.; Huchet, M.; Ferrandis, E.; Reed, M. J.; Purohit, A.; Potter, B. V. Novel inhibitors of 17beta-hydroxysteroid dehydrogenase type 1: templates for design. *Bioorg. Med. Chem.* **2008**, *16*, 4438-4456.
- (24) Frotscher, M.; Ziegler, E.; Marchais-Oberwinkler, S.; Kruchten, P.; Neugebauer, A.; Fetzer, L.; Scherer, C.; Müller-Vieira, U.; Messinger, J.; Thole, H.; Hartmann, R. W. Design, synthesis and biological evaluation of (hydroxyphenyl)-naphthalene and quinoline derivatives: potent and selective non steroidal inhibitors of 17beta-hydroxysteroid dehydrogenase type 1 (17beta-HSD1) for the treatment of estrogen-dependent diseases. *J. Med. Chem.* **2008**, *51*, 2158-2169.
- (25) Marchais-Oberwinkler, S.; Kruchten, P.; Frotscher, M.; Ziegler, E.; Neugebauer, A.; Bhoga, U. D.; Bey, E.; Müller-Vieira, U.; Messinger, J.; Thole, H.; Hartmann, R. W. Substituted 6-phenyl-2-naphthols. Potent and

- selective non-steroidal inhibitors of 17 β -hydroxysteroid dehydrogenase type 1 (17 β -HSD1): design, synthesis, biological evaluation and pharmacokinetics. *J. Med. Chem.* **2008**, *51*, 4685-4698.
- (26) Marchais-Oberwinkler, S.; Frotscher, M.; Ziegler, E.; Werth, R.; Kruchten, P.; Messinger, J.; Thole, H.; Hartmann, R. W. Structure–activity study in the class of 6-(3-hydroxyphenyl)naphthalenes leading to an optimization of a pharmacophore model for 17 β -hydroxysteroid dehydrogenase type 1 (17 β -HSD1) inhibitors. *Mol. Cell. Endocrinol.* **2009**, *301*, 205-211.
- (27) Bey, E.; Marchais-Oberwinkler, S.; Kruchten, P.; Frotscher, M.; Werth, R.; Oster, A.; Algül, O.; Neugebauer, A.; Hartmann, R. W. Design, synthesis and biological evaluation of bis(hydroxyphenyl) azoles as potent and selective non-steroidal inhibitors of 17 β -hydroxysteroid dehydrogenase type 1 (17 β -HSD1) for the treatment of estrogen-dependent diseases. *Bioorg. Med. Chem.* **2008**, *16*, 6423-6435.
- (28) Bey, E.; Marchais-Oberwinkler, S.; Werth, R.; Negri, M.; Al-Soud, Y. A.; Kruchten, P.; Oster, A.; Frotscher, M.; Birk, B.; Hartmann, R. W. Design, synthesis, biological evaluation and pharmacokinetics of bis(hydroxyphenyl) substituted azoles, thiophenes, benzenes and aza-benzenes as potent and selective non-steroidal inhibitors of 17 β -hydroxysteroid dehydrogenase type 1 (17 β -HSD1). *J. Med. Chem.* **2008**, *51*, 6725-6739.
- (29) Kruchten, P.; Werth, R.; Bey, E.; Oster, A.; Marchais-Oberwinkler, S.; Frotscher, M.; Hartmann, R. W. Selective inhibition of 17 β -hydroxysteroid dehydrogenase type 1 (17 β -HSD1) reduces estrogen responsive cell growth of T-47D breast cancer cells. *J. Steroid Biochem. Mol. Biol.* **2009**, *114*, 200-206.
- (30) Kruchten, P.; Werth, R.; Marchais-Oberwinkler, S.; Bey, E.; Ziegler, E.; Oster, A.; Frotscher, M.; Hartmann, R. W. Development of biological assays for the identification of selective inhibitors of estradiol formation from estrone in rat liver preparations. *C. R. Chim.* **2009**, doi:10.1016/j.crci.2009.05.005.
- (31) Kruchten, P.; Werth, R.; Marchais-Oberwinkler, S.; Frotscher, M.; Hartmann, R. W. Development of a biological screening system for the evaluation of highly active and selective 17 β -HSD1-inhibitors as potential therapeutic agents. *Mol. Cell. Endocrinol.* **2009**, *301*, 154-157.
- (32) Al-Soud, Y. A.; Bey, E.; Oster, A.; Marchais-Oberwinkler, S.; Werth, R.; Kruchten, P.; Frotscher, M.; Hartmann, R. W. The role of the heterocycle in bis(hydroxyphenyl) triazoles for inhibition of 17 β -hydroxysteroid dehydrogenase (17 β -HSD) type 1 and type 2. *Mol. Cell. Endocrinol.* **2009**, *301*, 212-215.
- (33) Ghosh, D.; Pletnev, V. Z.; Zhu, D. W.; Wawrzak, Z.; Duax, W. L.; Pangborn, W.; Labrie, F.; Lin, S.-X. Structure of human estrogenic 17 β -hydroxysteroid dehydrogenase at 2.20 Å resolution. *Structure* **1995**, *3*, 503-513.
- (34) Azzi, A.; Rehse, P. H.; Zhu, D. W.; Campbell, R. L.; Labrie, F.; Lin, S.-X. Crystal structure of human estrogenic 17 β -hydroxysteroid dehydrogenase complexed with 17 β -estradiol. *Nat. Struct. Biol.* **1996**, *3*, 665-668.
- (35) Breton, R.; Housset, D.; Mazza, C.; Fontecilla-Camps, J. C. The structure of a complex of human 17 β -hydroxysteroid dehydrogenase with estradiol and NADP⁺ identifies two principal targets for the design of inhibitors. *Structure* **1996**, *4*, 905-915.
- (36) Mazza, C. Human type I 17 β -hydroxysteroid dehydrogenase: site directed mutagenesis and X-Ray crystallography structure-function analysis PhD Thesis, Université Joseph Fourier: Grenoble, 1997.
- (37) Qiu, W.; Campbell, R. L.; Gangloff, A.; Dupuis, P.; Boivin, R. P.; Tremblay, M. R.; Poirier, D.; Lin, S.-X. A concerted, rational design of type 1 17 β -hydroxysteroid dehydrogenase inhibitors: estradiol-adenosine hybrids with high affinity. *FASEB J.* **2002**, *16*, 1829-1831.
- (38) Miyaura, N.; Suzuki, A. The palladium catalysed cross-coupling reaction of phenylboronic acid with haloarenes in the presence of bases. *Synth. Commun.* **1995**, *11*, 513-519.
- (39) Togo, H.; Nogami, G.; Yokoyama, M. Synthetic application of poly[styrene(iodoso diacetate)]. *Synlett* **1998**, *5*, 534-536.
- (40) Emmons, W. D. The utility of phosphonate carbanions in olefin synthesis. *J. Am. Chem. Soc.* **1961**, *83*, 1733-1738.
- (41) Pascal, C.; Dubois, J.; Guénard, D.; Guéritte, F. Synthesis of biphenyls mimicking the structure of the antimitotic rhazinilam. *J. Org. Chem.* **1998**, *63*, 6414-6420.
- (42) Hwang, K.-J.; O'Neil, J. P.; Katzenellenbogen, J. A. 5,6,11,12-Tetrahydrochrysenes: synthesis of rigid stilbene systems designed to be fluorescent ligands for the estrogen receptor. *J. Org. Chem.* **1992**, *57*, 1262-1271.

- (43) Sherbet, D. P.; Guryev, O. L.; Papari-Zareei, M.; Mizrahi, D.; Rambally, S.; Akbar, S.; Auchus, R. J. Biochemical factors governing the steady-state estrone/estradiol ratios catalyzed by human 17beta-hydroxysteroid dehydrogenases types 1 and 2 in HEK-293 cells. *Endocrinology* **2009**, *150*, 4154-4162.
- (44) Sherbet, D. P.; Papari-Zareei, M.; Khan, N.; Sharma, K. K.; Brandmaier, A.; Rambally, S.; Chattopadhyay, A.; Andersson, S.; Agarwal, A. K.; Auchus, R. J. Cofactors, redox state, and directional preferences of hydroxysteroid dehydrogenases. *Mol. Cell. Endocrinol.* **2007**, *265-266*, 83-88.
- (45) Bruno, I. J.; Cole, J. C.; Lommerse, J. P. M.; Rowland, R. S.; Taylor, T.; Verdonk, M. L. Isostar: A library of information about non-bonded interactions. *J. Comput. Chem.* **1997**, *11*, 523-537.
- (46) Haggmann, W. K. The many roles for fluorine in medicinal chemistry. *J. Med. Chem.* **2008**, *51*, 4359-4369.
- (47) Bohm, H. J.; Banner, D.; Bendels, S.; Kansy, M.; Kuhn, B.; Muller, K.; Obst-Sander, U.; Stahl, M. Fluorine in medicinal chemistry. *ChemBioChem* **2004**, *5*, 637-643.
- (48) Muller, K.; Faeh, C.; Diederich, F. Fluorine in pharmaceuticals: looking beyond intuition. *Science* **2007**, *317*, 1881-1886.
- (49) Poirier, D.; Boivin, R. P.; Tremblay, M. R.; Bérubé, M.; Qiu, W.; Lin, S.-X. Estradiol-adenosine hybrid compounds designed to inhibit type 1 17beta-hydroxysteroid dehydrogenase. *J. Med. Chem.* **2005**, *48*, 8134-8147.
- (50) Bérubé, M.; Poirier, D. Synthesis of simplified hybrid inhibitors of type 1 17beta-hydroxysteroid dehydrogenase via cross-metathesis and Sonogashira coupling reactions. *Org. Lett.* **2004**, *6*, 3127-3130.
- (51) Fournier, D.; Poirier, D.; Mazumdar, M.; Lin, S.-X. Design and synthesis of bisubstrate inhibitors of type 1 17beta-hydroxysteroid dehydrogenase: Overview and perspectives. *Eur. J. Med. Chem.* **2008**, *43*, 2298-2306.
- (52) Hartman, J.; Lindberg, K.; Morani, A.; Inzunza, J.; Strom, A.; Gustafsson, J. A. Estrogen receptor beta inhibits angiogenesis and growth of T47D breast cancer xenografts. *Cancer Res.* **2006**, *66*, 11207-11213.
- (53) Smith, G.; Mikkelsen, G.; Eskildsen, J.; Bundgaard, C. The synthesis and SAR of 2-arylsulfanylphenyl-1-oxyalkylamino acids as GlyT-1 inhibitors. *Bioorg. Med. Chem.* **2006**, *16*, 3981-3884.
- (54) Pfahl, M.; Al-Shamma, H. A.; Fanjul, A.; Pleyne, D. P. M.; Spruce, L. W.; Wiemann, T. R.; Ibarra, J. B.; Tachdjian, C. Preparation of benzylidenethiazolidenediones and analogs as antitumor agents, 2002.
- (55) Duggan, H. M. E.; Leroux, F. G. M.; Malagu, K.; Martin, N. M. B.; Menear, K. A.; Smith, G. C. M. 2-Methylmorpholine-substituted pyrido-, pyrazo- and pyrimidopyrimidine derivatives as mTOR inhibitors and their preparation, pharmaceutical compositions and use in the treatment of cancer, 2008.
- (56) Zhu, D. W.; Lee, X.; Breton, R.; Ghosh, D.; Pangborn, W.; Duax, W. L.; Lin, S.-X. Crystallization and preliminary X-ray diffraction analysis of the complex of human placental 17beta-hydroxysteroid dehydrogenase with NADP⁺. *J. Mol. Biol.* **1993**, *234*, 242-244.
- (57) Lin, S.-X.; Yang, F.; Jin, J. Z.; Breton, R.; Zhu, D. W.; Luu-The, V.; Labrie, F. Subunit identity of the dimeric 17beta-hydroxysteroid dehydrogenase from human placenta. *J. Biol. Chem.* **1992**, *267*, 16182-16187.
- (58) Sam, K. M.; Auger, S.; Luu-The, V.; Poirier, D. Steroidal spiro-gamma-lactones that inhibit 17beta-hydroxysteroid dehydrogenase activity in human placental microsomes. *J. Med. Chem.* **1995**, *38*, 4518-4528.
- (59) Sam, K. M.; Boivin, R. P.; Tremblay, M. R.; Auger, S.; Poirier, D. C16 and C17 derivatives of estradiol as inhibitors of 17beta-hydroxysteroid dehydrogenase type 1: chemical synthesis and structure-activity relationships. *Drug. Des. Discov.* **1998**, *15*, 157-180.
- (60) Zimmermann, J.; Liebl, R.; von Angerer, E. 2,5-Diphenylfuran-based pure antiestrogens with selectivity for the estrogen receptor alpha. *J. Steroid Biochem. Mol. Biol.* **2005**, *94*, 57-66.
- (61) Denizot, F.; Lang, R. Rapid colorimetric assay for cell growth and survival. Modifications to the tetrazolium dye procedure giving improved sensitivity and reliability. *J. Immunol. Methods* **1986**, *89*, 271-277.
- (62) Berman, H. M.; Westbrook, J.; Feng, Z.; Gilliland, G.; Bhat, T. N.; Weissig, H.; Shindyalov, I. N.; Bourne, P. E. The Protein Data Bank. *Nucleic Acids Res.* **2000**, *28*, 235-242.
- (63) Davis, I. W.; Leaver-Fay, A.; Chen, V. B.; Block, J. N.; Kapral, G. J.; Wang, X.; Murray, L. W.; Arendall, W. B.; Snoeyink, J.; Richardson, J. S.; Richardson, D. C. MolProbity: all-atom contacts and structure validation for proteins and nucleic acids. *Nucleic Acids Res.* **2007**, *35*, W375-383.
- (64) Frisch, M. J.; Trucks, G. W.; Schlegel, H. B.; Scuseria, G. E.; Robb, M. A.; Cheeseman, J. R.; Montgomery, J. A. J.; Vreven, T.; Kudin, K. N.; Burant, J. C.; Millam, J. M.; Lyengar, S. S.; Tomasi, J.; Barone, V.; Mennucci, B.; Cossi, M.; Scalmani, G.; Rega, N.; Petersson, G. A.; Nakatsuji, H.; Hada, M.; Ehara, M.; Toyota, K.; Fukuda, R.; Hasegawa, J.; Ishida, M.; Nakajima, T.; Honda, Y.; Kitao, O.; Nakai, H.; Klene, M.; Li, X.; Knox, J. E.; Hratchian, H. P.; Cross, J. B.; Bakken, V.; Adamo, C.; Jaramillo, J.; Gomperts, R.; Stratmann, R. E.; Yazyev, O.; Austin, A. J.; Cammi, R.; Pomelli, C.; Ochterski, J. W.; Ayala, P. Y.;

- Morokuma, K.; Voth, G. A.; Salvador, P.; Dannenberg, J. J.; Zakrzewski, V. G.; Dapprich, S.; Daniels, A. D.; Strain, M. C.; Farkas, O.; Malick, D. K.; Rabuck, A. D.; Raghavachari, K.; Foresman, J. B.; Ortiz, J. V.; Cui, Q.; Baboul, A. G.; Clifford, S.; Cioslowski, J.; Stefanov, B. B.; Liu, G.; Liashenko, A.; Piskorz, P.; Komaromi, I.; Martin, R. L.; Fox, D. J.; Keith, T.; Al-Laham, M. A.; Peng, C. Y.; Nanayakkara, A.; Challacombe, M.; Gill, P. M. W.; Johnson, B.; Chen, W.; Wong, M. W.; Gonzalez, C.; Pople, J. A.; Gaussian, Inc.: Pittsburgh, PA.
- (65) Bayly, C. I.; Cieplak, P.; Cornell, W. D.; Kollman, P. A. A well behaved electrostatic potential based method using charge restraints for determining atom-centered charges: the RESP model. *J. Phys. Chem.* **1993**, *97*, 10269-10280.
- (66) Jones, G.; Willett, P.; Glen, R. C.; Leach, A. R.; Taylor, R. Development and validation of a genetic algorithm for flexible docking. *J. Mol. Biol.* **1997**, *267*, 727-748.
- (67) Morris, G. M.; Goodsell, D. S.; Halliday, R. S.; Huey, R.; Hart, W. E.; Belew, R. K.; Olson, A. J. Automated docking using a Lamarckian genetic algorithm and empirical binding free energy function. *J. Comput. Chem.* **1998**, *19*, 1639-1662.
- (68) Huey, R.; Morris, G. M.; Olson, A. J.; Goodsell, D. S. A semiempirical free energy force field with charge-based desolvation. *J. Comput. Chem.* **2007**, *28*, 1145-1152.
- (69) Dennington, I.; Roy, K. T.; Millam, J.; Eppinnett, K.; Howell, W. L.; Gilliland, R. *GaussView*; 3.0 ed.; Semichem Inc., Shawnee Mission.

3.3.5.3. Paper XI.

Dynamic motion investigation of 17 β -HSD1 provides deep insights in enzyme kinetics and ligand binding.

Matthias Negri, Maurizio Recanatini and Rolf W. Hartmann

Submitted 2010

Abstract

Bisubstrate enzymes, such as 17 β -hydroxysteroid dehydrogenase type 1 (17 β -HSD1), exist in solution as an ensemble of conformations. 17 β -HSD1 catalyzes the last step of the biosynthesis of estradiol and, thus, it is a potentially attractive target for breast cancer treatment. To elucidate the conformational transitions of its catalytic cycle, a structural analysis of all available crystal structures was performed and representative conformations were assigned to each step of the putative kinetic mechanism. To best cover the conformational space, all-atom MD simulations and free energy calculations were performed, using the four crystallographic structures best describing apoform, opened, occluded and closed state of 17 β -HSD1 as starting structure. With three of them binary and ternary complexes were built with NADPH and NADPH-estrone, respectively, while two were investigated as apoform. Remarkably, the comparison of the eight long range trajectories resulting from this multi-trajectory/-complex approach revealed an essential role for backbone and side chain motions, especially of the β F α G'-loop, in cofactor and substrate binding. Thus, a selected-fit mechanism is suggested for 17 β -HSD1, where ligand-binding induced concerted motions of the FG-segment and the C-terminal part guide the enzyme along its preferred catalytic pathway. Overall, we could assign enzyme conformations to the five steps of the random bi-bi kinetic cycle of 17 β -HSD1, identifying its preferred pathway. This study provides a useful guideline for other enzymes, characterized by a rigid core and a flexible region directing their catalysis.

Cytoplasmic proteins are present in solution as an ensemble of conformations, which are in a dynamic equilibrium, strongly influenced by the presence of ligands (in case of enzymes: cofactors, substrates, inhibitors, or other proteins). This is especially true for enzymes following a bisubstrate kinetic, like *E. coli* dihydrofolate reductase (DHFR) and human 17 β -hydroxysteroid dehydrogenase type 1 (17 β -HSD1), where concerted dynamic motions are necessary between the enzyme conformations responsible for specific kinetic steps. An in-depth knowledge of both protein dynamic and its influence on ligand binding could effectively speed up rational drug design (1). These new drugs might act not only by competing with the substrate for its binding site, but also by inducing a dynamic dysfunction of the enzyme by hindering the switch between its conformations.

In estrogen target cells 17 β -HSD1 catalyzes the NADPH-dependent reduction of estrone (E1) to the biologically highly potent 17 β -estradiol (E2) (2-3) (Fig. 1). It has been shown that in post-menopausal women with hormone-dependent breast cancer tumor proliferation is driven by increased levels of E2 (4-5). As 17 β -HSD1 is often overexpressed in breast tumor cells, it is considered as a novel therapeutic target (6-9).

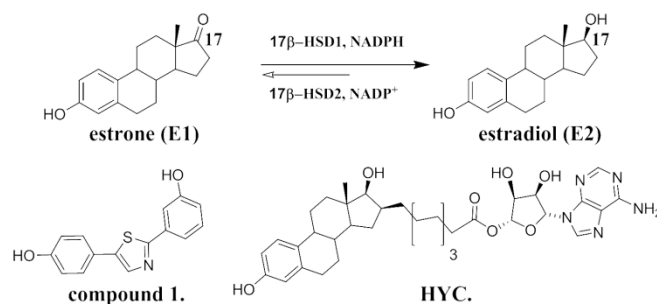


Fig. 1. Reduction from E1 to E2 and non-steroidal and steroidal inhibitors.

Recently, Cooper et al. elucidated the complete kinetic mechanism for the rat liver 3 α -HSD and could assign different enzyme forms to the specific reaction coordinates (10). 3 α -HSD and nearly all other HSD enzymes are described to follow a sequential ordered bi-bi kinetic mechanism, where the cofactor enters first and exits last. The kinetic mechanism of 17 β -HSD1 is still not fully clarified, although it has been reported to follow a rapid equilibrium random bi-bi mechanism, a peculiarity compared to other HSDs (11-13). The high NADPH/NADP⁺ gradient (>500:1) and the excess of NADPH with respect to E1 *in vivo*, as well as the thermodynamically favoured NADPH oxidation (14-15), suggest the presence of NADPH in the enzyme prior to steroid binding. Asn114, Ser142, Tyr155 and Lys159 form the catalytic tetrad of 17 β -HSD1, conserved in many HSD enzymes, and are involved in the *pro*-S hydride transfer from NADPH to the α -face of the C17 carbon as well as in the proton transfer between the OH group of Tyr155 and the C17 oxygen of E1 (16) (Fig. S1).

Remarkably, the catalytic reaction of 17 β -HSD1 is principally reversible; it is unidirectional, however *in vivo*, because of the abundance of NADPH. No crystal structure of the ternary complex enzyme (E)-NADPH-E1 exists, probably because of the very fast transfer rate observed for the reduction of E1 (k_{cat} 1.5s⁻¹) (17). E2 has a similar binding affinity to 17 β -HSD1 as E1, as well as a comparable k_{cat} , but due to the excess of NADPH the backward reaction E2 to E1 does not take place, thus explaining the several E-NADP⁺-E2 complexes.

Steroidal and non-steroidal inhibitors of 17 β -HSD1 have been reported (Fig. 1) (6-8, 18-22). The former mimic the substrate and are supposed to bind in the substrate binding site (SUB), a narrow hydrophobic tunnel. They are stabilized by hydrogen bonds with Tyr155/Ser142 and His221/Glu282, located on both ends of the pocket, and, further, by hydrophobic contacts. Recently, Poirier et al. published a series of hybrid inhibitors, based on a E1/E2 core with substituents of various lengths in C16 position (22). These inhibitors occupy both substrate (SUB) and cofactor binding site (COF), competing with E1 and NADPH, as demonstrated by the binary complex E-HYC (PDB entry 1i5r). Up to now no crystallographic data exists describing the binding mode of non-steroidal inhibitors, although computational studies performed by various groups suggested some classes of non-steroidals to bind like their steroidal analogues in the SUB (6-8, 23-24) and others to occupy only partially the SUB protruding into the COF, like compound **1** (20).

Herein, we present the first, to our knowledge, computational investigation of the kinetic mechanism of 17 β -HSD1, one of thirteen 17 β -HSDs belonging to the short-chain dehydrogenases/reductases (SDR), a large superfamily of NAD(P)H-dependent enzymes. Furthermore, the linkage between representative enzyme conformations and the five steps described for the random bi-bi mechanism, an in-depth computational analysis of the flexible β F α G'-loop, and its role in enzyme catalysis and in ligand binding were elucidated. Thus, a multi-trajectory/-complex molecular dynamic (MD) strategy was followed, based on four different enzyme conformations. Molecular mechanics Poisson-Boltzmann surface area (MM-PBSA) methods (25), in combination with normal-mode analysis (NMODE) (26), were exploited to calculate the free energies of the complexes. These substantiated our kinetic hypothesis and helped to determine the best enzyme conformation for binding of E1 and NADPH, respectively.

Results and Discussion.

Structural analysis of human 17 β -HSD1 crystal structures. 17 β -HSD1 is a homodimeric protein and shows the typical rigid β - α - β fold of the SDR-family with a core of parallel β -strands fanning across the center and α -helices draped on the outside (27), resulting in a rigid COF at the N-terminus and a structurally variable C-terminus, hosting the SUB. The structurally conserved region comprises Rossmann fold and GxxxGxG motif (G is glycine and x any other residue), characteristic of oxidation/reduction enzymes that bind nicotinamide cofactors, plus the YxxxK sequence (Y is Tyr155 and K Lys159) that participates in catalysis. In sharp contrast to other 17 β -HSDs, type 1 is characterized by a long, flexible β F α G'-loop and a C-terminal helix, both delimiting the SUB and probably involved in enzymatic catalysis and in entrance and exit mechanisms of small molecules.

Seventeen crystal structures of 17 β -HSD1 are available in the Protein Data Bank (PDB; Nov.2009) as apoform, binary or ternary complex (Tab. S1). The loop residues Thr190-Gly198 of the PDB entry 1fdt (28) are modeled in two different conformations and have been considered as two different conformer, denoted hereafter as 1fdtA and 1fdtB. Superimposition of all crystals gives a mean backbone RMSD (root mean-square distance) of ≈ 0.5 Å (all-atom RMSD ≈ 1.5 Å). The only flexible part is the above mentioned β F α G'-loop, which adopts different conformations, strongly modulating shape and volume of the active site (including both COF and SUB). Seven of

these crystal structures are incomplete, missing mainly the loop residues Phe192-Val196, while the remaining eleven show high b-factor values for this area, an additional hint for flexibility. In the fully resolved structures the loop occurs as a disordered random coil, but in some of them it is folded to a turn-helix-turn motif. Moreover, the loop is found in a stable orientation only for ternary complexes, which have enzyme, cofactor and steroidal product or inhibitor fully resolved (1a27, 1fdtA, 1fdtB, 1equA and 1fduC; cluster c12 in Fig.2). For all other crystal structures no univocal loop conformation could be ascribed to the presence of either cofactor or ligand. Nevertheless, this multiplicity of conformations suggests various substates for 17 β -HSD1, which are subjected to fast dynamic motions and secondary structure rearrangements of the loop. Most of the binary complexes E-E2 are fully resolved, while E-NAD(P)⁺ complexes lack part of the β F α G'-loop and no binary complex with NADPH or with E1 exists at all (Tab. S1). The numerous fully resolved E-E2 complexes suggest E2 to bind stronger to the enzyme than NADPH, which becomes tighter bound only after the steroid has entered the cavity and the loop has changed its conformation.

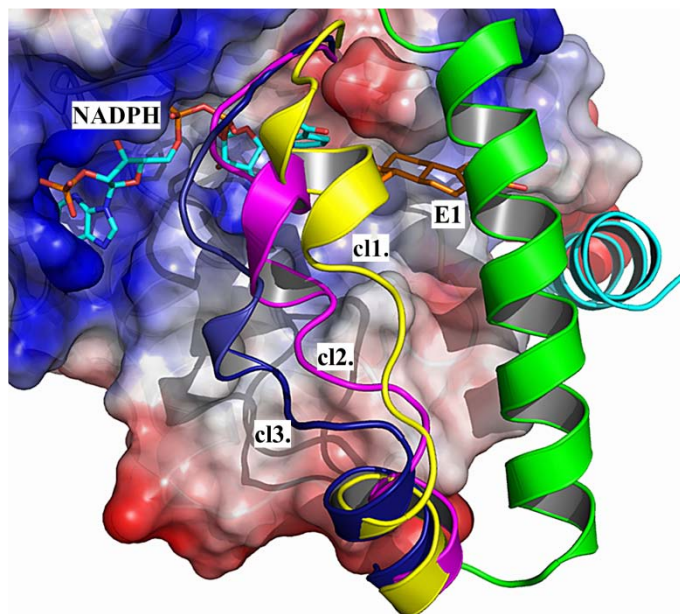


Fig. 2. Representative structures of the three β F α G'-loop conformations **c11** (yellow, 1iol), **c12** (magenta, 1a27) and **c13** (blue, 1i5r), clustered according to the backbone RMSD of the five residues Phe192-Val196. β F α G'-loop, α G'-helix (green) and C-terminal helix (cyan) are rendered as cartoon, NADPH and E1 as sticks and the rest of the enzyme (active site) as electrostatic surface.

The eleven full-length crystal structures of 17 β -HSD1 are superimposed and clustered according to the backbone RMSD (mean value \approx 3 Å) of the five loop residues Phe192 -Val196. Three clusters c11, c12 and c13 (Fig. 2; representative structures: 1iol, 1a27 and 1i5r, respectively) could be identified, as well as the presence of three gates, two close to the loop (gate 1 and 2) and a third one (gate 3) close to the C-terminal helix (Fig. 3). However, this backbone classification disregards active site volume changes and is limited to ascribe the presence of opened gates for the three clusters c11-c13. Thus, clustering was repeated taking into account all atoms of the same loop residues, which resulted in a mean RMSD value \approx 6 Å. Five clusters could be identified (Fig. 3 and S2) and Phe192, in particular, emerged as an important marker for the conformational variations, since its side chain presented the largest RMSD deviation (\approx 10 Å), as it rotates for about 200 degrees around the loop axis: it turns from the inner cavity, where it occludes the SUB and stabilizes the substrate in the correct position for hydride transfer (1fdtB), toward the outside, where it chaperones E1/E2 or the cofactor in and out of the active site (1fdtA). These two extremes in the orientation of the side chain of Phe192 correspond to the major changes of the active site volumes of all wild type E-NADPH-E2 complexes, where the volume ratio SUB/COF changes from 30:70 in 1fdtB to 37:63 in 1fdtA (Tab. S1).

Rapid equilibrium random bi-bi kinetic cycle – a hypothesis. Since 17 β -HSD1 is described to follow a five-step random bi-bi kinetic mechanism (Fig. 3 and S3), we tried to assign an enzyme conformation to each step and to explain the specific role played by the flexible loop for each enzyme form present along its preferred reaction pathway. As stated before, we assume that NADPH will bind first, inducing a conformational rearrangement of the

β F α G⁷-loop, which would allow and favour the successive entrance and binding of E1. Therefore, the loop needs to move toward the COF (1bhs – **step 1**), opening gate 2. This will be closed again, after E1 enters (1i5r – **step 2**) and the loop slides back to its starting point. Now, Phe192 and Met193 stabilize the substrate in an optimal position for the pro-S hydride transfer, allowing the formation of the first ternary complex. The catalytic reaction takes place (1a27 – **step 3**), and subsequently the loop moves toward the SUB (1i0l, 1fdtA – **step 4**) opening gate 1, the egress path for NADP⁺, which leaves the active site. The steroid is still stabilized in the SUB, shielded by Phe192 and Met193. In **step 5**, the steroid moves out of the active site through gate 3 (1fdtB). Interestingly, for all five substates the loop residues and Phe226 on the α G⁷-helix are oriented in a way to avoid solvent accessibility to the SUB.

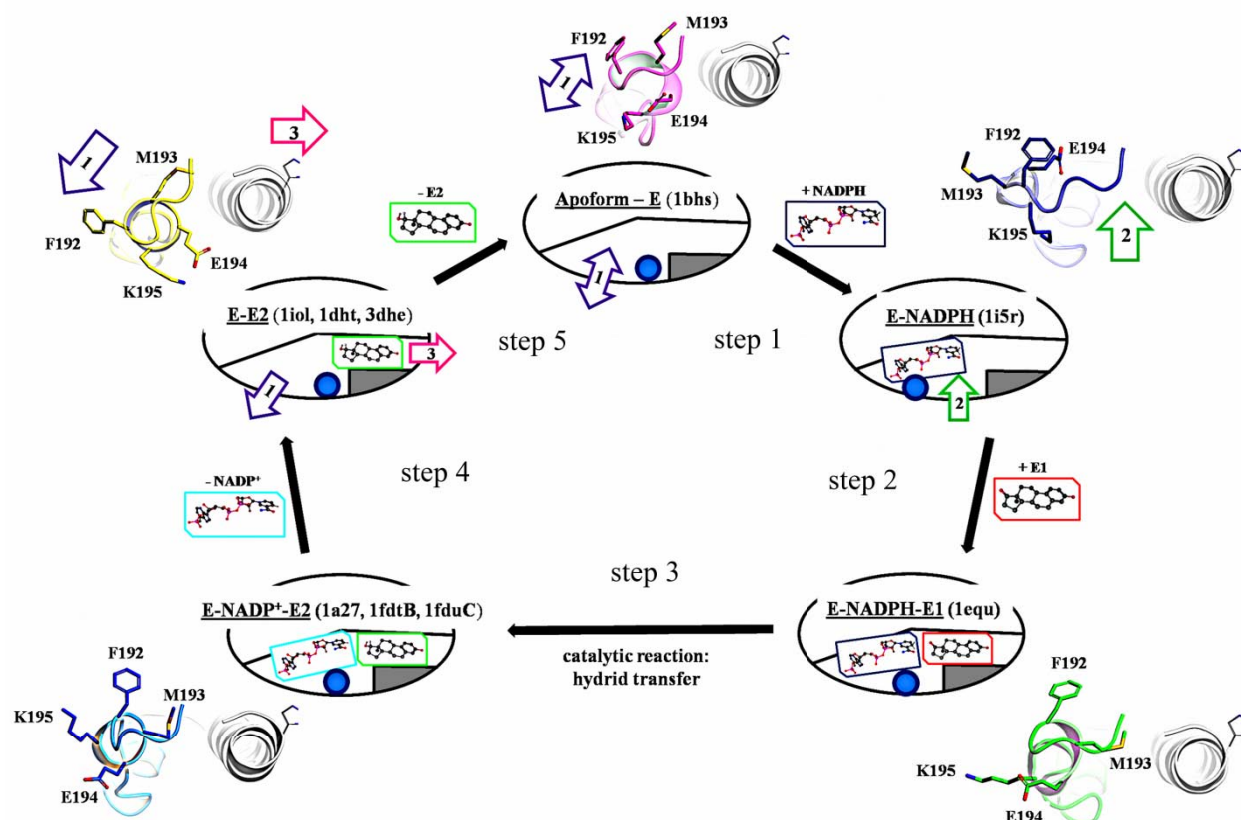


Fig. 3. Random bi-bi kinetic cycle of 17 β -HSD1. To each step one or more crystal structures were assigned. Side chains of the β F α G⁷-loop residues Phe192-Lys195 are rendered as sticks and the orientation of the loop (blue ball) with respect to the α G⁷ helix (in gray) is shown as cartoon. The arrows 1-3 indicate the entrance and egress gates identified along the reaction pathway. 1fdtA is not included in the balloon of **step 4** due to its different loop axis orientation with respect to 1i0l.

Validation of the catalytic cycle by means of molecular dynamic simulations. MD simulations have been proven to be very useful tools in the analysis of dynamic motions of enzymes with flexible loops, which play a prominent role in either the catalytic cycle and/or ligand binding, as for example for *E. coli* DHFR (1, 29) or Cdk2 (cyclin-dependent kinase type 2) (30). Moreover, the predictive capacity of MDs can be increased by free energy calculations and normal mode analysis. Herein, we apply these techniques pursuing as a main goal to substantiate the assignment of different enzyme conformations of 17 β -HSD1 to the five steps encountered along the catalytic pathway and to determine complexes representing the transition states. To this end, eight MD simulations (models I-III; *SI Text*) were designed based on the crystal structures 1fdtA, 1i5r, 1fdtB, and 1bhs, which differ strongly in the orientation of the β F α G⁷-loop (Fig. S4). In fact, the enzyme was investigated in its opened-state (1fdtA) - characterized by a fused COF and SUB and by Phe192 turned outward, in a semi-opened/occluded state (1i5r) - with the loop shifted toward the COF and Phe192 more buried than in 1fdtA, and in its closed-state (1fdtB) - mimicking the catalytic moment with a closed SUB and Phe192 pointing inward perpendicular to the catalytic Tyr155. The MD simulations of apoform E (A), binary E-NADPH (B) and ternary complexes E-NADPH-E1 (C) of 17 β -HSD1 were evaluated in terms of geometry (RMSD) and energy stability of the complexes, ligand and secondary structure displacement with respect to the starting pose, and the time required to reach a stable RMSD and energy plateau. For

each stable sector of the MD trajectories longer than 4 ns snapshots were collected every 30th frame (every 30 ps) and used to calculate absolute free energy (ΔG) and relative binding affinity (ΔG_{bind}) by means of MM-PBSA methods and NMODE. Thus, in order to determine whether a preferential enzyme conformation exists for the binding of NADPH and E1, we compared ΔG and ΔG_{bind} values of the binary complexes B1-B3 and of the ternary C1-C3, respectively (Tab. 1).

Tab. 1. Free energy calculations for the stable trajectories of the MD simulations B1-B3 and C1-C3 by means of MM-PBSA and NMODE.

PDB code	MD code	ELE		VDW		GAS		PBSOL		PBTOT		TSTOT		ΔG
		mean	std	mean	std	mean	std	mean	std	mean	std	mean	std	
enzyme-NADPH														
1fdtA	B1	-380.08	75.8	-42.87	4.5	-371.65	74.7	386.95	68.8	15.3	12.6	-20.23	20.3	-35.53
1i5r	B2	-484.85	75.0	-70.11	6.5	-554.96	75.5	510.69	62.8	-44.27	16.5	-34.92	21.8	-9.35
1fdtB	B3	-358.75	53.8	-74.54	5.4	-433.29	54.5	411.6	50.2	-21.69	8.9	-37.16	20.1	-15.47
enzyme-NADPH-E1														
1fdtA	C1	0.35	4.5	-38.8	2.0	-38.58	4.6	18.12	5.4	-20.47	5.0	-17.87	22.2	-2.6
1i5r	C2	-12.75	6.3	-36.81	2.8	-49.53	6.3	25.88	5.7	-23.65	4.0	-22.69	20.1	-0.96
1fdtB	C3	-23.43	2.3	-36.75	2.8	-60.29	2.9	31.99	2.2	-28.3	2.8	-19.99	24.3	8.31

(ELE) electrostatic contribution in gas phase; (VDW) Van der Waals contribution in gas phase; (GAS) free energy in vacuum; (PBSOL) solvation energy; (PBTOT) relative free binding energy (ΔG_{bind}); (TSTOT) entropic contribution; (ΔG) absolute free binding energy; (mean) mean value; (std) standard deviation; all energies expressed in kcal/mol.

For **step 1** two MD simulations were performed with the enzyme only (1bhs – A1, 1fdtB – A2; Fig. S5). In the apoform crystal structure 1bhs (A1) the fully resolved $\beta F\alpha G'$ -loop lies in cluster c11, presents a turn-helix-turn motif and the side chains of its residues are oriented along its axis. Thus, a 12 ns MD A1 was performed in order to verify the reliability of 1bhs as **step 1** enzyme conformation. Remarkably, the loop evolved toward cluster c12, shielding the COF and especially where the nicotinamide moiety is found. This led to a large active site suitable to host both cofactor and ligand. The enzyme showed the tendency to preserve the hydrophobic character of the SUB, turning the side chains of the apolar residues inward, especially of the aromatic ones, which occlude the SUB and avoid water to be placed in there. Met193 was deeply buried in the SUB, occupying the space where steroids are normally placed. On the contrary, all polar residues belonging to the FG segment and the C-terminal helix turned outside to form ion-pairs responsible for the closure of gate 2 and 3. The final stable complex of this MD has to be considered as a transition state of **step 1**, presenting an accessible COF, suitable to host NADPH, and an occluded SUB, not ready to accommodate the substrate. Moreover, the $\beta F\alpha G'$ -loop would drift toward the COF, in concert to NADPH entrance, resulting in a progressive closure of the COF (gate 1) and accessibility of the SUB (1i5r).

The second MD A2 was performed on the apoform of the closed-state conformation 1fdtB, stripped of both cofactor and steroid. The aim was to investigate whether the starting enzyme conformations of A1 and A2 lead to different final tertiary structures or if they converge to a common folding and loop axis orientation. However, already after 1 ns of simulation a marked change in the tertiary structure of the 1fdtB apoform was observed involving FG segment and C-terminal helix. Phe192 remained turned inward, while Met193 rotated toward the $\alpha G'$ -helix, becoming responsible for the disruption of the $\alpha G'$ -helix. Thus, the two simulations did not converge to a common conformation; moreover, the final complex of A2 resulted in a partially unfolded structure. This indicates that the presence of either cofactor or ligand is necessary to assure a correct transition between the five steps of the enzymatic cycle.

For **step 2**, three 9 ns MDs were carried out on the binary complex E-NADPH (B) and another three, lasting 10 ns, on the ternary complex E-NADPH-E1 (C), with the enzyme in its opened (1fdtA - B1, C1), semi-opened (1i5r - B2, C2) and closed (1fdtB - B3, C3) state, respectively. The aim was to obtain insights into the role played by the loop in the stabilization of NADPH, the shielding of the SUB and the stabilization of E1.

Simulation B2 (1i5r-NADPH) was characterized by a quickly reached, very long stable RMSD plateau (Fig. S6), indicating a good stability of the complex. Also the loop showed a stable RMSD profile, although, while the lower part (Glu194-Ser199) still remained close to the cofactor in cluster c13, the upper part (Thr190-Met193) drifted

toward the αG^{\prime} -helix. One can see here a direct consequence of the outward rotation of Phe226, responsible to sustain the nicotinamide moiety in the starting complex, which is involved in opening gate 2, a prerequisite for E1 entrance. The loop was folded to a short helix and stabilized by the ion-pair Lys195 and 2'-phosphate of the cofactor, which trapped the adenosine moiety. In the final structure the upper part of the loop, placed in cluster cl2, occluded part of gate 2, reducing the solvent accessible surface and preserving the hydrophobic character of the SUB. Nevertheless, a hydrophobic tunnel remained between loop and helix, suitable for steroid transition. The complex stability of B2 is also reflected by a good free energy ΔG (-9.35 kcal/mol) with respect to the positive values of B1 and B3 (Tab. 1), which substantiates our structural hypothesis for catalytic **step 2**.

The MD of the ternary complex 1i5r-NADPH-E1 (C2) describes very well the expected loop motion from cluster cl3, shielding the COF, to cluster cl2 (Fig. 4). Despite a suboptimal free energy (-0.96 kcal/mol) compared to that of the closed-state complex C3 (-8.31 kcal/mol), we consider the MD C2 as a valuable simulation of the transition state of **step 2** from a binary state to the ternary complex (Fig. 4B). Effectively, this simulation ended in a stable complex with E1 properly bound in the SUB and with the loop oriented in cl2 occluding the active site.

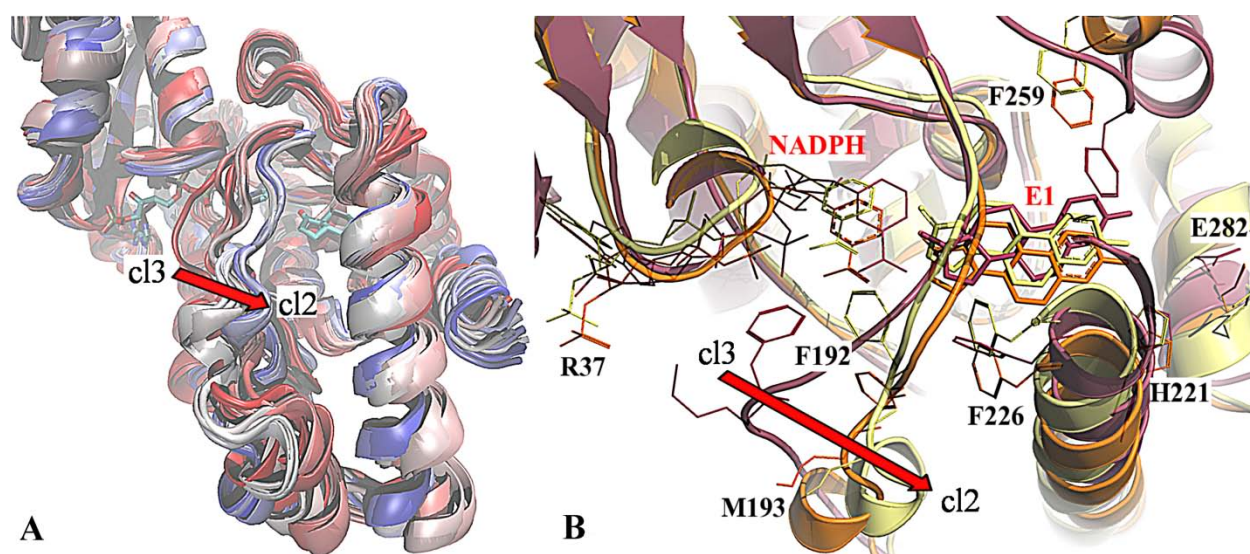


Fig. 4. Motion of the $\beta F\alpha G'$ -loop in MD C2 (1i5r) from cluster cl3 to cl2. (A) Overlay of multiple snapshots of the trajectory C2 (color-coded in a range from red to blue, according to start and end of the MD, respectively). (B) Important active site residues of the initial (violet, **step 1**), stable (orange, **step 2**) and final complex (yellow) are rendered as sticks.

For **step 3**, no tertiary structure rearrangements were expected, since in this step the hydride transfer takes place. Nevertheless, the three MDs of the ternary complex E-NADPH-E1 (C1-C3; Fig. S7) highlight very well the important role of Phe192 and Met193 in stabilizing E1 close to the cofactor to ensure an optimal distance necessary for hydride transfer. When these residues were turned outward, as happened for the opened and the semi-opened complexes, 1fdtA-NADPH-E1 (C1) and 1i5r-NADPH-E1 (C2) respectively, E1 had more space and was less stably bound. A combined analysis of the dynamic simulations C1 and C3 (1fdtB-NADPH-E1), which, despite of an opposite orientation of the side chains of the loop residues, present the loop axis (main chain) in the same starting conformation (cluster cl2), leads us to suggest a fine-tuned entrance mechanism for E1. Thus, the MDs C1 and C3 were prolonged for ≈ 6 ns, with the purpose to evaluate the propensity of the substrate to escape. The RMSD values of MD C1 rose in this extended part, related to a large $\beta F\alpha G'$ -loop motion to shield the active site, whereas they decreased for the closed-state simulation C3 (Fig. 5A). Although, the second part of the simulation C3 was characterized by slow concerted motions of FG-segment and C-terminal helix, as shown by the gradual increase of the loop RMSD (Fig. 5B), which opened gate 2 and 3 with an increase of ΔG from -2.6 (at 10 ns) to -6.02 kcal/mol (at 16 ns). In the opened-state MD C1, we observed the progressive loss of the hydrogen bonds to Ser142 and His221, typical for steroid binding in the SUB, facilitated by the outward rotation of Met193, Phe192, and Phe226. E1 drifted beneath the cofactor slowly turning its D-ring toward gate 2, now opened, and bound to Lys195. Thus, backward analysis of simulation B1 suggests a “pull-and-push” mechanism, in which E1 seems to enter the binding site through gate 2, pulled by the inward rotation of Lys195 to which the steroid is bound with the C17 carbonyl.

Once E1 is in the SUB, this bond is released, Lys195 rotates toward the 2'-phosphate and Phe192 turns inward below the cofactor (1fdtB), pushing E1 in the SUB. Other residues delimiting gate 2 also adapted to the steroid, in particular Phe226, which turned from the outside (final complex of MD C1) to the inner cavity, closing gate 2 and stabilizing E1. The catalytic residues Ser142, Tyr155, and Lys159 showed small RMSD values for all three ternary complexes, even after 10 ns of dynamics (Fig. S7D). This is in accordance to experimental site-directed mutagenesis studies (31), where the enzymatic activity was abolished because of the mutation of one or more of these residues. Moreover, the conformational stability of these residues suggested them to be essential for the postulated catalytic mechanism (Fig. S1) (32), while other regions, for example the β F α G'-loop, seem to be the driving force that keeps the catalytic cycle running. Interestingly, the trajectories observed for Phe192, Lys195 and Phe226 in the three simulations C1-C3 confirmed this implication in ligand stabilization and expulsion. Furthermore, the poses of these residues in the three MDs overlap nicely with their orientation in the eighteen enzyme conformations and fitted very well with the conclusion of Mazza et al. (33), who suggested a direct involvement of Lys195 and Phe192 in the catalysis.

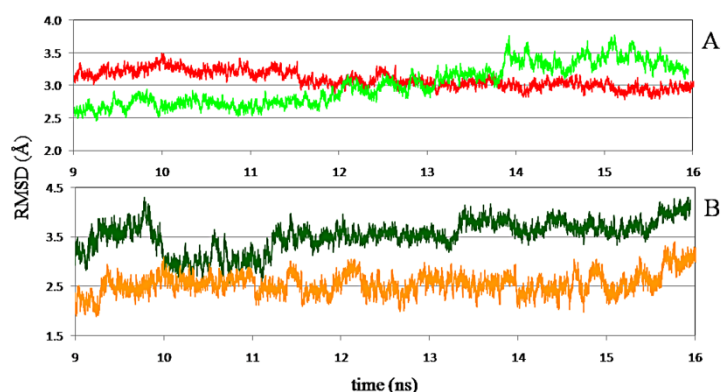


Fig. 5. Analysis of the last 7 ns of the MDs C1 (1fdtA) and C3 (1fdtB). (A) Time-dependent all-atom RMSD for all residues of complexes C1 (light green) and C3 (red) and (B) for the β F α G'-loop residues only of C1 (dark green) and C3 (orange).

Phe192 was observed to play a very important role for steroid stabilization, but also in the catalytic reaction. In most ternary complexes with E1, Phe192 pointed perpendicular toward Tyr155. In this T-shaped conformation, Phe192 is likely to increase the acidity of the phenol group of the catalytic Tyr155 from a pK_a of ca 9 to 6 (34), which facilitates the hydride transfer to the estrone. The final pose of Phe192 in C2 and C3 is consistent with this observation and enforces its role in protecting the nicotinamide moiety and activating the catalysis.

In **step 4** we expected to see the loop shift further toward the α G'-helix, opening gate 1, and NADP(H) to leave the COF. We considered both the simulations C1-C3 and B1-B3. Two of them were meaningful: 1fdtB-NADPH-E1 (C3), which confirmed the loop motion with subsequent opening of gate 1 and the drift of E2 toward gate 3; and 1fdtA-NADPH (B1), which showed the egress path of the cofactor due to gate 1 enlargement.

Although at this stage the steroid should be E2, we considered for **step 4** the simulations C1-C3, where E1 and NADPH were used instead of E2 and NADP⁺. We consider this approximation as acceptable, because no differences between the hydrogen bond patterns of E1 and E2 with 17 β -HSD1 exist and because forcefield based methods, such as MD simulation, are not sensitive enough to handle the electrostatic differences between ligand and cofactor forms (20). In all complexes, E1 was placed in the same pose, analogous to that of E2 in the crystals. Although the MDs C1-C3 reached a stable RMSD plateau after already 4 ns (Fig. S7), maintaining E1 placed in the SUB, the ΔG values for the stable segments varied notably for the three simulations (Tab.1). The MD of the ternary complex C3 best described **step 4**, with a ΔG of -8.31 kcal/mol: E1 maintained its hydrogen bonds to Ser142/Tyr155 for the first 10 ns of the simulation C3, until being pushed out of the SUB through gate 3 in the following 6 ns due to the loop motion toward the α G'-helix (Fig. 6).

Moreover, in simulation 1fdtA-NADPH (B1), characterized at its beginning by a wide access to the COF due to the outward rotated Phe192, we observed a concerted opening of gate 1 and closing of gate 2 due to the shift of the loop axis toward the α G'-helix. Thus, after a gradual increase in the first 5 ns, the all-atom RMSD reached a plateau and maintained it until the end of the simulation. Differently, the cofactor RMSD continued to rise (Fig. S6D), in

accordance to the movement of NADPH out of the COF, which was facilitated by the outward rotated Arg37, not burying the adenosine moiety in the COF anymore. Notably, the cofactor-stabilizing role of Arg37 had been previously demonstrated by site-directed mutagenesis studies (15). The α G'-helix rotated slightly rightward for about 30 degrees, adapting its residues to those of the loop. In this motion, His221 moved outward, breaking the salt bridge with Glu282 and enlarging gate 3. The free energy of complex B1 (+35.53 kcal/mol) clearly indicates that this enzyme conformation is disfavoured to stabilize NADPH, which ends up solvent exposed, suggesting complex B1 to be a good model to simulate the exit of the cofactor in **step 4**.

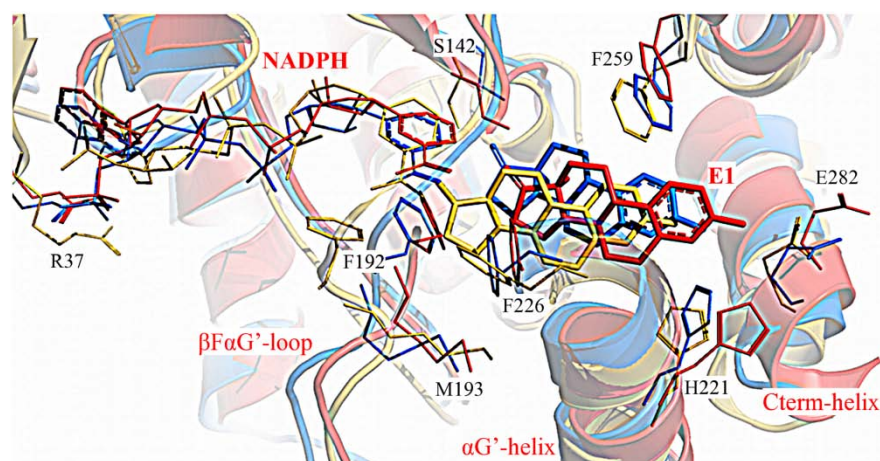


Fig. 6. Overlay of the representative structures of the initial position (yellow), the stable segment (blue, **step 3**) and the extended part (red, **step 5**) of the MD C3 (1fdtB).

In **step 5** the exit of the product is required as well as a side-chain rearrangement to shield the empty SUB. This has already been observed for the last 7 ns of MD C3 (Fig. 5), where E2 drifted to exit gate 3, pushed by motions of the loop axis and by the rotation of the apolar residues Phe192, Met193, Phe226, and Phe259 into the SUB (Fig. 6). Moreover, with the progression of E1 to the end of the tunnel His221 and Glu282 turned outward enlarging gate 3. The loop remained close to the α G'-helix, revealing broad gates 1 and 3 and an occluded gate 2, as observed for 1bhs, the representative crystal for **step 1**.

Conclusions.

The combined analysis of the crystal structures and of the biochemical data present in literature resulted in the identification of a preferred pathway for the random bi-bi kinetic cycle of 17 β -HSD1. Thus, a multi-trajectory MD approach and free energy calculations were employed to substantiate the catalytic cycle. MD simulations were performed to gain a more complete set of protein conformers, in particular of those with a relatively high energy and which often are transition states between two kinetic steps. When ligands bind to such enzyme forms, they push the new complex into a favorable low energy conformation and influence so the choice of the catalytic pathway. The identification of such saddle points is therefore crucial for an accurate study of the kinetic-related motions of the enzyme.

Kinetic cycle and ligand-binding related motions of *E. coli* DHFR were intensively studied by means of both experimental and computational methods. The former (such as site-directed mutagenesis, isothermal calorimetry, NMR dispersion, crystallography, etc.) constituted the basis for the understanding of DHFR functionality and catalysis. Differently, computational methods (such as MD simulations, thermal fluctuation, thermodynamic integration, etc.) were applied with success in order to elucidate protein plasticity and allosteric mechanism, but also to address new strategies in drug design, as for example the inhibition of *E. coli* DHFR by functional disruption, where the enzyme is frozen in a conformer that stops the kinetic cycle. Especially MD simulations resulted as a sophisticated tool to investigate transition steps and enzyme motions influenced by starting conformation and ligand binding.

Very recently, a binary and a ternary complex of 17 β -HSD1 (PDB entry 3hb4 and 3hb5) with the potent E2-derived inhibitor E2B were published (36). In the ternary structure the β F α G'-loop was oriented in cluster c12, in analogy to all other ternary complexes, confirming its importance in ligand stabilization, in particular of Phe192 and Met193.

Small RMSD variations were observed for the catalytic residues Ser142, Tyr155 and Lys159 in all MDs, suggesting other regions of the enzyme to be responsible for the proceeding of the five-step catalytic cycle. Site-directed mutagenesis studies indicated for His221 and Glu282 a prominent role in substrate recognition, but not in catalysis (31, 33). The motions of His221 observed in the simulations were in agreement with these results and allowed interesting conclusions regarding the role of His221 in substrate recognition and with respect to its chaperone function in guiding E1 out of the SUB (Fig. 6). The analysis of the trajectories of the eight MD simulations revealed the essential role for backbone and side chain motions, in particular of the flexible β F α G'-loop, in cofactor and substrate binding, and the existence of distinguished conformer ensembles related to the single steps of the catalysis. Thus, it suggested 17 β -HSD1 to follow a selected-fit mechanism (36): E1 or NADPH binds to a transition state of the enzyme and induces concerted conformational rearrangements of FG-segment and C-terminal part, which guide the enzyme along its preferred catalytic pathway.

Our multi-trajectory approach allowed an accurate assignment of enzyme conformers to each postulated step of the catalytic cycle of 17 β -HSD1. It laid the basis not only for a deeper understanding of the kinetic mechanism, but also for more general strategies applicable in flexible protein drug discovery. Due to the facts that many enzymes are characterized by multiple transition conformations, and that some of them are inhibited by functional disruption, it became apparent why an exhaustive enzyme conformer search has to be considered as a necessity in computational protein functional studies.

Methods.

A detailed description of all of methods is given in *SI Text*.

Initial coordinates for the MDs were taken from the crystal structures 1fdtA, 1i5r, 1fdtB and 1bhs, respectively, and prepared with the BIOPOLYMER module of SYBYLv8.0 (Sybyl, Tripos Inc., St. Louis, Missouri, USA). The crystallographic E2 and NADP⁺ were transformed into E1 and NADPH, except for 1i5r, where E1 and NADPH were merged from 1fdt after superimposition of all crystals. RESP charges were applied to E1, while for NADPH the parameters of Ulf Ryde (<http://www.teokem.lu.se/~ulf/>) were taken. All systems were solvated in a truncated octahedron box of waters with a buffer of 10 Å and neutralized with counterions with the xLeap module of the AMBER9 suite (37), and then minimized.

MD simulations were performed by means of AMBER 9.0 with constant temperature and periodic boundary conditions. The systems were equilibrated at constant volume (NVT) with restraints on protein heavy atoms, NADPH and E1, whereas the production runs were performed at constant pressure (NPT). The Amber99SB force field (38) was applied for the proteins. Free energies were calculated by means of MM-PBSA and NMODE of the AMBER9 suite.

The RMSD analysis of the trajectories of the MDs was done with PTRAJ module of the AMBER toolset, and the backbone and side chain classification was performed with the CONSENSUS utility of the Homology module of MOE (www.chemcomp.com).

Acknowledgments. We thank Dr. Sandrine Oberwinkler-Marchais and Dr. Matthias Engel for helpful discussion. This study is part of the PhD thesis of MN, performed in “co-tutele” between the University of Bologna and Saarland University.

Footnotes. Author contributions: M.N. designed research; R.W.H. and M.R. supervised M.N.; M.N. performed research; M.N. analyzed data; and M.N., M.R. and R.W.H. wrote the paper.

The authors declare no conflict of interest. Supplementary informations are available from the online PNAS-homepage.

References.

- (1) Lerner MG, Bowman AL, Carlson HA (2007) Incorporating dynamics in *E. coli* Dihydrofolate reductase enhances structure-based drug discovery. *J Chem Inf Model* 47:2358-2365.
- (2) Labrie F, et al. (1997) The key role of 17 β -hydroxysteroid dehydrogenases in sex steroid biology. *Steroids* 62:148-158.

- (3) Miettinen MM, Mustonen MV, Poutanen MH, Isomaa VV, Vihko RK. (1996) Human 17 β -hydroxysteroid dehydrogenase type 1 and type 2 isoenzymes have opposite activities in cultured cells and characteristic cell- and tissue-specific expression. *Biochem J* 314:839–845.
- (4) Sasano H, et al. (1996) Aromatase and 17 β -hydroxysteroid dehydrogenase type 1 in human breast carcinoma. *J Clin Endocrinol Metab* 11:4042–4046.
- (5) Miyoshi Y, et al. (2001) Involvement of up-regulation of 17 β -hydroxysteroid dehydrogenase type 1 in maintenance of intratumoral high estradiol levels in postmenopausal breast cancers. *Int J Cancer* 94:685–689.
- (6) Frotscher M, et al. (2008) Design, synthesis, and biological evaluation of (hydroxyphenyl)naphthalene and -quinoline derivatives: potent and selective nonsteroidal inhibitors of 17 β -hydroxysteroid dehydrogenase type 1 (17 β -HSD1) for the treatment of estrogen-dependent diseases. *J Med Chem* 51:2158–2169.
- (7) Marchais-Oberwinkler S, et al. (2008) Substituted 6-phenyl-2-naphthols. Potent and selective nonsteroidal inhibitors of 17 β -hydroxysteroid dehydrogenase type 1 (17 β -HSD1): design, synthesis, biological evaluation, and pharmacokinetics. *J Med Chem* 51:4685–4698.
- (8) Day JM, Tutill HJ, Purohit A, Reed MJ (2008) Design and validation of specific inhibitors of 17 β -hydroxysteroid dehydrogenases for therapeutic application in breast and prostate cancer, and in endometriosis. *Endocr Relat Cancer* 15:665–692.
- (9) Kruchten P, et al. (2009) Selective inhibition of 17 β -hydroxysteroid dehydrogenase type 1 (17 β -HSD1) reduces estrogen responsive cell growth of T47-D breast cancer cells. *J Steroid Biochem Mol Biol* 114:200–206.
- (10) Cooper WC, Jin Y, Penning TM (2007) Elucidation of a complete kinetic mechanism for a mammalian hydroxysteroid dehydrogenase (HSD) and identification of all enzyme forms on the reaction coordinate: the example of rat liver 3 α -HSD (AKR1C9). *J Biol Chem* 282:33848–33493.
- (11) Betz G (1971) Reaction mechanism of 17 β -estradiol dehydrogenase determined by equilibrium rate exchange. *J Biol Chem* 246:2063–2068.
- (12) Sherbet DP, et al. (2007) Cofactors, redox state, and directional preferences of hydroxysteroid dehydrogenases. *Mol Cell Endocrinol* 265–266:83–88.
- (13) Penning TM (1997) Molecular endocrinology of hydroxysteroid dehydrogenases. *Endocrin Rev* 18:281–305.
- (14) Agarwal AK, Auchus RJ (2005) Minireview: Cellular redox state regulates hydroxysteroid dehydrogenase activity and intracellular hormone potency. *Endocrinology* 146:2531–2538.
- (15) Sherbet DP, et al. (2009) Biochemical factors governing the steady-state estrone/estradiol ratios catalyzed by human 17 β -hydroxysteroid dehydrogenases types 1 and 2 in HEK-293 cells. *Endocrinology* 150: 4154–4162.
- (16) Ghosh D, et al. (1995). Structure of human estrogenic 17 β -hydroxysteroid dehydrogenase at 2.20 Å resolution. *Structure* 3:503–513.
- (17) Gangloff A, Garneau A, Huang Y-W, Yang F, Lin S-X (2001) Human oestrogenic 17 β -hydroxysteroid dehydrogenase specificity: enzyme regulation through an NADPH-dependent substrate inhibition towards the highly specific oestrone reduction. *Biochem J* 356:269–276.
- (18) Brozic P, Lanisnik Risner T, Gobec S (2008) Inhibitors of 17 β -hydroxysteroid dehydrogenase type 1. *Curr Med Chem* 15:137–150.
- (19) Bey E, et al. (2008) Design, synthesis, biological evaluation and pharmacokinetics of bis(hydroxyphenyl) substituted azoles, thiophenes, benzenes, and aza-benzenes as potent and selective nonsteroidal inhibitors of 17 β -hydroxysteroid dehydrogenase type 1 (17 β -HSD1). *J Med Chem* 51:6725–6739.
- (20) Bey E, et al. (2009) New insights into the SAR and binding modes of bis(hydroxyphenyl)thiophenes and -benzenes: influence of additional substituents on 17 β -hydroxysteroid dehydrogenase type 1 (17 β -HSD1) inhibitory activity and selectivity. *J Med Chem* 52:6724–6743.
- (21) Poirier D (2009) Advances in development of inhibitors of 17 β -hydroxysteroid dehydrogenases. *Anticancer Agents Med Chem* 9:642–660.
- (22) Poirier D, et al. (2005) Estradiol-adenosine hybrid compounds designed to inhibit type 1 17 β -hydroxysteroid dehydrogenase. *J Med Chem* 48:8134–8147.
- (23) Karkola S, Lilienkamp A, Wähälä K (2008) A 3D QSAR model of 17 β -HSD1 inhibitors based on a thieno[2,3-d]pyrimidin-4(3H)-one core applying molecular dynamics simulations and ligand-protein docking. *Chem Med Chem* 3:461–472.
- (24) Messinger J, et al. (2006) New inhibitors of 17 β -hydroxysteroid dehydrogenase type 1. *Mol Cell Endocrinol* 248:192–198.

- (25) Kollman PA, et al. (2000) Calculating structures and free energies of complex molecules: combining molecular mechanics and continuum models. *Acc Chem Res* 33:889-897.
- (26) Case DA, (1999) in *Rigidity Theory and Applications*, eds Thorpe MF, Duxbury PM (Plenum, New York), pp 329-344.
- (27) Jornvall H, et al. (1995) Short-chain dehydrogenases/reductases (SDR). *Biochemistry* 34:6003–6013.
- (28) Breton R, Housset D, Mazza C, Fontecilla-Camps JC (1996) The structure of a complex of human 17 β -hydroxysteroid dehydrogenase with estradiol and NADP⁺ identifies two principal targets for the design of inhibitors. *Structure* 4:905-915.
- (29) Mauldin RV, Carroll MJ, Lee AL (2009) Dynamic dysfunction in dihydrofolate reductase results from antifolate drug binding: modulation of dynamics within a structural state. *Structure* 17:386–394.
- (30) Bakan A, Bahar I (2009) The intrinsic dynamics of enzymes plays a dominant role in determining the structural changes induced upon inhibitor binding. *Proc Natl Acad Sci USA* 106:14349-14354.
- (31) Puranen T, Poutanen M, Ghosh D, Vihko P, Vihko R (1997) Characterization of structural and functional properties of human 17 β -hydroxysteroid dehydrogenase type 1 using recombinant enzymes and site-directed mutagenesis. *Mol Endocrinol* 11:77-86.
- (32) Bennett MJ, Schlegel BP, Jez JM, Penning TM, Lewis M (1996) Structure of 3 α -hydroxysteroid/dihydrodiol dehydrogenase complexed with NADP⁺. *Biochemistry* 35:10702-10711.
- (33) Mazza C, Breton R, Housset D, Fontecilla-Camps JC (1998) Unusual Charge Stabilization of NADP⁺ in 17 β -Hydroxysteroid Dehydrogenase. *J Biol Chem* 273:8145–8152.
- (34) Ibarra CA, Chowdhury P, Petrich JW, Atkins WM (2003) The anomalous pK_a of Tyr9 in Glutathione S-Transferase A1-1 Catalyzes Product Release. *J Biol Chem* 278:19257–19265.
- (35) Mazumdar M, et al. (2009) Binary and ternary crystal structure analyses of a novel inhibitor with 17 β -HSD type 1: a lead compound for breast cancer therapy. *Biochem J* 424:357-366.
- (36) Weikl TR, von Deuster C (2009) Selected-fit versus induced-fit protein binding: kinetic differences and mutational analysis. *Proteins* 75:104-110.
- (37) Case DA, et al. (2006) Amber 9, University of California, San Francisco.
- (38) Hornak V, et al. (2006) Comparison of multiple Amber force fields and development of improved protein backbone parameters. *Proteins* 65:712–725.

3.3.6. Conclusions and Outlook

The analysis of the crystal structures of 17 β -HSD1 resulted in the hypothesis of a random bi-bi kinetic cycle, which was substantiated by a set of MD simulations performed on apoform, binary and ternary complexes between 17 β -HSD1, NADPH and substrate estrone (E1). For each step of the cycle an enzyme conformation was identified. Moreover, insights were gained into the high adaptability of the loop to different steps and its importance in stabilizing the cofactor and substrate.

Docking studies for the class of bis(hydroxyphenyl)-arenes on a small ensemble of enzyme conformations of 17 β -HSD1 led to the identification of two plausible binding modes: a steroidal binding mode and an alternative one. MDs were applied to validate these two binding modes, resulting in compound **1** (representative for this class of 17 β -HSD1 inhibitors) placed preferentially in the alternative binding mode, synergically interacting with the nicotinamide moiety of NADPH.

A global picture emerged by combining the results of the MD studies and the quantum-chemical investigations of the MEPs of 5 catalytic residues-NADPH-inhibitor complexes suggesting for this class of inhibitors a new inhibition mechanism with respect to what observed for steroidal inhibitors. They seemed to dysfunction the enzyme dynamics, due to the simultaneous binding to active site and cofactor, strongly influenced by electrostatics, which could “freeze” the loop in a particular conformation, stabilizing the enzyme in a “half-switching” state.

Concluding it can be stated that the application of different computational techniques, namely X-ray clustering, molecular docking, MD simulations and quantum-chemical studies, resulted in very valuable results which helped pushing rational drug design forward and ensured insights in the kinetic cycle of 17 β -HSD1 and the dynamic motions characterizing the enzyme. Nevertheless, still some work should be performed.

From the computational point of view at least one approach would be advisable: steered or REMD simulations with E1 and compound **1**, respectively, could help investigating the entrance and egress pathways, as well as the concerted β F α G'-motions as a consequence of the interactions occurring between enzyme, cofactor and E1 or compound **1**. The results of such simulations would complete and validate the results presented in this doctoral thesis and in the papers **IX-XI**.

From a biochemical point of view, site-directed mutagenesis studies focused on the loop residues Phe192-Lys195 and on Phe226, placed on the α G'-helix, could validate the hypothetical catalytic cycle described in this thesis and shed some new light on the role played by these residues in enzyme catalysis and ligand binding. Through concerted mutations the chaperone role of the β F α G'-loop should be clarified.

The computational approach applied on 17 β -HSD1 and presented in this thesis has to be seen in a more general perspective, namely as a guideline for drug design and biomolecular studies on similar enzymes. In particular, analogous studies might be helpful to study the dynamic behavior of members of the very large SDR/HSD family. These are characterized by highly flexible domains strongly influencing the space of the active site and subjected to conformational rearrangements as a consequence of their role in the various kinetic steps.

3.4 Congestive heart failure – selective CYP11B2 inhibition

3.4.1. Pharmacophore-model – evolution and consequences for drug design

In the CYP11B2 project the *in silico* technique primarily used was the pharmacophore-modelling.

In paper XII a first pharmacophore (ph4) model was built based upon a series of indane-, naphthalene- and tetrahydronaphthalene-derivatives. On the basis of a global superimposition, with a careful look to the aromatic nitrogen and its lone pair, a pharmacophore model could be established consisting of four pharmacophore points (Fig. 39).

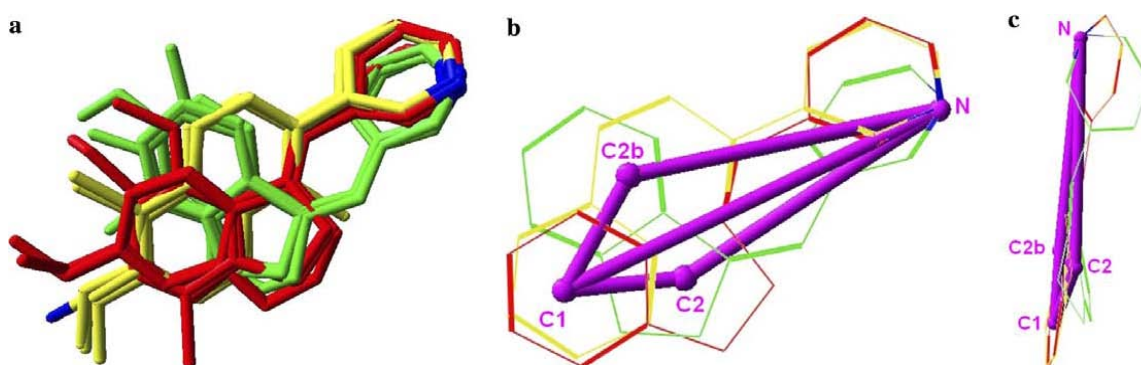


Figure 39. First pharmacophore model, with the four pharmacophore points (N: heterocyclic nitrogen, C1: ring centroid, C2: ring centroid, C2b: ring centroid).

This pharmacophore model resulted as a valuable tool in the further development of potent non-steroidal aldosterone synthetase inhibitors, leading to an increase of the molecular complexity.

Subsequently, this first pharmacophore model was expanded by including non-steroidal aromatase inhibitors with some CYP11B2-inhibitory potency, leading so to a new pharmacophore model (ph4 model) (Fig. 40), used as starting point for the design of new inhibitors. One aromatic (HY3) and three acceptor (AA) features were added to the first model, indicating that an additional part of the active site of the enzyme could be targeted as well.

Combined ligand-based (ph4 model) and structure-based (docking simulations) virtual screening led in paper XIV to the development of a new class of pyridynaphthalene derivatives with extended carbocyclic skeleton. Derivatives with *para*-functionalized benzyl moiety in 3-position of the naphthalene molecular scaffold thoroughly satisfied the spatial constraints imposed by the pharmacophore model and turned out to be highly potent aldosterone synthase inhibitors. The most active compound, *para*-cyanobenzyl derivative 17 (paper XIV), displayed nanomolar potency at the target enzyme ($IC_{50} = 2.7$ nM)

The selectivity versus CYP11B1 (up to a factor of 900) which is especially remarkable with respect to the high homology of the two CYP11B isoforms was found to be a consequence of *para*-substitution and hence of exploiting the AA3b pharmacophoric feature as well.

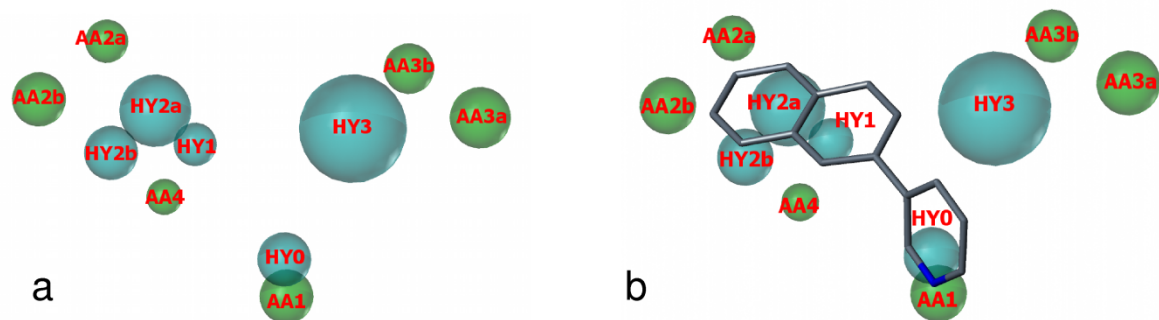


Figure 40. Pharmacophore model (a) and compound **1** (paper XIV) mapped to the pharmacophore model (b). The newly identified hydrophobic feature HY3 as well as the acceptor atom features AA3a and AA3b are not exploited by inhibitors with a naphthalene molecular scaffold. Pharmacophoric features are color-coded: cyan for hydrophobic regions (HY0–HY3) and green for acceptor atom features (AA1–4).

3.4.2. MEP maps and rotational energy barriers

In paper XIII molecular electrostatic potential investigations and rotational energy calculations led to a series of pyridynaphthalene derivatives with a substituted heterocyclic moiety with reduced CYP1A2 inhibition. Interesting structure-activity relationships could be observed with respect to electrostatic properties (Fig. 41). Compounds bearing protic substituents in 5'-position rather poorly inhibited CYP11B2 whereas bioisosteric exchange by aprotic residues gave rise to highly potent aldosterone synthase inhibitors, e.g., the inhibitory potency increased by a factor of 40 from carboxamide **17** ($IC_{50} = 94$ nM) to the ethanone **18** ($IC_{50} = 2.1$ nM). Figure 41 shows the MEP maps of compounds **17**, **10**, and **21** and their bioisosteric analogues **18**, **11**, and **22**. In the pyridine moiety of compounds **17**, **10**, and **21**, showing low inhibitory potency, areas with a positive ESP are present, while for the highly potent bioisosters, these areas display less positive values with a more uniformly distributed electron charge. Hence, the difference in the electrostatic potential distribution is a reasonable explanation for the varying potency within this set of compounds.

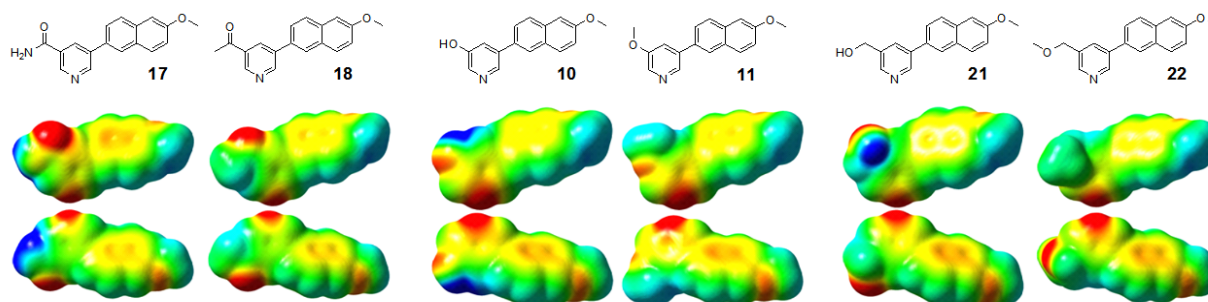


Figure 41. MEP of compounds **17**, **18**, **10**, **11**, **21**, and **22** (front and back view). The electrostatic potential surfaces were plotted with GaussView 3.0 in a range of -18.83 kcal/mol (red) to $+21.96$ kcal/mol (blue).

In the same paper we investigated also the rotational energy barriers with respect to the planarity between heterocycle and naphthalene core. It clearly emerged that the isoquinoline constrains the rotation around the carbon–carbon bond between the heterocycle and the naphthalene, especially in presence of the additional *ortho*-methyl groups in **29** and **30** (paper XIII), with rotational

barriers higher than 35 kcal/mol. Thus, a coplanar conformation for the isochinoline-substituted compounds becomes energetically disfavored compared to the pyridine analogues and the sterically demanding heterocycle rotates out of the naphthalene plane. This loss of planarity is a reasonable explanation for the reduced inhibitory potency since both CYP1A2 substrates and inhibitors are usually small-volume molecules with a planar shape (e.g., caffeine and furafylline). An even more drastic effect on the CYP1A2 potency was observed in case of the dihydronaphthalene type compounds, where the partly saturated core structure becomes flexible and disturbs the planarity. Since aromaticity has been identified to correlate positively with CYP1A2 inhibition in recent QSAR studies,¹³⁹ factors other than steric might play an additional role for the decreased CYP1A2 inhibition, e.g., disturbed π - π -stacking contacts with aromatic amino acids in the CYP1A2 binding pocket due to the reduced number of aromatic carbons.

3.4.3. Articles published in CYP11B2 project – paper XII-XIV

3.4.3.1. Paper XII.

Development and evaluation of a pharmacophore model for inhibitors of aldosterone synthase (CYP11B2).

Sarah Ulmschneider, Matthias Negri, Marieke Voets and Rolf W. Hartmann

This article is protected by copyrights of ‘Bioorganic and Medicinal Chemistry Letters.’

Bioorg. Med. Chem. Lett. **2006**, *16*, 25–30

Abstract

Recently, we proposed inhibition of aldosterone synthase (CYP11B2) as a novel strategy for the treatment of congestive heart failure and myocardial fibrosis and synthesized a large number of inhibitors. In this work, a pharmacophore model for CYP11B2 inhibitors was developed by superimposition of active and non-active compounds. This model was confirmed by the synthesis of two pyridyl substituted acenaphthene derivatives (**A**, **B**). This new class of compounds as well as the pharmacophore could be helpful for the discovery of novel inhibitors.

Aldosterone synthase (CYP11B2) is the key enzyme of mineralocorticoid biosynthesis. It catalyzes the conversion of 11-deoxycorticosterone to the most potent mineralocorticoid aldosterone.¹ Pathological elevations in plasma aldosterone levels increase blood pressure and play a detrimental role in cardiovascular diseases.² In two recent clinical studies, the aldosterone receptor antagonists spironolactone and eplerenone were found to reduce mortality in patients with chronic congestive heart failure and in patients after myocardial infarction, respectively.^{3,4} The treatment with these antagonists however, is accompanied with severe side effects like hyperkalemia.⁵ A new pharmacological approach for the treatment of hyperaldosteronism, congestive heart failure, and myocardial fibrosis was recently suggested by us: inhibition of aldosterone formation with CYP11B2-inhibitors.^{6,7} Non-steroidal, selective inhibitors are to be preferred, because they can be expected to have less side effects on the endocrine system. The inhibitors must not affect other P450 (CYP) enzymes. In case of 11- β -hydroxylase (key enzyme of glucocorticoid biosynthesis, CYP11B1) this was very difficult to achieve, since it has a sequence homology of more than 93% compared to CYP11B2.⁸ Therefore we initiated a drug discovery program^{6,7} which finally resulted in potent and selective inhibitors originating from three classes of compounds: *E*- and *Z*- heterocyclic substituted methylene-tetrahydronaphthalenes and -indanes and heterocyclic substituted naphthalene derivatives.⁹⁻¹¹

Here, we describe a pharmacophore model to get insight in the 3-dimensional shape of the binding pocket. Compounds named ‘inhibitors’ were highly active in V79MZh11B2 cells,¹² expressing human CYP11B2 (IC₅₀ values < 100 nM).⁹⁻¹¹ ‘Non-inhibitors’ showed little to no activity (IC₅₀ values > 300 nM).⁹⁻¹¹

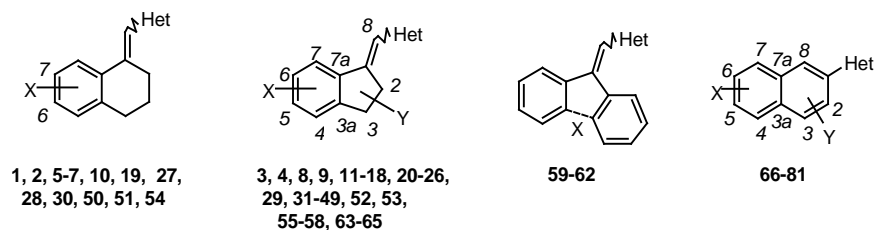
These compounds are supposed to occupy the substrate binding site in the apoprotein moiety. They also complex with their aromatic nitrogen (pharmacophore point N, Fig. 1b) the iron ion of the heme, which is located in the active site as well. This complexation mechanism does not only increase binding affinity of the inhibitors but also prevents oxygen activation at the heme, which is required for the catalytic process. No X-ray structure of CYP11B2, which is located in the inner mitochondrial membrane, is available. Homology approach based protein models have been improved continuously,^{9-11,13} but still are of limited predictive value.

The compounds shown in Table 1 were first built in Sybyl 7.0 (Tripos Associates; Inc., St. Louis, MO 2001, USA) and then optimized in conjugate-gradient modus. Subsequently all molecules underwent a conformational analysis with MacroModel V7.0 (1999 Schrödinger, Inc.) and were energy-minimized in MMFF94s¹⁴ forcefield as

implemented in Sybyl 7.0. A dielectric constant of 1.0 has been used throughout and the optimizations have been terminated at a gradient of 0.001 kcal/mol. After defining the ring centroids for each compound of the three classes

(C1, C2, and C2b, Fig. 1b), the compounds 17–39 - with the exception of the non-inhibitors - were first superimposed on compounds 20 and 21 with Sybyl by a three-point-fit strategy using the very same atoms for E-(red) and Z-(green) 3-pyridyl substituted tetrahydronaphthalenes and -indanes (Fig. 1a).¹⁵

Table 1. Inhibitors and non-inhibitors of aldosterone synthase (CYP11B2)



no	X, Y	Het ^a	Isomer	IC ₅₀ [nM] ^b	no	X, Y	Het ^a	Isomer	IC ₅₀ [nM] ^b	no	X, Y	Het ^a	Isomer	IC ₅₀ [nM] ^b
1	H	Im	E	25	28	6-OMe	3-Py	Z	878	55	6-Me	4-Py	E	>500
2	H	Im	Z	10	29	6-OMe	3-Py	E	>500	56	6-Me	4-Py	Z	>500
3	H	Im	E	41	30	6,7-diOMe	3-Py	E	>500	57	5-F	Pyrim	E	27
4	H	Im	Z	11	31	5-OEt	3-Py	E	79	58	5-F	Pyrim	Z	>500
5	7-CN	Im	E	>500	32	5-OBn	3-Py	E	>500	59	bond	3-Py	-	>500
6	7-CN	Im	Z	13	33	6-Me	3-Py	E	>500	60	no bond	3-Py	-	>500
7	6-CN	Im	Z	23	34	6-Me	3-Py	Z	>500	61	bond	4-Py	-	>500
8	5-CN	Im	E	36	35	4-Me	3-Py	Z	>500	62	no bond	4-Py	-	>500
9	5-CN	Im	Z	36	36	4-F	3-Py	E	21	63	3-Me	3-Py	E	>500
10	7-Cl	Im	E	47	37	4-Cl	3-Py	E	9	64	3-Me	3-Py	Z	>500
11	5-F	Im	E	17	38	4-Cl	3-Py	Z	31	65	3-Phenyl	3-Py	E	>500
12	5-F	Im	Z	14	39	7-OMe	3-Py	E	27	66	H	3-Py	-	28
13	5-Cl	Im	E	89	40	H	4-Py	E	>500	67	5-OH	3-Py	-	23
14	5-Cl	Im	Z	4	41	H	4-Py	Z	931	68	5-OMe	3-Py	-	6
15	5-Br	Im	E	93	42	5-F	4-Py	E	1098	69	5-OEt	3-Py	-	12
16	5-Br	Im	Z	10	43	5-F	4-Py	Z	34	70	5-OPr	3-Py	-	>500
17	H	3-Py	E	11	44	5-Cl	4-Py	E	1515	71	5-OBn	3-Py	-	>500
18	H	3-Py	Z	92	45	5-Cl	4-Py	Z	301	72	5-COOMe	3-Py	-	72
19	H	3-Py	E	22	46	5-Br	4-Py	E	2640	73	5-Br	3-Py	-	15
20	5-F	3-Py	E	7	47	5-Br	4-Py	Z	484	74	5-CN	3-Py	-	3
21	5-F	3-Py	Z	11	48	5-OMe	4-Py	E	>500	75	6-OMe	3-Py	-	>500
22	5-Cl	3-Py	E	26	49	5-OMe	4-Py	Z	>500	76	4-Cl, 5-OMe	3-Py	-	13
23	5-Cl	3-Py	Z	73	50	6-OMe	4-Py	E	>500	77	4-Cl, 5-OMe, 8-Cl	3-Py	-	28
24	5-Br	3-Py	E	37	51	6-OMe	4-Py	Z	>500	78	4-Br, 5-OMe	3-Py	-	33
25	5-OMe	3-Py	E	34	52	6-OMe	4-Py	E	>500	79	4-(3-Pyridyl), 2,3-	3-Py	-	>500
26	5-OMe	3-Py	Z	26	53	6-OMe	4-Py	Z	>500	80	Benzene-annelated	3-Py	-	>500
27	6-OMe	3-Py	E	57	54	6,7-diOMe	4-Py	E	>500	81	5-OMe	4-Py	-	>500

^a Heterocycle: Im= imidazole, 3-Py= 3-pyridine, 4-Py= 4-pyridine, Pyrim= pyrimidine;

^b Activity determined in V79MZh 11B2 cells as described.⁹⁻¹¹

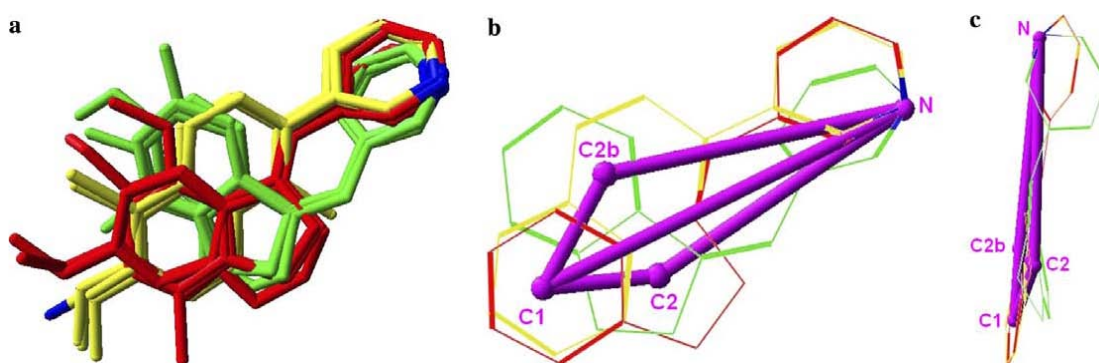
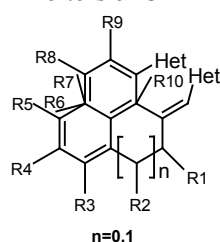


Figure 1. Superimposition of compounds: (a) alignment of inhibitors from **17** to **39** and **66** to **81** (see Table 1); (b) skeletal structure of the pharmacophore model: overlay of the unsubstituted 2-(3-pyridyl) naphthalene (**66** yellow) and the unsubstituted E- and Z-3-pyridylmethylene-indane (**17** and **18**; red and green); the pharmacophore (magenta) is built by connecting the ring centroids (**C1**, **C2**, and **C2b**) and the aromatic nitrogen **N**; (c) sideview of the pharmacophore.

The naphthalene inhibitors (**66–69**, **72–74**, and **76–78**; yellow, Fig. 1a) were aligned with both E- and Z-(3-pyridyl)methylene-indanes and -tetrahydronaphthalenes, respectively.^{16,17} These naphthalenes as well as the E and Z-imidazolyl substituted tetrahydronaphthalene and -indane inhibitors (not shown) fitted very well into the pharmacophore (Fig. 1b). The superimposition of non-inhibitors - using the same procedure as applied for the inhibitors - revealed that the corresponding substituents did not match with the model (Table 2).

Table 2. Substitution patterns of inhibitors and non-inhibitors of CYP11B2



$n=0,1$
 Inhibitors: Het= 3-Pyridine, Imidazole, Pyrimidine
 Non-Inhibitors: Het= 4-Pyridine

R	appropriate substituents	inappropriate substituents
R ¹	H, CH ₃ ,	Phenyl, anellated rings (R ¹ to R ²)
R ²	-	-
R ³	H, F, Cl, CH ₃ , OMe	-
R ⁴	H, F, Cl, Br, CN, OH, OMe, OEt, COOMe	OPr, OBn
R ⁵	H, Cl, Br	Me, OMe, CN, 3-Pyridyl
R ⁶	H, Cl	-
R ⁷	H, OMe	-
R ⁸	H, F, Cl, Br, CN, OMe	anellated rings (R ⁸ to R ⁹)
R ⁹	H, CN	Me
R ¹⁰	Cl	-

The pharmacophore model (Fig. 1b) was built on four pharmacophore points, chosen on the basis of the global superimposition (Fig. 1):

- **N**: heterocyclic nitrogen (all inhibitors).
- **C1**: ring centroid (E-(3-pyridyl)methylene-tetrahydronaphthalenes and -indanes and naphthalenederivatives).
- **C2**: ring centroid (E- and Z-(3-pyridyl)-methyleneindanes and -tetrahydronaphthalenes).
- **C2b**: ring centroid (Z-(3-pyridyl)methylene-tetrahydronaphthalenes and -indanes and naphthalenederivatives).

Each compound fits with three of these points and has nitrogen N in common. The lone pair of the heterocyclic nitrogen of all compounds has to point in almost the same direction (Fig. 1a) for complexing the heme iron. The three ring centroids (**C1**, **C2**, and **C2b**) are located in one plane, **P0**, forming a planar three-ring-system (acenaphthene or dihydro-phenalene), while the aromatic nitrogen N is located slightly above plane **P0** (see geometric parameters, Table 3). Actually, the whole pharmacophore seems to be quite planar.

Table 3. Geometric parameters of the pharmacophore

Distances (Å)		Angles (°)		Angles respect to the planes (°)	
C1–C2	2.0–2.3	C1–N–C2	12.5–15	P0–P1	13.3
C1–C2b	2.2–2.4	C1–N–C2b	10–12	P0–P2	11.9
C2–C2b	2.1–2.3	C2–N–C2b	23.5–25	P1–P2	157.8
C1–N	7.1–8.1				
C2–N	5.2–6.0				
C2b–N	5.2–6.4				

where:

- **P0**: plane containing **C1**, **C2**, and **C2b**;
- **P1**: plane containing **C1**, **N**, and **C2**;
- **P2**: plane containing **C1**, **N**, and **C2b**;
- **P3**: plane containing **C2**, **N**, and **C2b**.

The steric features of active and non-active CYP11B2-inhibitors were further explored by the ‘steric inclusion area (SIA)’ and the ‘steric exclusion area (SEA)’, respectively (Figs. 2a and b). The SIA is mainly located in the region of substituents R3, R4 and R8 (see Table 2). Larger groups as formic acid methyl ester can only be introduced in position R4 (**72**), whereas position R8 is of limited size. The SEA is located at the non-aromatic ring and the exocyclic double bond of the *Z*-isomer (substituents R1 and R2, Table 2). Additionally, large substituents as benzyloxy- or 3-pyridyl-groups in the region of R4 and R5 are not suitable for proper inhibitor binding (**32** and **79**). The SEA is also located close to R9, since methyl-groups lead to a strong decrease of activity (**34**).

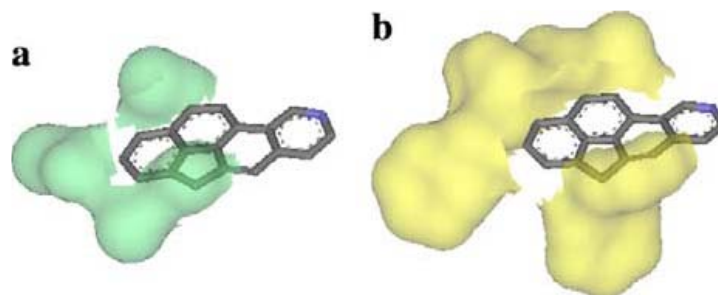
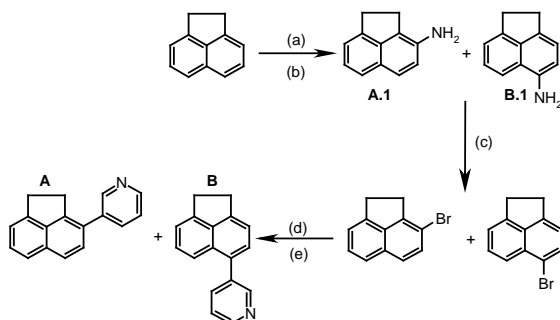


Figure 2. Unsubstituted hybrid-structure with: a) the steric inclusion area (SIA); b) the steric exclusion area (SEA).

To validate the model, a compound was generated as a hybrid structure of the used *E*- and *Z*-isomers as well as the naphthalene compounds, the acenaphthene derivative (**A**). Compound **A** was synthesized in four steps: nitration of acenaphthene¹⁶ and subsequently hydrogenation¹⁷ leading to a mixture of two isomers: 3- and 5-aminoacenaphthene. In the following Sandmeyer reaction the bromo derivatives were formed and used for Suzuki coupling with 3-pyridine boronic acid. The resulting mixture was subsequently chromatographed and the isomers **A** and **B** were isolated (Scheme 1).

Scheme 1.



Reagents and Conditions: (a) HNO_3 , in acetic anhydride, 20 h at 10°C ; (b) H_2 , Pt/C (5%), in THF; (c) 1. NaNO_2 , in HBr, 0°C , 2. CuBr, in HBr/toluene, 0°C , addition of the diazonium salt, 10 min at 0°C , 2h at 100°C ; (d) Na_2CO_3 -solution, 3-pyridine-boronic acid, in methanol, tetrakis(triphenyl-phosphin)palladium, N_2 , reflux, 12 h; (e) separation of A and B using column chromatography.

Both isomers were tested for activity in V79 cells,¹² expressing human CYP11B2.⁶ The IC_{50} values of the compounds are given in Table 4.

Table 4. Biological evaluation of hybrid compounds A and B

Compound	IC_{50} -value [nM] ^a		Selectivity ^d
	CYP11B1 ^b	CYP11B2 ^c	
A	2452	10	245
B	2896	14	207

^a Mean value of four determinations, standard deviation less than 20%. ^b Hamster fibroblasts (V79 cells) expressing human CYP11B1; substrate deoxycorticosterone, 100 nM. ^c Hamster fibroblasts (V79 cells) expressing human CYP11B2; substrate deoxycorticosterone, 100 nM; ^d IC_{50} CYP11B1/ IC_{50} CYP11B2.

As expected compound A exhibited strong inhibitory activity ($\text{IC}_{50} = 10$ nM), thus confirming the validity of the pharmacophore model. Surprisingly the isomer B was also very potent. This can be explained by the alignment of the acenaphthene derivatives A and B (Fig. 3). The compounds display a very similar shape, they only differ in the position of the non-aromatic cyclopentene-ring.

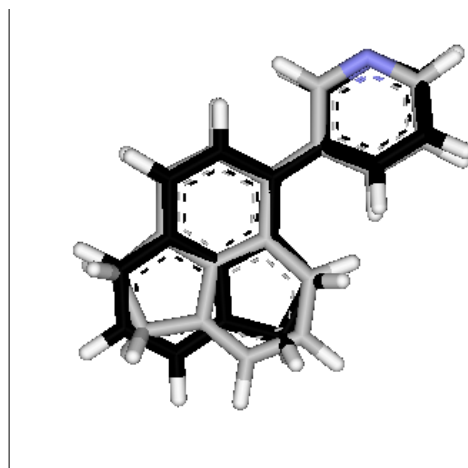


Figure 3. Alignment of hybrid compound A (black) and its isomer B (grey).

After having discovered the acenaphthene isomers as highly potent lead compounds we wanted to know about their selectivity towards CYP11B1 (Table 4). Both inhibitors showed little inhibition of CYP11B1 which makes them interesting candidates for further development.

Summarizing, the first pharmacophore model for inhibitors of aldosterone synthase (CYP11B2) was built by superimposition of a series of compounds synthesized by our group. This pharmacophore could be confirmed by synthesis and biological evaluation of two hybrid compounds derived from the model.

Acknowledgements. We thank the Deutsche Forschungsgemeinschaft (Ha 1513/6), the Saarland Ministry of Education, Culture and Science (ETTT Project) and the Fonds der Chemischen Industrie for financial support. Sarah Ulmschneider is grateful to the Fonds der Chemischen Industrie and the Bundesministerium für Bildung und Forschung for a scholarship (Kekule's grant).

Supplementary data. Supplementary data associated with this article can be found in the online version at doi:10.1016/j.bmcl.2005.09.059.

References and notes

- (1) Kawamoto, T.; Mitsuuchi, Y.; Toda, K.; Yokoyama, Y.; Miyahara, K.; Miura, S.; Ohnishi, T.; Ichikawa, Y.; Nakao, K.; Imura, H. *Proc. Natl. Acad. Sci. U S A* **1992**, *89*, 1458-1462.
- (2) Brilla, C. G. *Cardiovasc. Res.* **2000**, *47*, 1-3.
- (3) Pitt, B.; Remme, W.; Zannad, F.; Neaton, J.; Martinez, F.; Roniker, B.; Bittman, R.; Hurley, S.; Kleiman, J.; Gatlin, M. *N. Engl. J. Med.* **2003**, *348*, 1309-1321.
- (4) Pitt, B.; Zannad, F.; Remme, W. J.; Cody, R.; Castaigne, A.; Perez, A.; Palensky, J.; Wittes, J. *N. Engl. J. Med.* **1999**, *341*, 709-717.
- (5) Christ, M.; Grimm, W.; Maisch, B. *Internist (Berl)* **2004**, *45*, 347-354.
- (6) Ehmer, P. B.; Bureik, M.; Bernhardt, R.; Müller, U.; Hartmann, R. W. *J. Steroid Biochem. Mol. Biol.* **2002**, *81*, 173-179.
- (7) Hartmann, R. W.; Müller, U.; Ehmer, P. B. *Eur. J. Med. Chem.* **2003**, *38*, 363-366.
- (8) Pilon, C.; Mulatero, P.; Barzon, L.; Veglio, F.; Garrone, C.; Boscaro, M.; Sonino, N.; Fallo, F. *J. Clin. Endocrinol. Metab.* **1999**, *84*, 4228-4231.
- (9) Voets, M.; Antes, I.; Scherer, C.; Biemel, K.; Barassin, C.; Marchais-Oberwinkler, S.; Hartmann, R. W. *J. Med. Chem.* **2005**, submitted.
- (10) Ulmschneider, S.; Müller-Vieira, U.; Klein, C. D.; Hartmann, R. W.; Antes, I.; Lengauer, T. *J. Med. Chem.* **2005**, *48*, 1563-1575.
- (11) Ulmschneider, S.; Müller-Vieira, U.; Mitrenga, M.; Hartmann, R. W.; Oberwinkler-Marchais, S.; Klein, C. D.; Bureik, M.; Bernhardt, R.; Antes, I.; Lengauer, T. *J. Med. Chem.* **2004**, *48*, 1796-1805.
- (12) Denner, K.; Doehmer, J.; Bernhardt, R. *Endocr. Res.* **1995**, *21*, 443-448.
- (13) Belkina, N. V.; Lisurek, M.; Ivanov, A. S.; Bernhardt, R. *J Inorg Biochem* **2001**, *87*, 197-207.
- (14) Halgren, T. A. *J. Comput. Chem.* **1999**, *20*, 730.
- (15) Alignment was performed as follows: E-(3-pyridyl) methylene-indanes and -tetrahydronaphthalenes (aromatic nitrogen N, centroid C2, C7a or C8a, respectively), Z-(3-pyridyl)methylene-indanes and -tetrahydronaphthalenes (aromatic nitrogen N, centroid C2, C3a or C4a, respectively).
- (16) Alignment was performed as follows: E-(3-pyridyl) methylene-indanes and -tetrahydronaphthalenes (aromatic nitrogen N, centroid C1, C7a or C8a, respectively), 3-pyridyl substituted naphthalenes (aromatic nitrogen N, centroid C1, C7a).
- (17) Alignment was performed as follows: Z-(3-pyridyl) methylene-indanes and -tetrahydronaphthalenes (aromatic nitrogen N, centroid C2b, C3a or C4a, respectively), 3-pyridyl substituted naphthalenes (aromatic nitrogen N, centroid C2b, C7a).
- (18) Chen, M.; Hu, Y.; Shen, Y. *Ranliao Gongye* **2001**, *38*, 21-23.
- (19) Friedman, O. M.; Gofstein, R. M.; Seligman, A. M. *J. Am. Chem. Soc.* **1949**, *71*, 3010-3013.

3.4.3.2. Paper XIII.

Overcoming Undesirable CYP1A2 Inhibition of Pyridyl-naphthalene Type Aldosterone Synthase Inhibitors: Influence of Heteroaryl Derivatization on Potency and Selectivity Inhibitors.

Ralf Heim, Simon Lucas, Cornelia M. Grombein, Christina Ries, Katarzyna E. Schewe, Matthias Negri, Ursula Müller-Vieira, Barbara Birk, and Rolf W. Hartmann

This article is protected by copyrights of 'Journal of Medicinal Chemistry.'

J. Med. Chem. **2008**, 51, 5064–5074.

Abstract

Recently, we reported on the development of potent and selective inhibitors of aldosterone synthase (CYP11B2) for the treatment of congestive heart failure and myocardial fibrosis. A major drawback of these non-steroidal compounds was a strong inhibition of the hepatic drug-metabolizing enzyme CYP1A2. In the present study, we examined the influence of substituents in the heterocycle of lead structures with a naphthalene molecular scaffold to overcome this unwanted side effect. With respect to CYP11B2 inhibition, some substituents induced a dramatic increase in inhibitory potency. The methoxyalkyl derivatives **22** and **26** are the most potent CYP11B2 inhibitors up to now ($IC_{50} = 0.2$ nM). Most compounds also clearly discriminated between CYP11B2 and CYP11B1 and the CYP1A2 potency significantly decreased in some cases (e.g., isoquinoline derivative **30** displayed only 6 % CYP1A2 inhibition at 2 μ M concentration). Furthermore, isoquinoline derivative **28** proved to be capable of passing the gastrointestinal tract and reached the general circulation after peroral administration to male Wistar rats.

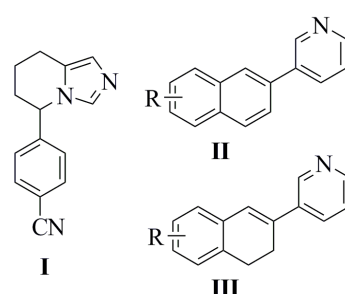
Introduction

The most important circulating mineralocorticoid aldosterone is secreted by the zona glomerulosa of the adrenal gland and is to a minor extent also synthesized in the cardiovascular system.¹ The hormone plays a key role in the electrolyte and fluid homeostasis and thus for the regulation of blood pressure. Its biosynthesis is accomplished by the mitochondrial cytochrome P450 enzyme aldosterone synthase (CYP11B2) and proceeds via catalytic oxidation of the substrate 11-deoxycorticosterone to corticosterone and subsequently to aldosterone.² The adrenal aldosterone synthesis is regulated by several physiological parameters such as the renin-angiotensin-aldosterone system (RAAS) and the plasma potassium concentration. Chronically elevated plasma aldosterone levels increase the blood pressure and are closely associated with certain forms of myocardial fibrosis and congestive heart failure.³ An insufficient renal flow chronically activates the RAAS and aldosterone is excessively released. The therapeutic benefit of reducing aldosterone effects by use of the mineralocorticoid receptor (MR) antagonists spironolactone and eplerenone has been reported in two recent clinical studies (RALES and EPHEBUS).^{4,5} The studies showed that treatment with these antagonists reduces mortality in patients with chronic congestive heart failure and in patients after myocardial infarction, respectively. Spironolactone, however, showed severe side effects presumably due to its steroidal structure.^{4,6} Although the development of non-steroidal aldosterone receptor antagonists has been reported recently,⁷ several issues associated with the unaffected and pathophysiologically elevated plasma aldosterone levels remain unsolved by this therapeutic strategy such as the up-regulation of the mineralocorticoid receptor expression⁸ and non-genomic aldosterone effects.⁹ A novel approach for the treatment of diseases affected by elevated aldosterone levels is the blockade of aldosterone biosynthesis by inhibition of CYP11B2.^{10,11} Aldosterone synthase has previously been proposed as a potential pharmacological target,¹² and preliminary work focused on the development of steroidal inhibitors, i.e., progesterone¹³ and deoxycorticosterone¹⁴ derivatives with unsaturated C₁₈-substituents. These compounds were found to be mechanism-based inhibitors binding covalently to the active site of bovine CYP11B, however, data on inhibitory action towards human enzyme are essentially absent in these studies. The strategy of inhibiting the aldosterone formation has two main advantages compared to MR antagonism. First, there is no non-steroidal inhibitor of a steroidogenic CYP enzyme known to have affinity to a steroid receptor. For this reason, fewer side effects on the endocrine system should be expected. Furthermore, CYP11B2 inhibition can

reduce the pathologically elevated aldosterone levels whereas the latter remain unaffected by interfering one step later at the receptor level. By this approach, however, it is a challenge to reach selectivity versus other CYP enzymes. Taking into consideration that the key enzyme of glucocorticoid biosynthesis, 11 β -hydroxylase (CYP11B1), and CYP11B2 have a sequence homology of more than 93 %, ¹⁵ the selectivity issue becomes especially critical for the design of CYP11B2 inhibitors.

The aromatase (CYP19) inhibitor fadrozole (**I**, Chart 1) which is used in the therapy of breast cancer was found to significantly reduce the corticoid formation. ¹⁶ This compound is a potent inhibitor of CYP11B2 displaying an IC₅₀ value of 1 nM (Table 1). The R(+)-enantiomer of fadrozole (FAD 286) was recently shown to reduce mortality and to ameliorate angiotensin II-induced organ damage in transgenic rats overexpressing both the human renin and angiotensinogen genes. ¹⁷ These findings underline the potential therapeutic utility of aldosterone synthase inhibition, and up to now, several structurally modified fadrozole derivatives are investigated as CYP11B2 inhibitors. ^{18,19} Recently, the development of imidazolyl- and pyridylmethylenetetrahydronaphthalenes and -indanes as highly active and in some cases selective CYP11B2 inhibitors has been described by our group. ^{20,21} By keeping the pharmacophore and rigidization of the core structure, pyridine substituted naphthalenes ²² **II** and dihydronaphthalenes ²³ **III** were shown to be potent and selective CYP11B2 inhibitors (Chart 1). Combining the structural features of these substance classes to a hybrid core structure led to pyridine substituted acenaphthenes as potent CYP11B2 inhibitors with remarkable selectivity. ²⁴ Furthermore, most of the naphthalene and dihydronaphthalene type compounds exhibited a favorable selectivity profile versus selected hepatic CYP enzymes. However, they turned out to be potent inhibitors of the hepatic CYP1A2 enzyme (see examples **1**, **3**, and **4** in Table 1). CYP1A2 makes up about 10 % of the overall cytochrome P450 content in the liver and metabolizes aromatic and heterocyclic amines as well as polycyclic aromatic hydrocarbons. ²⁵ This experimental result turned these naphthalene type aldosterone synthase inhibitors into unsuitable drug candidates since adverse drug-drug interactions are mainly caused by inhibition of hepatic cytochrome P450 enzymes and have to be avoided in either case. In our preceding studies, the attention was focused on the optimization of the naphthalene skeleton, the substitution pattern of the heme complexing 3-pyridine moiety, however, was not investigated in detail. Herein, we describe the synthesis of a series of naphthalenes and dihydronaphthalenes with various substituents in the pyridine heterocycle to examine their influence on potency and selectivity (Table 1). The biological activity of the synthesized compounds was determined *in vitro* on human CYP11B2 for potency and human CYP11B1 and CYP1A2 for selectivity. In addition, selected compounds were tested for inhibitory activity at human CYP17 (17 α -hydroxylase-C17,20-lyase), CYP19, and selected hepatic CYP enzymes (CYP2B6, CYP2C9, CYP2C19, CYP2D6, CYP3A4). The *in vivo* pharmacokinetic profile of two promising compounds was determined in a cassette dosing experiment using male Wistar rats.

Chart 1. Non-steroidal inhibitors of CYP11B2.

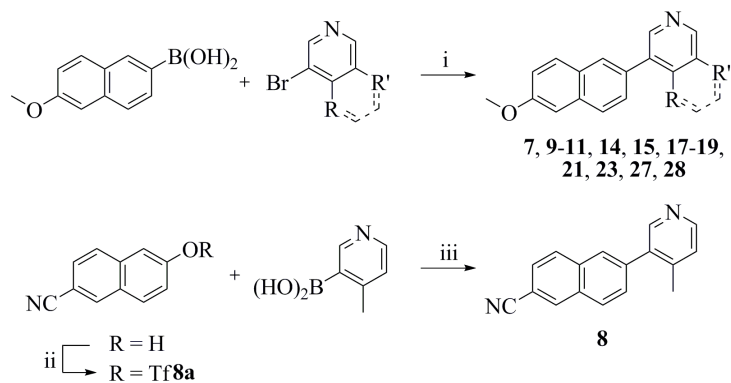


Results

Chemistry

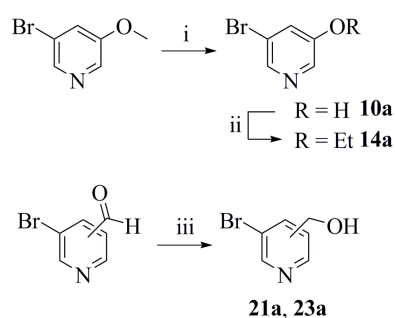
The key step for the synthesis of pyridine substituted naphthalenes was a Suzuki cross coupling (Scheme 1). ²⁶ A microwave enhanced method developed by van der Eycken et al. was chosen for this purpose. ²⁷ By applying this method, various substituted bromopyridines were coupled with 6-methoxy-2-naphthaleneboronic acid to afford compounds **7**, **9–11**, **14**, **15**, **17–19**, **21**, **23**, **27**, and **28**. Compound **8** was obtained by coupling of 4-methyl-3-pyridineboronic acid with triflate **8a** which was accessible by treating 6-cyano-2-naphthol with Tf₂NPh and K₂CO₃ in THF under microwave irradiation. ²⁸ The bromopyridines could be derivatized prior to Suzuki coupling according to Scheme 2 to provide heterocycles bearing a hydroxy, ethoxy or hydroxymethyl substituent (**10a**, **14a**, **21a**, and **23a**). ²⁹

Scheme 1.



Reagents and conditions: i) Pd(PPh₃)₄, DMF, aq. NaHCO₃, μ w, 150 °C; ii) Tf₂NPh, K₂CO₃, THF, μ w, 120 °C; iii) Pd(dppf)Cl₂, toluene/acetone, aq. Na₂CO₃, μ w, 150 °C.

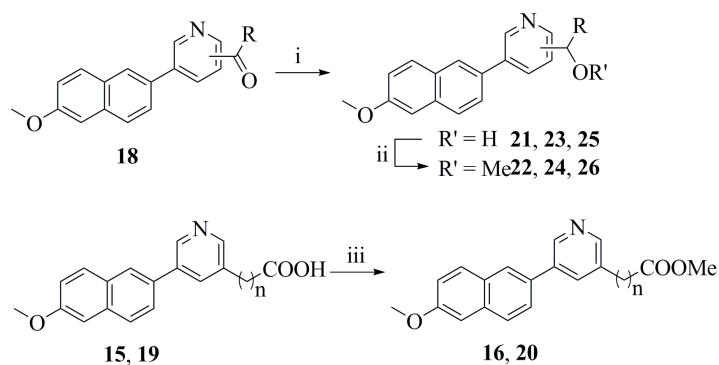
Scheme 2.



Reagents and conditions: i) conc. HBr, reflux; ii) EtBr, K₂CO₃, DMF, rt; iii) NaBH₄, methanol, 0 °C.

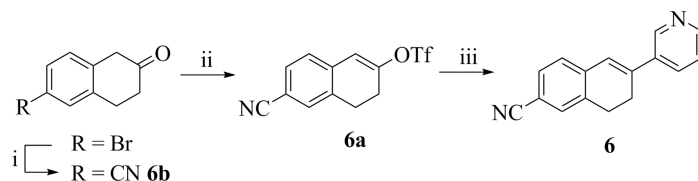
For compounds **21–26**, the substitution pattern was modified after the cross-coupling reaction as shown in Scheme 3 by sodium borohydride reduction and optional methylation. Esterification of the carboxylic acids **15** and **19** by refluxing in methanol under acid catalysis afforded the corresponding methyl esters **16** and **20**. The synthesis of 6-cyanodihydronaphthalene **6** was accomplished by the sequence shown in Scheme 4. Using 6-bromo-2-tetralone, Pd-catalyzed cyanation³⁰ led to intermediate **6b** which was transformed into the alkenyltriflate **6a** by deprotonation with KHMDS and subsequent treatment with Tf₂NPh.³¹ Compound **6a** underwent Suzuki coupling with 3-pyridineboronic acid to afford **6**.

Scheme 3.



Reagents and conditions: i) NaBH₄, methanol, 0 °C; ii) MeI, NaH, THF, rt; iii) methanol, H₂SO₄, reflux.

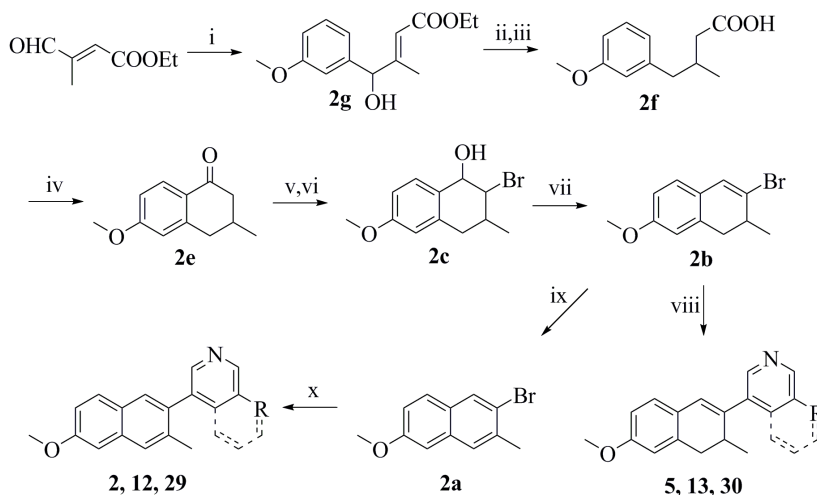
Scheme 4.



Reagents and conditions: i) $\text{Zn}(\text{CN})_2$, $\text{Pd}(\text{PPh}_3)_4$, DMF, 100 °C; ii) $\text{ Tf}_2\text{NPh}$, KHMDS, THF/toluene, -78 °C; iii) 3-pyridineboronic acid, $\text{Pd}(\text{PPh}_3)_4$, DMF, aq. NaHCO_3 , μw , 150 °C.

The naphthalenes **2**, **12**, **29** and the dihydronaphthalenes **5**, **13**, **30** were obtained as shown in Scheme 5. The sequence for the synthesis of intermediate **2e** was described previously and was only slightly modified by us (see supplementary material).³² Regioselective α -bromination was accomplished by treating **2e** with CuBr_2 in refluxing ethyl acetate/ CHCl_3 .³³ After a subsequent reduction/elimination step,²³ the intermediate alkenylbromide **2b** underwent Suzuki coupling³⁴ with the appropriate boronic acid to afford the dihydronaphthalenes **5**, **13**, and **30**. The corresponding naphthalenes **2**, **12**, and **29** were obtained by aromatization of **2b** with DDQ in refluxing toluene³⁵ followed by Suzuki coupling.²⁷ The synthesis of compounds **1**, **3**, and **4** has been reported previously by our group.^{22,23}

Scheme 5.

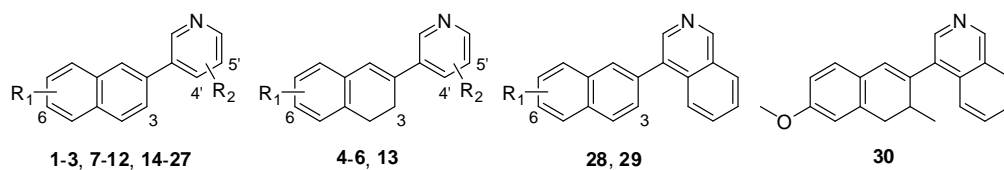


Reagents and conditions: i) 3-methoxyphenylmagnesium bromide, THF, -5 °C; ii) KOH, NaOH/water, reflux; iii) H_2 , Pd/C, AcOH, 60 °C; iv) $(\text{COCl})_2$, CH_2Cl_2 , rt, then AlCl_3 , CH_2Cl_2 , -10 °C; v) CuBr_2 , ethyl acetate/ CHCl_3 , reflux; vi) NaBH_4 , methanol, 0 °C; vii) *p*-toluenesulfonic acid, toluene, reflux; viii) boronic acid, $\text{Pd}(\text{OAc})_2$, TBAB, acetone, aq. Na_2CO_3 , μw , 150 °C; ix) DDQ, toluene, reflux; x) boronic acid, $\text{Pd}(\text{PPh}_3)_4$, DMF, aq. NaHCO_3 , μw , 150 °C.

Biological Results

Inhibition of Human Adrenal Corticoid Producing CYP11B2 and CYP11B1 *In Vitro* (Table 1). The inhibitory activities of the compounds were determined in V79 MZh cells expressing either human CYP11B2 or CYP11B1.^{10,36} The V79 MZh cells were incubated with [^{14}C]-deoxycorticosterone as substrate and the inhibitor at different concentrations. The product formation was monitored by HPTLC using a phosphoimager. Fadrozole, an aromatase (CYP19) inhibitor with proven ability to reduce corticoid formation *in vitro* and *in vivo* was used as a reference compound (CYP11B2, $\text{IC}_{50} = 1$ nM; CYP11B1, $\text{IC}_{50} = 10$ nM).¹⁶

Most of the substituted pyridynaphthalenes showed a high inhibitory activity at the target enzyme CYP11B2 with IC_{50} values in the low nanomolar range (Table 1). Some of the compounds displayed subnanomolar potency ($\text{IC}_{50} < 1$ nM) and turned out to be even stronger aldosterone synthase inhibitors than the reference substance fadrozole. The methoxyalkyl substituted compounds **22** and **26** exhibited IC_{50} values of 0.2 nM each. Hence, they are 5-fold more active than fadrozole ($\text{IC}_{50} = 1$ nM) and 30-fold more active than the unsubstituted parent compound **1** ($\text{IC}_{50} = 6.2$ nM). However, derivatization by polar and acidic residues in 5'-position resulted in a decrease in potency. This particularly applies to the carboxylic acids **15** and **19** showing no or only low inhibitory activity and to a minor extent also to the phenolic compound **10** and the carboxamide **17** with IC_{50} values of 94 nM each.

Table 1. Inhibition of human adrenal CYP11B2, CYP11B1 and human CYP1A2 *in vitro*

compd	R ₁	R ₂	IC ₅₀ value ^a (nM)		selectivity factor ^d	% inhibition ^e CYP1A2 ^f
			V79 11B2 ^b	V79 11B1 ^c		
			hCYP11B2	hCYP11B1		
1 ^g	6-OMe	H	6.2	1577	254	98
2	6-OMe-3-Me	H	7.0	1047	150	93
3 ^g	6-CN	H	2.9	691	239	97
4 ^g	6-OMe	H	2.1	578	275	98
5	6-OMe-3-Me	H	3.3	248	79	73
6	6-CN	H	4.5	461	103	91
7	6-OMe	4'-Me	0.8	114	143	98
8	6-CN	4'-Me	0.6	52	87	86
9	6-OMe	4'-NH ₂	13	1521	117	58
10	6-OMe	5'-OH	94	8925	95	93
11	6-OMe	5'-OMe	4.2	238	57	91
12	6-OMe-3-Me	5'-OMe	3.8	875	230	91
13	6-OMe-3-Me	5'-OMe	1.2	100	83	18
14	6-OMe	5'-OEt	5.1	373	73	85
15	6-OMe	5'-COOH	n.a. ^h	n.d.	n.d.	n.d.
16	6-OMe	5'-COOMe	0.8	15	19	n.d.
17	6-OMe	5'-CONH ₂	94	41557	442	n.d.
18	6-OMe	5'-COMe	2.1	255	121	80
19	6-OMe	5'-CH ₂ COOH	1216	37796	31	n.d.
20	6-OMe	5'-CH ₂ COOMe	6.9	199	29	n.d.
21	6-OMe	5'-CH ₂ OH	9.1	614	68	93
22	6-OMe	5'-CH ₂ OMe	0.2	31	155	83
23	6-OMe	4'-CH ₂ OH	22	1760	80	92
24	6-OMe	4'-CH ₂ OMe	2.2	435	198	97
25	6-OMe	5'-CH(OH)Me	0.5	99	198	78
26	6-OMe	5'-CH(OMe)Me	0.2	10	50	n.d.
27	6-OMe	5'-Ph	4.8	151	32	n.d.
28	6-OMe	-	0.6	67	112	57
29	6-OMe-3-Me	-	3.1	843	272	45
30	-	-	0.5	64	128	6
fadrozole	-	-	1.0	10	10	8

^a Mean value of four experiments, standard deviation usually less than 25 %, n.d. = not determined. ^b Hamster fibroblasts expressing human CYP11B2; substrate deoxycorticosterone, 100 nM. ^c Hamster fibroblasts expressing human CYP11B1; substrate deoxycorticosterone, 100 nM. ^d IC₅₀ CYP11B1/IC₅₀ CYP11B2. ^e Mean value of two experiments, standard deviation less than 5 %; n.d. = not determined. ^f Recombinantly expressed enzyme from baculovirus-infected insect microsomes (Supersomes); inhibitor concentration, 2.0 μM; furafylline, 55 % inhibition. ^g These compounds were described previously.^{22,23} ^h n.a. = no activity (7 % inhibition at an inhibitor concentration of 500 nM).

Beside introduction of small residues in 4'- and 5'-position, an extension of the heterocyclic moiety by a condensed phenyl ring afforded the extraordinary potent isoquinoline compounds **28–30** with IC_{50} values in the range of 0.5–3.1 nM. Even the sterically demanding 5'-phenyl residue of compound **27** was still tolerated (IC_{50} = 4.8 nM). In general, changing the carbocyclic core (naphthalene, 3-methyl- or dihydro-derivative) while simultaneously keeping the substitution pattern of the heterocycle had only little effect on the CYP11B2 inhibition as shown by the series **11–13** (IC_{50} = 1.2–4.2 nM) and **28–30** (IC_{50} = 0.5–3.1 nM). With regard to the inhibitory activity at the highly homologous CYP11B1, most of the tested compounds were less active than at CYP11B2. However, a noticeable inhibition with IC_{50} values in the range of 10–100 nM was observed in some cases. In particular, the 5'-methoxyalkylpyridine derivatives **22** (IC_{50} = 31 nM) and **26** (IC_{50} = 10 nM) as well as the methyl ester **16** (IC_{50} = 15 nM) turned out to be potent CYP11B1 inhibitors. Although introduction of substituents in the heterocyclic moiety mostly resulted in a moderate decrease in selectivity compared to the unsubstituted derivatives, the selectivity factors were still high for most of the tested compounds (factor 100–200). In case of 6-methoxy-3-methylnaphthalene **2**, the introduction of substituents in the heterocyclic moiety led to an enhanced selectivity. A methoxy substituent in 5'-position as accomplished in compound **12** increased the selectivity factor from 150 to 230 and the isoquinoline derivative **29** proved to be one of the most selective CYP11B2 inhibitors of the series with a selectivity factor of 272, thus being 27-fold more selective than fadrozole (selectivity factor = 10).

Inhibition of Hepatic and Steroidogenic CYP Enzymes (Tables 1 and 2). In order to further examine the influence of heteroaryl substitution on selectivity, the compounds were tested for inhibition of the hepatic CYP1A2 enzyme. CYP1A2 was strongly inhibited by all previous CYP11B2 inhibitors of the naphthalene and dihydronaphthalene type with unsubstituted heme-coordinating heterocycle, e.g., **1–4** exhibited more than 90 % inhibition at an inhibitor concentration of 2 μ M (Table 1). With regard to the potent CYP1A2 inhibitor **1**, derivatization of the heterocycle gave rise to compounds with a slightly reduced inhibitory potency, e.g., compounds **14**, **18**, **22**, and **25** displaying approximately 80 % inhibition. A pronounced decrease of CYP1A2 inhibition was observed in case of compounds **9**, **13**, and **29–30** (6–57 %). However, the dihydronaphthalenes **6**, **13**, and **30** turned out to be chemically unstable and decomposition in DMSO solution was observed after storage at 2 °C (~80 % purity after three days) yielding considerable amounts of the aromatized analogues and traces of unidentified degradation products. Therefore, they were not taken into account for further biological evaluations despite their outstanding CYP1A2 selectivity. The CYP1A2 inhibition of some compounds was not determined at all due to either a low CYP11B2 potency (**15**, **17**, and **19**) or low CYP11B1 selectivity (**16**, **20**, **26**, and **27**).

For a set of four structurally diverse compounds (**9**, **11**, **18**, and **28**), an extended selectivity profile including inhibition of the steroidogenic enzymes CYP17 and CYP19 as well as inhibition of some crucial hepatic CYP enzymes (CYP2B6, CYP2C9, CYP2C19, CYP2D6, CYP3A4) was determined (Table 2). The inhibition of CYP17 was determined with the 50,000 *g* sediment of the *E. coli* homogenate recombinantly expressing human CYP17, progesterone (25 μ M) as substrate, and the inhibitors at a concentration of 2 μ M.³⁷ The tested compounds turned out to be moderately potent inhibitors of CYP17. The inhibition values ranked around 40 % corresponding with IC_{50} values of approximately 2000 nM or higher. The inhibition of CYP19 at an inhibitor concentration of 500 nM was determined *in vitro* by use of human placental microsomes and [1β -³H]androstenedione as substrate as described by Thompson and Siiteri³⁸ using our modification.³⁹ In this assay, no inhibition of CYP19 was observed for compounds **11**, **18**, and **28**. Only the amino substituted compound **9** displayed a moderate inhibition of 47 %. The IC_{50} values of the compounds for the inhibition of the hepatic CYP enzymes CYP1A2, CYP2B6, CYP2C9, CYP2C19, CYP2D6, and CYP3A4 were determined using recombinantly expressed enzymes from baculovirus-infected insect microsomes (Supersomes). The values of the CYP1A2 inhibition matched well the previously determined percental inhibition (Table 1). Methoxy compound **11** with 91 % inhibition at 500 nM turned out to be a potent CYP1A2 inhibitor (IC_{50} = 83 nM) whereas the inhibitory potency decreased to 488 nM in case of the ketone derivative **18**. A pronounced selectivity regarding the CYP1A2 inhibition was observed in case of compounds **9** and **28** with IC_{50} values of approximately 1.5 μ M. In most cases, the other investigated CYP enzymes were unaffected, e.g., IC_{50} values of **9** were greater than 10 μ M versus CYP2B6, CYP2C9, CYP2C19, CYP2D6, and CYP3A4.

Table 2. Inhibition of selected steroidogenic and hepatic CYP enzymes *in vitro*

compd	% inhibition ^a		IC ₅₀ value ^b (nM)					
	CYP17 ^c	CYP19 ^d	CYP1A2 ^{e,f}	CYP2B6 ^{e,g}	CYP2C9 ^{e,h}	CYP2C19 ^{e,i}	CYP2D6 ^{e,j}	CYP3A4 ^{e,k}
9	42	47	1420	> 50000	48970	45800	11100	21070
11	41	14	83	> 25000	1888	> 25000	> 25000	1913
18	36	< 5	488	> 50000	> 200000	> 200000	> 200000	9070
28	39	7	1619	16540	1270	3540	33110	3540

^a Mean value of four experiments, standard deviation less than 10 %. ^b Mean value of two experiments, standard deviation less than 5 %. ^c *E. coli* expressing human CYP17; substrate progesterone, 25 μM; inhibitor concentration 2.0 μM; ketoconazole, IC₅₀ = 2780 nM. ^d Human placental CYP19; substrate androstenedione, 500 nM, inhibitor concentration 500 nM; fadrozole, IC₅₀ = 30 nM. ^e Recombinantly expressed enzymes from baculovirus-infected insect microsomes (Supersomes). ^f Furafylline, IC₅₀ = 2419 nM. ^g Tranylcyromine, IC₅₀ = 6240 nM. ^h Sulfaphenazole, IC₅₀ = 318 nM. ⁱ Tranylcyromine, IC₅₀ = 5950 nM. ^j Quinidine, IC₅₀ = 14 nM. ^k Ketoconazole, IC₅₀ = 57 nM.

Pharmacokinetic Profile of Compounds 1, 9, and 28 (Table 3). The pharmacokinetic profile of compounds **9** and **28** was determined after peroral application to male Wistar rats and compared to the unsubstituted parent compound **1**. After administration of a 5 mg/kg dose in a cassette (N = 5), plasma samples were collected over 24 h and plasma concentrations were determined by HPLC-MS/MS. Fadrozole which was used as a reference compound displayed the highest plasma levels (AUC_{0-∞} = 3575 ng·h/mL), followed by **1** (1544 ng·h/mL) and **28** (762 ng·h/mL). At all sampling points, the amounts of **9** detected were found below the limit of quantification (1.5 ng per mL plasma). This experimental result may be either due to a fast metabolism of the aromatic amine or due to a lacking ability of this compound to permeate the cell membrane under physiological conditions. The half-lives were between 2.2–5.4 h in which the elimination of fadrozole occurs faster than the elimination of the naphthalenes **1** and **28**. Compound **28** is slowly absorbed as indicated by the t_{max} of 6 h whereas **1** is absorbed as fast as fadrozole (t_{max} = 1 h). Furthermore, no obvious sign of toxicity was noted in any animal over the duration of the experiment (24 h).

Table 3. Pharmacokinetic profile of compounds **1**, **9**, and **28**

compd ^a	t _{1/2 z} (h) ^b	t _{max} (h) ^c	C _{max} (ng/mL) ^d	AUC _{0-∞} (ng·h/mL) ^e
1	5.4	1.0	222	1544
9	n.d. ^f	n.d. ^f	< 1.5 ^g	n.d. ^f
28	3.2	6.0	81	762
fadrozole	2.2	1.0	454	3575

^a All compounds were applied perorally at a dose of 5 mg per kg body weight in four different cassette dosing experiments using male Wistar rats. ^b Terminal half-life. ^c Time of maximal concentration. ^d Maximal concentration. ^e Area under the curve. ^f n.d. = not detectable. ^g Below the limit of quantification.

Discussion and Conclusion

The results obtained in the present study revealed that a variety of substituents in 4'- and 5'-position is tolerated with regard to the CYP11B2 potency. Most of the tested compounds were more potent than the unsubstituted parent compounds and IC₅₀ values less than 1 nM were observed in 7 cases (e.g., **22** and **26**, IC₅₀ = 0.2 nM). Some of the compounds were also potent CYP11B1 inhibitors (e.g., **26**, IC₅₀ = 10 nM). Interestingly, a precise relationship between the inhibition of CYP11B2 and CYP11B1 was observed: An increased or decreased inhibitory activity at the one enzyme was accompanied by an increased or decreased inhibitory activity at the other enzyme. For instance, based on the unsubstituted parent compound **1**, introduction of the methoxyalkyl substituent in compound **26** resulted in an enhanced inhibition of both CYP11B2 (IC₅₀ = 0.2 nM) and CYP11B1 (IC₅₀ = 10 nM), whereas introduction of the hydroxy group in compound **10** resulted in a decreased inhibitory potency at both CYP11B isoforms in a comparable order of magnitude (CYP11B2, IC₅₀ = 94 nM; CYP11B1, IC₅₀ = 8925 nM). This trend becomes particularly evident when plotting the CYP11B2 versus the CYP11B1 pIC₅₀ values of the compounds presented in Table 1 revealing a reasonable linear correlation (r² = 0.86, n = 29). The finding that it is to some extent possible to change the inhibitory potency by the heteroaryl derivatization without significantly changing the selectivity versus either CYP11B2 or CYP11B1 is an indication that the inhibitor binding proceeds via similar protein-inhibitor interactions of the heterocyclic moiety with both CYP11B isoforms. Contrariwise, it has been

shown earlier by us that variation of the carbocyclic skeleton instead of the heterocycle can significantly influence the selectivity. Therefore, no correlation is observed for a plot of the CYP11B2 and CYP11B1 pIC₅₀ values of the naphthalenes²² and dihydronaphthalenes²³ described previously by us that are functionalized with an unsubstituted 3-pyridine as heme complexing heterocycle ($r^2 = 0.30$, $n = 20$). Consistent with these findings, it can be assumed that both enzymes, CYP11B2 and CYP11B1, are structurally more diverse in the naphthalene binding site than in the heterocyclic binding site. Interesting structure-activity relationships could also be observed with respect to electronic properties. Compounds bearing protic substituents in 5'-position rather poorly inhibited CYP11B2 whereas bioisosteric exchange by aprotic residues gave rise to highly potent aldosterone synthase inhibitors, e.g., the inhibitory potency increased by a factor of 40 from carboxamide **17** (IC₅₀ = 94 nM) to the ethanone **18** (IC₅₀ = 2.1 nM). A comparable increase of potency was observed when the protic hydroxy group was replaced by the aprotic methoxy group, e.g., the IC₅₀ value decreased by a factor of 20 in case of compound **11** compared to the phenol **10** or by a factor of 40 in case of compound **22** compared to the primary alcohol **21**. Similarly, the methyl esters **16** and **20** were more active than the corresponding carboxylic acids **15** and **19**. However, a lack of membrane permeability must be taken into consideration as an alternative explanation. Figure 1 shows the molecular electrostatic potentials (MEP) mapped on the electron density surface of compounds **17**, **10**, and **21** and their bioisosteric analogues **18**, **11**, and **22**. Both the shape and the geometry of the compounds as well as the electrostatic potential distribution in the naphthalene moiety are very similar. In addition, all compounds contain a region in which the nitrogen of the pyridine ring presents a negative potential. However, areas with a distinct positive potential in the pyridine moiety are present in compounds **17**, **10**, and **21** showing low inhibitory potency. In case of the highly potent bioisosters, these areas display less positive potential values with a more uniformly distributed electron charge. Hence, the difference in the electrostatic potential distribution is a reasonable explanation for the varying binding behavior within this set of compounds.

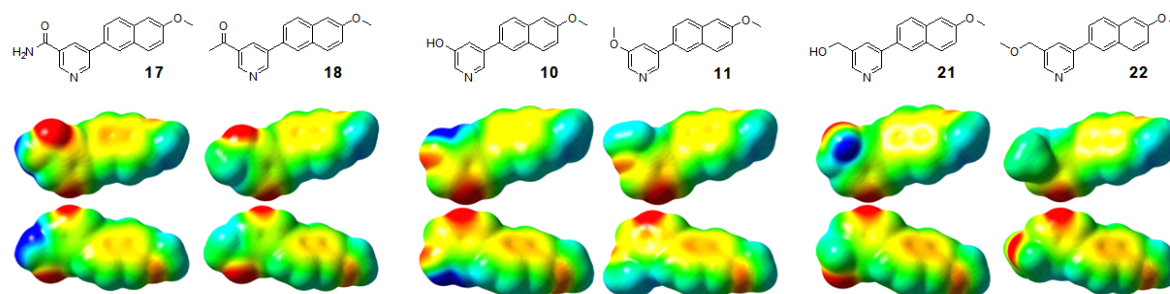


Figure 1. MEP of compounds **17**, **18**, **10**, **11**, **21**, and **22** (front and back view). The electrostatic potential surfaces were plotted with GaussView 3.0 in a range of -18.83 kcal/mol (red) to $+21.96$ kcal/mol (blue).

The heteroaryl derivatization had also a noticeable influence on the CYP1A2 potency of the compounds. Most of the substituted derivatives were still inhibiting CYP1A2 for more than 90 % at a concentration of 2 μ M. With respect to the compounds with a 6-methoxynaphthalene core, a slight decrease to approximately 80 % inhibition was observed in some cases. This effect was due to the introduction of substituents in 5'-position of the heterocycle. While no decrease of CYP1A2 inhibition was observed in case of the rather small substituents in compounds **10**, **11**, and **21** (hydroxy, methoxy, and hydroxymethyl), a slight increase of the sterical bulk in compounds **14**, **18**, **22**, and **25** (ethoxy, acetyl, methoxymethyl, and hydroxyethyl) resulted in a decrease in CYP1A2 inhibition to 78–85 %. On the other hand, some derivatives proved to be significantly less active with approximately 50 % inhibition of CYP1A2, including the 4'-amino-substituted compound **9** and the isoquinoline **28** with IC₅₀ values of 1420 nM and 1619 nM, respectively. The effect of changing 3-pyridine by 4-isoquinoline as heme-complexing heterocycle is particularly noteworthy. The three isoquinoline derivatives **28**, **29**, and **30** are considerably less active at CYP1A2 (6–57 % inhibition) than their unsubstituted analogues **1**, **2**, and **5** (73–98 % inhibition). An explanation might be found in the geometry of these molecules. The isoquinoline constrains the rotation around the carbon–carbon bond between the heterocycle and the naphthalene, especially in presence of the additional *ortho*-methyl groups in **29** and **30**. Thus, a coplanar conformation becomes energetically disfavored compared to the pyridine analogues and the sterically demanding heterocycle rotates out of the naphthalene plane. This loss of planarity is a reasonable explanation for the reduced inhibitory potency since both CYP1A2 substrates and inhibitors are usually small-volume molecules with a planar shape (e.g., caffeine⁴⁰ and furafylline⁴¹). An even more drastic effect on the

CYP1A2 potency was observed in case of the dihydronaphthalene type compounds. While the unsubstituted parent compound **5** exhibited 74 % inhibition, introduction of the methoxy substituent in compound **13** led to a reduction to 18 % and the isoquinoline derivative **30** displayed only 6 % inhibition. The partly saturated core structure becomes flexible and disturbs the planarity. Factors other than steric might play an additional role for the decreased CYP1A2 inhibition, e.g., disturbed π - π -stacking contacts with aromatic amino acids in the CYP1A2 binding pocket due to the reduced number of aromatic carbons. Aromaticity has been identified to correlate positively with CYP1A2 inhibition in recent QSAR studies.⁴² As dihydronaphthalenes **13** and **30** were found to be unstable in DMSO solution, the low potencies might be due to substance degradation. However, the decomposition (~20 % after three days) afforded mainly the aromatized naphthalene analogues, i.e., **12** and **29** both displaying higher CYP1A2 inhibition than **13** and **30**.

In conclusion, we have shown that modifying the lead compounds **I** and **II** by introduction of substituents in the heterocyclic moiety has a clear effect on the activity and selectivity profile. Some substituents induced a significant increase in inhibitory potency versus CYP11B2. Compounds **22** and **26** with subnanomolar IC₅₀ values are the most potent aldosterone synthase inhibitors so far. The undesirable high CYP1A2 inhibition that is present in the previously investigated derivatives could be overcome by certain residues, giving rise to compounds with an advantageous overall selectivity profile. It was also demonstrated that the naphthalene type aldosterone synthase inhibitors **1** and **28** were able to cross the gastrointestinal tract and reached the general circulation. Presently, the elucidated concepts are used to systematically modify other lead structures whereof some are under investigation for their ability to reduce aldosterone levels *in vivo*.

Experimental Section

Chemical and Analytical Methods. Melting points were measured on a Mettler FP1 melting point apparatus and are uncorrected. ¹H NMR and ¹³C spectra were recorded on a Bruker DRX-500 instrument. Chemical shifts are given in parts per million (ppm), and tetramethylsilane (TMS) was used as internal standard for spectra obtained in DMSO-*d*₆ and CDCl₃. All coupling constants (*J*) are given in hertz. Mass spectra (LC/MS) were measured on a TSQ Quantum (Thermo Electron Corporation) instrument with a RP18 100-3 column (Macherey Nagel) and with water/acetonitrile mixtures as eluents. Elemental analyses were carried out at the Department of Chemistry, University of Saarbrücken. Reagents were used as obtained from commercial suppliers without further purification. Solvents were distilled before use. Dry solvents were obtained by distillation from appropriate drying reagents and stored over molecular sieves. Flash chromatography was performed on silica gel 40 (35/40–63/70 μ m) with hexane/ethyl acetate mixtures as eluents, and the reaction progress was determined by thin-layer chromatography analyses on Alugram SIL G/UV254 (Macherey Nagel). Visualization was accomplished with UV light and KMnO₄ solution. All microwave irradiation experiments were carried out in a CEM-Discover monomode microwave apparatus.

The following compounds were prepared according to previously described procedures: 6-Methoxy-3-methyl-3,4-dihydronaphthalen-1(2*H*)-one (**2e**),³² (2*E*)-4-hydroxy-4-(3-methoxyphenyl)-3-methyl-2-butenoic acid (**2g**),³² 5-bromopyridin-3-ol (**10a**).²⁹

Synthesis of the Target Compounds

Procedure A.²⁷ Pyridine boronic acid (0.75 mmol, 1 equivalent), aryl bromide or -triflate (0.9–1.3 equivalents), and tetrakis(triphenylphosphane)palladium(0) (43 mg, 37.5 μ mol, 5 mol %) were suspended in 1.5 mL DMF in a 10 mL septum-capped tube containing a stirring magnet. To this was added a solution of NaHCO₃ (189 mg, 2.25 mmol, 3 equivalents) in 1.5 mL water and the vial was sealed with a Teflon cap. The mixture was irradiated with microwaves for 15 min at a temperature of 150 °C with an initial irradiation power of 100 W. After the reaction, the vial was cooled to 40 °C, the crude mixture was partitioned between ethyl acetate and water and the aqueous layer was extracted three times with ethyl acetate. The combined organic layers were dried over MgSO₄ and the solvents were removed *in vacuo*. The coupling products were obtained after flash chromatography on silica gel (petroleum ether/ethyl acetate mixtures) and/or crystallization. If an oil was obtained, it was transferred into the hydrochloride salt by 1N HCl solution in diethyl ether.

Procedure B.³⁴ In a microwave tube alkenyl bromide **7** (1 equivalent), pyridine boronic acid (1.3 equivalent), tetrabutylammonium bromide (1 equivalent), sodium carbonate (3.5 equivalents) and palladium acetate (1.5 mol %) were suspended in water/acetone 3.5/3 to give a 0.15 M solution of bromide **7** under an atmosphere of nitrogen. The

septum sealed vessel was irradiated under stirring and simultaneous cooling for 15 min at 150 °C with an initial irradiation power of 150 W. The reaction mixture was cooled to room temperature, diluted with a saturated ammonium chloride solution and extracted several times with diethyl ether. The combined extracts were washed with brine, dried over MgSO₄, concentrated and purified by flash chromatography on silica gel. The resulting oil was transferred into the hydrochloride salt by a 5-6 N HCl solution in 2-propanol and crystallized from ethanol.

Procedure C. To a suspension of NaH (1.15 equivalents, 60 % dispersion in oil) in 5 mL dry THF at was added dropwise a solution of alcohol (1 equivalent) in 5 mL THF at room temperature under an atmosphere of nitrogen. After hydrogen evolution ceased, a solution of methyl iodide (3.3 equivalents) in 5 mL THF was added dropwise, and the resulting mixture was stirred for 5 h at room temperature. The mixture was then treated with saturated aqueous NH₄Cl solution and extracted three times with ethyl acetate. The combined organic layers were washed with water and brine, dried over MgSO₄ and the solvent was evaporated in vacuo. The crude product was flash chromatographed on silica gel (petroleum ether/ethyl acetate mixtures) to afford the pure methylether. If an oil was obtained, it was transferred into the hydrochloride salt by 1N HCl solution in diethyl ether.

Procedure D. To a 0.05 M solution of carbonyl compound in dry methanol was added sodium borohydride (2 equivalents). The reaction mixture was stirred for 1 h, diluted with diethylether and treated with saturated aqueous NaHCO₃ solution. The mixture was then extracted three times with ethyl acetate, washed twice with saturated aqueous NaHCO₃ solution and once with brine and dried over MgSO₄. The filtrate was concentrated in vacuo, and the residue was filtered through a short pad of silica gel or flash chromatographed on silica gel (petroleum ether/ethyl acetate mixtures) to afford the corresponding alcohols.

3-(6-Methoxy-3-methylnaphthalen-2-yl)pyridine (2) was obtained according to procedure A starting from **2a** (377 mg, 1.50 mmol) and 3-pyridineboronic acid (240 mg, 1.95 mmol) after flash chromatography on silica gel (petroleum ether/ethyl acetate, 4/1, *R_f* = 0.16) as a white solid (304 mg, 1.22 mmol, 81 %), mp 106–107 °C. MS *m/z* 250.06 (MH⁺). Anal. (C₁₇H₁₅NO) C, H, N.

3-(6-Methoxy-3-methyl-3,4-dihydronaphthalen-2-yl)pyridine (5) was obtained according to procedure B starting from **2b** (127 mg, 0.50 mmol) and 3-pyridineboronic acid (80 mg, 0.65 mmol) after flash chromatography on silica gel (petroleum ether/ethyl acetate, 4/1, *R_f* = 0.20), precipitation as HCl salt and **crystallization** from ethanol as a white solid (50 mg, 0.17 mmol, 35 %), mp (HCl salt) 186–187 °C. MS *m/z* 252.02 (MH⁺). Anal. (C₁₇H₁₇NO·HCl·0.2H₂O) C, H, N.

6-(Pyridin-3-yl)-7,8-dihydronaphthalene-2-carbonitrile (6) was prepared according to procedure A starting from 3-pyridineboronic acid (107 mg, 0.87 mmol) and **6a** (189 mg, 0.62 mmol). After flash chromatography on silica gel (petroleum ether/ethyl acetate, 2/1, *R_f* = 0.10) pure **6** was obtained as a white, crystalline solid (100 mg, 0.43 mmol, 69 %). Treatment with hydrochloride acid (0.1 N in Et₂O) yielded the hydrochloride salt of **6** (110 mg, 0.41 mmol, 66 %) as a white solid, mp (HCl salt) 264–268 °C. MS *m/z* 223.23 (MH⁺). Anal. (C₁₆H₁₂N₂·HCl·0.4H₂O) C, H, N.

3-(6-Methoxynaphthalen-2-yl)-4-methylpyridine (7) was prepared according to procedure A starting from 6-methoxy-2-naphthaleneboronic acid (131 mg, 0.65 mmol) and 3-bromo-4-methylpyridine (86 mg, 0.50 mmol). After flash chromatography on silica gel (petroleum ether/ethyl acetate, 7/3, *R_f* = 0.10) pure **7** was obtained as a white solid (65 mg, 0.26 mmol, 52 %), mp (HCl salt) 172–174 °C. MS *m/z* 250.30 (MH⁺). Anal. (C₁₇H₁₅NO·HCl·0.1H₂O) C, H, N.

6-(4-Methylpyridin-3-yl)-2-naphthonitrile (8). Triflate **8a** (151 mg, 0.50 mmol), 4-methyl-3-pyridineboronic acid (89 mg, 0.65 mmol), K₂CO₃ (138 mg, 1.0 mmol) and Pd(dppf)Cl₂ (37 mg, 0.05 mmol) were suspended in 4.0 mL of a 4:4:1 mixture of toluene/acetone/water. This mixture was heated to 125 °C by microwave irradiation for 15 minutes (initial irradiation power 150 W). After cooling to room temperature, 15 mL of distilled water were added and the reaction mixture was extracted four times with 10 mL of Et₂O. After washing the combined organic fractions with water (twice) and brine, drying over MgSO₄ and evaporation of the solvent crude product **8** was obtained as a yellow solid (127 mg). Further purification by flash chromatography on silica gel (**petroleum ether/ethyl acetate, 2/5, *R_f* = 0.20**) and subsequent crystallization of the free base as hydrochloride salt gave 52 mg (0.19 mmol, 37 %) of pure **8** (HCl salt) as an yellowish solid, mp (HCl salt) decomposition above 210 °C. MS *m/z* 245.30 (MH⁺). Anal. (C₁₇H₁₂N₂·HCl·0.5H₂O) C, H, N.

3-(6-Methoxynaphthalen-2-yl)pyridin-4-amine (9) was prepared according to procedure A starting from 6-methoxy-2-naphthaleneboronic acid (131 mg, 0.65 mmol) and 3-bromopyridin-4-amine (86 mg, 0.50 mmol). After crystallization from acetone pure **9** was obtained as a white solid (39 mg, 0.16 mmol, 31 %), mp 155–156 °C. MS *m/z* 251.28 (MH⁺). Anal. (C₁₆H₁₄N₂O) C, H, N.

5-(6-Methoxynaphthalen-2-yl)pyridin-3-ol (10) was prepared according to procedure A starting from 6-methoxy-2-naphthaleneboronic acid (131 mg, 0.65 mmol) and **10a** (87 mg, 0.50 mmol). After crystallization from acetone/diethyl ether pure **10** was obtained as an off-white solid (86 mg, 0.34 mmol, 68 %), mp 172–175 °C. MS m/z 252.02 (MH⁺). Anal. (C₁₆H₁₃NO₂·0.7H₂O) C, H, N: calcd, 5.31, found, 5.79.

3-Methoxy-5-(6-methoxynaphthalen-2-yl)pyridine (11) was prepared according to procedure A starting from 6-methoxy-2-naphthaleneboronic acid (131 mg, 0.65 mmol) and 3-bromo-5-methoxypyridine (94 mg, 0.50 mmol). After flash chromatography on silica gel (petroleum ether/ethyl acetate, 7/3, R_f = 0.10) pure **11** was obtained as a white solid (80 mg, 0.30 mmol, 60 %), mp (HCl salt) 211–214 °C. ¹H-NMR (500 MHz, CD₃OD): δ = 3.96 (s, 3H), 4.15 (s, 3H), 7.23 (dd, ³ J = 9.1 Hz, ⁴ J = 2.5 Hz, 1H), 7.32 (d, ⁴ J = 2.2 Hz, 1H), 7.85 (dd, ³ J = 8.5 Hz, ⁴ J = 1.9 Hz, 1H), 7.92 (d, ³ J = 8.8 Hz, 1H), 7.97 (d, ³ J = 8.5 Hz, 1H), 8.29 (d, ⁴ J = 1.5 Hz, 1H), 8.52 (s, 1H), 8.54 (s, 1H), 8.86 (s, 1H). ¹³C-NMR (125 MHz, CD₃OD): δ = 57.9, 58.3, 108.5, 120.9, 121.9, 128.1, 128.5, 130.2, 131.4, 132.5, 134.5, 136.7, 138.9, 139.1, 142.6, 158.4, 160.4. MS m/z 266.26 (MH⁺). Anal. (C₁₇H₁₅NO₂·HCl·0.3H₂O) C, H, N.

3-Methoxy-5-(6-methoxy-3-methylnaphthalen-2-yl)pyridine (12) was obtained according to procedure A starting from **2a** (377 mg, 1.50 mmol) and 5-methoxy-3-pyridineboronic acid (298 mg, 1.95 mmol) after flash chromatography on silica gel (petroleum ether/ethyl acetate, 3/1, R_f = 0.16) as a white solid (328 mg, 1.17 mmol, 78 %), mp 106–107 °C. ¹H-NMR (500 MHz, CDCl₃): δ = 2.40 (s, 3H), 3.91 (s, 3H), 3.94 (s, 3H), 7.12 (m, 2H), 7.23 (dd, ⁴ J = 2.8 Hz, ⁴ J = 1.9 Hz, 1H), 7.62 (s, 1H), 7.64 (s, 1H), 7.71 (d, ³ J = 8.8 Hz, 1H), 8.28 (d, ⁴ J = 1.9 Hz, 1H), 8.33 (d, ⁴ J = 2.8 Hz, 1H). ¹³C-NMR (125 MHz, CDCl₃): δ = 21.0, 55.3, 55.6, 104.9, 118.6, 121.5, 127.4, 127.5, 128.6, 129.2, 134.1, 134.4, 134.5, 135.8, 138.0, 142.6, 155.2, 158.1. MS m/z 280.08 (MH⁺). Anal. (C₁₈H₁₇NO₂) C, H, N.

3-Methoxy-5-(6-methoxy-3-methyl-3,4-dihydronaphthalen-2-yl)pyridine (13) was obtained according to procedure B starting from **2b** (253 mg, 1.00 mmol) and 5-methoxy-3-pyridineboronic acid (199 mg, 1.30 mmol) after flash chromatography on silica gel (petroleum ether/ethyl acetate, 4/1, R_f = 0.14), precipitation as HCl salt and crystallization from ethanol as a yellow solid (84 mg, 0.26 mmol, 26 %), mp (HCl salt) 181–182 °C. ¹H-NMR (500 MHz, CD₃OD): δ = 0.94 (d, ³ J = 7.0 Hz, 3H), 2.71 (dd, ² J = 15.3 Hz, ³ J = 1.2 Hz, 1H), 3.02 (m, 1H), 3.13 (dd, ² J = 15.5 Hz, ³ J = 6.4 Hz, 1H), 3.74 (s, 3H), 4.01 (s, 3H), 6.72 (m, 2H), 7.15 (d, ³ J = 8.2 Hz, 1H), 7.19 (s, 1H), 8.22 (m, 1H), 8.34 (d, ⁴ J = 2.4 Hz, 1H), 8.59 (d, ⁴ J = 1.5 Hz, 1H). ¹³C-NMR (125 MHz, CD₃OD): δ = 17.8, 30.6, 36.7, 55.8, 57.9, 112.9, 115.6, 116.6, 127.0, 127.2, 127.8, 129.8, 130.3, 132.3, 137.1, 137.2, 150.9, 160.1. MS m/z 281.96 (MH⁺). Anal. (C₁₈H₁₉NO₂·HCl·0.2H₂O) C, H, N.

3-Ethoxy-5-(6-methoxynaphthalen-2-yl)pyridine (14) was prepared according to procedure A starting from 6-methoxy-2-naphthaleneboronic acid (131 mg, 0.65 mmol) and **14a** (101 mg, 0.50 mmol). After crystallization from ethyl acetate/petroleum ether pure **14** was obtained as a white solid (33 mg, 0.17 mmol, 23 %), mp decomposition above 130 °C. MS m/z 280.05 (MH⁺). Anal. (C₁₈H₁₇NO₂·0.2H₂O) C, H, N.

5-(6-Methoxynaphthalen-2-yl)pyridine-3-carboxylic acid (15) was prepared according to procedure A starting from 6-methoxy-2-naphthaleneboronic acid (131 mg, 0.65 mmol) and 5-bromonicotinic acid (101 mg, 0.50 mmol). After crystallization from methanol/water pure **15** was obtained as an off-white solid (74 mg, 0.26 mmol, 53 %), mp decomposition above 300 °C. MS m/z 279.98 (MH⁺). Anal. (C₁₇H₁₃NO₃·HCl·0.3H₂O) C, H, N.

Methyl 5-(6-methoxynaphthalen-2-yl)pyridine-3-carboxylate (16). Carboxylic acid **15** (45 mg, 0.16 mmol) was dissolved in 20 mL dry methanol and 0.05 mL concentrated H₂SO₄ (98%) was added. The whole mixture was refluxed for 10 h and thereafter the excess methanol was distilled off. The residue was taken up in 50 mL ethyl acetate and the organic layer was washed several times with 5 % aqueous Na₂CO₃ solution, water and brine. After drying over MgSO₄, the solvent was evaporated in vacuo. After flash chromatography on silica gel (petroleum ether/ethyl acetate, 7/3, R_f = 0.34) pure **16** was obtained as an off-white solid (28 mg, 0.10 mmol, 60 %), mp 150–151 °C. MS m/z 293.97 (MH⁺). Anal. (C₁₈H₁₄NO₃) C, H, N.

5-(6-Methoxynaphthalen-2-yl)pyridine-3-carboxamide (17) was prepared according to procedure A starting from 6-methoxy-2-naphthaleneboronic acid (131 mg, 0.65 mmol) and 5-bromonicotinamide (92 mg, 0.50 mmol). After crystallization from acetone/diethyl ether pure **17** was obtained as a white solid (55 mg, 0.20 mmol, 40 %), mp 245–247 °C. MS m/z 279.07 (MH⁺). Anal. (C₁₇H₁₄N₂O₂) C, H, N.

1-[5-(6-Methoxynaphthalen-2-yl)pyridin-3-yl]ethanone (18) was prepared according to procedure A starting from 6-methoxy-2-naphthaleneboronic acid (131 mg, 0.65 mmol) and 3-acetyl-5-bromopyridine (100 mg, 0.50 mmol). After crystallization from acetone/diethyl ether pure **18** was obtained as a white solid (75 mg, 0.27 mmol, 54 %), mp 159–160 °C. MS m/z 278.09 (MH⁺). Anal. (C₁₈H₁₅NO₂·0.1H₂O) C, H, N.

[5-(6-Methoxynaphthalen-2-yl)pyridin-3-yl]acetic acid (19) was prepared according to procedure A starting from 6-methoxy-2-naphthaleneboronic acid (131 mg, 0.65 mmol) and 5-bromo-3-pyridineacetic acid (108 mg, 0.50 mmol). After crystallization from methanol/water pure **19** was obtained as a white solid (70 mg, 0.24 mmol, 48 %), mp decomposition above 210 °C. MS m/z 293.97 (MH⁺). Anal. (C₁₈H₁₅NO₃·0.5H₂O) C, H, N.

Methyl [5-(6-methoxynaphthalen-2-yl)pyridin-3-yl]acetate (20) was prepared as described for **16** starting from **19** (145 mg, 0.49 mmol). After flash chromatography on silica gel (petroleum ether/ethyl acetate, 1/1, R_f = 0.18) pure **20** was obtained as a white solid (81 mg, 0.26 mmol, 53 %), mp 145–146 °C. MS m/z 308.04 (MH⁺). Anal. (C₁₉H₁₇NO₃) C: calcd, 74.25, found, 74.72, H, N.

[5-(6-Methoxynaphthalen-2-yl)pyridin-3-yl]methanol (21) was prepared according to procedure A starting from 6-methoxy-2-naphthaleneboronic acid (131 mg, 0.65 mmol) and **21a** (94 mg, 0.50 mmol). After crystallization from acetone/diethyl ether pure **21** was obtained as a white solid (86 mg, 0.32 mmol, 65 %), mp 193–194 °C. MS m/z 266.05 (MH⁺). Anal. (C₁₇H₁₅NO₂·0.1H₂O) C, H, N.

3-(Methoxymethyl)-5-(6-methoxynaphthalen-2-yl)pyridine (22) was prepared according to procedure C starting from **21** (150 mg, 0.57 mmol) using methyl iodide (82 μ L, 1.32 mmol). After flash chromatography on silica gel (petroleum ether/ethyl acetate, 1/1, R_f = 0.22) pure **22** was obtained as an off-white solid (80 mg, 0.29 mmol, 50 %), mp 121–122 °C. MS m/z 279.91 (MH⁺). Anal. (C₁₈H₁₇NO₂) C, H, N.

[4-(6-Methoxynaphthalen-2-yl)pyridin-3-yl]methanol (23) was prepared according to procedure A starting from 6-methoxy-2-naphthaleneboronic acid (131 mg, 0.65 mmol) and **23a** (94 mg, 0.50 mmol). After crystallization from acetone/diethyl ether pure **23** was obtained as a white solid (90 mg, 0.34 mmol, 68 %), mp decomposition above 240 °C. MS m/z 266.05 (MH⁺). Anal. (C₁₇H₁₅NO₂·0.2H₂O) C, H, N.

4-(Methoxymethyl)-3-(6-methoxynaphthalen-2-yl)pyridine (24) was prepared according to procedure C starting from **23** (150 mg, 0.57 mmol) using methyl iodide (82 μ L, 1.32 mmol). After flash chromatography on silica gel (petroleum ether/ethyl acetate, 1/1, R_f = 0.23) pure **24** was obtained as an off-white solid (74 mg, 0.26 mmol, 46 %), mp (HCl salt) 174–177 °C. MS m/z 279.91 (MH⁺). Anal. (C₁₈H₁₇NO₂·0.2H₂O) C, H, N.

1-[5-(6-Methoxynaphthalen-2-yl)-pyridin-3-yl]ethanol (25) was prepared according to procedure D starting from **18** (50 mg, 0.18 mmol) using NaBH₄ (8.0 mg, 0.21 mmol). After flash chromatography on silica gel (petroleum ether/ethyl acetate, 1/1, R_f = 0.24) pure **25** was obtained as a white solid (28 mg, 0.10 mmol, 56 %), mp 154–155 °C. MS m/z 280.05 (MH⁺). Anal. (C₁₈H₁₇NO₂) C, H, N.

3-(1-Methoxyethyl)-5-(6-methoxynaphthalen-2-yl)pyridine (26) was prepared according to procedure C starting from **25** (70 mg, 0.25 mmol) using methyl iodide (41 μ L, 0.66 mmol). After flash chromatography on silica gel (petroleum ether/ethyl acetate, 1/1, R_f = 0.23) pure **26** was obtained as a yellowish solid (26 mg, 0.08 mmol, 35 %), mp 124–125 °C. MS m/z 294.11 (MH⁺). Anal. (C₁₉H₁₉NO₂) C, H, N.

3-(6-Methoxynaphthalen-2-yl)-5-phenylpyridine (27) was prepared according to procedure A starting from 6-methoxy-2-naphthaleneboronic acid (394 mg, 1.95 mmol) and 3-bromo-5-phenylpyridine (351 mg, 1.50 mmol). After flash chromatography on silica gel (petroleum ether/ethyl acetate, 2/1, R_f = 0.23) pure **27** was obtained as a white, crystalline solid (455 mg, 1.46 mmol, 97 %), mp 216–217 °C. MS m/z 312.09 (MH⁺). Anal. (C₂₂H₁₇NO·0.4H₂O) C, H, N.

4-(6-Methoxynaphthalen-2-yl)isoquinoline (28) was prepared according to procedure A starting from 6-methoxy-2-naphthaleneboronic acid (131 mg, 0.65 mmol) and 4-bromoisoquinoline (104 mg, 0.50 mmol). After flash chromatography on silica gel (petroleum ether/ethyl acetate, 7/3, R_f = 0.21) pure **28** was obtained as a white solid (44 mg, 0.16 mmol, 31 %), mp 185–186 °C. MS m/z 286.07 (MH⁺). Anal. (C₂₀H₁₅NO·0.1H₂O) C, H, N.

4-(6-Methoxy-3-methylnaphthalen-2-yl)isoquinoline (29) was obtained according to procedure A starting from **2a** (377 mg, 1.50 mmol) and 4-isoquinolineboronic acid (337 mg, 1.95 mmol) after flash chromatography on silica gel (dichloromethane/methanol 99/1, R_f = 0.26) as yellow oil which solidified with diethyl ether as a pale yellow solid (178 mg, 0.59 mmol, 40 %), mp 156–157 °C. MS m/z 300.10 (MH⁺). Anal. (C₂₁H₁₁NO) C, H, N.

4-(6-Methoxy-3-methyl-3,4-dihydronaphthalen-2-yl)isoquinoline (30) was obtained according to procedure B starting from **2b** (253 mg, 1.00 mmol) and 4-isoquinolineboronic acid (225 mg, 1.30 mmol) after two flash chromatographical separations on silica gel (petroleum ether/ethyl acetate, 5/1, R_f = 0.20 and dichloromethane/methanol 99/1, R_f = 0.27) and precipitation as HCl salt as a yellow solid (112 mg, 0.33 mmol, 17 %), mp 149–150 °C. MS m/z 302.18 (MH⁺). Anal. (C₂₁H₁₉NO·HCl·0.2H₂O) C, H, N.

Biological Methods. 1. Enzyme Preparations. CYP17 and CYP19 preparations were obtained by described methods: the 50,000 g sediment of *E. coli* expressing human CYP17³⁷ and microsomes from human placenta for CYP19.³⁹ **2. Enzyme Assays.** The following enzyme assays were performed as previously described: CYP17³⁷ and CYP19.³⁹ **3. Activity and Selectivity Assay Using V79 Cells.** V79 MZh 11B1 and V79 MZh 11B2 cells³⁶ were incubated with [4-¹⁴C]-11-deoxycorticosterone as substrate and inhibitor in at least three different concentrations. The enzyme reactions were stopped by addition of ethyl acetate. After vigorous shaking and a centrifugation step (10,000 g, 2 min), the steroids were extracted into the organic phase, which was then separated. The conversion of the substrate was analyzed by HPTLC and a phosphoimaging system as described.^{10,22} **4. Inhibition of Human Hepatic CYP Enzymes.** The recombinantly expressed enzymes from baculovirus-infected insect microsomes (Supersomes) were used and the manufacturer's instructions (www.gentest.com) were followed. **5. In Vivo Pharmacokinetics.** Animal trials were conducted in accordance with institutional and international ethical guidelines for the use of laboratory animals. Male Wistar rats weighing 317–322 g (Janvier, France) were housed in a temperature-controlled room (20–22 °C) and maintained in a 12 h light/12 h dark cycle. Food and water were available *ad libitum*. The animals were anaesthetised with a ketamine (135mg/kg)/xylazine (10mg/kg) mixture, and cannulated with silicone tubing via the right jugular vein. Prior to the first blood sampling, animals were connected to a counterbalanced system and tubing, to perform blood sampling in the freely moving rat. Separate stock solutions (5 mg/mL) were prepared for the tested compounds in Labrasol/Water (1:1; v/v), leading to a clear solution. Immediately before application, the cassette dosing mixture was prepared by adding equal volumes of the 5 stock solutions to end up with a final concentration of 1 mg/mL for each compound. The mixture was applied perorally to 3 rats with an injection volume of 5 mL/kg (Time 0). 400 µL of blood were taken via jugularis catheter 1 hour before application and then 1 and 2 hours after application. Immediately, equal volume (400 µL) of 0.9 % NaCl (37 °C) was re-injected intravenously to keep the blood volume stable. 4, 6, 8, 10 and 24 hours after application 250 µL of blood were sampled without balancing the blood volume. Blood samples were centrifuged at 3000 g for 10 minutes at 4 °C. Plasma was harvested and kept at –20 °C until analysis. The mean of absolute plasma concentrations (±SEM) was calculated for the 3 rats and the regression was performed on group mean values. The pharmacokinetic analysis was performed using a noncompartment model (PK Solutions 2.0, Summit Research Services). HPLC-MS/MS analysis and quantification of the samples was carried out on a Surveyor-HPLC-system coupled with a TSQ Quantum (ThermoFinnigan) triple quadrupole mass spectrometer equipped with an electrospray interface (ESI).

Computational Methods. MEP. For each docked compound geometry optimization was performed at the B3LYP/6-31G* density functional levels by means of the Gaussian03 software and the molecular electrostatic potential (MEP) maps were plotted using GaussView3, the 3-D molecular graphics package of Gaussian.⁴³ These electrostatic potential surfaces were generated by mapping 6-31G* electrostatic potentials onto surfaces of molecular electron density (isovalue = 0.002 electron/Å).⁴⁴

Acknowledgement. We thank Ms. Gertrud Schmitt and Ms. Jeannine Jung for their help in performing the *in vitro* tests. S. L. is grateful to Saarland University for a scholarship (Landesgraduierten-Förderung). Thanks are due to Prof. J. J. Rob Hermans, University of Maastricht, The Netherlands, for supplying the V79 CYP11B1 cells, and Prof. Rita Bernhardt, Saarland University, for supplying the V79 CYP11B2 cells.

Supporting Information Available: Individual plasma levels of each compound and animal, graphs and equations of the linear regression of pIC₅₀ values, NMR-spectroscopic data of compounds **2**, **5–10**, **14–30**, full experimental details and spectroscopic characterization of the reaction intermediates **2a–2d**, **2f**, **6a**, **6b**, **8a**, **14a**, **21a**, **23a**, elemental analysis results of compounds **2**, **5–30**. This information is available free of charge via the Internet at <http://pubs.acs.org>.

References

- (1) (a) Takeda Y. Vascular synthesis of aldosterone: role in hypertension. *Mol. Cell. Endocrinol.* **2004**, *217*, 75–79. (b) Davies, E.; MacKenzie, S. M. Extra-adrenal production of corticosteroids. *Clin. Exp. Pharmacol. Physiol.* **2003**, *30*, 437–445.
- (2) Kawamoto, T.; Mitsuuchi, Y.; Toda, K.; Yokoyama, Y.; Miyahara, K.; Miura, S.; Ohnishi, T.; Ichikawa, Y.; Nakao, K.; Imura, H.; Ulick, S.; Shizuta, Y. Role of steroid 11β-hydroxylase and steroid 18-hydroxylase in

- the biosynthesis of glucocorticoids and mineralocorticoids in humans. *Proc. Natl. Acad. Sci. U.S.A.* **1992**, *89*, 1458–1462.
- (3) (a) Brilla, C. G. Renin-angiotensin-aldosterone system and myocardial fibrosis. *Cardiovasc. Res.* **2000**, *47*, 1–3. (b) Lijnen, P.; Petrov, V. Induction of cardiac fibrosis by aldosterone. *J. Mol. Cell. Cardiol.* **2000**, *32*, 865–879.
 - (4) Pitt, B.; Zannad, F.; Remme, W. J.; Cody, R.; Castaigne, A.; Perez, A.; Palensky, J.; Wittes, J. The effect of spironolactone on morbidity and mortality in patients with severe heart failure. *N. Engl. J. Med.* **1999**, *341*, 709–717.
 - (5) Pitt, B.; Remme, W.; Zannad, F.; Neaton, J.; Martinez, F.; Roniker, B.; Bittman, R.; Hurley, S.; Kleiman, J.; Gatlin, M. Eplerenone, a selective aldosterone blocker, in patients with left ventricular dysfunction after myocardial infarction. *N. Eng. J. Med.* **2003**, *348*, 1309–1321.
 - (6) Khan, N. U. A.; Movahed, A. The role of aldosterone and aldosterone-receptor antagonists in heart failure. *Rev. Cardiovasc. Med.* **2004**, *5*, 71–81.
 - (7) Bell, M. G.; Gernert, D. L.; Grese, T. A.; Belvo, M. D.; Borromeo, P. S.; Kelley, S. A.; Kennedy, J. H.; Kolis, S. P.; Lander, P. A.; Richey, R.; Sharp, V. S.; Stephenson, G. A.; Williams, J. D.; Yu, H.; Zimmerman, K. M.; Steinberg, M. I.; Jadhav, P. K. (S)-N-{3-[1-Cyclopropyl-1-(2,4-difluoro-phenyl)-ethyl]-1H-indol-7-yl}-methanesulfonamide: A potent, nonsteroidal, functional antagonist of the mineralocorticoid receptor. *J. Med. Chem.* **2007**, *50*, 6443–6445.
 - (8) (a) Delcayre, C.; Swynghedauw, B. Molecular mechanisms of myocardial remodeling. The role of aldosterone. *J. Mol. Cell. Cardiol.* **2002**, *34*, 1577–1584. (b) de Resende, M. M.; Kauser, K.; Mill, J. G. Regulation of cardiac and renal mineralocorticoid receptor expression by captopril following myocardial infarction in rats. *Life Sci.* **2006**, *78*, 3066–3073.
 - (9) (a) Wehling, M. Specific, nongenomic actions of steroid hormones. *Annu. Rev. Physiol.* **1997**, *59*, 365–393. (b) Lösel, R.; Wehling, M. Nongenomic actions of steroid hormones. *Nature Rev. Mol. Cell. Biol.* **2003**, *4*, 46–55. (c) Chai, W.; Garrelds, I. M.; Arulmani, U.; Schoemaker, R. G.; Lamers, J. M. J.; Danser, A. H. J.; Genomic and nongenomic effects of aldosterone in the rat heart: Why is spironolactone cardioprotective? *Br. J. Pharmacol.* **2005**, *145*, 664–671. (d) Chai, W.; Garrelds, I. M.; de Vries, R.; Batenburg, W. W.; van Kats, J. P.; Danser, A. H. J. Nongenomic effects of aldosterone in the human heart: Interaction with angiotensin II. *Hypertension* **2005**, *46*, 701–706.
 - (10) Ehmer, P. B.; Bureik, M.; Bernhardt, R.; Müller, U.; Hartmann, R. W. Development of a test system for inhibitors of human aldosterone synthase (CYP11B2): Screening in fission yeast and evaluation of selectivity in V79 cells. *J. Steroid Biochem. Mol. Biol.* **2002**, *81*, 173–179.
 - (11) Hartmann, R. W.; Müller, U.; Ehmer, P. B. Discovery of selective CYP11B2 (aldosterone synthase) inhibitors for the therapy of congestive heart failure and myocardial fibrosis. *Eur. J. Med. Chem.* **2003**, *38*, 363–366.
 - (12) (a) Yamakita, N.; Chiou, S.; Gomez-Sanchez, C. E. Inhibition of aldosterone biosynthesis by 18-ethynyl-deoxycorticosterone. *Endocrinology* **1991**, *129*, 2361–2366. (b) Hartmann, R. W. Selective inhibition of steroidogenic P450 enzymes: Current status and future perspectives. *Eur. J. Pharm. Sci.* **1994**, *2*, 15–16.
 - (13) (a) Viger, A.; Coustal, S.; Perard, S.; Piffeteau, A.; Marquet, A. 18-Substituted progesterone derivatives as inhibitors of aldosterone biosynthesis. *J. Steroid Biochem.* **1989**, *33*, 119–124. (b) Delorme, C.; Piffeteau, A.; Viger, A.; Marquet, A. Inhibition of bovine cytochrome P-450_{11β} by 18-unsaturated progesterone derivatives. *Eur. J. Biochem.* **1995**, *232*, 247–256. (c) Delome, C.; Piffeteau, A.; Sobrio, F.; Marquet, A. Mechanism-based inactivation of bovine cytochrome P-450_{11β} by 18-unsaturated progesterone derivatives. *Eur. J. Biochem.* **1997**, *248*, 252–260.
 - (14) Davioud, E.; Piffeteau, A.; Delorme, C.; Coustal, S.; Marquet, A. 18-Vinyldeoxycorticosterone: a potent inhibitor of the bovine cytochrome P-450_{11β}. *Bioorg. Med. Chem.* **1998**, *6*, 1781–1788.
 - (15) Taymans, S. E.; Pack, S.; Pak, E.; Torpy, D. J.; Zhuang, Z.; Stratakis, C. A. Human CYP11B2 (aldosterone synthase) maps to chromosome 8q24.3. *J. Clin. Endocrinol. Metab.* **1998**, *83*, 1033–1036.
 - (16) (a) Häusler, A.; Monnet, G.; Borer, C.; Bhatnagar, A. S. Evidence that corticosterone is not an obligatory intermediate in aldosterone biosynthesis in the rat adrenal. *J. Steroid Biochem.* **1989**, *34*, 567–570. (b) Demers, L. M.; Melby, J. C.; Wilson, T. E.; Lipton, A.; Harvey, H. A.; Santen, R. J. The effects of CGS 16949A, an aromatase inhibitor on adrenal mineralocorticoid biosynthesis. *J. Clin. Endocrinol. Metab.* **1990**, *70*, 1162–1166.

- (17) Fiebeler, A.; Nussberger, J.; Shagdarsuren, E.; Rong, S.; Hilfenhaus, G.; Al-Saadi, N.; Dechend, R.; Wellner, M.; Meiners, S.; Maser-Gluth, C.; Jeng, A. Y.; Webb, R. L.; Luft, F. C.; Muller, D. N. Aldosterone synthase inhibitor ameliorates angiotensin II-induced organ damage. *Circulation* **2005**, *111*, 3087–3094.
- (18) (a) Ksander, G.; Hu, Q.-Y. Fused imidazole derivatives for the treatment of disorders mediated by aldosterone synthase and/or 11 β -hydroxylase and/or aromatase. PCT Int. Appl. WO2008027284, 2008. (b) Papillon J.; Ksander, G. M.; Hu, Q.-Y. Preparation of tetrahydroimidazo[1,5-a]pyrazine derivatives as aldosterone synthase and/or 11 β -hydroxylase inhibitors. PCT Int. Appl. WO2007139992, 2007. (c) Adams, C.; Papillon, J.; Ksander, G. M. Preparation of imidazole derivatives as aldosterone synthase inhibitors. PCT Int. Appl. WO2007117982, 2007. (d) Ksander, G. M.; Meredith, E.; Monovich, L. G.; Papillon, J.; Firooznia, F.; Hu, Q.-Y. Preparation of condensed imidazole derivatives for the inhibition of aldosterone synthase and aromatase. PCT Int. Appl. WO2007024945, 2007. (e) Firooznia, F. Preparation of imidazo[1,5a]pyridine derivatives for treatment of aldosterone mediated diseases. PCT Int. Appl. WO2004046145, 2004. (f) McKenna, J. Preparation of imidazopyrazines and imidazodiazepines as agents for the treatment of aldosterone mediated conditions. PCT Int. Appl. WO2004014914, 2004.
- (19) (a) Herold, P.; Mah, R.; Tschinke, V.; Stojanovic, A.; Marti, C.; Jelakovic, S.; Stutz, S. Preparation of imidazo compounds as aldosterone synthase inhibitors. PCT Int. Appl. WO2007116099, 2007. (b) Herold, P.; Mah, R.; Tschinke, V.; Stojanovic, A.; Marti, C.; Jelakovic, S.; Bennacer, B.; Stutz, S. Preparation of spiro-imidazo derivatives as aldosterone synthase inhibitors. PCT Int. Appl. WO2007116098, 2007. (c) Herold, P.; Mah, R.; Tschinke, V.; Stojanovic, A.; Marti, C.; Stutz, S. Preparation of imidazo compounds as aldosterone synthase inhibitors. PCT Int. Appl. WO2007116097, 2007. (d) Herold, P.; Mah, R.; Tschinke, V.; Quirnbach, M.; Marti, C.; Stojanovic, A.; Stutz, S. Preparation of fused imidazoles as aldosterone synthase inhibitors. PCT Int. Appl. WO2007065942, 2007. (e) Herold, P.; Mah, R.; Tschinke, V.; Stojanovic, A.; Marti, C.; Jotterand, N.; Schumacher, C.; Quirnbach, M. Preparation of heterocyclic spiro-compounds as aldosterone synthase inhibitors. PCT Int. Appl. WO2006128853, 2006. (f) Herold, P.; Mah, R.; Tschinke, V.; Stojanovic, A.; Marti, C.; Jotterand, N.; Schumacher, C.; Quirnbach, M. Preparation of heterocyclic spiro-compounds as aldosterone synthase inhibitors. PCT Int. Appl. WO2006128852, 2006. (g) Herold, P.; Mah, R.; Tschinke, V.; Stojanovic, A.; Marti, C.; Jotterand, N.; Schumacher, C.; Quirnbach, M. Preparation of fused imidazoles as aldosterone synthase inhibitors. PCT Int. Appl. WO2006128851, 2006. (h) Herold, P.; Mah, R.; Tschinke, V.; Schumacher, C.; Marti, C.; Quirnbach, M. Preparation of fused heterocycles as aldosterone synthase inhibitors. PCT Int. Appl. WO2006005726, 2006. (i) Herold, P.; Mah, R.; Tschinke, V.; Schumacher, C.; Quirnbach, M. Preparation of imidazopyridines and related analogs as aldosterone synthase inhibitors. PCT Int. Appl. WO2005118557, 2005. (j) Herold, P.; Mah, R.; Tschinke, V.; Schumacher, C.; Quirnbach, M. Preparation of tetrahydro-imidazo[1,5-a]pyridin derivatives as aldosterone synthase inhibitors. PCT Int. Appl. WO2005118581, 2005. (k) Herold, P.; Mah, R.; Tschinke, V.; Schumacher, C.; Behnke, D.; Quirnbach, M. Preparation of nitrogen-containing heterobicyclic compounds as aldosterone synthase inhibitors. PCT Int. Appl. WO2005118541, 2005.
- (20) Ulmschneider, S.; Müller-Vieira, U.; Mitrenga, M.; Hartmann, R. W.; Oberwinkler-Marchais, S.; Klein, C. D.; Bureik, M.; Bernhardt, R.; Antes, I.; Lengauer, T. Synthesis and evaluation of imidazolylmethylenetetrahydronaphthalenes and imidazolylmethyleneindanes: Potent inhibitors of aldosterone synthase. *J. Med. Chem.* **2005**, *48*, 1796–1805.
- (21) Ulmschneider, S.; Müller-Vieira, U.; Klein, C. D.; Antes, I.; Lengauer, T.; Hartmann, R. W. Synthesis and evaluation of (pyridylmethylene)tetrahydronaphthalenes/-indanes and structurally modified derivatives: Potent and selective inhibitors of aldosterone synthase. *J. Med. Chem.* **2005**, *48*, 1563–1575.
- (22) Voets, M.; Antes, I.; Scherer, C.; Müller-Vieira, U.; Biemel, K.; Barassin, C.; Oberwinkler-Marchais, S.; Hartmann, R. W. Heteroaryl substituted naphthalenes and structurally modified derivatives: Selective inhibitors of CYP11B2 for the treatment of congestive heart failure and myocardial fibrosis. *J. Med. Chem.* **2005**, *48*, 6632–6642.
- (23) Voets, M.; Antes, I.; Scherer, C.; Müller-Vieira, U.; Biemel, K.; Oberwinkler-Marchais, S.; Hartmann, R. W. Synthesis and evaluation of heteroaryl-substituted dihydronaphthalenes and indenes: Potent and selective inhibitors of aldosterone synthase (CYP11B2) for the treatment of congestive heart failure and myocardial fibrosis. *J. Med. Chem.* **2006**, *49*, 2222–2231.
- (24) Ulmschneider, S.; Negri, M.; Voets, M.; Hartmann, R. W. Development and evaluation of a pharmacophore model for inhibitors of aldosterone synthase (CYP11B2). *Bioorg. Med. Chem. Lett.* **2006**, *16*, 25–30.

- (25) (a) Eaton, D. L.; Gallagher, E. P.; Bammler, T. K.; Kunze, K. L. Role of cytochrome P4501A2 in chemical carcinogenesis: Implications for human variability in expression and enzyme activity. *Pharmacogenetics* **1995**, *5*, 259–274. (b) Guengerich, F.; Parikh, A.; Turesky, R. J.; Josephy, P. D. Interindividual differences in the metabolism of environmental toxicants: Cytochrome P450 1A2 as a prototype. *Mutat. Res.* **1999**, *428*, 115–124.
- (26) Miyaura, N.; Suzuki, A. Palladium-catalyzed cross-coupling reactions of organoboron compounds. *Chem. Rev.* **1995**, *95*, 2457–2483.
- (27) Appukkuttan, P.; Orts, A. B.; Chandran, R. P.; Goeman, J. L.; van der Eycken, J.; Dehaen, W.; van der Eycken, E. Generation of a small library of highly electron-rich 2-(hetero)aryl-substituted phenethylamines by the Suzuki-Miyaura reaction: A short synthesis of an apogalanthamine analogue. *Eur. J. Org. Chem.* **2004**, 3277–3285.
- (28) Bengtson, A.; Hallberg, A.; Larhed, M. Fast synthesis of aryl triflates with controlled microwave heating. *Org. Lett.* **2002**, *4*, 1231–1233.
- (29) Kertesz, D. J.; Martin, M.; Palmer, W. S. Process for preparing pyridazinone compounds. PCT Int. Appl. WO2005100323, 2005.
- (30) Lézé, M.-P.; Le Borgne, M.; Pinson, P.; Paluszczak, A.; Duflos, M.; Le Baut, G.; Hartmann, R. W. Synthesis and biological evaluation of 5-[(aryl)(1H-imidazol-1-yl)methyl]-1H-indoles: Potent and selective aromatase inhibitors. *Bioorg. Med. Chem. Lett.* **2006**, *16*, 1134–1137.
- (31) Carreño, M. C.; García-Cerrada, S.; Urbano, A. From central to helical chirality: Synthesis of P and M enantiomers of [5]helicenequinones and bisquinones from (SS)-2-(p-tolylsulfanyl)-1,4-benzoquinone. *Chem. Eur. J.* **2003**, *9*, 4118–4131.
- (32) Heyer, D.; Fang, J.; Navas III, F.; Katamreddy, S. R.; Peckham, J. P.; Turnbull, P. S.; Miller, A. B.; Akwabi-Ameyaw, A. Chemical compounds. PCT Int. Appl. WO2006002185, 2006.
- (33) Fitzgerald, D. H.; Muirhead, K. M.; Botting, N. P. A comparative study on the inhibition of human and bacterial kynureninase by novel bicyclic kynurenine analogues. *Bioorg. Med. Chem.* **2001**, *9*, 983–989.
- (34) (a) Leadbeater, N. E.; Marco, M. Ligand-free palladium catalysis of the suzuki reaction in water using microwave heating. *Org. Lett.* **2002**, *4*, 2973–2976. (b) Liu, L.; Zhang, Y.; Xin, B. Synthesis of biaryls and polyaryls by ligand-free suzuki reaction in aqueous phase. *J. Org. Chem.* **2006**, *71*, 3994–3997.
- (35) Li, D.; Zhao, B.; Sim, S.; Li, T.; Liu, A.; Liu, L. F.; LaVoie, E. J. 8,9-Methylenedioxybenzo[*i*]-phenanthridines: Topoisomerase I-targeting activity and cytotoxicity. *Bioorg. Med. Chem.* **2003**, *11*, 3795–3805.
- (36) (a) Denner, K.; Bernhardt, R. Inhibition studies of steroid conversions mediated by human CYP11B1 and CYP11B2 expressed in cell cultures. In *Oxygen Homeostasis and Its Dynamics*, 1st ed.; Ishimura, Y., Shimada, H., Suematsu, M., Eds.; Springer-Verlag: Tokyo, Berlin, Heidelberg, New York, 1998; pp 231–236. (b) Denner, K.; Doehmer, J.; Bernhardt, R. Cloning of CYP11B1 and CYP11B2 from normal human adrenal and their functional expression in COS-7 and V79 chinese hamster cells. *Endocr. Res.* **1995**, *21*, 443–448. (c) Böttner, B.; Denner, K.; Bernhardt, R. Conferring aldosterone synthesis to human CYP11B1 by replacing key amino acid residues with CYP11B2-specific ones. *Eur. J. Biochem.* **1998**, *252*, 458–466.
- (37) (a) Ehmer, P. B.; Jose, J.; Hartmann, R. W. Development of a simple and rapid assay for the evaluation of inhibitors of human 17 α -hydroxylase-C_{17,20}-lyase (P450c17) by coexpression of P450c17 with NADPH-cytochrome-P450-reductase in *Escherichia coli*. *J. Steroid Biochem. Mol. Biol.* **2000**, *75*, 57–63; (b) Hutschenreuter, T. U.; Ehmer, P. B.; Hartmann, R. W. Synthesis of hydroxy derivatives of highly potent nonsteroidal CYP17 inhibitors as potential metabolites and evaluation of their activity by a non cellular assay using recombinant enzyme. *J. Enzyme Inhib. Med. Chem.* **2004**, *19*, 17–32.
- (38) Thompson, E. A.; Siiteri, P. K. Utilization of oxygen and reduced nicotinamide adenine dinucleotide phosphate by human placental microsomes during aromatization of androstenedione. *J. Biol. Chem.* **1974**, *249*, 5364–5372.
- (39) Hartmann, R. W.; Batzl, C. Aromatase inhibitors. Synthesis and evaluation of mammary tumor inhibiting activity of 3-alkylated 3-(4-aminophenyl)piperidine-2,6-diones. *J. Med. Chem.* **1986**, *29*, 1362–1369.
- (40) Butler, M. A.; Iwasaki, M.; Guengerich, F. P.; Kadlubar, F. F. Human cytochrome P-450_{PA} (P-450IA2), the phenacetin O-deethylase, is primarily responsible for the hepatic 3-demethylation of caffeine and N-oxidation of carcinogenic arylamines. *Proc. Natl. Acad. Sci. U.S.A.* **1989**, *86*, 7696–7700.
- (41) Sesardic, D.; Boobis, A. R.; Murray, B. P.; Murray, S.; Segura, J.; de la Torre, R.; Davies, D. S. Furfurylline is a potent and selective inhibitor of cytochrome P450IA2 in man. *Br. J. Clin. Pharmacol.* **1990**, *29*, 651–663.

- (42) (a) Chohan, K. K.; Paine, S. W.; Mistry, J.; Barton, P.; Davis, A. M. A rapid computational filter for cytochrome P450 1A2 inhibition potential of compound libraries. *J. Med. Chem.* **2005**, *48*, 5154–5161. (b) Korhonen, L. E.; Rahnasto, M.; Mähönen, N. J.; Wittekindt, C.; Poso, A.; Juvonen, R. O.; Raunio, H. Predictive three-dimensional quantitative structure-activity relationship of cytochrome P450 1A2 inhibitors. *J. Med. Chem.* **2005**, *48*, 3808–3815.
- (43) GaussView, Version 3.0, Dennington I.; Roy, Keith, T.; Millam, J.; Eppinnett, K.; Hovell, W. L.; Gilliland, R.; Semichem, Inc., Shawnee Mission, KS, **2003**.
- (44) Petti, M. A.; Shepodd, T. J.; Barrans, R. E.; Dougherty, D. A. "Hydrophobic" binding of water-soluble guests by high-symmetry, chiral hosts. An electron-rich receptor site with a general affinity for quaternary ammonium compounds and electron-deficient π systems. *J. Am. Chem. Soc.* **1988**, *110*, 6825–6840.

3.4.3.3. Paper XIV.

Novel aldosterone synthase inhibitors with extended carbocyclic skeleton by a combined ligand-based and structure-based drug design approach

Simon Lucas, Ralf Heim, Matthias Negri, Iris Antes, Christina Ries, Katarzyna E. Schewe, Alessandra Bisi, Silvia Gobbi, and Rolf W. Hartmann

This article is protected by copyrights of 'Journal of Medicinal Chemistry.'

J. Med. Chem. **2008**, 51, 6138–6149.

Abstract

Pharmacophore modeling of a series of aldosterone synthase (CYP11B2) inhibitors triggered the design of compounds **11** and **12** by extending a previously established naphthalene molecular scaffold (e.g., present in molecules **1** and **2**) via introduction of a phenyl or benzyl residue in 3-position. These additional aromatic moieties have been hypothesized to fit into the newly identified hydrophobic pharmacophore feature HY3. Subsequent docking studies in our refined CYP11B2 protein model have been performed prior to synthesis to estimate the inhibitory properties of the proposed molecules. While phenyl-substituted compound **11** ($IC_{50} > 500$ nM) did not dock under the given pharmacophore constraint (i.e., the Fe(heme)-N(ligand) interaction), benzyl-substituted compound **12** ($IC_{50} = 154$ nM) was found to exploit a previously unexplored sub-pocket of the inhibitor binding site. By structural optimization based on the pharmacophore hypothesis, 25 novel compounds were synthesized, amongst them highly potent CYP11B2 inhibitors (e.g., **17**, $IC_{50} = 2.7$ nM) with pronounced selectivity toward the most important steroidogenic and hepatic CYP enzymes

Introduction

Aldosterone synthase (CYP11B2), a mitochondrial cytochrome P450 enzyme that is localized mainly in the adrenal cortex, is the key enzyme of mineralocorticoid biosynthesis. It catalyzes the terminal three oxidation steps in the biogenesis of aldosterone in humans.¹ This hormone is the most important circulating mineralocorticoid and plays a crucial role in the electrolyte and fluid homeostasis mainly by binding to epithelial mineralocorticoid receptors (MR) promoting sodium reabsorption and potassium secretion. Since the sodium movement is followed by water via osmosis, aldosterone is a key regulator of blood volume and blood pressure. Abnormally increased plasma levels of aldosterone have been diagnosed in different cardiovascular diseases such as elevated blood pressure, congestive heart failure, and myocardial fibrosis.² Inhibitors of the angiotensin-converting enzyme (ACE) which are in use for the treatment of hypertension and congestive heart failure can initially induce a down-regulation of circulating aldosterone. However, increased levels of aldosterone are frequently observed after several months of therapy.³ This phenomenon termed 'aldosterone escape' is a limiting factor of ACE inhibitors and shows that novel therapeutic concepts combating the effects of elevated aldosterone levels are needed. Two recent clinical studies (RALES and EPHEBUS) demonstrated that treatment with mineralocorticoid receptor antagonists in addition to the standard therapy resulted in a decrease of mortality in patients with chronic congestive heart failure and in patients after myocardial infarction, respectively.^{4,5} The use of spironolactone, however, is accompanied by severe progestational and antiandrogenic side effects due to its affinity to other steroid receptors. Moreover, the elevated plasma aldosterone concentrations are left unaffected on a pathological level which raises several issues. First, the elevated aldosterone plasma levels do not induce a homologous down-regulation but an up-regulation of the aldosterone receptor.⁶ This fact complicates a long-term therapy as MR antagonists are likely to become ineffective. Furthermore, the high concentrations promote nongenomic actions of aldosterone which are in general not blocked by receptor antagonists.⁷ Pathological aldosterone concentrations have been identified to induce a negative inotropic effect in human trabeculae and to potentiate the vasoconstrictor effect of angiotensinII in coronary arteries in rapid, nongenomic manner.⁸ Thus, aldosterone is intrinsically capable to further deteriorate heart function by acting nongenomically.

A novel therapeutic strategy with potential to overcome the drawbacks of MR antagonists is the blockade of aldosterone formation, preferably by inhibiting CYP11B2, the key enzyme of its biosynthesis. Aldosterone synthase has been proposed as a potential pharmacological target by our group as early as 1994,⁹ followed soon thereafter by the hypothesis that inhibitors of CYP11B2 could serve as drugs for the treatment of hyperaldosteronism, congestive heart failure and myocardial fibrosis.^{10,11} Consequent structural optimization of a hit discovered by a compound library screening led to a series of nonsteroidal aldosterone synthase inhibitors with high selectivity toward other cytochrome P450 enzymes.¹²⁻¹⁵

In the present study, we describe the design and synthesis of a series of 3-benzyl-substituted pyridyl-naphthalenes and structurally related compounds (Chart 1) by a combined ligand-based and structure-based drug design approach as well as the determination of their biological activity regarding human CYP11B2 for potency. Selectivity is a prerequisite for a CYP11B2 inhibitor, especially with regard to other cytochrome P450 enzymes as they are likely to interact with other CYP enzymes in a similar way (e.g., by complexation of the heme iron). Taking into consideration that the key enzyme of glucocorticoid biosynthesis, 11 β -hydroxylase (CYP11B1), and CYP11B2 have a sequence homology of approximately 93 %, ¹⁶ the selectivity issue becomes especially critical for the design of CYP11B2 inhibitors. On that account, all compounds were tested for their inhibitory potency versus CYP11B1 to determine their selectivity. A set of compounds was additionally tested for inhibitory activity versus the steroidogenic enzymes CYP17 (17 α -hydroxylase-C17,20-lyase) and CYP19 (aromatase) as well as selected hepatic drug-metabolizing CYP enzymes (CYP1A2, CYP2B6, CYP2C9, CYP2C19, CYP2D6, and CYP3A4).

Results

Inhibitor Design Concept

In our search for new lead compounds as CYP11B2 inhibitors structurally differing from the previously discovered pyridyl-naphthalenes such as **1** and **2**,¹⁴ we identified imidazolylmethylene-substituted flavones (e.g., **3-10**) to be aldosterone synthase inhibitors with moderate to high inhibitory potency by compound library screening (Table 1). These compounds that originally have been described as aromatase inhibitors¹⁷ display CYP11B2 inhibition in a range of 73–94 % at a concentration of 500 nM with methoxy-functionalized **6** being most active (IC₅₀ = 11 nM), albeit without showing selectivity versus the highly homologous CYP11B1 (see supplementary material for selectivity data).

Chart 1. Title Compounds

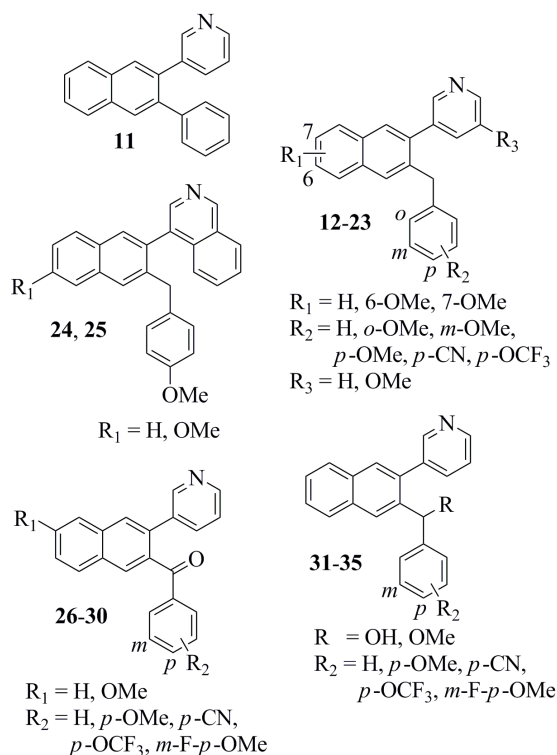
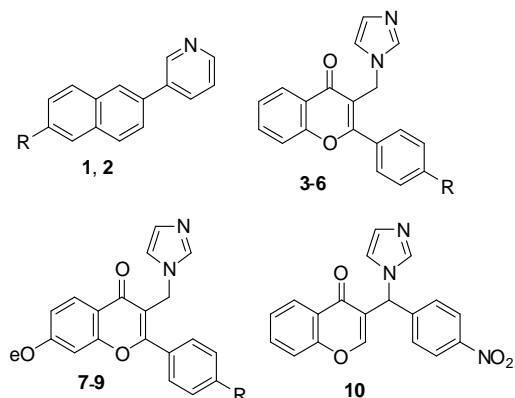


Table 1. Inhibition of Human Adrenal CYP11B2 *in vitro* (Compounds 1–10)

compd	R	% inhibition ^a CYP11B2 ^b	
		[IC ₅₀ (nM)] ^c	
1	H	92	[28]
2	OMe	91	[6.2]
3	H	88	[28]
4	NO ₂	81	[95]
5	Br	90	[25]
6	OMe	94	[11]
7	H	86	[124]
8	Br	80	[n.d.]
9	NO ₂	73	[n.d.]
10		77	[187]

^a Mean value of at least two experiments, standard deviation usually less than 10 %; inhibitor concentration, 500 nM. ^b Hamster fibroblasts expressing human CYP11B2; substrate deoxycorticosterone, 100 nM. ^c Mean value of at least four experiments, standard deviation usually less than 25 %, n.d. = not determined; fadrozole, IC₅₀ = 1 nM.

Recently, a pharmacophore model for aldosterone synthase inhibitors was built by superimposition of a series of heteroaryl-substituted methyleneindanes^{12,13} and naphthalenes^{14,15} synthesized in our laboratory and subsequently validated by pyridine-substituted acenaphthenes as hybrid structures that fit into the four identified pharmacophoric points (i.e., a heterocyclic nitrogen and three ring centroids).¹⁸ The most potent compounds of the latter substance classes together with the most potent flavone type inhibitors were used as training set for the generation of an extended pharmacophore model by applying the GALAHAD¹⁹ pharmacophore generation module of SYBYL molecular modeling software. In the top ranked pharmacophore model, best in three of the most indicative ranking criteria of this software (Pareto ranking,²⁰ Specificity, and Mol-query), the earlier pharmacophoric points¹⁸ were confirmed, namely the hydrophobic features HY0, HY1, HY2a, HY2b as well as the acceptor atom features AA1, AA2a, and AA2b (Figure 1).

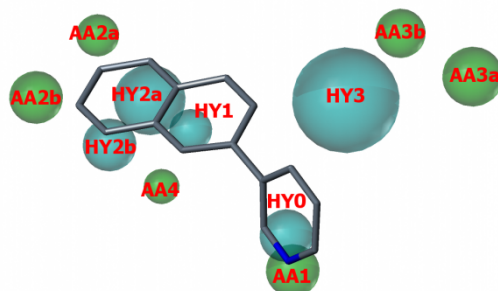
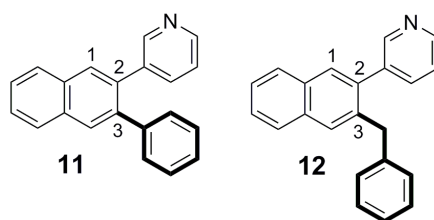


Figure 1. Compound 1 mapped to the pharmacophore model. The newly identified hydrophobic feature HY3 as well as the acceptor atom features AA3a and AA3b are not exploited by inhibitors with a naphthalene molecular scaffold. Pharmacophoric features are color-coded: cyan for hydrophobic regions (HY0–HY3) and green for acceptor atom features (AA1–4).

A novel and voluminous hydrophobic area HY3 was identified next to HY1, along with the acceptor atom features AA3a and AA3b (see supplementary material for exact pharmacophore geometric properties) as well as an additional acceptor atom feature AA4. Rationalizing the given information, the two sample compounds **11** and **12** (Chart 2) were designed by modifying our previously reported naphthalene derivatives **1** and **2** to exploit the newly discovered pharmacophoric feature HY3. As suggested by the model and visualized in Figure 1, introduction of a hydrophobic substituent in 3-position of the naphthalene skeleton should be favorable to exploit the voluminous hydrophobic feature HY3 of the pharmacophore. The phenyl residue directly bound to the naphthalene core in compound **11** creates a conformationally constrained structure in which both rotational degrees of freedom of the two aryl–aryl bonds are limited since they are located *ortho* to each other. The benzyl motive in compound **12** leads to an increased flexibility of the spatial property distribution by rotation around the two benzylic carbon–carbon bonds. Furthermore, the aromatic ring moves apart from the naphthalene core by one methylene unit.

Chart 2. Proposed Lead Structures **11** and **12**.



In order to elucidate the role of conformational flexibility and the exact position of the aryl moiety for optimal inhibitor binding, docking studies were performed (Figure 2). For this purpose, we used the CYP11B2 protein model that has been built¹² and subsequently validated^{13–15} by our group as well as the same docking calculations that have been performed in these studies.

Previous investigations have identified the binding affinity to the target enzyme to be highly dependent on the geometry of the coordinative bond between the heme iron and the heterocyclic nitrogen. An angle of the Fe–N straight line with the porphyrin plane close to 90° (i.e., the heterocyclic nitrogen lone pair arranges perpendicular to the heme group) provides an optimal orbital overlap corresponding to a high inhibitory potency.^{14,15} The analysis of the docking mode of compound **3** led to the identification of a new sub-pocket which interacts with the aryl moiety (Figure 2a). This sub-pocket was not considered as potential binding site during our previous design efforts due to the fact that the formerly investigated compounds such as **2** did not occupy this binding site (Figure 2b). The above considerations led to the design of compounds **11** and **12**. Both compounds combine the pyridynaphthalene skeleton of compound **1** with an additional aryl motive which should be able to interact with the newly identified sub-pocket. However, compound **11** proved to be too rigid to fit into the binding site and could thus not be docked successfully into the binding pocket under the given pharmacophore constraint, that is the Fe(heme)-N(ligand) interaction. A directed heme-Fe–N interaction was defined perpendicular to the heme-plane. This pharmacophore constraint was applied to ensure the right binding mode of the inhibitors with the heme-cofactor. The constraint requires the existence of an inhibitor-nitrogen-atom on the surface of an interaction cone with a 20 degree radius, which has its origin at the Fe-atom and points perpendicular to the heme-plane (with a length of 2.2 Å). Obviously, the conformationally restricted phenyl moiety of compound **11** undergoes repulsive interaction with amino acids of the binding pocket or with the heme-cofactor under the above mentioned constraint (i.e., when the pyridine moiety forms a coordinative bond to the heme iron), thus preventing that the molecule successfully docks into the CYP11B2 protein model. Contrariwise, the 3-benzyl substituted analog **12** is more flexible due to an additional methylene spacer between the two ring systems and thus fitted adequately into the binding site (Figure 2c). From these docking results we concluded that the methylene group of the potential inhibitor should provide the flexibility necessary to adapt to the binding site geometry.

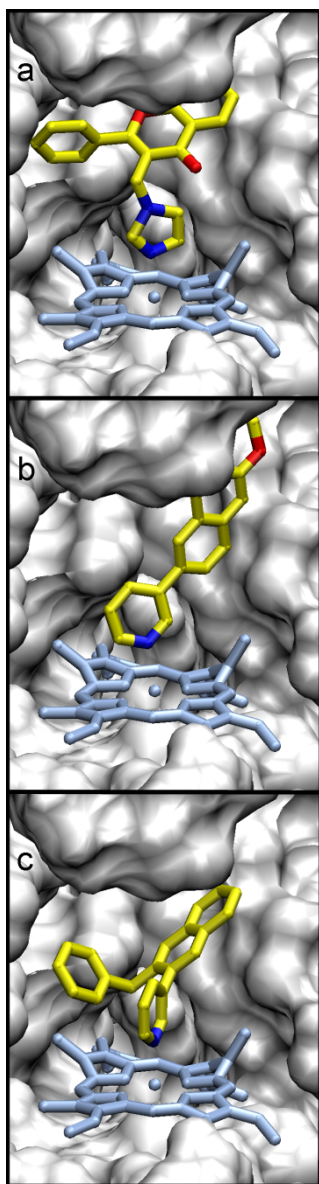


Figure 2. Structure of the CYP11B2–inhibitor complexes of **3** (a), **2** (b) and **12** (c). Surface of the binding pocket (grey) surrounding the inhibitor and the heme co-factor (light blue). The inhibitors are presented in yellow; nitrogen atoms are colored in blue and oxygen atoms are in red. Unlike **2**, the inhibitors **3** and **12** exploit an additional sub-pocket of the inhibitor binding site.

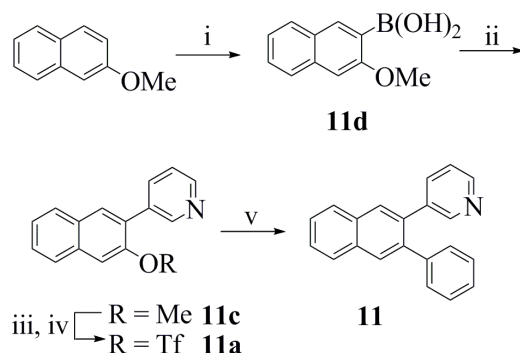
Chemistry

The phenyl-substituted pyridynaphthalene **11** was obtained as shown in Scheme 1 by two subsequent Suzuki coupling²¹ steps, whereof the first proceeded between 3-bromopyridine and 3-methoxy-2-naphthaleneboronic acid **11d**. The boronic acid **11d** was accessible by *ortho*-lithiation of 2-methoxynaphthalene and in situ addition of trimethylborate as described previously.²² After demethylation of **11c** by refluxing in concentrated hydrobromic acid, the intermediate naphthol was transferred into the triflate **11a** by a microwave-enhanced method described by Bengtson et al.²³ A second Suzuki coupling using controlled microwave heating afforded compound **11**.²⁴

The benzyl-substituted derivatives **12–16**, **19**, and **21–25** were synthesized by the route shown in Scheme 2. Starting from a 3-hydroxy-2-naphthoic acid, few functional group inversions led to the carbaldehydes **12e–14e**. These transformations were performed by a 4-step sequence starting with an esterification²⁵ and subsequent introduction of a protection group to the naphthalene hydroxy group of **12h** and **13h** (i.e., methyl in **12g** or benzyl in **13g** and **14g**).²⁶ Lithium borohydride reduction²⁷ followed by TEMPO oxidation²⁸ (of primary alcohol **12f**) or Parik-Doehring oxidation²⁹ (of **13f** and **14f**) afforded the corresponding carbaldehydes **12e–14e**. Grignard reaction with

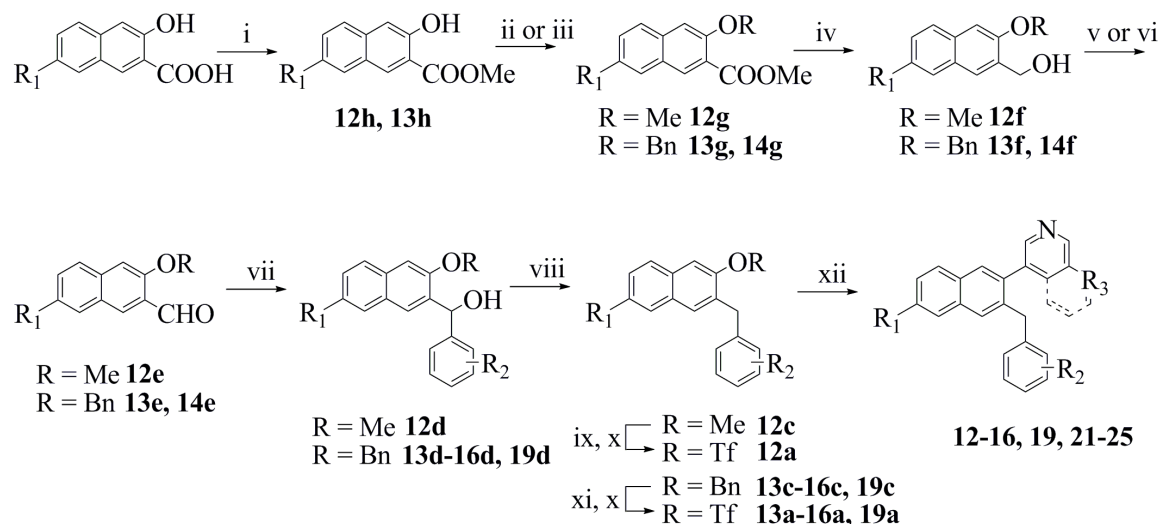
various substituted phenylmagnesium halogenides afforded the phenyl-naphthylalcohols **12d–16d**, and **19d**. Hydrogenolytic removal of the hydroxy group was accomplished by treatment with NaBH₄ and AlCl₃ in refluxing THF.³⁰ After deprotection using BBr₃ (for de-methylation of **12c**) or ammonium formate under Pd-catalysis³¹ (for de-benzylation of **13c–16c**, and **19c**) and subsequent triflate formation,²³ the heterocycle was introduced by microwave-enhanced Suzuki coupling²⁴ giving rise to the benzyl-substituted pyridyl-naphthalenes **12–16**, **19**, and **21–25**.

Scheme 1^a



^a Reagents and conditions: i) *n*BuLi, B(OMe)₃, THF, -78 °C, then HCl/water; ii) 3-bromopyridine, Pd(PPh₃)₄, toluene/ethanol, aq. Na₂CO₃, reflux; iii) conc. HBr, reflux; iv) Tf₂NPh, K₂CO₂, THF, μ w, 120 °C; v) phenylboronic acid, Pd(PPh₃)₄, aq. NaHCO₃, DMF, μ w, 150 °C.

Scheme 2^a

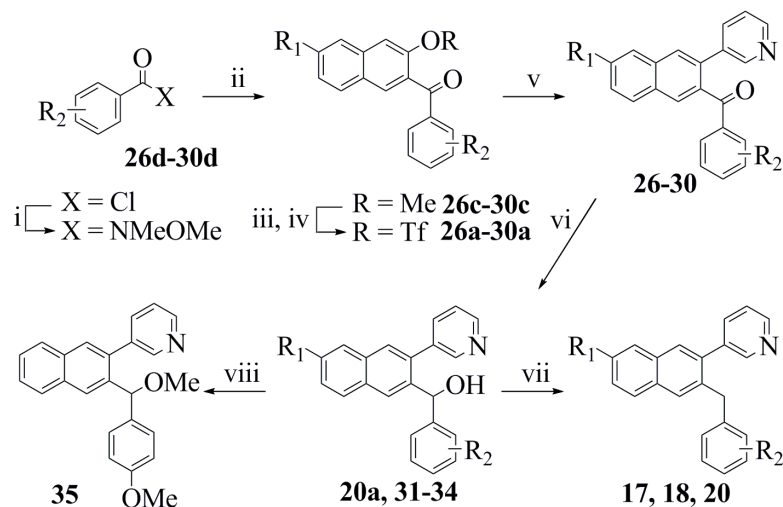


^a Reagents and conditions: i) methanol, H₂SO₄, reflux; ii) MeI, K₂CO₃, 18-crown-6, acetone, reflux (for R = Me); iii) BnBr, K₂CO₃, 18-crown-6, acetone, reflux (for R = Bn); iv) LiBH₄, THF/toluene, reflux; v) NCS, TEMPO, *n*Bu₄NCl, aq. Na₂CO₃/NaHCO₃, CH₂Cl₂; rt (for R = Me); vi) SO₃·py, NEt₃, DMSO, rt (for R = Bn); vii) ArMgX, THF, 0 °C, then aq. NH₄Cl; viii) NaBH₄, AlCl₃, THF, reflux; ix) BBr₃, CH₂Cl₂, -20 °C; x) Tf₂NPh, K₂CO₂, THF, μ w, 120 °C; xi) ammonium formate, Pd/C, THF/methanol, reflux; xii) heteroarylboronic acid, Pd(PPh₃)₄, aq. NaHCO₃, DMF, μ w, 150 °C.

Alternatively, the benzyl-substituted pyridyl-naphthalenes **17**, **18**, and **20** were obtained by the route shown in Scheme 3. Applying the presented transformations afforded the benzoyl-substituted derivatives **26–30** and the corresponding hydroxymethylene analogues **31–34** as reaction intermediates. The sequence toward the 3-benzoyl-substituted 2-naphthols **26b–30b** was reported previously by Li et al. and starts with an *ortho*-lithiation of 2-methoxy- or 2,7-dimethoxynaphthalene, followed by in situ addition of a Weinreb amide. Regioselective demethylation of the obtained methanones **26c–30c** at the naphthalene-position *ortho* to the benzoyl residue was accomplished by treatment with BCl₃/*n*Bu₄NI at -78 °C.³² After triflate formation, a 3-pyridyl residue was introduced by Suzuki coupling to afford compounds **26–30**. The corresponding alcohols **20a** and **31–34** were obtained by sodium borohydride reduction. The methyl ether **35** was synthesized by treating **31** with methyl iodide and NaH in THF. The benzyl-substituted pyridyl-naphthalenes **17**, **18**, and **20** were obtained by in situ iodotrimethyl-

silane mediated reduction.^{33,34} However, reduction by this method did not succeed in the case of **32**, neither by other commonly used hydrogenolysis protocols.^{30,35}

Scheme 3^a



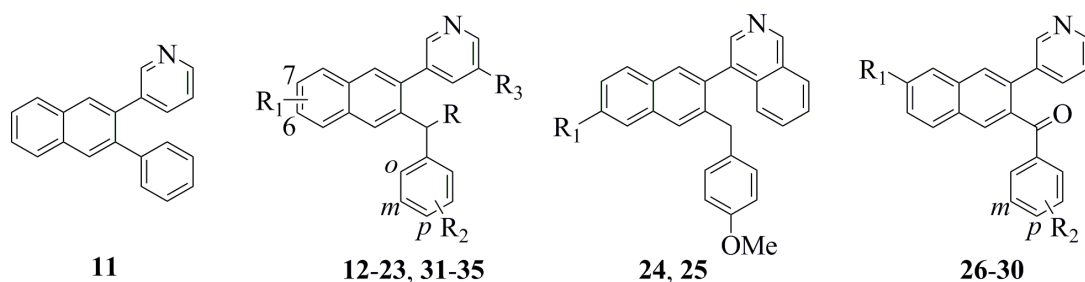
^a Reagents and conditions: i) *N,O*-dimethylhydroxylamine hydrochloride, NEt₃, CH₂Cl₂, rt; ii) *n*BuLi, 2-methoxynaphthalene (for R₁ = H) or 2,7-dimethoxynaphthalene (for R₁ = OMe), TMEDA, THF, -78 °C, then HCl/water; iii) BCl₃, *n*Bu₄NI, CH₂Cl₂, -78 °C to rt; iv) Tf₂O, pyridine, CH₂Cl₂, 0 °C; v) pyridineboronic acid, Pd(PPh₃)₄, aq. Na₂CO₃, toluene/ethanol, reflux; vi) NaBH₄, methanol, 0 °C; vii) Me₃SiCl, NaI, CH₃CN, 55 °C; viii) MeI, NaH, THF, rt.

Biological Results

Inhibition of Human Adrenal Corticoid Producing CYP11B2 and CYP11B1 In Vitro (Table 2). The inhibitory activities of the compounds were determined in V79 MZh cells expressing either human CYP11B2 or CYP11B1.^{10,36} The V79 MZh cells were incubated with [¹⁴C]-deoxycorticosterone as substrate and the inhibitor in different concentrations. The product formation was monitored by HPTLC using a phosphoimager. Fadrozole, an aromatase (CYP19) inhibitor with proven ability to reduce corticoid formation in vitro³⁷ and in vivo³⁸ was used as a reference (CYP11B2, IC₅₀ = 1 nM; CYP11B1, IC₅₀ = 10 nM).

Compound **11** with a phenyl residue directly bound to the naphthalene core shows no significant activity at the target enzyme with only 8 % inhibition at an inhibitor concentration of 500 nM (Table 2). Insertion of a methylene linker into the biaryl bond results in an increased inhibitory potency at CYP11B2 in compound **12** (IC₅₀ = 154 nM). Introduction of a methoxy residue in *ortho*- or *meta*-position of the benzylic moiety as accomplished in compounds **14** and **15** results in a significantly decreased inhibitory potency whereas the same substituent in *para*-position gives rise to the highly potent CYP11B2 inhibitor **16** (IC₅₀ = 7.8 nM) with pronounced selectivity versus CYP11B1 (IC₅₀ = 2804). The cyano and trifluoromethoxy-substituted analogues **17** and **18** are highly potent as well and about 700-fold and 900-fold more selective for CYP11B2. Derivatization of the naphthalene core by a methoxy group is readily tolerated in 6-position as accomplished in compounds **13**, **19**, **22**, **23**, and **25**. The inhibitory profile of the 6-methoxy derivatives regarding the two CYP11B isoforms is thereby comparable to the corresponding hydrogen analogues with a slightly increased selectivity factor in most cases. On the other hand, introduction of methoxy in 7-position results in a decrease of the inhibition to less than 40 % at an inhibitor concentration of 500 nM (**20** and **30**). Modification of the pyridine moiety which has recently been shown to increase the activity and selectivity of naphthalene type CYP11B2 inhibitors³⁹ affords compounds **21–25** with IC₅₀ values in the range of 3–24 nM. Replacing the methylene linker by a carbonyl group as accomplished in compounds **26–29** results in a slightly reduced inhibitory potency (IC₅₀ = 16–118 nM), albeit the high CYP11B1 selectivity is retained (factor 200–500). Introducing hydroxymethylene (**31–34**) or methoxymethylene (**35**) as linker between the aryls leads to a significant loss of inhibitory activity to approximately 60 % at an inhibitor concentration of 500 nM in the case of compounds **31–34** and to an almost complete loss in the case of compound **35**.

Table 2. Inhibition of Human Adrenal CYP11B2 and CYP11B1 In Vitro (Compounds 11–35)



compd	R ₁	R ₂	R ₃	R	%		IC ₅₀ value ^b (nM)		selectivity factor ^e
					V79 hCYP11B2 ^c	11B2 ^c	V79 hCYP11B2 ^c	11B1 ^d	
11					8		n.d.	n.d.	n.d.
12	H	H	H	H	76		154	953	6
13	6-OMe	H	H	H	85		53	640	12
14	H	<i>o</i> -OMe	H	H	24		n.d.	n.d.	n.d.
15	H	<i>m</i> -OMe	H	H	62		n.d.	n.d.	n.d.
16	H	<i>p</i> -OMe	H	H	89		7.8	2804	359
17	H	<i>p</i> -CN	H	H	93		2.7	1956	724
18	H	<i>p</i> -OCF ₃	H	H	95		3.9	3559	913
19	6-OMe	<i>p</i> -OMe	H	H	95		11	4329	394
20	7-OMe	<i>p</i> -OMe	H	H	35		n.d.	n.d.	n.d.
21	H	<i>p</i> -OMe	OMe	H	93		7.7	1811	235
22	6-OMe	<i>p</i> -OMe	OMe	H	96		7.6	2452	322
23	6-OMe	H	OMe	H	90		24	2936	122
24	H				98		3.0	785	262
25	OMe				94		5.0	735	147
26	H	<i>p</i> -OMe	H		79		119	24003	202
27	H	<i>m</i> -F- <i>p</i> -OMe	H		78		65	19816	305
28	H	<i>p</i> -CN	H		88		30	9639	321
29	H	<i>p</i> -OCF ₃	H		91		28	11307	404
30	OMe	<i>p</i> -OMe	H		25		n.d.	n.d.	n.d.
31	H	<i>p</i> -OMe	H	OH	57		n.d.	n.d.	n.d.
32	H	<i>m</i> -F- <i>p</i> -OMe	H	OH	51		n.d.	n.d.	n.d.
33	H	<i>p</i> -CN	H	OH	59		n.d.	n.d.	n.d.
34	H	<i>p</i> -OCF ₃	H	OH	63		n.d.	n.d.	n.d.
35	H	<i>p</i> -OMe	H	OM	23		n.d.	n.d.	n.d.
fadrozol					-		1	10	10

^a Mean value of at least two experiments, standard deviation usually less than 10 %; inhibitor concentration, 500 nM. ^b Mean value of at least four experiments, standard deviation usually less than 25 %, n.d. = not determined. ^c Hamster fibroblasts expressing human CYP11B2; substrate deoxycorticosterone, 100 nM. ^d Hamster fibroblasts expressing human CYP11B1; substrate deoxycorticosterone, 100 nM. ^e IC₅₀ CYP11B1/IC₅₀ CYP11B2, n.d. = not determined.

Inhibition of Steroidogenic and Hepatic CYP Enzymes (Tables 3 and 4). A set of 12 compounds was investigated for inhibition of the steroidogenic enzymes CYP17 and CYP19 (Table 3). The inhibition of CYP17 was investigated using the 50,000 g sediment of the *E. coli* homogenate recombinantly expressing human CYP17 and progesterone (25 μ M) as substrate.⁴⁰ The inhibition values were measured at an inhibitor concentration of 2 μ M. In general, the compounds show no or only little inhibition of less than 25 %. As an exception, compound **22** exhibits 51 % inhibition which is in the range of the reference ketoconazole (IC_{50} = 2780 nM). The inhibition of CYP19 at an inhibitor concentration of 500 nM was determined in vitro with human placental microsomes and [1β - 3 H]androstenedione as substrate as described by Thompson and Siiteri⁴¹ using our modification.⁴² Most of the compounds display only a moderate aromatase inhibition of less than 40 % whereof four compounds do not inhibit CYP19 at all (**21**, **24**, **25**, and **28**). The *para*-cyano-substituted derivative **17** shows a pronounced activity (60 %) and introduction of methoxy in 6-position of the naphthalene core as accomplished in compounds **19**, **22**, and **23** results likewise in a remarkably increased inhibition. Most notably, compound **19** is a highly potent CYP19 inhibitor exhibiting an IC_{50} value of 38 nM, thus being almost as active as the reference fadrozole (IC_{50} = 30 nM).

Table 3. Inhibition of Human CYP17 and CYP19 *in vitro*

compd	% inhibition ^a		compd	% inhibition ^a	
	CYP17 ^b	CYP19 ^c		CYP17 ^b	CYP19 ^c
16	< 5	39	23	26	73
17	25	60	24	< 5	< 5
18	10	45	25	21	6
19	< 5	92 ^d	26	5	19
21	28	6	28	7	< 5
22	51	49	29	8	17

^a Mean value of three experiments, standard deviation usually less than 10 %. ^b *E. coli* expressing human CYP17; substrate progesterone, 25 μ M; inhibitor concentration, 2.0 μ M; ketoconazole, IC_{50} = 2.78 μ M. ^c Human placental CYP19; substrate androstenedione, 500 nM; inhibitor concentration, 500 nM; fadrozole, IC_{50} = 30 nM. ^d IC_{50} = 38 nM.

A selectivity profile relating to inhibition of crucial hepatic CYP enzymes (CYP1A2, CYP2B6, CYP2C9, CYP2C19, CYP2D6, and CYP3A4) was determined for compounds **16**, **17**, **19**, and **28** by use of recombinantly expressed enzymes from baculovirus-infected insect microsomes. Table 4 shows the inhibition at a concentration of 10 μ M and 1 μ M. It becomes apparent that some enzymes are affected only to a minor degree by all compounds including CYP2B6 and CYP2D6. On the other hand, CYP2C9 is strongly inhibited in most cases. The benzoyl derivative **28** with less than 40 % inhibition at 1 μ M concentration at all CYP enzymes is the most selective compound within this series. The worst selectivity profile is observed in the case of **19** inhibiting CYP2C9, CYP2C19, and CYP3A4 with pronounced potency.

Table 4. Inhibition of Selected Hepatic CYP Enzymes *in vitro*

compd	% inhibition ^a											
	CYP1A2 ^{b,c}		CYP2B6 ^{b,d}		CYP2C9 ^{b,e}		CYP2C19 ^{b,f}		CYP2D6 ^{b,g}		CYP3A4 ^{b,h}	
	10	1 μ M	10	1 μ M	10	1 μ M	10	1 μ M	10	1 μ M	10	1
16	77	23	48	< 5	92	51	32	< 5	6	< 5	79	30
17	83	41	69	24	96	78	87	62	62	23	17	9
19	59	13	61	8	98 ⁱ	96 ⁱ	96	74	7	< 5	89	60
28	47	22	43	14	74	35	43	< 5	51	23	62	23

^a Mean value of two experiments, standard deviation usually less than 10 %. ^b Recombinantly expressed enzymes from baculovirus-infected insect microsomes (Supersomes). ^c Furafylline, IC_{50} = 2.42 μ M. ^d Tranilcypromine, IC_{50} = 6.24 μ M. ^e Sulfaphenazole, IC_{50} = 318 nM. ^f Tranilcypromine, IC_{50} = 5.95 μ M. ^g Quinidine, IC_{50} = 14 nM. ^h Ketoconazole, IC_{50} = 57 nM. ⁱ IC_{50} = 64 nM.

Discussion and Conclusion

The inhibitor design concept of the present study triggered the synthesis of compounds **11** and **12** as potential new lead structures by extending a previously established naphthalene molecular scaffold via introduction of a phenyl or benzyl residue in 3-position. Subsequently, docking studies in our CYP11B2 protein model were performed in order to check for spatial consistency with the pharmacophore hypothesis. It was found that while phenyl-substituted **11** did not dock under the given pharmacophore constraint (Fe(heme)-N(ligand) interaction), benzyl-substituted **12** adequately fits into the binding site by exploiting a previously unexplored sub-pocket. These findings were confirmed by experimental results showing that 3-phenyl-substituted pyridylnaphthalene **11** exhibits no significant CYP11B2 inhibition in vitro. In accordance with the docking results, benzyl analog **12** is a moderately potent aldosterone synthase inhibitor ($IC_{50} = 154$ nM). The selectivity versus CYP11B1, however, is rather poor with an only 6-fold increased IC_{50} value compared to CYP11B2. The following lead optimization was accomplished by considering the SAR results obtained previously from the structures of the known inhibitors which have been used for the generation of the pharmacophore model (e.g., **1–10**). Methoxy substitution in compound **6** afforded the most active compound of the flavone series ($IC_{50} = 11$ nM) and was therefore chosen as a model substituent to figure out the optimal substituent position in the benzyl moiety of **12**. In case of the pyridylnaphthalenes, methoxy in 6-position as accomplished in **2** proved to be favorable in terms of both inhibitory potency and selectivity.¹⁴

Within the present set of compounds, interesting structure-activity and structure-selectivity relationships can be observed, particularly with regard to the benzyl and the naphthalene moieties. The benzylic part of the investigated molecules represents a pivotal region for structural optimization and is to a great extent dependent on the position of substituents in terms of both inhibitory activity and selectivity toward the highly homologous CYP11B1. Placing methoxy in *ortho*- or *meta*-position of the benzyl residue significantly reduces the inhibitory potency. Most notably, the inhibition decreases to 24 % at an inhibitor concentration of 500 nM in case of *ortho*-methoxy-derivatized compound **14**. Contrariwise, methoxy in *para*-position as accomplished in compound **16** increases the CYP11B2 activity by a factor of 20 compared to the hydrogen analog **12** and the selectivity toward CYP11B1 clearly improves (selectivity factor = 359). The experimental observations can be explained by the docking results of compounds **16** and **19**, both bearing a *para*-methoxy group (Figure 3). The introduction of this substituent into the benzyl moiety as accomplished in **16** leads to interactions of the compound with the residues of Pro452, Val339, and Thr279, thus stabilizing the complex formed by coordination of the heme iron by the heterocyclic nitrogen considerably (Figure 3a). In compound **19**, a second methoxy group was introduced at the 6-position of the naphthalene scaffold (Figure 3b). This leads to no additional stabilization of the complex, but to a slightly increased selectivity versus CYP11B1. The same trend was observed previously for the binding properties of a series of substituted pyridylnaphthalenes.^{14,15} The *para*-cyano and *para*-trifluoromethoxy derivatives **17** and **18** are likewise highly potent and display IC_{50} values of 2.7 nM and 3.9 nM, respectively, which corroborates the importance of *para*-substitution for activity. Keeping in mind the high homology of the two CYP11B isoforms, the selectivity factors relating to CYP11B1 inhibition of the latter compounds are particularly noteworthy. Compound **17** displays an approximately 700-fold and compound **18** a 900-fold stronger inhibition of CYP11B2 versus CYP11B1.

In the naphthalene molecular scaffold, introduction of a methoxy substituent in 7-position results in a decreased inhibitory potency (**20**, **30**) whereas the same substituent is readily tolerated in 6-position and even slightly increases the CYP11B1 selectivity in most cases. Figure 4 shows the 6-methoxy substituted derivative **19** mapped to the pharmacophore model. It is obvious that this compound nearly perfectly exploits both the well known (HY0, HY1, HY2a, AA1, AA2a) and the newly identified (HY3, AA3b) interaction areas which is reflected by the high inhibitory potency of this compound and underlines the predictive power of our pharmacophore hypothesis.

The *para*-methoxy group in the benzyl moiety of **19** which has been found to be responsible for both high inhibitory activity at CYP11B2 and selectivity versus CYP11B1 fits to the acceptor atom feature AA3b. Hence, targeting this interaction area is a promising strategy in the future design of potent and selective aldosterone synthase inhibitors. With respect to the selectivity profile relating to inhibition of several other CYP enzymes, it becomes apparent that 6-methoxylation endows the benzylnaphthalenes with an increased inhibitory potency at CYP19 as in the case of compounds **19**, **22**, and **23**, for example 6-methoxy derivative **19** is a highly potent CYP19 inhibitor displaying an activity similar to fadrozole. In addition, the latter compound strongly inhibits several hepatic CYP enzymes (i.e., CYP2C9, CYP2C19, and CYP3A4).

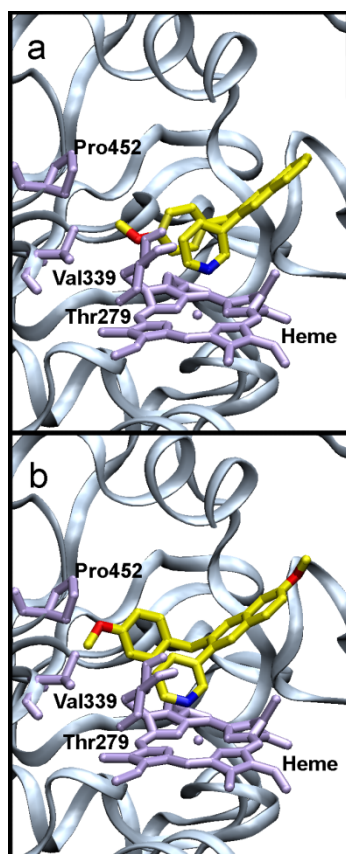


Figure 3. Structure of the CYP11B2 binding pocket with the docked inhibitors **16** (a) and **19** (b). Details of the active site, showing inhibitor, heme co-factor and the interacting residues of Pro452, Val339, and Thr279.

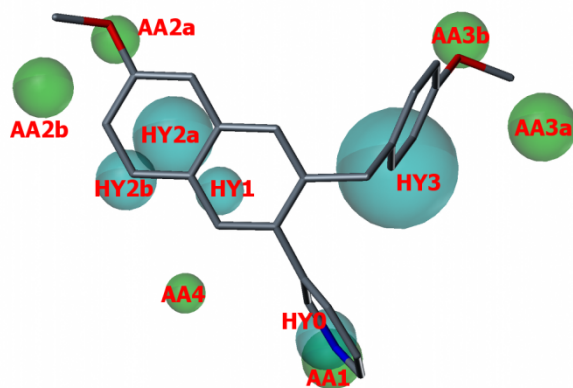


Figure 4. Compound **19** shows an enhanced fit to the pharmacophore hypothesis compared to **1** by additionally exploiting the features HY3 and AA3b. Pharmacophoric features are color-coded: Cyan for hydrophobic regions (HY0–HY3) and green for acceptor atom features (AA1–4).

Varying the substitution pattern of the pyridine site induces no distinct changes of the CYP11B2 potency in case of **21** and **22**. Again, 6-methoxylation in compound **22** increases the selectivity versus CYP11B1 compared to **21**. A slightly decreased selectivity versus CYP11B1 is observable in case of the isoquinoline derivatives **24** and **25** due to a moderate increase in CYP11B1 potency ($IC_{50} < 1000$ nM) which corresponds to previously observed results within the pyridynaphthalene series.³⁹ Contrary to the finding that 6-methoxylation effects a slightly improved selectivity (as shown in previous studies^{14,15} and observed in case of compounds **13**, **19**, and **22** compared to **12**, **16**, and **21**), the 6-methoxynaphthalene compound **25** is less selective than the hydrogen analog **24**. Derivatization of the methylene linker in compounds **26–35** leads to a decrease in inhibitory potency. The carbonyl analogues **26**, **28**, and **29** are slightly less active than their methylene analogues. On the other hand, CYP11B1 inhibition is reduced to the same degree and the high selectivity is maintained. Again, *para*-trifluoromethoxy has the strongest effect on the

inhibitory discrimination between the two CYP11B isoforms and derivative **29** is approximately 400-fold less active at CYP11B1 compared to CYP11B2. In case of the *para*-cyanobenzoyl compound **28**, a decreased inhibition of the sex-hormone producing CYP17, CYP19 as well as the hepatic CYP1A2, CYP2B6, CYP2C9, CYP2C19, and CYP2D6 enzymes is found compared to the benzyl analog **17**, thus providing an advantageous overall CYP selectivity profile for this compound. Other variations of the methylene moiety as accomplished in the hydroxy- and methoxymethylene derivatives **30–35** lead to a pronounced decrease of inhibitory activity compared to the unsubstituted analogues. These compounds display 51–63 % inhibition at an inhibitor concentration of 500 nM in case of hydroxy substitution (**30–34**) and only 23 % in case of methoxy substitution (**35**). Obviously, the decrease in potency with increasing substituent size (hydrogen < carbonyl < hydroxy < methoxy) reflects the increase of steric repulsion between the aryl–aryl spacer and the enzyme parts (i.e., Leu343 and heme co-factor) separating the naphthalene binding site from the sub-pocket interacting with the benzyl residue.

In summary, it has been shown that our CYP11B2 pharmacophore model has predictive power to identify prospective lead structures. Based on the results of the pharmacophore model, a new class of pyridylnaphthalene derivatives with extended carbocyclic skeleton was synthesized. Derivatives with *para*-functionalized benzyl moiety in 3-position of the naphthalene molecular scaffold thoroughly satisfied the spatial constraints imposed by the pharmacophore model and turned out to be highly potent aldosterone synthase inhibitors. The most active compound, *para*-cyanobenzyl derivative **17**, displayed nanomolar potency at the target enzyme ($IC_{50} = 2.7$ nM). In addition, docking studies using our CYP11B2 protein model proved to be a useful tool to estimate the inhibitory properties of proposed new molecules and to explain structure-activity relationships. The binding behavior of compounds **11** and **12** was adequately predicted by the docking results. Furthermore, it was shown that the high inhibitory potency of the *para*-substituted derivative **16** is the outcome of stabilizing interactions with the residues of Pro452, Val339, and Thr279. The selectivity versus CYP11B1 (up to a factor of 900) which is especially remarkable with respect to the high homology of the two CYP11B isoforms was found to be a consequence of *para*-substitution and hence of exploiting the AA3b pharmacophoric feature as well. Currently, further studies are underway to evaluate selected compounds for their *in vivo* properties.

Experimental Section

Chemical and Analytical Methods. Melting points were measured on a Mettler FP1 melting point apparatus and are uncorrected. 1H NMR and ^{13}C spectra were recorded on a Bruker DRX-500 instrument. Chemical shifts are given in parts per million (ppm), and tetramethylsilane (TMS) was used as internal standard for spectra obtained in $DMSO-d_6$ and $CDCl_3$. All coupling constants (J) are given in Hertz. Mass spectra (LC/MS) were measured on a TSQ Quantum (Thermo Electron Corporation) instrument with a RP18 100-3 column (Macherey Nagel) and with water/acetonitrile mixtures as eluents. Elemental analyses were carried out at the Department of Chemistry, University of Saarbrücken. Reagents were used as obtained from commercial suppliers without further purification. Solvents were distilled before use. Dry solvents were obtained by distillation from appropriate drying reagents and stored over molecular sieves. Flash chromatography was performed on silica gel 40 (35/40–63/70 μM) with petroleum ether/ethyl acetate mixtures as eluents, and the reaction progress was determined by thin-layer chromatography analyses on Alugram SIL G/UV254 (Macherey Nagel). Visualization was accomplished with UV light and $KMnO_4$ solution. All microwave irradiation experiments were carried out in a CEM-Discover monomode microwave apparatus.

The following compounds were prepared according to previously described procedures: 3-(3-methoxynaphthalen-2-yl)pyridine (**11c**),¹⁴ (3-methoxynaphthalen-2-yl)boronic acid (**11d**),²² methyl 3-methoxynaphthalen-2-carboxylate (**12g**),²⁶ methyl 3-hydroxynaphthalen-2-carboxylate (**12h**),²⁵ (3-hydroxynaphthalen-2-yl)(4-methoxyphenyl)methanone (**26b**),³² (3-methoxynaphthalen-2-yl)(4-methoxyphenyl)methanone (**26c**),³² *N*,4-Dimethoxy-*N*-methylbenzamide (**26d**),³² 4-[(3-hydroxynaphthalen-2-yl)carbonyl]benzotrile (**28b**),³² 4-[(3-methoxynaphthalen-2-yl)carbonyl]benzotrile (**28c**),³² 4-Cyano-*N*-methoxy-*N*-methylbenzamide (**28d**).³²

Synthesis of the Target Compounds

Procedure A.²⁴ Boronic acid (0.75 mmol, 1 equivalent), aryl bromide or -triflate (0.9–1.3 equivalents), and tetrakis(triphenylphosphane)palladium(0) (43 mg, 37.5 μmol , 5 mol %) were suspended in 1.5 mL DMF in a 10 mL septum-capped tube containing a stirring magnet. To this was added a solution of $NaHCO_3$ (189 mg, 2.25 mmol, 3 equivalents) in 1.5 mL water and the vial was sealed with a Teflon cap. The mixture was irradiated with

microwaves for 15 min at a temperature of 150 °C with an initial irradiation power of 100 W. After the reaction, the vial was cooled to 40 °C, the crude mixture was partitioned between ethyl acetate and water and the aqueous layer was extracted three times with ethyl acetate. The combined organic layers were dried over MgSO₄ and the solvents were removed in vacuo. The coupling products were obtained after flash chromatography on silica gel (petroleum ether/ethyl acetate mixtures) and/or crystallization. If an oil was obtained, it was dissolved in diethyl ether/methanol and transferred into the hydrochloride salt by 1N HCl solution in isopropanol/diethyl ether, followed by filtration and optional crystallization from acetone. Analytical data refer to the free base unless otherwise noted.

Procedure B. Boronic acid (1 equivalent), aryl bromide or -triflate (1.3–1.5 equivalents), and tetrakis(triphenylphosphane)palladium(0) (5 mol %) were suspended in toluene/ethanol 4/1 to give a 0.07–0.1 M solution of boronic acid under an atmosphere of nitrogen. To this was added a 1 N aqueous solution of Na₂CO₃ (6 equivalents). The mixture was then refluxed for 12–18 h, cooled to room temperature, diluted with water and extracted several times with ethyl acetate. The combined extracts were dried over MgSO₄, concentrated and purified by flash chromatography on silica gel (petroleum ether/ethyl acetate mixtures) and/or crystallization. If an oil was obtained, it was dissolved in diethyl ether/methanol and transferred into the hydrochloride salt by 1N HCl solution in isopropanol/diethyl ether, followed by filtration and optional crystallization from acetone. Analytical data refer to the free base unless otherwise noted.

Procedure C.^{33,34} To a 0.6 M solution of NaI (6 equivalents) in acetonitrile was added chlorotrimethylsilane (6 equivalents) at room temperature, and the mixture was stirred for 30 min before cooling to 0 °C with an ice-water bath. Then, a 1 M solution of the phenyl naphthyl alcohol (1 equivalent) in acetonitrile was added dropwise. After complete addition the mixture was heated at 55 °C for 3 h. After recooling to room temperature, the reaction was quenched by addition of saturated aqueous NaHCO₃ solution. The layers were separated, and the aqueous layer extracted twice with ethyl acetate. The combined organic layers were washed with a solution of Na₂S₂O₃, water and brine. The extracts were dried over MgSO₄, concentrated and purified by flash chromatography on silica gel (petroleum ether/ethyl acetate mixtures). If an oil was obtained, it was dissolved in diethyl ether/methanol and transferred into the hydrochloride salt by 1N HCl solution in isopropanol/diethyl ether, followed by filtration and optional crystallization from acetone. Analytical data refer to the free base unless otherwise noted.

Procedure D. To a 0.05 M solution of benzoynaphthalene in dry methanol was added sodium borohydride (2 equivalents) at such a rate as to maintain the internal reaction temperature below 5 °C. The reaction mixture was stirred for 1 h, diluted with diethylether and treated with saturated aqueous NaHCO₃ solution. The mixture was then extracted three times with ethyl acetate, washed twice with saturated aqueous NaHCO₃ solution and once with brine and dried over MgSO₄. The filtrate was concentrated in vacuo, and the residue was flash chromatographed on silica gel (petroleum ether/ethyl acetate mixtures) to afford the corresponding alcohols.

3-(3-Phenyl naphthalen-2-yl)pyridine (11) was obtained according to procedure A from **11a** (657 mg, 1.86 mmol) and phenylboronic acid (854 mg, 4.00 mmol) after flash chromatography on silica gel (petroleum ether/ethyl acetate, 7/3, *R_f* = 0.22) as a colorless oil (195 mg, 0.69 mmol, 37 %), precipitation of the hydrochloride salt afforded a highly hygroscopic solid, mp (HCl salt) 106–109 °C. MS *m/z* 282.70 (MH⁺). Anal. (C₂₁H₁₅N·HCl·1.5H₂O) C, H, N.

3-(3-Benzyl naphthalen-2-yl)pyridine (12) was obtained according to procedure A from **12a** (433 mg, 1.18 mmol) and 3-pyridineboronic acid (105 mg, 0.85 mmol) after flash chromatography on silica gel (petroleum ether/ethyl acetate, 4/1, *R_f* = 0.19) as a colorless oil (186 mg, 0.63 mmol, 74 %), mp (HCl salt) 197–198 °C. MS *m/z* 296.14 (MH⁺). Anal. (C₂₂H₁₇N·HCl·0.6H₂O) C, H, N.

3-(3-Benzyl-6-methoxynaphthalen-2-yl)pyridine (13) was obtained according to procedure A from **13a** (462 mg, 1.17 mmol) and 3-pyridineboronic acid (100 mg, 0.81 mmol) after flash chromatography on silica gel (petroleum ether/ethyl acetate, 4/1, *R_f* = 0.18) as a colorless oil (196 mg, 0.60 mmol, 74 %), mp (HCl salt) 170–172 °C. MS *m/z* 326.09 (MH⁺). Anal. (C₂₃H₁₉NO·HCl·0.6H₂O) C, H, N.

3-[3-(2-Methoxybenzyl)naphthalen-2-yl]pyridine (14) was obtained according to procedure A from **14a** (462 mg, 1.17 mmol) and 3-pyridineboronic acid (100 mg, 0.81 mmol) after flash chromatography on silica gel (petroleum ether/ethyl acetate, 7/3, *R_f* = 0.26) as colorless oil (161 mg, 0.50 mmol, 61 %), mp (HCl salt) 214–216 °C. MS *m/z* 326.02 (MH⁺). Anal. (C₂₃H₁₉NO·HCl·0.6H₂O) C, H, N.

3-[3-(3-Methoxybenzyl)naphthalen-2-yl]pyridine (15) was obtained according to procedure A from **15a** (433 mg, 1.09 mmol) and 3-pyridineboronic acid (92 mg, 0.75 mmol) after flash chromatography on silica gel (petroleum

ether/ethyl acetate, 4/1, $R_f = 0.13$) as a colorless oil (162 mg, 0.50 mmol, 66 %), mp (HCl salt) 161–162 °C. MS m/z 326.02 (MH^+). Anal. ($C_{23}H_{19}NO \cdot HCl \cdot 0.6H_2O$) C, H, N.

3-[3-(4-Methoxybenzyl)naphthalen-2-yl]pyridine (16) was obtained according to procedure A from **16a** (476 mg, 1.20 mmol) and 3-pyridineboronic acid (92 mg, 0.75 mmol) after flash chromatography on silica gel (petroleum ether/ethyl acetate, 4/1, $R_f = 0.14$) as a colorless oil (199 mg, 0.56 mmol, 75 %), mp (HCl salt) 180–182 °C. 1H -NMR (500 MHz, $CDCl_3$): $\delta = 3.75$ (s, 3H), 4.00 (s, 2H), 6.72 (d, $^3J = 8.8$ Hz, 2H), 6.82 (d, $^3J = 8.8$ Hz, 2H), 7.26 (ddd, $^3J = 7.9$ Hz, $^3J = 4.7$ Hz, $^5J = 0.9$ Hz, 1H), 7.45–7.52 (m, 3H), 7.68 (s, 1H), 7.70 (s, 1H), 7.79–7.83 (m, 2H), 8.55 (dd, $^4J = 2.2$ Hz, $^5J = 0.9$ Hz, 1H), 8.59 (dd, $^3J = 4.7$ Hz, $^4J = 1.9$ Hz, 1H). ^{13}C -NMR (125 MHz, $CDCl_3$): $\delta = 39.0, 55.2, 113.7, 122.7, 126.0, 126.4, 127.3, 127.6, 128.9, 129.4, 129.7, 132.0, 132.4, 133.1, 136.6, 137.06, 137.13, 148.2, 149.9, 157.9$. MS m/z 326.16 (MH^+). Anal. ($C_{23}H_{19}NO \cdot HCl \cdot 0.6H_2O$) C, H, N.

4-(3-Pyridin-3-yl-naphthalen-2-ylmethyl)benzotrile (17) was obtained according to procedure C from **33** (841 mg, 2.50 mmol), sodium iodide (2.25 g, 15.0 mmol) and chlorotrimethylsilane (1.63 g, 15.0 mmol) after flash chromatography on silica gel (petroleum ether/ethyl acetate, 7/3, $R_f = 0.15$) as a colorless oil (486 mg, 1.52 mmol, 61 %), mp (HCl salt) 130–131 °C. MS m/z 321.33 (MH^+). Anal. ($C_{23}H_{16}N_2 \cdot HCl \cdot 0.8H_2O$) C, H, N.

3-[3-(4-Trifluoromethoxybenzyl)naphthalen-2-yl]pyridine (18) was obtained according to procedure C from **34** (395 mg, 1.00 mmol), sodium iodide (899 mg, 6.0 mmol) and chlorotrimethylsilane (652 mg, 6.0 mmol) after flash chromatography on silica gel (petroleum ether/ethyl acetate, 4/1, $R_f = 0.28$) as a colorless oil (292 mg, 0.77 mmol, 77 %), precipitation of the hydrochloride salt afforded a highly hygroscopic solid, mp (HCl salt) 139–142 °C. MS m/z 379.90 (MH^+). Anal. ($C_{24}H_{17}F_3NO \cdot HCl \cdot 0.2H_2O$) C, H, N.

3-[6-Methoxy-3-(4-methoxybenzyl)naphthalen-2-yl]pyridine (19) was obtained according to procedure A from **19a** (512 mg, 1.20 mmol) and 3-pyridineboronic acid (113 mg, 0.92 mmol) after flash chromatography on silica gel (petroleum ether/ethyl acetate, 7/3, $R_f = 0.18$) as a colorless oil (189 mg, 0.55 mmol, 60 %), mp (HCl salt) 114–115 °C. 1H -NMR (500 MHz, $CDCl_3$): $\delta = 3.75$ (s, 3H), 3.91 (s, 3H), 3.98 (s, 2H), 6.73 (d, $^3J = 8.5$ Hz, 2H), 6.84 (d, $^3J = 8.5$ Hz, 2H), 7.09 (d, $^4J = 2.5$ Hz, 1H), 7.13 (dd, $^3J = 9.0$ Hz, $^4J = 2.5$ Hz, 1H), 7.25 (dd, $^3J = 8.0$ Hz, $^3J = 4.8$ Hz, 1H), 7.51 (m, 1H), 7.57 (s, 1H), 7.60 (s, 1H), 7.71 (d, $^3J = 8.9$ Hz, 1H), 8.54 (d, $^4J = 1.9$ Hz, 1H), 8.56 (dd, $^3J = 4.8$ Hz, $^4J = 1.5$ Hz, 1H). ^{13}C -NMR (125 MHz, $CDCl_3$): $\delta = 38.9, 55.2, 55.3, 105.2, 113.7, 119.0, 122.8, 127.5, 127.8, 129.1, 129.2, 129.8, 132.6, 134.4, 134.8, 136.8, 137.3, 137.6, 148.1, 150.1, 157.9, 158.1$. MS m/z 356.25 (MH^+). Anal. ($C_{24}H_{21}NO_2 \cdot HCl \cdot 0.8H_2O$) C, H, N.

3-[7-Methoxy-3-(4-methoxybenzyl)naphthalen-2-yl]pyridine (20) was obtained according to procedure C from **20a** (400 mg, 1.08 mmol), sodium iodide (1.65 g, 11.0 mmol) and chlorotrimethylsilane (1.20 g, 11.0 mmol) after flash chromatography on silica gel (petroleum ether/ethyl acetate, 7/3, $R_f = 0.11$) as a colorless oil (148 mg, 0.42 mmol, 39 %), mp (HCl salt) 101–103 °C. MS m/z 356.04 (MH^+). Anal. ($C_{24}H_{21}NO_2 \cdot HCl \cdot 0.1H_2O$) C, H, N.

3-Methoxy-5-[3-(4-methoxybenzyl)naphthalen-2-yl]pyridine (21) was obtained according to procedure A from **16a** (396 mg, 1.00 mmol) and 5-methoxy-3-pyridineboronic acid acid (130 mg, 0.85 mmol) after flash chromatography on silica gel (petroleum ether/ethyl acetate, 7/3, $R_f = 0.21$) as a colorless oil (149 mg, 0.42 mmol, 49 %), mp (HCl salt) 106–108 °C. MS m/z 356.09 (MH^+). Anal. ($C_{24}H_{21}NO_2 \cdot HCl \cdot 0.5H_2O$) C, H, N.

3-Methoxy-5-[6-methoxy-3-(4-methoxybenzyl)naphthalen-2-yl]pyridine (22) was obtained according to procedure A from **19a** (426 mg, 1.00 mmol) and 5-methoxy-3-pyridineboronic acid acid (130 mg, 0.85 mmol) after flash chromatography on silica gel (petroleum ether/ethyl acetate, 7/3, $R_f = 0.18$) as colorless plates (244 mg, 0.63 mmol, 75 %), mp 129–130 °C. MS m/z 385.91 (MH^+). Anal. ($C_{25}H_{23}NO_3$) C, H, N.

3-(3-Benzyl-6-methoxynaphthalen-2-yl)5-methoxypyridine (23) was obtained according to procedure A from **13a** (396 mg, 1.00 mmol) and 5-methoxy-3-pyridineboronic acid acid (130 mg, 0.85 mmol) after flash chromatography on silica gel (petroleum ether/ethyl acetate, 7/3, $R_f = 0.21$) as a colorless oil (221 mg, 0.62 mmol, 73 %), mp (HCl salt) 119–121 °C. MS m/z 356.09 (MH^+). Anal. ($C_{24}H_{21}NO_2 \cdot HCl \cdot 0.2H_2O$) C, H, N.

4-[3-(4-Methoxybenzyl)naphthalen-2-yl]isoquinoline (24) was obtained according to procedure A from **16a** (396 mg, 1.00 mmol) and 4-isoquinolineboronic acid (130 mg, 0.75 mmol) after flash chromatography on silica gel (petroleum ether/ethyl acetate, 7/3, $R_f = 0.20$) as a colorless oil (178 mg, 0.47 mmol, 63 %), mp (HCl salt) 202–203 °C. MS m/z 376.12 (MH^+). Anal. ($C_{27}H_{21}NO \cdot HCl \cdot 0.5H_2O$) C, H, N.

4-[6-Methoxy-3-(4-methoxybenzyl)naphthalen-2-yl]isoquinoline (25) was obtained according to procedure A from **19a** (456 mg, 1.07 mmol) and 4-isoquinolineboronic acid (130 mg, 0.75 mmol) after flash chromatography on silica gel (petroleum ether/ethyl acetate, 7/3, $R_f = 0.18$) and crystallization from acetone/diethyl ether as colorless plates (178 mg, 0.44 mmol, 59 %), mp 158–159 °C. MS m/z 406.00 (MH^+). Anal. ($C_{28}H_{23}NO_2$) C, H, N.

(4-Methoxyphenyl)(3-pyridin-3-yl-naphthalen-2-yl)methanone (26) was obtained according to procedure B from **26a** (4.02 g, 9.80 mmol) and 3-pyridineboronic acid (1.02 g, 8.33 mmol) after flash chromatography on silica

gel (petroleum ether/ethyl acetate, 1/1, $R_f = 0.22$) as an off-white solid (2.66 g, 7.84 mmol, 94 %), mp 69–72 °C. MS m/z 340.07 (MH^+). Anal. ($C_{23}H_{17}NO_2 \cdot 0.2H_2O$) C, H, N.

(3-Fluoro-4-methoxyphenyl)(3-pyridin-3-yl-naphthalen-2-yl)methanone (27) was obtained according to procedure B from **27a** (4.19 g, 9.78 mmol) and 3-pyridineboronic acid (1.02 g, 8.33 mmol) after flash chromatography on silica gel (petroleum ether/ethyl acetate, 1/1, $R_f = 0.16$) as an off-white solid (2.52 g, 7.05 mmol, 85 %), mp 96–97 °C. MS m/z 358.00 (MH^+). Anal. ($C_{23}H_{16}FNO_2 \cdot 0.1H_2O$) C, H, N.

4-(3-Pyridin-3-yl-naphthalene-2-carbonyl)benzotrile (28) was obtained according to procedure B from **28a** (3.0 g, 7.40 mmol) and 3-pyridineboronic acid (1.0 g, 8.20 mmol) after flash chromatography on silica gel (petroleum ether/ethyl acetate, 7/3, $R_f = 0.15$) as yellowish needles (1.67 g, 5.0 mmol, 68 %), mp 135–136 °C. MS m/z 335.05 (MH^+). Anal. ($C_{23}H_{14}N_2O \cdot 0.1H_2O$) C, H, N.

(3-Pyridin-3-yl-naphthalen-2-yl)(4-trifluoromethoxyphenyl)methanone (29) was obtained according to procedure B from **29a** (4.57 g, 9.84 mmol) and 3-pyridineboronic acid (1.02 g, 8.33 mmol) after flash chromatography on silica gel (petroleum ether/ethyl acetate, 7/3, $R_f = 0.20$) as a colorless oil (3.20 g, 8.14 mmol, 98 %), precipitation of the hydrochloride salt afforded a highly hygroscopic solid, mp (HCl salt) 116–118 °C. MS m/z 393.89 (MH^+). Anal. ($C_{23}H_{14}F_3NO_2 \cdot HCl$) C, H, N.

(4-Methoxyphenyl)(6-methoxy-3-pyridin-3-yl-naphthalen-2-yl)methanone (30) was obtained according to procedure B from **30a** (1.54 g, 3.50 mmol) and 3-pyridineboronic acid (374 mg, 3.0 mmol) after flash chromatography on silica gel (petroleum ether/ethyl acetate, 1/1, $R_f = 0.08$) and crystallization from methanol as a white solid (723 mg, 1.96 mmol, 65 %), mp 140–141 °C. MS m/z 370.10 (MH^+). Anal. ($C_{24}H_{19}NO_3 \cdot 0.2H_2O$) C, H, N.

(4-Methoxyphenyl)(3-pyridin-3-yl-naphthalen-2-yl)methanol (31) was obtained according to procedure D from **26** (1.02 g, 3.0 mmol) and sodium borohydride (226 mg, 6.0 mmol) after flash chromatography on silica gel (petroleum ether/ethyl acetate, 1/1, $R_f = 0.18$) as a colorless solid (597 mg, 1.75 mmol, 58 %), mp 77–78 °C. MS m/z 342.10 (MH^+). Anal. ($C_{23}H_{19}NO_2 \cdot 0.3H_2O$) C, H, N.

(3-Fluoro-4-methoxyphenyl)(3-pyridin-3-yl-naphthalen-2-yl)methanol (32) was obtained according to procedure D from **27** (2.11 g, 5.91 mmol) and sodium borohydride (246 mg, 6.50 mmol) after flash chromatography on silica gel (petroleum ether/ethyl acetate, 1/1, $R_f = 0.19$) as a yellowish solid (543 mg, 1.51 mmol, 26 %), mp 75–76 °C. MS m/z 359.96 (MH^+). Anal. ($C_{23}H_{18}FNO_2 \cdot 0.5H_2O$) C, H, N.

4-[Hydroxy-(3-pyridin-3-yl-naphthalen-2-yl)methyl]benzotrile (33) was obtained according to procedure D from **28** (1.46 g, 4.37 mmol) and sodium borohydride (182 mg, 4.80 mmol) after flash chromatography on silica gel (petroleum ether/ethyl acetate, 1/1, $R_f = 0.16$) as a colorless solid (1.22 g, 3.63 mmol, 83 %), mp 101–103 °C. MS m/z 336.93 (MH^+). Anal. ($C_{23}H_{16}N_2O \cdot 0.5H_2O$) C, H, N.

(3-Pyridin-3-yl-naphthalen-2-yl)(4-trifluoromethoxyphenyl)methanol (34) was obtained according to Procedure D from **29** (2.80 g, 7.12 mmol) and sodium borohydride (295 mg, 7.80 mmol) after flash chromatography on silica gel (petroleum ether/ethyl acetate, 1/1, $R_f = 0.32$) as a colorless solid (1.86 g, 4.70 mmol, 66 %), mp 65–66 °C. MS m/z 396.20 (MH^+). Anal. ($C_{23}H_{16}F_3NO_2 \cdot 0.2H_2O$) C, H, N.

3-{3-[Methoxy-(4-methoxyphenyl)methyl]naphthalen-2-yl}pyridine (35). To a suspension of NaH (40 mg, 1.0 mmol, 60% dispersion in oil) in 5 mL dry THF at was added dropwise a solution of **31** (300 mg, 0.88 mmol) in 5 mL THF at room temperature under an atmosphere of nitrogen. After hydrogen evolution ceased, a solution of methyl iodide (59 μ L, 0.95 mmol) in 5 mL THF was added dropwise, and the resulting mixture was stirred for 5 h at room temperature. After 2 h an additional 59 μ L methyl iodide was added. The mixture was then treated with saturated aqueous NH_4Cl solution and extracted three times with ethyl acetate. The combined organic layers were washed with water and brine, dried over $MgSO_4$ and the solvent was evaporated in vacuo. **35** was obtained after flash chromatography on silica gel (petroleum ether/ethyl acetate, 1/1, $R_f = 0.39$) as colorless oil (226 mg, 0.64 mmol, 72 %), mp (HCl salt) 113–114 °C. MS m/z 356.11 (MH^+). Anal. ($C_{24}H_{21}NO_2 \cdot HCl \cdot 0.7H_2O$) C, H, N.

Biological Methods. 1. Enzyme Preparations. CYP17 and CYP19 preparations were obtained by described methods: the 50,000 g sediment of *E. coli* expressing human CYP17⁴⁰ and microsomes from human placenta for CYP19.⁴² **2. Enzyme Assays.** The following enzyme assays were performed as previously described: CYP17⁴⁰ and CYP19.⁴² **3. Activity and Selectivity Assay Using V79 Cells.** V79 MZh 11B1 and V79 MZh 11B2 cells³⁶ were incubated with [4-¹⁴C]-11-deoxycorticosterone as substrate and inhibitor in at least three different concentrations. The enzyme reactions were stopped by addition of ethyl acetate. After vigorous shaking and a centrifugation step (10,000 g, 2 min), the steroids were extracted into the organic phase, which was then separated. The conversion of the substrate was analyzed by HPTLC and a phosphoimaging system as described.^{10,36} **4. Inhibition of Human**

Hepatic CYP Enzymes. The recombinantly expressed enzymes from baculovirus-infected insect microsomes (Supersomes) were used and the manufacturer's instructions (www.gentest.com) were followed.

Computational Methods. 1. Pharmacophore Modeling. The most potent compounds of the heteroaryl substituted methyleneindane and naphthalene derivatives and the most potent flavones were selected as training set (see supplementary material for composition of the training set) for the generation of an extended pharmacophore model. GALAHAD,¹⁹ the pharmacophore generation module of SYBYL 7.3.2 (Sybyl, Tripos Inc., St. Louis, Missouri, USA), was used to generate pharmacophore hypotheses of the series of inhibitors from hypermolecules incorporating the structural information of the dataset and alignments from sets of ligand molecules. In the genetic algorithm, default values were used. In the present case, 100 models were generated and the best 20 pharmacophore-hypotheses were saved. GALAHAD takes into account energetics, steric similarity, and pharmacophoric overlap, while accommodating conformational flexibility, ambiguous stereochemistry, alternative ring configurations, multiple partial match constraints, and alternative feature mappings among molecules. All the other molecules of the library were then aligned using each of the 20 pharmacophores as a template, and the best pharmacophore was selected. The top ranked model was the best in three of the most indicative ranking criteria of the used software (Pareto ranking,²⁰ Specificity, and Mol-query). An additional donor site feature not shown in the figures) was manually added to simulate the complexation of the heme iron by the sp²-hybridized nitrogen (AA1) in order to fix the orientation of the lone pair of the sp²-hybridized nitrogen. This refined pharmacophore model was selected as molecular query for the alignment of our database library. The core of the pharmacophoric scheme is formed by five hydrophobic features (HY0, HY1, HY2a, HY2b) and the acceptor atom (AA) spheres represent the H-bond acceptors. In some cases, the acceptor feature AA2a overlapped a donor feature (data not shown), indicating the presence of an OH function. The final pharmacophore model consists of 12 pharmacophoric features: 4 essential ones (HY0, AA1, HY1), necessary for basal inhibitory potency, and 8 partial matches (HY2, HY2b, AA2a, AA2b, HY3, AA3a, AA3b, and AA4). **2. Protein Modeling and Docking.** Using the resolved human cytochrome CYP2C9 structure (PDB code: 1OG5)⁴³ as template, a homology model was build and refined for CYP11B2. This work has been described in more detail by our group in four recent papers.¹²⁻¹⁵ In this study selected compounds were docked into the refined homology model using FlexX-Pharm.⁴⁴ A pharmacophore constraint was applied to ensure the right binding mode of the inhibitors with the heme-cofactor. For this purpose the standard Fe-N interaction parameters of FlexX^{45,46} were modified and a directed heme-Fe-N interaction was defined perpendicular to the heme-plane. The constraint requires the existence of an inhibitor-nitrogen-atom on the surface of an interaction cone with a 20 degree radius, which has its origin at the Fe-atom and points perpendicular to the heme-plane (with a length of 2.2 Å). Only docking solutions were accepted, which fulfill this constraint. For all other ligand-protein interactions the standard FlexX interaction parameters and geometries were used. The protein-ligand interactions were analyzed using the FlexX software.

Acknowledgement. We thank Gertrud Schmitt and Jeannine Jung for their help in performing the in vitro tests. The investigation of the hepatic CYP profile by Dr. Ursula Müller-Vieira, Pharmacelsus CRO, Saarbrücken, is highly appreciated. S. L. is grateful to Saarland University for a scholarship (Landesgraduiererten-Förderung). Thanks are due to Prof. J. J. Rob Hermans, University of Maastricht, The Netherlands, for supplying the V79 CYP11B1 cells, and Prof. Rita Bernhardt, Saarland University, for supplying the V79 CYP11B2 cells.

Supporting Information Available: Additional inhibitory data of compounds **1–10** (CYP11B1 inhibition and selectivity factors), NMR spectroscopic data of the target compounds **11–15, 17, 18, 20–35**, full experimental details and spectroscopic characterization of the reaction intermediates **11a–16a, 19a, 20a, 26a–30a, 11b–16b, 19b, 26b–30b, 11c–16c, 19c, 11d–16d, 19d, 26d–30d, 12e–14e, 12f–14f, 12g–14g, 12h, 13h**, elemental analysis results and purity data (LC/MS) of compounds **11–35**, pharmacophore modeling training set and pharmacophore geometric properties. This information is available free of charge via the Internet at <http://pubs.acs.org>.

References.

- (1) Kawamoto, T.; Mitsuuchi, Y.; Toda, K.; Yokoyama, Y.; Miyahara, K.; Miura, S.; Ohnishi, T.; Ichikawa, Y.; Nakao, K.; Imura, H.; Ulick, S.; Shizuta, Y. Role of steroid 11 β -hydroxylase and steroid 18-hydroxylase in the biosynthesis of glucocorticoids and mineralocorticoids in humans. *Proc. Natl. Acad. Sci. U.S.A.* **1992**, *89*, 1458–1462.

- (2) (a) Brilla, C. G. Renin-angiotensin-aldosterone system and myocardial fibrosis. *Cardiovasc. Res.* **2000**, *47*, 1–3. (b) Lijnen, P.; Petrov, V. Induction of cardiac fibrosis by aldosterone. *J. Mol. Cell. Cardiol.* **2000**, *32*, 865–879.
- (3) (a) Struthers, A. D. Aldosterone escape during angiotensin-converting enzyme inhibitor therapy in chronic heart failure. *J. Card. Fail.* **1996**, *2*, 47–54. (b) Sato, A.; Saruta, T. Aldosterone escape during angiotensin-converting enzyme inhibitor therapy in essential hypertensive patients with left ventricular hypertrophy. *J. Int. Med. Res.* **2001**, *29*, 13–21.
- (4) Pitt, B.; Zannad, F.; Remme, W. J.; Cody, R.; Castaigne, A.; Perez, A.; Palensky, J.; Wittes, J. The effect of spironolactone on morbidity and mortality in patients with severe heart failure. *N. Engl. J. Med.* **1999**, *341*, 709–717.
- (5) Pitt, B.; Remme, W.; Zannad, F.; Neaton, J.; Martinez, F.; Roniker, B.; Bittman, R.; Hurley, S.; Kleiman, J.; Gatlin, M. Eplerenone, a selective aldosterone blocker, in patients with left ventricular dysfunction after myocardial infarction. *N. Eng. J. Med.* **2003**, *348*, 1309–1321.
- (6) Delcayre, C.; Swynghedauw, B. Molecular mechanisms of myocardial remodeling. The role of aldosterone. *J. Mol. Cell. Cardiol.* **2002**, *34*, 1577–1584.
- (7) (a) Wehling, M. Specific, nongenomic actions of steroid hormones. *Annu. Rev. Physiol.* **1997**, *59*, 365–393. (b) Lösel, R.; Wehling, M. Nongenomic actions of steroid hormones. *Nature Rev. Mol. Cell. Biol.* **2003**, *4*, 46–55.
- (8) Chai, W.; Garrelds, I. M.; de Vries, R.; Batenburg, W. W.; van Kats, J. P.; Danser, A. H. J. Nongenomic effects of aldosterone in the human heart: Interaction with angiotensin II. *Hypertension* **2005**, *46*, 701–706.
- (9) Hartmann, R. W. Selective inhibition of steroidogenic P450 enzymes: Current status and future perspectives. *Eur. J. Pharm. Sci.* **1994**, *2*, 15–16.
- (10) Ehmer, P. B.; Bureik, M.; Bernhardt, R.; Müller, U.; Hartmann, R. W. Development of a test system for inhibitors of human aldosterone synthase (CYP11B2): Screening in fission yeast and evaluation of selectivity in V79 cells. *J. Steroid Biochem. Mol. Biol.* **2002**, *81*, 173–179.
- (11) Hartmann, R. W.; Müller, U.; Ehmer, P. B. Discovery of selective CYP11B2 (aldosterone synthase) inhibitors for the therapy of congestive heart failure and myocardial fibrosis. *Eur. J. Med. Chem.* **2003**, *38*, 363–366.
- (12) Ulmschneider, S.; Müller-Vieira, U.; Mitrenga, M.; Hartmann, R. W.; Oberwinkler-Marchais, S.; Klein, C. D.; Bureik, M.; Bernhardt, R.; Antes, I.; Lengauer, T. Synthesis and evaluation of imidazolymethylenetetrahydronaphthalenes and imidazolymethyleneindanes: Potent inhibitors of aldosterone synthase. *J. Med. Chem.* **2005**, *48*, 1796–1805.
- (13) Ulmschneider, S.; Müller-Vieira, U.; Klein, C. D.; Antes, I.; Lengauer, T.; Hartmann, R. W. Synthesis and evaluation of (pyridylmethylene)tetrahydronaphthalenes/-indanes and structurally modified derivatives: Potent and selective inhibitors of aldosterone synthase. *J. Med. Chem.* **2005**, *48*, 1563–1575.
- (14) Voets, M.; Antes, I.; Scherer, C.; Müller-Vieira, U.; Biemel, K.; Barassin, C.; Oberwinkler-Marchais, S.; Hartmann, R. W. Heteroaryl substituted naphthalenes and structurally modified derivatives: Selective inhibitors of CYP11B2 for the treatment of congestive heart failure and myocardial fibrosis. *J. Med. Chem.* **2005**, *48*, 6632–6642.
- (15) Voets, M.; Antes, I.; Scherer, C.; Müller-Vieira, U.; Biemel, K.; Oberwinkler-Marchais, S.; Hartmann, R. W. Synthesis and evaluation of heteroaryl-substituted dihydronaphthalenes and indenes: Potent and selective inhibitors of aldosterone synthase (CYP11B2) for the treatment of congestive heart failure and myocardial fibrosis. *J. Med. Chem.* **2006**, *49*, 2222–2231.
- (16) Taymans, S. E.; Pack, S.; Pak, E.; Torpy, D. J.; Zhuang, Z.; Stratakis, C. A. Human CYP11B2 (aldosterone synthase) maps to chromosome 8q24.3. *J. Clin. Endocrinol. Metab.* **1998**, *83*, 1033–1036.
- (17) (a) Cavalli, A.; Bisi, A.; Bertucci, C.; Rosini, C.; Paluszczak, A.; Gobbi, S.; Giorgio, E.; Rampa, A.; Belluti, F.; Piazza, L.; Valenti, P.; Hartmann, R. W.; Recanatini, M. Enantioselective nonsteroidal aromatase inhibitors identified through a multidisciplinary medicinal chemistry approach. *J. Med. Chem.* **2005**, *48*, 7282–7289. (b) Gobbi, S.; Cavalli, A.; Rampa, A.; Belluti, F.; Piazza, L.; Paluszczak, A.; Hartmann, R. W.; Recanatini, M.; Bisi, A. Lead optimization providing a series of flavone derivatives as potent nonsteroidal inhibitors of the cytochrome P450 aromatase enzyme. *J. Med. Chem.* **2006**, *49*, 4777–4780.
- (18) Ulmschneider, S.; Negri, M.; Voets, M.; Hartmann, R. W. Development and evaluation of a pharmacophore model for inhibitors of aldosterone synthase (CYP11B2). *Bioorg. Med. Chem. Lett.* **2006**, *16*, 25–30.

- (19) (a) Richmond, N. J.; Abrams, C. A.; Wolohan, P. R.; Abrahamian, E.; Willett, P.; Clark, R. D. GALAHAD: 1. Pharmacophore identification by hypermolecular alignment of ligands in 3D. *J. Comput. Aided Mol. Des.* **2006**, *20*, 567–587. (b) Shepphird, J. K.; Clark, R. D. A marriage made in torsional space: Using GALAHAD models to drive pharmacophore multiplet searches. *J. Comput. Aided Mol. Des.* **2006**, *20*, 763–771. (c) <http://www.tripos.com>.
- (20) Gillet, V. J.; Willett, P.; Fleming, P. J.; Green, D. V. S. Designing focused libraries using MoSELECT. *J. Mol. Graph. Model.* **2003**, *20*, 491–498.
- (21) Miyaura, N.; Suzuki, A. Palladium-catalyzed cross-coupling reactions of organoboron compounds. *Chem. Rev.* **1995**, *95*, 2457–2483.
- (22) Chowdhury, S.; Georghiou, P. E. Synthesis and properties of a new member of the calixnaphthalene family: A C₂-symmetrical endo-calix[4]naphthalene. *J. Org. Chem.* **2002**, *67*, 6808–6811.
- (23) Bengtson, A.; Hallberg, A.; Larhed, M. Fast synthesis of aryl triflates with controlled microwave heating. *Org. Lett.* **2002**, *4*, 1231–1233.
- (24) Appukkuttan, P.; Orts, A. B.; Chandran, R., P.; Goeman, J. L.; van der Eycken, J.; Dehaen, W.; van der Eycken, E. Generation of a small library of highly electron-rich 2-(hetero)aryl-substituted phenethylamines by the Suzuki-Miyaura reaction: A short synthesis of an apogalanthamine analogue. *Eur. J. Org. Chem.* **2004**, 3277–3285.
- (25) Miller, L. E.; Hanneman, W. W.; St. John, W. L.; Smeby, R. R. The reactivity of the methyl group in 2-methyl-3-nitronaphthalene. *J. Am. Chem. Soc.* **1954**, *76*, 296–297.
- (26) Wu, K.-C.; Lin, Y.-S.; Yeh, Y.-S.; Chen, C.-Y.; Ahmed, M. O.; Chou, P.-T.; Hon, Y.-S. Design and synthesis of intramolecular hydrogen bonding systems. Their application in metal cation sensing based on excited-state proton transfer reaction. *Tetrahedron* **2004**, *60*, 11861–11868.
- (27) Brown, H. C.; Narasimhan, S.; Choi, Y. M.; Selective reductions. 30. Effect of cation and solvent on the reactivity of saline borohydrides for reduction of carboxylic esters. Improved procedures for the conversion of esters to alcohols by metal borohydrides. *J. Org. Chem.* **1982**, *47*, 4702–4708.
- (28) Einhorn, J.; Einhorn, C.; Ratajczak, F.; Pierre, J.-L. Efficient and highly selective oxidation of primary alcohols to aldehydes by N-chlorosuccinimide mediated by oxoammonium salts. *J. Org. Chem.* **1996**, *61*, 7452–7454.
- (29) Parikh, J. R.; Doering, W. v. E. Sulfur trioxide in the oxidation of alcohols by dimethyl sulfoxide. *J. Am. Chem. Soc.* **1967**, *89*, 5505–5507.
- (30) Ono, A.; Suzuki, N.; Kamimura, J. Hydrogenolysis of diaryl and aryl alkyl ketones and carbinols by sodium borohydride and anhydrous aluminum(III) chloride. *Synthesis* **1987**, 736–738.
- (31) Bieg, T.; Szeja, W. Removal of O-benzyl protective groups by catalytic transfer hydrogenation. *Synthesis* **1985**, 76–77.
- (32) Li, X.; Hewgley, J. B.; Mulrooney, C. A.; Yang, J.; Kozlowski, M. C. Enantioselective oxidative biaryl coupling reactions catalyzed by 1,5-diazadecalin metal complexes: Efficient formation of chiral functionalized BINOL derivatives. *J. Org. Chem.* **2003**, *68*, 5500–5511.
- (33) Stoner, E. J.; Cothron, D. A.; Balmer, M. K.; Roden, B. A. Benzylolation via tandem Grignard reaction-iodotrimethylsilane (TMSI) mediated reduction. *Tetrahedron* **1995**, *51*, 11043–11062.
- (34) Cain, G. A.; Holler, E. R. Extended scope of in situ iodotrimethylsilane mediated selective reduction of benzylic alcohols. *Chem. Commun.* **2001**, 1168–1169.
- (35) (a) Nakamura, H.; Wu, C.; Inouye, S.; Murai, A. Design, synthesis, and evaluation of the transition-state inhibitors of coelenterazine bioluminescence: Probing the chiral environment of active site. *J. Am. Chem. Soc.* **2001**, *123*, 1523–1524. (b) Gribble, G. W.; Leese, R. M.; Evans, B. E. Reactions of sodium borohydride in acidic media; IV. Reduction of diarylmethanols and triarylmethanols in trifluoroacetic acid. *Synthesis* **1977**, 172–176.
- (36) (a) Denner, K.; Bernhardt, R. Inhibition studies of steroid conversions mediated by human CYP11B1 and CYP11B2 expressed in cell cultures. In *Oxygen Homeostasis and Its Dynamics*, 1st ed.; Ishimura, Y., Shimada, H., Suematsu, M., Eds.; Springer-Verlag: Tokyo, Berlin, Heidelberg, New York, 1998; pp 231–236. (b) Denner, K.; Doehmer, J.; Bernhardt, R. Cloning of CYP11B1 and CYP11B2 from normal human adrenal and their functional expression in COS-7 and V79 chinese hamster cells. *Endocr. Res.* **1995**, *21*, 443–448. (c) Böttner, B.; Denner, K.; Bernhardt, R. Conferring aldosterone synthesis to human CYP11B1 by replacing key amino acid residues with CYP11B2-specific ones. *Eur. J. Biochem.* **1998**, *252*, 458–466.

- (37) Lamberts, S. W.; Bruining, H. A.; Marzouk, H.; Zuiderwijk, J.; Uitterlinden, P.; Blijd, J. J.; Hackeng, W. H.; de Jong, F. H. The new aromatase inhibitor CGS-16949A suppresses aldosterone and cortisol production by human adrenal cells in vitro. *J. Clin. Endocrinol. Metab.* **1989**, *69*, 896–901.
- (38) Demers, L. M.; Melby, J. C.; Wilson, T. E.; Lipton, A.; Harvey, H. A.; Santen, R. J. The effects of CGS 16949A, an aromatase inhibitor on adrenal mineralocorticoid biosynthesis. *J. Clin. Endocrinol. Metab.* **1990**, *70*, 1162–1166.
- (39) Heim, R.; Lucas, S.; Grombein, C. M.; Ries, C.; Schewe, K. E.; Negri, M.; Müller-Vieira, U.; Birk, B.; Hartmann, R. W. Overcoming undesirable CYP1A2 inhibition of pyridyl-naphthalene type aldosterone synthase inhibitors: Influence of heteroaryl derivatization on potency and selectivity. *J. Med. Chem.* **2008**, *51*, 5064–5074.
- (40) (a) Ehmer, P. B.; Jose, J.; Hartmann, R. W. Development of a simple and rapid assay for the evaluation of inhibitors of human 17 α -hydroxylase-C_{17,20}-lyase (P450c17) by coexpression of P450c17 with NADPH-cytochrome-P450-reductase in *Escherichia coli*. *J. Steroid Biochem. Mol. Biol.* **2000**, *75*, 57–63; (b) Hutschenreuter, T. U.; Ehmer, P. B.; Hartmann, R. W. Synthesis of hydroxy derivatives of highly potent nonsteroidal CYP17 inhibitors as potential metabolites and evaluation of their activity by a non cellular assay using recombinant enzyme. *J. Enzyme Inhib. Med. Chem.* **2004**, *19*, 17–32.
- (41) Thompson, E. A.; Siiteri, P. K. Utilization of oxygen and reduced nicotinamide adenine dinucleotide phosphate by human placental microsomes during aromatization of androstenedione. *J. Biol. Chem.* **1974**, *249*, 5364–5372.
- (42) Hartmann, R. W.; Batzl, C. Aromatase inhibitors. Synthesis and evaluation of mammary tumor inhibiting activity of 3-alkylated 3-(4-aminophenyl)piperidine-2,6-diones. *J. Med. Chem.* **1986**, *29*, 1362–1369.
- (43) Williams, P. A.; Cosme, J.; Ward, A.; Angove, H. C.; Matak Vinkovic, D.; Jhoti, H. Crystal structure of human cytochrome P4502C9 with bound warfarin. *Nature* **2003**, *424*, 464–468.
- (44) Hindle, S. A.; Rarey, M.; Buning, C.; Lengauer, T. Flexible docking under pharmacophore type constraints. *J. Comput. Aided Mol. Des.* **2002**, *16*, 129–149.
- (45) Rarey, M.; Kramer, B.; Lengauer, T.; Klebe, G. A fast flexible docking method using an incremental construction algorithm. *J. Mol. Biol.* **1996**, *261*, 470–489.
- (46) Rarey, M.; Kramer, B.; Lengauer, T. Multiple automatic base selection: Protein-ligand docking based on incremental construction without manual intervention. *J. Comput. Aided Mol. Des.* **1997**, *11*, 369–384.

3.4.4. Conclusions and Outlook.

In this project two pharmacophore models have been established, which resulted very helpful in the drug design process. Especially the second pharmacophore (paper **XIV**), in combination with docking studies, led to the development of a new class of aldosterone synthase inhibitors with an increased molecular complexity and a very good selectivity and activity profile.

Nevertheless, in the light of already newly synthesized inhibitors of CYP11B2, not included in the two pharmacophores presented herein, and of the recently solved crystal structure of aromatase, first steroidogenic CYP enzyme crystallized so far, two main computational approaches could be advisable for the future.

In first line, the pharmacophore model should be extended by including the above mentioned new inhibitor classes developed in house, but also by including inhibitors published in literature and included in patents of Speedel and Novartis. Especially the stereospecific characteristics of the chiral inhibitors should be addressed, since these are often responsible for selectivity between CYP11B2, CYP11B1 and aromatase (i.e. R/S-fadrozole).

Most of the homology models of CYP11B2 reported in literature are based on bacterial CYP enzymes as templates or at best on a hepatic mammalian (CYP2C9) one. The aromatase x-ray structure 3EQM might be a valid alternative for the creation of a new homology model of CYP11B2 and CYP11B1. This should take into consideration the inhibitors subject of paper **XIII** and **XIV** and in some extend also the high flexibility characterizing the BC-loop, FG-segment and C-terminal region of the CYP enzymes.

A high gain of informations useful in drug design could be expected from these two suggested approaches, which are already an ongoing work in our research group.

Chapter Four. GENERAL CONCLUSIONS.

Several pathologies related to the fields of oncology, congestive heart failure and blood pressure regulation are steroid hormone-dependent. Thus, steroidogenic enzymes involved in the last steps of the biosynthesis of the steroidal hormones could be indicated as valid pharmaceutical targets. Currently several inhibitors of such enzymes are used in clinics or at least in clinical trials, but most of them are based on a steroidal scaffold, which might implicate systemic side effects and reduced target selectivities.

In this work, several computational methodologies were applied in order to rationalize and increase the knowledge of the three-dimensional structure of the active site of four steroidogenic enzymes, namely CYP17, CYP19, CYP11B2 and 17 β -HSD1, as well as to investigate the fundamental functional and structural features required by different classes of non-steroidal inhibitors of the mentioned enzymes in order to reach high potency and good selectivity. The final aim was to speed up the rational drug design process of non-steroidal lead candidates to be applied in hormone-dependent pathologies, like breast and prostate cancer, endometriosis, congestive heart failure and hypertension.

As a part of this thesis the tridimensional structure of the androgen-producing enzyme cytochrome P450 17 (17 α -hydroxylase/17,20-lyase) was built using as a core template the mammalian CYP2C9 crystal structure. Further, this homology model of CYP17 could plausibly explain the binding mode of the substrate pregnenolone and the differences in the binding affinities of different classes of non-steroidal CYP17 inhibitors as an output of docking studies. This substantially speeded up the drug design process of a new non-steroidal inhibitors of CYP17, resulting in an increase of their molecular complexity and inhibitory potency.

An analogous study has been performed on aromatase, where a series of imidazolylmethylene-benzophenones was investigated by docking studies performed on the aromatase model (PDB entry 1tqa). This investigation sustained the development of new non-steroidal AI presenting with a very high inhibitory potency.

A combination of ligand- and structure based techniques was used in the CYP11B2 project, which resulted into two pharmacophore models with a good predictive capacity, and into a new class of aldosterone synthase inhibitors with an increased selectivity versus the highly homologous isoform CYP11B1 and the hepatic CYP enzymes in general. These pharmacophore models, in particular the second one, might be suitable for virtual screening of 3D databases, searching for new lead candidates.

In the 17 β -HSD1 project, an in-depth structural analysis of existing crystal structures was the basis for mechanistic studies concerning the catalytic cycle, as well as for the drug design process. The combination of molecular dynamic simulations, quantum chemical investigations, and docking studies led to the hypothesis of the kinetic cycle of the enzyme and to the identification of an alternative binding mode for a class of non-steroidal 17 β -HSD1 inhibitors, which might act by functional disruption of the enzyme.

Altogether, this work shows the power of computational methodologies in modern macromolecular, as well as drug design research, especially when these methods are used in combination. They are a perfect complement to traditional medicinal chemistry and can

contribute strongly to the multidisciplinary research efforts in the field of steroidogenic enzymes and hormone-dependent diseases.

Chapter Five. BIBLIOGRAPHY.

Steroidogenesis:

1. <http://commons.wikimedia.org/w/thumb.php?f=Steroidogenesis.svg>
2. Miller WL. (1988) Molecular biology of steroid hormone synthesis. *Endocr Rev.* 9:295–318.
3. Copland JA, Sheffield-Moore M, Koldzic-Zivanovic N, Gentry S, Lamprou G, Tzortzatou-Stathopoulou F, Zoumpourlis V, Urban RJ, Vlahopoulos SA. (2009) Sex steroid receptors in skeletal differentiation and epithelial neoplasia: is tissue-specific intervention possible? *Bioessays* 31:629-641.
4. <http://themedicalbiochemistrypage.org/images/adrenalsteroidsynthesis.jpg>
5. <http://themedicalbiochemistrypage.org/images/malesexhormones.jpg>

Endocrinology vs intracrinology:

6. Labrie F, Van Luu-The, Lin SX, Simard J, Labrie C, El-Alfy M, Pelletier G, Bélanger A. (2000) Intracrinology and 17 β -HSD dehydrogenases *J Mol Endocrinol.* 25:1–16.
7. a) Labrie C, Belanger A, Labrie F. (1988) Androgenic activity of dehydroepiandrosterone and androstenedione in the rat ventral prostate. *Endocrinology* 123(3):1412-7. b) Labrie F, Dupont A, Belanger A. (1985) Complete androgen blockade for the treatment of prostate cancer. *Important Adv Oncol.* 193-217. c) Labrie F. (1991) Intracrinology *Mol Cell Endocrinol.* 78:C113-C118.
8. Sasano H, Suzuki T, Miki Y, Moriya T. (2008) Intracrinology of estrogens and androgens in breast carcinoma. *J Steroid Biochem Mol Biol.* 108:181–185.
9. Hayat MJ, Howlader N, Reichman ME, Edwards BK. (2007) Cancer statistics, trends, and multiple primary cancer analyses from the surveillance, epidemiology, and end results (SEER) program. *Oncologist* 12:20-37.
10. Jemal A, Siegel R, Ward E, Hao Y, Xu J, Murray T, Thun MJ. (2008) Cancer statistics, 2008. *CA Cancer J Clin.* 58:71-96.
11. Ferlay J, Autier P, Boniol M, Heanue M, Colombet M, Boyle P. (2007) Estimates of the cancer incidence and mortality in Europe in 2006. *Ann Oncol.* 18:581-592.
12. Labrie F, Bélanger A, Simard J, Van Luu-The, Labrie C. (1995) DHEA and peripheral androgen and estrogen formation: intracrinology. *Ann N Y Acad Sci.* 774:16-28.
13. Labrie F, Dupont A, Belanger A, Lacoursiere Y, Raynaud JP, Husson JM, Gareau J, Fazekas ATA, Sandow J, Monfette G, Girard JG, Emond J, Houle JG. (1983) New approach in the treatment of prostate cancer: Complete instead of partial withdrawal of androgens. *The Prostate.* 4:579-594.
14. Labrie F, Bélanger A, Cusan L, Seguin C, Pelletier G, Kelly PA, Reeves JJ, Lefebvre FA, Lemay A, Gourdeau Y, Raynaud JP. (1980) Antifertility Effects of LHRH Agonists in the Male. *J Androl.* 1:209-228.
15. Labrie F, Dupont A, Belanger A, Cusan L, Lacoursiere Y, Monfette G, Laberge JG, Emond JP, Fazekas AT, Raynaud JP, Husson JM. (1982) New hormonal therapy in prostatic carcinoma: combined treatment with LHRH agonist and an antiandrogen. *Clin Invest Med.* 5:267–275.
16. Pienta KJ, Bradley D. (2006) Mechanisms underlying the development of androgen-independent prostate cancer. *Clin Cancer Res.* 12:1665-1671.
17. Kitamura M, Buczko E, Dufau ML. (1991) Dissociation of hydroxylase and lyase activities by site-directed mutagenesis of the rat P45017 alpha. *Mol Endocrinol.* 5:1373–1380.

18. Roach M 3rd, Bae K, Speight J, Wolkov HB, Rubin P, Lee RJ, Lawton C, Valicenti R, Grignon D, Pilepich MV. (2008) Short-term neoadjuvant androgen deprivation therapy and external-beam radiotherapy for locally advanced prostate cancer: long-term results of RTOG 8610. *J Clin Oncol.* 26, 585–591.
19. Simpson ER, Mahendroo MS, Means GD, Kilgore MW, Hinshelwood MM, Graham-Lorence S, Amarneh B, Ito Y, Fisher CR, Michael MD, Mendelson CR, Bulun SE. (1994) Aromatase cytochrome P450, the enzyme responsible for estrogen biosynthesis. *Endocr Rev.* 15:342–355.
20. a) Buzdar A, Jonat W, Howell A, Jones SE, Blomqvist C, Vogel CL, Eiermann W, Wolter JM, Azab M, Webster A, Plourde PV. (1996) Anastrozole, a potent and selective aromatase inhibitor, versus megestrol acetate in postmenopausal women with advanced breast cancer: results of overview analysis of two phase III trials. Arimidex Study Group. *J Clin Oncol.* 14:2000-2011. b) Buzdar A, Douma J, Davidson N, Elledge R, Morgan M, Smith R, Porter L, Nabholz J, Xiang X, Brady C. (2001) Phase III, Multicenter, Double-Blind, Randomized Study of Letrozole, an Aromatase Inhibitor, for Advanced Breast Cancer Versus Megestrol Acetate. *J Clin Oncol.* 19:3357-3366.
21. Travis RC, Key TJ. (2003) Oestrogen exposure and breast cancer risk. *Breast Cancer Res.* 5:239-247.
22. Lower EE, Blau R, Gazder P, Stahl DL. (1999) The effect of estrogen usage on the subsequent hormone receptor status of primary breast cancer. *Breast Cancer Res Treat.* 58:205-211.
23. a) Nelson HD, Fu R, Griffin JC, Nygren P, Smith ME, Humphrey L. (2009) Systematic review: comparative effectiveness of medications to reduce risk for primary breast cancer. *Ann Intern Med.* 151:703-15, W226-W235. b) Mathew J, Asgeirsson KS, Jackson LR, Cheung KL, Robertson JF. (2009) Neoadjuvant endocrine treatment in primary breast cancer - review of literature. *Breast* 18:339-344.
24. Rotanski K. (1860) Über Uterusdrüsen - Neubildung in Uterus und Ovarialsarkomen. *Zentralblatt der Gesellschaft der Ärzte in Wien* 37:577-593.
25. a) Bulun SE, Zeitoun K, Sasano H, Simpson ER. (1999) Aromatase in aging women. *Seminars in reproductive Endocrinology* 17:349–358. b) Bulun SE, Zeitoun K, Takayama K, Noble L, Michael D, Simpson E, Johns A, Putman M, Sasano H. (1999) Estrogen production in endometriosis and use of aromatase inhibitors to treat endometriosis. *Endocr Relat Cancer* 6:293-301.
26. Attar E, Bulun SE. (2006) Aromatase and other steroidogenic genes in endometriosis: translational aspects. *Hum Reprod Update* 12:49-56.
27. a) Sampson JA. (1927) Peritoneal endometriosis due to the menstrual dissemination of endometrial tissue into the peritoneal cavity. *Am J Obstet Gynecol.* 14:422. b) Giudice LC, Kao LC. (2004) Endometriosis. *Lancet* 364:1789-1799.
28. Ferrero S, Ragni N, Remorgida V. (2006) Antiangiogenic therapies in endometriosis. *Br J Pharmacol.* 149:133-135.
29. Bush NJ. (2007) Advances in hormonal therapy for breast cancer. *Semin Oncol Nurs.* 23:46-54.
30. Berkley KJ, Rapkin AJ, Papka RE. (2005) The pains of endometriosis. *Science* 308:1587-1589.
31. Cowie MR, Mosterel A, Wood DA, Deckers JW, Poole-Wilson PA, Grobbee DE. (1997) The epidemiology of heart failure. *Eur Heart J.* 18:208–225.
32. Connell JM, Davies E. (2005) The new biology of aldosterone. *J Endocrinol.* 186:1-20.
33. Schiffrin EL. (2004) The Many Targets of Aldosterone. *Hypertension* 43:938-940.
34. Delcayre C, Silvestre JS, Garnier A, Oubenaissa A, Cailmail S, Tatara E, Swynghedauw B, Robert V. (2000) Cardiac aldosterone production and ventricular remodeling. *Kidney Int.* 57:1346–1351.
35. Struthers AD. (2002) Aldosterone: cardiovascular assault. *Am Heart J.* 144:2-7.
36. Satoh M, Nakamura M, Saitoh H, Satoh H, Akatsu T, Iwasaka J, Masuda T, Hiramori K. (2002) Aldosterone synthase (CYP11B2) expression and myocardial fibrosis in the failing human heart. *Clin Sci. (Lond.)* 102:381–386.

37. a) The CONSENSUS trial study group. (1987) Effects of enalapril on mortality in severe congestive heart failure. Results of the cooperative north scandinavian enalapril survival study (CONSENSUS). *N Engl J Med.* 316:1429–1435. b) Kjekshus J, Swedberg K, Snapinn S. (1992) Effects of enalapril on long-term mortality in severe congestive heart failure. *Am J Cardiol.* 69:103–107.
38. SOLVD Investigators. (1991) Effect of enalapril on survival in patients with reduced left ventricular ejection fractions and congestive heart failure. *N Engl J Med.* 325:293-302.
39. a) Struthers AD. (1996) Aldosterone escape during angiotensin-converting enzyme inhibitor therapy in chronic heart failure. *J Card Fail.* 2:47–54. b) Sato A, Saruta T. (2001) Aldosterone escape during angiotensin-converting enzyme inhibitor therapy in essential hypertensive patients with left ventricular hypertrophy. *J Int Med Res.* 29:13–21.
40. Pitt B, Zannad F, Remme WJ, Cody R, Castaigne A, Perez A, Palensky J, Wittes J. (1999) The effect of spironolactone on morbidity and mortality in patients with severe heart failure. Randomized Aldactone Evaluation Study Investigators. *N Engl J Med.* 341:709-717.
41. a) Pitt B, Williams G, Remme WJ, Martinez F, Lopez-Sendon J, Zannad F, Neaton J, Roniker B, Hurley S, Burns D, Bittman R, Kleiman J. (2001) The EPHEsus trial: eplerenone in patients with heart failure due to systolic dysfunction complicating acute myocardial infarction. Eplerenone Post-AMI Heart Failure Efficacy and Survival Study. *Cardiovasc Drugs Ther.* 15:79-87. b) Pitt B, Remme WJ, Zannad F, Neaton J, Martinez F, Roniker B, Bittman R, Hurley S, Kleiman J, Gatlin M. (2003) Eplerenone a selective aldosterone blocker in patients with left ventricular dysfunction after myocardial infarction. *N Engl J Med.* 348:1309-1321. c) Adamopoulos C, Ahmed A, Fay R, Angioi M, Filippatos G, Vincent J, Pitt B, Zannad F. (2009) Timing of Eplerenone Initiation and Outcomes in Patients With Heart Failure After Acute Myocardial Infarction Complicated by Left Ventricular Systolic Dysfunction: Insights From the EPHEsus Trial. *Eur J Heart Fail.* 11:1099-1105.
42. Christ M, Grimm W, Maisch B. (2004) Significance of aldosterone antagonist therapy. *Internist (Berl).* 45:347-354.
43. Hartmann RW. (1994) Selective inhibition of steroidogenic P450 enzymes: Current status and future perspectives. *Eur J Pharm Sci.* 2:15-16.
44. Hartmann RW, Müller U, Ehmer PB. (2003) Discovery of selective CYP11B2 (aldosterone synthase) inhibitors for the therapy of congestive heart failure and myocardial fibrosis. *Eur J Med Chem.* 38:363-366.
45. a) Menard J. (2004) The 45-year story of the development of an anti-aldosterone more specific than spironolactone. *Mol Cell Endocrinol.* 217:45–52. b) Krum H, Nolly H, Workman D, He W, Roniker B, Krause S, Fakouhi K. (2002) Efficacy of eplerenone added to renin-angiotensin blockade in hypertensive patients. *Hypertension* 40:117-123. c) Rousseau MF, Gurne O, Duprez D, Van Mieghem W, Robert A, Ahn S, Galanti L, Ketelslegers J-M, Belgian RALES Investigators. (2002) Beneficial neurohormonal profile of spironolactone in severe congestive heart failure: Results from the RALES neurohormonal substudy. *J Am Coll Cardiol.* 40:1596-1601.
46. a) Wehling M. (1997) Specific, nongenomic actions of steroid hormones. *Annu Rev Physiol.* 59:365-393. b) Lösel R, Wehling M. (2003) Nongenomic actions of steroid hormones. *Nature Rev Mol Cell Biol.* 4:46-55. c) Haseroth K, Gerdes D, Berger S, Feuring M, Günther A, Herbst C, Christ M, Wehling M. (1999) Rapid nongenomic effects of aldosterone in mineralocorticoid-receptor-knockout mice. *Biochem Biophys Res Commun.* 266:257-261.

Cytochromes P450:

47. a) Poulos TL, Johnson EF in *Cytochrome P450: Structure Mechanism and Biochemistry* 3rd edn (ed. Ortiz de Montellano, P.) 87–114 (Kluwer Academic/Plenum, 2004). b) Michael W. King, PhD <http://themedicalbiochemistrypage.org/steroid-hormones.html>. c) <http://p450.abc.hu>.
48. Guengerich FP. (2004) Cytochrome P450: what have we learned and what are the future issues. *Drug Metab Rev.* 36:159-197.

49. Wade RC, Winn PJ, Schlichting E, Sudarko. (2004) A survey of active site access channels in cytochromes P450. *J Inorg Biochem.* 98:1175-1182.
50. Meunier B, de Visser SP, Shaik S. (2004) Mechanism of oxidation reactions catalyzed by cytochrome P450 enzymes. *Chem Rev.* 104:3947-3980.
51. a) Schleinkofer K, Sudarko, Winn PJ, Ludemann SK, Wade RC. (2005) Do mammalian cytochrome P450s show multiple ligand access pathways and ligand channelling? *EMBO reports* 6:584-589. b) Winn PJ, Ludemann SK, Gauges R, Lounnas V, Wade RC. (2002) Comparison of the dynamics of substrate access channels in three cytochrome P450s reveals different opening mechanisms and a novel functional role for a buried arginine. *Proc Natl Acad Sci USA* 99:5361-5366.
52. Wade RC, Motiejunas D, Schleinkofer K, Sudarko, Winn PJ, Banerjee A, Kaniakin A, Jung C. (2005) Multiple molecular recognition mechanisms. Cytochrome P450 - A case study. *BBA Proteins Proteom.* 1754:239-244.
53. Roumen LL, Sanders MPA, Koen P, Hilbers PAJ, Plate R, Custers E, de Gooyer M, Smits JFM, Beugels I, Emmen J, Ottenheijm HCJ, Leysen D, Hermans JJR. (2007) Construction of 3D models of the CYP11B family as a tool to predict ligand binding characteristics *J Comput Aided Mol Des.* 21:455-471.
54. Ristau O, Jung C. (1991) Binding sites of pyridine in cytochrome P-450cam. *Biochim Biophys Acta* 1078:321-325.
55. Miller WL. (2009) Androgen synthesis in adrenarche. *Rev Endocr Metab Disord* 10:3-17.
56. Gotoh O. (1992) Substrate recognition sites in cytochrome P450 family 2 (CYP2) proteins inferred from comparative analyses of amino acid and coding nucleotide sequences. *J Biol Chem.* 267:83-90.
57. Biason-Lauber A, Kempken B, Werder E, Forest MG, Einaudi S, Ranke MB, Matsuo N, Brunelli V, Schoenle EJ, Zachmann M. (2000) 17 α -hydroxylase/17,20-lyase deficiency as a model to study enzymatic activity regulation: role of phosphorylation. *J Clin Endocrinol Metab.* 85:1226-1231.
58. a) Lee-Robichaud P, Shyadehi AZ, Wright JN, Akhtar ME, Akhtar M. (1995) Mechanistic kinship between hydroxylation and desaturation reactions: acyl-carbon bond cleavage promoted by pig and human CYP17 (P-450(17) α ; 17 α -hydroxylase-17,20-lyase). *Biochemistry* 34:14104-14113. b) Lee-Robichaud P, Kaderbhai MA, Kaderbhai N, Wright JN, Akhtar M. (1997) Interaction of human CYP17 (P-450(17) α), 17 α -hydroxylase-17,20-lyase) with cytochrome b5: importance of the orientation of the hydrophobic domain of cytochrome b5. *Biochem J.* 321:857-863. c) Lee-Robichaud P, Akhtar ME, Akhtar M. (1998) Control of androgen biosynthesis in the human through the interaction of Arg347 and Arg358 of CYP17 with cytochrome b5. *Biochem J.* 332:293-296. d) Lee-Robichaud P, Akhtar ME, Wright JN, Sheikh QI, Akhtar M. (2004) The cationic charges on Arg347, Arg358 and Arg449 of human cytochrome P450c17 (CYP17) are essential for the enzyme's cytochrome b5-dependent acyl-carbon cleavage activities. *J Steroid Biochem Mol Biol.* 92:119-130.
59. a) Auchus RJ, Miller WL. (1999) Molecular modeling of human P450c17 (17 α -hydroxylase/17,20-lyase): insights into reaction mechanisms and effects of mutations. *Mol Endocrinol.* 13:1169-1182. b) Lewis DFV, Lee-Robichaud P. (1998) Molecular modelling of steroidogenic cytochromes P450 from families CYP11, CYP17, CYP19 and CYP21 based on the CYP102 crystal structure. *J Steroid Biochem Mol Biol.* 66:217-233. c) Schappach A. and Hölftje HD. (2001) Molecular modelling of 17 α -hydroxylase-17,20-lyase. *Pharmazie* 56:435-442.
60. Miller WL, Auchus RJ, Geller DH. (1997) The regulation of 17, 20 lyase activity. *Steroids* 62:133-142.
61. Miller WL, Geller DH, Auchus RJ. (1998) The molecular basis of isolated 17,20 lyase deficiency. *Endocrin Res.* 24:817-825.
62. Auchus RJ, Rainey WE. (2004) Adrenarche – physiology, biochemistry and human disease. *Clin Endocrinol.* 60:288-296.
63. Flück CE, Miller WL, Auchus RJ. (2003) 17, 20-Lyase Activity of Cytochrome P450c17. *J Clin Endocrinol Metab.* 88:3762-3766.
64. Yap TA, Carden CP, Attard G, de Bono JS. (2008) Targeting CYP17: established and novel approaches in prostate cancer. *Curr Opin Pharmacol.* 8:449-457.

65. Ghosh D, Griswold J, Erman M, Pangborn W. (2009) Structural basis for androgen specificity and oestrogen synthesis in human aromatase. *Nature* 457:219-224.
66. Bulun SE, Lin Z, Imir G, Amin S, Demura M, Yilmaz B, Martin R, Utsunomiya H, Thung S, Gurates B, Tamura M, Langoi D, Deb S. (2005) Regulation of aromatase expression in estrogen-responsive breast and uterine disease: From bench to treatment. *Pharmacol Rev.* 57:359-383.
67. Simpson E, Mahendroo M, Means G, Kilgore M, Hinshelwood M, Graham-Lorence S, Amarneh B, Ito Y, Fisher C, Michael M. (1994) Aromatase cytochrome P450, the enzyme responsible for estrogen biosynthesis. *Endocr Rev.* 15:342-355.
68. Miller WR, Mullen P, Sourdaine P, Watson C, Dixon JM, Telford J. (1997) Regulation of aromatase activity within the breast. *J Steroid Biochem Mol Biol.* 61:193-202.
69. Brodie A, Njar V, Macedo LF, Vasaitis TS, Sabnis G. (2009) The Coffey Lecture: Steroidogenic enzyme inhibitors and hormone dependent cancer. *Urologic Oncology: Seminars and Original Investigations* 27:53-63.
70. a) Hartmann RW, Batzl C. (1986) Aromatase inhibitors. Synthesis and evaluation of mammary tumor inhibiting activity of 3-alkylated 3-(4-aminophenyl)piperidine-2,6-diones. *J Med Chem.* 29:1362-1369. b) Bayer H, Batzl C, Hartmann RW, Mannschreck A. (1991) New aromatase inhibitors. Synthesis and biological activity of pyridyl-substituted tetralone derivatives. *J Med Chem.* 34:2685-2691. c) Hartmann RW, Bayer H, Grün GL, Sergejew T, Bartz U, Mitrenga M. (1995) Pyridyl-substituted tetrahydrocyclopropa[a]naphthalenes: highly active and selective inhibitors of P450 arom. *J Med Chem.* 38:2103-2111. c) Wächter GA, Hartmann RW, Sergejew T, Grün GL, Ledergerber D. (1996) Tetrahydro-naphthalenes: Influence of heterocyclic substituents on inhibition of steroidogenic enzymes P450 arom and P450 17. *J Med Chem.* 39:834-841. d) Recanatini M, Bisi A, Cavalli A, Belluti F, Gobbi S, Rampa A, Valenti P, Palzer M, Paluszczak A, Hartmann RW. (2001) A new class of non steroidal aromatase inhibitors: Design and synthesis of chromone and xanthone derivatives, and inhibition of P450 enzymes aromatase and 17 α -hydroxylase/C17,20-lyase. *J Med Chem.* 44:672-680. e) Gobbi S, Cavalli A, Rampa A, Belluti F, Piazza L, Paluszczak A, Hartmann RW, Recanatini M, Bisi A. (2006) Lead optimization providing a series of flavone derivatives as potent nonsteroidal inhibitors of the cytochrome P450 aromatase enzyme. *J Med Chem.* 49:4777-80.
71. Hartmann RW. (1986) Influence of alkyl chain ramification on estradiol receptor binding affinity and intrinsic activity of 1,2-dialkylated 1,2-bis(4- or 3-hydroxyphenyl)ethane estrogens and antiestrogens. *J Med Chem.* 29:1668-1674. b) Schwarz W, Hartmann RW, Engel J, Schneider MR, Schönenberger H. (1989) Ester derivatives of the mammary-tumor-inhibiting antiestrogen 2,3-bis(2-fluoro-4-hydroxyphenyl)-2,3-dimethylbutane. *J Cancer Res Clin Oncol.* 115:161-165. c) Hartmann RW, Kranzfelder G, von Angerer E, Schönenberger H. (1980) Antiestrogens. Synthesis and evaluation of mammary tumor inhibiting activity of 1,1,2,2-tetraalkyl-1,2-diphenylethanes. *J Med Chem.* 23:841-8. d) Katzenellenbogen BS, Katzenellenbogen JA. (2000) Estrogen receptor transcription and transactivation: Estrogen receptor alpha and estrogen receptor beta - regulation by selective estrogen receptor modulators and importance in breast cancer. *Breast Cancer Res.* 2:335-344. e) Cummings FJ, Bhardwaj S. (2002) Estrogen receptor antagonists: Progress in hormonal therapy for metastatic breast cancer. *Clin Ther.* 24:C59-C60. f) Riggs BL, Hartmann LC. (2003) Selective estrogen-receptor modulators - mechanisms of action and application to clinical practice. *N Engl J Med.* 348:618-629.
72. Baum M, Budzar AU, Cuzick J, Forbes J, Houghton JH, Klijn JG, Sahmoud T. (2002) Anastrozole alone or in combination with tamoxifen vs. tamoxifen alone for adjuvant treatment of postmenopausal women with early breast cancer: First results of the ATAC randomized trial. *Lancet* 359: 2131-2139.
73. Kawamoto T, Mitsuuchi Y, Toda K, Yokoyama Y, Miyahara K, Miura S, Ohnishi T, Ichikawa Y, Nakao K, Imura H. (1992) Role of steroid 11 β -hydroxylase and steroid 18-hydroxylase in the biosynthesis of glucocorticoids and mineralocorticoids in humans. *Proc Natl Acad Sci. USA* 89:1458-1462.
74. Lisurek M, Bernhardt R. (2004) Modulation of aldosterone and cortisol synthesis on the molecular level. *Mol Cell Endocrinol.* 215:149-159.

75. a) Bureik M, Lisurek M, Bernhardt R. (2002) The human steroid hydroxylases CYP11B1 and CYP11B2. *Chem Biol.* 383:1537–1551. b) Belkina NV, Lisurek M, Ivanov AS, Bernhardt R. (2001) Modelling of 3D structures of cytochromes P450 11B1 and 11B2. *J Inorg Biochem.* 87:197–207.
76. Fisher A, Friel EC, Bernhardt R, Gomez-Sanchez C, Connell JM, Fraser R, Davies E. (2001) Effects of 18-hydroxylated steroids on corticosteroid production by human aldosterone synthase and 11 β -hydroxylase. *J Clin Endocrinol Metab.* 86:4326–4329.
77. a) Böttner B, Schrauber H, Bernhardt R. (1996) Engineering a mineralocorticoid- to a glucocorticoid-synthesizing cytochrome P450. *J Biol Chem.* 271:8028–8033. (b) Böttner B, Denner K, Bernhardt R. (1998) Conferring aldosterone synthesis to human CYP11B1 by replacing key amino acid residues with CYP11B2-specific ones. *Eur J Biochem.* 252:458–466.
78. Ulmschneider S, Müller-Vieira U, Klein CD, Antes I, Lengauer T, Hartmann RW. (2005) Synthesis and evaluation of (pyridylmethylene)tetrahydronaphthalenes/-indanes and structurally modified derivatives: Potent and selective inhibitors of aldosterone synthase. *J Med Chem.* 48:1563–1575.
79. Ulmschneider S, Müller-Vieira U, Mitrenga M, Hartmann RW, Oberwinkler-Marchais S, Klein CD, Bureik M, Bernhardt R, Antes I, Lengauer T. (2005) Synthesis and evaluation of (imidazolylmethylene)tetrahydronaphthalenes and (imidazolylmethylene)indanes: Potent inhibitors of aldosterone synthase. *J Med Chem.* 48:1796–1805.
80. a) Brilla CG. (2000) Renin-angiotensin-aldosterone system and myocardial fibrosis. *Cardiovasc Res.* 47:1-3. (b) Brilla CG. (2000) Aldosterone and myocardial fibrosis in heart failure. *Herz* 25:299-306. (c) Lijnen P, Petrov V. (2000) Induction of cardiac fibrosis by aldosterone. *J Mol Cell Cardiol.* 32:865-879.
81. a) Connell JMC, Davies E. (2005) The new biology of aldosterone. *J Endocrinol.* 186:1-20. b) Cole MA, Kalman BA, Pace TW, Topczewski F, Lowrey MJ, Spencer RL. (2000) Selective blockade of the mineralocorticoid receptor impairs hypothalamic-pituitary-adrenal axis expression of habituation. *J Neuroendocrinol.* 12:1034-1042.
82. a) Ehmer PB, Bureik M, Bernhardt R, Müller U, Hartmann RW. (2002) Development of a test system for inhibitors of human aldosterone synthase (CYP11B2): screening in fission yeast and evaluation of selectivity in V79 cells. *J Steroid Biochem Mol Biol.* 81:173-179. b) Hartmann RW, Müller U, Ehmer PB. (2003) Discovery of selective CYP11B2 (aldosterone synthase) inhibitors for the therapy of congestive heart failure and myocardial fibrosis. *Eur J Med Chem.* 38:363-366.

Hydroxysteroid dehydrogenases (HSDs):

83. Penning TM. (1996) 17 β -hydroxysteroid dehydrogenase: inhibitors and inhibitor design. *Endocr Relat Cancer* 3:41-56.
84. Agarwal AK, Auchus RJ. (2005) Cellular redox state regulates hydroxysteroid dehydrogenase activity and intracellular hormone potency. *Endocrinology* 146:2531–2538.
85. a) Jornvall H, Persson B, Krook M, Atrian S, Gonzalez-Duarte R, Jeffery J, Ghosh D. (1995) Short-chain dehydrogenases/reductases (SDR). *Biochemistry* 34:6003-6013. b) Bray EJ, Marsden BD, Oppermann U. (2009) The human short-chain dehydrogenase/reductase (SDR) superfamily: A bioinformatics summary *Chem Biol Interact.* 178:99–109.
86. Puranen TJ, Poutanen MH, Peltoketo HE, Vihko PT, Vihko RK. (1994) Site-directed mutagenesis of the putative active site of human 17 beta-hydroxysteroid dehydrogenase type 1. *Biochem J.* 304:289-293.
87. Penning TM. (1997) Molecular endocrinology of hydroxysteroid dehydrogenases. *Endocr Rev.* 18:281-305.
88. a) El-Alfy M, Luu-The V, Huang XF, Berger L, Labrie F, Pelletier G. (1999) Localization of type 5 17 β -hydroxysteroid dehydrogenase, 3 β -hydroxysteroid dehydrogenase, and androgen receptor in the human prostate by in situ hybridization and immunocytochemistry. *Endocrinology* 140:1481–1491. b) Penning TM, Burczynski ME, Jez JM, Hung CF, Lin HK, Ma H, Moore M, Palackal N, Ratnam K. (2000) Human 3 α -hydroxysteroid dehydrogenase isoforms (AKR1C1–AKR1C4) of the aldo-keto reductase superfamily:

functional plasticity and tissue distribution reveals roles in the inactivation and formation of male and female sex hormones. *Biochem J.* 351:67–77.

89. Moeller G, Adamski J. (2006) Multifunctionality of human 17 β -hydroxysteroid dehydrogenases. *Mol Cell Endocrinol.* 248:47-55.
90. Lukacik P, Kavanagh KL, Oppermann, U. (2006) Structure and function of human 17beta-hydroxysteroid dehydrogenases. *Mol Cell Endocrinol.* 248:61-71.
91. Möller G, Adamski J. (2009) Integrated view on 17 β -hydroxysteroid dehydrogenases. *Mol Cell Endocrinol.* 301:7–19.
92. a) Sherbet DP, Papari-Zareei M.; Khan N, Sharma KK, Brandmaier A, Rambally, S Chattopadhyay, A, Andersson S, Agarwal AK, Auchus RJ. (2003) Cofactors, redox state, and directional preferences of hydroxysteroid dehydrogenases. *Mol Cell Endocrinol.* 265-266, 83-88; b) Williamson DH, Lund P, Krebs HA. (1967) The redox state of free nicotinamide-adenine dinucleotide in the cytoplasm and mitochondria of rat liver. *Biochem J.* 103, 514-527.
93. a) Pletnev VZ; Weeks CM; Duax WL. (2004) Rational proteomics II: electrostatic nature of cofactor preference in the short-chain oxidoreductase (SCOR) enzyme family. *Proteins* 57:294-301. b) Mazza C, Breton R, Housset D, Fontecilla-Camps JC. (1998) Unusual charge stabilization of NADP⁺ in 17beta-hydroxysteroid dehydrogenase. *J Biol Chem.* 273:8145-8152.
94. a) Chen Z, Lee WR, Chang SH. (1991) Role of aspartic acid 38 in the cofactor specificity of drosophila alcohol dehydrogenase. *Eur J Biochem.* 202:263-267. b) Huang YW, Pineau I, Chang HJ, Azzi A, Bellemare V, Laberge S, Lin S. X. (2001) Critical residues for the specificity of cofactors and substrates in human estrogenic 17beta-hydroxysteroid dehydrogenase 1: variants designed from the three-dimensional structure of the enzyme. *Mol Endocrinol.* 15:2010-2020.
95. Scrutton NS, Berry A, Perham RN. (1990) Redesign of the coenzyme specificity of a dehydrogenase by protein engineering. *Nature* 343:38-43.
96. Langer LJ, Engel LL. (1958) Human placental estradiol-17 β dehydrogenase I. Concentration, characterization and assay. *J Biol Chem.* 233:583-588.
97. Lin S-X, Yang F, Jin JZ, Breton R, Zhu DW, Luu-The V, Labrie F. (1992) Subunit identity of the dimeric 17 β -hydroxysteroid dehydrogenase from human placenta. *J Biol Chem.* 267:16182-16187.
98. Peltoketo H, Isomaa V, Maentausta O, Vihko R. (1988) Complete amino acid sequence of human placental 17 β -hydroxysteroid dehydrogenase deduced from cDNA. *FEBS Lett.* 239:73-77.
99. Poutanen M, Isomaa V, Peltoketo H, Vihko R. (1995) Role of 17 β -hydroxysteroid dehydrogenase type 1 in endocrine and intracrine estradiol biosynthesis. *J Steroid Biochem Mol Biol.* 55:525-532.
100. Sawetawan C, Milewich L, Word A, Carr B, Rainey W. (1994) Compartmentalization to type 1 17 β -hydroxysteroid oxidoreductase in the human ovary. *Mol Cell Endocrinol.* 99:161-168.
101. Fournet-Dulguerov N, MacLusky N, Leranath C. (1987) Immunohistochemical localization of aromatase cytochrome P-450 and estradiol dehydrogenase in the syncytiotrophoblast of the human placenta. *J Clin Endocrinol Metab.* 65:757-764.
102. Labrie F, Luu-The V, Labrie C, Belanger A, Simard J, Lin S-X, Pelletier G. (2003) Endocrine and intracrine sources of androgens in women: Inhibition of breast cancer and other roles of androgens and their precursor dehydroepiandrosterone. *Endocr Rev.* 24:152–182.
103. Ghosh D, Pletnev VZ, Zhu DW, Wawrzak Z, Duax WL, Pangborn W, Labrie F, Lin S-X. (1995) Structure of human estrogenic 17 β -hydroxysteroid dehydrogenase at 2.20 Å resolution. *Structure* 3:503-513.
104. Luu-The V, Zhang Y, Poirier D, Labrie F. (1995) Characteristics of human types 1, 2 and 3 17 beta-hydroxysteroid dehydrogenase activities: oxidation/reduction and inhibition. *J Steroid Biochem Mol Biol.* 55:581-587.

105. Poutanen M, Miettinen M, Vihko R. (1993) Differential estrogen substrate specificities for transiently expressed human placental 17 β -hydroxysteroid dehydrogenase and an endogenous enzyme expressed in cultured COS-m6 cells. *Endocrinology* 133:2639-2644.
106. Han Q, Campbell RL, Gangloff A, Huang YW, Lin S-X. (2000) Dehydroepiandrosterone and dihydrotestosterone recognition by human estrogenic 17 β -hydroxysteroid dehydrogenase. C-18/C-19 steroid discrimination and enzyme-induced strain. *J Biol Chem.* 275:1105-1111.
107. Puranen T, Poutanen M, Peltoketo HE, Vihko PT, Vihko RK. (1994) Site directed mutagenesis of the putative active site of human 17 β -hydroxysteroid dehydrogenase type 1. *Biochem J.* 304:289-293.
108. Puranen T, Poutanen M, Ghosh D, Vihko P, Vihko R. (1997) Characterization of structural and functional properties of human 17 β -hydroxysteroid dehydrogenase type 1 using recombinant enzymes and site-directed mutagenesis. *Mol Endocrinol.* 11:77-86.
109. Brown WM, Metzger LE, Barlow JP, Hunsaker LA, Deck LM, Royer RE, Van der Jagt DL. (2003) 17 β -hydroxysteroid dehydrogenase type 1: computational design of active site inhibitors targeted to the Rossmann fold *Chem Biol Interact.* 143-144:481-491.
110. Qiu W, Campbell RL, Gangloff A, Dupuis P, Boivin RP, Tremblay MR, Poirier D, Lin S-X. (2002) A concerted, rational design of type 1 17 β -hydroxysteroid dehydrogenase inhibitors: estradiol-adenosine hybrids with high affinity. *FASEB J.* 16:1829-1831.

Aims, Results, Discussion:

111. a) Davidson NE, Lippman ME. (1989) The role of estrogens in growth regulation of breast cancer. *Crit Rev Oncog.* 1:89-111. b) Bernstein L, Ross RK. (1993) Endogenous hormones and breast cancer risk. *Epidemiol Rev.* 15:48-65.
112. a) Poulin R, Labrie F. (1986) Stimulation of cell proliferation and estrogenic response by adrenal C19- Δ 5-steroids in the ZR-75-1 human breast cancer cell line. *Cancer Res.* 46: 4933-4937. b) Labrie F, Simard J, de Launoit Y, Poulin R, Thériault C, Dumont M, Dauvois S, Martel C, Li S. (1992) Androgens and breast cancer. *Cancer Detect Prev.* 16:31-38.
113. Sanderson JT. (2006) The Steroid Hormone Biosynthesis Pathway as a Target for Endocrine-Disrupting Chemicals. *Toxicol Sci.* 94:3-21.
114. Lin D, Zhang LH, Chiao E, Miller WL. (1994) Modeling and mutagenesis of the active site of human P450c17. *Mol Endocrinol.* 8:392-402.
115. a) Laughton CA, Neidle S, Zvelebil MJ, Sternberg MJ. (1990) A molecular model for the enzyme cytochrome P450(17 α), a major target for the chemotherapy of prostatic cancer. *Biochem Biophys Res Comm.* 171:1160-1167. b) Burke DF, Laughton CA, Neidle S. (1997) Homology modelling of the enzyme P450 17 α -hydroxylase/17,20-lyase - a target for prostate cancer chemotherapy - from the crystal structure of P450BM-3. *Anticancer Drug Des.* 12:113-123.
116. Tomlinson ES, Lewis DF, Maggs JL, Kroemer HK, Park BK, Back DJ. (1997) In vitro metabolism of dexamethasone (DEX) in human liver and kidney: the involvement of CYP3A4 and CYP17 (17,20 lyase) and molecular modelling studies. *Biochem Pharmacol.* 54:605-611.
117. Altschul S, Madden T, Schaffer A, Zhang J, Zhang Z, Miller W, Lipman D. (1997) Gapped BLAST and PSI-BLAST: a new generation of protein database search programs. *Nucl Acids Res.* 25:3389-3402.
118. a) Lundström J, Rychlewski L, Bujnicki J, Elofsson A. (2001) Pcons: A neural-network-based consensus predictor that improves fold recognition. *Protein Sci.* 10:2354-2362. b) Wallner B, Fang H, Elofsson A. (2003) Automatic consensus based fold recognition using Pcons, ProQ and Pmodeller. *Proteins* 53(S6):534-541. c) Wallner B, Elofsson A. (2005) Pcons5: combining consensus, structural evaluation and fold recognition scores. *Bioinformatics* 21:4248-54.
119. a) Bryson K, McGuffin LJ, Marsden RL, Ward JJ, Sodhi JS, Jones DT. (2005) Protein structure prediction servers at University College London. *Nucl Acids Res.* 33:W36-38. b) Jones DT. (1999) Protein secondary

- structure prediction based on position-specific scoring matrices. *J Mol Biol.* 292:195-202. c) McGuffin LJ, Bryson K, Jones, D.T. (2000) The PSIPRED protein structure prediction server. *Bioinformatics* 16:404-405.
120. Armougom F, Moretti S, Poirot O, Audic S, Dumas P, Schaeli B, Keduas V, Notredame C. (2006) Espresso: automatic incorporation of structural information in multiple sequence alignments using 3D-Coffee. *Nucl Acids Res.* 34:W604-W608.
 121. Notredame C, Higgins DG, Heringa J. (2000) T-Coffee: A novel method for fast and accurate multiple sequence alignment. *J Mol Biol.* 302:205-217.
 122. Lee-Robichaud P, Akhtar ME, Akhtar M. (1998) An analysis of the role of active site protic residues of cytochrome P-450s: mechanistic and mutational studies on 17 α -hydroxylase-17,20-lyase (P-45017 α also CYP17). *Biochem J.* 330:967-974.
 123. Sherbet DP, Tiosano D, Kwist KM, Hochberg Z, Auchus RJ. (2003) CYP17 mutation E305G causes isolated 17,20-lyase deficiency by selectively altering substrate binding. *J Biol Chem.* 278:48563-48569.
 124. a) Eswar N, Marti-Renom MA, Webb B, Madhusudhan MS, Eramian D, Shen M, Pieper U, Sali A. (2006) Comparative protein structure modeling with MODELLER. Current protocols in bioinformatics. *John Wiley & Sons, Inc., Supplement 15, 5.6.1-5.6.30.* b) Marti-Renom MA, Stuart A, Fiser A, Sánchez R, Melo F, Sali A. (2000) Comparative protein structure modeling of genes and genomes. *Annu Rev Biophys Biomol Struct.* 29:291-325. c) Sali A, Blundell TL. (1993) Comparative protein modelling by satisfaction of spatial restraints. *J Mol Biol.* 234:779-815. d) Fiser A, Do RK, Sali A. (2000) Modeling of loops in protein structures. *Protein Sci.* 9:1753-1773.
 125. a) Case DA, Cheatham TE III, Darden T, Gohlke H, Luo R, Merz KM Jr, Onufriev A, Simmerling C, Wang B, Woods R. (2005) The Amber biomolecular simulation programs. *J Computat Chem.* 26:1668-1688. b) Wang JM, Wolf RM, Caldwell JW, Kollman PA, Case DA (2004) Development and testing of a general amber force field. *J Comput Chem.* 25:1157-1174. c) Case DA, Darden TA, Cheatham TE, Simmerling CL, Wang J, Duke RE, Luo R, Mrtz KM, Pearlman DA, Crowley M, Walker RC, Zhang W, Wang B, Hayik S, Roitberg A, Seabra G, Wong KF, Paesani F, Wu X, Brozell S, Tsui V, Gohlke H, Yang L, Tan C, Mongan J, Hornak V, Cui G, Beroza P, Mathews DH, Schafmeister C, Ross WS, Kollman PA. Amber 9, University of California, San Francisco 2006.
 126. Favia AD, Cavalli A, Masetti M, Carotti A, Recanatini M. (2006) Three-dimensional model of the human aromatase enzyme and density functional parameterization of the iron-containing protoporphyrin IX for a molecular dynamics study of heme-cysteinato cytochromes. *Proteins* 62:1074-1087.
 127. Jones G, Willett P, Glen RC, Leach AR, Taylor R. (1997) Development and validation of a genetic algorithm for flexible docking. *J Mol Biol.* 267:727-748.
 128. Politzer P, Laurence PR, Jayasuriya K. (1985) Molecular electrostatic potentials: An effective tool for the elucidation of biochemical phenomena. *Environmental Health Perspectives* 61:191-202.
 129. Berman HM, Westbrook J, Feng Z, Gilliland G, Bhat TN, Weissig H, Shindyalov IN, Bourne PE. (2000) The Protein Data Bank. *Nucl Acids Res.* 28:235-242.
 130. Dundas J, Ouyang Z, Tseng J, Binkowski A, Turpaz Y, Liang J. (2006) CASTp: computed atlas of surface topography of proteins with structural and topographical mapping of functionally annotated residues. *Nucl Acids Res.* 34:W116-W118.
 131. Krebs WG, Gerstein M. (2000) The morph server: a standardized system for analyzing and visualizing macromolecular motions in a database framework. *Nucl Acids Res.* 28:1665-75.
 132. a) Betz G. (1971) Reaction mechanism of 17 β -estradiol dehydrogenase determined by equilibrium rate exchange. *J Biol Chem.* 246:2063-2068. b) Sherbet DP, Papari-Zareei M, Khan N, Sharma KK, Brandmaier A, Rambally S, Chattopadhyay A, Andersson S, Agarwal AK, Auchus RJ. (2007) Cofactors, redox state, and directional preferences of hydroxysteroid dehydrogenases. *Mol Cell Endocrinol.* 265-266:83-88.

133. Cooper WC, Jin Y, Penning TM (2007) Elucidation of a complete kinetic mechanism for a mammalian hydroxysteroid dehydrogenase (HSD) and identification of all enzyme forms on the reaction coordinate: the example of rat liver 3 α -HSD (AKR1C9). *J Biol Chem.* 282:33848-33493.
134. Sherbet DP, Guryev OL, Papari-Zareei M, Mizrachi D, Rambally S, Akbar S, Auchus RJ. (2009) biochemical factors governing the steady-state estrone/estradiol ratios catalyzed by human 17 β -hydroxysteroid dehydrogenases types 1 and 2 in HEK-293 cells. *Endocrinology* 150:4154–4162.
135. Rafi SB, Cui G, Song K, Cheng X, Tonge PJ, Simmerling C. (2006) Insight through molecular mechanics Poisson-Boltzmann surface area calculations into the binding affinity of triclosan and three analogues for FabI, the E. coli enoyl reductase. *J Med Chem.* 49:4574-80.
136. Bey E, Marchais-Oberwinkler S, Kruchten P, Frotscher M, Werth R, Oster A, Algül O, Neugebauer A, Hartmann RW. (2008) Design, synthesis and biological evaluation of bis(hydroxyphenyl) azoles as potent and selective non-steroidal inhibitors of 17 β -hydroxysteroid dehydrogenase type 1 (17 β -HSD1) for the treatment of estrogen-dependent diseases. *Bioorg Med Chem.* 16:6423-6435.
137. Frisch MJ, Trucks GWS, HB, Scuseria GE, RobbMA, Cheeseman JR, Montgomery JA Jr, Vreven T, Kudin KN, Burant JC, Millam JM, Iyengar SS, Tomasi J, Barone V, Mennucci B, Cossi M, Scalmani G, Rega N, Petersson GA, Nakatsuji H, Hada M, Ehara M, Toyota K, Fukuda R, Hasegawa J, Ishida M, Nakajima T, Honda Y, Kitao O, Nakai H, Klene M, Li X, Knox JE, Hratchian HP, Cross JB, Bakken V, Adamo C, Jaramillo J, Gomperts R, Stratmann RE, Yazyev O, Austin AJ, Cammi R, Pomelli C, Ochterski JW, Ayala PY, Morokuma K, Voth GA, Salvador P, Dannenberg JJ, Zakrzewski VG, Dapprich S, Daniels AD, Strain MC, Farkas O, Malick DK, Rabuck AD, Raghavachari K, Foresman JB, Ortiz JV, Cui Q, Baboul AG, Clifford S, Cioslowski J, Stefanov BB, Liu G, Liashenko A, Piskorz P, Komaromi I, Martin RL, Fox DJ, Keith T, Al-Laham MA, Peng CY, Nanayakkara A, Challacombe M, Gill PMW, Johnson B, Chen W, Wong MWG, Pople JA: Gaussian, Inc.: Pittsburgh, PA: (2003).
138. Dennington I, Roy KT, Millam J, Eppinnett K, Howell WL, Gilliland R: GaussView, 3.0; Semichem Inc., Shawnee Mission (2003).
139. a) Chohan KK, Paine SW, Mistry J, Barton P, Davis AM. (2005) A rapid computational filter for cytochrome P450 1A2 inhibition potential of compound libraries. *J Med Chem.* 48:5154–5161. (b) Korhonen LE, Rahnasto M, Mähönen NJ, Wittekindt C, Poso A, Juvonen RO, Raunio H. (2005) Predictive three-dimensional quantitative structure-activity relationship of cytochrome P450 1A2 inhibitors. *J Med Chem.* 48:3808–3815.

Chapter Six. ACKNOWLEDGEMENTS.

Well, last but not least, the most difficult part... my acknowledgements.

The many thanks, expressions of gratitude, and reminding do not follow a precise order, but are listed as my heart and mind told, thus.. no one should blame me if he or she is ranked more toward the bottom or even not explicitly mentioned. Thanks for understanding.

I'd like to start in a classic manner by expressing my deepest gratitude to my beloved wife Monika and my mother Getrud (or isn't Trudi more appropriate ??!) for their moral and emotional support in these last four years, lamost five. These years were not always easy, because each exile, even if in a wonderful place with persons one is loving, can end up in a golden cage.. (and I am NOT referring to our marriage, Monika). Beside this, I'd never imagined to marry ones, and considering that it passed just a blink of an eye between we met and we became parents, well, I think we managed the this time great, my dearest, and I am looking forward to spend another long long time with you, ti amo Moni.

Thereafter, due to strict chronological appearance, I'd like to embrace my son Amor Leonard (I know you will neither read nor understand these english lines, now, but perhaps later on in your life.. and for what is worth of, I already tell you every day how much I love you and I please spending my time with you.. thus, hurry up and 'all'arrembaggio, capitano'!). He was fundamental for my thesis, because every time I was neglecting my duties he pushed me forward to take the bull by the horns. Of course, by god.. (??) it were not always bed of roses with him, but hey, as I recently read: children are nothing else than angels without wings (fallen ones, I would add), so..

Another big thanks goes to Alessandro, my italian emigrant companion (or 'compagno'), with whom I spent nights disputing on science, politics and not-belonging stuff, as well as to Stefan. I am really gratefull having met two friends like them here, which helped me overcome my Italy-nostalgia, the lack of sun and heat, ... In particular, Stefan, I'd like to thank you for welcoming me in Saarland and Teutons-country, for the great times together, even though I've always lost in squash, damn! Concluding with close relatives in Saarland, I've to mention Rita (whithout you I would have to renounce to a plenty of great meels and Italian cuisine), my stepmother Ulla, always supportive and present when help was needed, and concluding my former flatmates Nicole, Kathrin and David (guys, even if we have barely seen us in the last time, I'll never forget you).

Concluced with "family", my gratitude goes to Prof. Rolf Hartmann (for one time I'll forget the W.) and Prof. Maurizio Recanatini. I'll never forget the 'passionate' discussions with Prof. Hartmann, which without any doubt forged my character (it's hard to slow down when one is stubborn, but I had to!..) and my way of working and scientific thinking; nevertheless, more then ones I had to fight down a "Rolf!", blazing its trail out of my mouth in the heat of the dispute. After all, I think that I have learned a lot, and perhaps that I could also contribute to a better working by bringin in my creativity, and for that I'll risk a "Thank you, Rolf!", coming from the heart.

Since I'm starting to get into confidence, a big thanks goes also to Maurizio. Without your encouragements, help and support I'd never been able to manage my thesis, to spend part of it (too less!) in Bologna and to learn on how to stand on my feets (scientifically speaking).. and this considering you are from Trento! I did not regret ones my decision to do my diploma thesis in the QSAR and modeling lab in Bologna (long time ago) and if I finally "PhD"-myself, well part of the credits deserve to you. By the way, I wish also to thank Andrea Cavalli for his generosity and our fruitful discussions and I'm looking forward for further good cooperations.

An important period of my PhD was embossed by two of my group leaders, Carsten Jagusch and Ralf Heim. Both of you showed me the importance of loyalty and team-work and how strong a group has to work together to reach its goals. Therefore, and not to forget due to several pleasant evenings spent drinking a bottle of wine, you deserve my friendship and gratitude.

Same has to said about the former lab 1 members,Erika, Mariano, Marcel and Ulli, ouff, our Friday after-works were simply great! I'm very thankful for all your precious advices (not only in synthesis) and the long discussion we had about work, love and life.

I wish to thank all my former and present co-workers, in Saarbrücken as well as in Bologna, which had the patience to follow me along the tortuous paths of my mind, and in particular the biology group (Christina, Martina, Sabrina, Sigrid, Patricia, etc.), Emmanuel, Sandrine, Matthias, Adriane, Vittorio, Luisa, etc. They really supported me each time I had to deal with biological aspects (kinetics, testings, etc) or computational approaches concerning my work.

A special thanks then goes to Corina and Martina, the right hands of our "chief" in Saarbrücken. Corina, enjoy becoming a mama and if you will rise your daughter like you were supporting us, well, then I think she'll become a great girl.

Well, to all other AK-Hartmann and QSAR-lab members: listing all of you in the space left is pretty hard, especially because I hate simply setting up lists.. but you all have my gratitude and friendship for the years spend together.. sometimes they were a bit harsh, more often nice and pleased, and this is how I will remind them.

Last annotation goes to my far-far-away friends: Raby, Alex, Max, Paolino, Andi, Paolo, Luke, Heini, etc etc etc.. you are the reason why I don't feel lonely even if I live far-far away. Every time I'm back home or to Italy, it's like we have seen us the day before.. I appreciate and are really grateful that our friendship had last so long, and I hope it will still be like that.

Well, that's all folks.

Matthias

Chapter Seven. APPENDIX

APPENDIX A. CYP families in humans

57 genes divided among 18 families of cytochrome P450 genes and 43 subfamilies.

Family	Function	Members	Names
CYP1	drug and steroid (especially estrogen) metabolism	3 subfamilies, 3 genes, 1 pseudogene	CYP1A1, CYP1A2, CYP1B1
CYP2	drug and steroid metabolism	13 subfamilies, 16 genes, 16 pseudogenes	CYP2A6, CYP2A7, CYP2A13, CYP2B6, CYP2C8, CYP2C9, CYP2C18, CYP2C19, CYP2D6, CYP2E1, CYP2F1, CYP2J2, CYP2R1, CYP2S1, CYP2U1, CYP2W1
CYP3	drug and steroid (including testosterone) metabolism	1 subfamily, 4 genes, 2 pseudogenes	CYP3A4, CYP3A5, CYP3A7, CYP3A43
CYP4	arachidonic acid or fatty acid metabolism	6 subfamilies, 11 genes, 10 pseudogenes	CYP4A11, CYP4A22, CYP4B1, CYP4F2, CYP4F3, CYP4F8, CYP4F11, CYP4F12, CYP4F22, CYP4V2, CYP4X1, CYP4Z1
CYP5	thromboxane A ₂ synthase	1 subfamily, 1 gene	CYP5A1
CYP7	bile acid biosynthesis 7-alpha hydroxylase of steroid nucleus	2 subfamilies, 2 genes	CYP7A1, CYP7B1
CYP8	<i>varied</i>	2 subfamilies, 2 genes	CYP8A1 (prostacyclin synthase), CYP8B1 (bile acid biosynthesis)
CYP11	steroid biosynthesis	2 subfamilies, 3 genes	CYP11A1, CYP11B1, CYP11B2
CYP17	steroid biosynthesis, 17-alpha hydroxylase	1 subfamily, 1 gene	CYP17A1
CYP19	steroid biosynthesis: aromatase synthesizes estrogen	1 subfamily, 1 gene	CYP19A1
CYP20	unknown function	1 subfamily, 1 gene	CYP20A1
CYP21	steroid biosynthesis	2 subfamilies, 2 genes, 1 pseudogene	CYP21A2
CYP24	vitamin D degradation	1 subfamily, 1 gene	CYP24A1
CYP26	retinoic acid hydroxylase	3 subfamilies, 3 genes	CYP26A1, CYP26B1, CYP26C1
CYP27	<i>varied</i>	3 subfamilies, 3 genes	CYP27A1 (bile acid biosynthesis), CYP27B1 (vitamin D3 1-alpha hydroxylase, activates vitamin D3), CYP27C1 (unknown function)
CYP39	7-alpha hydroxylation of 24-hydroxycholesterol	1 subfamily, 1 gene	CYP39A1
CYP46	cholesterol 24-hydroxylase	1 subfamily, 1 gene	CYP46A1
CYP51	cholesterol biosynthesis	1 subfamily, 1 gene, 3 pseudogenes	CYP51A1 (lanosterol 14-alpha demethylase)

APPENDIX B. Catalytic cycle of CYPs

1: The substrate binds to the active site of the enzyme, in close proximity to the heme group, on the side opposite to the peptide chain. The bound substrate induces a change in the conformation of the active site, often displacing a water molecule from the distal axial coordination position of the heme iron, and sometimes changing the state of the heme iron from low-spin to high-spin.

2: The change in the electronic state of the active site favors the transfer of an electron from NAD(P)H via cytochrome P450 reductase or another associated

This takes place by way of the electron transfer chain, as described above, reducing the ferric heme iron to the ferrous state.

3: Molecular oxygen binds covalently to the distal axial coordination position of the heme iron. The cysteine ligand is a better electron donor than histidine, with the oxygen consequently being activated to a greater extent than in other heme proteins. However, this sometimes allows the bond to dissociate, the so-called "decoupling reaction", releasing a reactive superoxide radical, interrupting the catalytic cycle.

4: A second electron is transferred via the electron-transport system, either from cytochrome P450 reductase, ferredoxins, or cytochrome b5, reducing the dioxygen adduct to a negatively charged peroxy group. This is a short-lived intermediate state.

5: The peroxy group formed in step 4 is rapidly protonated twice by local transfer from water or from surrounding amino-acid side chains, releasing one water molecule, and forming a highly reactive iron(V)-oxo species.

6: Depending on the substrate and enzyme involved, P450 enzymes can catalyse any of a wide variety of reactions. A hypothetical hydroxylation is shown in this illustration. After the product has been released from the active site, the enzyme returns to its original state, with a water molecule returning to occupy the distal coordination position of the iron nucleus.

S: An alternative route for mono-oxygenation is via the "peroxide shunt": interaction with single-oxygen donors such as peroxides and hypochlorites can lead directly to the formation of the iron-oxo intermediate, allowing the catalytic cycle to be completed without going through steps 3, 4 and 5. A hypothetical peroxide "XOOH" is shown in the diagram.

C: If carbon monoxide (CO) binds to reduced P450, the catalytic cycle is interrupted. This reaction yields the classic CO difference spectrum with a maximum at 450 nm.

